Characterisation and validation of *ex vivo* nasal epithelial cultures to investigate transmembrane protein 16A as a therapeutic avenue in cystic fibrosis

Dr Iram J Haq

MBBS, MRes, MRCPCH

Doctor of Philosophy

Institute of Cellular Medicine

Newcastle University

February 2019

Abstract

Cystic fibrosis (CF) is the most common genetic life-limiting disease in the UK. Strategies to correct dysfunctional CF transmembrane conductance regulator (CFTR) will not benefit all people with CF and alternative approaches are required. Transmembrane protein 16A (TMEM16A) was recently identified as an essential component of the epithelial calcium activated chloride channel (CaCC) and has potential to bypass effects of faulty CFTR. TMEM16A expression is confirmed in the adult airway, however, its presence in the paediatric airway was previously unknown. Robust experimental models are required to investigate such therapeutic avenues in children. Primary bronchial epithelial cells (PBECs) have been pivotal through their role in CFTR modulator development. Although primary nasal epithelial cells (PNECs) provide a more accessible paediatric model, their characterisation was previously undetermined.

To investigate the role of paediatric PNECs as a substitute for PBECs, I established a programme to sample both nasal and bronchial mucosal brushings from children with and without CF. These were used to develop differentiated paediatric cultures using strategies to optimise culture success by improving cell yield, promoting cell attachment and minimising infection. Epithelial properties of paediatric PNECs were confirmed in relation to tight junctional integrity and muco-ciliary differentiation. Ion transport assessment revealed that CFTR and CaCC expression were not different in PNECs versus PBECs in both non-CF and CF cultures. Low levels of TMEM16A expression were identified in the paediatric nasal and bronchial epithelium. Finally, application of a novel TMEM16A activating compound to the PNEC model demonstrated potential to enhance TMEM16A-mediated airway epithelial chloride transport.

This characterisation of *ex vivo* paediatric PNECs has provided evidence to support their role as a tool to investigate the CF airway. Inter-donor variability of PNEC ion transport properties is an important consideration for future investigation of novel therapeutic modulators of CFTR and alternative ‘non-CFTR’ airway epithelial channels.

Dedication

This thesis is dedicated to my friends and family

Acknowledgements

Firstly, I would like to acknowledge the children and parents who have participated in this study without whom this research would not have been possible. I am also grateful to members of the cystic fibrosis multi-disciplinary team, anaesthetists, surgical theatre and ward nursing staff at the Great North Children's Hospital who facilitated the collection of research material.

My project supervisors, Dr Malcolm Brodlie (ICM), Dr Chris Ward (ICM) and Dr Mike Gray (ICaMB) have provided constant guidance and mentorship throughout this PhD. Their diverse scientific disciplines ensured that I was well placed to carry out this work. They have helped me with ethical approval processes, study design, data interpretation and with my fellowship application.

I am hugely indebted to the support of Dr Brodlie, who has provided frequent and regular supervision over the last three years. In addition to his support with this PhD, his mentorship and guidance has enabled me to further develop my professional clinical academic career.

Within ICM, I am grateful to Professor John Simpson for welcoming me into the Respiratory Research Group and to all members for their general support. Professor Simpson and Professor Sophie Hambleton's guidance with PhD progression and fellowship interview preparation has been invaluable. Also within ICM, Dr Aaron Gardner provided support and training in immunofluorescence, confocal microscopy, quantitative real time polymerase chain reaction techniques and data analysis.

In ICaMB, I am grateful for the training provided by Dr Bernard Verdon with primary airway epithelial cell culture, Ussing chamber experiments, enzyme linked immunosorbent assay techniques, for feeding cells in my absence and for his constant support throughout this PhD. Professor Jeff Pearson has allowed me to utilise laboratory space and his group have provided friendly advice during this research. Dr Vinciane Saint-Criq has provided training and support with Ussing chamber techniques and data analysis. Dr Emily Mavin and Dr Jason Powell have provided training with enzyme linked immunosorbent assays.

Kasim Jiwa in the Sir William Leech Centre for Lung Research, Freeman Hospital has been instrumental to the preparation of paraffin embedded sectioned blocks of primary nasal and bronchial cell cultures and provided training in immunohistochemistry techniques.

I am grateful for the statistical advice provided by Vicky Ryan during the fellowship application process.

This research has been funded by a Wellcome Trust Clinical Research Training Fellowship. I would also like to acknowledge Professor Margarida Amaral (University of Lisbon, Portugal) and Professor Karl Kunzelmann (University of Regensberg, Germany) for their collaboration and provision of novel compounds and preliminary data.

As my educational supervisor for paediatric specialty training, Professor Nick Embleton has provided guidance and mentorship during my research and with my general progression as a paediatric trainee.

Finally, I would like to thank my close friends for their encouragement and support throughout my PhD. They have stayed beside me during my professional journey and provided me with the inspiration, motivation and self-belief to follow my career ambitions. I would also like to give thanks to my parents, who without their incredible hard work, dedication and encouragement early in my life, I would not be where I am today.

Declaration

I declare that I undertook the work described in this thesis between September 2015 until August 2018 full time within the Institute of Cellular Medicine, Institute for Cell and Molecular Biosciences and the Sir William Leech Laboratory, Freeman Hospital.

All laboratory work has been performed by myself under the supervision of my PhD supervisors with the exception of the following work detailed below.

Kasim Jiwa, Sir William Leech Laboratory, prepared the paraffin embedded cell culture sections for use with tinctorial staining. Staff of the Electron Microscopy Research Services, Newcastle University, performed all transmission and scanning electron microscopy work. JinHeng Lin, PhD student of Dr Mike Gray in the Institute for Cell and Molecular Biosciences, performed the intracellular calcium experimental work and assisted with data analysis. Preliminary work to identify and investigate the novel compounds using HT29 cells was performed by the lab groups of Professor Amaral (University Lisbon, Portugal) and Professor Kunzelmann (University of Regensberg, Germany).

Table of Contents

List of figures

List of tables

List of abbreviations

ABC	ATP binding cassette
ALI	Airway liquid interface
ANOVA	Analysis of variance
ASL	Airway surface liquid
ATP	Adenosine triphosphate
BAL	Bronchoalveolar lavage
BEBM	Bronchial epithelial basal medium
BEGM	Bronchial epithelial growth medium
BK	Large conductance potassium channel
BSA	Bovine serum albumin
Ca	Calcium
CaCC	Calcium activated chloride channel
cAMP	Cyclic adenosine monophosphate
cDNA	Complementary deoxyribonucleic acid
CF	Cystic fibrosis
CFTR	Cystic fibrosis transmembrane conductance regulator protein
Cl	Chloride
CLCA	Chloride channel accessory channel
CRISPR	Clustered regularly interspaced short palindromic repeats
CT	Computerised tomography
C_T	Cycle threshold
DMEM	Dulbecco’s Modified Eagle’s Medium
DNA	Deoxyribonucleic acid
EM	Electron microscopy
ENaC	Epithelial sodium channel

FCS	Fetal calf serum
FDA	Food and drug administration
FEV_1	Forced expiratory volume in 1 second
GCP	Good clinical practice
GNCH	Great North Children's Hospital
GPCR	G protein coupled receptor
HEK	Human embryonic kidney
ICL	Intracellular loop
IBMX	3-isobutyl-1-methylxanthine
IFN	Interferon
IL	Interleukin
IP_3	Inositol-1,4,5-triphosphate
IPSC	Induced pluripotent stem cells
IQR	Interquartile range
I_{sc}	Short circuit current
K	Potassium
MCC	Mucociliary clearance
MCL	Mucus layer
Mg	Magnesium
mRNA	Messenger ribonucleic acid
MSD	Membrane spanning domain
MUC	Mucin
Na	Sodium
NICE	National Institute of Clinical Excellence
NBD	Nuclear binding domain
NBS	Newborn screening

PBEC	Primary bronchial epithelial cell
PBS	Phosphate buffered saline
PBST	PBS and 0.05 % Tween 20
PCL	Periciliary layer
PD	Potential difference
PFA	Paraformaldehyde
PIP	Phosphatidylinositol phosphate
PKA	Protein kinase A
PNEC	Primary nasal epithelial cell
R	Regulatory domain
RNA	Ribonucleic acid
ROCK	Rho-associated protein kinase
RPMI	Roswell Park Memorial Institute
RT-qPCR	Quantitative real time polymerase chain reaction
SEM	Scanning electron microscopy
siRNA	Small interfering RNA
TEER	Transepithelial resistance
TEM	Transmission electron microscopy
TNF	Tumour necrosis factor
TMEM16A	Transmembrane protein 16A
UK	United Kingdom
UKCFGTC	UK CF Gene Therapy Consortium
UTP	Uridine triphosphate
Vte	Transepithelial voltage
YFP	Yellow fluorescence protein
($[Ca^{2+}]_I$	Intracellular calcium concentration

1 Chapter 1. Introduction

1.1 Cystic fibrosis

1.1.1 Overview: the significance of cystic fibrosis

Cystic Fibrosis (CF) is the most common life-limiting autosomal recessive disease affecting North Western European populations. Approximately 1 in 2500 newborns and over 10000 children and adults are affected in the United Kingdom (UK) (Cystic Fibrosis Trust, 2011). CF is increasingly recognised to occur in other populations worldwide, albeit at a much lower incidence (O'Sullivan and Freedman, 2009, Elborn, 2016).

The underlying defect in CF arises from mutations in the CF transmembrane conductance regulator *(CFTR)* gene (Riordan et al., 1989) . This encodes for a chloride channel predominantly expressed in epithelia, including the sweat gland, airway, gastrointestinal tract, pancreas and vas deferens. Although this gives rise to multisystem disease, morbidity and mortality is predominantly secondary to progressive respiratory pathology.

Significant advances in the understanding of CF pathophysiology and multidisciplinary clinical care have greatly contributed to improved survival outcomes. The current median age of survival is 45.1 years and the proportion of adults with CF is likely to increase over time (Elborn et al., 1991, Burgel et al., 2015). CF is managed nationally by specialist regional centres comprised of experienced clinicians, nurses, physiotherapists, dieticians and other relevant allied health professionals to provide high quality multidisciplinary treatment in accordance with CF Trust Standards of Care (Cystic Fibrosis Trust, 2011).

The CF national Newborn Screening Programme (NBS) was introduced in the UK in 2007 and has enabled early identification of disease and optimisation of clinical management. Nevertheless, the burden of care remains significant, comprising of intensive daily treatment regimens to improve quality of life and survival. Despite these efforts, progressive respiratory disease leads to eventual respiratory failure and either consideration for lung transplantation where feasible, or unfortunately death.

1.1.2 The genetic defect in cystic fibrosis

The *CFTR* gene was first cloned in 1989 (Riordan et al., 1989). It is located at position q31.2 on the long arm of chromosome 7 and encodes the transmembrane CFTR protein. CFTR is a member of the adenosine triphosphate (ATP)-binding cassette (ABC) transporter superfamily, which are characterised by direct ATP binding to enable cell membrane molecular transport.

CFTR is constructed from two homologous units and in total consists of five membrane domains (Figure 1). Each homologous unit has a membrane spanning domain (MSD), which forms the transmembrane ion channel pore. Unique to other ABC proteins which are active transporters, the CFTR pore is anion selective. Each MSD is connected to a cytoplasmic nucleotide binding domain (NBD). The two homologous units are linked by a regulatory (R) domain, which is phosphorylated by cyclic adenosine monophosphate (cAMP)-dependent activation of protein kinase A (PKA) (Hwang and Sheppard, 2009). R domain phosphorylation together with NBD-ATP binding and subsequent MSD conformational change results in CFTR activation and gating of chloride secretion (Vergani et al., 2005). However, the activation and regulation of CFTR is complex, with additional involvement of other factors including signalling proteins and protein kinases. These form large macromolecular complexes with CFTR and are involved in CFTR trafficking and function (Guggino and Stanton, 2006).

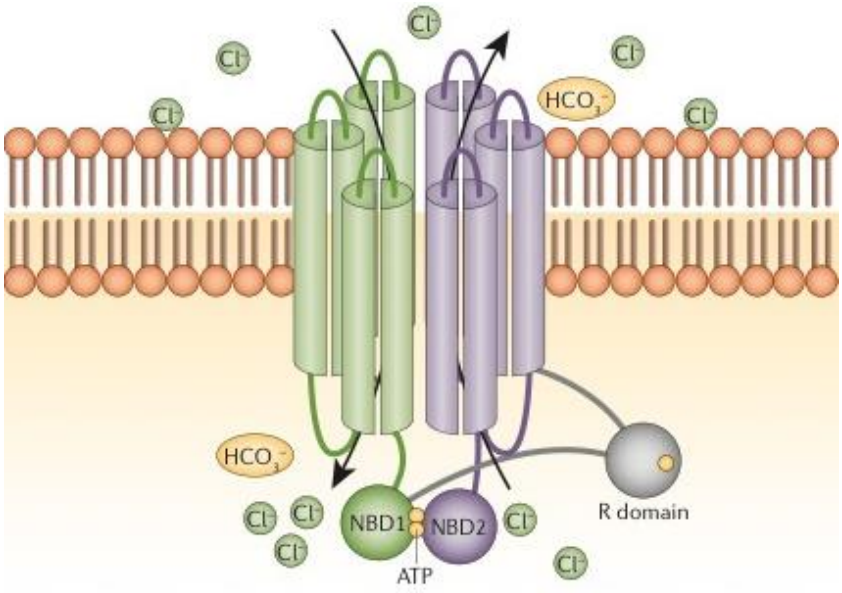

Figure 1: Structure of CFTR

Two MSDs form the ion channel pore across the membrane. These are each connected to an NBD (NBD1 and NBD2) within the cytoplasm. ATP binding to the NBDs coupled with R domain phosphorylation by cAMP-mediated PKA activation results in CFTR channel opening and chloride and bicarbonate secretion. Adapted from (Ratjen et al., 2015).

1.1.3 Classification of cystic fibrosis transmembrane conductance regulator (CFTR) mutations

Approximately 2000 *CFTR* mutations have been identified of which 200 have been confirmed as disease causing. The *F508del* (c.1521_1523delCTT) mutation is the most common in European populations with around 90 % of patients having at least one affected allele and 50 % of patients with two affected alleles in the UK (Zolin et al., 2017). *CFTR* mutations have been classified into six classes according to the underlying mechanisms involved in CFTR synthesis, trafficking and function, as demonstrated in Figure 2 and summarised in Table 1. Class I mutations arise from nonsense, frameshift or messenger ribonucleic acid (mRNA) splicing mutations. This produces premature termination signals resulting in absent protein production. Class II mutations occur as a result of dysfunctional CFTR processing and trafficking to the cell surface. In class III mutations, although CFTR is expressed at the cell surface, there is impaired channel gating due to defective NBD binding. Class IV mutations are a result of abnormalities in the channel pore, resulting in restricted ion transport and conductance defects. Low CFTR levels arise from splicing defects in class V mutations. With class VI mutations, there is instability of functional CFTR at the cell surface resulting in high turnover and reduced levels of CFTR. Despite this classification, some mutations are not confined to an individual class as exemplified by *F508del*. Here, phenylanine deletion at position 508 results in abnormal protein folding due to impaired NBD1 stability, giving rise to a class II mutation. However, this mutation also results in a gating defect as present in class III mutations (Okiyoneda et al., 2010). Furthermore, mutation classification is complicated by the existence of considerable phenotypic heterogeneity within individual mutation types and classes, suggesting a potential impact of other genotypic-phenotypic interactions arising from environmental, microbiological and non-CFTR effects.

Mutation Class	Nature of CFTR defect	Functional consequence	Example	Therapeutic Strategy
I	Protein synthesis	Reduced CFTR expression	Gly542X	Production correctors (ataluren)
II	Protein processing	Misfolded protein degraded in proteasome and not transported to cell surface	F508del	Corrector plus potentiator (lumacaftor plus ivacaftor)
III	Channel gating	Reduced/lack of channel opening	Gly551Asp	Potentiator (ivacaftor)
IV	Channel conductance	Misshaped CFTR pore restricts chloride movement	Arg551Asp	Potentiator (ivacaftor)
V	Reduced protein production	Very low levels of CFTR protein	3849 + 10kb C→T	No data available
VI	Increased cell surface turnover	Functional but unstable protein at cell surface	120del23	No data available

Table 1: *CFTR* mutation classes

Classification of *CFTR* mutations with implicated functional consequences.

Adapted from (Brodlie et al., 2015)

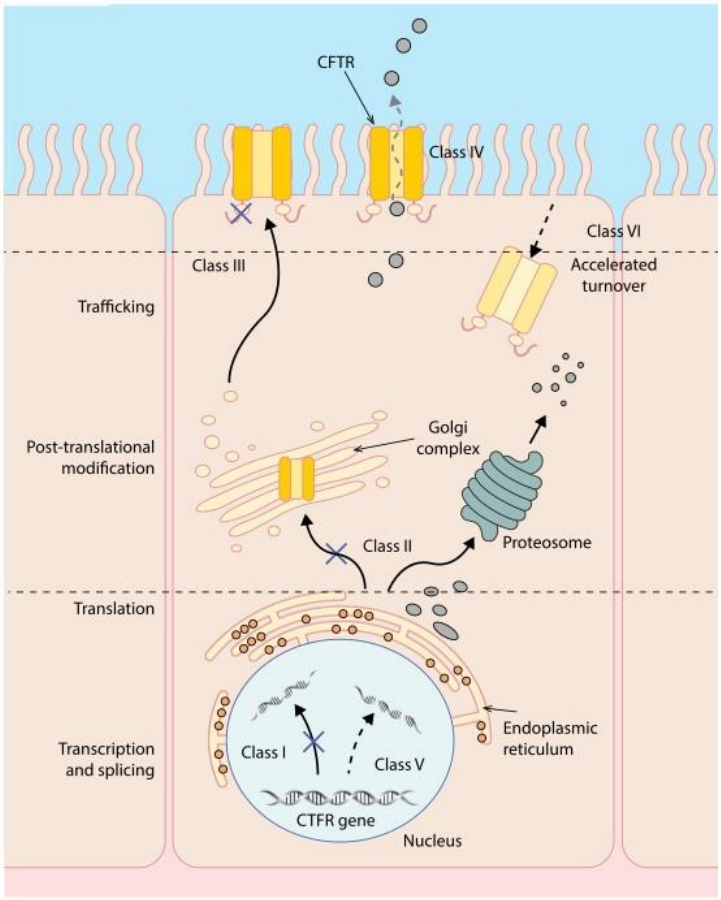

Figure 2: Schematic representation of *CFTR* mutation class

Class I mutations are caused by nonsense, frameshift or mRNA splicing mutations and produce premature termination signals resulting in absent CFTR production. Class II mutations arise from dysfunctional CFTR processing and failure of CFTR trafficking to the cell surface. CFTR is expressed at the cell surface in class III mutations, but impaired channel gating secondary to defective nucleotide binding leads to abnormal chloride epithelial transport. The CFTR channel pore is abnormal in class IV mutations leading to restricted chloride transport and conductance defects. Splicing defects in class V mutations lead to low CFTR levels. In class VI mutations, functional CFTR is unstable at the plasma membrane resulting in high CFTR turnover at the cell surface and reduced levels. Adapted from (Brodlie et al., 2015).

1.1.4 Pulmonary manifestations of cystic fibrosis

CFTR is expressed in multiple organs, giving rise to multisystem disease. Extra-pulmonary manifestations of CF are described in Table 2. Despite this multisystem pathology, progressive pulmonary disease is responsible for 95 % of all morbidity and mortality (Döring et al., 2007). Chronic endobronchial infection, neutrophilic inflammation, and retention of mucopurulent secretions lead to progressive bronchiectasis and eventual irreversible respiratory failure and death. Figure 3 shows radiographic features evident in CF lung disease.

Mainstays of CF therapy have targeted symptomatic relief by provision of stringent regimens of life-long courses of antibiotics, inhaled mucolytic agents and intensive chest physiotherapy. Despite these interventions, eventual respiratory failure results in early mortality unless lung transplantation is available as a feasible option. This has demonstrated survival of 50 % at 10 years post transplantation (Stephenson et al., 2015) . However, after transplantation, long term respiratory morbidity can occur and the burden associated with the extra-pulmonary features persists (Meachery et al., 2008, Stephenson et al., 2015).

Early respiratory infection is typically characterised by *Haemophilus influenza* and *Staphylococcus aureus* bacteria and associated with neutrophilic inflammation (O'Sullivan and Freedman, 2009). This progresses to infection dominated by *Pseudomonas aeruginosa,* which increases in prevalence with age. Initial non-mucoid *P. aeruginosa* strains can be eradicated with targeted aggressive treatment. However, with chronic infections, strains produce biofilms resistant to standard antibiotic therapy (Mathee et al., 1999, Pedersen et al., 1992, Pier et al., 1991). CF airways are susceptible to *P. aeruginosa* growth due to mucus stasis, impaired bacterial clearance, enhanced bacterial-epithelial attachment and the hypoxic microenvironment created by mucus plaques (Smith et al., 1996, Matsui et al., 2006, Worlitzsch et al., 2002). Chronic infection and colonisation is apparent in approximately 80 % of CF patients and causes significant morbidity and mortality (O'Sullivan and Freedman, 2009, Cystic Fibrosis Trust, 2004). Acquisition of resistant strains leads to ongoing neutrophilic inflammation, severe bronchiectasis, decline in lung function and eventual mortality (O'Sullivan and Freedman, 2009). Eradiation is of paramount importance and measures are required to specifically prevent the perpetual pulmonary decline associated with *P. aeruginosa*.

System	Disease Manifestation	Treatment
Gastrointestinal	Meconium ileus (15 % newborns)	Gastrografin enema, surgery
	Distal intestinal obstruction syndrome (15 % adults affected)	As for meconium ileus
	Gastro-oesophageal reflux	Proton pump inhibitors, pro-kinetics, surgery (fundoplication)
	Rectal prolapse	Pancreatic enzyme supplements, surgery
	Increased malignancy	Tumour-specific management
	Pancreatic exocrine insufficiency (90-95 % children affected)	Pancreatic enzyme supplements, fat soluble vitamins (A, D, E, K), dietary intervention
	CF related diabetes (50 % adults affected)	Insulin
	Pancreatitis	Supportive management (intravenous fluids, analgesia)
	CF related liver disease	Vitamin K, ursodeoxycholic acid, transplantation
Upper respiratory tract	Chronic rhinosinusitis +/- nasal polyps	Topical steroids, surgery
Bones	Osteoporosis	Vitamin D, calcium, exercise
Reproductive	Congenital bilateral absence of vas deferens and azoospermia	Fertility counselling and treatment where applicable
	Reduced fertility in females	As above

Table 2: Extra-pulmonary manifestations of CF disease

(Houwen et al., 2010, Moran et al., 2009, Alexander et al., 2008)

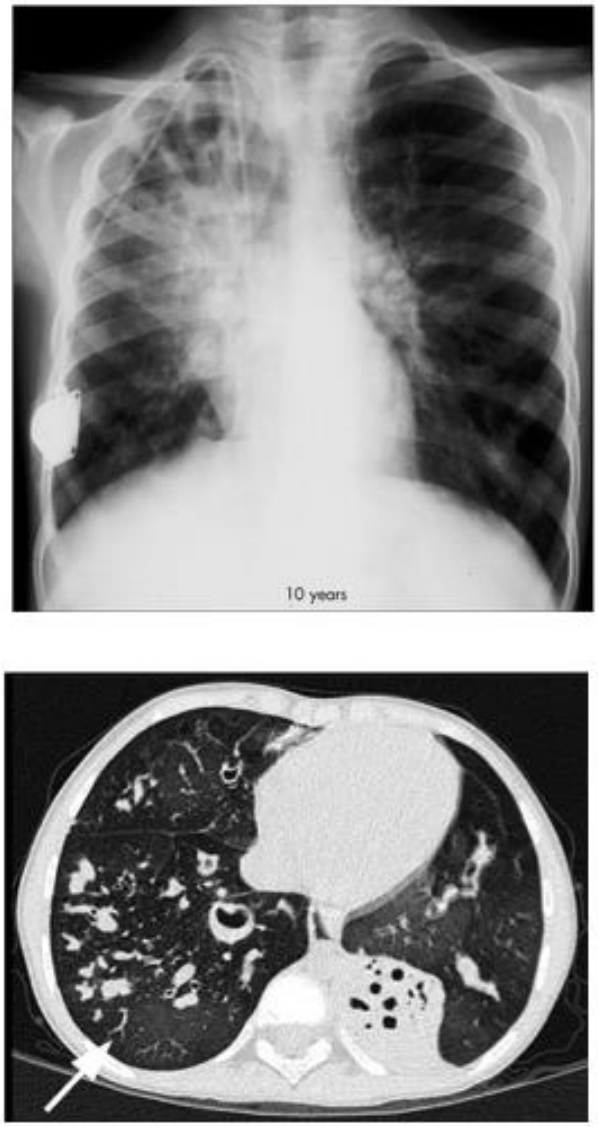

Figure 3: Radiographic features of CF lung disease

Chest x-ray (A) of a 10-year-old child showing evidence of bronchiectasis with collapse and consolidation affecting the right upper lobe. High resolution computerised tomography scan (B) of a teenager with end-stage CF demonstrating extensive severe bronchiectasis with bronchial wall thickening and dilatation. The characteristic “tree-in bud” sign (arrow) is a feature of bronchial luminal mucus plugging and impaction (Rossi and Owens, 2005).

1.1.5 Early lung disease in cystic fibrosis

The lungs of newborn babies are thought to be free of respiratory damage or infection with rapid progression to pulmonary inflammation evident early in infancy. An American study of 16 CF infants (aged 12 months and younger) showed evidence of neutrophil accumulation, detectable free neutrophil elastase activity and increased levels of interleukin (IL)-8 in bronchoalveolar lavage (BAL) fluid compared to control infants (Khan et al., 1995b). Interestingly this inflammatory response was also evident in BAL sampled from infants free of both common and CF-related respiratory pathogens, suggesting evidence of respiratory inflammation before infectious insult. A more recent study carried out by the Australian Respiratory Early Surveillance Team for CF of 125 children in Perth and Melbourne showed that 8.5 % of infants had radiographic evidence of bronchiectasis on computerised tomography (CT) scan in the first year of life with an increased prevalence of 36 % by 4 years of age (Stick et al., 2009). This prevalence increased with age, where 56 % of children had features of bronchiectasis by their fifth year of life. Although this latter study is may have covered a wide geographic area and treatment practices could vary to those in the UK, the represented demographic and patient management are likely to be characteristic of the developed world.

Recent animal studies have challenged the idea that the CF lung is normal at birth. The development of a CF piglet model has enabled investigation of disease in newborn piglets, which share similarities with human babies including meconium ileus, exocrine pancreatic dysfunction and progression to CF pulmonary inflammation and infection in the first few weeks to months of life (Adam et al., 2013). Using this model, CF piglets displayed radiographic evidence of air trapping and airflow obstruction before the onset of infection, inflammation and mucus obstruction. Structural airway abnormalities, relating to the tracheal and carina, have been found in newborn CF piglets, with potential implications on increased deposition of particulate matter and bacteria together with exacerbation of airway mucus obstruction (Awadalla et al., 2014). However, the piglets investigated in these studies were *CFTR*$^{-/-}$ and likely to represent a more severe pathology to that seen in humans with a small degree of residual CFTR function, as is seen with the most common *F508del* mutation.

1.2 The airway epithelium in cystic fibrosis

1.2.1 The healthy airway epithelium

The airway epithelium plays an essential role in lung host defence through mucus secretion and clearance of unwanted inhaled pathogens and particulate matter. It is largely comprised of basal, secretory and ciliated cells. Airway composition varies with distal progression towards the lung alveolar surface. Early bronchi are cartilaginous, contrary to narrower bronchioles originating from the 10th airway generation that contain smooth muscle (Fischer and Widdicombe, 2006). Large airways are characterised by a pseudostratified columnar epithelium, whereas lower respiratory bronchioles are cuboidal.

Basal cells are attached to the basement membrane and predominate in larger conducting airways. They serve as progenitors for mucous and ciliated cells and provide attachment via hemidesmosomes of other columnar epithelial cells to the basement membrane (Evans et al., 1989). In lower respiratory bronchioles, club cells (previously referred to as Clara cells) provide this stem cell function.

There is a predominance of submucosal glands in large airways, goblet cells in lower airways and club cells in respiratory bronchioles (Verkman et al., 2003). This anatomical location reflects underlying roles in airway defence, where goblet cells protect against large particulate matter and club cells against toxic gases (Widdicombe and Wine, 2015, Fischer and Widdicombe, 2006). Ciliated cells account for around half of all airway epithelial types and are essential for airway mucus clearance along the mucociliary escalator from the airways to the throat where mucus is swallowed or expectorated (Knight and Holgate, 2003).

1.2.2 The airway surface liquid

The airway surface liquid (ASL) is a thin layer of fluid above the apical (luminal) surface of airway epithelial cells. It contains water, inorganic ions, proteins, lipids and mucins and provides a barrier between inspired and expired air. ASL volume, pH, ionic and nutrient composition are tightly controlled by the airway epithelium and regulation of its composition is important for mucociliary clearance (MCC) and antimicrobial function (Haq et al., 2015). Antimicrobial factors including β-defensins, lactoferrin and lysozymes contained within the ASL are involved in innate and

adaptive host mechanisms that protect the airways from inhaled pathogens (Pezzulo et al., 2012).

ASL hydration is regulated predominantly by CFTR-mediated chloride secretion, which provides the net driving force and generation of an osmotic gradient for water movement towards the airway lumen (Figure 4). The epithelial sodium channel (ENaC) is also important in regulating ASL volume through its role in sodium absorption (Randell et al., 2006).

There are two distinct layers within the ASL as shown in Figure 5 (Widdicombe and Wine, 2015). The 7 μm periciliary layer (PCL) lies adjacent to the airway epithelial cell and surrounds the extended cilial length (Widdicombe and Widdicombe, 1995). An adequate PCL volume is required for efficient ciliary beat and MCC. Above this sits the mucus layer (MCL) which contains large gel-forming mucins, including MUC5B and MUC5AC, produced by secretory submucosal glands and goblet cells respectively (Groneberg et al., 2002).

Until recently, the ‘gel-on-liquid’ ASL model was proposed, describing these large gel-forming mucins contained within the MCL sitting above an aqueous PCL (Widdicombe and Widdicombe, 1995). However, this concept did not explain the distinct PCL and MCL layers. Recent investigation using PBECs has described an alternative ‘gel-on-brush’ model (Button et al., 2012). Here, the PCL contains large macromolecular mucins, including MUC1 and MUC4, adhered to cilia, microvilli and the epithelial surface (Button et al., 2012). This dense meshwork increases with proximity to the epithelial surface, preventing penetration of larger MCL macromolecules and certain infectious agents from entering the PCL. These tethered macromolecules regulate PCL hydration by generating an osmotic pressure and modulus. In a healthy airway, the MCL has a lower osmotic modulus, enabling water entry into the MCL, preserving PCL hydration.

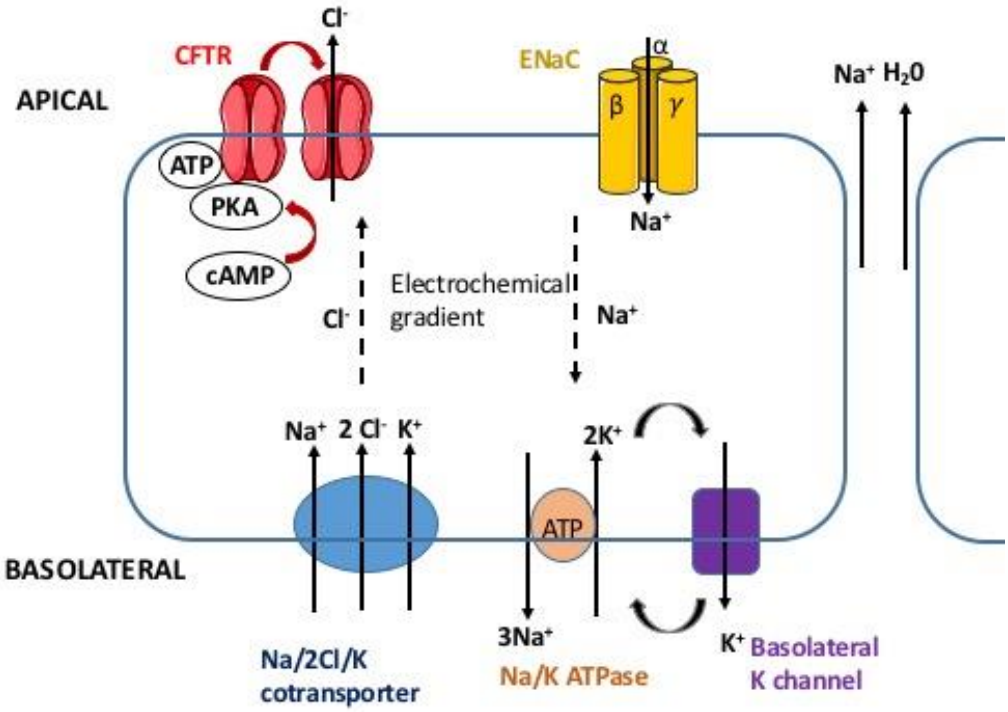

Figure 4: Airway epithelial ion transport mechanisms

Chloride (Cl^-) enters and accumulates in the airway epithelial cell via the basolateral Na/K/2Cl co-transporter. Sodium (Na^+) entering via the Na/K/2Cl cotransporter is removed by the Na/K-ATPase pump. Basolateral potassium (K^+) channels recycle K^+, which hyperpolarises the basolateral membrane and provides the electrochemical driving force for chloride exit into the ASL. Apical chloride exit generates an electrical gradient for paracellular sodium secretion. Together with chloride secretion, this creates an osmotic gradient leading to paracellular and transcellular water (H_2O) secretion.

ENaC absorbs sodium from the ASL. Sodium is actively exchanged for potassium by the basolateral Na/K/ATPase pump. The secretory effect of CFTR together with ENaC-mediated sodium absorption maintain overall ASL hydration.

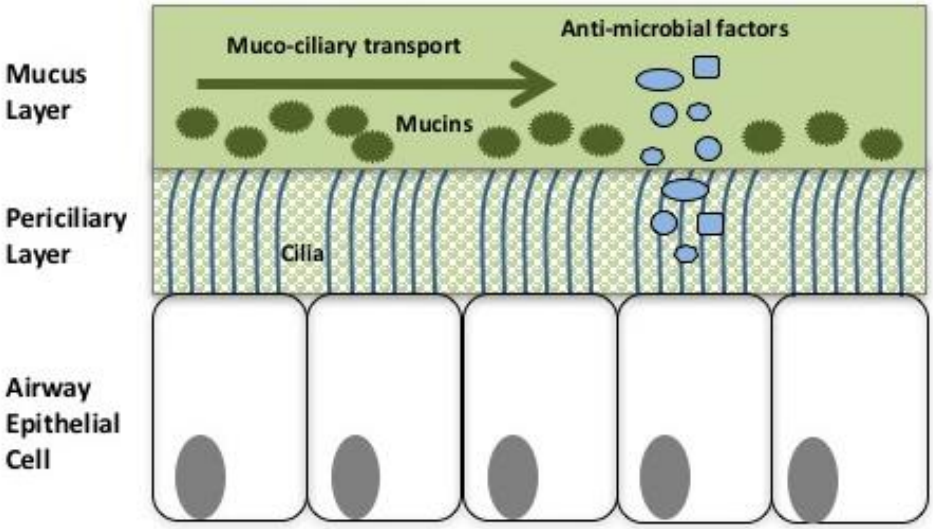

Figure 5: Schematic representation of the healthy airway epithelium

In the healthy airway the airway surface liquid (ASL) consists of the periciliary and mucus layers (PCL and MCL). The tight meshwork of mucins within the PCL prevents entry of the large macromolecular mucins from the MCL. The greater osmotic modulus created by this meshwork also preserves PCL hydration status. The ASL also contains antimicrobial factors important for airway innate host defence.

1.2.3 The airway surface liquid in cystic fibrosis

Dysfunctional CFTR reduces chloride and bicarbonate transport into the lumen. This leads to sodium and water compartmental shifts, producing a dehydrated airway surface and thick mucopurulent secretions. In this dehydrated ASL, water preferentially leaves the MCL, which increases its concentration and osmotic modulus. Eventually, in a severely dehydrated CF airway, the MCL osmotic modulus exceeds that of the PCL (Button et al., 2012). Preservation of PCL hydration is compromised, resulting in its dehydration and compression by the MCL. PCL dehydration leads to cilial compression, reduced ciliary beat frequency, impaired MCC and progressive airway infection and inflammation (Figure 6).

Given CFTR's role in bicarbonate transport, it has been hypothesised that the CF ASL is acidic, which in turn contributes to respiratory bacterial infection. Many ASL antimicrobial factors are pH sensitive and their function is impaired at an acidic pH (Nakayama et al., 2002). Bacterial killing has been reduced in the acidic ASL of the transgenic CF pig model, which can be restored to wild type function by increasing the pH from 6.9 to 7.4 using aerosolised sodium bicarbonate (Pezzulo et al., 2012).

Assessment of ASL pH in cultured primary airway epithelial cells using pH-sensitive electrodes showed an increased rate of ASL acidification over time in CF cultures, with differences in pH maintained after 24 hours (Coakley et al., 2003). Interestingly, although the cultures were studied after 14 days of confluence and time in culture, the initial pH values were similar in both CF and non-CF cultures.

In vivo nasal pH assessment in neonates using nasal pH probes demonstrated a more acidic pH in CF versus non-CF babies (pH 5.2 ± 0.3 versus 6.4 ± 0.2) (Abou Alaiwa et al., 2014). Although a relative difference in pH was found between both groups, it is interesting to note that the absolute values found using this technique were both acidic. Using the same method, no differences were found in children or adults with or without CF. The authors suggested that early changes in ASL pH could trigger airway disease and that ongoing disease airway remodelling may reduce these pH differences over time, accounting for the lack of acidic pH seen in older populations (Abou Alaiwa et al., 2014).

Further *in vivo* studies, including recent investigation using pH-sensitive fibre-optic probes and earlier studies utilising pH probes (used for the diagnosis of gastro-

oesophageal reflux) have not found any differences in ASL pH between children with and without CF (Schultz et al., 2017, McShane et al., 2003).

These findings are contrary to those using exhaled breath condensate and the CF pig model, where ASL acidification was significant in CF subjects (Tate et al., 2002, Pezzulo et al., 2012). A key challenge in addressing the question of potential ASL acidification has been largely accounted for by variations in detection methods, species variability and practical difficulties involved in maintaining accurate pH assessment both *in vivo* and in *ex vivo* systems. Furthermore, there is notable variation in the absolute pH values determined in different studies, perhaps warranting appreciation of relative rather than absolute pH changes in CF versus non-CF comparisons. However, given these recent findings, it is possible that CFTR dysfunction does not result in ASL acidification.

In addition to its potential effect on ASL pH, bicarbonate is also required for mucus secretion and clearance. Lack of CFTR-dependent bicarbonate transport increases mucus viscosity, leading to dysfunctional MCC without affecting ASL hydration (Birket et al., 2014). In CF murine intestinal tissue depleted of bicarbonate, mucus is denser and more impenetrable compared to wild-type controls, requiring more rigorous methods for epithelial removal (Gustafsson et al., 2012). Lack of bicarbonate secretion may reduce calcium chelation, which is required for the unfolding of mucin aggregates secreted from goblet cells and expansion and formation of a mucus gel (Gustafsson et al., 2012). Given similarities with the properties of key mucins in the respiratory and intestinal environments, these principles could apply to the CF respiratory epithelium.

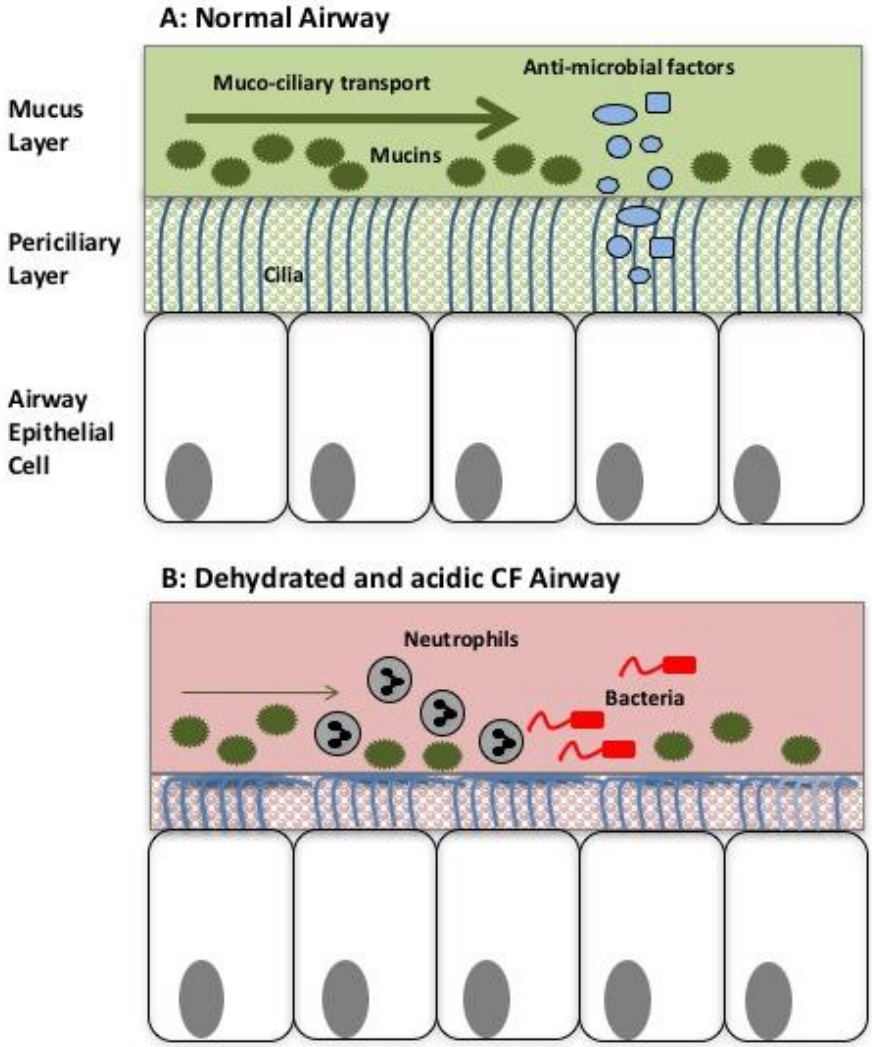

Figure 6: Schematic representation of the CF airway epithelium

Normal airway (A) as previously described. In the dehydrated CF airway (B), water leaves the MCL, eventually increasing its osmotic modulus. In a severely dehydrated airway, such as in CF, water eventually leaves the PCL, causing cilial compression and dysfunction. The acidic environment impairs antimicrobial function and increases mucus viscosity. These processes lead to MCC impairment and subsequent bacterial inflammation and infection. Adapted from (Haq et al., 2015)

1.3 Recent advances in cystic fibrosis therapy

1.3.1 Overview

The mainstays of CF treatment include stringent treatment regimens of chest physiotherapy, life-long courses of antibiotics, pancreatic enzyme supplements, inhaled mucolytic agents and intensive chest physiotherapy. However, such strategies have not corrected the underlying defect and eventual respiratory failure is characteristic of the disease.

The well-recognised phenotypic heterogeneity in CF, even amongst individuals with identical *CFTR* genotypes, has greatly challenged traditional strategies for therapy, with significant variations in disease progression and treatment response. However, greater understanding of *CFTR* mutation classes has driven the investigation and development of small molecule targeted therapy, which has revolutionised the approach for CF therapeutics in the last ten years.

1.3.2 Gene therapy

Since the cloning of *CFTR* in 1989, direct targeting of defective CFTR with gene therapy has remained an attractive option. Direct introduction of wild-type *CFTR* into CF airway epithelial cells has the potential to increase functional *CFTR* expression (Alton et al., 2015). Recent developments led by the UK CF Gene Therapy Consortium (UKCFGTC) focused on a non-viral vector approach using a deoxyribonucleic acid (DNA)-liposome complex for wild-type *CFTR* airway delivery. In a phase IIb randomised double-blind placebo-controlled trial, this approach revealed modest improvements in lung function, as measured by percentage predicted forced expiratory volume in 1 second (FEV_1), of 3.7 % (p=0.046), similar to responses seen with lumacaftor/ivacaftor therapy (Alton et al., 2015). However, considerable heterogeneity was evident amongst responders in the UK multi-centre gene therapy trial highlighting potential challenges with the development of agents that adequately penetrate the airway surface in a range of disease severities (Alton et al., 2015). Phenotypic variation may account for these differences, raising the possibility that a combination of strategies involving targeted precision medicine with gene therapy may be required to produce adequate treatment effects. Early phase clinical trials led by the UKCFGTC are currently underway to investigate a novel viral

vector based on *in vitro* work in murine and human airway liquid interface (ALI) cultures and results are awaited (Alton et al., 2017). This approach hopes to overcome recognised limitations of standard viral vector approaches, which include the need to damage the epithelium to enable transduction and inducing a host immune response resulting in subsequent loss of activity and expression (Alton et al., 2017).

1.3.3 Targeted small molecule therapy

Targeted small molecule therapy for specific mutation classes has been a major advancement in CF therapy, most notably with the development of a small molecule CFTR potentiator, ivacaftor, targeting the Gly551Asp *CFTR* mutation. (Figure 7). *In vitro* investigation of airway epithelia expressing this mutation revealed improvements in chloride transport, ASL height (and therefore hydration) and cilial function (Van Goor et al., 2009a). Phase III clinical trials showed significant improvements in lung function accompanied by benefits in sweat chloride, respiratory symptoms, reduced pulmonary exacerbations and hospital stay (Ramsey et al., 2011, Davies et al., 2013, McKone et al.). Ivacaftor was commissioned for UK use in 2012 in patients aged over 6 years with at least one Gly551Asp allele and the European Union has approved usage with a rarer Class III mutation.

Phase III trials investigating combination therapy of ivacaftor with the CFTR corrector, lumacaftor, for patients with the most common *CFTR* mutation, F508del, aged 12 years and over and also in younger patients aged 6 to 11 years showed statistically significant improvements in lung function (Wainwright et al., 2015, Ratjen et al., 2017) . This received US Food and Drug Administration (FDA) approval in 2015. However, improvements in FEV_1 of around 2 % were modest in comparison to ivacaftor for patients with Gly551Asp where the mean improvement was 10 % (Wainwright et al., 2015).

More recently, the EVOLVE phase III trial of a novel small molecule corrector, tezacaftor, in combination with ivacaftor demonstrated an increase in percentage predicted FEV_1 of 4 % from baseline versus placebo in F508del homozygous patients, thereby providing improved benefit and fewer adverse events compared to the lumacaftor/ivacaftor combination (Taylor-Cousar et al., 2017). Furthermore, a 6.8 % improvement was evident in heterozygote subjects with one F508del mutation and

a residual function mutation (Rowe et al., 2017). This combination therapy has now achieved US FDA approval. Investigations involving triple therapy of ivacaftor, tezacaftor and a third novel compound are underway for patients with one copy of F508del and one copy of a Class I-III ‘minimal function’ mutation (Vertex Pharamceuticals Incorporated, 2018).

Despite its benefits of targeted small molecule therapy, ivacaftor does not benefit approximately 90 % of people with CF. The lumacaftor/ivacaftor combination (Orkambi™) for patients with at least one F508del copy was granted UK licence in 2015, but has not achieved approval by the National Institute for Health and Care and Excellence (NICE), on the grounds of cost-effectiveness and lack of long-term data. Future approaches are likely to involve a combination of small molecules tailored towards restoring specific aspects of CFTR function. Employment of small molecule precision therapy is likely to be an expensive option, exemplified by ivacaftor which costs £180,000 per patient annually (Brodlie et al., 2015, Whiting et al., 2014).

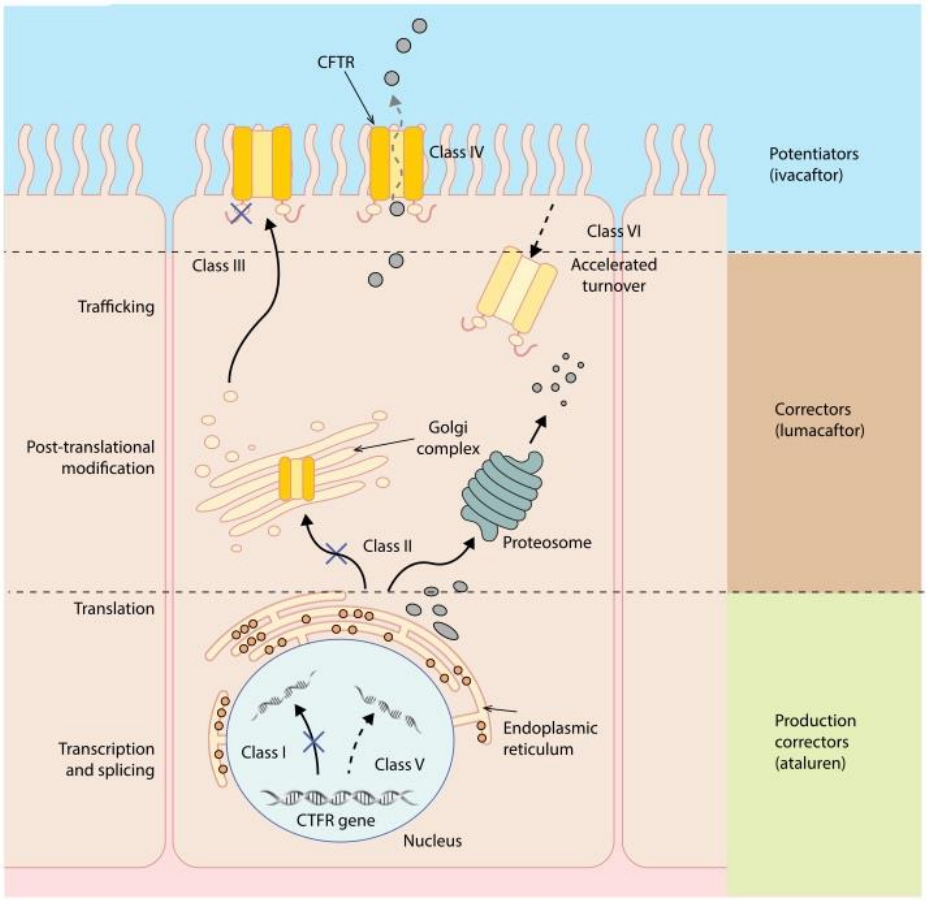

Figure 7: Small molecule targeted treatment strategies for *CFTR* mutation classes

The potentiator, ivacaftor increases CFTR function at the airway epithelial surface by increasing the opening probability of Gly551Asp-CFTR channel. Correctors, such as lumacaftor and tezacaftor, enhance intracellular processing and delivery of mutant CFTR to the cell surface. The production corrector, ataluren, promotes read-through of premature mRNA termination codons and increases CFTR production. However, ataluren failed to show significant improvements in FEV_1 in a Phase III trial (Kerem et al., 2014). Adapted from Brodlie *et al.* (Brodlie et al., 2015).

1.4 Experimental models in cystic fibrosis

1.4.1 Overview

Valid experimental models are required to help further our understanding of early CF pathophysiology and potential therapeutic options. Early investigation of disease processes is of paramount importance, particularly in the context of research involving children. With the recent recognition of 'theraptyping' as a strategy to characterise responses to current and emerging CFTR modulator compounds in individuals with CF, there is a significant need to develop reliable patient-derived models (Clancy et al., 2018).

Identification of the underlying genetic defect has enabled the development of knockout animal models to help develop understanding of *in vivo* disease pathogenesis and investigate the effects of novel therapies. Cellular based *in vitro* models have provided an insight into distinct epithelial functions particularly in the context of CF airway disease. Strategies for utilisation of specific research models largely depend on resource availability and the specific focus of CF research.

1.4.2 Animal models

Huge efforts have been made to produce CF mouse models to investigate pathophysiology, variations in genetic defects and new therapeutic strategies. Several loss of function CF knockout mice models were initially generated using homologous recombination of *CFTR* in mouse embryonic stem cells (Snouwaert et al., 1992, Ratcliff et al., 1993, Rozmahe et al., 1996). Later murine models employed the introduction of specific CF causing mutations, including F508del and Gly551Asp, thus providing more focussed *in vivo* phenotypic disease profiling compared with *CFTR*-null mice models. (Colledge et al., 1995, Zeiher et al., 1995, Delaney et al., 1996).

Despite the significant contribution of murine models to CF research over the last 20 years, differences between mice and humans greatly limits their translation and application into human disease (Table 3). Similarities exist with intestinal pathology, whereby CF mice display obstruction, malabsorption, cryptal mucus and chronic gut inflammation. However, the majority of CF mouse models do not show signs of spontaneous bacterial lung infection, inflammation or lower airway disease

(Snouwaert et al., 1992, Ratcliff et al., 1993, Delaney et al., 1996, Kent et al., 1996). Mice lack respiratory bronchioles and therefore small airway pathology (Pack et al., 1981). In humans, trachea and major bronchi are characterised by submucosal glands and goblet cells predominate proximal airways. In mice, however, there is relative paucity of mucus producing epithelial cells (Pack et al., 1981). Submucosal glands are confined to the trachea and proximal airways are comprised of club cells (Rosen et al., 2018). Intrinsic differences in airway composition, respiratory physiology, innate immune response and alternative chloride channel expression are all possible explanations for differences seen (Grubb et al., 1994, Scholte et al., 2004).

An alternative CF mouse model has been genetically engineered to overexpress the β-ENaC subunit. These mice display a phenotype more in keeping with human CF respiratory disease, with evidence of impaired mucociliary clearance, airway mucus obstruction, neutrophilic inflammation and bacterial infection (Mall et al., 2004) . Although this has helped overcome some challenges faced with CF mouse models, it remains limited by intrinsic species differences and retention of normal CFTR provides limited translation to human CF disease. Chronic sodium hyperabsorption and ASL depletion has led to the development of pulmonary emphysema and eosinophilic inflammation in β-ENaC mice, suggesting that this model may be more applicable for the investigation of chronic obstructive pulmonary disease (Mall et al., 2008).

Pigs and ferrets have more recently been employed in CF research, largely due to closer similarities in respiratory anatomy and disease phenotype compared with humans as described in Table 3 (Rogers et al., 2008, Sun et al., 2010). Furthermore, these models display extra-pulmonary manifestations of CF including hepatic disease and pancreatic exocrine insufficiency. Although valuable in complementing and increasing our understanding of CF pathophysiology, particularly in early CF lung disease, maintenance and application of these models requires immense resource and expertise.

CF disease phenotype	Human	Mouse	Rat	Pig	Ferret	Rabbit
Spontaneous respiratory infections	Present	Absent	Absent	Present	Present	Unknown
Growth impairment	Present	Present	Present	Present	Present	Present
Intestinal manifestations	Present	Present	Present	Present	Present	Present
Pancreatic dysfunction:						
Exocrine	Present	Absent	Absent	Present	Present	Unknown
Endocrine	Present	Absent	Unknown	Present	Present	Unknown
Hepatic disease	Present	Absent	Unknown	Present	Present	Unknown
Biliary disease	Present	Absent	-	Present	Present	Unknown

Table 3: Comparable CF disease phenotypes in experimental animal models

CF disease phenotypes in different animal models. Rats do not possess a gall bladder and many phenotypes in the rat and rabbit are currently unknown.

Adapted from (Rosen et al., 2018)

1.4.3 Cellular models

More accessible *in vitro* models have been developed to complement understanding of CF pathophysiology and aid development of targeted CF therapy. Immortalised cell lines are generated from epithelial carcinomas or transformation of epithelial cells with viral, chemical or physical agents. Their extended lifespan, enhanced proliferation and relative homogeneity have helped to overcome some of the limitations of primary airway epithelial cells and proved beneficial with the investigation of inflammatory processes, mucus phenotypes and therapeutic responses in epithelial diseases such as CF (Gruenert et al., 1995). A large number of immortalised cell lines have been developed which vary in their epithelial characteristics (Gruenert et al., 2004). However, limitations of this model include associated karyotype instability, which can generate subpopulations of cells that do not retain the phenotype of interest (Gruenert et al., 2004). The process of transformation and multiple passages also affects expression and differentiation of key epithelial characteristics including cell polarity, cilia formation and tight junctions (Gruenert et al., 2004).

1.4.4 Gene-editing and induced pluripotent stem cells

Gene editing techniques are being developed with the aim of repairing individual *CFTR* mutations using a number of systems. One system utilises the Cas9 protein derived from clustered regularly interspaced short palindromic repeats (CRISPR) bacterial adaptive immune systems (Wang et al., 2016). Cas9 is used as an RNA-guided endonuclease to create a double strand break in close proximity to the DNA site to be repaired (Harrison et al., 2018). Other systems use other nucleases including zinc-finger and transcription activator-like effector nucleases (Wang et al., 2016).

Once the double stranded break is made, the cell's endogenous homology-directed repair pathways are exploited to replace the mutant sequence with a donor corrected molecule containing the desired DNA sequence. The breaks are repaired by non-homologous end joining whereby DNA is joined by creating small insertions or deletions. However, this technique is limited by its relatively low level of precision. To optimise technique efficiency and broaden gene-editing application to all *CFTR* mutations, homology-independent targeted integration (HITI) methods are currently

being investigated to incorporate larger segments of DNA into the *CFTR* sequence with improved efficiency (Harrison et al., 2018). These technologies also carry a risk of inserting a double stranded break into similar DNA sequences within the genome (Harrison et al., 2018). However, these “off target” effects may be reduced by optimising guide RNA design and Cas9 modification (Chen et al., 2017, Fu et al., 2014).

Although these techniques are very much still in the experimental stage, translation into human cells will have potential to repair *CFTR* in disease-affected cells. Gene editing technologies can also be applied to induced pluripotent stem cells (IPSCs). IPSCs have been genetically engineered from patient-derived samples, including hair, blood and mucus and clonally expanded in high numbers to produce differentiated cells of CF-affected tissues, including the respiratory epithelia (Huang et al., 2014). Incorporation of gene editing into IPSCs can be used to investigate CF disease modelling and enable high throughout assessment of novel therapies.

1.4.5 The role of primary airway epithelial cells in cystic fibrosis research

Ex vivo culture of primary airway epithelial cells has improved our understanding of respiratory diseases, airway inflammatory mechanisms and neoplastic processes. They have been pivotal in CF research, where they provide a physiologically relevant model to study treatment responses such as ivacaftor and gene therapy (Van Goor et al., 2009a). Application of the air liquid interface (ALI) model has enabled *ex vivo* development of a muco-ciliary phenotype that is more representative of the *in vivo* pseudostratified columnar airway epithelium compared to submerged, undifferentiated cultures and allows comprehensive investigation of airway epithelial function (Fulcher et al., 2005).

Primary bronchial epithelial cells (PBECs) can be isolated from explanted CF lung tissue. Although transplantation may be performed in children, it is more common in adolescents or adults with end-stage disease. PBECs can also be harvested from bronchial brushings and tissue collected during bronchoscopic procedures (McNamara et al., 2008, Brodlie et al., 2010). In paediatric research, this requires a general anaesthetic and often the clinical need for bronchoscopy to avoid unnecessary procedures in this young patient group.

1.4.6 Primary nasal epithelial cells in cystic fibrosis research

The necessity for paediatric CF research is increasingly recognised and has previously been challenged by methods that are invasive and limited by experimental material. Given the possibility of early pathological changes, a robust strategy for timely investigation of disease processes and potential treatments is of paramount importance. In contrast to the invasive procedures required for PBEC collection, primary nasal epithelial cells (PNECs) can be cultured from nasal mucosal brushings. Clinical PNEC collection for congenital ciliary disorder diagnosis is a well-established procedure and generally well tolerated by awake children. PNECs would therefore be hugely beneficial in facilitating longitudinal sampling from children of different ages, CF genotypes and disease severity in multiple settings.

The nose forms part of the conducting component of the respiratory tract, which is also comprised of the mouth, pharynx, larynx, trachea, bronchi and respiratory bronchioles. The gas exchanging component of the respiratory system is represented by the terminal respiratory bronchioles and corresponding alveoli. The larynx traditionally forms the physical barrier between the upper and lower respiratory tracts (Gaga et al., 2001). Within the nose, the internal cavity is separated by the nasal septum. Three bony ridges, or turbinates, project from the lateral wall of each side of the internal cavities. These increase the surface area of the narrow interior cavity to promote warming and humidification of inspired air. Turbulent flow within this component enables filtration and trapping of large inhaled particulate matter. Nasal mucosal brushings for PNEC culture are generally sampled from the inferior nasal turbinate surface (de Courcey et al., 2012). Methods of acquisition for both PBECs and PNECs are shown in Figure 8.

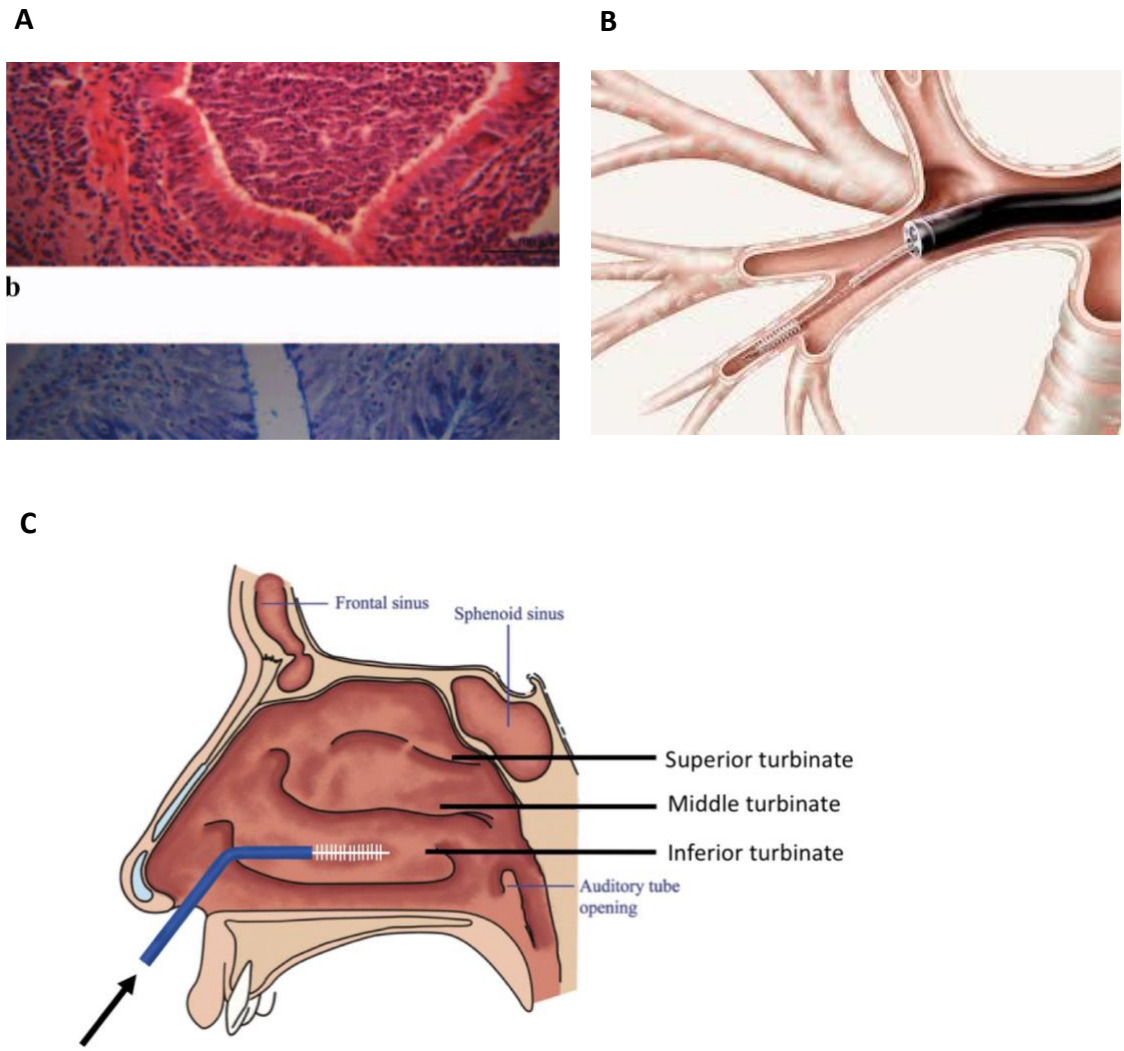

Figure 8: Methods for the acquisition of bronchial and nasal epithelial cells

Bronchial epithelial cells can be acquired by brushing the bronchial mucosal surface from explanted CF lung tissue (A) or during flexible bronchoscopy (B) using a cytology brush (Brodlie et al., 2010, Olympus, 2017) Alternatively, nasal epithelial cells can sampled from nasal mucosal brushings taken from the inferior nasal turbinate surface (C); image adapted from (Sahin-Yilmaz and Naclerio, 2011).

The nasal epithelium composition reflects its underlying role in conditioning air together with providing a barrier against infective and noxious substances. The epithelium begins as stratified, keratinised, and squamous with gradual transition into a pseudostratified, ciliated columnar epithelium (Gaga et al., 2001). It shares histological similarities with the bronchial epithelium including the presence of goblet cells, ciliated cells, non-ciliated cells, basal cells, connective tissue and inflammatory cells (Serrano et al., 2005). However, despite the concept of a “united airway”, it is important to consider the distinct functions of the nose and bronchi (Gaga et al., 2001). In contrast to the nose, the bronchial epithelium plays a key role in MCC and filters smaller particulate matter, and unlike the nasal epithelium also contains serous and club cells.

Studies directly comparing PNECs with PBECs have been performed in a range of respiratory disorders, however studies are limited in CF. A comparison of ALI PNECs and PBECs isolated from 21 adult patients with chronic obstructive pulmonary disease demonstrated greater levels of basal and stimulated IL-8 release, but IL-8 levels were positively correlated in both groups (Comer et al., 2012). With respect to the culture process, PBECs reached confluence after a longer period of time. This latter finding was also apparent in a further study comparing inflammatory responses between submerged PBECs and PNECs isolated from adults with respiratory tumours, interstitial lung disease, sarcoidosis and children with persistent chest x-ray changes, recurrent stridor, wheeze or cough, asthma and bronchopulmonary dysplasia (McDougall et al., 2008). Investigation of a combination of paired and unpaired PBECs and PNECs in this study showed similar morphology with analogous levels of stimulated inflammatory mediator release including IL-8, IL-6, granulocyte colony-stimulating factor and vascular endothelial growth factor (McDougall et al., 2008). Paired analysis of PBEC and PNEC ALI cultures from 9 children with asthma and atopy and 6 healthy children have shown lower proportions of ciliated cells in PNECs but similar stimulated inflammatory responses (Guo-Parke et al., 2013, Pringle et al., 2012). Inflammatory responses following respiratory syncytial virus exposure were similar in bronchial and nasal cultures.

Micro-array global gene expression analysis of CF and non-CF nasal and bronchial epithelia revealed similar proportions of differentially expressed genes between the tissue types in each group (Ogilvie et al., 2011). However, patterns of differential

gene expression were different in bronchial versus nasal cultures (Ogilvie et al., 2011). This was attributed to potential lower levels of chronic disease and airway remodelling seen in the CF nose compared with the lungs. The differentially expressed genes in the CF nasal and bronchial epithelium included those involved in cellular movement and signalling. This differed to the non-CF group, where cell growth, proliferation and tissue maintenance were of higher relevance (Ogilvie et al., 2011). These findings suggest that the nose and lower airways have varying roles in disease and in CF. However, although the non-CF nasal and bronchial epithelia were paired from the same participants, the CF group were mostly unpaired and therefore susceptible to inter-donor variability. Furthermore, non-epithelial inflammatory cells isolated from the bronchial cultures, particularly in the CF group, may have accounted for some of the differences seen.

Interestingly in the same study, 863 genes were differentially expressed between CF and non-CF bronchial epithelia, with predominance evident in inflammatory pathways, cell signalling and cellular movement (Ogilvie et al., 2011). This was in contrast to the CF and non-CF nasal epithelium, where only 15 genes were differentially expressed, with enriched expression in amino acid metabolism and cell morphology. Another large-scale analysis found only 26 genes to be differentially expressed in well differentiated CF versus non-CF tracheal and bronchial cultures (Zabner et al., 2005). Despite the functional crossover, differentially expressed genes were not identical in both studies. Methodological variations could account for this difference, including airway epithelial cell collection technique, culture conditions, RNA sequencing and threshold setting for selecting ‘significant’ genes.

PNECs are increasingly being employed in respiratory research and nasal cells have predicted electrophysiological and ion transport properties (de Courcey et al., 2012). Nevertheless, there are no direct comparisons of PBECs and PNECs from paired participants and comprehensive analysis of paediatric cultures remains limited. This knowledge would be hugely beneficial in determining the role of PNECs in translational research and personalised paediatric treatment, which is likely to predominate future CF therapy.

1.5 Alternative 'non CFTR' targets in cystic fibrosis lung disease

1.5.1 Overview

Although measures are underway to improve upon existing corrector therapy for rescue the *F508de*l mutation, alternative strategies are required to benefit all people with CF, regardless of *CFTR* mutation type. One potential option is to correct ASL abnormalities that play a key role in CF pathogenesis. In addition to CFTR there are other plasma membrane channels and transporters including ENaC, alternative chloride channels, anion exchangers, potassium channels and aquaporins. Targeting these "by-pass" channels could compensate for abnormalities seen in the CF ASL with ion transport, solute trafficking, pH and volume and may provide potential therapeutic strategies for all people with CF.

1.5.2 The epithelial sodium channel

ENaC is expressed in the apical aspect of absorptive epithelia including the conducting airways, distal nephron, sweat gland and distal colon (Canessa et al., 1994). It is a transmembrane protein consisting of three homologous subunits, α, β and ɣ, which form the channel pore for the amiloride-sensitive low conductance sodium channel (Canessa et al., 1994). An additional fourth subunit, δ, expressed in the brain, pancreas and urogenital tract, can replace the α subunit to enhance ENaC activity (Waldmann et al., 1995, Wichmann et al., 2018).

In respiratory epithelia, ENaC-mediated sodium absorption generates a transepithelial potential difference providing the driving force for water and chloride absorption via a paracellular shunt pathway (Mall and Galietta, 2015). The basolateral Na/K/ATPase channel (Figure 4) actively pumps sodium out of the epithelial cell in exchange for potassium. The balance between ENaC's absorptive function together with CFTR-mediated chloride secretion maintains ASL hydration.

In addition to the absence of CFTR's secretory function in CF, ASL dehydration is thought to be further confounded by ENaC upregulation in the absence of CFTR. This results in sodium hyper-absorption and further ASL dehydration. There are several lines of evidence to suggest this including cAMP-dependent CFTR ENaC regulation (Stutts et al., 1995). *In vitro* assessment of short circuit current (I_{sc}) in response to amiloride, an ENaC inhibitor, in nasal tissue has shown a larger

decrease in I_{sc} in CF versus non CF subjects suggesting a greater ENaC presence in CF (Boucher et al., 1986). Furthermore, a greater amiloride-sensitive nasal potential difference (PD) is evident in CF subjects versus healthy controls (Knowles et al., 1983). Interestingly, transgenic mice over-expressing the β-ENaC subunit display a CF phenotype with ASL dehydration, impaired MCC and neutrophilic lung inflammation (Mall et al., 2004). However, transgenic human-CFTR expression in these mice has not corrected airway disease (Grubb et al., 2012).

Endogenous serine proteases such as neutrophil elastase, which is abundant in CF, may contribute to ENaC upregulation in disease (Gaillard et al., 2010). Importantly, ENaC dysfunction has not been demonstrated in all experimental models of CF leaving the CFTR/ENaC relationship under ongoing debate (Gentzsch et al., 2010).

Several strategies have been employed to target ENaC inhibition for CF therapy as a means to restoring ASL hydration. A double-blinded crossover trial involving aerosol delivery of an ENaC inhibitor, amiloride, did not show significant improvements in lung function due to its relative low potency and rapid airway absorption (Knowles et al., 1990). More potent derivatives of amiloride were also rapidly cleared or absorbed from the airway both *in vitro* and in *in vivo* sheep models (Hirsh et al., 2004). Further clinical trials are underway for alternative ENaC inhibitors developed via high throughput screening approaches and the results of these are currently awaited.

Protease inhibitors have also been employed to downregulate ENaC. More recently, early phase clinical trials have commenced to investigate the effects of a Spx-101, a peptide mimetic of the endogenous protease inhibitor short palate lung and nasal clone 1 (SPLUNC1). By direct binding with ENaC, SPLUNC1 prevents ENaC proteolytic cleavage and activation by serine proteases (Garcia-Caballero et al., 2009). Spx-101 promoted ENaC internalisation in bronchial cell culture models and improved MCC in the β-ENaC mouse and sheep models (Walker et al., 2017). Gene silencing by the introduction of small interfering RNA (siRNA) could be an alternative method for ENaC inhibition. Indeed nanoparticle formulations for siRNA delivery targeting the α-ENaC subunit have been investigated in primary airway epithelial cells and shown effective silencing (Manunta et al., 2017). This airway focussed approach would reduce systemic effects of ENaC inhibition and provides an attractive therapeutic option. However, it is in the very early stages of development and will require careful consideration of optimum dose and delivery.

1.5.3 Calcium activated chloride channels

Correction of chloride (and bicarbonate) transport may provide a superior approach to truly compensate for defective ion transport in CF. Calcium activated chloride channels (CaCCs) were described as an alternative CFTR-independent route for epithelial chloride secretion in the early 1990s. Stimulation with nucleotide triphosphates, including ATP and uridine triphosphate (UTP), both in PNECs and by *in vivo* nasal PD measurement, revealed large increases in chloride secretion (Knowles et al., 1991, Mason et al., 1991). Nasal PD measurement is non-invasive and reflects transepithelial ion transport. It involves sequential perfusion of compounds across the nasal epithelial surface. Amiloride is initially applied to block the absorptive effect of ENaC prior to perfusion with compounds targeting the channel of interest. In this case, amiloride-containing solutions of ATP, UTP, adenosine and uridine were added to activate CaCCs and the resultant increase in PD was calculated (Knowles et al., 1991). Interestingly nasal PD elevation following nucleotide addition was greater in CF versus non-CF participants. This finding has been complemented by the relatively mild murine CF lung phenotype and attributed to the presence of non CFTR-dependent calcium regulated chloride transport (Clarke et al., 1994).

CaCCs were first described in *Xenopus* oocytes where fertilisation caused CaCC opening and subsequent membrane depolarisation (Miledi, 1982). In humans, CaCCs are required for epithelial secretion, smooth muscle contraction and sensory transduction (Hartzell et al., 2004). Increases in cytosolic calcium concentration by physiological ligands including ATP, UTP, acetylcholine, histamine, endothelin I and angiotensin II, results in halide secretion, with relative permeability as follows: iodide > bromide > chloride > fluoride (Hartzell et al., 2004, Qu and Hartzell, 2000). Although CaCC function has been well characterised for many years, the molecular identity was only recently described. A number of candidates including integral membrane bestrophin proteins and the calcium-sensitive chloride accessory protein family (CLCA) did not satisfy the hallmark criteria of CaCCs including activation by micromolar intracellular calcium concentrations and voltage-dependent modulation of channel activity.

1.6 Transmembrane protein 16A (TMEM16A)

1.6.1 TMEM16A: a component of the calcium activated chloride channel

Transmembrane protein 16A (TMEM16A) was recently discovered as an essential component of CaCC by three independent research groups in 2008 (Yang et al., 2008, Caputo et al., 2008, Schroeder et al., 2008). Endogenous CaCCs are required to generate a fertilisation potential that prevents polyspermia in *Xenopus* oocytes. However, this is not the case in the polyspermic *Axolotl* salamander oocytes. Using this knowledge, Schroeder *et al.* injected mRNA extracted from *Xenopus* oocytes into *Axolotl* oocytes resulting in the generation of large CaCC currents and eventual identification of a single complementary deoxyribonucleic acid (cDNA) clone bearing the TMEM16A coding sequence (Schroeder et al., 2008).

Th-2 cytokines such as IL-4 and IL-13 have been shown to upregulate calcium dependent chloride secretion in PBECs (Danahay et al., 2002, Galietta et al., 2002). Utilising this concept, Caputo *et al.* performed a microarray-based gene approach in IL-4 treated and untreated PBECs to identify proteins with corresponding *mRNA* upregulation. Subsequent siRNA gene silencing in relevant pancreatic and bronchial derived cell lines and PBECs revealed TMEM16A to be responsible for calcium mediated chloride secretion (Caputo et al., 2008).

In the same year, after performing a search of public domain databases for putative transmembrane proteins, Yang *et al.* identified TMEM16A as a potential candidate for CaCC in view of its multiple MSDs and ten human homologues (Yang et al., 2008). Expression of mouse TMEM16A (which shares homology with human TMEM16A) in the human embryonic kidney 293T (HEK293T) cell line demonstrated TMEM16A-mediated chloride currents similar to endogenously activated CaCCs. These results were confirmed by siRNA knockdown in mouse salivary glands (Yang et al., 2008). In this study, TMEM16A was activated by increases in intracellular calcium and its anion permeability was consistent with endogenous CaCCs (Yang et al., 2008).

1.6.2 Structure and function of TMEM16A

TMEM16A is a member of the TMEM16 family, which is comprised of ten proteins, otherwise known as the anoctamins. These proteins typically have between 800 and 1000 amino acid residues and are predominantly scramblases involved in membrane lipid movement. However, a smaller number, including the closely related TMEM16A and TMEM16B, proteins, function as CaCC ion channels (Schroeder et al., 2008). TMEM16A is widely expressed in secretory epithelial cells, including the airway, pancreas, kidney, retina, salivary glands and gastrointestinal tract (Yang et al., 2008, Ousingsawat et al., 2009). TMEM16B is expressed in neuronal cells including olfactory neurons and photoreceptors (Stephan et al., 2009, Stöhr et al., 2009).

TMEM16A consists of eight transmembrane domains with intracellularly located amino and carboxyl termini (Figure 9A). Of its ten family members, TMEM16A is closely related to TMEM16B as evident in the phylogenetic tree in Figure 9B. As characteristic of CaCCs, TMEM16A is activated by G protein coupled receptor (GPCR) purinergic P2Y stimulation, via ligands such as ATP and UTP. This increases inositol-1,4,5-triphosphate (IP_3) production by phospholipase C, resulting in calcium release from intracellular stores (Figure 10A). Activation occurs with cytosolic free calcium concentrations of 0.2 – 1.0 μM and channel activity is further modulated by membrane potential (Hartzell et al., 2004). At this concentration range, the resultant stimulated current is outwardly rectifying and time-dependent.

Mutational studies involving the replacement of three highly conserved positively charged amino acid residues with negatively charged glutamate residues have confirmed the region spanning the re-entrant loop between the fifth and sixth transmembrane domains to be the pore-forming region (Yang et al., 2008). Recent work investigating the transmembrane domains of mouse TMEM16A using cryo-electron microscopy has identified ten highly conserved pore-lining residues that affect anion selectivity in addition to a cluster of seven residues that regulate channel gating and stability in open and closed states (Dang et al., 2017).

The exact mechanism for calcium binding in TMEM16A remains unclear. A highly conserved region within the first intracellular loop (ICL1) of five negatively charged glutamic acid residues resembling the ‘calcium bowl’ in large conductance calcium activated potassium (BK) channels was initially proposed as a calcium binding site

(Schreiber and Salkoff, 1997). Although ablation of this region has not shown significant effects on channel sensitivity, this region may be important for channel and voltage modulation (Xiao et al., 2011).

The third intracellular loop (ICL3) has since been suggested to be essential for calcium activation. Replacement of this region in a chimera containing the ICL3 of TMEM16B has reduced calcium affinity by almost 8-fold compared to wild-type TMEM16A (Scudieri et al., 2013). This has been confirmed by calcium insensitivity in a mutant form of TMEM16A whereby ICL3 was deleted (Lee et al., 2015b). Further investigation based on homology modelling has shown ICL3 to be comprised of two oppositely charged parallel helices that interact with each other in a calcium dependent manner (Lee et al., 2015b). These studies have suggested that under resting conditions, the positively charged helix holds the negatively charged calcium-sensor helix in place, which is pushed away from the positive helix upon calcium ion attachment (Figure 10B). Mutations in both helices has reduced TMEM16A calcium sensitivity with no apparent effect on channel voltage sensitivity (Lee et al., 2015b). The proposed putative calcium binding site is comprised of two glutamic acid residues at positions 702 and 705, with alterations in calcium sensitivity evident in mutagenesis of these residues (Yu et al., 2012).

Four splicing variants of TMEM16A have been identified. Activation of an alternative promoter in variant *a* results in missing transcripts in the first 116 amino acids (Ferrera et al., 2009). Variants *b, c and d* can arise from exon inclusion or skipping involving exons 6b, 13 and 15 which code for short protein regions of 22, 4 and 26 amino acids respectively (Ferrera et al., 2009). Variants *a* and *b* are localised on the N-terminus; *c* and *d* are located within ICL1 (Caputo et al., 2008). The isoform, TMEM16A(*0*) lacks all splice variants and is significantly shorter than TMEM16A(*abcd)*, with 840 amino acids compared with 1008 (Caputo et al., 2008).

Splicing variants may arise from cell proliferation, differentiation or pathological processes and play a functional role in regulating calcium transport in dependent tissues (Ferrera et al., 2009). Implications of these variants have been investigated using the halide sensitive yellow fluorescence protein (YFP) assay. This can be used as a measure of CaCC sensitivity and works on the above-mentioned principle of CaCC anion selectivity (iodide > bromide > chloride). Cells loaded with YFP are placed into an iodide rich solution and challenged with a calcium agonist.

Subsequent iodide influx results in rapid YFP fluorescence, the rate of which is proportional to CaCC activity. Using this assay in human embryonic kidney cells together with whole cell patch clamp analysis of ion transport, functional variability is evident with splicing variants. The *ac* variant has a four-fold higher affinity for calcium compared to *abc*, indicating that the *b* segment has a higher threshold for calcium sensitivity. The *ab* variant significantly reduces CaCC activity, while the *d* segment has no effect on CaCC variability (Ferrera et al., 2009). Importantly, splicing variants can either exhibit tissue specificity of be co-expressed within the same tissues. Alternative splicing bears important physiological relevance in regulating CaCC sensitivity and voltage dependence, which may explain variations seen in different cell and tissue types.

TMEM16A channel gating by direct calcium binding has been challenged by the possibility that additional accessory CaCC sensors, such as calmodulin, may be involved in channel function. Specific calmodulin inhibitors have decreased TMEM16A(*abc)* activation and the *b* segment has been put forward as a calmodulin binding site (Tian et al., 2011). Investigation in human embryonic kidney (HEK) 293T cells has shown that the calcium dependent calmodulin-TMEM16A interaction increases relative bicarbonate channel permeability (Jung et al., 2013). However, calcium dependent TMEM16A activation remains strongly present in absence of the *b* variant and opposing results are evident with calmodulin inhibition (Xiao et al., 2011). More recent work has shown that although calmodulin may be involved in channel modulation, it is not required for TMEM16A activation and that gating occurs with direct calcium-TMEM16A binding (Yu et al., 2014). In view of these conflicting findings, further investigation is clearly required to ascertain the precise TMEM16A mechanisms involved in calcium binding, channel gating and modulation.

A

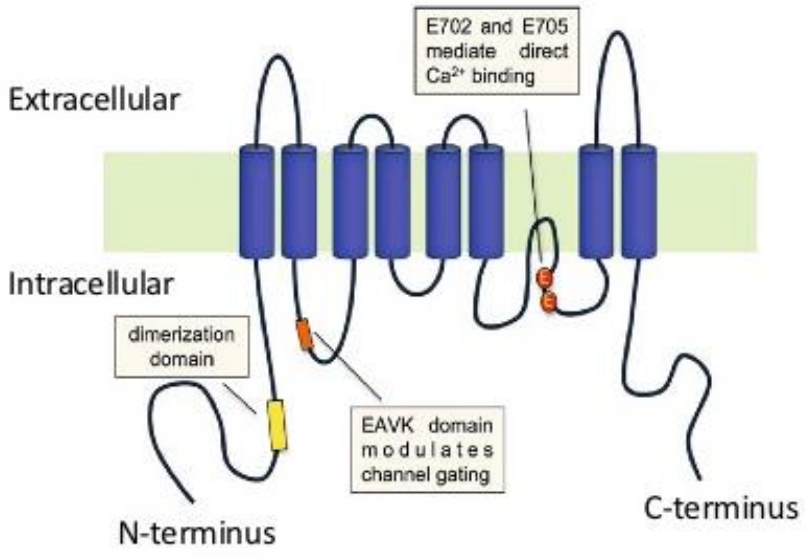

B

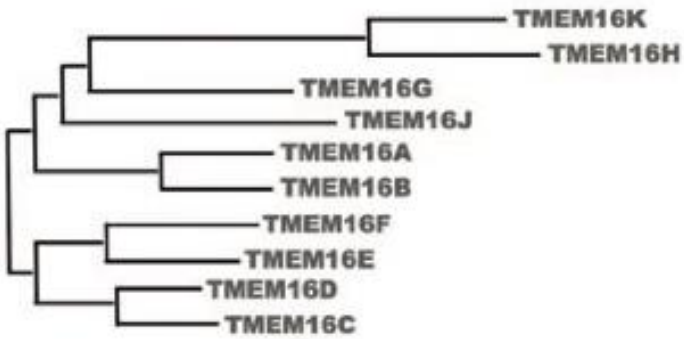

Figure 9: TMEM16A structure

Predicted topology for TMEM16A is shown in A consisting of eight transmembrane domains with intracellular C and N termini and a re-entrant loop between the fifth and sixth domains. A region in the ICL3 contains two glutamic acid residues E702 and E705 which may be involved in calcium binding. The EAVK sequence in ICL1 at positions 448-551 may be important for modulation of channel opening (Scudieri and Galietta, 2016). Phylogenetic tree of TMEM16A proteins is shown in B. TMEM16A and TMEM16B are close paralogues (Scudieri et al., 2012b).

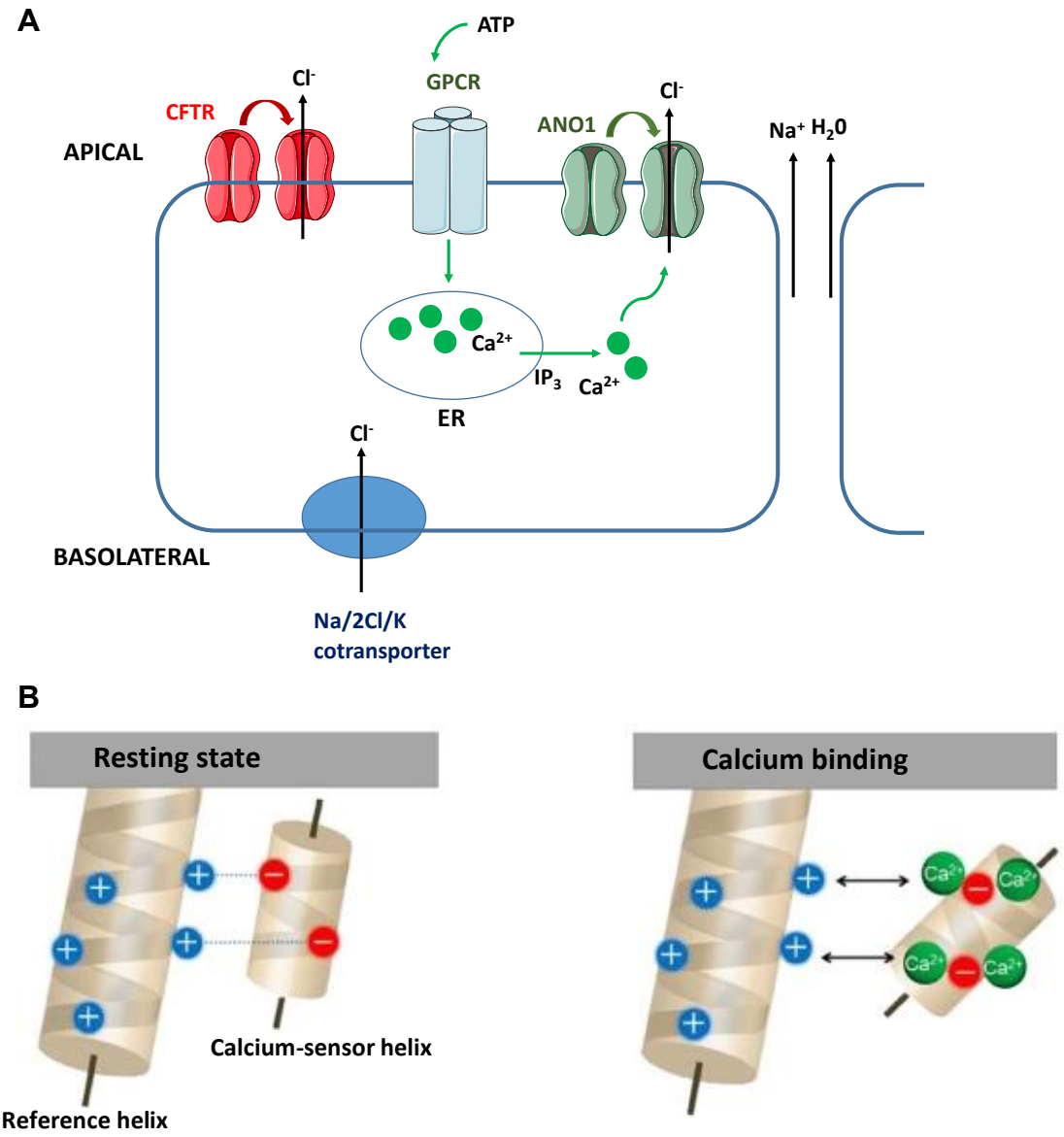

Figure 10: Mechanisms for TMEM16A activation

A: Stimulation of luminal G protein coupled receptor (GPCR) receptors by ligands such as ATP and UTP causes an increase in IP_3 production by phospholipase C and subsequent release of calcium from intracellular stores, such as the endoplasmic reticulum (ER). This increase in intracellular calcium activates TMEM16A and resultant chloride (and bicarbonate) secretion.

B: The two helices in third intracellular loop are oppositely charged. In the resting state (A), the positively charged reference helix holds the negatively charged calcium-sensor helix in place. Upon calcium ion attachment (B), the calcium-sensor helix is pushed away. Mutations in these regions result in reduced overall calcium ion sensitivity (Lee et al., 2015b)

1.6.3 TMEM16A relevance in the airway epithelium

In the adult human airway, TMEM16A is expressed in the apical bronchial epithelium and in submucosal glands as shown in Figure 11 (Ousingsawat et al., 2009). TMEM16A knockout mice have demonstrated defective tracheal airway calcium dependent chloride transport and a CF-like phenotype with impaired MCC and suggestions of inadequate airway hydration (Rock et al., 2009, Ousingsawat et al., 2009). siRNA-knockdown in PBECs has shown TMEM16A to be a major component of calcium activated chloride transport in the airway (Ousingsawat et al., 2009).

In addition to the upregulation of CaCC and TMEM16A, IL-4 and IL-13 increase the abundance of mucus-secreting goblet cells (Scudieri et al., 2012a, Zhang et al., 2013, Gorrieri et al., 2016). In the context of a 'pro-inflammatory' CF airway, this has significance for anion secretion, ASL regulation, mucus secretion and MCC (Caputo et al., 2008, Scudieri et al., 2012a, Lin et al., 2015). Studies investigating epithelial repair in CF PBECs have also shown that TMEM16A is required for cell proliferation and migration (Ruffin et al., 2013). In this study, a reduction in chloride activity was evident in CF versus wild type PBECs, which was attributed to reduced levels of *TMEM16A* mRNA and protein expression in CF PBECs.

TMEM16A displays permeability to bicarbonate in addition to chloride, and like CFTR, this is less than the channel's permeability to chloride (Jung et al., 2013, Ni et al., 2014, Tang et al., 2009). This function could be of relevance in correcting pH abnormalities in the CF airway, if indeed the CF airway is acidic (Jung et al., 2013). Bicarbonate is also required for the expansion of mucus granules and mucin secretion (Garcia et al., 2009, Gustafsson et al., 2012). TMEM16A-mediated bicarbonate secretion may be of physiological relevance in promoting MCC via enhancing mucin release from goblet cells.

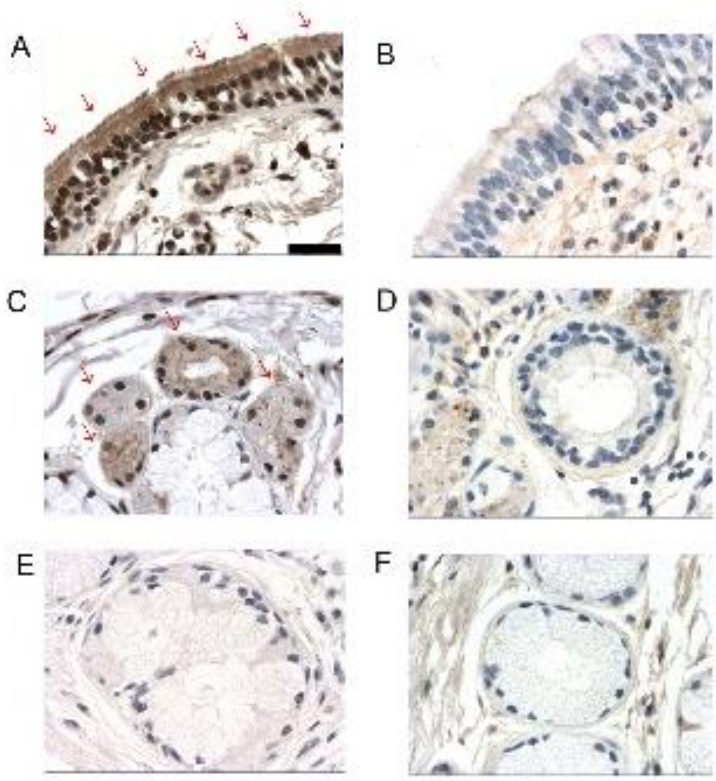

Figure 11: Expression of TMEM16A in human adult airways

Apical expression of TMEM16A in the epithelium of a mid-size bronchus (A) and in the serous submucosal glands (C). Lack of expression noted in larger mucus ducts (E). Negative controls demonstrated in B, D and F (Ousingsawat et al., 2009)

1.6.4 Airway interactions of TMEM16A and CFTR

CFTR has numerous stimulatory and inhibitory interactions with other cellular proteins involved in receptor or cell signalling. It is possible that CFTR interacts with TMEM16A to regulate secretory processes in the CF airway. CFTR has inhibited endogenous CaCC activity in *Xenopus* oocytes and bovine pulmonary artery endothelium (Kunzelmann et al., 1997, Wei et al., 1999). The purinergic CaCC response is enhanced in CF airway tissue and epithelial cells from both mice and humans (Knowles et al., 1991, Clarke et al., 1994, Mall et al., 2003, Ousingsawat et al., 2011). Basal and increased expression of CFTR has inhibited TMEM16A-mediated chloride secretion in a human bronchial epithelial cell line, with complete abolishment of TMEM16A activity following CFTR activation (Ousingsawat et al., 2011). Notably, in this study, TMEM16A over-expression has reduced CFTR-induced currents (Ousingsawat et al., 2011).

There are several explanations for the interactions between CFTR and TMEM16A. These include i) recognised effects of intracellular calcium on the enzymatic regulation of intracellular cAMP; ii) purinergic receptor-mediated increase in cAMP and calcium; iii) regulation of intracellular calcium by cAMP-affected proteins; and iv) CFTR-mediated GPCR translocation to the plasma membrane leading to an increase in calcium and subsequent TMEM16A activation (Namkung et al., 2010b, Kunzelmann et al., 2012).

1.6.5 Exploring TMEM16A modulation as a target for CF therapy

Despite the increase in CaCC activity noted in CF experimental models, it is clear from the presence of severe lung disease in CF that physiological activity alone is not sufficient to compensate for dysfunctional CFTR. This may be explained by the transient nature of CaCC activation and its relatively minor contributory role in chloride secretion relative to CFTR. However, modification of TMEM16A activity is an attractive target to bypass dysfunctional CFTR and correct chloride and bicarbonate transport, with potential to improve the underlying ASL pH and volume abnormalities evident in CF.

Clinical trials have investigated the effects of the investigational compound denufusol, a P2Y receptor agonist that stimulates CaCC-mediated chloride

secretion. Early phase trials revealed significantly improved lung function in patients with mild impairments in lung function after nebulised denufusol treatment for 28 days. In a subsequent phase III placebo controlled double blinded trial (TIGER-1) there was a 2 % improvement in percentage predicted FEV_1 after denufusol treatment for 28 weeks, but this effect was modest and no improvements in secondary outcomes of pulmonary exacerbations, quality of life scores and hospitalisation were seen (Deterding et al., 2005). A further clinical trial was carried out to assess the efficacy of denufusol over a longer treatment period (Ratjen et al., 2012). No significant benefits in lung function were seen following a 48-week treatment period. This lack of clinical efficacy was attributed to the possibility that denufusol has a relatively short half-life in pulmonary tissue compared with *in vitro* assessment, despite nebulised administration three times daily. Furthermore, the study was performed in patients with relatively mild lung function, and benefits may not have been apparent in this patient population.

Targeting TMEM16A is likely to be challenging in view of its wide expression and risk of off-target effects. In addition to the epithelia, TMEM16A is expressed in smooth muscle cells in the airway, reproductive and gastrointestinal tracts (Huang et al., 2009, Gallos et al., 2013). Furthermore, TMEM16A overexpression has been shown in certain human cancers including gastrointestinal stromal tumours and head and neck cancers, and it may be of relevance in tumour metastasis (Wang et al., 2017). This effect varies in different cell types, potentially due to distinct differences in activation of cell signalling pathways by TMEM16A, which has been extensively described in the review by Wang et al.

Although some of these more widespread effects of TMEM16A activation could in some part be limited by direct airway delivery of a CF therapeutic compound, the potential effects on smooth muscle and airway hyper-responsiveness are of serious relevance (Zhang et al., 2013). A greater understanding of precise channel function and gating mechanisms will be essential to enable targeted modulation of TMEM16A to prevent this significant off-target effect. An additional layer of complexity also lies with the variation in TMEM16A tissue expression and varying levels of CaCC activity described in different cells. However, alternative ANO1 splicing may be relevant for the investigation of pharmacological agents to modify physiological processes and off-target effects that arise from these variations.

1.7 Research aims and objectives

1.7.1 Hypotheses

There is limited evidence directly comparing the functional characteristics of PBECs and PNECs isolated from children with and without CF. If their properties are similar, PNEC use in paediatric CF research will be hugely beneficial.

Although TMEM16A expression has been investigated in adult cultured epithelial cells, lung tissue and other models, it's relevance in children is yet to be determined. Given the role of TMEM16A in epithelial chloride and bicarbonate transport, modification of TMEM16A function may be a potential therapeutic strategy in CF.

The work carried out in this PhD has aimed to address the following hypotheses:

1. PNECs can be used as a suitable drug discovery tool in CF.
2. TMEM16A is expressed in paediatric PNECs and PBECs, where it is involved in calcium activated chloride transport.
3. Paediatric PNECs can be used to investigate the effects of novel TMEM16A activators including their potential to compensate for defective CFTR-mediated ion transport that is evident in CF.

1.7.2 Aims and objectives

The specific aims of this work were to:

1. Sample PNECs and PBECs from children with and without CF who are attending the Great North Children's Hospital to establish paediatric ALI culture models.
2. Characterise and compare the epithelial and electrophysiological profiles of fully differentiated PBECs and PNECs derived from children with and without CF to further validate PNEC suitability as a paediatric drug discovery tool.
3. Investigate TMEM16A expression and its involvement in endogenous CaCC function in paediatric CF PNECs and PBECs.
4. Comparatively assess novel small molecule TMEM16A activator effects on ion transport in these cellular models as a potential therapeutic avenue to bypass dysfunctional CFTR.

2 Chapter 2 Materials and Methods

2.1 Research ethics and consent

Ethical approval was granted by the Newcastle and North Tyneside 1 Research Ethics Committee on 8th September 2015 (reference: 15/NE/0215) following an application by myself with Drs Malcolm Brodlie, Chris Ward and Mike Gray. Research and Development Department approval was granted by the Newcastle upon Tyne NHS Foundations Trust (reference: 7494).

Written consent was obtained by myself from parents of children with and without CF undergoing clinical bronchoscopy at the Great North Children's Hospital (GNCH) in Newcastle upon Tyne. Parent and age appropriate participant information leaflets were designed by myself for participants with and without CF and are shown in Appendix A.

2.2 Air liquid interface culture of paediatric primary nasal and bronchial epithelial cells

2.2.1 Collection of paediatric nasal brushings

Children with CF undergoing clinical bronchoscopy under the care of the paediatric respiratory team at GNCH were recruited into the study. Children without a clinical diagnosis of CF and, where performed a negative CF NBS, undergoing clinical bronchoscopy for the investigation of other respiratory indications were recruited as non-CF controls.

After administration of general anaesthesia, nasal brushings were collected by brushing the inferior nasal turbinate of each nostril with a 2 mm disposable cytology brushes (Conmed 129R) using a rotary and linear movement for 10 seconds. The brushes were placed into 10 mL of Roswell Park Memorial Institute (RPMI) 1640 medium (Sigma-Aldrich) for transfer to the laboratory for processing. This was performed prior to flexible bronchoscopy.

2.2.2 Collection of paediatric bronchial brushings

Bronchial brushings were collected during flexible bronchoscopy after the performing clinician had visualised the airways and obtained all clinically indicated samples. A

sheathed bronchial cytology brush was inserted into the channel port and carefully advanced. Upon direct visualisation of the brush tip at a 2nd or 3rd generation bronchus, the brush was unsheathed, and the bronchial surface was carefully brushed using a similar rotary and linear movement to that used for the acquisition of nasal brushings. The size of bronchoscopic brush (2 mm brush as above, or 1.2 mm, Olympus BC-203D-2006) was determined by the internal channel diameter of the flexible bronchoscope (Table 4), which had been selected at the discretion of the performing physician and dependent upon the age and size of the child. After brushing, the cytology brush was re-sheathed and the bronchoscope was withdrawn with the brush in situ, cut and placed into 10ml of RPMI 1640 medium for transfer to the laboratory for processing.

Flexible bronchoscope outer diameter (mm)	**Compatible cytology brush (mm)**
2.2 (Neonates and infants)	1.2
2.8 (Infants)	1.2
3.5 (Young children)	1.2
4.4 (Older children)	2.0

Table 4: Compatibility of paediatric flexible bronchoscope with bronchoscopic cytology brush size

Neonates are defined as children under 1 month of age; infants are children under the age of 1 year.

2.2.3 Harvesting of paediatric primary nasal and bronchial epithelial cells

Tissue culture was performed using a Class II biological safety cabinet. Methods were based on those previously described (Fulcher et al., 2005, Forrest et al., 2005, Brodlie et al., 2010). Brushings were gently agitated in collection medium, ensuring complete removal of epithelial cells, which were centrifuged in collection medium at 200 x g for 7 minutes at 10 °C. The supernatant was discarded and the remaining cell pellet re-suspended in 1 mL of Bronchial Epithelial Growth Medium (BEGM) (Lonza) supplemented with single quots (Lonza) and antimicrobials (Table 5).

The combined nasal cell suspension was seeded into a 25 cm^2 tissue culture flask (Corning), pre-coated with 30 μg/mL collagen (Purecol, Advanced Biomatrix) and primed with 4 mL of BEGM.

The bronchial cell suspension isolated from the single brushing was seeded into a 12.5 cm^2 tissue culture flask (Corning), pre-coated with a mix of 30 μg/mL collagen (Purecol), 10 μg/mL bovine serum albumin (BSA) (Sigma-Aldrich) and 10 μg/mL fibronectin (Sigma-Aldrich) and primed with 1.5 mL of BEGM.

Flasks were incubated at 37 °C, in 5 % carbon dioxide (CO_2) and cells were monitored daily for growth and infection. BEGM media was supplemented with 100 μg/mL Primocin (Invivogen) to provide additional antimicrobial cover for the first 72 to 96 hours. Media was replaced with standard antimicrobials (Table 5) and exchanged every 48 hours.

Cells were passaged at 80 – 90 % confluency and processed as previously described (Brodlie et al., 2010). BEGM was removed from the flasks and either 2.5 mL or 5 mL of 0.05 % trypsin/0.02 % ethylene diamine tetracetic acid (EDTA) (Sigma-Aldrich) added to the 12.5 or 25 cm^2 flask respectively and incubated at 37 °C. After cell detachment, an equal volume of RPMI containing 10 % fetal calf serum (FCS, Sigma-Aldrich) was added to neutralise the trypsin and centrifuged at 200 x g for 7 minutes at 10 °C. The resultant supernatant was discarded and the pellet re-suspended in BEGM. Cells were seeded onto the apical compartment of pre-collagen coated and medium-primed Transwell (Corning) semipermeable clear polyester membranes (6.5 mm diameter, 0.4 μm pore size) in 100 μL BEGM aiming for a density of 60,000-80,000 cells per membrane (180,000 – 240,000 cells/cm^2).

600 µL of BEGM was added to the Transwell basolateral compartments. The apical medium was exchanged the following day to remove unattached epithelial cells and both the apical and basolateral medium was exchanged every 48 hours. Cells were visualised daily and air lifted after attaining confluence at 48 to 72 hours.

Component	Volume
Bronchial Epithelium Basal Medium	500 mL
Bovine pituitary extract	2 mL
Retinoic acid	500 µL
Insulin	500 µL
Hydrocortisone	500 µL
Transferrin	500 µL
Epinephrine	500 µL
Human epidermal growth factor	500 µL
Tri-iodothyronine	500 µL
Gentamicin/amphotericin	500 µL
Penicillin/Streptomycin *	5 mL (final concentration Penicillin 100U/mL, Streptomycin 100 µg/mL

Table 5: Components of BEGM medium

Components supplied by Lonza (concentrations not published).

* Supplied by Sigma-Aldrich

2.2.4 Air liquid interface culture

The apical medium was removed and basolateral BEGM medium replaced with differentiation medium. This consisted of a 50:50 mix of BEGM basal medium with Dulbecco's Modified Eagle's Medium (DMEM-high glucose) (Lonza) supplemented with single quots as described in Table 5, with the exception of retinoic acid, added at 100 ng/ml, human epidermal growth factor, added at 0.5 ng/mL and gentamicin/amphotericin which was omitted. Calcium chloride was supplemented with 500 μL of 1 M solution in 500 mL of DMEM. Cells were regularly visualised using light microscopy for leakage and membrane integrity. Basolateral medium was exchanged every 48 hours. The apical surface was washed weekly using phosphate buffered saline (PBS) (Sigma). Resultant washings were stored at -80 °C for future analysis. Figure 12 provides a summary of the ALI culture process.

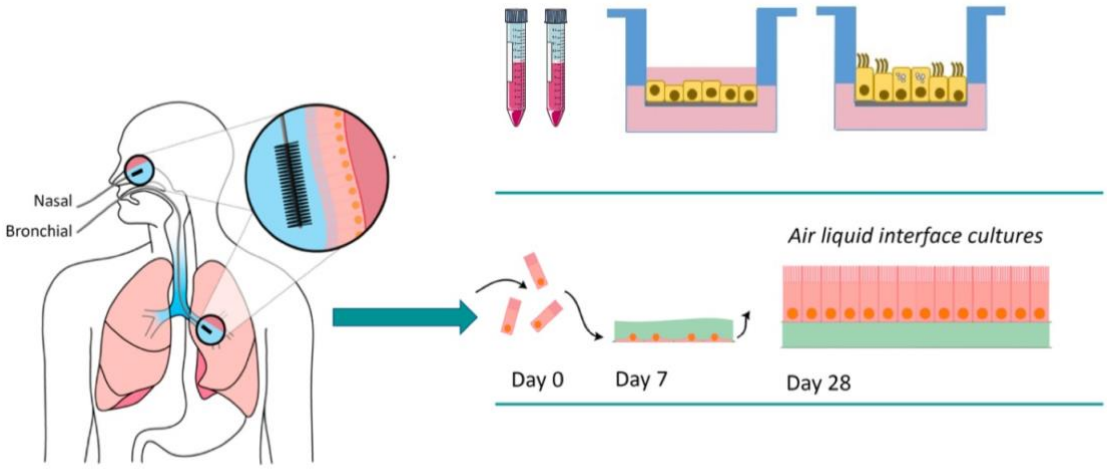

Figure 12: Air liquid interface culture methods

Sampled nasal and bronchial brushings were collected into RPMI medium and transported to the laboratory. After processing, the resultant cell pellets were re-suspended into tissue culture flasks. After attaining 80-90 % confluency, cells were seeded onto semipermeable membrane supports and initially submerged with BEGM. Cells were air lifted when confluent to enable differentiation to a pseudostratified, ciliated columnar airway epithelium.

2.3 Characterisation of differentiated paediatric nasal and bronchial epithelial cultures

2.3.1 Transepithelial electrical resistance

Weekly serial transepithelial resistance (TEER) measurements were performed to assess tight junction integrity according to the manufacturer's instructions (STX2 electrodes, EVOM2TM Epithelial Voltohmmeter, World Precision Instruments (WPI)) Pre-warmed PBS (100 μL) was added to the apical compartment of each membrane and cultures were incubated and allowed to equilibrate at 37 ºC for 20 minutes. TEER measurement was also performed on a 'blank' membrane without seeded cells in each plate to provide the background level of resistance and this value was subtracted from each measurement. The final calculation of TEER was performed as follows:

TEER ($\Omega.cm^2$) = (TEER value – blank value) x culture insert surface area

2.3.2 Electron microscopy

Electron microscopy (EM) was performed by the EM Research Service, Newcastle University. After fixation, nasal and bronchial ALI cultures were prepared as below by the EM Research Service. For scanning electron microscopy (SEM) differentiated ALI cultures were fixed with glutaraldehyde in Sorenson's Phosphate Buffer (overnight minimum) and rinsed several times in the buffer. Fixed cultures were dehydrated through graded alcohols in ethanol as follows: 25 %, 50 %, 75 %, 100 % and 100 % ethanol and dried. Cultures were mounted on an aluminium stub and gold coated. SEM was performed by the EM Research Service using a Tescan Vega LMU scanning electron microscope and digital images collected with Tescan supplied software.

For transmission electron microscopy (TEM), differentiated cultures were fixed firstly with glutaraldehyde in sodium cacodylate buffer, followed by osmium tetroxide. Fixed cultures were dehydrated through graded acetone as follows: 25 %, 50 %, 75 %, 100 % and 100 % acetone and embedded in resin. Sections of 0.5 μm were cut using an ultramicrotome, stretched with chloroform and mounted on copper grids. The grids were examined by the EM Research Service using a Philips CM100 Compustage

(FE1) transmission electron microscope and digital images were collected using an AMT CCD camera (Deben).

2.3.3 Fixation of air liquid interface cultures in paraformaldehyde

Differentiated cultures at 28d ALI were washed with 100 μL PBS and fixed in 4 % paraformaldehyde (PFA, Sigma-Aldrich) for 20 minutes. PBS was applied to the surface of fixed cultures, which were maintained at 2-4 °C until ready for paraffin embedding and histological assessment.

2.3.4 Preparation of paraffin-embedded sections

Paraffin-embedded sections were prepared by a HCPC registered biomedical scientist (Kasim Jiwa, Sir William Leech laboratory, Freeman hospital) as follows:

PFA-fixed ALI cultured membranes were cut away and detached from their inserts using a scalpel. The membranes were divided into 2 semi-circles and placed into labelled cassettes for histology processing. Membranes were dehydrated by immersing the cassette through graded alcohols, with a 20-minute interval for each concentration of alcohol (70 %, 80 %, 95 % and 99 %). The membranes were submerged twice in xylene solvent for 20 minutes and infiltrated using a molten paraffin wax bath for 2 hours at 60 ºC.

Processed membranes were externally embedded into paraffin blocks and cross sections were cut at 5 μm using a microtome. Sections were dewaxed in xylene for 10 minutes and dehydrated in graded alcohol (99 %, 99 % and 95 %).

2.3.5 Haematoxylin and eosin staining

This was performed on paraffin embedded sections of ALI cultures to enable histological assessment of epithelial morphology. Sections were dewaxed in xylene twice for 5 minutes and rehydrated in 99% and 95% alcohol for 1 minute each. After washing in distilled water, freshly filtered Harris Haemaotoxylin (Thermofisher) was applied to the sections for 2 minutes. Sections were washed in tap water for 3 min and checked microscopically for nuclear staining. A counterstain with Eosin Y (Thermofisher) was applied for 2 minutes. Sections were washed well and

dehydrated through graded alcohols using 95 %, 99 % and 99 % ethanol for 30 seconds each. Pertex (Leica Biosystems) was used to mount the slides.

2.3.6 Periodic acid-Schiff staining

This was performed to stain for mucin glycoproteins within the epithelium of paraffin embedded sections of ALI cultures. Sections were dewaxed, rehydrated and washed as described in section 2.3.5. 1 % Periodic Acid (Sigma-Aldrich) was applied to sections for 10 minutes. Sections were rinsed in distilled water before applying Schiff's reagent (Sigma-Aldrich) for 10 minutes. After rinsing in tap water, Harris Haematoxylin (Thermofisher) was applied for 1 minute. Sections were washed, dehydrated and mounted.

2.3.7 Alcian blue/periodic acid-Schiff staining

This staining was performed to differentiate between acidic and neutral mucin glycoproteins within the epithelium of paraffin embedded sections of ALI cultures. Sections were dewaxed, rehydrated and washed as described in section 2.3.5. Sections were incubated with 0.1 % diastase (VWR) for 30 minutes and washed with tap water. PAS staining was then performed as above.

2.3.8 Zona-occludins immunofluorescence

This was performed to assess for the presence of tight junctions in PFA-fixed ALI cultures. Cultured cells were rinsed in PBS and blocked with 3 % BSA for 1 hour. Cells were washed in PBS and 0.05 % Tween 20 (Sigma-Aldrich) (PBST) and the mouse monoclonal zona-occludins antibody (ZO-1A12, Thermofisher,) was applied at 1:100 dilution in 3 % BSA overnight at 4 °C. Cells were washed in PBST before applying the secondary goat ant-mouse antibody (Alexa Fluor 488 A-11001, Thermofisher) at a 1:1000 dilution in 1 % BSA for 60 minutes at room temperature. Cells were light protected from this stage. Cells were washed in PBST and DAPI was applied for nuclear staining at 1:1000 dilution in PBS for 5 minutes. Cells were washed in PBS and mounted with Mowiol for assessment by confocal microscopy. Control experiments were also performed in the absence of primary and secondary antibodies.

2.3.9 Alpha-acetylated tubulin immunofluorescence

This was performed to assess for the presence of cilia in PFA-fixed ALI cultures. Cultured cells were rinsed in PBS and blocked with 2 % BSA/0.04 % Triton X (Sigma-Aldrich) for 1 hour. Cells were washed in PBST and the mouse monoclonal alpha (α)-acetylated tubulin antibody (T7451, Sigma-Aldrich,) was applied at 1:500 dilution in 2 % BSA/0.04 % Triton X (Sigma-Aldrich) overnight at 4 °C. Cells were then washed in PBST before applying the secondary goat anti-mouse antibody (Alexa Fluor 594 A-11032, Thermofisher) at a 1:1000 dilution in 1 % BSA for 60 minutes at room temperature. Cells were light protected from this stage. Cells were washed in PBST and DAPI (Sigma-Aldrich) was applied for nuclear staining at 1:1000 dilution in PBS for 5 minutes. Cells were washed in PBS and mounted with Mowiol (Sigma-Aldrich) for assessment by confocal microscopy. Control experiments were also performed in the absence of primary and secondary antibodies.

2.3.10 TMEM16A immunofluorescence

This was performed to assess for the presence of TMEM16A in PFA-fixed ALI cultures and based on methods described by Benedetto et al (Benedetto et al., 2017). Cultured cells were rinsed in PBS and blocked with 2 % BSA/0.04 % Triton X for 1 hour. Cells were washed in PBST and the rabbit polyclonal TMEM16A antibody (GWB-MP178G, Genway Biotech) was applied at 1:100 dilution in 2 % BSA/0.04 % Triton X overnight at 4 °C. Cells were washed in PBST before applying the secondary goat ant-rabbit antibody (Alexa Fluor 488 A-11034, Thermofisher) at a 1:1000 dilution in 1 % BSA for 60 minutes at room temperature. Cells were light protected from this stage. Cells were washed in PBST and DAPI was applied for nuclear staining at 1:1000 dilution in PBS for 5 minutes. Cells were washed in PBS and mounted with Mowiol for assessment by confocal microscopy. Control experiments were also performed in the absence of primary and secondary antibodies.

All antibody characteristics used for the above immunofluorescent techniques are summarised in Table 6.

Primary antibody	Target	Type	Host	Dilution	Secondary antibody
T7451	α-acetylated tubulin	Monoclonal	Mouse	1:500	A-11032 (AF 594)
ZO-1A12	Zona occludins	Monoclonal	Mouse	1:100	A-11001 (AF 488)
GWB-MP178G	TMEM16A	Polyclonal	Rabbit	1:100	A-11034 (AF 488)

Table 6: Primary antibodies used in immunofluorescent work

Abbreviations: AF Alexa Fluor

2.3.11 Confocal microscopy

ALI cultures stained with the above immunofluorescence methods were visualised using a Nikon A1 plus confocal microscope at either 20x or 40x magnification utilising a numerical aperture of 0.75 mm or 1.3 mm respectively. Scanning speed was consistent, with typically 40 optical x-y sections for all images acquired. Pre-set lasers and filters were used to assess the fluorescence for DAPI-stained nuclei at an excitation wavelength of 405 nm. To visualise the specific targets, pre-set lasers and filters were used to excite at either 488 or 594 nm depending upon the secondary antibody used (Table 6).

2.3.12 Quantification of TMEM16A positive immunofluorescence

This was performed using ImageJ software using a two-step process. Quantification of immunofluorescence was first determined using ImageJ to calculate the area of fluorescence intensity as shown in Figure 13. The number of cells were then calculated by identification of the number of DAPI stained nuclei. This enabled the assessment of area of fluorescence intensity per cell for each ALI culture.

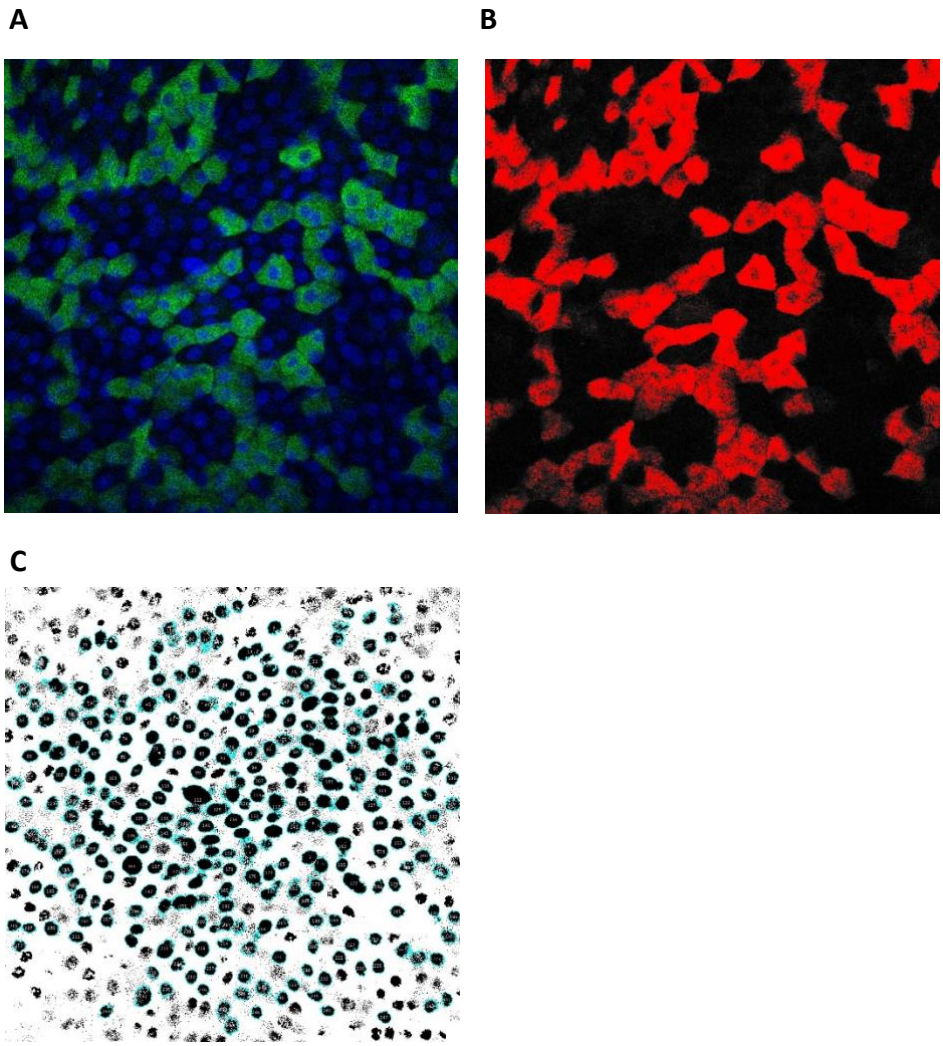

Figure 13: Quantification of TMEM16A immunofluorescence

Air liquid interface PNEC cultures derived from a CF donor were treated with IL-4 (to upregulate TMEM16A expression) and were fixed in 4 % paraformaldehyde and assessed for the presence of TMEM16A with immunofluorescence techniques as described above. Images were obtained using confocal microscopy, with positive TMEM16A staining (green) and nuclei stained with DAPI (blue) as shown in A. ImageJ software was used to select out and quantify the area of positive TMEM16A staining or the area of fluorescence (A.U) as shown in B (red). The number of cells were quantified, as shown in C, and used to calculate the final A.U per cell.

2.4 Enzyme linked immunosorbent assays of bronchoalveolar lavage and air liquid interface cell culture supernatants

2.4.1 Bronchoalveolar lavage collection and processing

Bronchoalveolar lavage (BAL) was collected from children at the time of clinical bronchoscopy. The volume of 0.9 % saline instilled and choice of BAL site was determined by the performing clinician and based on European Respiratory Society taskforce guidelines (de Blic et al., 2000). BAL was performed by gently positioning the tip of the bronchoscope in the selected position and instilling the designated volume of saline. Fluid was aspirated into a sterile suction trap and transported to the laboratory for immediate processing.

The BAL sample was centrifuged at 1250 rpm (183 x g) for 6 minutes at 4 ºC (Mistral 3000i). The supernatant decanted and centrifuged at 2500 rpm (743 x g) for 6 minutes at 4 ºC. The final supernatant was divided into 500 µL aliquots and stored at -80 ºC for later analysis.

2.4.2 Mucin 5AC assessment

An indirect enzyme linked immunosorbent assay (ELISA) was used for the detection of MUC5AC in supernatants harvested from ALI cell cultures at 28d ALI. MUC5AC standard (harvested from purified pig gastric mucin) was diluted in PBS and applied at 100 µL in duplicate into standard wells of a 96 well microtitre plate (Thermofisher) in the range of 0 -10 µg/ml. Cell culture supernatants were diluted in PBS using a 1:2, 1:5 or 1:10 dilution or applied neat at 100 µL into wells in duplicate. Samples and standards were allowed to develop overnight. Plates were emptied and washed three times in 400 µL of PBST (Sigma-Aldrich). Wash steps were repeated after each ELISA protocol step. Unoccupied binding sites were blocked with 300 µL 1 % casein (Sigma-Aldrich) in PBS for 2 hours. The primary antibody (45M1 mouse anti-human MUC5AC, Thermofisher) was diluted 1:1000 in 0.1 % casein/PBST and added at 100 µl for 2 hours. The secondary antibody (horseradish peroxidase-conjugated polyclonal goat anti-mouse antibody; Dako) was diluted 1:5000 and added at 100 µL for 2 hours. Finally, peroxidase substrate ABTS (2,2'-azino-bis(3-ethylbenzthiazoline-6-sulphonic acid; Sigma-Aldrich) was added at 100 µL and left to

develop for 30 minutes. Absorbance at 405 nm was measured using a plate reader (M200, Infinite, Männendorf). The lower limit of detection was 0.156 μg/mL.

2.4.3 Mesoscale Discovery multiplex cytokine analysis

Meso Scale Discovery (MSD) technology was used to quantify cytokines in ALI cell culture and BAL supernatants using the validated human V-PLEX platform (K15067L-1 kit, Meso Scale Diagnostics), specifically measuring interleukin (IL)-17A, IL-6, IL-1β, tumour necrosis factor (TNF)-α, interferon (IFN)-γ, IL-14 and IL-13 according to the manufacturer's instructions. Quantification of IL-8 was performed of ALI culture and BAL supernatants diluted at 1:100 using a U-PLEX human IL-8 kit (K151RAD-1m, Meso Scale Diagnostics) according to the manufacturer's instructions. The lower limits of detection for each cytokine were as follows: IL-4 0.06 pg/mL, IL-6 0.33 pg/mL, IL-17A 2.1 pg/mL, IL-1β 0.15 pg/mL, IFN-γ 1.7 pg/mL, TNF-α 0.54 pg/mL and IL-8 0.15 pg/mL.

2.5 Ussing chamber short circuit current measurement

The Ussing chamber was developed by Hans Ussing in the 1940s as a technique to measure short circuit current (I_{sc}) as an indicator of net transepithelial ion transport (Ussing and Zerahn, 1951).

Experiments were performed using non-perfused Ussing chambers controlled by the VCC MC8 (Voltage Current Clamp MultiChannel, Physiologic Instruments, Inc.). A schematic representation of an Ussing chamber system is shown in Figure 14. Prior to each experiment, 'blank' semi-permeable supports, without cultured cells, were mounted into the system to offset the potential difference and fluid resistance between the two chambers. Semi-permeable supports of differentiated ALI cultures were then mounted into the chambers and bathed both apically and basolaterally in 5mL of Krebs solution. Experiments were performed in a 125 mM chloride containing Krebs solution unless otherwise specified, whereby either 40 mM or 0 mM chloride Krebs solutions were used. The composition of these solutions are shown below in Table 7. Chambers were gassed with 5 % CO_2/95 % O_2 and maintained at pH 7.4 and 37ºC. Each chamber was connected to an Ag/AgCl pellet voltage sensing electrode and an Ag wire current passing electrode. These were connected to the chamber by agar bridges in 3 M KCl.

To measure I_{sc}, transepithelial voltage (Vte) was clamped to 0 mV and the injected current, required to maintain Vte to 0 mV, was continuously measured and recorded using the Acquire and Analyze software (Harvard Apparatus). Under these conditions, the injected I_{sc} was a direct measure of net ion transport across the epithelial monolayer. The transepithelial electrical resistance (TEER) was also continuously recorded using the same software by intermittently clamping the Vte to 5 mV and TEER calculated using Ohm's law.

After a 20-minute period of stabilisation, pharmacological reagents of interest were added to either the apical or basolateral compartments (depending upon individual mechanisms of action) and the resultant effect on I_{sc} was assessed. For all experiments, the protocol consisted of initial apical amiloride addition (100 μM, Tocris) to inhibit ENaC. This was followed by apical addition of forskolin (10 μM, Tocris) as a cAMP activator of CFTR, which was subsequently inhibited with apical $CFTR_{inh}$-172 (20 μM, Tocris). Finally, UTP (100 μM, Sigma-Aldrich) was apically

added as a purinergic agonist for CaCC activation. A representative Ussing chamber trace derived from a non-CF ALI culture is shown in Figure 15A.

The resultant amiloride-sensitive I_{sc} was calculated as shown in Figure 15B. This was performed by first determining the baseline I_{sc} by calculating the mean I_{sc} values for 1 minute prior to amiloride addition. The minimum I_{sc} value after amiloride addition was next determined using GraphPad Prism software and subtracted from the calculated baseline to obtain the resultant amiloride-sensitive I_{sc}. Responses to forskolin, $CFTR_{inh}$-172 and UTP were calculated using a similar approach as shown also in Figure 15B. In addition, the total current calculated from the area under the curve (AUC) using GraphPad Prism software, was used to assess the total UTP-induced I_{sc} response (Figure 15C).

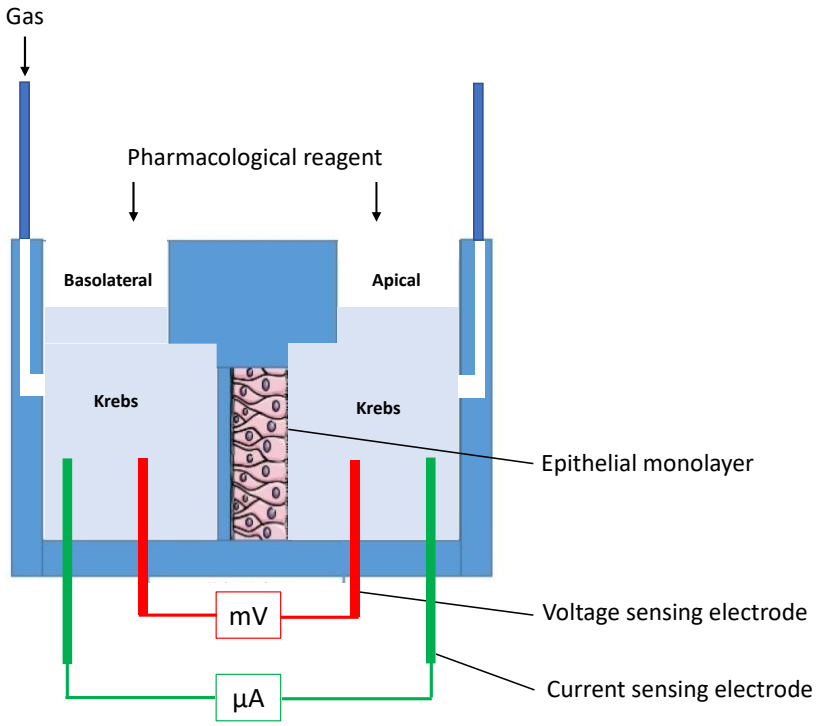

Figure 14: Schematic representation of Ussing chamber

PNEC and PBEC ALI differentiated cultures grown on semi-permeable supports were mounted in the Ussing chamber. The epithelial monolayer was bathed apically and basolaterally with 5 mL of Krebs solution. Each chamber was connected to voltage and current sensing electrodes. The I_{sc} required to clamp the V_{te} to 0 mV was recorded. Pharmacological reagents were added to the apical or basolateral compartments and resultant changes in I_{sc} and R_T were assessed.

125 mM chloride	40 mM chloride	0 mM chloride
25 mM $NaHCO_3$	25 mM $NaHCO_3$	25 mM $NaHCO_3$
115 mM NaCl	31 mM NaCl	115 mM Na gluconate
5 mM KCl	84 mM Na gluconate	2.5 mM K_2SO_4
1 mM $CaCl_2$	5 mM KCl	6 mM Ca gluconate
1 mM $MgCl_2$	1 mM $CaCl_2$	1 mM Mg gluconate
	1 mM $MgCl_2$	

Table 7: Composition of Krebs solutions used for Ussing chamber experiments

10 mM D-glucose was added to all solutions on the day of experiments.

Abbreviations: $CaCl_2$: calcium chloride; KCl: potassium chloride; K_2SO_4 potassium sulphate; $MgCl_2$: magnesium chloride; NaCl: sodium chloride; $NaHCO_3$: sodium bicarbonate.

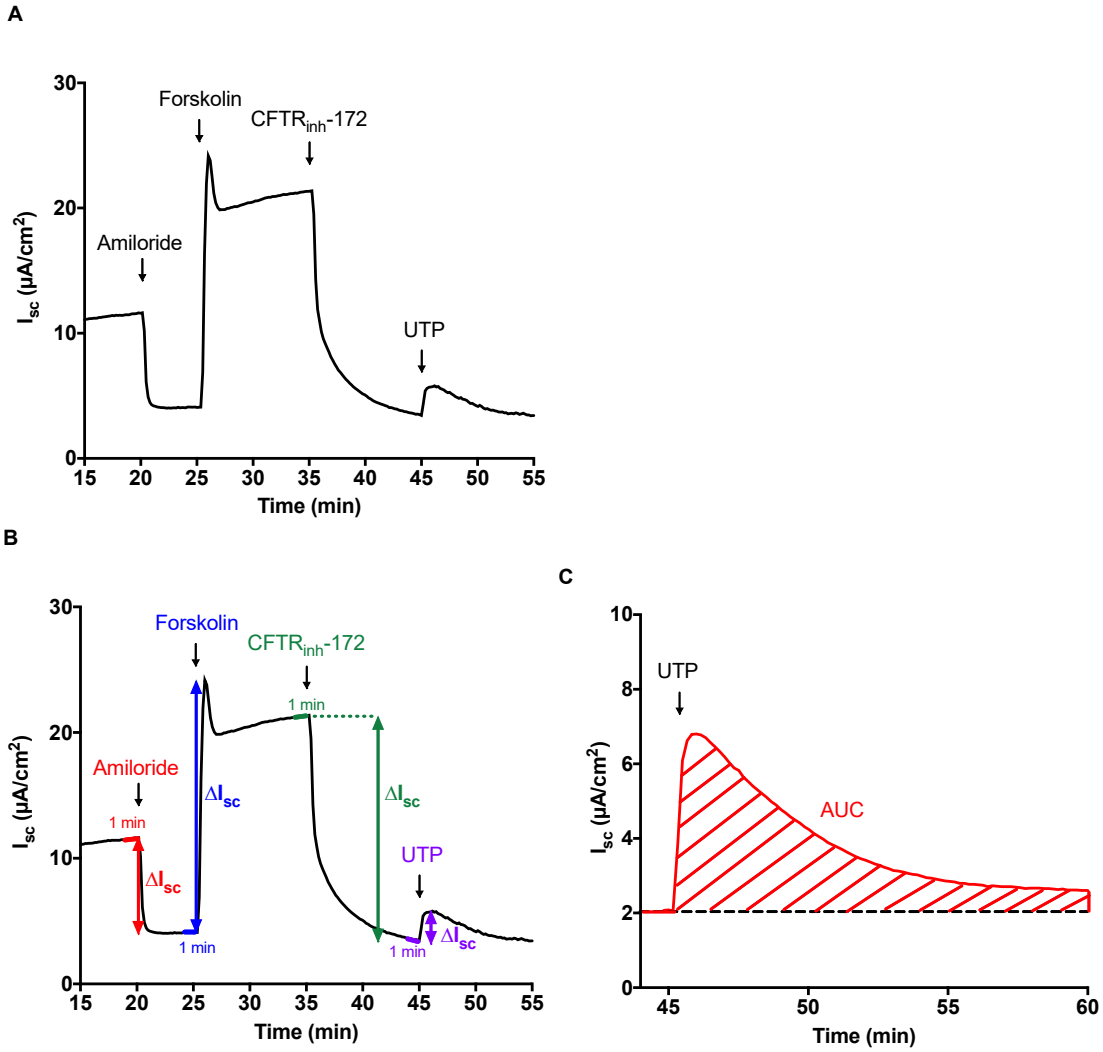

Figure 15: Representative short circuit current responses to amiloride, forskolin and $CFTR_{inh}$-172 and calculated changes in responses in ALI cultures derived from a non-CF donor

Representative short circuit current (I_{sc}) trace showing responses to amiloride, forskolin, $CFTR_{inh}$-172 and UTP are shown in A. The minimum I_{sc} value after amiloride addition (determined with GraphPad Prism software) was subtracted from the calculated baseline 1 minute prior to amiloride addition to obtain the resultant amiloride-sensitive I_{sc} (red). Similarly, the forskolin-induced I_{sc} was obtained by subtracting the mean baseline I_{sc} 1 minute prior to forskolin addition from the maximum peak response to forskolin (blue). I_{sc} responses to $CFTR_{inh}$-172 (green) and UTP (purple) were calculated using the same approach. The area under the curve (AUC) was analysed using GraphPad Prism software and used to assess the total UTP-induced I_{sc} response (C).

2.6 Intracellular calcium assessment

Nasal epithelial cells were submerged and cultured on 25 mm glass coverslips (VWR) at a seeding density of 6 x 10^5 per coverslip and investigated after achieving 80-90 % confluence.

All intracellular calcium measurements were performed by JinHeng Lin (PhD student, Newcastle University). Cells were washed in NaHEPES buffered solution (containing in mM: 130 NaCl, 5 KCl, 1 $CaCl_2$, 1 $MgCl_2$, 10 NaHEPES and 10 D-glucose, pH 7.4) and incubated with 5 μM Fura-2 AM for 1 hour. The dye was removed and cells were incubated in NaHEPES for a further 15 minutes to enable dye de-esterification. Cells were then mounted onto a Nikon microscope at room temperature and imaged with a Nikon fluor x 40 oil immersion objective with a numerical aperture of 1.3. A NaHEPES solution was perfused across the cells at a rate of 3 mL/min. Cells were alternately excited at 340 nm and 380 nm for 0.25 s each continuously, and emitted light was collected at 510 nm and recorded using InCyt PM-2 software (Biopress Online). The changes in the ratio of 340 nm:380 nm emission were proportional to changes in intracellular calcium ($[Ca^{2+}]_I$).

2.7 Quantitative real time polymerase chain reaction

2.7.1 Extraction of RNA and cDNA synthesis

Quantitative real-time polymerase chain reaction (RT-qPCR) was used as a technique to investigate the expression of genes of interest. This was performed by first extracting total RNA from paediatric differentiated non-CF and CF PNEC and PBEC ALI cultures using the standard protocol of the AllPrep RNA/Protein kit (Qiagen) as shown below in Figure 16. After extraction, RNA was eluted in 20 μL of RNAase-free water (Thermofisher). The NanoDrop One UV-Vis spectrophotometer (Thermofisher) was used to determine the concentration (by ultraviolet absorbance at 260 nm) and purity (ratio of 260:280 nm absorbance) of the extracted RNA. Total RNA was converted to cDNA using a random hexamer primer, dNTP mix, reverse transcriptase buffer, RiboLock RNAase inhibitor and maxima reverse transcriptase (Thermofisher) which were incubated with the RNA for 10 minutes at 25 °C followed by 30 minutes at 50 °C and terminated by heating at 85 °C for 5 minutes.

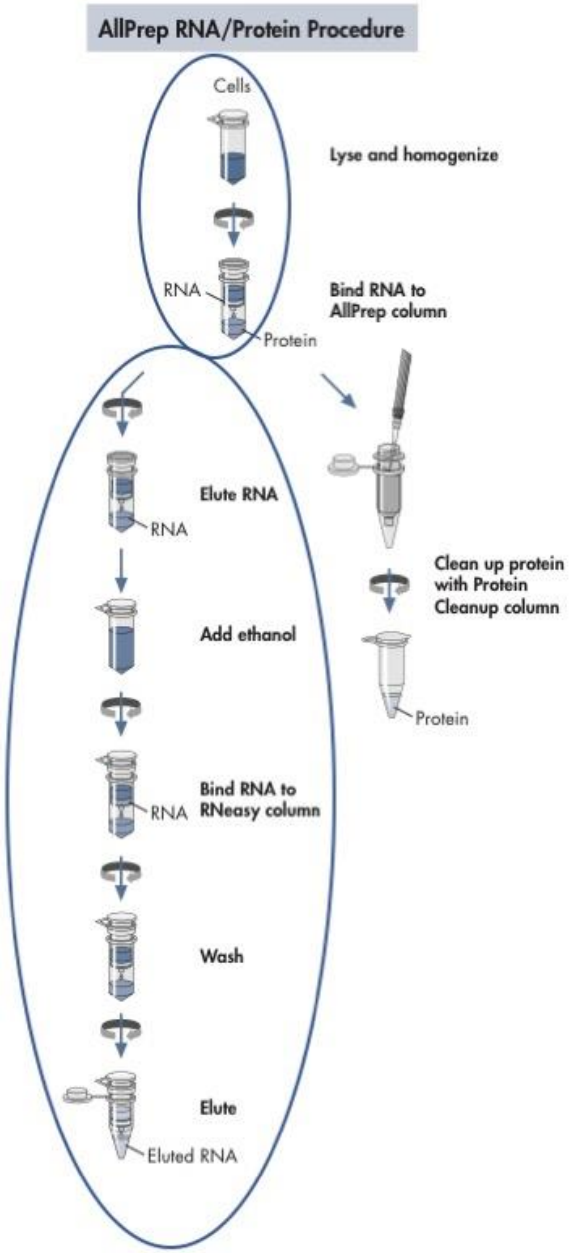

Figure 16: Protocol for RNA extraction from differentiated ALI cultures

RNA was extracted from differentiated PNEC and PBEC ALI cultures using the AllPrep RNA/Protein kit (Qiagen) as highlighted within the blue circles. After extraction, the RNA was eluted into 20 μL of RNAase free water for subsequent conversion to cDNA. Image adapted from AllPrep RNA/Protein handbook (Qiagen, 2014).

2.7.2 Quantitative real-time polymerase chain reaction (SYBR™ Green)

RT-qPCR was performed using the QuantStudio 3 Real Time PCR machine (Thermofisher). A final reaction volume was produced containing 45 ng of cDNA, 0.3 μL (200 μM) of each forward and reverse primers, 7.5 μL of PowerUp™ SYBR™ Green Master Mix (Thermofisher) and RNAase free water to make a final volume of 15 μL. Primer sequences for all genes of interest are shown in Table 8 and Table 9. GAPDH was used as the reference house-keeping gene and cDNA derived from an internal reference control was used in each RT-qPCR plate to enable comparisons across different plate preparations.

Amplifications were performed starting with an initial denaturation step at 95 °C for 10 minutes followed by the PCR phase comprising of 40 cycles of denaturation at 95 °C for 10 seconds and a combined primer annealing/extension at 60 °C and 72 °C for 20 seconds each. At the end of each PCR, a melting curve was generated with 95 °C for 15 seconds followed by 60 °C for 1 minute and dissociation at 95 °C for 15 seconds. This process has been summarised in Figure 17. Template negative controls and assessment of melt curve analysis (Figure 17) were used to determine the absence of DNA contamination.

Target	Sequence	Amplicon length (bp)
GAPDH*	F: 5'-TGCACCACCAACTGCTTAGC-3'	87
	R: 5'-TGCACCACCAACTGCTTAGC-3'	
CFTR*	F: 5'-CACTGCTGGTATGCTCTCCA-3’	237
	R: 5'-CACTGCTGGTATGCTCTCCA-3’	
TMEM16A*	F: 5'-TGCATGGTCCCGTTCTTACT-3’	376
	R: 5'-TGCATGGTCCCGTTCTTACT-3’	
MUC5AC*	F: 5'-CAGCCACGTCCCCTTCAATA-3’	64
	R: 5'-CAGCCACGTCCCCTTCAATA-3’	
MUC5B*	F: 5′-GCAACACCCTCCTCTAGCAC-3′	120
	R: 5′-AGGTGTTGTCCCTGGAGTTG-3′	
α-ENaC†	F: 5’-CAGCCCATACCAGGTCTCAT-3’	221
	R: 5’-ATGGTGGTGTTGTTGCAGAA-3’	
β-ENaC†	F: 5’-TCCTACCCTCGTCCCTACCT-3’	151
	R: 5’-CCAGGAAGGAGAAAACCACA-3’	
γ-ENaC†	F: 5’-ACCACCAGCCATGGTCTAAG-3’	211
	R: 5’-GTTCAGGTCCCGGGATTTAT-3’	

Table 8: Primer sequences for genes encoding epithelial channels of interest

Abbreviations: F: forward; R: reverse.

* In house primers designed in Dr Mike Gray’s lab using Primer3web (http://primer3.ut.ee/) and verified with Primer Blast (https://www.ncbi.nlm.nih.gov/tools/primer-blast/). † Sequences obtained from (Lee et al., 2015a) and verified with Primer Blast.

Target	Sequence	Amplicon length (bp)
ZO-1	F: 5'-ACCAGTAAGTCGTCCTGATCC-3'	128
	R: 5'-TCGGCCAAATCTTCTCACTCC -3'	
CDH1	F: 5'-ATTTTTCCCTCGACACCCGAT-3’	109
	R: 5'-TCCCAGGCGTAGACCAAGA-3’	
EpCAM	F: 5’-AATCGTCAATGCCAGTGTACTT-3’	178
	R: 5’-TCTCATCGCAGTCAGGATCATAA-3’	
Foxj1	F: 5'-TCGTATGCCACGCTCATCTG-3’	183
	R: 5'-CTCCCGAGGCACTTTGATGA-3’	
TUBA1A	F: 5'-CTATGTGCCGCAGGTTCTCT-3’	119
	R: 5'-CTCACGCATGGTTGCTGCTT-3’	

Table 9: Primer sequences for genes encoding epithelial markers of interest

Abbreviations: F: forward; R: reverse.

All primers were in house primers designed in Dr Brodlie’s lab using Primer3web (http://primer3.ut.ee/) and verified with Primer Blast (https://www.ncbi.nlm.nih.gov/tools/primer-blast/).

A

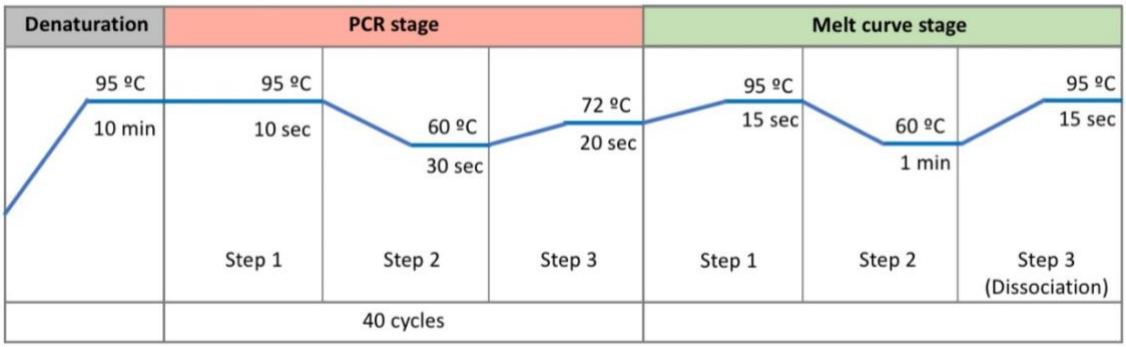

B

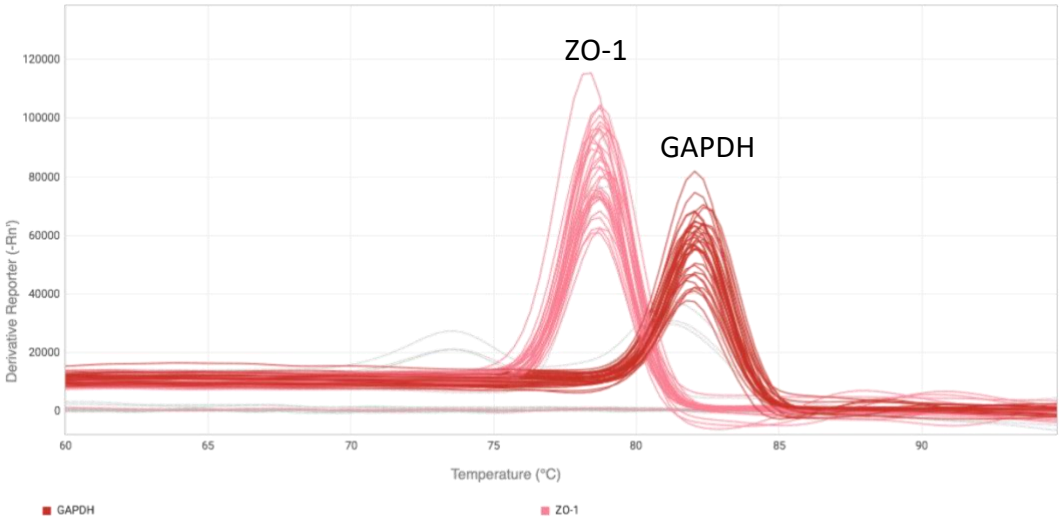

Figure 17: Process for real time quantitative polymerase chain reaction and melt curve analysis

The protocol used for real time quantitative polymerase chain reaction (RT-qPCR) is shown in A, with the initial denaturation, followed by the PCR and melt curve stages. Representative melt curve analysis graph after RT-qPCR with primers for zona-occludins 1 (ZO-1; pink) and GAPDH (red) is shown in B, showing single peaks for each gene indicating the production of pure DNA amplification products.

2.7.3 Analysis of real-time quantitative polymerase chain reaction

The Design and Analysis Application Software (Thermofisher) was used to determine the threshold cycle (C_T) for expression analysis of each gene of interest in samples investigated. This was used to determine the relative quantification of each gene, using the comparative C_T method whereby the ΔC_T (relative to GAPDH) was first calculated as follows:

Equation 1: $\Delta C_T = C_{T\ \text{gene of interest}} - C_{T\ \text{GAPDH}}$

These ΔC_T values were normalised to the internal reference control sample to enable comparison across experimental plates. To determine the relative fold change for each gene between two different groups (e.g. non-CF PBECs non-CF PBECs), the $2^{-\Delta\Delta CT}$ method was used, whereby the relative fold change was calculated as follows:

Equation 2: $\Delta\Delta C_T = \Delta C_{T\ \text{non-CF PNECs}} - \Delta C_{T\ \text{non-CF PBECs}}$

Equation 3: Relative fold change = $2^{-\Delta\Delta CT}$

A challenge of using patient derived samples is the difficulty in justifying and assigning a particular sample from one group to compare with another (Schmittgen and Livak, 2008). To overcome this in relation to equation 2, the ΔC_T for the first group (in this case non-CF PNECs) was determined by calculating the mean ΔC_T for all non-CF PNECs. Individual ΔC_T values for samples in the second group (in this case non-CF PBECs) were subtracted from this to ascertain the $\Delta\Delta C_T$ for each non-CF PBEC sample. The mean of these values was determined, and applied to equation 3 to derive the relative fold change between the two groups. This approach is exemplified in Table 10 and was used for all grouped data analyses of mRNA expression in this PhD.

Although this analysis determined the relative fold change between two groups, this calculation did not incorporate SD for the calculated ΔC_T values for each individual sample. To overcome this, $2^{-\Delta CT}$ (i.e. relating to equation 1) values were also calculated for each sample to enable the calculation of the median $\pm$ IQR for each group from the individual patient sample values. This provided relative gene expression data and an alternative analysis of the spread of data (Schmittgen and Livak, 2008).

Non-CF PNECs ΔC_T	**Non-CF PBECs ΔC_T**	**$\Delta\Delta C_T$**	**Relative fold change ($2^{-\Delta\Delta CT}$)**
		(10.3 - non-CF PBECs ΔC_T)	
10.1	9.1	-1.3	2.4
9.5	8.0	-2.4	5.2
10.7	15.8	5.4	0.0
11.3	12.4	2.1	0.2
8.4	11.3	0.9	0.5
10.4	13.1	2.7	0.2
12.4	14.7	4.4	0.1
9.8	13.5	3.2	0.1
Mean: 10.3			**Mean fold change: 1.1 ± 1.9**

Table 10: Exemplification of relative fold change calculation for *TMEM16A* expression in non-CF PNECs versus PBECs

Abbreviations: C_T cycle threshold.

$\Delta C_T = C_T$ TMEM16A - C_T GAPDH.

$\Delta\Delta C_T$ as described above i.e. mean ΔC_T non-CF PNECs - ΔC_T non-CF PBECs.

Relative fold change is $2^{-\Delta\Delta C_T}$.

In this example, the mean relative fold change for TMEM16A in non-CF PBECs versus non-CF PNECs is 1.1 ± SD 1.9.

2.8 Statistical analysis

Prism version 7.0 for Mac (GraphPad software, CA, USA) was used to perform all statistical analyses and prepare graphical representations of data. The Shapiro-Wilk test was applied to assess the normality of data. Normally distributed data is presented as the mean ± standard deviation (SD) in text and figures and analysed using the unpaired t test or one-way analysis of variance (ANOVA) with post hoc Bonferroni's multiple comparison test in accordance with the data set. Non-normally distributed data is presented as the median ± interquartile range (IQR) in text and figures and analysed using the Mann Whitney test or Kruskal-Wallis analysis of variance with Dunn's post hoc analysis of variance in accordance with the data set. Statistical tests used for data analysis are detailed in the figure legends. Data was considered to be statistically significant at p-values of less than 0.05.

3 Chapter 3 Development and characterisation of differentiated primary nasal and bronchial epithelial cell cultures derived from children with and without CF

3.1 Introduction

As discussed earlier in the thesis, primary airway epithelial cells have been pivotal to enable further investigation of pathological processes in CF in addition to facilitating drug discovery (Van Goor et al., 2009a). The culture of both primary bronchial and nasal epithelial cells are established techniques that are performed by many CF research groups.

In children, bronchial epithelial cells are harvested either during a bronchoscopy, which requires a general anaesthetic, or at transplantation, which is an infrequent occurrence thereby limiting available samples for research. Nasal epithelial cells provide a more attractive experimental model, given the relative ease of sampling and potential for application in a range of CF disease severities, genotypes and clinical settings. Despite the uptake of nasal culture use in CF research, there are very few comparisons of nasal and bronchial epithelial characteristics. Indeed, it is still recognised amongst the CF research community that further comparative assessment with bronchial epithelial cells is very much needed (Clancy et al., 2018). Furthermore, with the evolution of 'theratyping' to investigate specific effects of *CFTR* variants on CFTR function and therapeutic response, there is considerable need for robust, reliable, patient-derived experimental models to deliver effective personalised CF care.

Establishment of this resource in Newcastle will enable the investigation of the research aims and objectives outlined in this thesis. Furthermore, if successful, it will be valuable for the progression of paediatric CF research in Newcastle. With a regional CF paediatric patient population of around 180 children, the current infrastructure is well suited to facilitating this process.

3.2 Hypotheses

This chapter will involve the investigation of the following hypothesis:

- Paediatric PNECs will have similar epithelial characteristics to PBECs and are therefore a representative model for CF research.

3.3 Aims

The specific aims of the work detailed in this chapter were to:

- establish a programme to enable the sampling of elective nasal and bronchial brushings from children already attending the GNCH for a clinically-indicated bronchoscopy
- develop and optimise methods to obtain PNEC and PBEC ALI cultures from brushings isolated from children with and without CF and non-CF participants
- assess the morphology of successfully established ALI cultures including investigation of epithelial integrity and mucociliary phenotypes

3.4 Results

3.4.1 Establishment of a programme to harvest paediatric nasal and bronchial brushings

To establish this programme at GNCH and Newcastle University, I coordinated the necessary ethical approval in accordance with the Integrated Research Application System and Research Ethics Committee review. I developed the research protocol together with parent and age-appropriate participant information sheets (see Appendix A for relevant ethical approval documentation, consent forms and parent and participant information literature). The value of public engagement in research was highlighted through my participation in activities with the North East's Young People's Advisory Group for paediatric research relating to protocol design and updates of research progress.

Through my involvement in this research project, I obtained certification in Good Clinical Practice (GCP) relating to research in secondary care, issues relating to informed consent in paediatric research and the acquisition and use of human tissue. It was also necessary to acquire technical knowledge relating to the model and size of bronchoscopes used within the hospital and verify information regarding the compatibility of cytology brushes with existing equipment.

Nasal brushings can be sampled from awake children and is current practice at GNCH for the clinical diagnosis of primary ciliary disorders. However, for the purposes of this research and to enable the acquisition of both nasal and bronchial epithelial cells, both sets of brushings were sampled during a clinically-indicated bronchoscopy to minimise invasive procedures in children. It was essential to ensure that members of the paediatric CF multi-disciplinary team, paediatric anaesthetists and surgical theatre staff were well-informed throughout. They were instrumental in facilitating sampling of brushings through their exceptional co-operation and assistance throughout the period of participant recruitment.

3.4.2 Development and optimisation of differentiated paediatric primary nasal and bronchial epithelial air liquid interface cultures

Recruitment of paediatric participants for the work performed in this PhD took place between November 2015 until March 2018. Figures related to recruitment, brushings harvested and culture success are summarised in Figure 18. All parents and children with CF who were approached consented to their participation. For non-CF participants, parents and children declined on 5 occasions. A total of 29 CF and 20 non-CF participants were recruited. Clinical information and success rates of PNEC and PBEC cultures are summarised in Table 11 and Table 12. The median age of the non-CF group was lower than the CF group as shown in Figure 19 (non-CF: 3.2 years, range 0.8-15.7 versus CF: 5.4 years, 0.5-15.3) and there was a small preponderance for male children in both groups (CF: 55 %, non-CF 60 %). The majority (72 %) of CF participants were homozygous for the F508del mutation. The predominant indication for bronchoscopy in non-CF participants was for the investigation of recurrent chest infections, which occurred in 60% of cases.

Nasal brushings were sampled from all recruited participants (n=29 CF and 20 non-CF). Bronchial brushings were not sampled due to technical difficulties during the bronchoscopy in three cases and the procedure was not re-attempted (n=27 CF and 19 non-CF bronchial brushings). All bronchial brushings were harvested from the same anatomical generation of lobar bronchi. Either a 1.2 mm or 2.0 mm bronchial brush was used to harvest bronchial epithelial cells. This selection was at the discretion of the performing clinician and dependent upon the size of the child and the internal bronchoscope working channel diameter. A smaller 1.2 mm brush was used in 60 % of non-CF participants, with a lower frequency in CF participants of 43 %, in accordance with the increased age in this latter group.

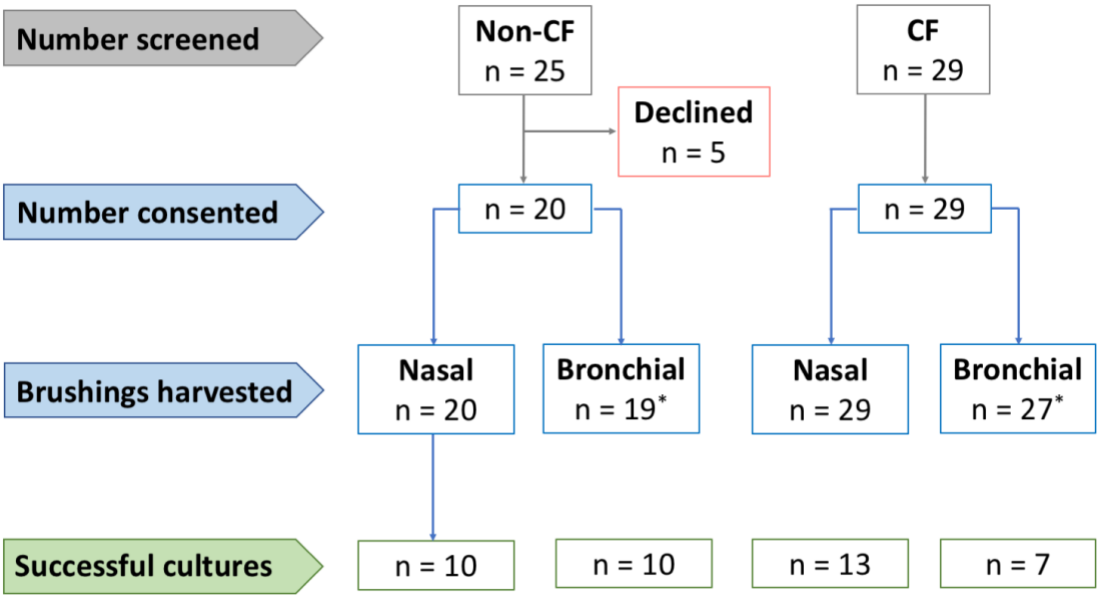

Figure 18: Participant recruitment and sampling of nasal and bronchial brushings from children with and without cystic fibrosis

* Bronchial brushings not sampled for technical reasons from 1 non-cystic fibrosis (CF) and 2 CF participants.

Sample	Genotype	Age (y)	Sex	Pancreatic function	Sweat test (mmol/L)	FEV_1 (% pred)	Relevant microbiology	PNEC success	PBEC success
PCF1	F508del/ G551D	2.9	M	PI	114	ND	*M. catarrhalis*	No [1]	No [1]
PCF2	F508del/2184delA	2.5	M	PI	117	ND	None	No [2]	No [2]
PCF3	F508del/F508del	9.3	M	PI	ND	96	None	Yes	No [3]
PCF4	F508del/F508del	12.5	F	PI	106	61	*A. fumigatus*	No [1]	NS
PCF5	F508del/F508del	1.3	F	PI	103	ND	None	Yes	NS
PCF6	F508del/F508del	0.6	M	PI	103	ND	None	No [3]	Yes
PCF7	F508del/F508del	12.2	M	PI	ND	80	None	No [4]	No [4]
PCF8	F508del/F508del	1.2	M	PI	Insufficient	ND	None	No [4]	No [4]
PCF9	F508del/F508del	3.9	M	PI	98	117	None	Yes	No [3]
PCF10	F508del/F508del	5.9	F	PI	112	62	None	Yes	No [3]
PCF11	F508del/F508del	0.5	F	PI	93	ND	Rhinovirus	Yes	No [1]
PCF12	F508del/F508del	5.4	F	PI	ND	71	None	Yes	No [5]
PCF13	F508del/Q493X	10.5	F	PI	105	95	*E. coli*	Yes	No [1]
PCF14	F508del/1138insG	15.3	M	PI	104	87	None	No [1]	Yes
PCF15	F508del/F508del	4.3	M	PI	ND	81	*H. influenzae*, *A. fumigatus*	Yes	No [5]
PCF16	F508del/F508del	3.3	M	PI	91	ND	None	No [6]	No [6]

PCF17	F508del/F508del	10.2	M	PI	118	104	None	No [6]	No [6]
PCF18	F508del/F508del	2.3	F	PI	106	ND	None	No [1]	Yes
PCF19	F508del/F508del	10.3	F	PI	NA	66	*Achromobacter*	Yes	No [5]
PCF20	F508del/1154insT	14.7	M	PI	NA	55	None	No [2]	No [2]
PCF21	F508del/F508del	0.9	M	PI	ND	ND	None	No [1]	No [1]
PCF22	F508del/F508del	11.4	F	PI	ND	98	*P. aeruginosa, A. fumigatus*	No [1]	Yes
PCF23	F508del/2896delA	5.7	F	PI	112	100	*Mycobacterium*	Yes	Yes
PCF24	F508del/R751L	6.4	M	PS	74	?	*B. cepacia*	No [1]	Yes
PCF25	F508del/F508del	5.7	M	PI	103	86	None	Yes	Yes
PCF26	F508del/G542X	5.3	M	PI	99	67	None	Yes	No [6]
PCF27*	F508del/F508del	3.2	F	PI	103	ND	None	No [1]	No [1]
PCF28†	F508del/F508del	5.6	M	PI	ND	89	*Mycobacterium*	Yes	No [3]
PCF29	F508del/F508del	4.6	F	PI	104	68	None	No [1]	No [3]

Table 11: Clinical details of CF participants

Abbreviations: y: years; M: male; F: female; PI: pancreatic insufficient; PS: pancreatic insufficient; pred: predicted; NA : not available; ND: not done; NS: not sampled (technical reasons). Relevant microbiology indicates results from sputum or cough swabs taken before bronchoscopy. * Same donor as PCF5. † Same donor as PCF15. Reasons for culture failure: 1 failure during ALI phase; 2 low brushing yield; 3 culture infection; 4 suspected toxicity; 5 problems with cell attachment; 6 undetermined cause.

Sample	Diagnosis	Age (y)	Sex	Sweat test (mmol/L)	FEV_1 (% pred)	Relevant microbiology	PNEC success	PBEC success
PWT1	Recurrent chest infections	2.0	M	ND	ND	None	Yes	No [1]
PWT2	Recurrent chest infections and wheeze	1.7	F	ND	ND	None	Yes	No [1]
PWT3	Recurrent chest infections and tracheitis	7.9	M	ND	110	ND	No [2]	Yes
PWT4	Recurrent chest infections	5.6	F	ND	ND	ND	Yes	NS
PWT5	Recurrent chest infections and wheeze	3.3	F	ND	ND	ND	No [1]	No [1]
PWT6	Recurrent wheeze	7.5	F	ND	ND	ND	Yes	Yes
PWT7	Recurrent chest infections	1.8	M	Normal	ND	None	No [2]	Yes
PWT8	Recurrent wheeze and tracheitis	3.1	F	Normal	ND	ND	Yes	Yes
PWT9	Recurrent wheeze	0.9	M	Normal	ND	None	Yes	Yes
PWT10	Recurrent chest infections and wheeze	2.8	F	Normal	ND	None	No [3]	Yes
PWT11	Recurrent chest infections	2.3	M	Normal	ND	ND	Yes	Yes
PWT12	Recurrent chest infections	0.8	M	ND	ND	RSV	No [6]	No [6]
PWT13	Recurrent chest infections	3.3	M	Normal	ND	ND	Yes	No [1]

PWT14	Recurrent chest infections and wheeze	1.3	M	ND	ND	ND	No [1]	No [1]
PWT15	Recurrent chest infections	1.1	M	ND	ND	*M. catarrhalis*	No [1]	No [1]
PWT16	Persistent cough	15.7	F	ND	108	ND	Yes	Yes
PWT17	Recurrent croup	13.4	M	ND	ND	ND	Yes	Yes
PWT18	Persistent cough Persistent CXR consolidation	3.8	F	ND	ND	ND	No [1]	No [1]
PWT19	Asthma Persistent cough	8.0	M	ND	115	None	No [1]	No [1]
PWT20	Recurrent chest infections	5.8	F	Normal	ND	*H. influenzae*	No [1]	Yes

Table 12: Clinical details of non-CF participants

Abbreviations: y: years; M: male; F: female; pred: predicted; ND: not done; NS: not sampled (technical reasons). Relevant microbiology indicates results from sputum or cough swabs taken before bronchoscopy. Reasons for culture failure: [1] failure during ALI phase; [2] low brushing yield; [3] culture infection; [4] suspected toxicity; [5] problems with cell attachment; [6] undetermined cause.

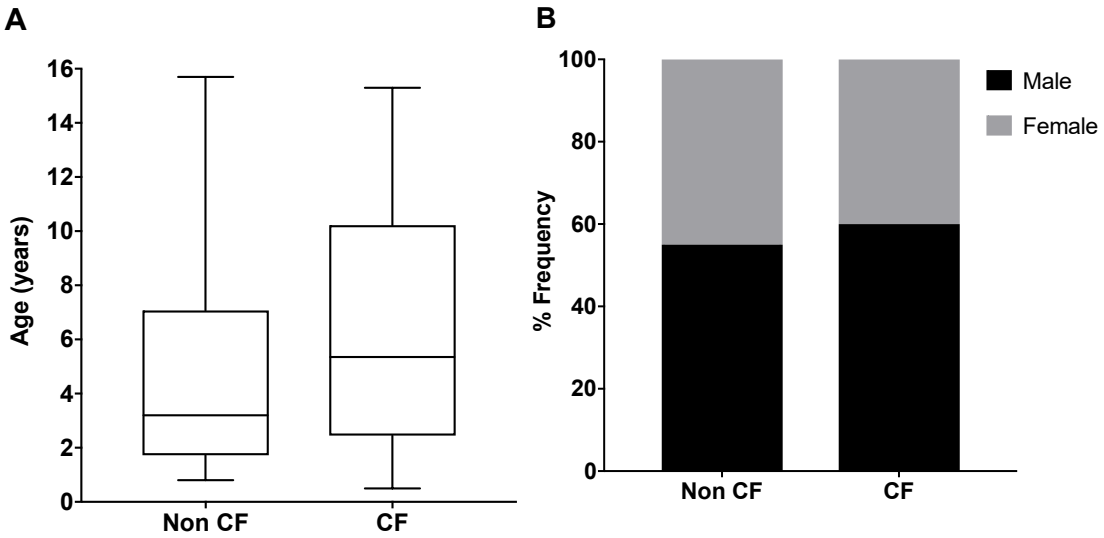

Figure 19: Participant demographics

The age (A) of recruited participants is presented as box plots showing median age ± 25th and 75th quartiles with whiskers indicating the maximum and minimum values. The sex (B) of recruited participants are presented in the bar graphs as percentage frequency.

3.5 Culture outcomes

3.5.1 Cell yield from nasal and bronchial brushings

Methods used for developing paediatric ALI cultures were derived from existing procedures within the research group for the culture of adult PBECs isolated from bronchoscopic brushings and explanted CF lung tissue (Fulcher et al., 2005, Brodlie et al., 2010, Forrest et al., 2005). Nasal cultures had not previously been developed. Published literature relating to methods described by other research groups was consulted to develop and optimise techniques for airway epithelial sampling in Newcastle (McDougall et al., 2008, McNamara et al., 2008, Guo-Parke et al., 2013).

Cell yield was assessed in 4 CF PBEC and PNEC pairs after brushings were harvested. All brushes compared were 2.0 mm in size and calculations were corrected for number of brushes used to sample epithelial cells. No differences were found in the median cell yield between PNECs and PBECs with 4.5 $x10^4$, IQR 2.3 to 6.7 $x10^4$ versus 3.5 $x10^4$, IQR 2.1 to 6.8 $x10^4$ cells respectively, p=0.89 (Figure 20).

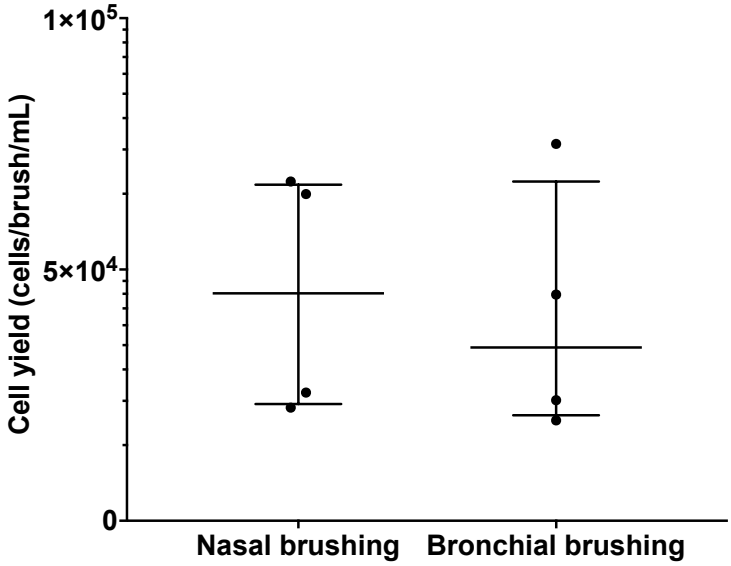

Figure 20: Cell yield isolated from nasal and bronchial brushings

The number of cells isolated from 4 CF nasal and 4 bronchial brushings harvested from CF participants was assessed using a haemocytometer. All brushes were 2.0 mm in size. Data is presented as median ±IQR and analysed using the Mann Whitney test, p=0.89.

3.5.2 Determinants of air liquid interface culture success

ALI cultures were successful in 13 of 29 (45 %) CF PNECs, 7 of 27 (26 %) CF PBECs, 10 of 20 (50 %) non-CF PNECs and 10 of 19 (53 %) non-CF PBECs. Paired cultures from the same individual donors were possible in 2 CF donors and 6 non-CF donors.

Culture outcomes and reasons for failure are summarised in Figure 21. Overall culture success rate was 42 %, with highest rates in non-CF PBECs of 53 %. During the initial stages of culture technique development, predominant reasons for failure were either technical or due to culture infection. Paediatric bronchial brushings to harvest PBECs had not previously been performed at GNCH. Technical reasons occurred early in recruitment (e.g. with donor PCF2) and included an inadequate brushing technique leading to low cell yield and subsequent problems with the initial expansion stage in tissue culture flasks.

Culture infection, both from the donor source and environmental contamination, can be problematic in cultures derived from CF patients (Garratt et al., 2014). All 7 incidences of culture infection occurred during the initial submerged expansion phase, of which 5 (71 %) occurred in CF PBECs with 1 infection in both CF PNEC and non-CF PNECs. Culture media was supplemented with penicillin/streptomycin with 18 PBEC and PNEC cultures isolated from the first 10 CF participants. Although bacterial infection was not an issue, all infected cultures displayed evidence of fungal infection on phase contrast microscopy (Figure 22).

The source of these infections was most likely due to environmental contamination since BAL microbiology from these donors was either bacterial or normal. Antimicrobials as detailed in Table 13 were subsequently added to PCF7 and PCF8 cultures to minimise infection. These antimicrobials are routinely used to culture CF PBECs isolated from end-stage diseased explanted lung tissue in the current lab environment (Brodlie et al., 2010). However, supplementation in paediatric cultures on this occasion resulted in universal cell death. The addition of a commercially available antimicrobial, Primocin, for the first 72 hours of culture significantly reduced infection rates from 22% prior to its application to 4 % in subsequent CF and non-CF cultures without detrimental effects on epithelial cell survival ($p=0.01$; Chi-squared test).

Problems with epithelial cell attachment were encountered with all bronchial cultures in the early phases of culture development affecting 15 % of CF PBECs overall. This difficulty was not evident with PNECs. Despite improvements with brushing technique and successful prevention of infection, cells failed to attach to the collagen-coated tissue culture flasks, leading to subsequent culture failure. Eventual modification of the substratum with the addition of fibronectin and 1 % BSA (as outlined in 2.2.3) improved cell attachment. Culture success rates for PBECs were re-calculated from the time of substratum modification and shown in Table 14. Evidently, there was a more pronounced improvement with CF PBEC culture success from 13 % to 42 % after the introduction of BSA/fibronectin. The success rate reduced for the non-CF PNECs, however this is likely to reflect the increase in culture numbers after this timepoint.

After the above-mentioned modifications, successful expansion and growth was achieved under submerged conditions enabling progression to ALI culture. Failure during the ALI phase occurred in 30 – 42 % of all cultures with the greatest incidence in non-CF PBECs (Figure 21).

Despite investigation for the presence of infection and maintenance of optimum culture conditions, no obvious explanations were apparent for the causes of ALI failure. However, cultures that took longer to reach confluence in the initial submerged expansion phase were more likely to fail at ALI as shown in Figure 23 A and B. This median time was significantly less in successful PNECs than those that failed at any stage of ALI (8.0d, IQR 7.0 to 8.0 versus 9.5d, IQR 8.3 to 12.0, p=0.0001) and was also apparent in PBECs (11.5d, IQR 10.0 to 13.3 versus 15.0d, IQR 12.3 to 18.6, p=0.008). This suggests that time to confluence is a useful marker of ALI culture success and therefore could help with early exclusion of cultures that are unlikely to progress during ALI.

As shown in Figure 23C, median time to confluence in successful non-CF PNECs was 8.0d (IQR 7.0 to 9.0) and significantly shorter that non-CF PBECs (11.5d, IQR 9.5 to 13.5, p=0.03). This difference was also apparent in successful CF cultures (PNECs: 7.0d, IQR 6.5 to 8.0 versus PBECs: 11.5d, IQR 10.3 to 135, p=0.01). No significant differences were found between cells harvested from the same anatomical sites.

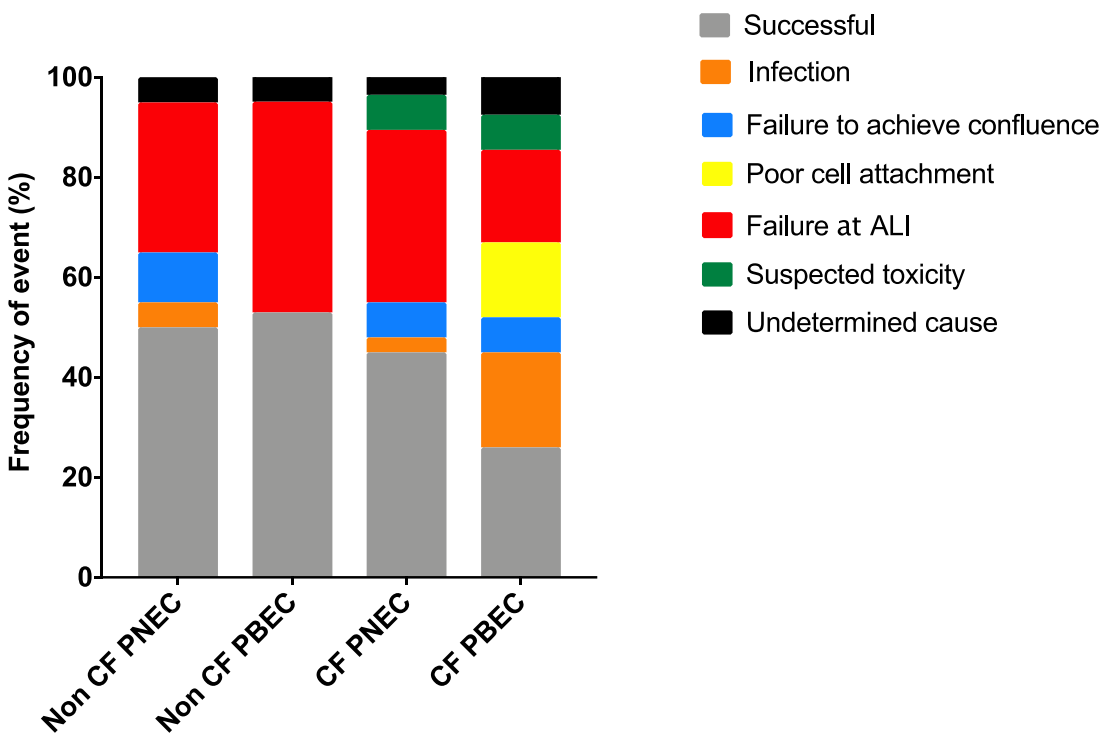

Figure 21: Outcomes of PNEC and PBEC air liquid interface cultures

Outcomes were compared in PNECs and PBECs cultures isolated from all non-CF and CF participants. These included ALI culture success, culture infection, failing to achieve confluence due to low cell yield, poor epithelial cell attachment during initial submerged expansion phase, failure during ALI culture, suspected toxicity from antimicrobials and finally reasons that were undetermined during the submerged expansion phase; n=20 non-CF PNECs, 19 non-CF PBECs, 29 CF PNECs and 27 CF PBECs.

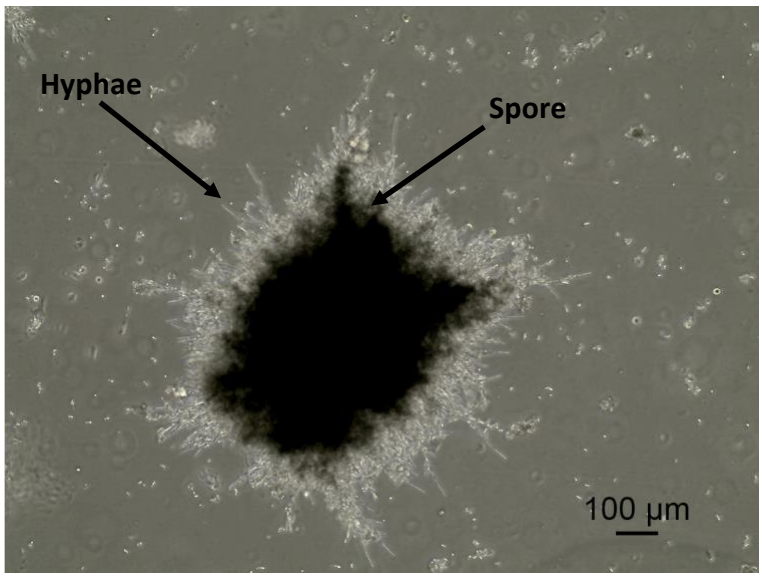

Figure 22: Fungal contamination of epithelial culture

Evidence of fungal contamination of submerged CF PBEC culture during the initial expansion phase as visible by phase contrast microscopy. This contaminant has a typical fungal appearance with evidence of central spore and surrounding hyphae.

Antimicrobial	Concentration
Ceftazidime	128 µg/mL
Tobramycin	16 µg/mL
Amphotericin B	4 µg/mL
Vancomycin	10 µg/mL
Voriconazole	10 µg/mL

Table 13: Working concentrations of supplementary antimicrobials used in culture growth media

	Non-CF n/N (%)	CF n/N (%)
Pre-modification		
PNEC	2/3 (67)	8/17 (47)
PBEC	1/3 (33)	2/15 (13)
Post modification		
PNEC	8/17 (47)	5/12 (42)
PBEC	9/16 (56)	5/12 (42)

Table 14: Culture success rates after timepoint of PBEC cell culture substratum modification

Abbreviations: n: number of cultures; N: total number of cultures

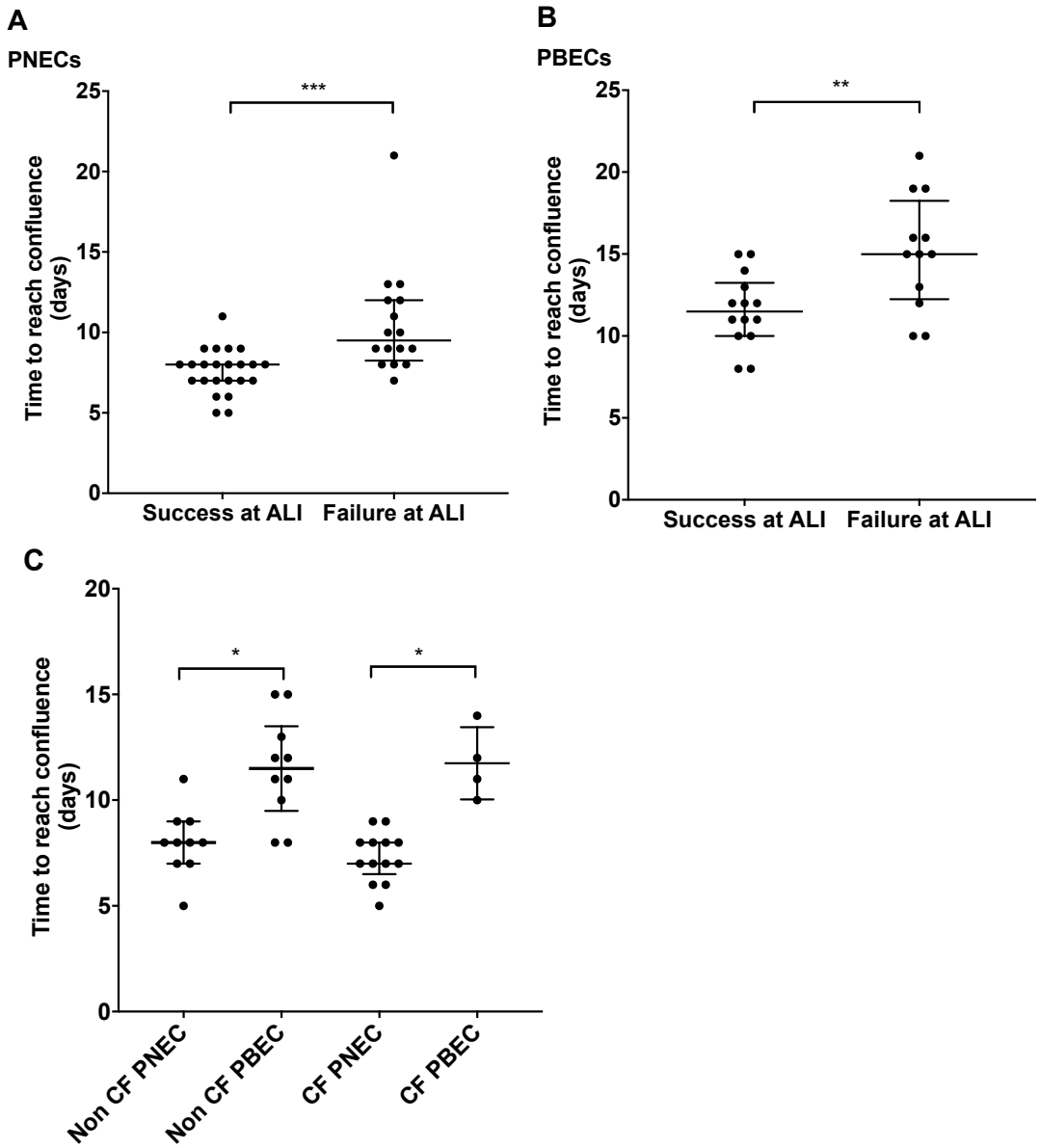

Figure 23: Time to reach confluence relative to culture success

Median time to achieve 80-90 % confluence was assessed in PNEC (A) and PBEC (B) submerged cultures in relation to ALI success. Data is presented as median ±IQR and analysed using the Mann-Whitney test; PNECs: p=0.0001; PBECs; p=0.0008); PNECs: n=23 successful; 16 unsuccessful; PBECs: n=14 successful, 12 unsuccessful. Median time was also assessed according to cell culture type in ALI cultures that were successful (C). Data is presented as median ±IQR and analysed using the Kruskall Wallis with Dunn's multiple comparison test; non-CF PNEC versus non-CF PBEC: p=0.03; CF PNECs versus CF PBECs: p=0.01; non-CF PNEC: n=10; non-CF PBEC: n=10; CF PNEC: n=13; CF PBEC: n=4.

3.6 Epithelial characteristics of differentiated paediatric primary nasal and bronchial epithelial cultures

3.6.1 Morphology

Immediately after brushing collection, clusters of epithelial cells were evident with active ciliary beating when viewed under phase contrast microscopy. Figure 24A demonstrates a representative image for a PNEC cell cluster the appearance of which was the same in harvested PBECs.

Culture morphology was assessed at regular intervals using phase contrast microscopy from submerged to ALI culture to monitor the epithelial appearance. After 2 days of submerged growth, cell attachment and growth of epithelial colonies were evident in both PBEC and PNEC cultures with similar epithelial morphology (Figure 24B and C). 80-90 % confluent submerged PBEC and PNEC cultures shared the characteristic ‘cobblestone’ appearance (Figure 25).

Assessment after 28d ALI revealed a tight epithelial monolayer that was ciliated and had evidence of mucus production at the culture surface (Figure 26).

Ultrastructural assessment of differentiated first passage PBECs and PNECs at 28d ALI culture was performed using TEM and confirmed the presence of a pseudostratified columnar epithelium comprising of ciliated, mucus-producing and basal cells (Figure 27).

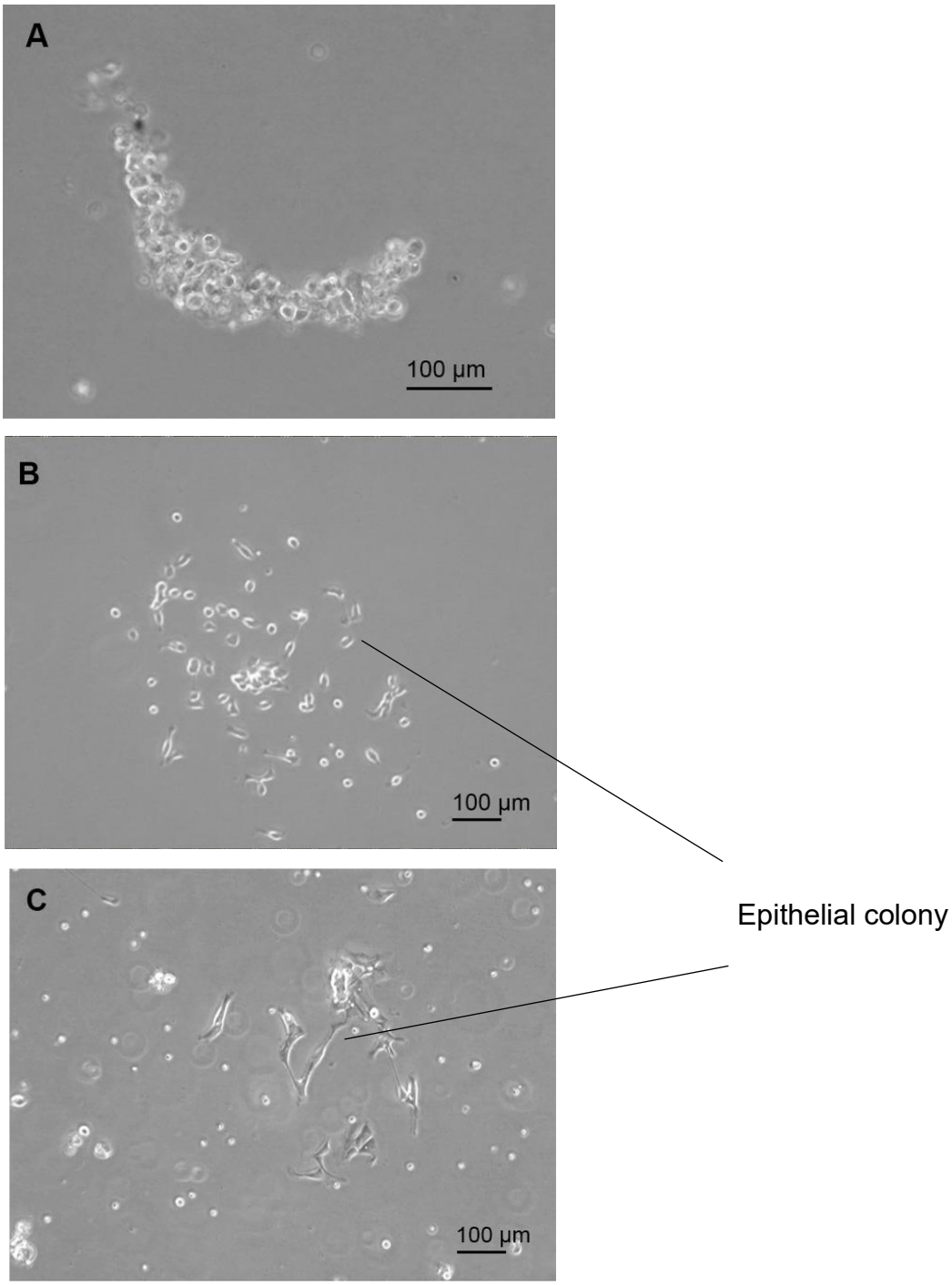

Figure 24: Phase contrast microscopy image of submerged epithelial cells immediately and 2 days after brushing

Representative image of epithelial cells after brushing collection is shown in A. Small colonies of nasal (B) and bronchial (C) epithelial cells are adherent to the collagen matrix and undergoing division and formation of epithelial colonies 2 days after brushing collection.

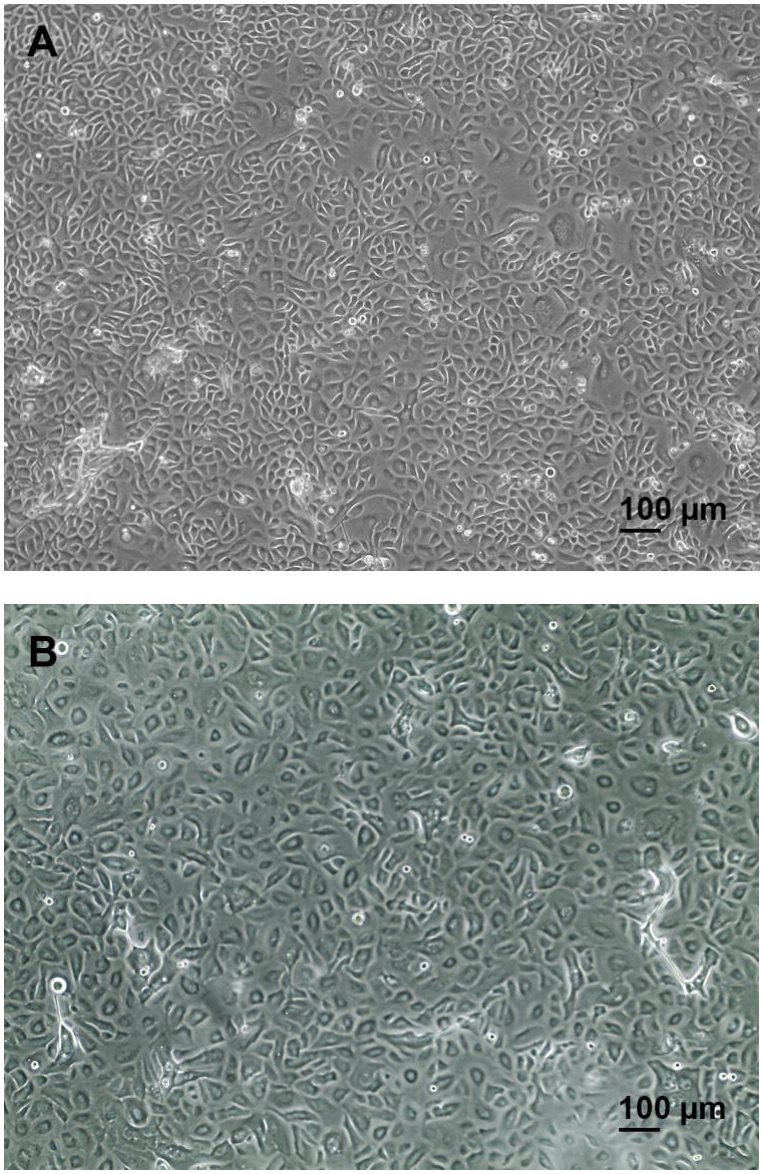

Figure 25: Morphology of confluent submerged airway epithelial cultures

Representative images of confluent submerged nasal (A) and bronchial (B) epithelial monolayers. Epithelial cells were grown to 80-90 % confluency before passage. At this stage, the epithelial cells demonstrated the typical “cobblestone” appearance.

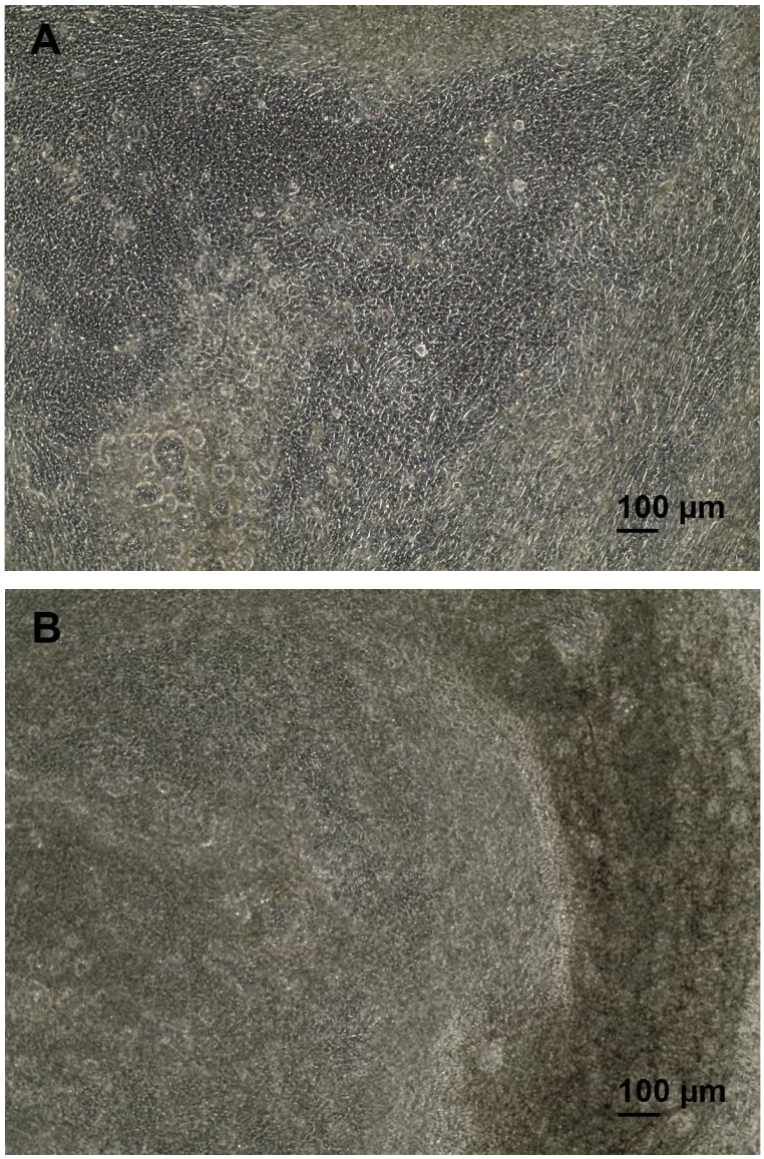

Figure 26: Representative phase contrast microscopy images of first passage PNEC and PBECs at 28d of ALI culture

Phase contrast images taken of Transwell inserts of PNEC (A) and PBECs (B) at 28d ALI to demonstrate the cellular morphology with tightly formed epithelial monolayers. There is a surface of mucus overlying the epithelia evident in both images and more prominent in the PBEC.

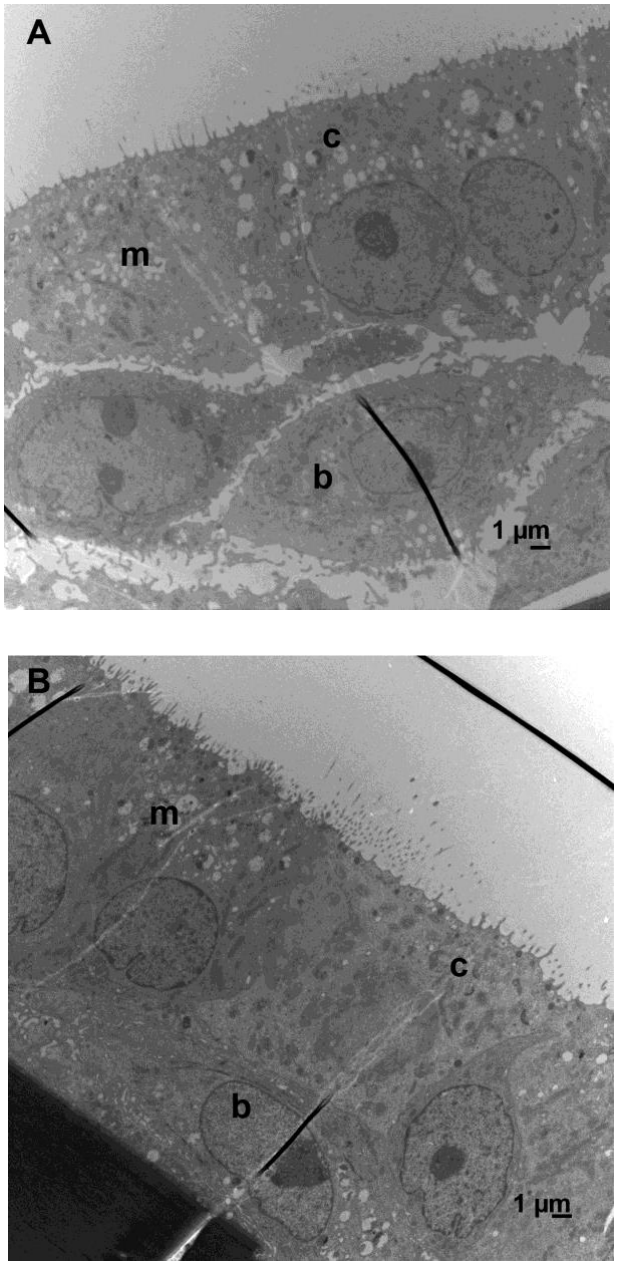

Figure 27: Assessment of epithelial differentiation of PNECs and PBECs using transmission electron microscopy

The images demonstrate the presence of ciliated (c), mucus producing (m) and basal (b) cells in differentiated PNEC (A) and PBEC (B) ALI cultures harvested from the non-CF PWT17 donor.

3.6.2 Haematoxylin and eosin staining

H&E tinctorial assessment of paraffin embedded sections of first passage PBEC and PNEC ALI cultures after 28d ALI demonstrated differentiated epithelial morphology (Figure 28).

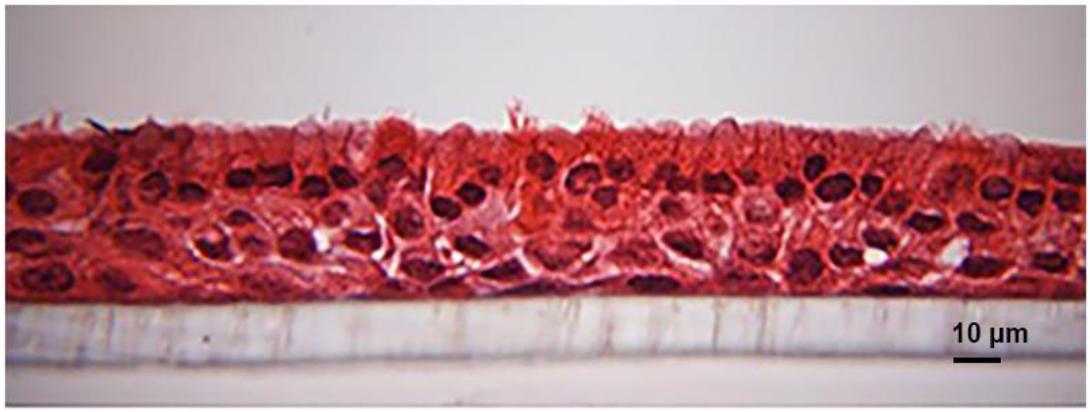

Figure 28: Haemaotoxylin and eosin tinctorial assessment of differentiated CF PNEC ALI culture

Paraffin-embedded PNEC culture sections at 28d ALI were stained with H&E to demonstrate epithelial morphology and differentiation.

3.6.3 Transepithelial electrical resistance measurement

TEER is the measurement of electrical resistance across a cellular monolayer and is a well-recognised technique to provide quantitative functional assessment of epithelial monolayer and tight junction integrity (Blume et al., 2010, Srinivasan et al., 2015). Tight junctions provide adhesive contact between neighbouring epithelia and regulate epithelial permeability and polarity (Hartsock and Nelson, 2008). In the context of this PhD, it was especially important to monitor TEER in ALI cultures designated for the subsequent profiling of ion transport and investigation of TMEM16A (as discussed later). In primary airway epithelia, a TEER close to 500 $\Omega.cm^2$ indicates suitability for *in vitro* assessment, however a lower limit of 150 $\Omega.cm^2$ has been acknowledged for application in Ussing chamber experiments (Lin et al., 2007, Fulcher et al., 2005). On review of the literature, practically cultures are deemed suitable for use at values above 300 - 400 $\Omega.cm^2$ (Guo-Parke et al., 2013, Tosoni et al., 2016).

TEER measurements of first passage PNEC and PBEC ALI cultures were made weekly (where possible) as previously described Chapter 2 section 2.3.1. All cultures demonstrated TEER increases over time, with peak values generally reached at 28d, (mean TEER of 459 – 1629 $\Omega.cm^2$). Significant changes were seen in all cultures at 28d compared with 21d ALI (Figure 29). PNEC cultures also showed significant differences at 21d. As shown in Figure 30, the overall mean TEER measurement was higher in CF PNECs and significantly greater at 21 and 28 d ALI than in CF PBECs (21d ALI: 1514 $\Omega.cm^2 \pm$ SD 698 versus 766 $\Omega.cm^2 \pm$ SD 221, p=0.02; 28d ALI: 1629 $\Omega.cm^2 \pm$ SD 674 versus 896 $\Omega.cm^2 \pm$ SD 294, p=0.02) and non-CF PNECs (21d ALI: 738 $\Omega.cm^2 \pm$ SD 9, p=0.005; 28d ALI: 848 $\Omega.cm^2 \pm$ SD 276, p=0.005).

Further comparisons were made between paired CF and non-CF cultures isolated from the same donor (Figure 31). In parallel with the grouped analysis, TEER in CF PNECs was significantly greater than the PBEC counterpart, but this significance was also apparent at 7 and 14d ALI. Furthermore, TEER was significantly greater in non-CF PNECs at all stages of ALI in comparison to their paired PBEC counterparts. The lack of significance in the grouped non-CF analysis may be attributable to the overall variability of TEER in these groups.

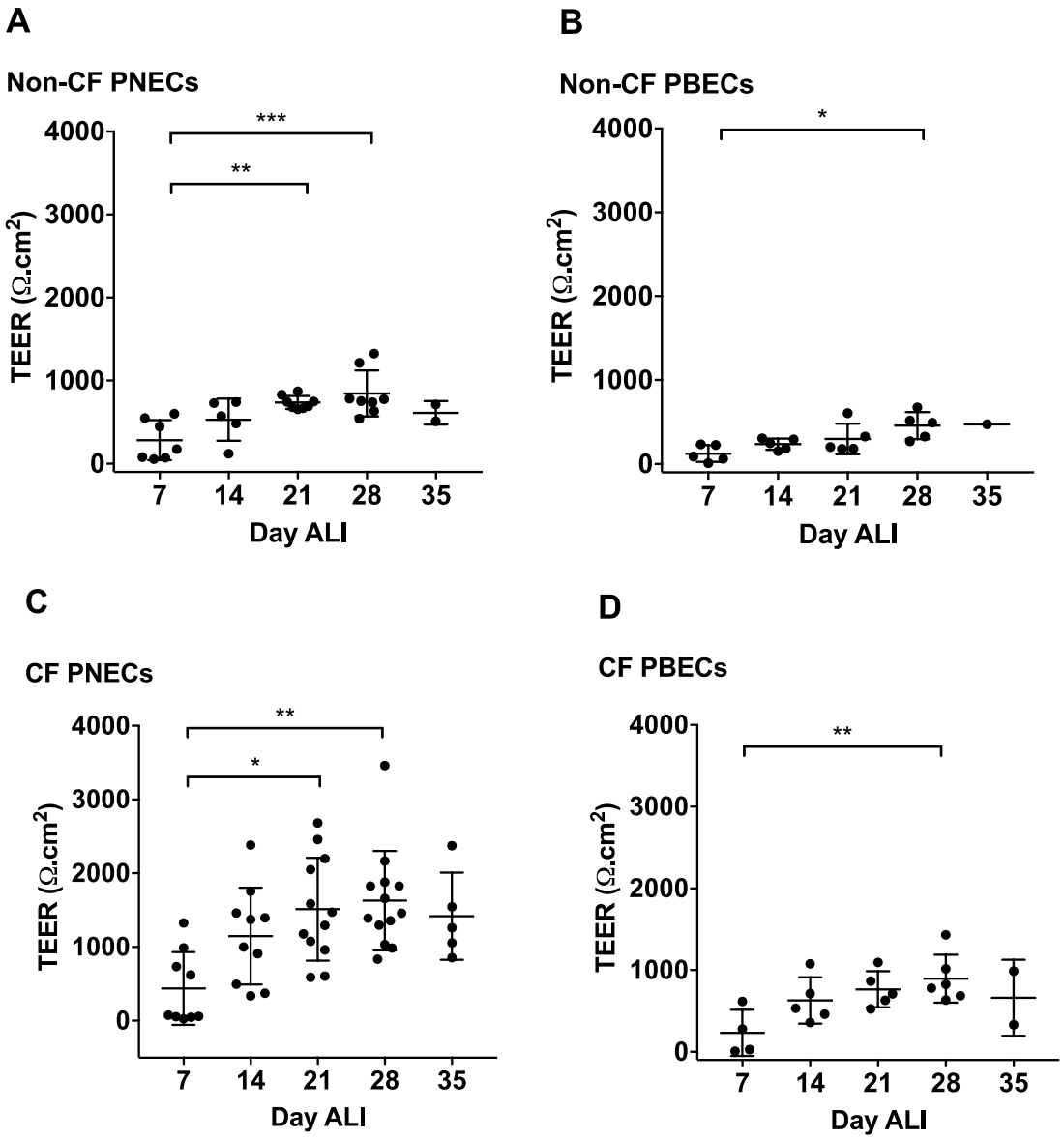

Figure 29: Transepithelial resistance measurement in differentiated paediatric PNEC and PBECs derived from non-CF and CF donors

Chopstick electrode measurements of transepithelial resistance (TEER) using an epithelial voltohmmeter (WPI) in first passage ALI non-CF PNECs (A), non-CF PBECs (B), CF PNECs (C) and non-CF PBECs (D). Each point represents the mean TEER reading for each culture. Data is presented as mean ± SD and analysed with one-way ANOVA with post hoc Bonferroni's multiple comparison test, non-CF PNEC: 7d v 21d p=0.004, 7d v 28d p=0.0005; non-CF PBEC: 7d v 28d p=0.01; CF PNEC: 7d v 21d p=0.004, 7d v 28d p=0.001; CF PBEC: 7d v 28d p=0.02. The range of n numbers at each timepoint are as follows: non-CF PNECs: 2-8; non-CF PBECs: 1-5; CF PNECs: 5-13; CF PBECs: 2-6.

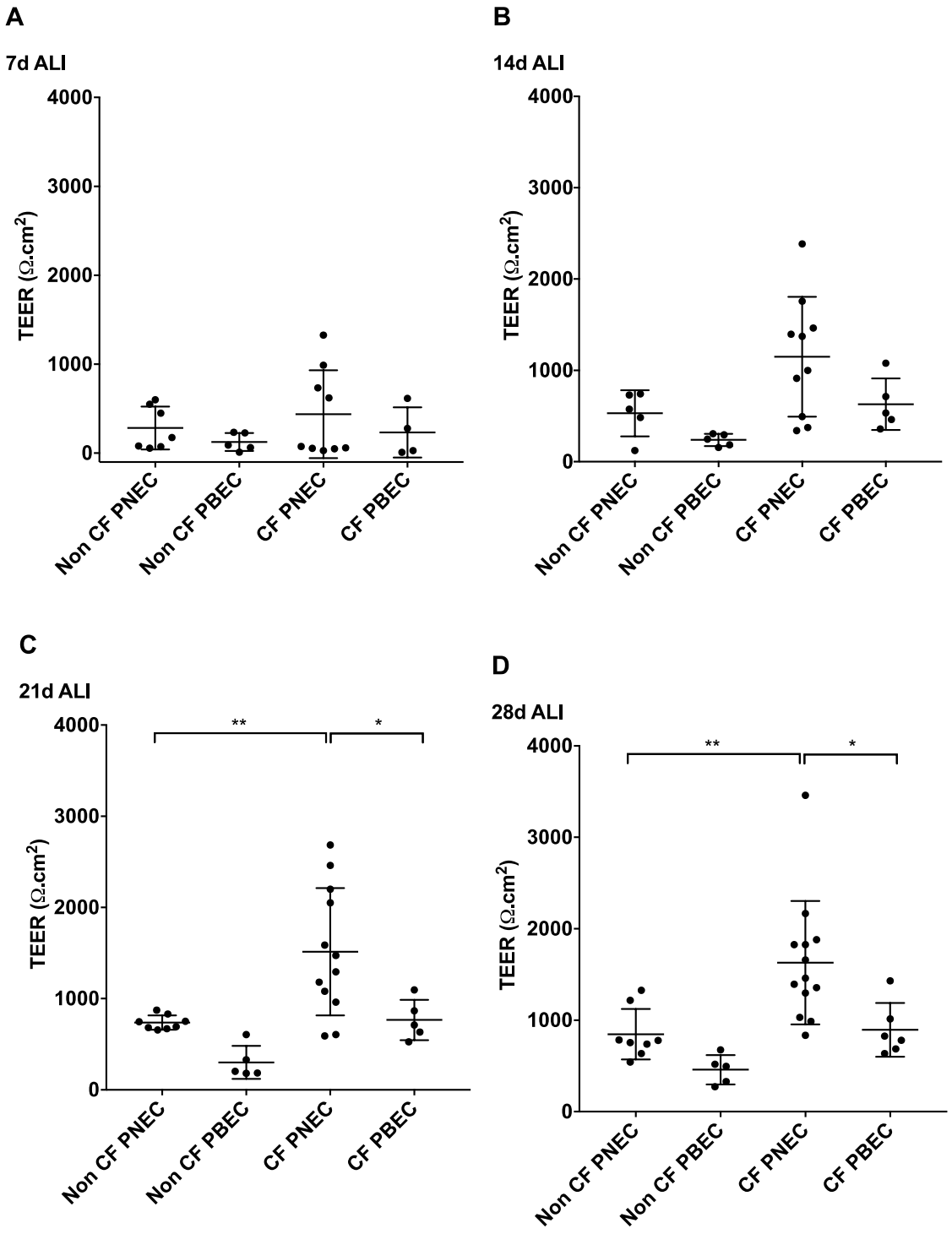

Figure 30: Comparison of transepithelial resistance measurements

Comparisons of TEER measurements were made at 7d (A), 14d (B), 21d (C) and 28d (D) ALI. Each point represents the mean TEER reading for each culture. Data is presented as mean ±S.D and analysed using one-way ANOVA with post hoc Bonferroni's multiple comparison test; * p=0.02, ** p=0.005 for C and D.

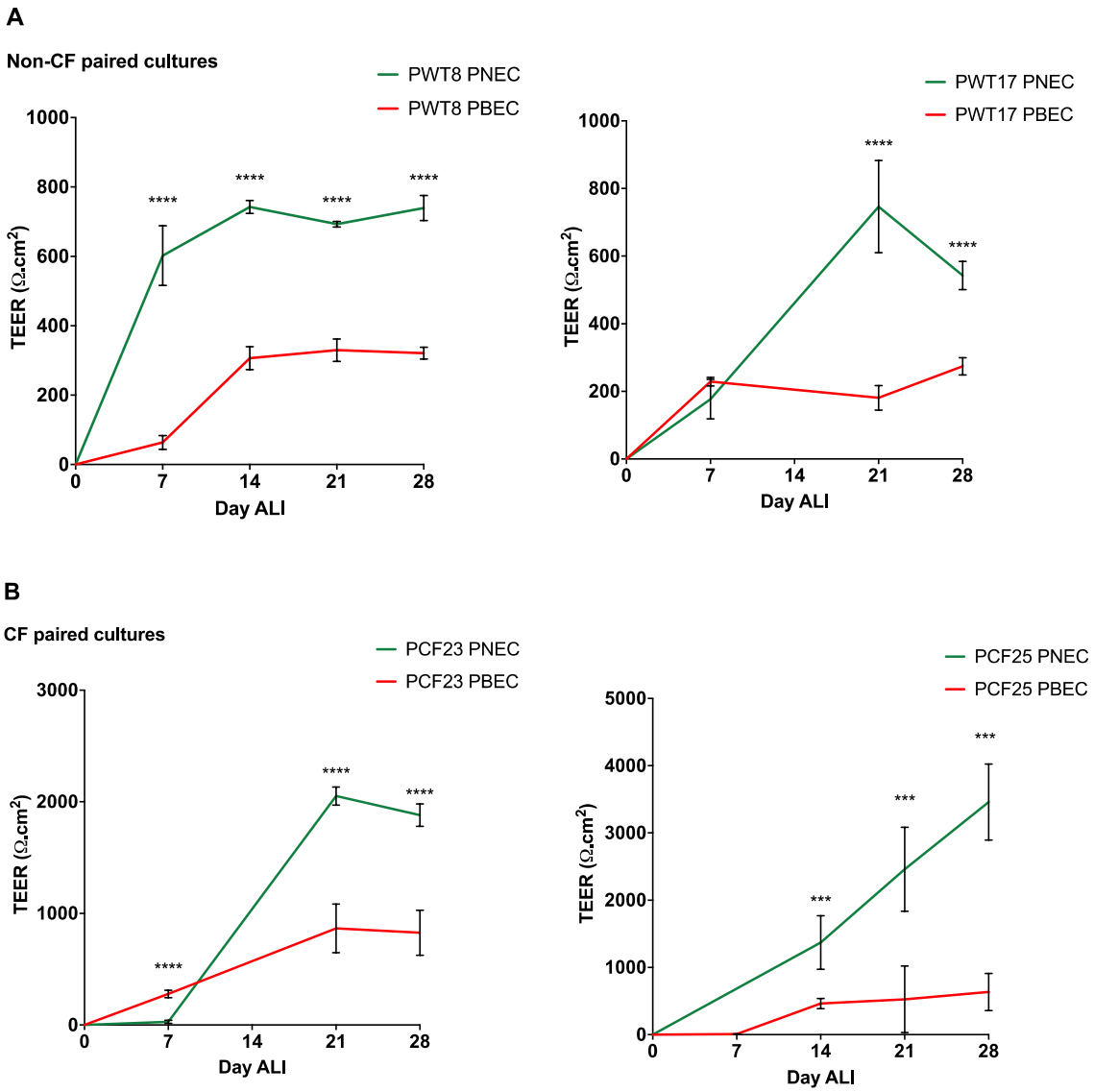

Figure 31: Transepithelial resistance assessment in paired PNEC and PBEC cultures

Weekly transepithelial resistance (TEER) measurements were compared in paired non-CF (A) and CF (B) PNECs and PBECs. Lines represent the mean TEER ± SD. Data analysed using unpaired t-test; ***p<0.001, ****p<0.0001.

3.6.4 Tight junctional proteins

Tight junctions are comprised of transmembrane occludin and claudin proteins, and cytoplasmic scaffolding proteins such as ZO-1, which provide connections between transmembrane and cytoplasmic proteins (Hartsock and Nelson, 2008). To further investigate the localisation of tight junctions in first passage ALI cultures, the presence of ZO-1 was investigated by immunofluorescence as demonstrated in Figure 32. Further evidence of tight junctional formation was confirmed by SEM as shown in Figure 33.

E-cadherin, a member of the cadherin transmembrane protein family, is required for the initiation and assembly of tight junction formation (Contreras et al., 2002). Tight junctional composition is regulated by the epithelial cell adhesion molecule (EpCAM) through its effects on claudin intra-cellular localisation and degradation (Wu et al., 2013). To determine variations in epithelial integrity between CF and non-CF nasal and bronchial cultures, mRNA expression profiles for *CDH1*, the gene encoding E-cadherin, *ZO-1* and *EpCAM* were investigated in first passage cultures at 28d ALI using RT-qPCR. Calculated $2^{-\Delta CT}$ values were used to represent the relative fold change of gene expression for each group assessed as shown in Figure 34. No differences with *ZO-1* and *CDH1* expression were found in all 4 groups.

EpCAM expression was increased in PBECs versus PNECs in both non-CF (7.4-fold) and CF groups (3.6-fold). Furthermore, *EpCAM* expression was increased by 12.6-fold in CF PBECs versus non-CF PBECs and by 8.4-fold in CF PNECs versus non-CF PNECs. However, no statistically significant differences were found between $2^{-\Delta CT}$ values for each group (Figure 35).

These results suggest that no differences in *ZO-1* and *CDH1* expression were evident at the mRNA level, between both non-CF and CF nasal and bronchial cultures. *EpCAM* expression was upregulated in PBECs versus PNECs in each disease group, but these changes were not significant. There was no correlation of gene expression with TEER (Figure 36), suggesting that they were not contributory to TEER variations evident in the cultures.

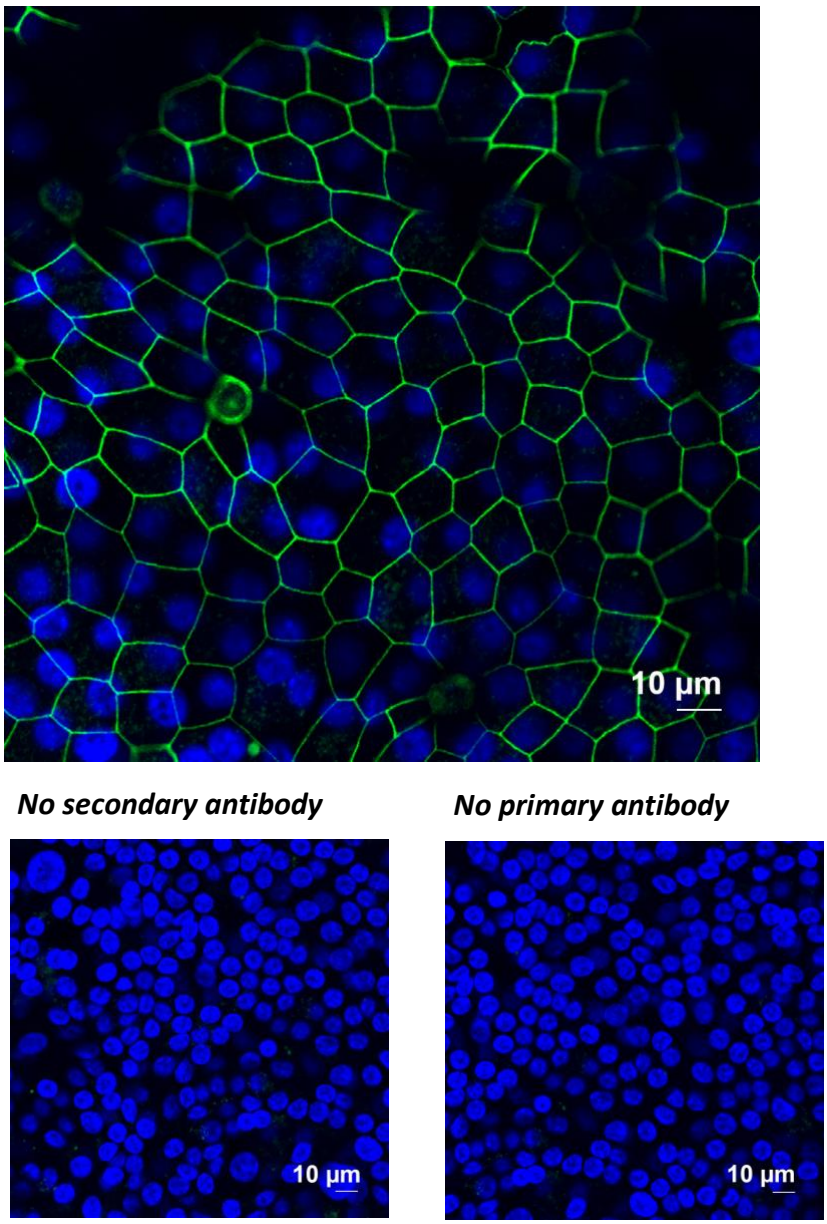

Figure 32: Assessment of ZO-1 by immunofluorescence in a PBEC derived from a CF donor at 28d of ALI culture

PBEC cultures derived from the CF PCF22 donor were fixed in 4 % PFA and assessed for ZO-1 (green) using immunofluorescence; nuclei stained with DAPI (blue). Images below show no secondary and no primary antibody controls.

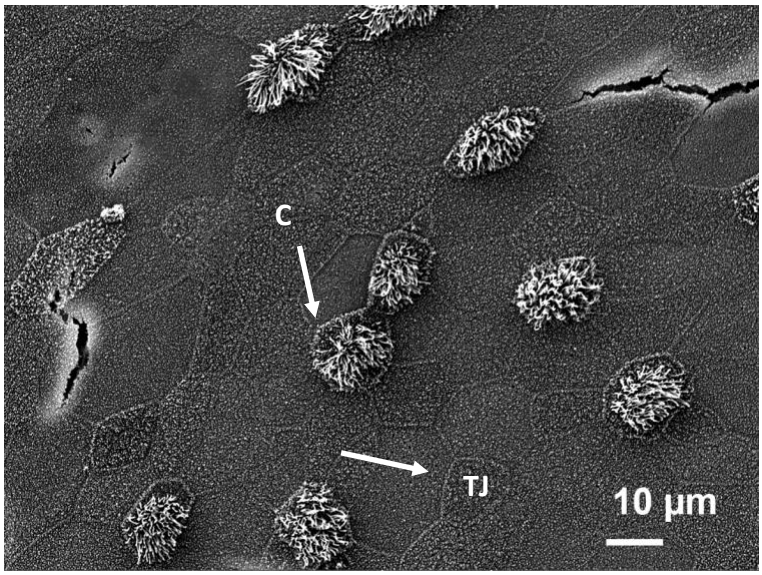

Figure 33: Tight junctions demonstrated by scanning electron microscopy

Scanning electron microscopy (SEM) image taken of a PNEC ALI culture derived from the non-CF PWT1 donor demonstrating location of tight junctions (TJ) and cilia (c).

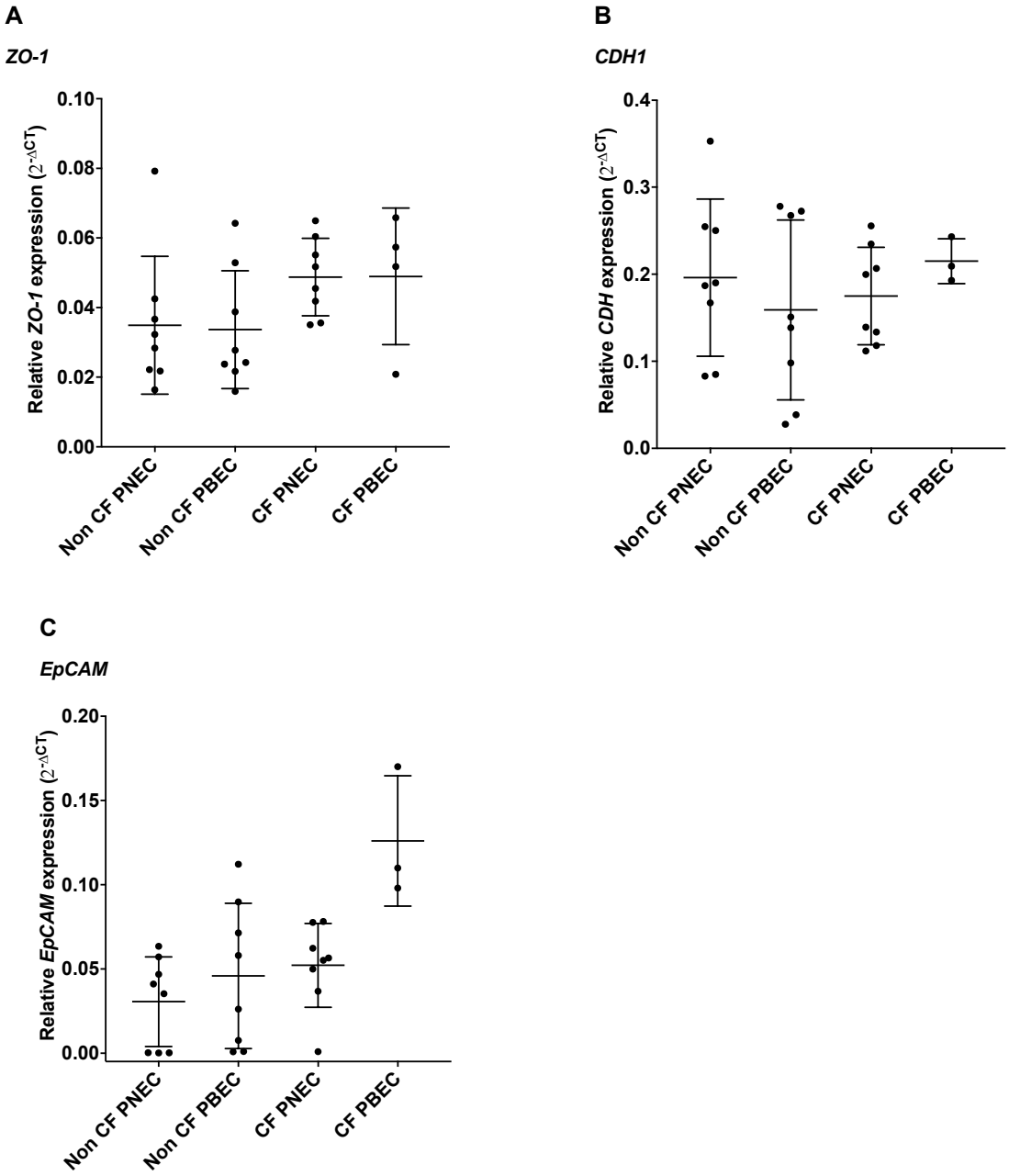

Figure 34: Relative gene expression of *ZO-1, CDH1* and *EpCAM* in first passage PNEC and PBEC ALI cultures

ZO-1 (A), *CDH* (B) and *EpCAM* (C) expression were assessed in differentiated cultures at 28d ALI using RT-qPCR. $2^{-\Delta CT}$ values were calculated to determine relative gene expression and complement data for relative fold change. Data is displayed as the median ±IQR and analysed with Kruskal-Wallis and post hoc Dunn's multiple comparison test with no statistical differences found; non-CF PNECs (n=8), non-CF PBECs (n=8); CF PNECs (n=8), CF PBECs (n=4 for *ZO-1*; n=3 for *CDH1* and *EpCAM*).

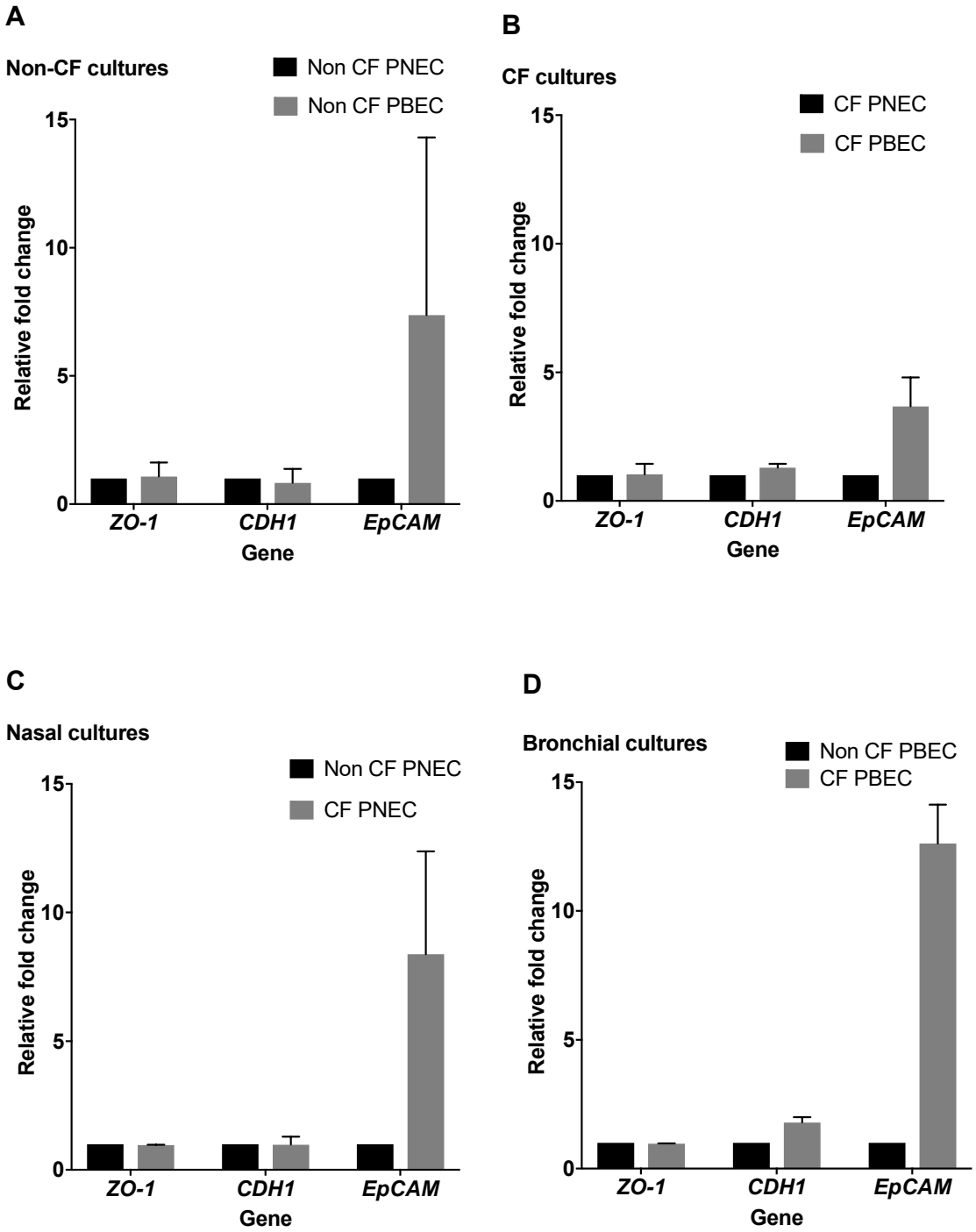

Figure 35: Relative fold change of *ZO-1*, *CDH1* and *EpCAM* in first passage PBEC and PNEC ALI cultures

Relative fold changes of *ZO-1, CDH1* and *EpCAM* were assessed in non-CF cultures (A), CF cultures (B), nasal cultures (C) and bronchial cultures (D) as assessed by RT-qPCR; non-CF PNECs (n=8), non-CF PBECs (n=8); CF PNECs (n=8), CF PBECs (n=4).

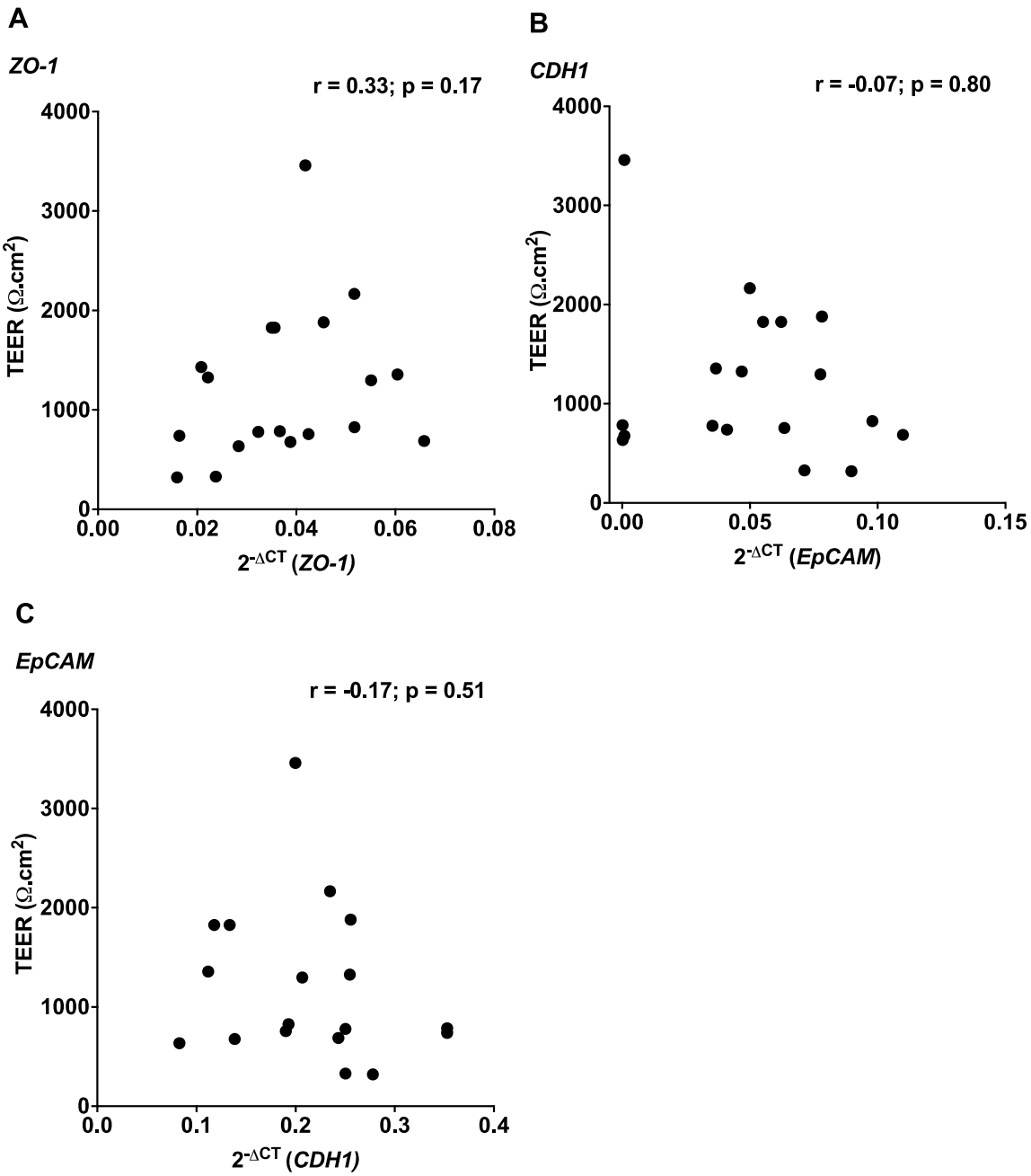

Figure 36: Correlation of tight junctional gene expression with transepithelial resistance in differentiated PNEC and PBEC ALI cultures

Spearman correlation analysis was performed for *ZO-1* (A), *CDH1* (B) and *EpCAM* (C) expression measured by $2^{-\Delta CT}$ with corresponding transepithelial (TEER) measurements of each culture taken at 28d ALI. Each point represents values for cultures derived from an individual donor. The correlation coefficient (r) was calculated whereby r of 1 indicated perfect correlation, 0 is no correlation and -1.0 refers to perfect inverse correlation; corresponding p values are shown; n=19.

3.6.5 The cilial phenotype

ALI cultures were monitored regularly for the presence of motile cilia by phase contrast microscopy. This occurred significantly earlier in PBECs than in PNECs as demonstrated in Figure 37 (mean 18d; ± SD 1.8 versus 23d ± SD 3.3, p=0.005).

Ciliated epithelia were confirmed in PFA-fixed ALI cultures by immunofluorescence assessment of α-acetylated tubulin after 28 days of ALI culture. α-tubulin is a major structural component of microtubules and its acetylation is required for microtubule stability (Rymut et al., 2013). Motile cilia express α-acetylated tubulin, which is widely used as a marker for cilial assessment in airway epithelial cultures (Jain et al., 2010, Rymut et al., 2013) . The representative image of immunofluorescent staining in a non-CF PBEC ALI culture shown in Figure 38 shows evidence of cilia in the apical aspect of the differentiated culture in 52 % of surface epithelial cells.

Cilia are typically membrane bound and contain the axoneme which forms the microtubule cytoskeleton (Satir and Christensen, 2007). Axonemes of multi-ciliated epithelial cells contain dynein arms whereby nine doublet microtubules surround a central pair of microtubules, known as the “9 + 2” dynein formation (Satir and Christensen, 2007). SEM and TEM images taken from ALI cultures demonstrate this dynein formation, providing further evidence for successful differentiation (Figure 39).

Comparative assessment of relevant cilial gene expression was performed using RT-qPCR of mRNA isolated from a cohort of differentiated PNECs and PBEC ALI cultures harvested from CF and non-CF donors at 28d ALI. Cilia are generally classified into two groups; primary cilia, which are solitary and non-motile, and motile cilia, which occur in clusters of 100 to 300 on the surface of apical epithelia (Jain et al., 2010). The cilial type changes with differentiation of ALI cultures with an abundance of primary cilia during early stages of ALI compared with a shift to a predominance of motile cilia in differentiated epithelia (Jain et al., 2010). Expression of *TUBA1A*, which encodes α-acetylated tubulin, was assessed to compliment the above immunofluorescence work. Expression of *Foxj1*, which encodes a transcription factor essential for motile ciliated cell differentiation, was also investigated in the same cohort of ALI cultures (Yu et al., 2008).

Comparative analysis of gene expression in PNECs and PBECs was performed to ascertain differences in relation to the nasal and bronchial airway epithelium. Despite the upregulation of *TUBA1A* expression by 6.6-fold and 4.1-fold in CF PBECs compared with CF PNECs and non-CF PBECs respectively, there was no significant increase in the corresponding $2^{-\Delta CT}$ analysis of relative gene expression (Figure 40 and Figure 41). There was a 5-fold upregulation in *TUBA1A* in non-CF PBECs versus their PNEC counterparts, but this was not accompanied by a significant increase in the corresponding $2^{-\Delta CT}$ analysis of relative gene expression. *Foxj1* expression was increased in non-CF and CF PBECs of 19.8 and 25.3 times respectively versus their nasal counterparts. This was accompanied with a significant increase in $2^{-\Delta CT}$ in CF PBECs versus CF PNECs (median 0.216 ±IQR 0.19-0.25 versus 0.013 ±IQR 0.002-0.05, p=0.05) and non-CF PNECs (0.003 ±IQR 0.001-0.01, p=0.006). Interestingly, there was a suggestion of *Foxj1* upregulation in non-CF versus CF cultures in both nasal (5.8-fold) and bronchial (12.8-fold) groups, but these were not significant. These results suggest a predominance for *Foxj1* expression in PBECs. Given the role of *Foxj1* for motile cilia development, this finding may reflect anatomical variations in cilial phenotypes and role in mucociliary clearance in the bronchial epithelium.

No significant differences were found in *TUBA1A* expression in CF cultures compared with non-CF cultures. Interestingly *Foxj1* was upregulated in CF PBECs compared with all PNECs.

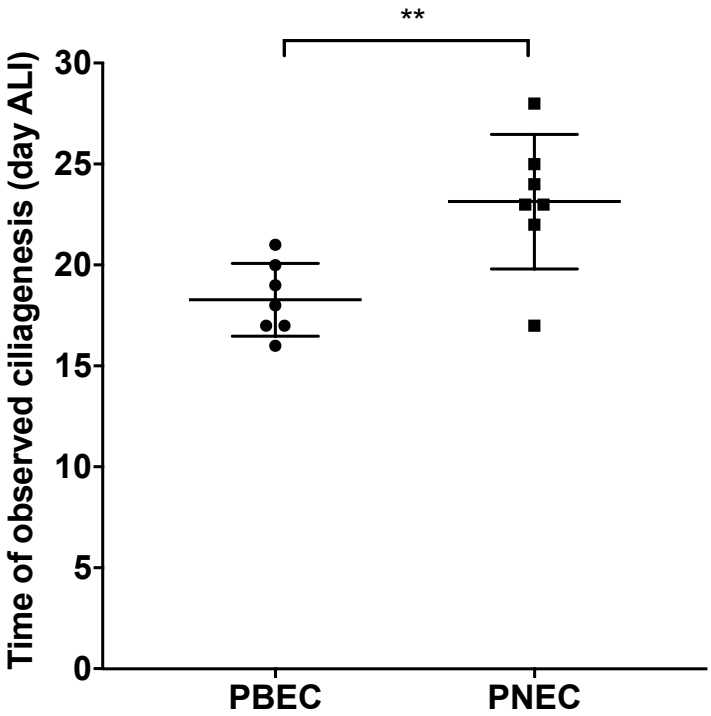

Figure 37: Observed time for motile cilia in differentiated PNEC and PBEC ALI cultures

Differentiated PNEC and PBEC ALI cultures were monitored daily for the detection of motile cilia with phase contrast microscopy. This occurred significantly earlier in non-CF PBECs versus PNECs. Each point represents cultures derived from an individual donor. Data is presented as mean ± SD and analysed using the unpaired t test; **p<0.01, n=7 for each culture type.

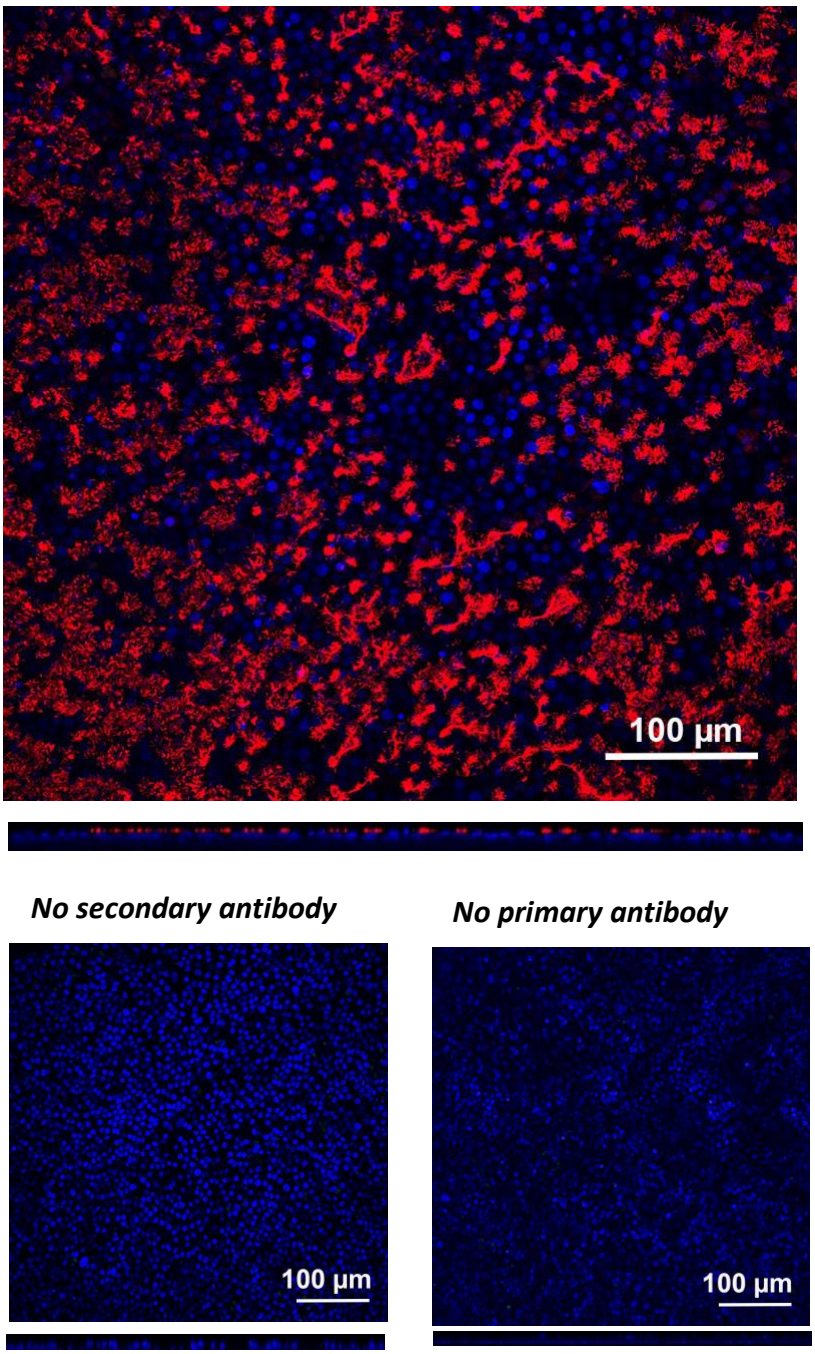

Figure 38: Immunofluorescent detection of α-acetylated tubulin in non-CF PBEC ALI culture

Representative image of a PBEC derived from a non-CF donor that was fixed in 4 % PFA after 28d ALI and assessed for α-acetylated tubulin (red) presence at the apical surface of epithelial cells. Nuclei are stained with DAPI (blue). The lower images represent no secondary and no primary antibody controls.

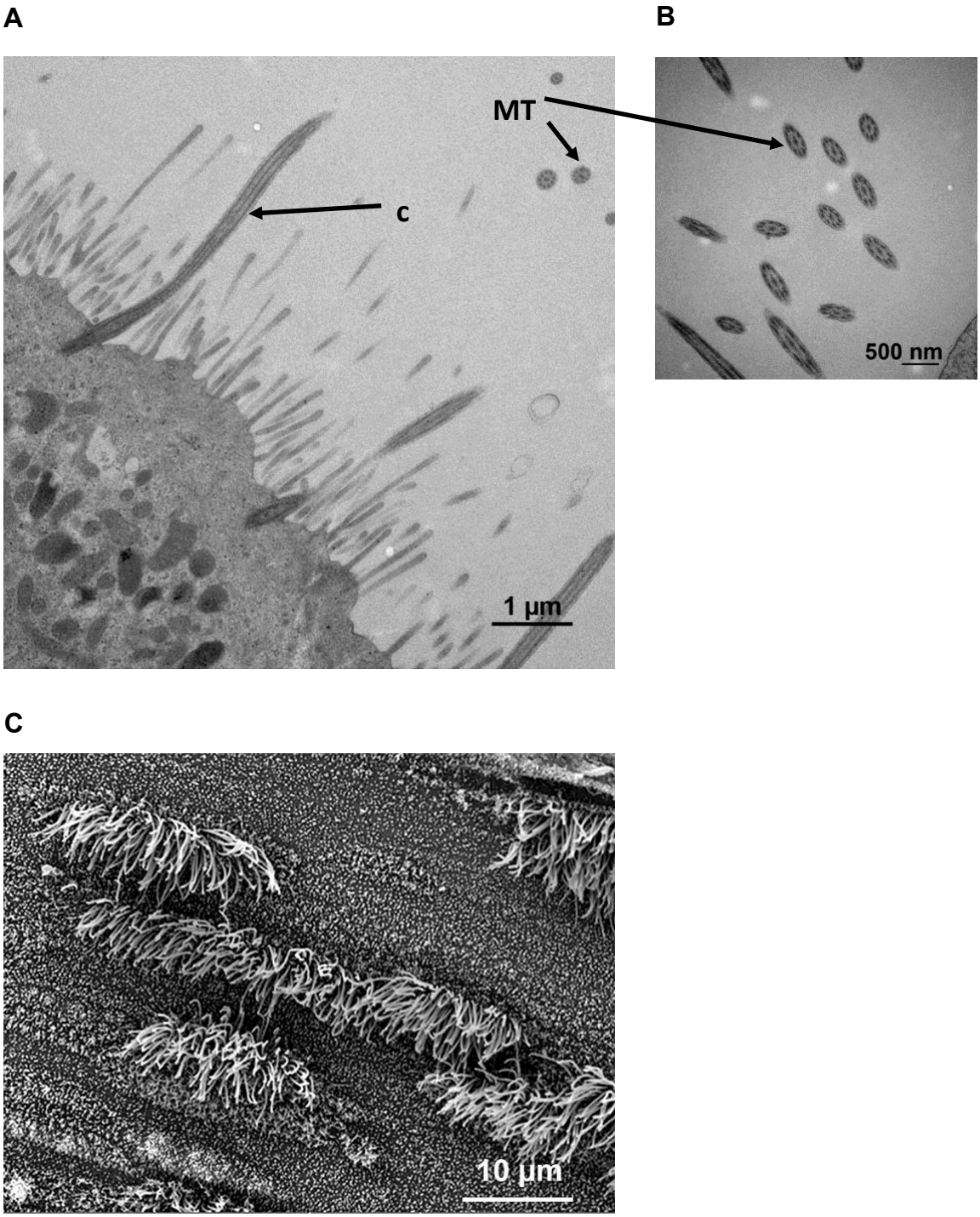

Figure 39: Assessment of cilia ultra-structure in PNEC cultures using electron microscopy

Transmission (A and B) and scanning (C) electron microscopy images demonstrate the presence of cilia (c) and structure at the apical surface of differentiated cultures at 28d ALI. There is evidence of the characteristic dynein microtubule (MT) formation as demonstrated in A and B.

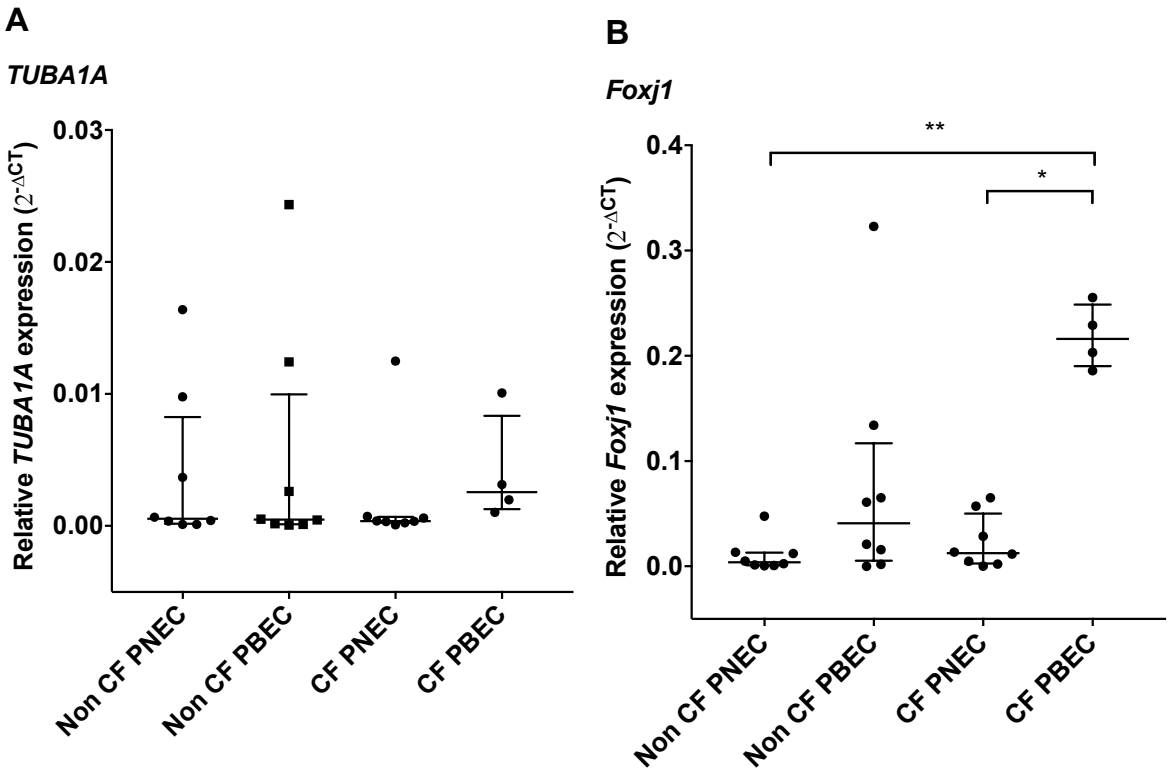

Figure 40: Relative gene expression of *TUBA1A* and *Foxj1* in PNEC and PBEC ALI cultures

TUBA1A (A) and *Foxj1* (B) expression were assessed in differentiated cultures at 28d ALI using RT-qPCR. $2^{-\Delta CT}$ values were calculated to determine relative gene expression and complement the data for relative fold change and provide statistical comparisons. Each point represents cultures derived from individual donors. Data is displayed as the median ±IQR and analysed with Kruskal-Wallis with post hoc Dunn's multiple comparison test; **p=0.005, *p=0.05; non-CF PNECs (n=8), non-CF PBECs (n=8); CF PNECs (n=8), CF PBECs (n=4).

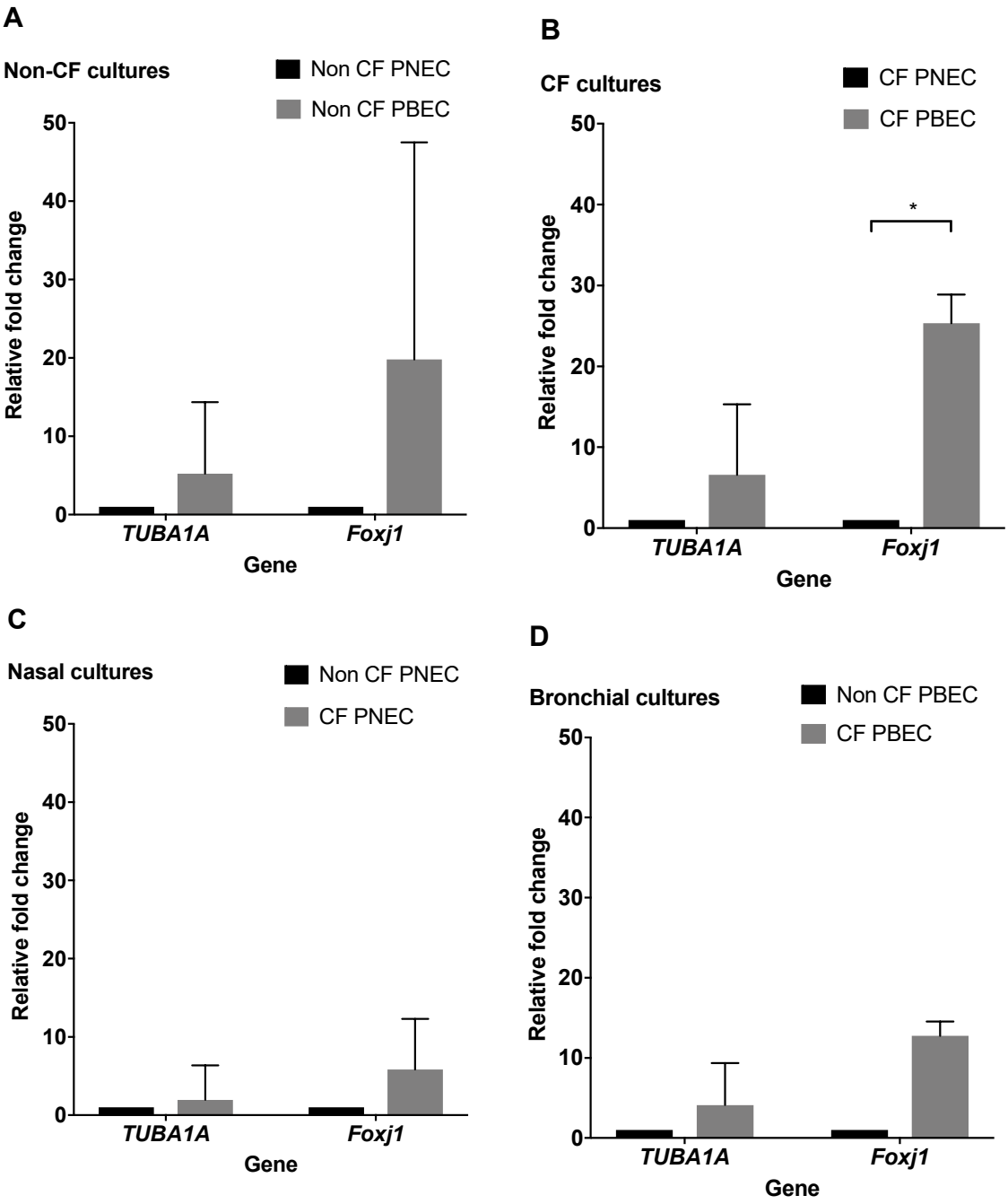

Figure 41: Relative fold change of *TUBA1A* and *Foxj1* in PNEC and PBEC ALI cultures

Relative fold changes of *TUBA1A* and *Foxj1* expression were compared in non-CF cultures (A), CF cultures (B), nasal cultures (C) and bronchial cultures (D) as assessed by RT-qPCR; non-CF PNECs (n=8), non-CF PBECs (n=8); CF PNECs (n=8), CF PBECs (n=4); *p=0.05 (refers to the corresponding $2^{-\Delta CT}$ analysis in Figure 40).

3.6.6 The mucus phenotype

It was possible to visualise mucus production on the surface of ALI cultures with the naked eye and on phase contrast microscopy (Figure 42A). To further confirm this, first passage ALI cultures were stained with Periodic acid-Schiff's stain to demonstrate the presence of glycoproteins and with the addition of Alcian Blue to confirm this as acidic mucin glycoproteins (Figure 42B and C).

MUC5AC and MUC5B are the predominant gel-forming mucins secreted in airway epithelial cells. Concentration of MUC5AC in apical washings harvested from differentiated ALI cultures at 28d ALI was investigated by indirect ELISA (Figure 43).

Final concentrations were corrected for the dilutional factor taking into account the predicted volume of the ASL (10 μL) relative to the volume used for apical washing (Harvey et al., 2011). Concentrations were lowest in non-CF PNECs (median 65.1 μg/mL, IQR 46.5 to 93.7) and although higher concentrations were evident in non-CF PBECs (165.9 μg/mL, IQR 127.4 to 172.3), this difference was not significant (p=0.23). The highest median concentration of MUC5AC was evident in CF PBECs (343.2 μg/mL, IQR 236.5 to 368.2), which was significantly greater than the concentration in CF PNECs (68.3 μg/mL, IQR 38.8 to 148.8, p=0.03). Comparisons in paired PBEC and PNECs isolated from the same donors suggested higher MUC5AC concentrations in PBECs in both CF and non-CF cultures (non-CF PBEC: 155.2 ±24.3 versus non-CF PNEC: 46.0 μg/mL ± SD 12.1; CF PBEC 343.2 ± SD 15.4 versus CF PNEC: 90.9 ± SD 75.4), however statistical analyses were not possible due to the low donor numbers (Figure 43).

MUC5AC and *MUC5B* mRNA expression was also assessed in ALI cultures using RT-qPCR (Figure 44). No significant differences were found with either *MUC5AC* or *MUC5B* expression in CF and non-CF cultures in both PBECs and PNECs.

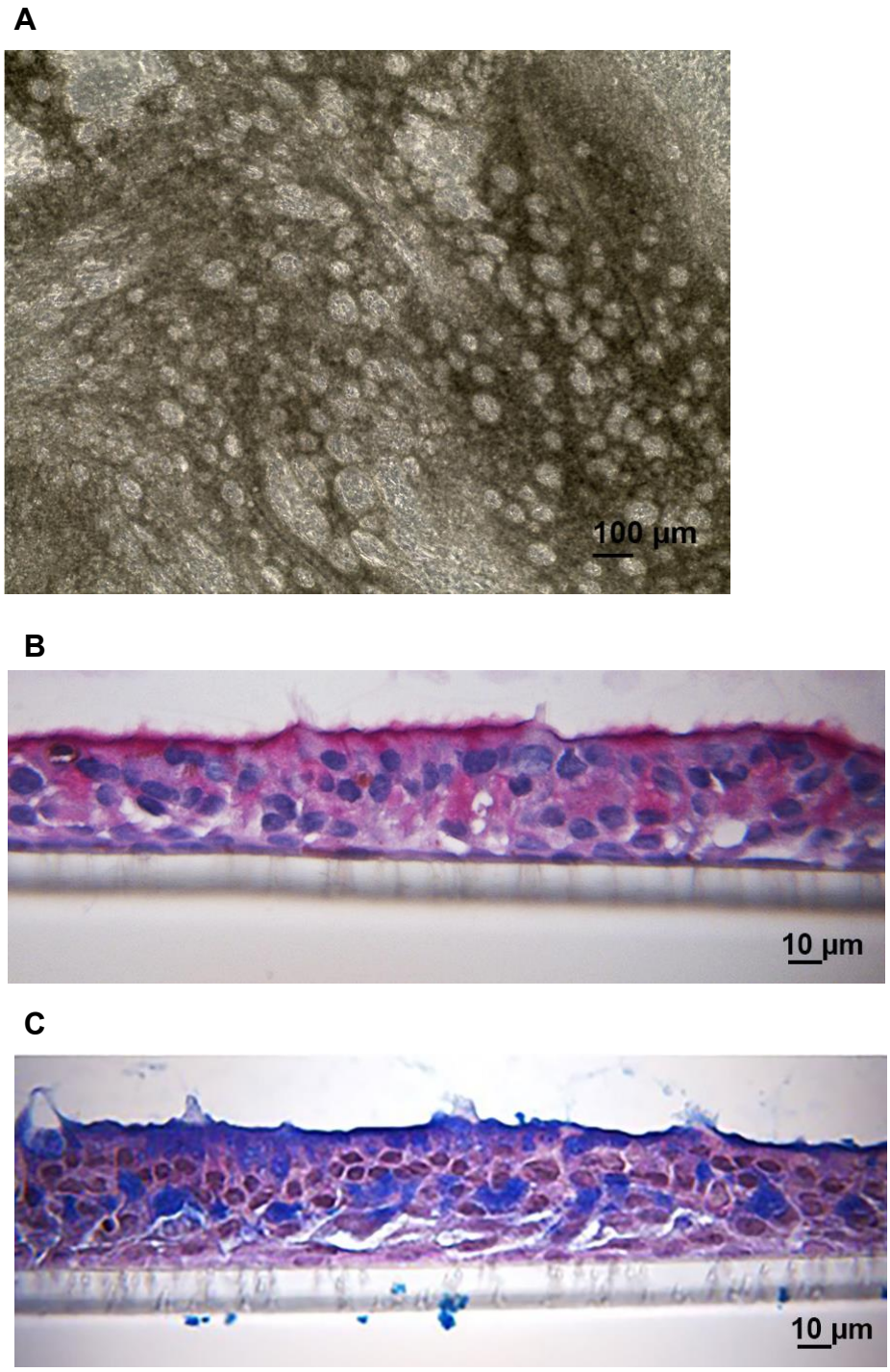

Figure 42: Mucus production by differentiated ALI cultures

Phase contrast appearance of ALI cultures (A) with secretory droplets and mucus material overlying the surface of the epithelial monolayer. Paraffin-embedded ALI sections were stained with Periodic-acid Schiff's (PAS) reagent (B) to demonstrate glycoprotein presence as shown by the magenta staining localised to the apical epithelium and mucus secreting cells. PAS staining with Alcian Blue (C) confirmed the presence of acidic mucin glycoproteins as shown by the blue staining.

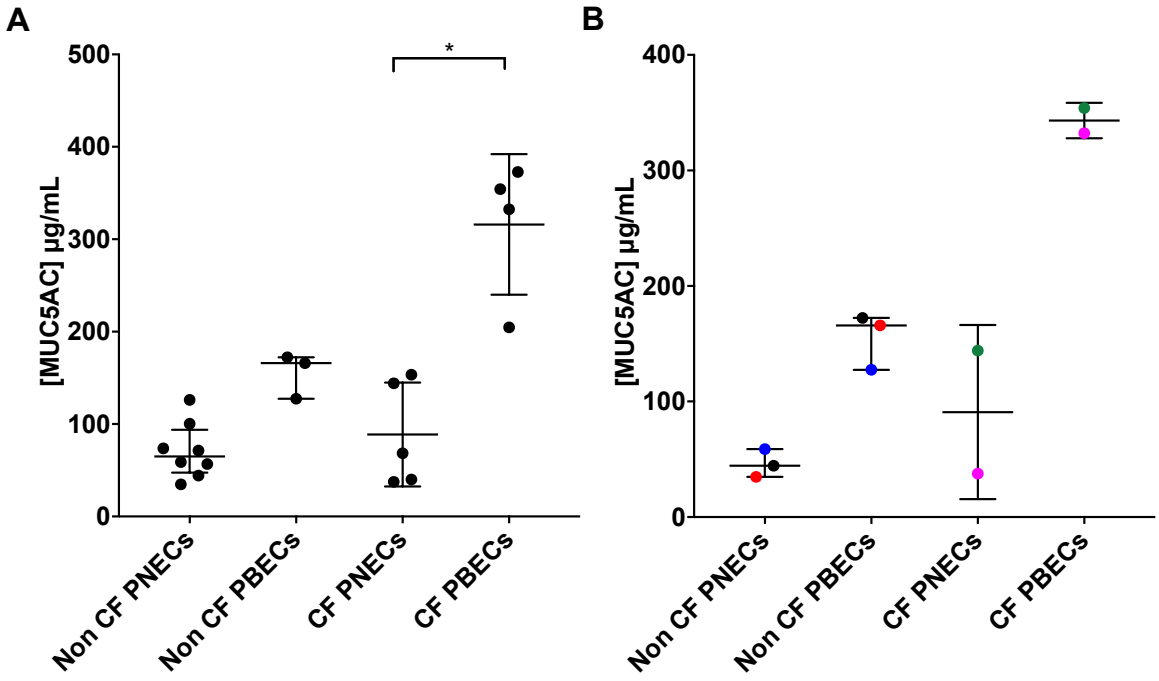

Figure 43: Concentration of MUC5AC in PNEC and PBEC ALI cultures

An indirect ELISA was performed to compare the concentration of MUC5AC in apical washings harvested from first passage ALI cultures at 28d ALI (A). Data is presented as mean ±S.D. and analysed using Kruskal-Wallis and Dunn's multiple comparison test; *p=0.03; non-CF PNECs n=8, non-CF PBECs n=3, CF PNECs n=5, CF PBECs n=4. Measurement of MUC5AC concentration in paired PBECs and PNECs isolated from the same donor, which are colour matched (B); n=3 non-CF donors, n=2 CF donors (statistical analysis not performed).

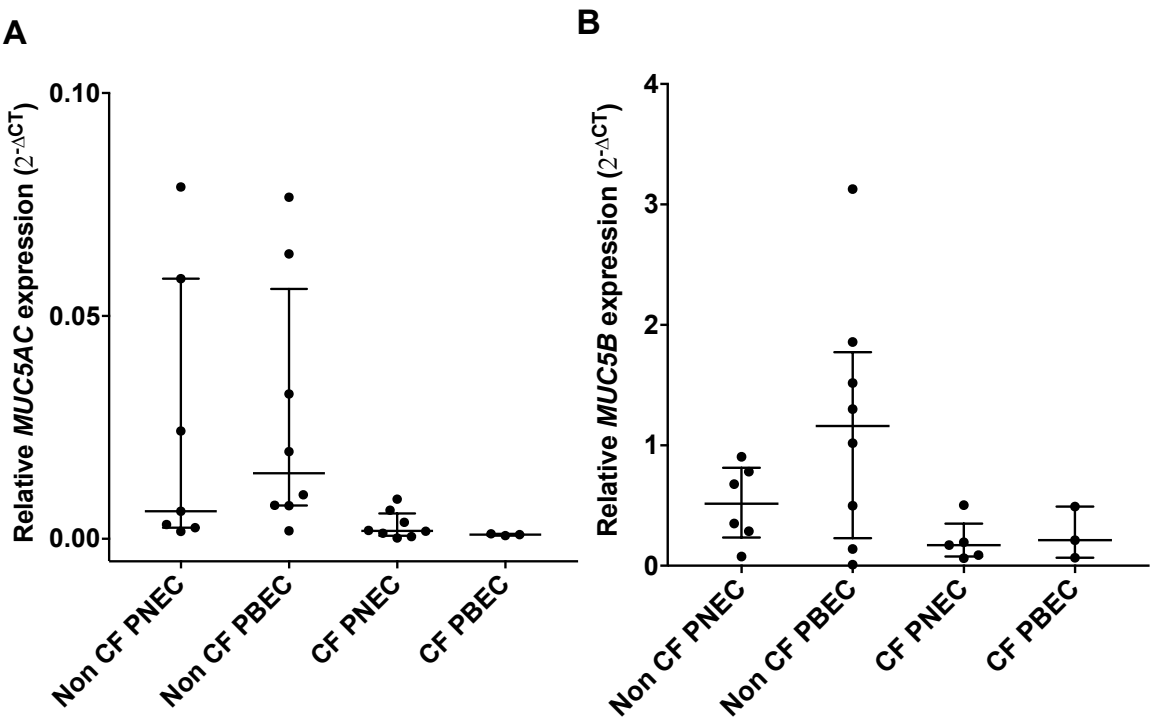

Figure 44: Relative gene expression of *MUC5AC* and *MUC5B* in PBEC and PNEC ALI cultures

MUC5AC (A) and *MUC5B* (B) expression were assessed in differentiated cultures at 28d ALI using RT-qPCR. $2^{-\Delta CT}$ values were calculated to determine relative changes in gene expression. Data is displayed as the median ±IQR. and analysed with Kruskall Wallis and Dunn's multiple comparison test with no statistical differences found; non-CF PNECs (n=7), non-CF PBECs (n=8); CF PNECs (n=8), CF PBECs (n=3).

3.6.7 The nasal and bronchial airway inflammatory profile

The airway inflammatory environment of children with CF is abnormal with increasing levels of IL-8 found previously in infants and inflammation recognised to occur early in life (Khan et al., 1995a, Pillarisetti et al., 2011). Other cytokines including IL-17A, IL-6 and IL-4 have been elevated in BAL and serum isolated from CF patients (Tan et al., 2011, Nixon et al., 1998, Bergin et al., 2013).

In this study, BAL samples were obtained from 16 non-CF and 12 CF participants. Of all 28 samples, 59 % BALs were obtained from the right middle lobe, 26 % the left lower lobe, 11 % the right lower lobe and 4 % from the left lingula. In all cases, 10mL of normal saline was instilled into the bronchoscope for lavage. The mean percentage return was 27 %, with a median return of 2.3mL (range 0.2 to 6.0mL). BAL supernatants were processed as described in Chapter 2 Methods section 2.4.3 and utilised for the investigation of the inflammatory profile of recruited participants. As previously described in Chapter 2 section 2.4.3, MSD technology was used to investigate a panel of cytokines using the V-PLEX (IL-17A, IL-6, IL-1β, TNF-α, IFN-γ, IL-14, IL-13) and U-PLEX (IL-8) ELISA-based assays.

The results are shown below in Figure 45 and Table 15 and are presented as the concentration of mediator per mL of BAL aspirate. Where cytokine levels were below the lower limit of detection a value equating to 50 % of the lower limit of detection value was assigned. Significantly greater levels of the following cytokines were found in CF versus non-CF BAL: IL-1β (p=0.04), IL-17A (p=0.007), IFN-γ (p=0.006), TNF-α (p=0.001), IL-6 (p=0.04); IL-4 (p=0.01) and IL-13 (p=0.001). No differences were evident with IL-8 (p=0.6) between the two groups.

Further subgroup analysis was performed to determine any relationship between BAL culture status and cytokine concentration. BAL microbiology culture results are shown in Table 16 with 75 % and 69 % of CF and non-CF showing positive results respectively. BAL cultures in each non-CF and CF groups were assigned as either culture positive or negative and comparisons were made for each cytokine (Figure 46 and Figure 47). Significant differences were found for IL-1β (p=0.003) and TNF-α (p=0.01) in the non-CF groups. Differences were not significant for any of the cytokines assessed in CF cultures between culture negative and positive samples. However, there was a suggested increase in IL-4, IL-13, IL-8, IL-17A and TNF-α in CF BAL culture positive samples.

This cytokine panel was also assessed in cell culture supernatants harvested from PNEC and PBEC cultures at 28d ALI to ascertain any relationship with the BAL data. ALI cell culture supernatants were harvested and the cytokine panel above was assessed as previously described. No significant differences were found with any of the cytokines assessed (Figure 48 and Table 17). Corresponding p values for statistical analyses performed are shown in Table 18. There was a suggested increase in levels of IL-17A and IL-1β in PBEC versus PNEC cultures in both non-CF and CF groups, however, these findings were not significant. Furthermore, the median IL-6 level was greatest in CF PBECs, but again this was not significant.

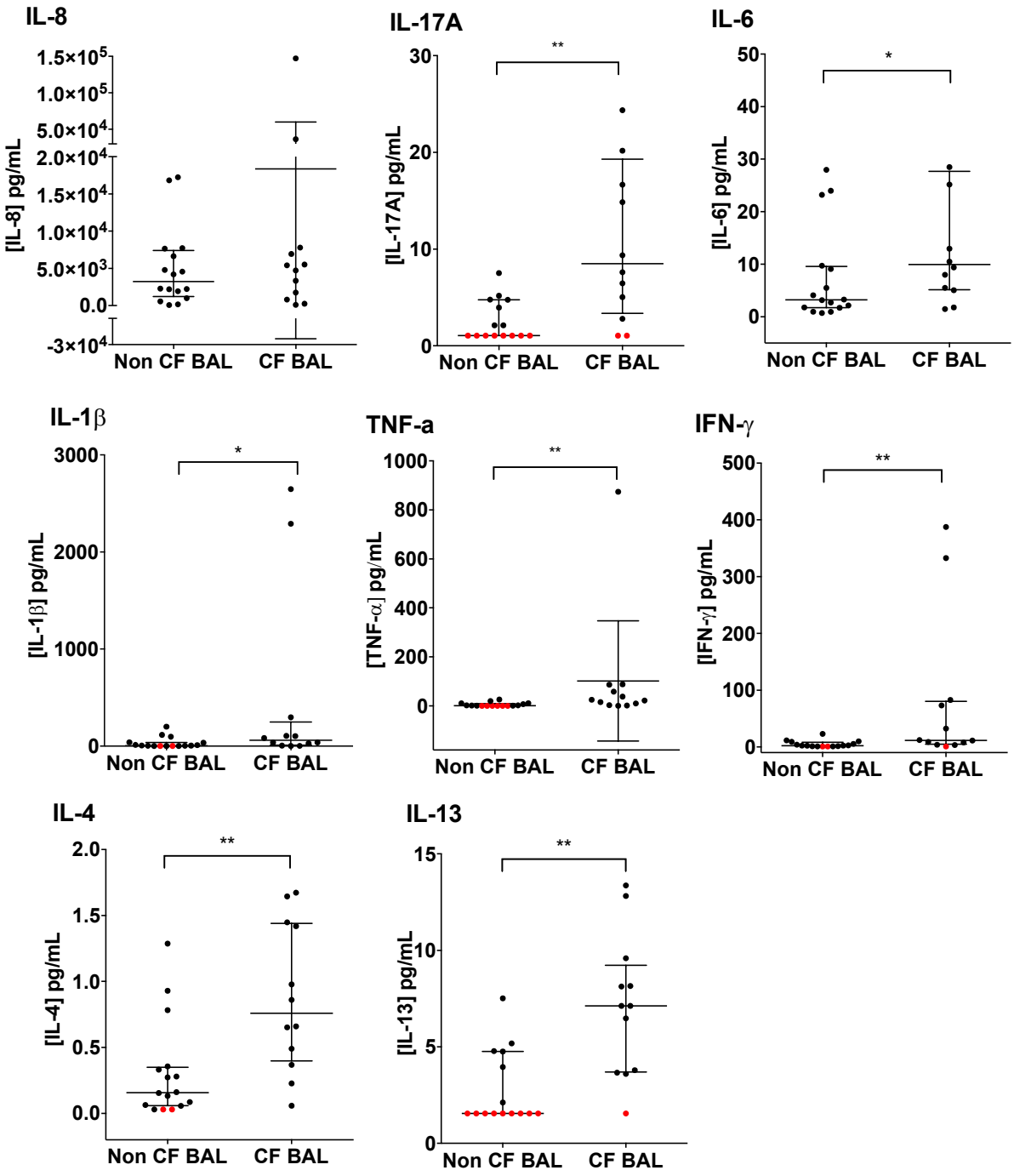

Figure 45: Inflammatory profile of bronchoalveolar lavage supernatants

The Meso Scale Discovery U-Plex assay was used to analyse IL-17A, IL-6, IL-1β, TNF-α, IFN-γ, IL-4 and IL-13 in BAL supernatants as described. The V-Plex assay was used to analyse IL-8. Points represents individual donors; red points are values < lower limit of detection. Bars represent median ± IQR. Data analysed with Mann-Whitney test; p values are shown in Table 15; non-CF: n=16; CF: n=12.

Cytokine	Non-CF BAL	CF BAL	p value
IL-8	3244 (1232 - 7409)	5073 (1055 - 7571)	0.6
IL-17A	1.1 (1.1 - 4.8)	8.5 (3.3 - 19.3)	0.002
IL-6	3.2 (1.7 - 9.6)	9.9 (5.2 - 27.7)	0.04
IL-1β	4.8 (0.5 - 37.2)	59.6 (3.4 - 19.3)	0.04
TNF-α	1.3 (0.2 - 9.5)	23.5 (5.0 - 79.4)	0.002
IFN-γ	2.5 (1.3 - 8.2)	11.8 (5.1 - 80.3)	0.006
IL-4	0.2 (0.06 - 0.4)	0.8 (0.4 - 1.4)	0.003
IL-13	1.6 (1.6 - 4.8)	7.1 (3.7 - 9.2)	0.001

Table 15: Cytokine concentrations in bronchoalveolar lavage supernatants

Abbreviations: BAL: bronchoalveolar lavage; IL interleukin; TNF tumour necrosis factor; IFN interferon.

Values are expressed as median ±IQR; units are pg/mL. Data analysed using Mann Whitney test and corresponding p values are shown; non-CF: n=16; CF: n=12.

CF BAL	Microbiology	Non-CF BAL	Microbiology
PCF15	*Mycobacterium spp.*	PWT1	*E. coli*
PCF16	*M. catarrhalis*	PWT2	No growth
PCF17	*Achromobacter*	PWT3	*H. influenza*
PCF18	No growth	PWT4	*M. catarrhalis*
PCF19	*Mycobacterium spp.*	PWT5	No growth
PCF20	*Proteus mirabilis*	PWT6	No growth
PCF21	No growth	PWT7	*H. influenza*
PCF22	*A. fumigatus*	PWT8	*H. influenza, M. catarrhalis*
PCF24	No growth	PWT9	*H. influenza*
PCF25	*P. aeruginosa*	PWT10	No growth
PCF26	*H. influenza*	PWT11	*M. catarrhalis, MRSA*
PCF27	*Aspergillus fumigatus*	PWT12	*K. pneumonaie*
		PWT13	*H. influenza, K. pneumonaie*
		PWT14	*H. influenza*
		PWT18	*H. influenza*
		PWT19	No growth

Table 16: Microbiology culture of bronchoalveolar lavage samples

Microbiology culture results of bronchoalveolar lavage (BAL) samples harvested for cytokine analysis.

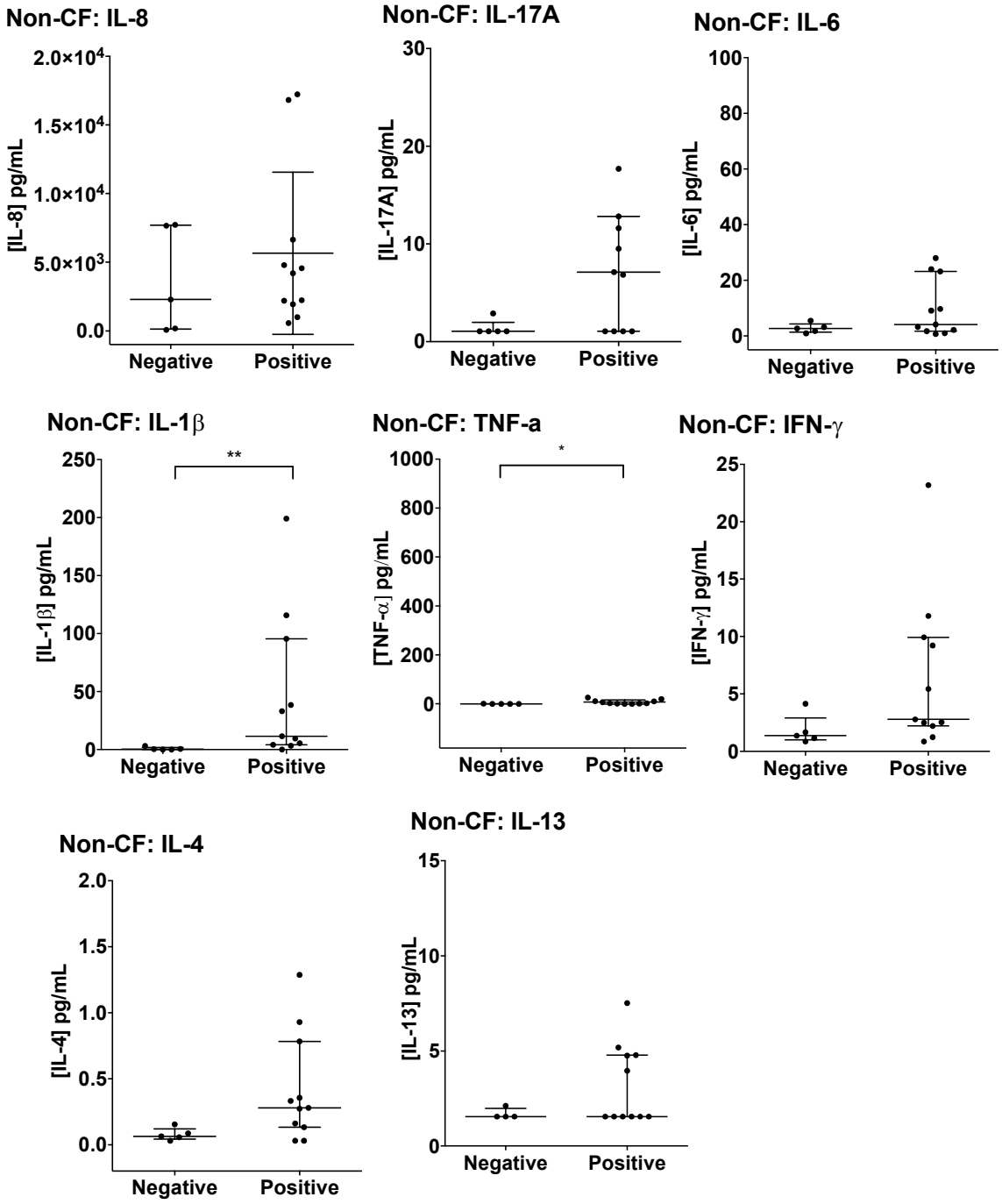

Figure 46: Assessment of cytokine profiles in culture negative and positive non-CF bronchoalveolar lavage supernatants

Concentrations of IL-8, IL-17A, IFN-γ, TNF-α, IL-1β, I L-6, IL-4 and IL-13 were compared in non-CF BAL supernatants as described to enable comparisons between culture negative and positive samples. Bars represent median ± IQR. Data analysed with Mann-Whitney test; p values: IL-8 0.7; IL-17A 0.06; IL-6 0.3, IL-1β 0.003; TNF-α 0.01; IFN-γ 0.07; IL-4 0.05; IL-13 0.3; n=16.

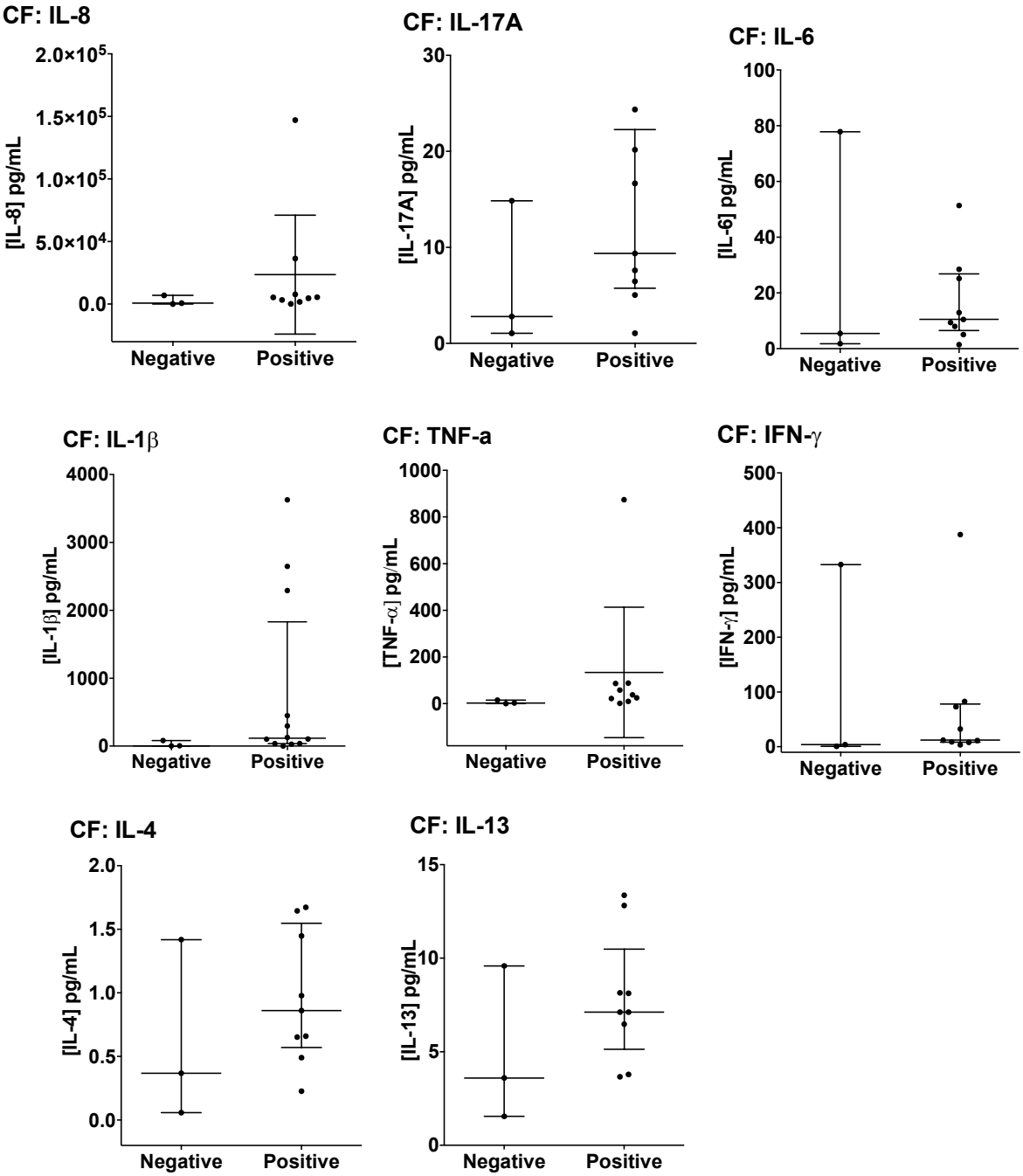

Figure 47: Assessment of cytokine profiles in culture negative and positive CF bronchoalveolar lavage supernatants

Concentrations of IL-8, IL-17A, IFN-γ, TNF-α, IL-1β, IL-6, IL-4 and IL-13 were compared in non-CF BAL supernatants as described to enable comparisons between culture negative and positive samples . Bars represent median ± IQR. Data analysed with Mann-Whitney test; p values: IL-8 0.3; IL-17A 0.2; IL-6 0.9, IL-1β 0.1; TNF-α 0.06; IFN-γ 0.5; IL-4 0.3; IL-13 0.3; n=12.

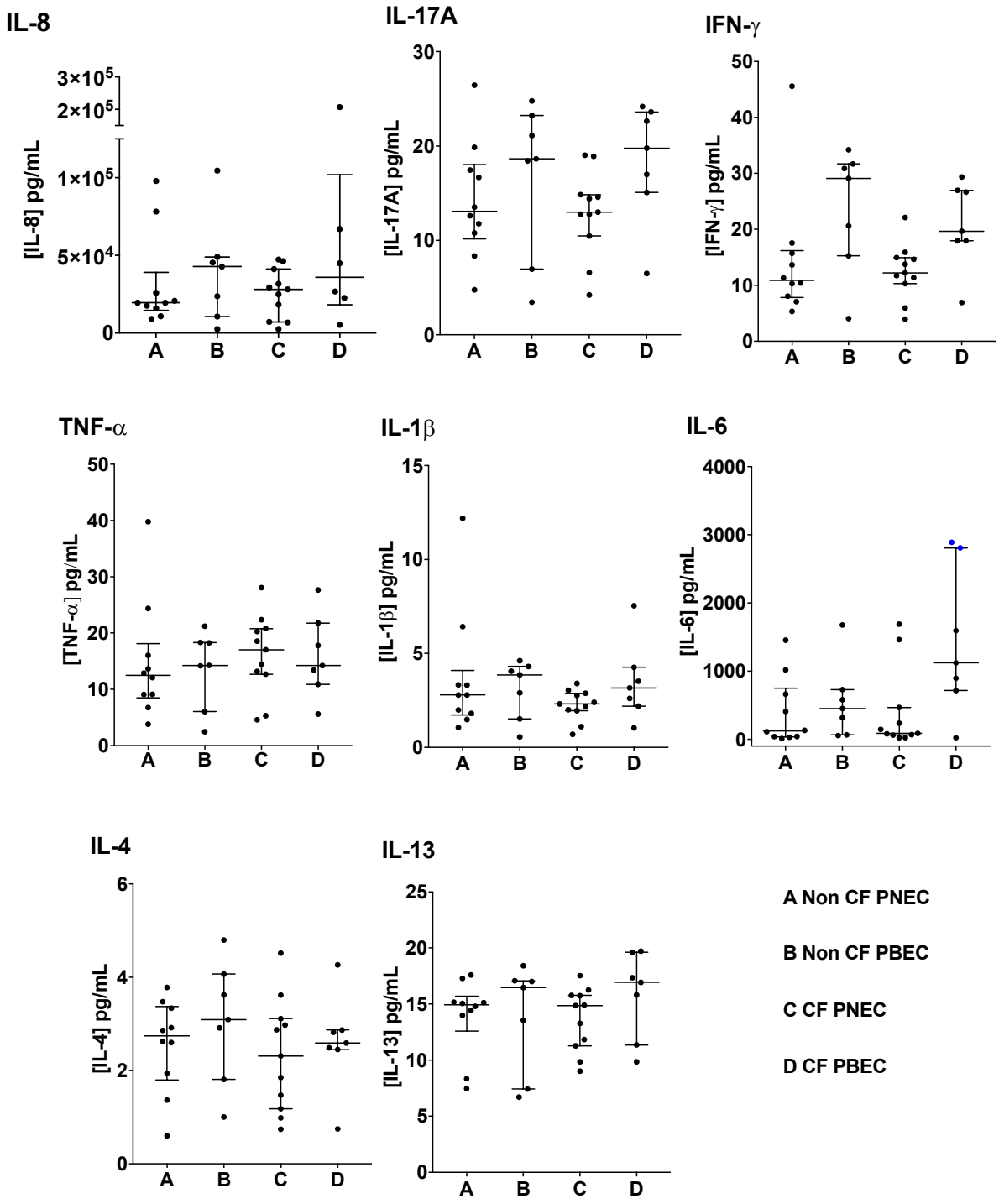

Figure 48: Inflammatory profile of cell culture supernatants

ALI cell culture supernatants were harvested from non-CF PNECs (A), non-CF PBECs (B), CF PNECs (C) and CF PBECs (D) and IL,8, IL-17A, IL-6, IL-1β, TNF-α, IFN-γ, IL-4 and IL-13 were assessed as described. Points represents individual donors; blue points are values > upper limit of detection. Bars represent median ± IQR. Data analysed with Kruskall-Wallis and Dunn's multiple comparison test with no significant differences found; A: n=10; B: n=7; C: n=11; D: n=6.

Cytokine	Non-CF PNEC	Non-CF PBEC	CF PNEC	CF PBEC
IL-8	19522 (14630 - 39043)	42813 (10686 - 48985)	28181 (7210 - 41225)	35836 (18342 - 101948)
IL-17A	13.1 (10.2 -18.1)	18.6 (7.0 - 23.2)	13.0 (10.5 -14.9)	19.8 (15.1 - 23.6)
IFN-γ	10.9 (7.8 - 16.2)	29.1 (15.3 - 31.7)	12.2 (10.3 - 15.0)	19.7 (18.0 - 27.0)
TNF-α	12.5 (8.5 - 18.1)	14.3 (6.1 - 18.3)	17.0 (12.7 - 20.8)	14.2 (10.9 - 21.8)
IL-1β	2.8 (1.7 - 4.1)	3.9 (1.5 - 4.3)	2.3 (2.0 - 2.9)	3.2 (2.2 - 4.3)
IL-6	122.4 (38.8 - 753.1)	452.8 (66.8 - 730.1)	87.6 (63.6 - 467.5)	1124 (715.8 - 2808)
IL-4	2.7 (1.8 - 3.4)	3.1 (1.8 - 4.1)	2.3 (1.2 - 3.1)	2.6 (2.5 - 2.9)
IL-13	14.9 (12.6 - 15.7)	16.5 (7.4 - 17.1)	14.9 (11.3 -15.8)	16.9 (11.3 - 19.6)

Table 17: Cytokine concentrations in cell culture supernatants

Abbreviations: IL interleukin; TNF tumour necrosis factor; IFN interferon.

Values are expressed as median ±IQR; units are pg/mL. Non-CF PNEC: n=10; non-CF PBEC: n=7; CF PNEC: n=11; CF PBEC: n=6.

Cytokine	Non-CF PNEC v PBEC	CF PNEC v PBEC	Nasal Non-CF v CF	Bronchial Non-CF v CF
IL-8	>0.99	>0.99	>0.99	>0.99
IL-17A	>0.99	0.2	>0.99	>0.99
IFN-γ	0.1	0.2	>0.99	>0.99
TNF-α	>0.99	>0.99	>0.99	>0.99
IL-1β	>0.99	0.6	>0.99	>0.99
IL-6	>0.99	0.1	>0.99	0.9
IL-4	>0.99	>0.99	>0.99	>0.99
IL-13	>0.99	0.5	>0.99	>0.99

Table 18: Statistical comparisons of cell culture supernatant cytokine profiles

Abbreviations: v versus; IL interleukin; TNF tumour necrosis factor; IFN interferon.

Data was analysed using the Kruskall-Wallis and Dunn's multiple comparison test. Corresponding p values for each cytokine assessed in each culture group are shown. Non-CF PNEC: n=10; non-CF PBEC: n=7; CF PNEC: n=11; CF PBEC: n=6.

3.7 Discussion

3.7.1 Feasibility of establishing a programme to harvest paediatric nasal and bronchial brushings

It can be challenging to establish a new programme for the acquisition of research samples within a hospital institution. However, this was achieved through early discussions with the clinical paediatric respiratory and CF MDT, the anaesthetic team and surgical theatre staff, who were all incredibly supportive and receptive to the research process.

Importantly, the research was discussed with parents and children with CF, to establish their overall perception and opinions of parent and participant information literature. For the majority of children without CF and some with CF, this has been their first exposure to flexible bronchoscopy and therefore a worrying and stressful time for parents. Sampling carries a relatively low risk of a small amount of bleeding from the brushing site in addition to the risks that are associated with the bronchoscopy itself. These are perceived as “low risk” interventions, however, it was important to respect parental perception of these associated risks and carefully adhere to GCP guidelines for research ethics and consent. Although it was explained that the children would not benefit directly from their participation, the parental response to their child’s involvement was incredibly receptive. Through this experience, I have been overwhelmed by the attitudes of parents and children towards this research from both the CF and non-CF groups.

3.7.2 Challenges faced with the tissue culture process

The success rates of establishing ALI cultures in this study are comparable to other similar studies involving children (Mosler et al., 2008, Garratt et al., 2014). Infection is a well-recognised complication of airway epithelial cell culture, particularly in the first 72 hours (Garratt et al., 2014). In a previous study performed to investigate determinants of paediatric CF bronchial culture outcomes, 28.9 % of cultures isolated from 260 brushings were infected. 25 % of cultures infected with fungus had relevant organisms isolated in corresponding BAL samples (Garratt et al., 2014). In this PhD study, rates were appreciably lower with only 7 % of all brushings displaying evidence of infection. All infections occurred in the absence of associated BAL fungal

microbiology, suggesting environmental contamination as opposed to contaminating airway flora.

The most significant challenges were faced with PBEC development, with lowest success rates in CF PBECs. Although type I collagen alone was appropriate for paediatric PNEC culture, PBECs required the addition of fibronectin and 1 % BSA to promote cell attachment after helpful discussion with colleagues in the tissue culture field. This approach was required only during the submerged expansion phase after which type I collagen alone was used in all culture inserts to maintain consistency with PNECs. Interestingly similar problems with cell attachment in CF culture using type 1 collagen alone have been previously reported by another group (Tosoni et al., 2016).

This problem was rectified prior to non-CF recruitment, and therefore it cannot be ascertained if this was limited specifically to bronchial culture. Type I collagen has been used for bronchial epithelial culture in the current lab setting and by other research groups (Fulcher et al., 2005, Brodlie et al., 2010, Yaghi et al., 2010, Comer et al., 2012). The basement membrane of airway epithelial cells contains type IV collagen and laminin in the lamina densa that are secreted by basal epithelial cells, below which lies the lamina reticularis composed of type III and IV collagen (Tam et al., 2011). Therefore, it is possible that PBECs may have attached better with the use of type IV collagen. Further investigation would be required to determine assessment of PBEC attachment to type IV collagen compared with type 1.

Neutrophil elastase is a protease released by neutrophils in the lung and plays a key role in the pathogenesis of CF lung disease. It is also implicated in degradation of the extracellular matrix by causing specific damage to structural proteins including collagen and fibronectin (Janoff et al., 1979, Downey et al., 2009). It is possible that this could have hindered epithelial cell attachment in CF PBECs, and additional exogenous fibronectin was required to promote adherence. To investigate this further, levels of neutrophil elastase and fibronectin production could be investigated to determine differences in the effects on the extracellular matrix and epithelial attachment in freshly brushed CF and non-CF bronchial and nasal samples. Furthermore, although not directly measured, all PBECs were more motile after collection due to vigorous cilia activity compared with PNECs, which may have further hindered epithelial attachment.

There were no clear reasons for failure during the ALI stage of culture, particularly after techniques were well established and standardised methods were employed for brushing technique, tissue culture equipment, seeding density, culture media and substrate choice. Mycoplasma infection is often insidious and associated with culture failure but was not present in unsuccessful cultures. Regular monitoring of incubator CO_2 levels was performed to ensure that incubation conditions were optimally maintained. Although anecdotal, discussions with other research groups regularly involved in airway epithelial culture have revealed shared experiences of ALI culture failure without apparent reason or isolated cause. Furthermore, there was a distinct problem with culture failure associated with specific media batches, however, the cause for this problem remains unknown despite liaising with the manufacturer.

The highest rates of failure at any stage of ALI were in non-CF PBECs. Around two thirds of these failed cultures were harvested with the smaller bronchial brush. Lower cell numbers require greater time for expansion and in view of the association between culture success and time to confluence, it is possible that the lower cell yield let to the development of poorer quality, senescent cells and subsequent culture failure. Furthermore, utilisation of larger brushes may have yielded more basal progenitor cells thereby facilitating subsequent differentiation. Detailed exploration into these potential causes would be time and resource intensive. Nevertheless, future sampling and culture success could be improved by sampling more than one bronchial brushing per participant.

3.7.3 Epithelial characterisation

In this chapter, differentiated ALI cultures have been characterised in terms of morphology and ability to form polarised epithelial monolayers that display ciliated and mucus phenotypes.

TEER measurements were highest in CF PNECs and although not statistically significant and likely limited by sample size, values were almost 2-fold greater in CF PBECs compared with non-CF PBECs. However, no apparent differences or correlations were found with expression of *ZO-1* and other genes involved in maintaining epithelial integrity between CF and non-CF cultures. This finding of increased CF-related TEER in conjunction with the absence of differences in ZO-1 has previously been reported in ALI cultures (Sajjan et al., 2004). These authors concluded that the overlying mucus layer in CF ALI cultures contributed to higher

TEER measurements with reduction of TEER to “non-CF values” after mucus removal with 3 % xylitol, which is a mucolytic agent (Sajjan et al., 2004).

TEER values were also greater in CF nasal cultures compared with their bronchial counterparts. There is little reported in the literature regarding direct TEER comparisons in CF PBECs and PNECs, however, comparatively high values have been reported in other studies involving PNECs (Tosoni et al., 2016).

Despite maintenance of consistent culture conditions including seeding density of epithelial cells there was considerable inter-donor variability in TEER measurements at all stages of ALI culture, particularly notable in CF PNECs with over a 4-fold difference between minimum and maximum mean values at 28d ALI. TEER measurement is temperature dependent with lower values evident at reduced temperatures and 37 °C being optimal to closely representative of the *in vivo* environment (Blume et al., 2010). To assess TEER, PBS was warmed to 37 °C, applied to the apical culture surface and incubated at 37 °C for 15 minutes before measurements were made. This approach was adopted for all TEER measurements to minimise temperature related variation and maintain consistency. Inter-donor variations in TEER have been previously described (Stewart et al., 2012, Tosoni et al., 2016). Consideration of these variations will be essential in the interpretation of ion transport profiles of cultured cells and the relevant responses to ion channel activators and inhibitors.

Successful ALI cultures were able to differentiate into ciliated epithelial cells. *Foxj1* expression was significantly greater in CF PBECs versus all PNECs. No differences were found with non-CF PBECs; however this could be accounted for by the greater variability in expression evident in this group. *Foxj1* promotes differentiation during later stages of ciliagenesis in epithelial cells already committed to cilial phenotypes (You et al., 2004). It is possible that greater levels of expression seen in CF PBECs could reflect the underlying role of cilial function in lower airways for MCC. However, previous studies have shown that ciliary beat frequency is higher in CF nasal versus bronchial epithelia (Alikadic et al., 2011). Furthermore, there is no evidence to suggest that there are differences in the percentage of ciliated cells in the two epithelial locations and this is supported by similar changes of *TUBA1A* expression in all ALI cultures. *Foxj1* is a marker of motility with increased expression at later stages of ALI (Jain et al., 2010). In this current study, observed ciliagenesis was determined later in PNECs by a mean of 5 days at 23d ALI. Given that gene expression analysis

was performed close to this time at 28d ALI, this may have missed later increases in *Foxj1* expression in PNECs. Analysis may have been better performed at a common time point after ciliagenesis as opposed to time in ALI culture to better differentiate between PNEC and PBEC expression. These findings could also be complemented by investigation of protein expression by immunofluorescence or Western blot techniques.

Although ALI cultures produced mucus, the amount produced and consistency varied between cultures. In CF cultures, it was much more adherent to the epithelial surface and difficult to remove. This was in contrast to the mucus produced by non-CF cultures, which was much easier to harvest. Therefore, it was difficult to make accurate direct comparisons of mucus produced by CF and non-CF cultures.

It has traditionally been challenging to investigate mucin concentrations in biological samples predominantly due to their large size and gel-forming characteristics (Henderson et al., 2014). As an alternative, apical washings were harvested from cultures and direct comparisons of mucin concentration were made using ELISA. This technique has previously been recommended for the investigation of mucins in airway epithelial cultures (Abdullah et al., 2012). Unfortunately, it was difficult to obtain reliable and consistent assessment of MUC5B concentration and this method does require further optimisation. MUC5AC was present in all ALI cultures with highest concentrations evident in washings harvested from CF PBECs. Hypersecretion of mucus is evident in CF lung disease secondary to goblet cell hyperplasia (Groneberg et al., 2002, Henderson et al., 2014). Although this was not formally assessed in these cultures, this could be a potential explanation for this finding.

RT-qPCR analysis did not reveal any differences in gene expression in all ALI cultures. Prior investigation involving non-CF cultures has also shown similar levels of *MUC5AC* and *MUC5B* in nasal versus bronchial cells (Bernacki et al., 1999). However, these findings contradict previous evidence of increased expression in tissue harvested from explanted CF lungs (Henderson et al., 2014). Therefore, these findings may signify that investigation in ALI cultures does not truly represent transcriptional changes evident *in vivo* which are likely affected by inflammatory mediators and insults in the CF airway environment. Furthermore, *mRNA* expression may not truly predict mucus properties of the airway, requiring alternative methods for investigation.

3.7.4 Assessment of the airway inflammatory environment

The inflammatory airway environment of non-CF and CF participants was investigated by assessing the cytokine profile of BAL supernatants. Results showed significant elevations of IL-17A, IFN-γ, TNF-α, IL-1β, IL-6, IL-4 and IL-13 in CF versus non-CF BAL supernatants. BAL neutrophil and IL-8 levels have previously been shown to be increased in asymptomatic children with CF, including in some children without positive respiratory cultures (Khan et al., 1995a). In this present study, IL-8 levels were elevated in both groups with no significant differences found. An important consideration is that the non-CF participants were not a healthy group, with problems including recurrent respiratory infections and symptoms of persistent of persistent bacterial bronchitis (PBB). In this group 69 % of children had positive BAL microbiology (compared with 75 % in the CF group). Elevated IL-8 levels together with features of neutrophilic inflammation have been found in BAL isolated from children with PBB and non-CF bronchiectasis, indicating that IL-8 elevation is not exclusively elevated in the CF airway (Marchant et al., 2008, Bergin et al., 2013).

The results found in this present study are in keeping with previous investigation in children, which has shown significantly elevated levels of Th1 (IFN-γ), Th2 (IL-13) and Th17 (IL-17A) and Th17 related cytokines (IL-6) in CF versus non-CF controls (Tiringer et al., 2013). These authors also found elevated levels of IL-5 and IL-1β and although they did not specifically investigate IL-4, levels of other Th2 cytokines were increased (Tiringer et al., 2013). In addition to IL-8, TNF-α, IL-6 and IL-17A are involved in modulation of the airway inflammatory response in CF (Taggart et al., 2000, Bergin et al., 2013, Tiringer et al., 2013). Importantly, the findings by Tiringer *et al* found that of the cytokines investigated in this PhD, IL-17A, IL-6, IL-1β, IL-8 and IL-13 significantly correlated with high resolution CT changes, with the additional finding of IL-17A and its correlation with relevant CF pathogens such as *Aspergillus* and *P. aeruginosa* (Tiringer et al., 2013). Furthermore, previous investigation in explanted CF lung tissue has demonstrated immunoreactivity for IL-17A in lavage specimens, with localisation to neutrophil and mononuclear cells, suggesting a role in neutrophil-mediated inflammation in the CF airway (Brodlie et al., 2011). Although not acutely unwell, all CF children in this present study were undergoing clinical bronchoscopy for recurrent respiratory symptoms that were not responding to standard antibiotic therapy, therefore there was an element of intercurrent respiratory illness in addition to chronic inflammatory changes that were part of their disease progression. BAL

samples were not comprehensively assessed for cytology and this would have complemented the supernatant findings and provided more detail of the airway inflammatory environment.

The same panel of cytokines were assessed in cell culture supernatants that were harvested from differentiated PNEC and PBECs at 28d ALI. No differences were apparent in all cytokines assessed in the non-CF and CF groups. Supernatants were harvested under unstimulated conditions, and the response to relevant stimuli, such as clinical *P. aeruginosa* isolates, was not assessed. This would have been useful to determine any parallels with the BAL data. Notably all cytokines measured were comparatively higher than the levels found in BAL and the exact cause for this is unclear. It is possible that the process of ALI culture or supernatant harvesting stimulated inflammatory responses in the epithelia. This could be investigated further with detailed exploration of cytokine expression and exploration of relative changes in cytokine concentrations to infective stimuli.

Although BAL cytokine analysis can provide a useful insight into the airway inflammatory environment, it is important to acknowledge the challenges faced with quantifying solute concentrations in BAL. It may be over-simplistic to assume that the aspirated volume of saline provides a representation of the ‘whole’ airway environment, particularly in light of recent evidence to suggest that regions are differentially affected by disease in CF (Li et al., 2012, Gutierrez et al., 2001). It is also difficult to determine how much solute found within the BAL is contained within the airway epithelial lining fluid and although this can be overcome by measuring the ratio of BAL to plasma solute concentration of urea and albumin, there are limitations with these methods and ratios can vary between disease groups (Walters and Gardiner, 1991). In this PhD, cytokine concentrations were expressed per mL of BAL aspirate. This approach was taken in the absence of matched participant serum samples and in view of the consistent approach that was taken with volume of saline instilled and techniques used for BAL collection.

3.8 Conclusion

In this chapter, I have demonstrated the ability to successfully establish a programme to culture nasal and bronchial epithelial cells from children with and without CF using an ALI technique to produce differentiated epithelial cells. In order to achieve this, it was necessary to overcome initial challenges with culture infection, low brushing epithelial yield and bronchial attachment in CF PBECs. Future ALI PBEC success is likely to be improved by multiple bronchial brush sampling to increase cell yield and culture success.

Although detailed assessment of cilial and mucus phenotypes were not performed in cultured cells, the above findings have confirmed the presence of differentiated ciliated and mucus producing PNEC and PBEC ALI cultures. These established techniques could be utilised to perform more extensive investigation of these parameters if required in the future.

The notable inter-donor variability in TEER may have relevance for the future analysis of ion transport profiles in cultured cells and will require recognition and careful consideration in analyses performed. However, with these considerations and based on the above findings, paediatric PNECs are a suitable experimental model to investigate the remaining aims and objectives outlined for this PhD.

4 Chapter 4: Functional characterisation of ion transport profiles in differentiated paediatric primary nasal and bronchial epithelial cultures derived from children with and without cystic fibrosis

4.1 Introduction

After having successfully established paediatric PNEC and PBEC ALI cultures and verified their epithelial characteristics, the next focus of this PhD was to perform a detailed investigation of the ion transport properties of these fully differentiated cells. This was important to firstly demonstrate the feasibility of utilising these cultures in Ussing chamber experiments and subsequent TMEM16A characterisation, and secondly to determine potential differences between PNEC and PBEC cultures.

Previous studies involving comparisons of PNEC and PBEC paediatric cultures have focussed on alternative functional measurements including stimulated cytokine responses and epithelial characteristics, however, these have not involved CF participants (McDougall et al., 2008, Thavagnanam et al., 2014). Studies assessing ion transport profiles in paediatric cultures are limited, with the publication of one paper during the compilation of this thesis (Brewington et al., 2018b). These authors concluded that paediatric CF PNEC cultures can be utilised in place of PBECs, with a particular focus on the utilisation of PNECs to investigate CFTR function and response to modulator therapy (Brewington et al., 2018b). Although there is now published data relating to this area of CF research, the findings in this PhD will help to build on this work. In view of early disease processes that are increasingly recognised in children with CF, research involving paediatric cultures is exceptionally valuable.

This chapter will explore the feasibility of using epithelial cultures established in this PhD for Ussing chamber experiments and investigate ENaC-mediated sodium absorption and chloride secretion by CFTR using this experimental technique.

4.2 Hypotheses

- Differentiated paediatric PNEC and PBEC ALI cultures can be used in Ussing chamber experiments to explore the function of ENaC and CFTR.
- There are no differences in ENaC and CFTR function in paediatric PNEC and PBEC ALI cultures therefore validating PNECs as a representative CF research model.

4.3 Aims

The specific aims of this chapter were to:

- assess the feasibility of using paediatric differentiated ALI PNEC and PBEC cultures in Ussing chamber experiments
- investigate the function and expression of ENaC and CFTR in paediatric differentiated ALI cultures and determine any differences between PNECs and PBECs derived from non-CF and CF participants

4.4 Results

4.4.1 Feasibility assessment of paediatric primary air liquid interface cultures for the profiling of ion transport

To determine the suitability of paediatric ALI cultures for analysis of ion transport properties, I_{sc} responses were investigated using Ussing chamber experiments as described in Chapter 2. Initial work was performed in PNECs due to early challenges faced with PBEC culture as described in Chapter 3.

To ascertain I_{sc} changes over time in ALI culture, responses were monitored from 28d until 45d ALI in one CF PNEC ALI culture, PCF3N (Figure 49). Although performed only once in each monolayer, due to limited availability of culture inserts, responses to each reagent were as predicted. Amiloride addition resulted in a reduction in I_{sc} due to ENaC inhibition. CFTR activation by forskolin was absent due to the isolation of these cultures from a homozygous F508del CF donor. A very small response to the CFTR inhibitor, $CFTR_{inh}$-172, was evident at 27d and 34d ALI. Finally, purinergic activation of CaCC by ATP increased I_{sc}. ATP was used in place of UTP during this early stage in the PhD.

Resultant I_{sc} responses to amiloride and ATP are shown in Figure 49. The amiloride-sensitive I_{sc} reduced over time in ALI culture with the peak response of -4.0 μA/cm^2 at 27d ALI, which had halved by 45d ALI. The ATP-induced I_{sc} was greatest at 34d ALI at 16.9 μA/cm^2, which reduced to 5.9 μA/cm^2 by 45d ALI.

These results demonstrated the feasibility of using paediatric PNECs to investigate I_{sc} responses with expected responses to each reagent. However, there was an apparent change in I_{sc} response over time in ALI culture, with peak responses seen at 27d and 34d to amiloride and ATP respectively. Responses to both reagents were reduced from 41d onwards. Therefore, these findings together with previous TEER assessment (as described in Chapter 3) informed the decision to make subsequent assessment of I_{sc} responses close to 28d ALI.

To maximise the usage of culture inserts available for experimental work, it was next determined whether repeated Ussing experiments could be performed on the same insert after a period of washing in between experiments. After performing the Ussing chamber experiment with the apical addition of amiloride, forskolin, $CFTR_{inh}$-172 and UTP as described in Chapter 2, the culture insert was washed in the Ussing chamber using a protocol of two additions and removal of Krebs solution to the apical and

basolateral compartments, a third addition of Krebs with a 30-minute period of gassing and final replacement of Krebs prior to repeating the experiment.

The effects of this protocol on tight junction integrity were assessed by measuring initial TEER before and after washing, as well TEER changes in response to amiloride, forskolin, $CFTR_{inh}$-172 and UTP on a CF PNEC (PCF5N) derived from a F508del homozygous participant at 14d and 21d ALI (Figure 50). The initial TEER at both 14d and 21d ALI in the first experimental run pre-washing was measured at 1667 $\Omega.cm^2$. At the end of the first experiment after UTP addition, the TEER was recorded at 1250 $\Omega.cm^2$ and 1000 $\Omega.cm^2$ at 14d and 21d respectively. After the washing protocol in run 2, TEER was reduced to 625 $\Omega.cm^2$ at 14d ALI and remained at 1000 $\Omega.cm^2$ at 21d ALI. Amiloride addition increased TEER in all circumstances due to ENaC-mediated inhibition of sodium absorption and a resultant decrease in transcellular conductance. However, the magnitude of this increase was reduced after washing at both 14d and 21d ALI, with an increase of 833 $\Omega.cm^2$ at both time points in run 1, versus an increase of 208 $\Omega.cm^2$ and 250 $\Omega.cm^2$ at 14d and 21d respectively. As predicted, there was no change in response to both forskolin and $CFTR_{inh}$-172 due to a lack of chloride conductance by dysfunctional CFTR at both timepoints before and after washing. UTP addition decreased TEER by 1250 $\Omega.cm^2$ and 1500 $\Omega.cm^2$ at 14d and 21d respectively during the first experimental run due to an increase in calcium-activated chloride conductance. However, this TEER reduction was less pronounced after washing at both timepoints with no change seen at 14d and a reduction of 200 $\Omega.cm^2$ at 21d ALI.

Overall, these results demonstrated the negative effect of repeated experiments and washing on tight junction integrity and the ability to make reliable comparisons using the same culture insert. Subsequent Ussing chamber experiments were therefore performed at around 28d ALI using fresh culture inserts for each experiment.

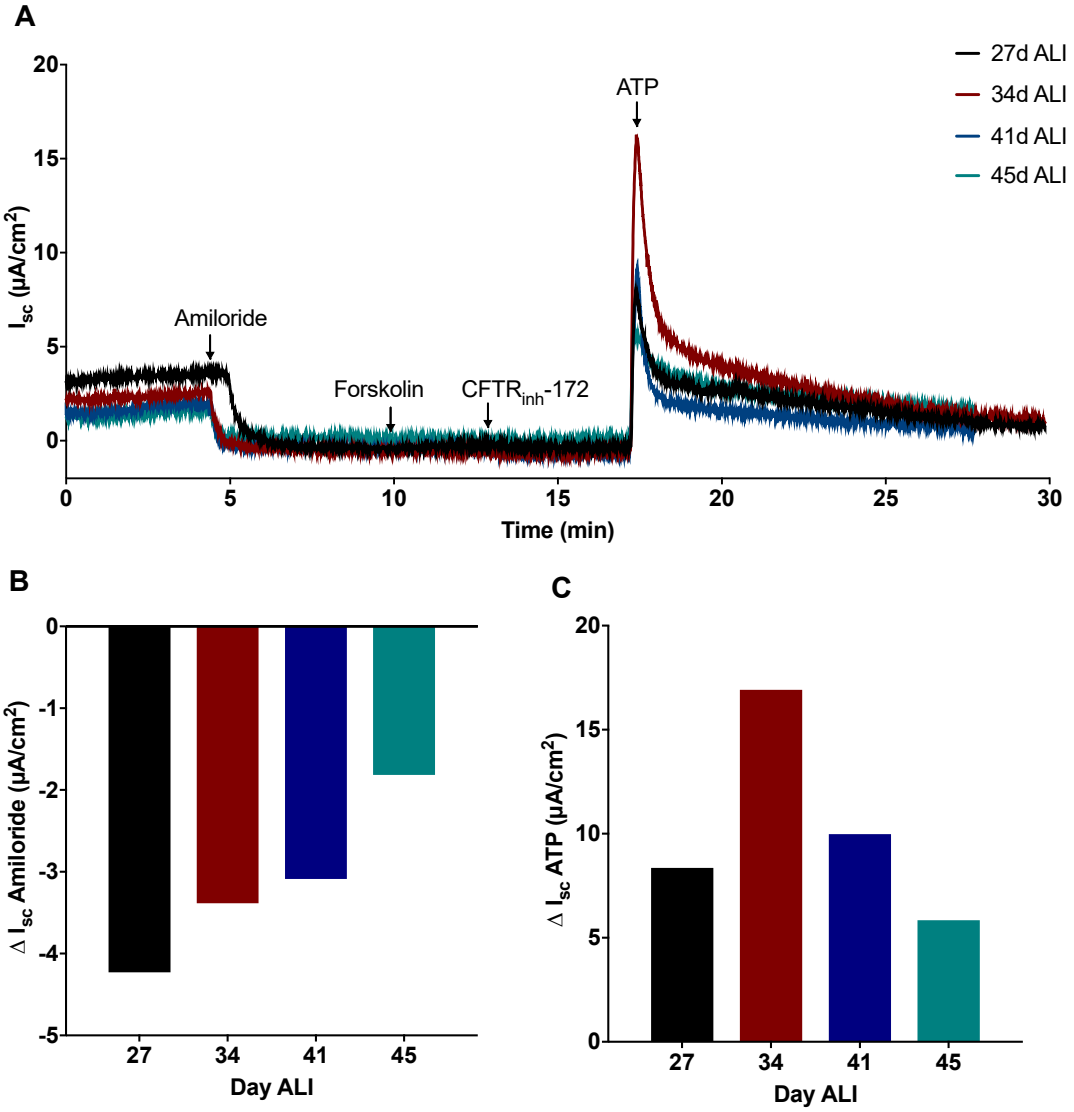

Figure 49 : Ussing chamber assessment of short circuit current responses over time in a CF PNEC culture

PNEC culture inserts derived from the CF PCF3 donor (F508del/F508del) were mounted in an Ussing chamber and bathed apically and basolaterally with a 125mM chloride Krebs solution. Short circuit current (I_{sc}) responses to the apical addition of amiloride (10 µM), forskolin (10 µM), $CFTR_{inh}$-172 (20 µM) and ATP (100 µM) were assessed at 27d (black), 34d (red), 41d (blue) and 45d (green) of ALI culture and shown in A. (There was a delay in amiloride addition at 27d ALI by 1 minute). Peak changes in short-circuit current (ΔI_{sc}) after amiloride and ATP addition at 27d (black), 34d (red), 41d (blue) and 45d (green) ALI were calculated and represented in B and C respectively; n=1 insert for each time point.

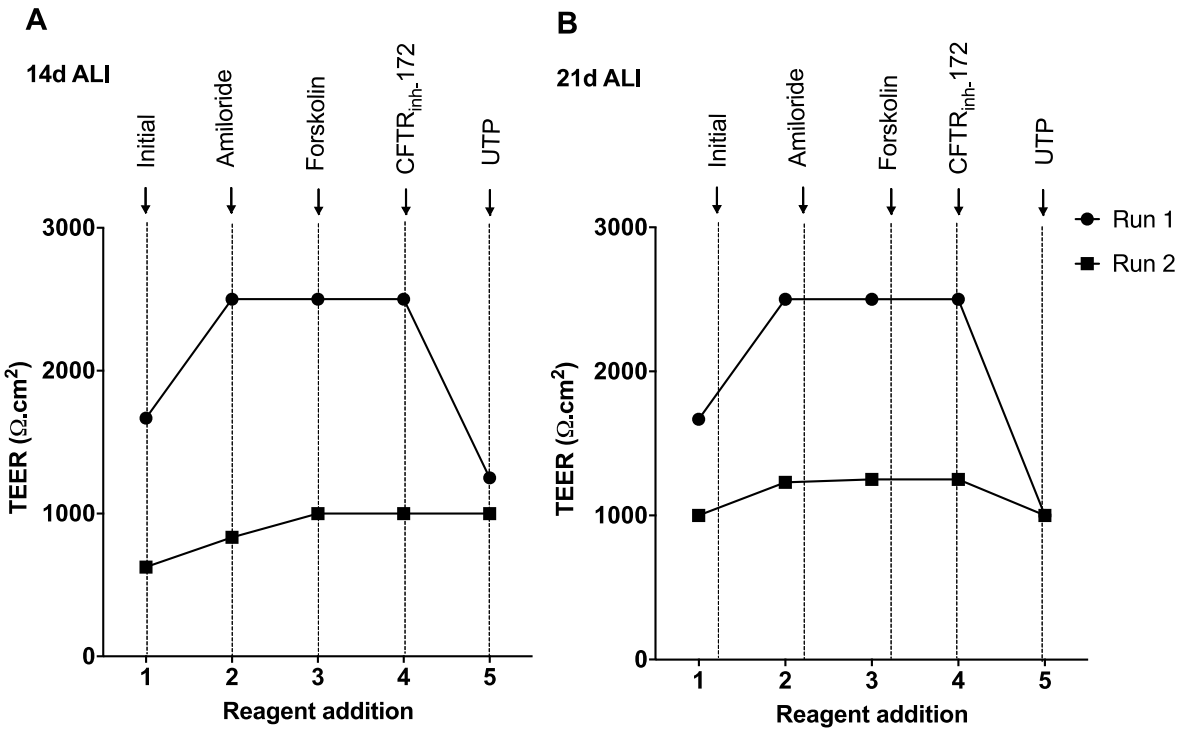

Figure 50: Effects of culture washing on TEER in Ussing chamber experiments in a CF PNEC culture

PNEC culture inserts derived from the CF PCF5 donor (F508del/F508del) at 28d ALI was mounted in the Ussing chamber to assess TEER response to amiloride (10 μM), forskolin (10 μM), $CFTR_{inh}$-172 (20 μM) and UTP (100 μM) at 14d ALI (Run 1) as shown in A. After washing the insert, the experiment was repeated to determine the effect of washing on TEER in response to individual reagents (Run 2). This was repeated at 21d ALI as demonstrated in B.

4.4.2 Investigation of epithelial sodium channel expression in differentiated paediatric primary airway epithelial cell cultures

In the airway epithelium, fluid absorption from the ASL is primarily mediated by the transport of sodium ions by ENaC at the apical membrane. Amiloride is a potent inhibitor of ENaC and can be utilised in electrophysiological studies to investigate epithelial ENaC function (Canessa et al., 1994, Mall et al., 1998).

Ussing chamber experiments were performed to investigate the functional expression of ENaC in paediatric differentiated PBEC and PNEC cultures from 25 to 33d ALI. A Krebs solution containing 125mM chloride was added to the apical and basolateral compartments and maintained at 5 % CO_2 and 37°C. After a 15-20 min period to enable baseline I_{sc} stabilisation, 10 μM amiloride was added to the apical compartment to inhibit ENaC activity. The resultant I_{sc} and TEER were measured as described in Chapter 2 section 2.5.

To exemplify the typical responses to amiloride in non-CF PNEC cultures, representative Ussing chamber traces for I_{sc} and TEER responses in PNECs derived from a non-CF donor are shown below in Figure 51. The resultant amiloride-sensitive I_{sc} and TEER were calculated as described in Chapter 2 section 2.5. In this non-CF PNEC culture, apical amiloride addition reduced the I_{sc} by -28.1μA/cm^2 due to inhibition of ENaC-mediated sodium absorption. As demonstrated in this figure, ENaC activity contributed to the majority of the initial resting I_{sc}. This was accompanied by a TEER increase of 417 Ω.cm^2 due to a reduction in sodium ion conductance.

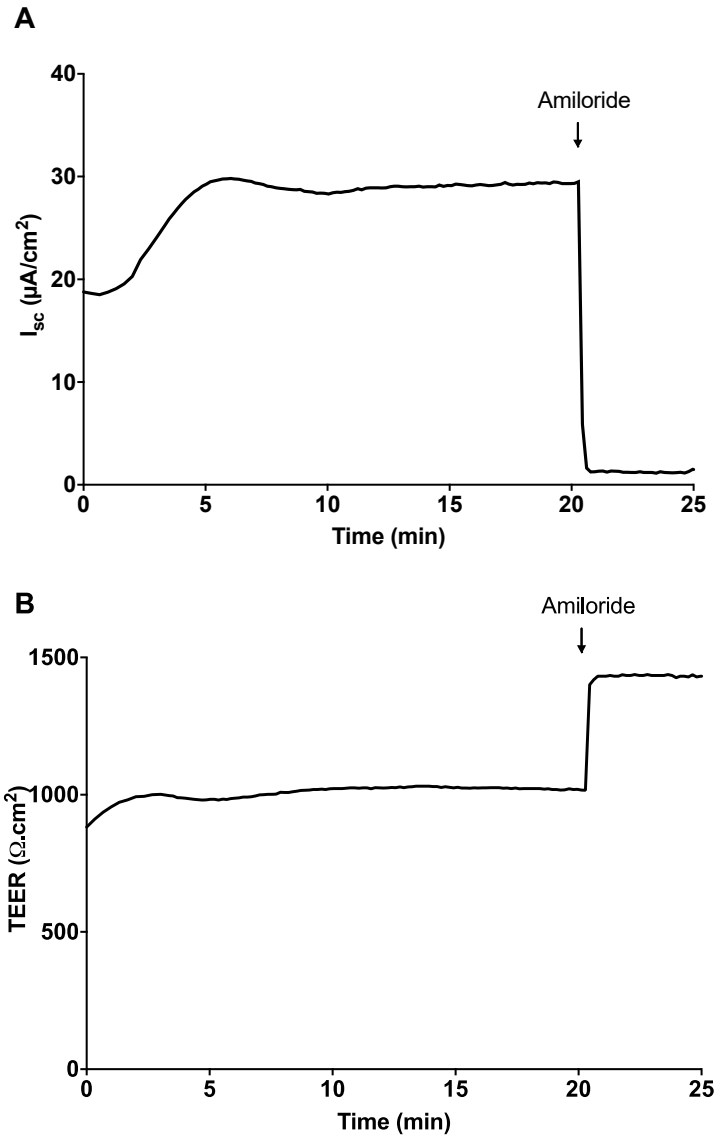

Figure 51: Representative Ussing chamber traces of short circuit current and transepithelial electrical resistance in response to amiloride addition in a non-CF PNEC culture

A PNEC culture derived from the non-CF PWT17 donor was mounted in the Ussing chamber and bathed apically and basolaterally in a 125 mM chloride Krebs solution. After a 20-minute period of stabilisation, 10 μM amiloride was added to the apical compartment. Resultant short circuit current (I_{sc}) and corresponding transepithelial electrical resistance (TEER) were recorded as shown in A and B respectively.

4.4.3 Assessment of epithelial sodium channel function

To determine if there were any functional differences in the amiloride-sensitive I_{sc} between PNEC and PBEC cultures isolated from non-CF and CF donors, Ussing chamber experiments were performed in 7 non-CF PNEC, 5 non-CF PBEC, 6 CF PNEC and 4 CF PBEC cultures from 25 to 33d ALI. Comparisons of the calculated amiloride-sensitive I_{sc} obtained from these cultures are shown in Figure 52.

In non-CF cultures, the amiloride-sensitive I_{sc} was significantly greater in PNECs versus PBECs (non-CF PNEC: median -25.2 $\mu A/cm^2$, IQR -17.1 to -44.9 versus non-CF PBEC: -7.4 $\mu A/cm^2$, IQR -4.4 to -9.6, p=0.008). In the non-CF PNEC group, cultures isolated from one particular donor demonstrated a large amiloride-sensitive current with a mean response of -115.4 $\mu A/cm^2 \pm$ SD 2.7. This result likely contributed to overall significance seen in differences between these two groups. Although there was a 2-fold increase in the amiloride-sensitive I_{sc} in CF nasal versus bronchial cultures, this was not statistically significant (CF PNEC: -16.9 $\mu A/cm^2$, IQR -12.8 to -20.7 versus CF PBEC: -8.2, IQR -2.6 to -10.4, p=0.38). Importantly, no differences were found in the median amiloride-sensitive I_{sc} in non-CF versus CF cultures in both PNEC and PBEC cultures (p>0.99 for both).

In this PhD study, epithelial cells were harvested from participants with a range of *CFTR* mutations. These mutations are shown relative to the amiloride-sensitive I_{sc} in Figure 52. *G542X* is a class 1 nonsense mutation that fails to produce full-length CFTR protein causing loss of channel function (Welsh and Smith, 1993). The 2986delA mutation is rare and poorly described in the literature, but clinically associated with a severe phenotype and pancreatic insufficiency. Therefore, all mutations investigated, aside from F508del/R751L, are associated with severe effects on CFTR function. With this in mind, the distribution of I_{sc} changes in response to amiloride were heterogeneous, with no obvious association with CF-disease severity and no effect of CF presence on ENaC expression.

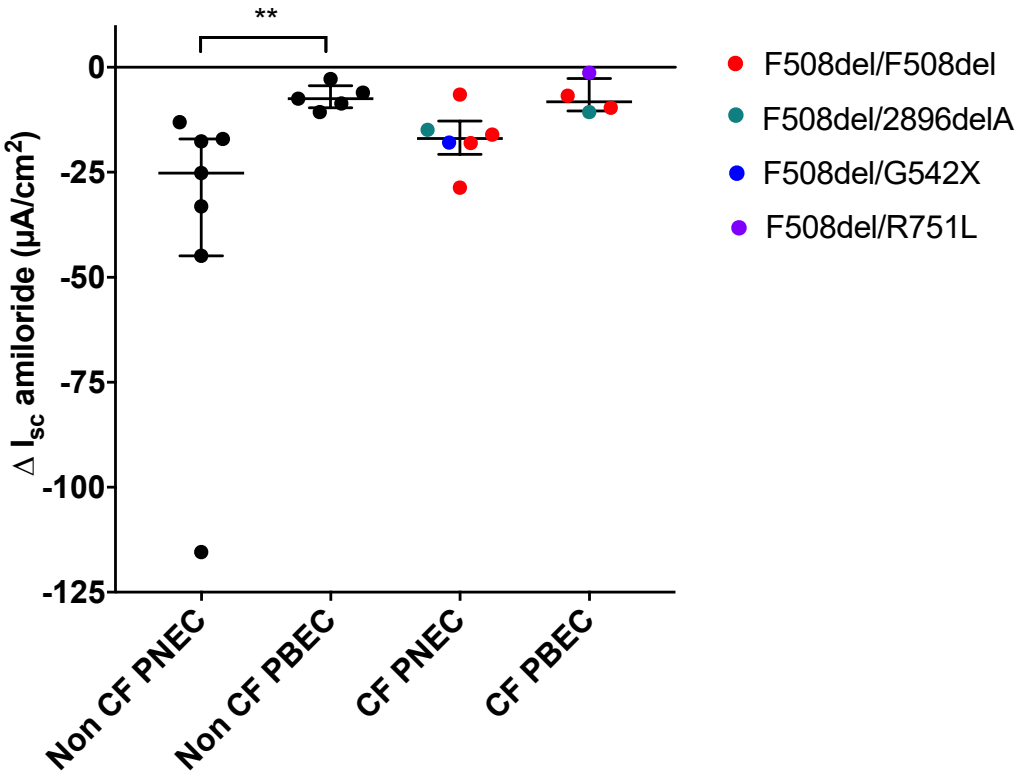

Figure 52: Assessment of amiloride-sensitive short circuit current in non-CF and CF PNEC and PBEC cultures

The amiloride-sensitive change in short circuit current (ΔI_{sc} amiloride) was assessed in differentiated PNEC and PBECs at 25 to 33d ALI in Ussing chamber experiments. Each point represents the mean amiloride-sensitive I_{sc} for each donor investigated. Data is presented as median ± IQR and analysed with Kruskal-Wallis and post hoc Dunn's multiple comparison test; **p=0.009; non-CF PNECs (n=7 donors, 25 inserts), non-CF PBECs (n=5 donors, 21 inserts), CF PNECs (n=6 donors, 20 inserts), CF PBECs (n=4 donors, 17 inserts). *CFTR* mutations for each donor are colour-coded as shown in the legend.

4.4.4 Assessment of epithelial sodium channel subunit expression

ENaC is composed of three homologous subunits, α, β and γ which together form the functional channel pore in the apical airway epithelium (Canessa et al., 1994). RT-qPCR analysis was performed in differentiated paediatric ALI cultures from 25 to 33d ALI to determine the relative mRNA expression of each subunit (Figure 53).

In non-CF cultures, no differences in *α-ENaC* were apparent in PNECs versus PBECs (1.0-fold change $\pm$0.7) as shown in Figure 53A. Overall there was a 2.3-fold $\pm$2.0 (mean $\pm$ SD) increase in *β-ENaC* expression in non-CF PBECs versus non-CF PNECs (Figure 53A). However, there was no significant increase in the corresponding $2^{-\Delta CT}$ analysis of relative gene expression (Figure 54B). There was a 1.5-fold $\pm$1.3 increase in *γ-ENaC* expression in non-CF PBECs versus PBECs (Figure 53A), however, the corresponding analysis of $2^{-\Delta CT}$ was not significant Figure 54C).

In CF cultures, there was a 1.7-fold $\pm$0.1 increase in *α-ENaC* expression in CF PBECs versus PNECs (Figure 53B). *β-ENaC* expression was similar in the two groups (1.1-fold $\pm$0.2). *γ-ENaC* expression was increased by 2.9-fold $\pm$2.5 in CF PBECs versus PNECs. However, again, these were not accompanied by statistical changes in gene expression assessed by $2^{-\Delta CT}$ analysis (Figure 54).

Gene expression and relative fold change analysis of each subunit was also performed to determine any differences between CF and non-CF cultures in the nasal and bronchial groups. In PNECs (Figure 53C), no differences were found in *α-ENaC* expression between CF and non-CF cultures (fold change of 1.0 $\pm$0.8). There was a 2.3-fold $\pm$2.0 increase in *β-ENaC* expression in CF versus non-CF PNECs. *γ-ENaC* expression was reduced in CF PNECs by 0.6-fold $\pm$0.3 relative to non-CF PNECs. There were no significant differences seen in $2^{-\Delta CT}$ analysis of gene expression for these comparisons (Figure 54). Assessment in bronchial cultures (Figure 53D) suggested increased expression of all three subunits in CF versus non-CF PBECs: *α-ENaC*: 1.5 $\pm$0.1, *β-ENaC*: 1.7 $\pm$0.5 and *γ-ENaC*: 1.6 $\pm$1.4. However, the $2^{-\Delta CT}$ analysis of gene expression for these analyses were not statistically significant, potentially attributable to the low sample numbers in the CF group (Figure 54).

Overall, the predominant subunit expressed by all ALI cultures was *α-ENaC,* with *γ-ENaC* expressed the least (Figure 55). However, there was considerable variability

evident in expression of all three subunits in all ALI cultures. To further highlight the evidence of this variability between disease and non-disease groups, the fold change of each subunit for each individual CF culture relative to the pooled expression for non-CF cultures has been presented below for PNECs (Figure 56A) and PBECs (Figure 56B). In the PNEC group, all cultures except PCF15N, PCF23N and PCF28N displayed an increase in at least one *ENaC* subunit expression. Notably, there was no consistency in the specific subunit that was elevated amongst CF cultures. The cultures which showed either similar or reduced fold changes were all isolated from children with severe disease genotypes (F508del/F508del and F508del/2896delA). Interestingly, PCF15N and PCF28N were isolated from the same F508del/F508del donor but sampled 1 year apart. Although the CF PBEC samples available for RT-qPCR investigation were small, it is evident from these 2 cultures that there was an increase in *ENaC* subunit expression in CF versus non-CF PBECs, again with variability of specific subunits between the 2 samples.

To determine any potential relationship of ENaC expression with functional activity, the correlation of each subunit with the amiloride-sensitive I_{sc} was investigated in differentiated ALI cultures where both experimental techniques were performed. Spearman rank correlation assessment of all ALI cultures did not reveal any relationship between *ENaC* subunit expression and amiloride-sensitive I_{sc} as demonstrated in Figure 57 (α-*ENaC*: r=-0.03, p=0.9; β-*ENaC:* r=-0.13, p=0.6; γ-*ENaC*: r=-0.22, p=0.39). Further subgroup analysis of each culture group did not reveal any correlations of ENaC subunit mRNA expression with amiloride-sensitive I_{sc} (not shown).

These findings show that in this cohort of ALI cultures, there was no correlation of *ENaC* subunit mRNA expression with functional ENaC assessment as investigated by the amiloride-sensitive I_{sc}.

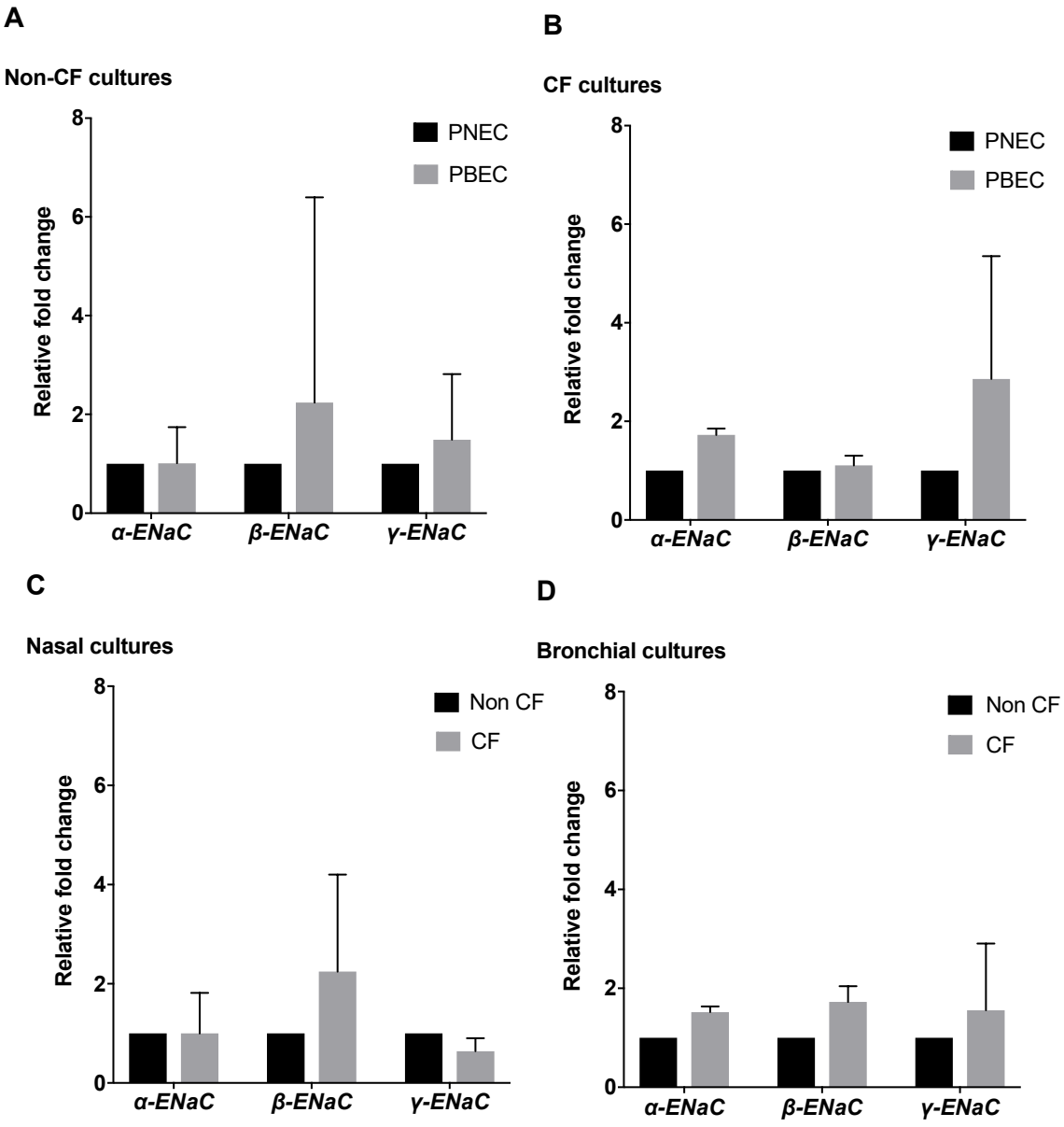

Figure 53: Relative fold change of *α-ENaC*, *β-ENaC* an d *γ-ENaC* in all cultures

Relative fold changes of *α-ENaC, β-ENaC* and *γ-ENaC* expression were determined in PBECs relative to PBECs in non-CF (A) and CF (B) PNEC (black) and PBEC (grey) cultures (B) as assessed by RT-qPCR. Comparisons were also made between CF relative to non-CF cultures in PNECs (C) and PBECs (D); non-CF PNECs: n=8 donors. Bars represent mean ± SD; non-CF PBECs: n=8 donors, CF PNECs: n=8 donors; CF PBECs: n=2 donors.

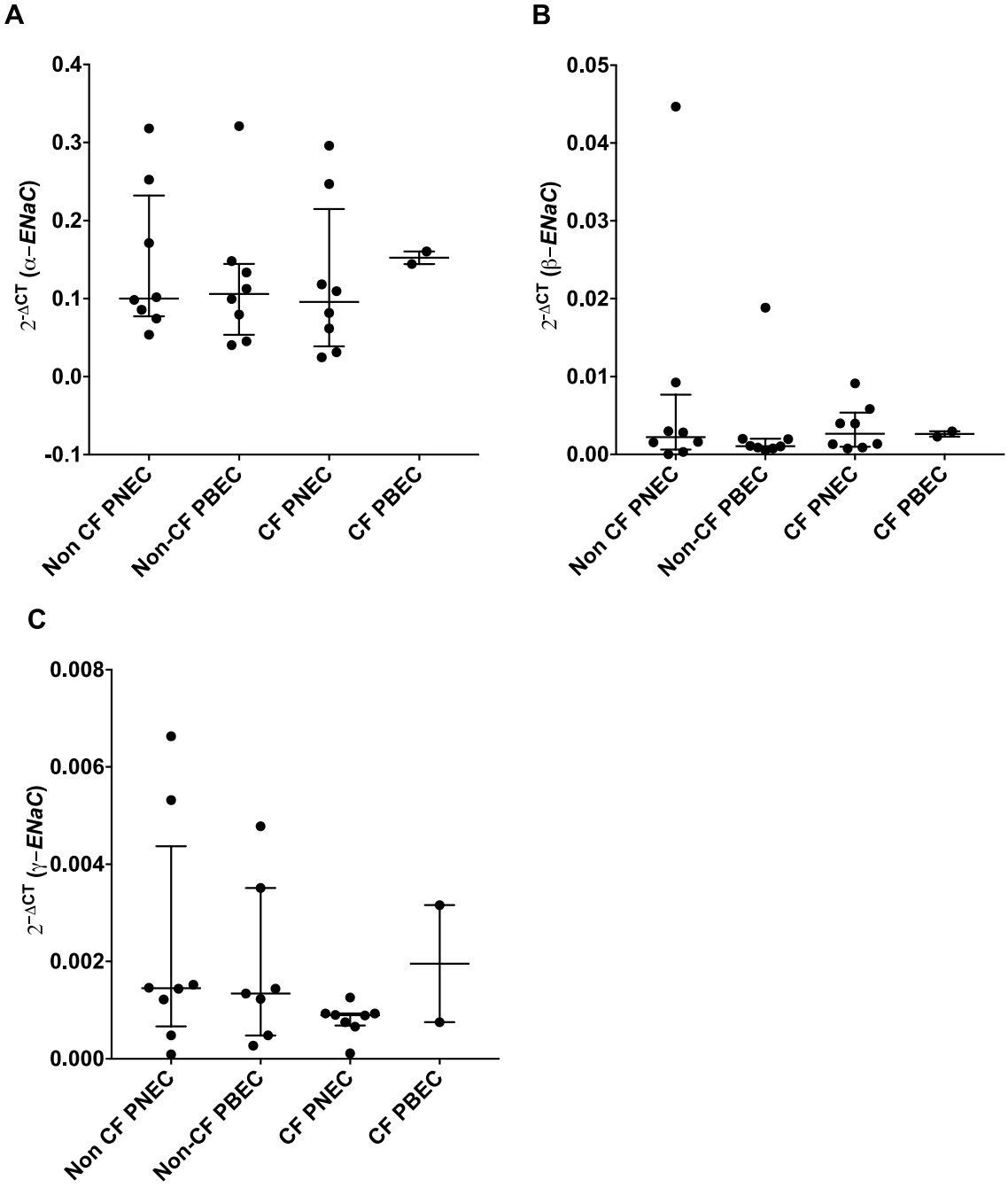

Figure 54: Relative gene expression of *α-ENaC*, *β-ENaC* and *γ-ENaC* in all non-CF and CF PNEC and PBEC cultures

α-ENaC (A), *β-ENaC* (B) and *γ-ENaC* (C) expression were assessed in differentiated cultures at around 28d ALI using RT-qPCR. $2^{-\Delta CT}$ values were calculated to determine relative gene expression and complement data for relative fold change. Data is displayed as the median ±IQR and analysed with Kruskal-Wallis and post hoc Dunn's multiple comparison test; p>0.99 for all comparisons; non-CF PNECs (n=8), non-CF PBECs (n=8, n=7 for *ENaC-γ*); CF PNECs (n=8), CF PBECs (n=2).

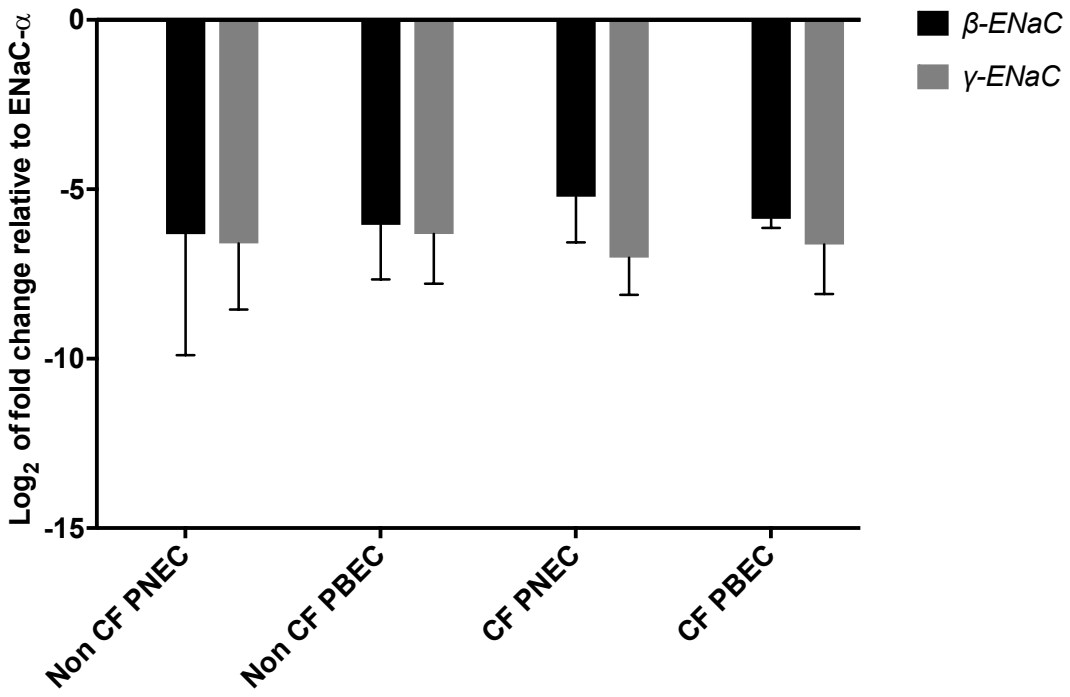

Figure 55: Log_2 fold change of *β-ENaC* and *γ-ENaC* relative to *α-ENaC* expression in all non-CF and CF PNEC and PBEC cultures

Relative fold change of *β-ENaC* and *γ-ENaC* relative to *α-ENaC* is demonstrated above by calculating the log_2 fold change of subunits in each culture group. Bars represent mean ± SD; non-CF PNECs (n=8), non-CF PBECs (n=8, n=7 for *ENaC-γ*); CF PNECs (n=8), CF PBECs (n=2).

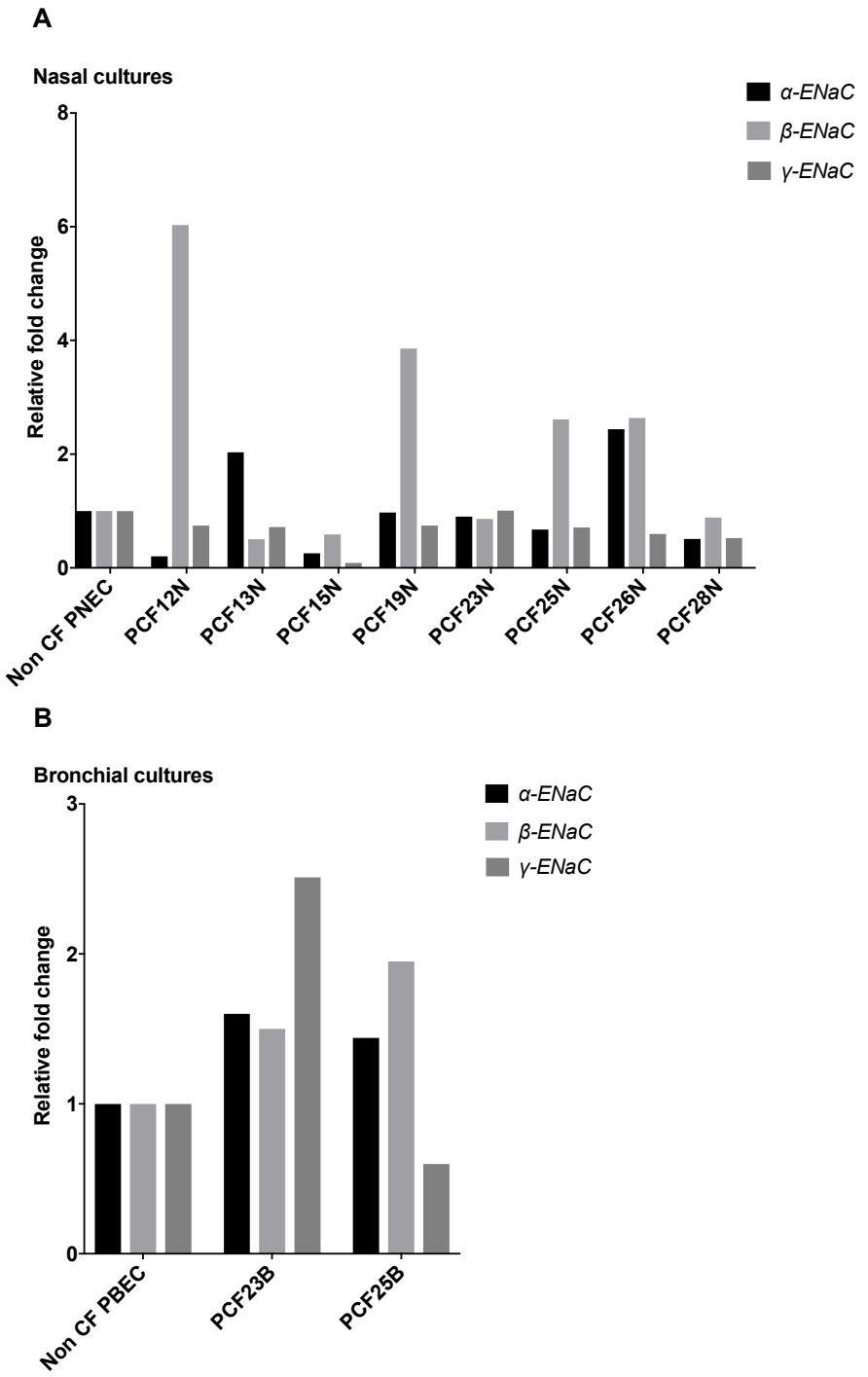

Figure 56: Relative fold change of *ENaC* subunit expression in CF cultures

Fold change of *ENaC* subunit expression in each CF PNEC culture was assessed relative to the pooled expression of non-CF PNECs as shown in A (n=8 non-CF PNECs, n=8 CF PNECs). Fold change of *ENaC* subunit expression in each CF PBEC culture was assessed relative to the pooled expression of non-CF PBECs as shown in B (n=8 non-CF PBECs, n=2 CF PBECs).

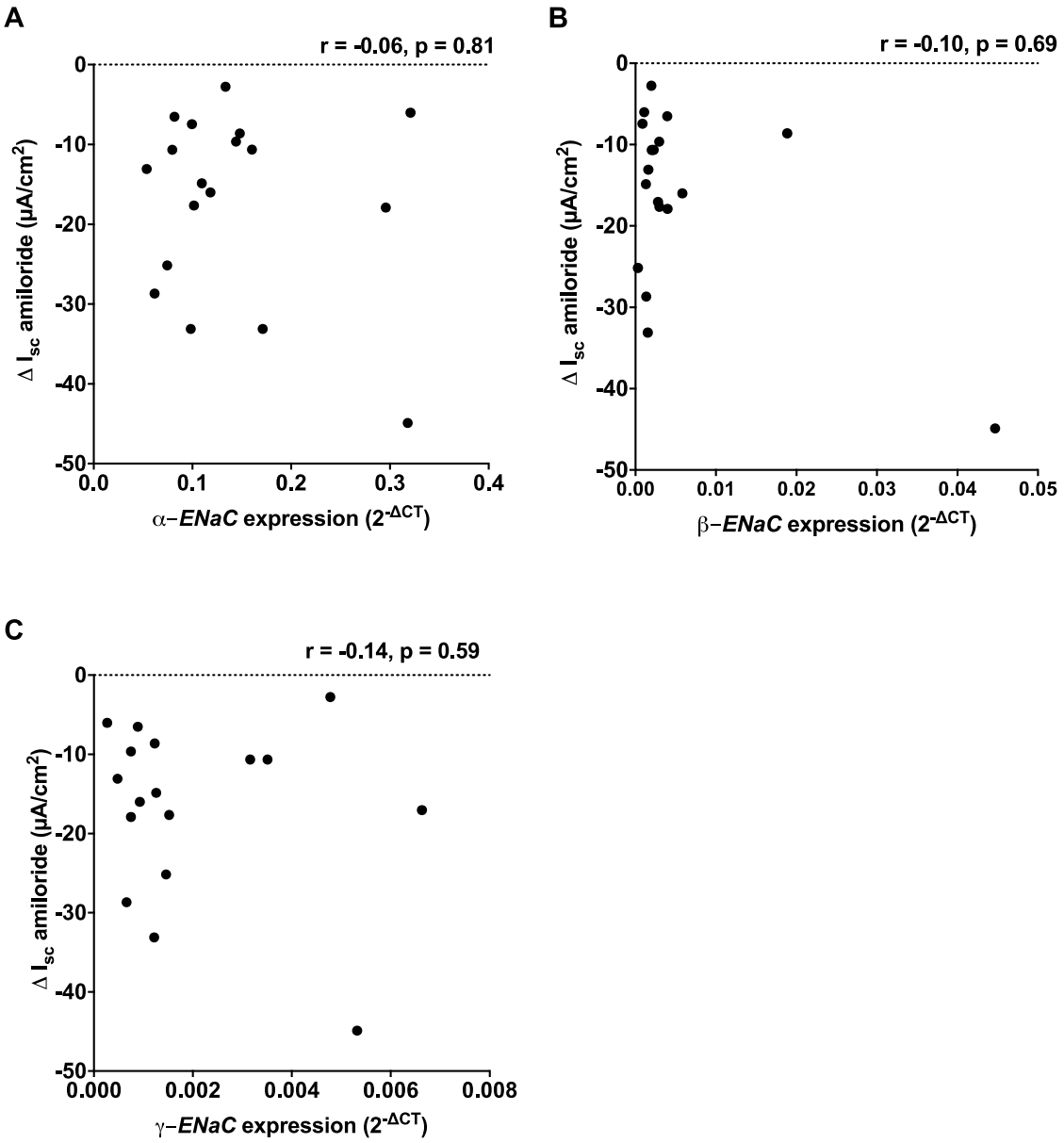

Figure 57 : Correlation of *α-ENaC* expression with the amiloride-sensitive short circuit current

Spearman analysis of correlation was performed for expression of *α-ENaC* (A), *β-ENaC* (B) and *γ-ENaC* (C) as measured by $2^{-\Delta CT}$ with corresponding assessment of amiloride-sensitive short circuit current (I_{sc}) in all CF and non-CF PNEC and PBEC cultures. The correlation coefficient (r) was calculated whereby r of 1.0 indicates perfect correlation, 0.0 is no correlation and -1.0 refers to perfect inverse correlation; n=18.

4.4.5 Assessment of epithelial sodium channel function and expression in paired primary nasal and bronchial epithelial cultures

It is possible that the variability in ENaC subunit *mRNA* expression and function across all differentiated ALI cultures could account for the lack of correlation seen. Therefore, further detailed investigation of ENaC function and subunit *mRNA* expression was performed in 3 paired PNEC/PBEC cultures isolated from the same non-CF donors (Figure 58 to Figure 60) and 2 paired PNEC/PBEC cultures from the same CF donors (Figure 61 and Figure 62) to ascertain any potential relationships.

In the 3 paired non-CF cultures, PWT8, PWT11 and PWT17, the amiloride-sensitive I_{sc} was greater in all PNEC cultures versus their PBEC counterparts. This effect was greatest in the PWT11 cultures: PNEC: median -33.8 $\mu A/cm^2$, IQR -29.5 to -36.4 versus PBEC: -2.7, IQR -2.4 to -3.2; p=0.004 (Figure 59). Increased PNEC I_{sc} responses were also statistically significant in PWT8 cultures (PNEC: -43.0 $\mu A/cm^2$, IQR -39.1 to -52.7 versus PBEC: -8.3, IQR -7.5 to -10.1, p=0.03) and PWT17 cultures (PNEC: -15.1, IQR -12.7 to -22.3 versus PBEC: -10.1, IQR -9.2 to -12.0, p=0.02) as shown in Figure 58 and Figure 60 below.

These changes were accompanied by increased α-*ENaC* expression in PNECs relative to PBEC cultures in all non-CF cultures as demonstrated in Figure 58 (PWT8), Figure 59 (PWT11) and Figure 60 (PWT17). The resultant percentage increase of α-*ENaC* expression in PNECs was +53 % in PWT8, +22 % in PWT11 and +22 % in PWT17. In PWT8, this was accompanied by increases in β-*ENaC* and γ-*ENaC* of +58 % and +77 % respectively in PNECs. Findings in all three subunits were less cohesive in PWT11 and 17, where expression of γ-*ENaC* decreased in PNECs by 4-fold and 2-fold respectively.

Comparative analysis of the amiloride-sensitive I_{sc} and *ENaC* expression was also investigated in 2 CF paired cultures, PCF23 and PCF25. As evident with the non-CF cultures, the amiloride-sensitive I_{sc} was increased in the PCF23 PNECs (Figure 61), but this difference was not statistically significant (PNEC: -13.8 $\mu A/cm^2$, IQR -9.9 to -19.5 versus PBEC: -10.6, IQR -9.5 to -12.0, p=0.06). Despite this increase in ENaC function in PNECs, there was a 1.5 to 3-fold decrease in expression of all three subunits.

In contrast to all other paired cultures, there were no significant differences in the amiloride-sensitive I_{sc} in PNECs and PBECs derived from the CF PCF25 donor as

shown in Figure 62 (PNEC: -6.4 μA/cm^2, IQR -3.9 to -9.0 versus -9.5, IQR -8.4 to -11.4, p=0.09). This was accompanied by a -76 % decrease in α-*ENaC* expression and increases in β-*ENaC* and γ-*ENaC* of +25 % and +15 % respectively.

Overall, these results suggest that in non-CF paired cultures, the amiloride-sensitive I_{sc} was consistently significantly greater in PNECs, with a suggestion of increased α-*ENaC* mRNA expression. These findings were not evident in all paired CF cultures, with variability in patterns of ENaC subunit expression. However, paired analysis was only possible in CF cultures derived from 2 donors, and warrants further investigation in more donors.

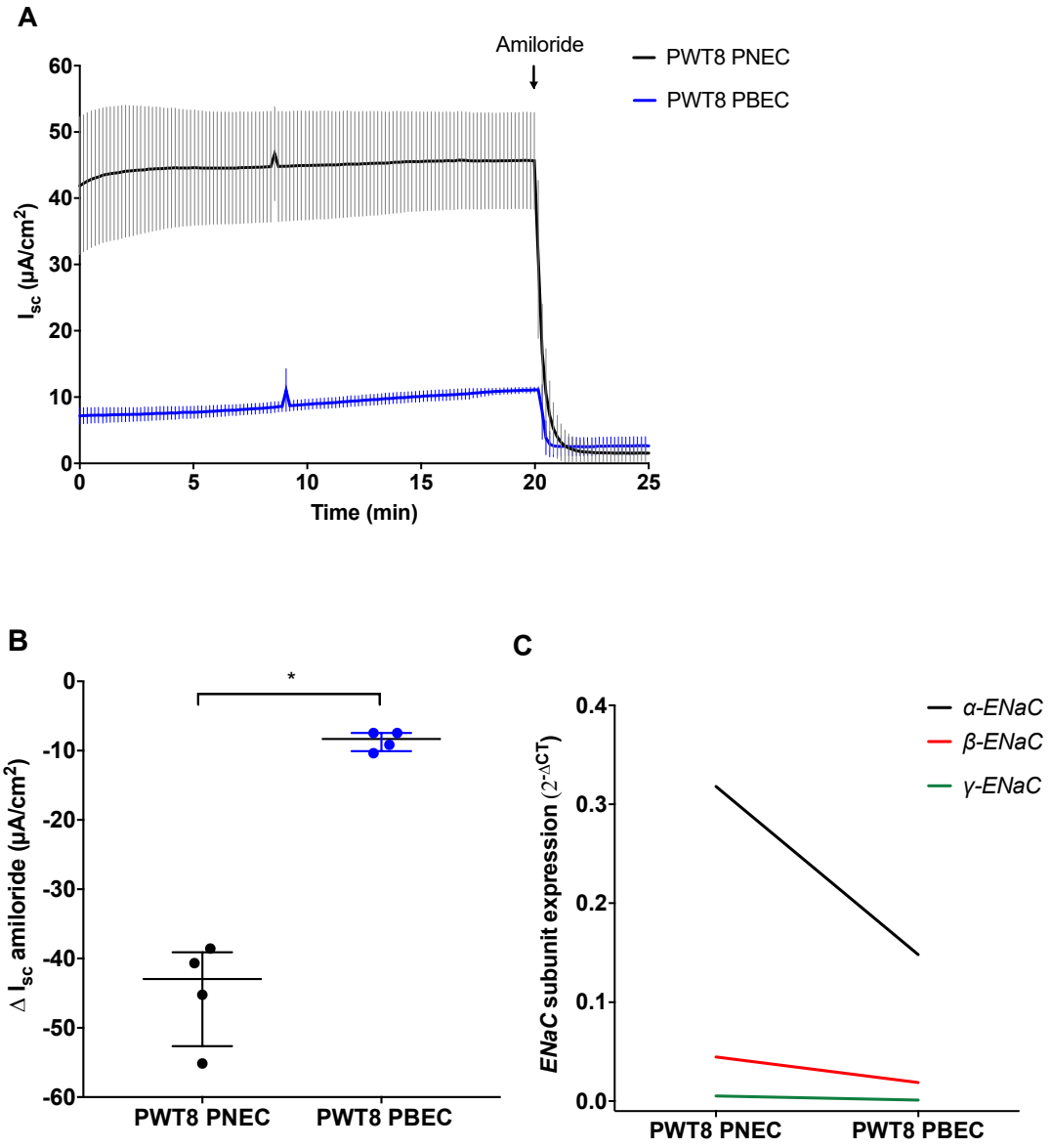

Figure 58: Paired assessment of amiloride-sensitive short circuit current and *ENaC* subunit expression in PNEC and PBEC cultures derived from the non-CF PWT8 donor

Ussing chamber traces for PNEC and PBEC cultures at 28 to 30d ALI isolated from the non-CF PWT8 donor are shown in A. The lines represent the mean short circuit current (I_{sc}) with error bars for the SD (PNEC in black, PBEC in blue). Corresponding amiloride-sensitive I_{sc} responses (ΔI_{sc} amiloride) are shown in B; data is presented as median ±IQR and analysed with Mann-Whitney test, *p=0.03; n=4 inserts for each culture type. mRNA expression of α (black), β (red) and γ-*ENaC* (green) are shown in C.

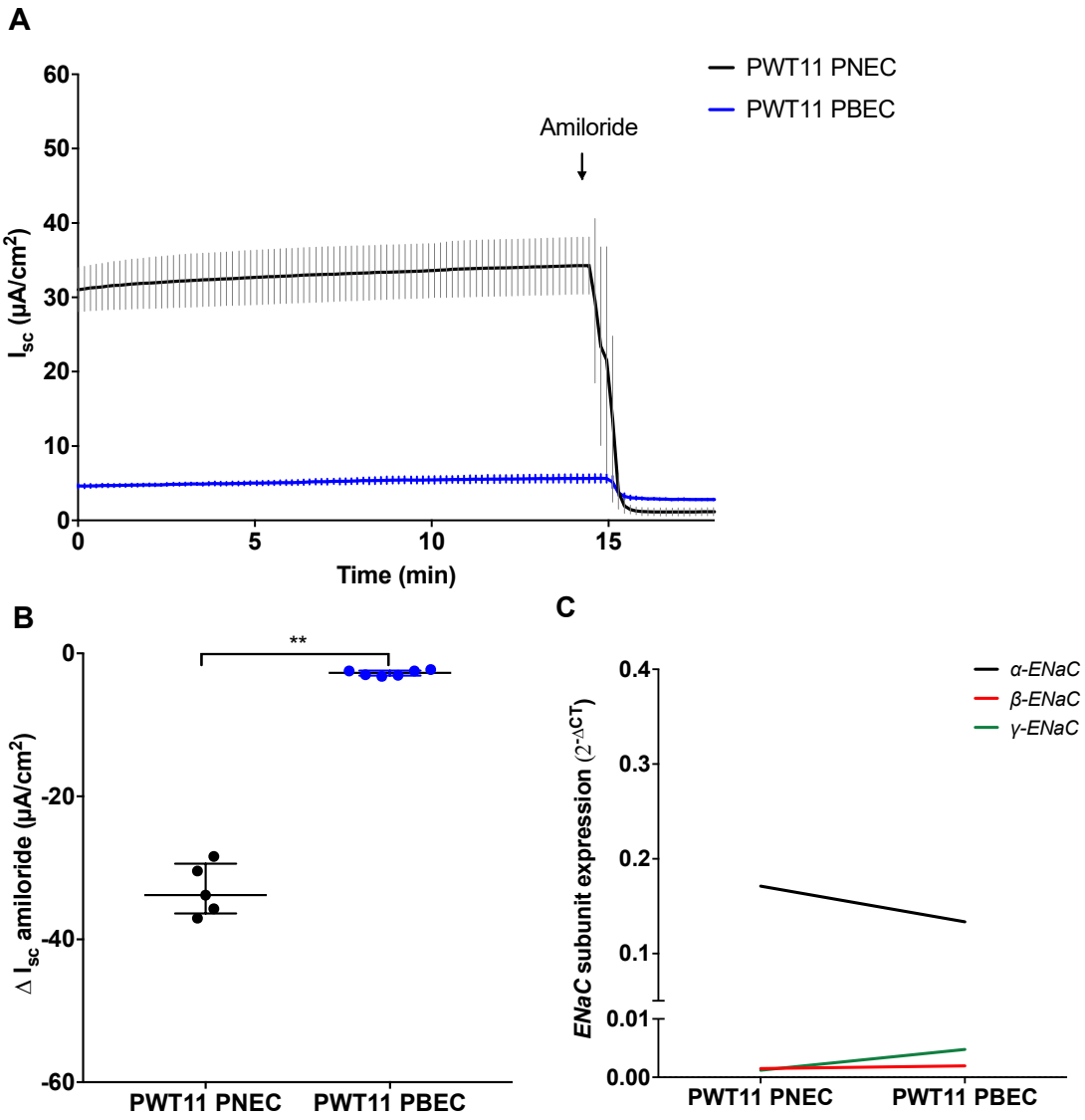

Figure 59: Paired assessment of amiloride-sensitive short circuit current and *ENaC* subunit expression in PNEC and PBEC cultures derived from the non-CF PWT11 donor

Ussing chamber traces for PNEC and PBEC cultures at 28 to 30d ALI isolated from the non-CF PWT11 donor are shown in A. The lines represent the mean short circuit current (I_{sc}) with error bars for the SD (PNEC in black, PBEC in blue). Corresponding amiloride-sensitive I_{sc} responses (ΔI_{sc} amiloride) are shown in B; data is presented as median ±IQR and analysed with Mann-Whitney test, **p=0.004; PNEC: n=5 inserts; PBEC: n=6 inserts. mRNA expression of α (black), β (red) and γ-*ENaC* (green) are shown in C.

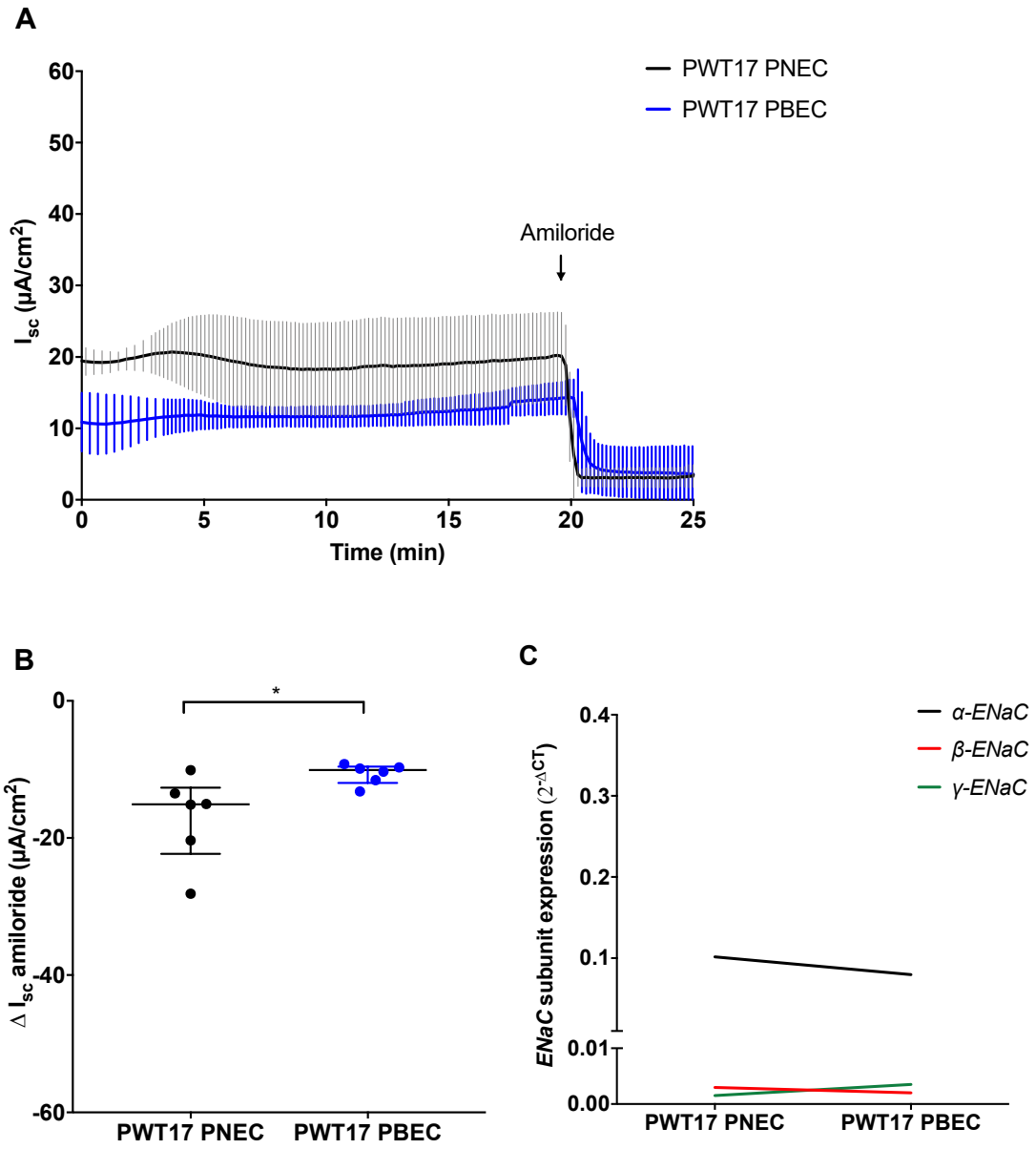

Figure 60: Paired assessment of amiloride-sensitive short circuit current in PNEC and PBEC cultures derived from the non-CF PWT17 donor

Ussing chamber traces for PNEC and PBEC cultures at 28 to 30d ALI isolated from the non-CF PWT17 donor are shown in A. The lines represent the mean short circuit current (I_{sc}) with error bars for the SD (PNEC in black, PBEC in blue). Corresponding amiloride-sensitive I_{sc} responses (ΔI_{sc} amiloride) are shown in B; data is presented as median ±IQR and analysed with Mann-Whitney test, *p=0.02; PNEC: n=6 insert for each culture type. mRNA expression of α (black), β (red) and γ-*ENaC* (green) are shown in C.

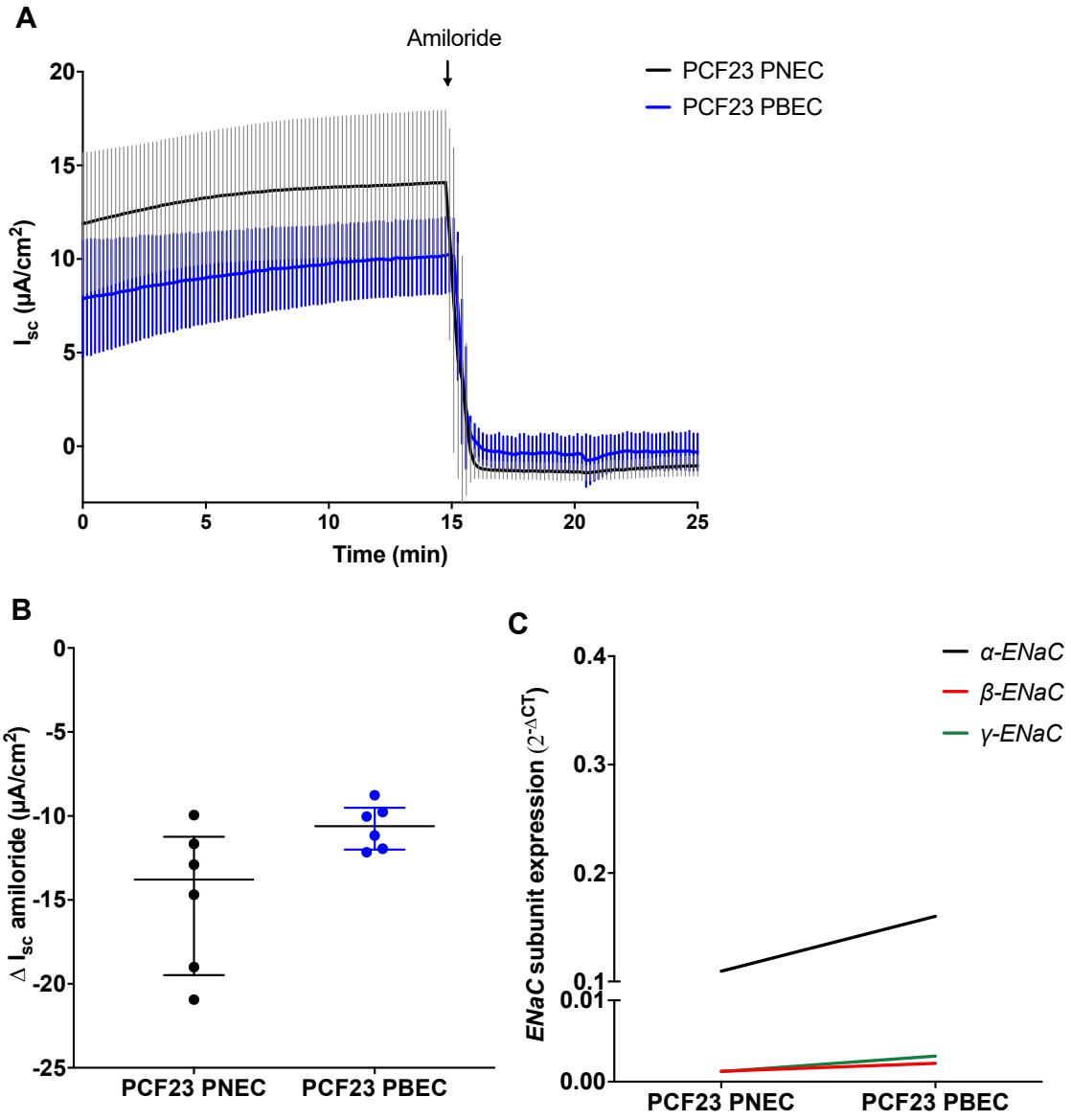

Figure 61: Paired assessment of amiloride-sensitive short circuit current in PNEC and PBEC cultures derived from the CF PCF23 donor

Ussing chamber traces for PNEC and PBEC cultures at 28 to 30d ALI isolated from the CF PCF23 donor (F508del/2896delA) are shown in A. The lines represent the mean short circuit current (I_{sc}) with error bars for the SD (PNEC in black, PBEC in blue). Corresponding amiloride-sensitive I_{sc} responses (ΔI_{sc} amiloride) are shown in B; data is presented as median ±IQR and analysed with Mann-Whitney test (no statistical differences found); n=6 inserts for each culture type. mRNA expression of α (black), β (red) and γ-*ENaC* (green) are shown in C.

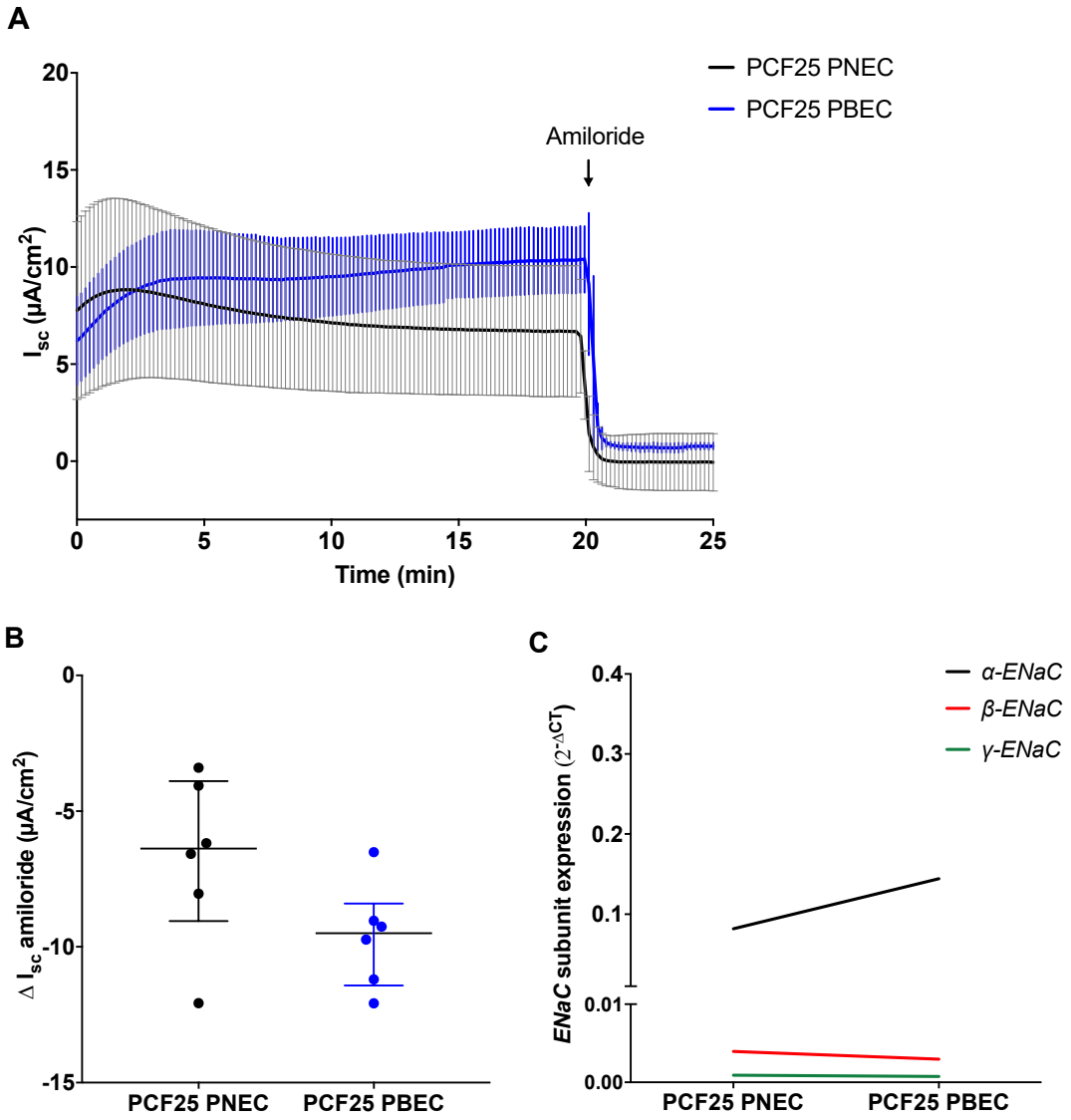

Figure 62: Paired assessment of amiloride-sensitive short circuit current in PNEC and PBEC cultures derived from the CF PCF25 donor

Ussing chamber traces for PNEC and PBEC cultures at 28 to 30d ALI isolated from the CF PCF25 donor (F508del/F508del) are shown in A. The lines represent the mean short circuit current (I_{sc}) with error bars for the SD (PNEC in black, PBEC in blue). Corresponding amiloride-sensitive I_{sc} responses (ΔI_{sc} amiloride) are shown in B; data is presented as median ±IQR and analysed with Mann-Whitney test (no statistical differences found); n=6 inserts for each culture type. PBEC: n=6 inserts. mRNA expression of α (black), β (red) and γ-*ENaC* (green) are shown in C.

4.4.6 Investigation of CFTR channel expression

Given the importance of CFTR-mediated chloride secretion in the airways, CFTR channel function was investigated in paediatric differentiated ALI cultures. This was performed firstly to verify the presence and absence of CFTR function in non-CF and CF cultures respectively, and secondly to compare PNEC with PBEC responses and determine the suitability of PNECs for CF research.

CFTR-mediated chloride secretion was assessed in paediatric differentiated ALI cultures from 25 to 33d ALI in Ussing chamber experiments as described in Chapter 2. In view of the significant contribution of ENaC to the basal I_{sc}, it was important to first inhibit ENaC before exploring CFTR function. Forskolin, an activator of cAMP, was applied to the apical compartment of the Ussing chamber to determine its effect on CFTR-mediated chloride secretion. After a period of 5 to 10 minutes to enable I_{sc} stabilisation, $CFTR_{inh}$-172 was applied apically for selective CFTR inhibition.

To exemplify responses to forskolin and $CFTR_{inh}$-172 on I_{sc} and TEER in non-CF cultures, Ussing chamber traces of PBECs isolated from the non-CF PWT8 donor are shown in Figure 63. A 125mM chloride Krebs solution was added to the apical and basolateral compartments and maintained at 5 % CO_2 and 37 °C. After a 20-minute period to enable basal I_{sc} stabilisation, 10 μM amiloride was added to the apical chamber to inhibit ENaC. This decreased I_{sc} by -7.6 $\mu A/cm^2$ and increased TEER by 189.7 $\Omega.cm^2$. Apical addition of 10 μM forskolin resulted in a robust and rapid I_{sc} increase of 18.6 $\mu A/cm^2$ (with an initial peak and eventual plateau) and TEER decrease of 174.0 $\Omega.cm^2$. $CFTR_{inh}$-172 (20 μM) was added apically to inhibit CFTR activity, which decreased I_{sc} by -15.6 $\mu A/cm^2$ and increased TEER by 413.3 $\Omega.cm^2$. This decline was initially rapid and followed by a more gradual response.

Forskolin and $CFTR_{inh}$-172 responses in CF cultures are shown in representative Ussing chamber traces from PBECs isolated from the CF PCF23 donor in Figure 64. This donor had the F508del/2896delA genotype, resulting in a severe clinical phenotype, pancreatic insufficiency and elevated diagnostic sweat chloride of 112 mmol/L. The mean magnitude of the amiloride-sensitive I_{sc} was -12.2 $\mu A/cm^2$ with an TEER increase of 148.9 $\Omega.cm^2$. As predicted, responses to CFTR activation and inhibition were minimal. Forskolin induced a very small increase in mean I_{sc} of +0.24 $\mu A/cm^2$ and a reduction of TEER by 35.3 $\Omega.cm^2$. The response to $CFTR_{inh}$-172 was small, with a change in mean I_{sc} of -0.7 $\mu A/cm^2$ and no change in TEER.

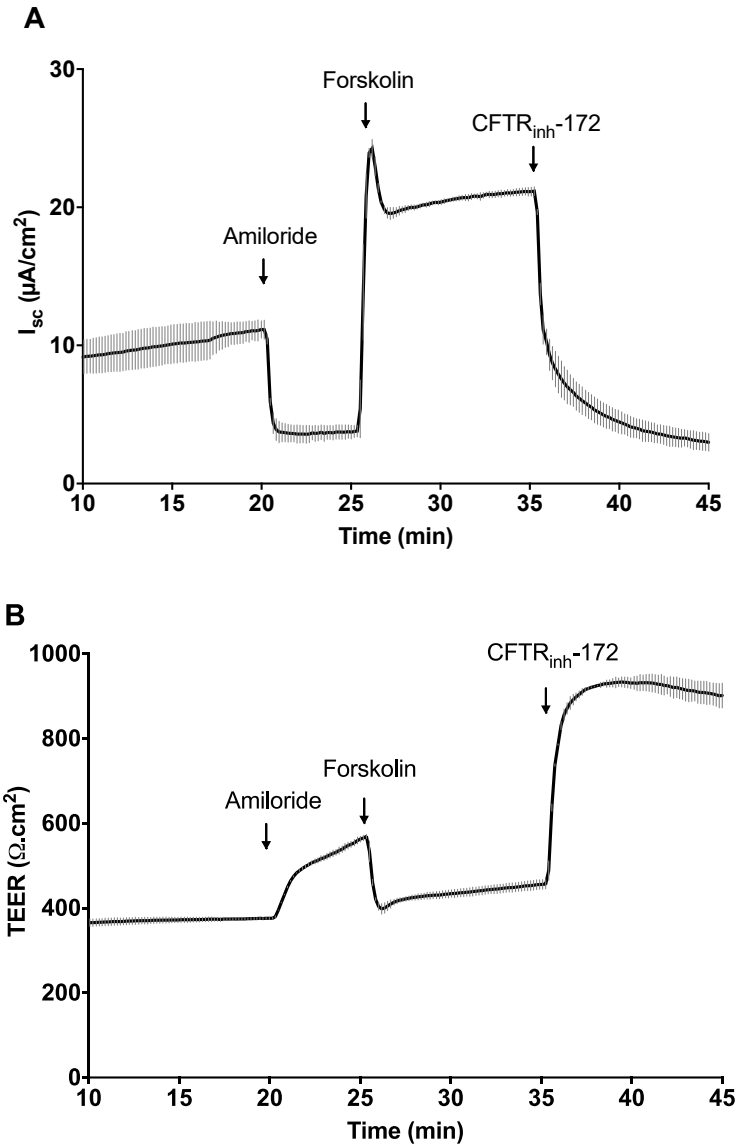

Figure 63: Representative Ussing chamber traces of short circuit current and transepithelial electrical resistance responses to forskolin and $CFTR_{inh}$-172 in a non-CF PBEC culture

A PBEC ALI culture insert derived from the non-CF PWT8 donor was mounted in the Ussing chamber and bathed apically and basolaterally in 125 mM chloride Krebs. After a 20-minute period of stabilisation, 10 μM amiloride was added to the apical compartment to inhibit ENaC. 10 μM forskolin and 20 μM $CFTR_{inh}$-172 were added apically at 25 and 35 minutes respectively. Resultant short circuit current (I_{sc}) and corresponding transepithelial electrical resistance (TEER) were measured as shown in A and B respectively. Lines mean responses in 2 inserts with error bars for the SD.

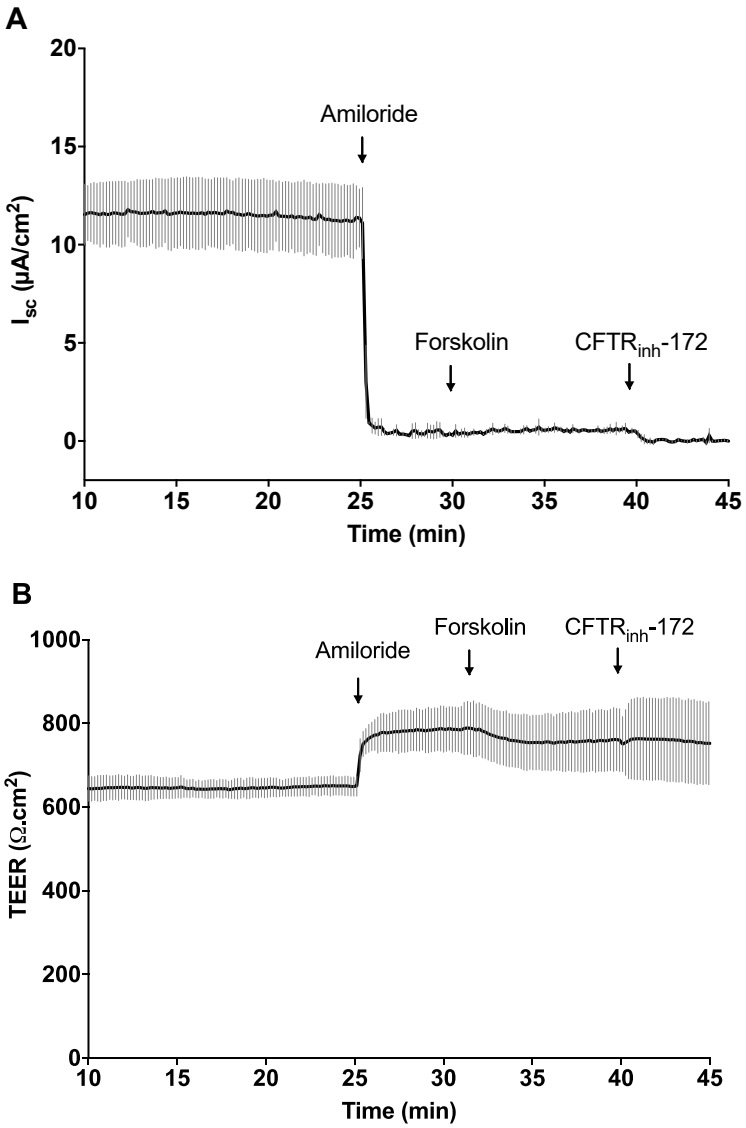

Figure 64: Representative Ussing chamber traces of short circuit current and transepithelial electrical resistance responses to forskolin and $CFTR_{inh}$-172 in a CF PBEC culture

A CF PBEC ALI culture insert (PCF23B) was mounted in the Ussing chamber and bathed apically and basolaterally in 125 mM chloride Krebs. After a 25-minute period of stabilisation, 10 μM amiloride was added to the apical compartment to inhibit ENaC. 10 μM forskolin and 20 μM $CFTR_{inh}$-172 were added apically at 30 and 40 minutes respectively. Resultant short circuit current (I_{sc}) and corresponding transepithelial electrical resistance (TEER) were measured as shown in A and B respectively. Lines mean responses in 2 inserts with error bars for the SD.

4.4.7 Assessment of CFTR function

To determine if there were any differences in I_{sc} responses to forskolin and $CFTR_{inh}$-172 between PNEC and PBEC cultures isolated from non-CF and CF donors, Ussing chamber experiments were performed in 7 non-CF PNEC, 5 non-CF PBEC, 6 CF PNEC and 4 CF PBEC cultures at 25 to 33d ALI. The calculated changes in I_{sc} in response to forskolin and $CFTR_{inh}$-172 are shown in Figure 65. CF donor responses have been colour-coded according to genotype.

In non-CF cultures, no significant differences were found with forskolin-induced I_{sc} responses in PNECs versus PBECs (non-CF PNECs: median 14.3 $\mu A/cm^2$, IQR 13.1 to 22.1 versus non-CF PBECs: 11.5 $\mu A/cm^2$, IQR 7.9 $\mu A/cm^2$ to 23.3, p>0.999). As shown in Figure 65, there were no differences in the $CFTR_{inh}$-172-sensitive I_{sc} in non-CF PNECs versus PBECs (non-CF PNECs: -12.6 $\mu A/cm^2$, IQR -11.5 to -22.2 versus -9.7 6 $\mu A/cm^2$, IQR -7.3 to -15.9, p>0.999). As evident from these results, there was considerable inter-donor variability in forskolin and $CFTR_{inh}$-172 responses in both groups.

In the CF group, no significant differences were found in the forskolin-induced I_{sc} (CF PNECs: median 0.05 $\mu A/cm^2$, IQR 0 to 0.5 versus CF PBECs: median 0.3 $\mu A/cm^2$, IQR 0.2 to 0.3, p>0.999) and $CFTR_{inh}$-172-sensitive I_{sc} (CF PNECs: median -0.2 $\mu A/cm^2$, IQR 0 to -0.3 versus CF PBECs: median -0.4 $\mu A/cm^2$, IQR -0.2 to -0.5, p>0.999). These results indicated no differences between responses to forskolin and $CFTR_{inh}$-172 in this cohort of PNECs and PBECs.

As expected, comparative assessment in nasal cultures showed significantly greater responses to forskolin (p=0.002) and $CFTR_{inh}$-172 (p=0.001) in non-CF PNECs compared with CF PNECs. Interestingly, these differences were not significant in non-CF versus CF PBECs (forskolin: p=0.2; $CFTR_{inh}$-172: p=0.3). There was a distinct outlier in the CF PBEC group showing a mean forskolin-induced I_{sc} of 4.4 $\mu A/cm^2$ ($\pm$ SD 4.0) and a CFTRinh-172-sensitive I_{sc} of -5.3 $\mu A/cm^2$ ($\pm$4.8). These cultures were derived from a donor with the F508del/R751L genotype (PCF24). Removal of this donor from the analysis did not affect the significance when analysed with the same statistical test (forskolin: p=0.2; $CFTR_{inh}$-172: 0.4). Lack of significance is most likely explained by the relatively small sample size of the CF PBEC group and highlights the need to explore this further in a larger number of donors.

Amongst CF PBEC cultures isolated from donors with severe mutations, a small-forskolin induced I_{sc} was evident ranging from 0.5 to 0.6 $\mu A/cm^2$ in PNECs and 0.2 to 0.3 $\mu A/cm^2$ in PBECs. A small $CFTR_{inh}$-172-sensitive I_{sc} was also evident in 4 PNECs (range -0.2 to -0.4 $\mu A/cm^2$) and 3 PBECs (-0.2 to -0.5 $\mu A/cm^2$). A representative Ussing chamber trace from a CF PBEC culture (PCF25 donor, F508del/F508del) is shown in Figure 66 to exemplify these small responses. Despite these changes in I_{sc}, the morphology of the waveform is clearly different to that seen in non-CF cultures (Figure 63) with a more gradual increase in forskolin-induced I_{sc} that is rapidly inhibited by $CFTR_{inh}$-172. Within this CF culture group, 4 cultures were isolated from F508del homozygous donors and 1 from the participant with F508/2896delA. These results suggest that cultures derived from participants harbouring severe disease-causing mutations can demonstrate residual, albeit small, CFTR functional activity.

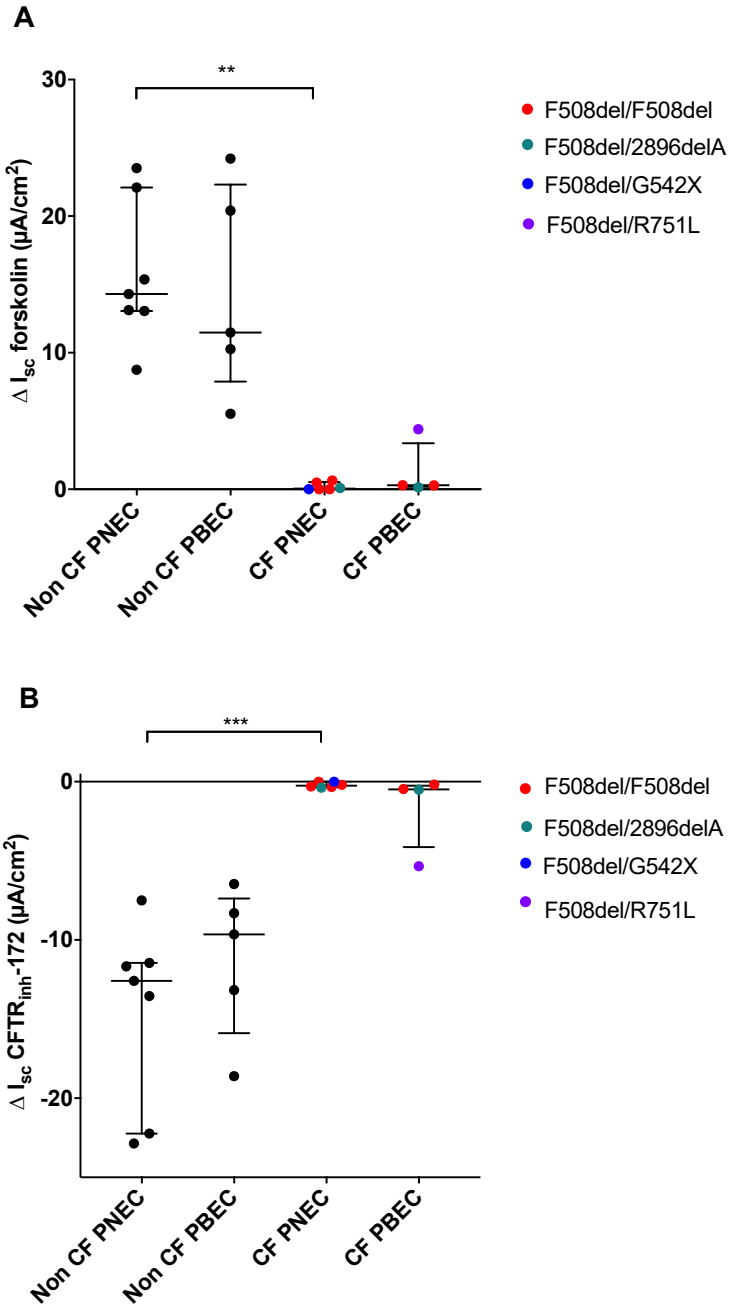

Figure 65: Assessment of short circuit current responses to forskolin and $CFTR_{inh}$-172 in non-CF and CF PNEC and PBEC cultures

The forskolin-induced (ΔI_{sc} forskolin; A) and $CFTR_{inh}$-172-sensitive (ΔI_{sc} $CFTR_{inh}$-172; B) changes in short circuit current were assessed in differentiated PNEC and PBECs at around 28d ALI culture using Ussing chamber experiments. Each point represents the mean ΔI_{sc} for each donor investigated. Data is presented as median ± IQR and analysed with Kruskal-Wallis and post hoc Dunn's multiple comparison test; A: **p=0.002; B: ***p=0.001. Non-CF PNECs (n=7 donors, 25 inserts), non-CF PBECs (n=5, 21 inserts), CF PNECs (n=6, 21 inserts), CF PBECs (n=4, 18 inserts). CF mutation types are colour coded as presented in the legend.

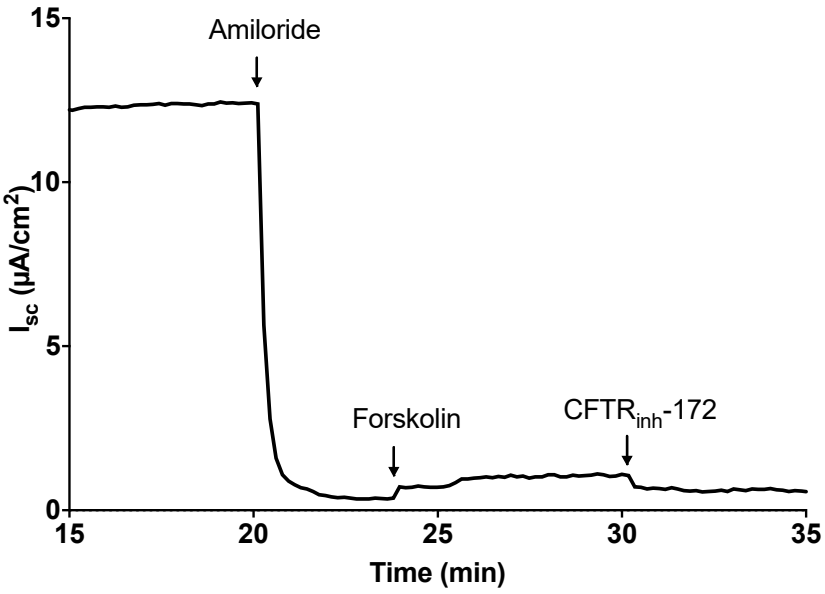

Figure 66: Representative Ussing chamber trace demonstrating residual CFTR activity in a CF PBEC culture

A PBEC ALI culture insert derived from the CF PCF25 donor (F508del/F508del) was mounted in the Ussing chamber and the resultant short circuit current (I_{sc}) was measured with cells bathed apically and basolaterally in 125 mM chloride Krebs. After a 20-minute period of stabilisation, 10 μM amiloride was added to the apical compartment to inhibit ENaC. 10 μM forskolin and 20 μM $CFTR_{inh}$-172 were added apically at 25 and 35 minutes respectively.

4.4.8 Assessment of CFTR function in paired primary nasal and bronchial epithelial cultures

To further investigate any potential differences in I_{sc} responses to forskolin and $CFTR_{inh}$-172 in PNEC and PBEC cultures, comparative assessments were made in 3 paired non-CF and 2 paired CF cultures.

Ussing chamber traces for cultures isolated from the non-CF PWT8 and PWT11 donors with corresponding calculated I_{sc} responses to forskolin and $CFTR_{inh}$-172 are depicted in Figure 67 and Figure 68. Here the shape of the forskolin-induced I_{sc} waveform differed consistently between PNEC and PBEC cultures. In both cases, PBECs demonstrated an initial peaked response, followed by a plateau. This peak was lacking in the PNEC counterparts and finding was not evident in PNEC/PBEC cultures isolated from PWT17 as shown in Figure 69, where the forskolin-induced I_{sc} waveforms were similar. Despite these variations, there were no significant differences found in the magnitude of the median forskolin-induced I_{sc} in paired cultures isolated from PWT8; PNEC median 23.6 $\mu A/cm^2$, IQR 21.9 to 25.0 versus PBEC: 24.3 $\mu A/cm^2$, IQR 20.4 to 27.9, $p > 0.999$ analysed by Mann-Whitney test), PWT11 (PNEC: median 14.6 $\mu A/cm^2$, IQR 10.0 to 15.3 versus PBEC: 11.3 $\mu A/cm^2$, IQR 4.8 to 18.6, $p>0.999$) and PWT17 (PNEC median 6.7 $\mu A/cm^2$, IQR 4.0 to 15.2 versus PBEC: 8.5 $\mu A/cm^2$, IQR 7.0 to 13.8, $p=0.39$).

Despite no differences in forskolin response, the $CFTR_{inh}$-172-sensitive I_{sc} was significantly greater in PNECs isolated from PWT8 compared with PBECs (PNEC: median -22.2 $\mu A/cm^2$, IQR -21.5 to -23.0 versus PBEC: -19.2 $\mu A/cm^2$, IQR -16.5 to -20.1, $p=0.03$). No significant differences were evident in the $CFTR_{inh}$-172-sensitive I_{sc} in cultures derived from PWT11 (PNEC: median -11.6 $\mu A/cm^2$, IQR -9.5 to -13.5 versus PBEC: -12.6 $\mu A/cm^2$, IQR -10.7 to -15.9, $p=0.4$) and PWT17 (PNEC: -6.0 $\mu A/cm^2$, IQR -3.8 to -12.5 versus PBEC: -6.2 $\mu A/cm^2$, IQR -4.9 to -7.9, $p > 0.999$).

Ussing chamber traces for paired I_{sc} responses in PNECs and PBECs isolated from the PCF23 and PCF25 donors with the corresponding calculated I_{sc} responses to forskolin and $CFTR_{inh}$-172 are shown in Figure 70 and Figure 71, respectively. PCF23 cultures did not demonstrate differences in response to forskolin (PNEC: median 0.33 $\mu A/cm2$, IQR 0.15 to 0.44 versus PBEC: 0.21 $\mu A/cm^2$, IQR 0.18 to 0.24, $p=0.31$) and $CFTR_{inh}$-172 (PNEC: median -0.37 $\mu A/cm2$, IQR -0.19 to -0.54 versus PBEC: -0.51 $\mu A/cm^2$, IQR -0.32 to -0.78, $p=0.31$).

This was in contrast to findings evident in cultures derived from PCF25, whereby the $CFTR_{inh}$-172-sensitve I_{sc} was significantly lower in PNECs (PNEC: -0.23 $\mu A/cm^2$, IQR -0.15 to -0.24 versus PBEC: -0.44 $\mu A/cm^2$, IQR -0.35 to -0.58, p=0.04). Although not significant, this was paralleled by a suggested smaller forskolin-induced I_{sc} response in PNECs (PNEC: 0.0 $\mu A/cm^2$, IQR 0 to 0.04 versus PBEC: 0.39 $\mu A/cm^2$, IQR 0.0 to 0.5, p=0.06). These differences are evident in the Ussing chamber traces demonstrated in Figure 71, whereby there is a small but present response to both forskolin and $CFTR_{inh}$-172 in the PCF25 PBEC cultures. Overall, these findings suggest that in cultures derived from both non-CF and CF cultures, there are no significant differences evident in response to forskolin. However, variations in $CFTR_{inh}$-172-senstive I_{sc} responses were evident.

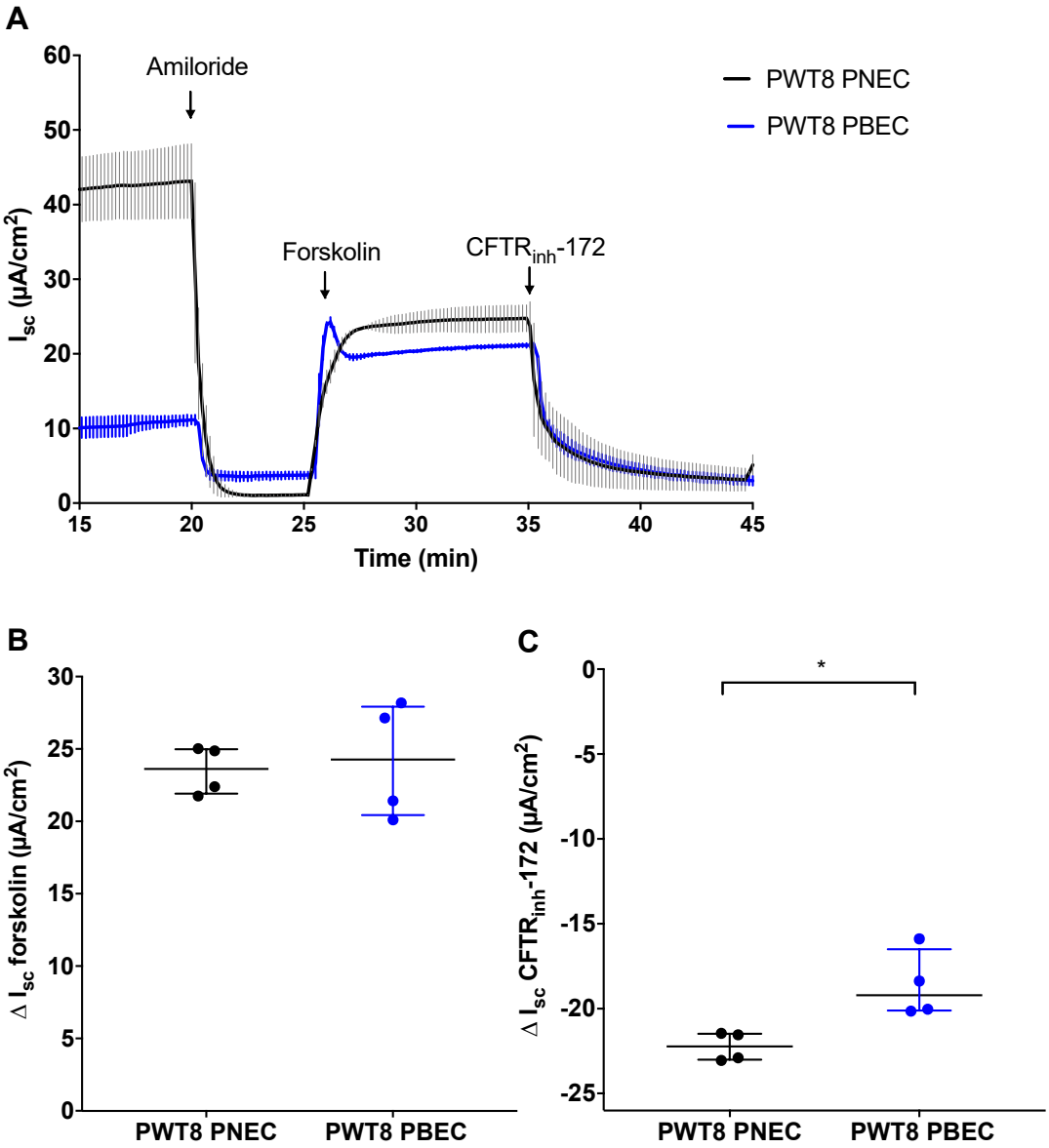

Figure 67 : Paired assessment of forskolin-induced and $CFTR_{inh}$-172-sensitive short circuit current in PNEC and PBEC cultures derived from the non-CF PWT8 donor

Ussing chamber traces for PNEC and PBEC cultures isolated from the non-CF PWT8 donor are shown in A. The lines represents the mean short circuit current (I_{sc}) with error bars for the SD (PNEC in black, PBEC in blue, n=2 inserts for each culture type). The change in I_{sc} (ΔI_{sc}) after forskolin (B) and $CFTR_{inh}$-172 (C) addition was calculated for each experiment. Data is presented as median ±IQR and analysed with Mann-Whitney test, *p=0.03; PNEC: n=4 inserts, PBEC: n=4 inserts.

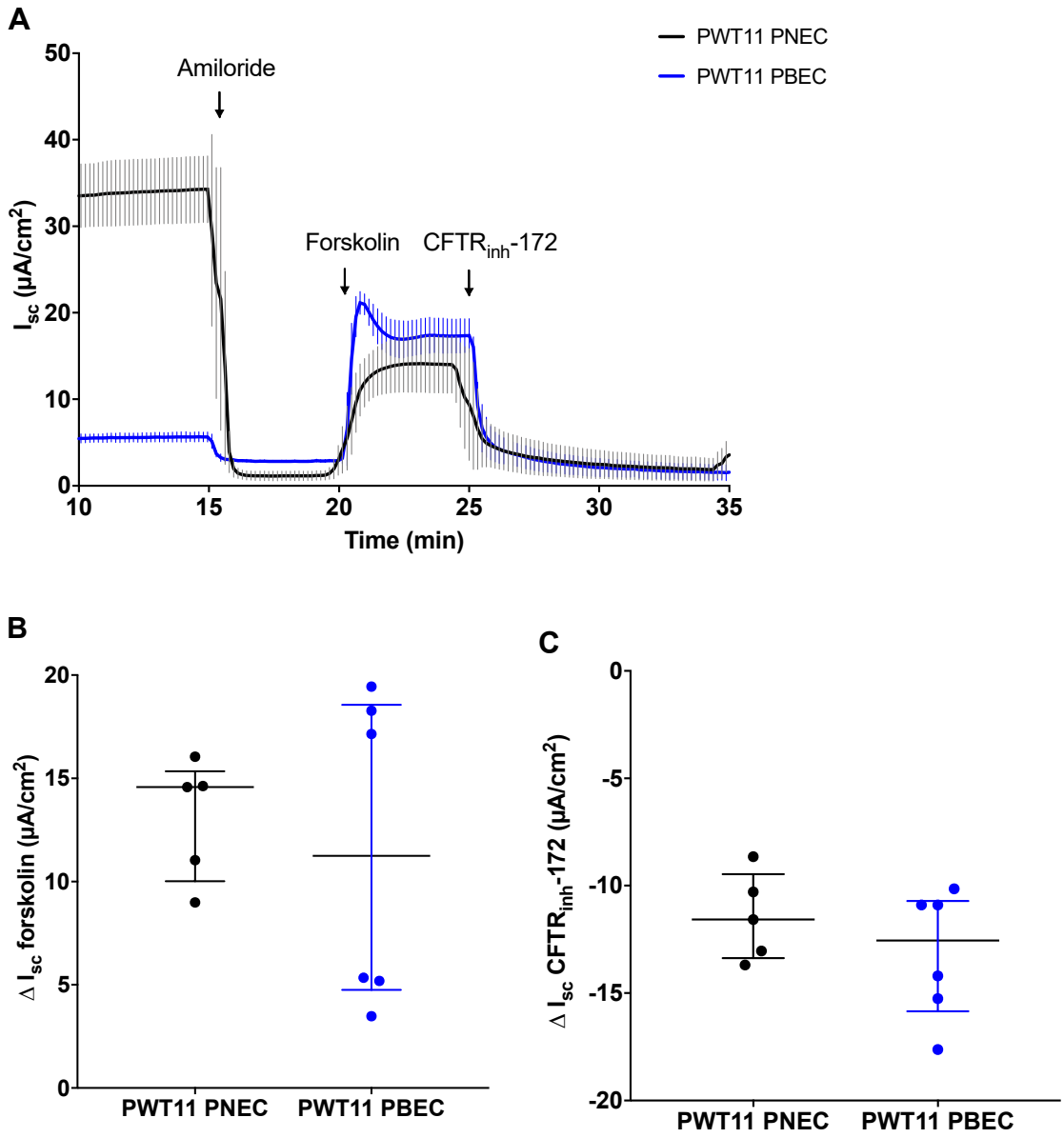

Figure 68: Paired assessment of forskolin-induced and $CFTR_{inh}$-172-sensitive short circuit current in PNEC and PBEC cultures derived from the non-CF PWT11 donor

Ussing chamber traces for PNEC and PBEC cultures isolated from the non-CF PWT11 donor are shown in A. The lines represents the mean short circuit current (I_{sc}) with error bars for the SD (PNEC in black, PBEC in blue, n=5 PNEC inserts, n=3 PBEC inserts). The change in I_{sc} (ΔI_{sc}) after forskolin (B) and $CFTR_{inh}$-172 (C) addition was calculated for each experiment. Data is presented as median ±IQR and analysed with Mann-Whitney test with no statistical differences found; PNEC: n=5 inserts, PBEC: n=6 inserts.

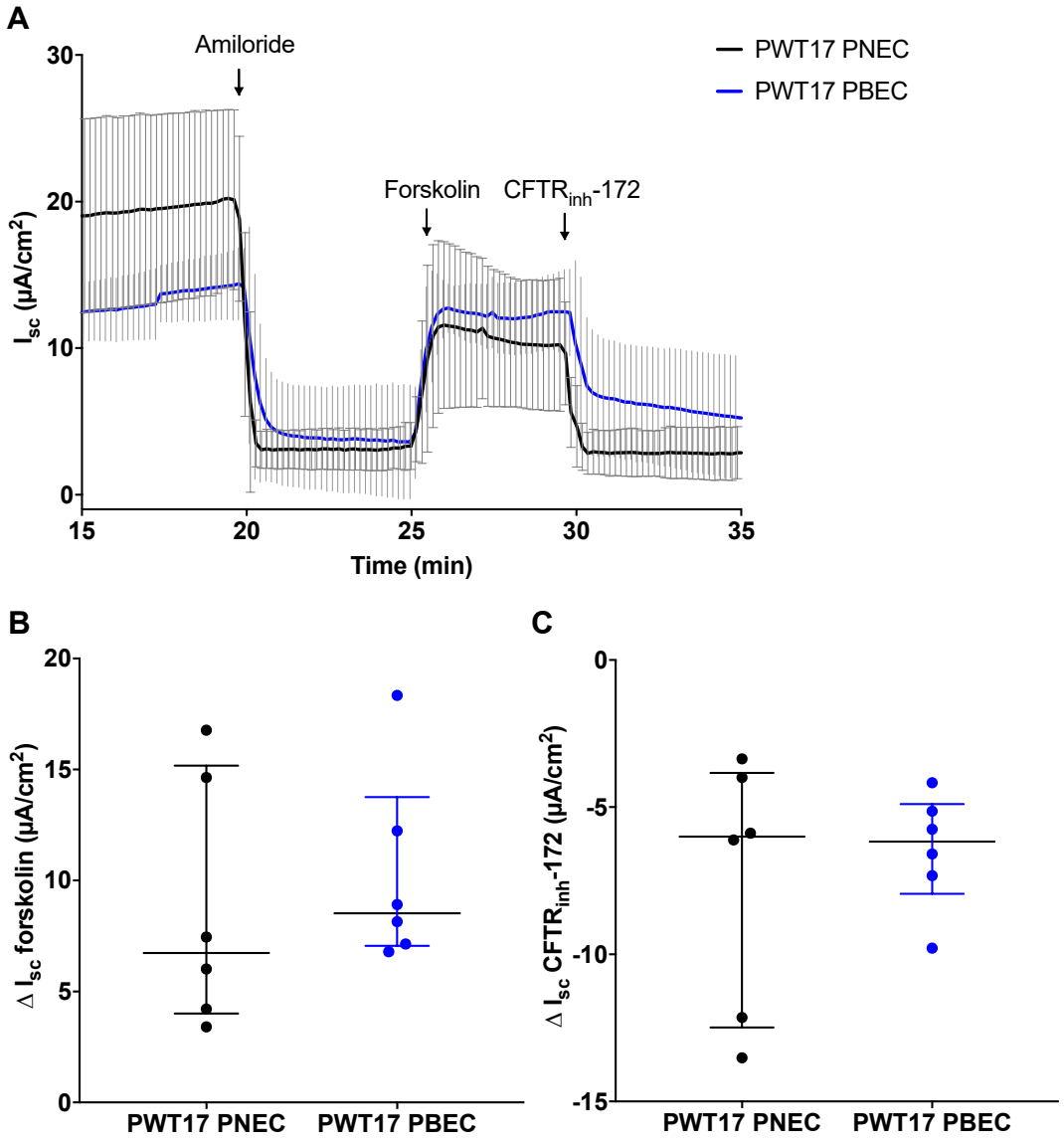

Figure 69: Paired assessment of short circuit current responses to forskolin and $CFTR_{inh}$-172 in PNEC and PBEC cultures derived from the non-CF PWT17 donor

Ussing chamber traces for PNEC and PBEC cultures isolated from the non-CF PWT17 donor are shown in A. The lines represents the mean short circuit current (I_{sc}) with error bars for the SD (PNEC in black, PBEC in blue, n=6 inserts for each culture type). The change in I_{sc} (ΔI_{sc}) after forskolin (B) and $CFTR_{inh}$-172 (C) addition was calculated for each experiment. Data is presented as median ±IQR and analysed with Mann-Whitney test with no statistical differences found, PNEC: n=6 inserts, PBEC: n=6 inserts.

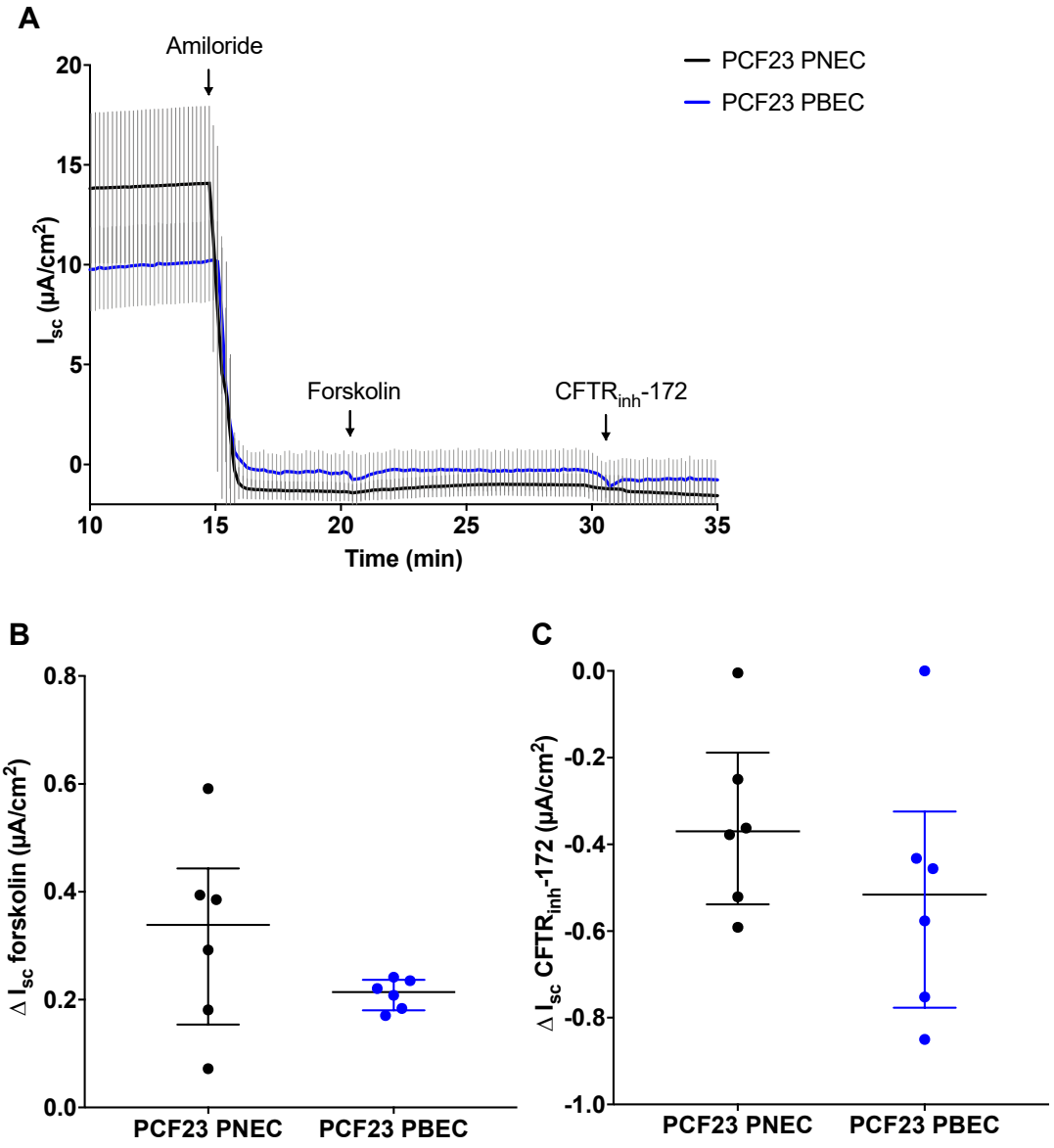

Figure 70: Paired assessment of short circuit current responses to forskolin and $CFTR_{inh}$-172 in PNEC and PBEC cultures derived from the CF PCF23 donor

Ussing chamber traces for PNEC and PBEC cultures isolated from the CF PCF23 donor (F508del/2896delA) are shown in A. The lines represents the mean short circuit current (I_{sc}) with error bars for the SD (PNEC in black, PBEC in blue, n=6 inserts for each culture type). The change in I_{sc} (ΔI_{sc}) after forskolin (B) and $CFTR_{inh}$-172 (C) addition was calculated for each experiment. Data is presented as median ±IQR and analysed with Mann-Whitney test with no statistical differences found, PNEC: n=6 inserts, PBEC: n=6 inserts.

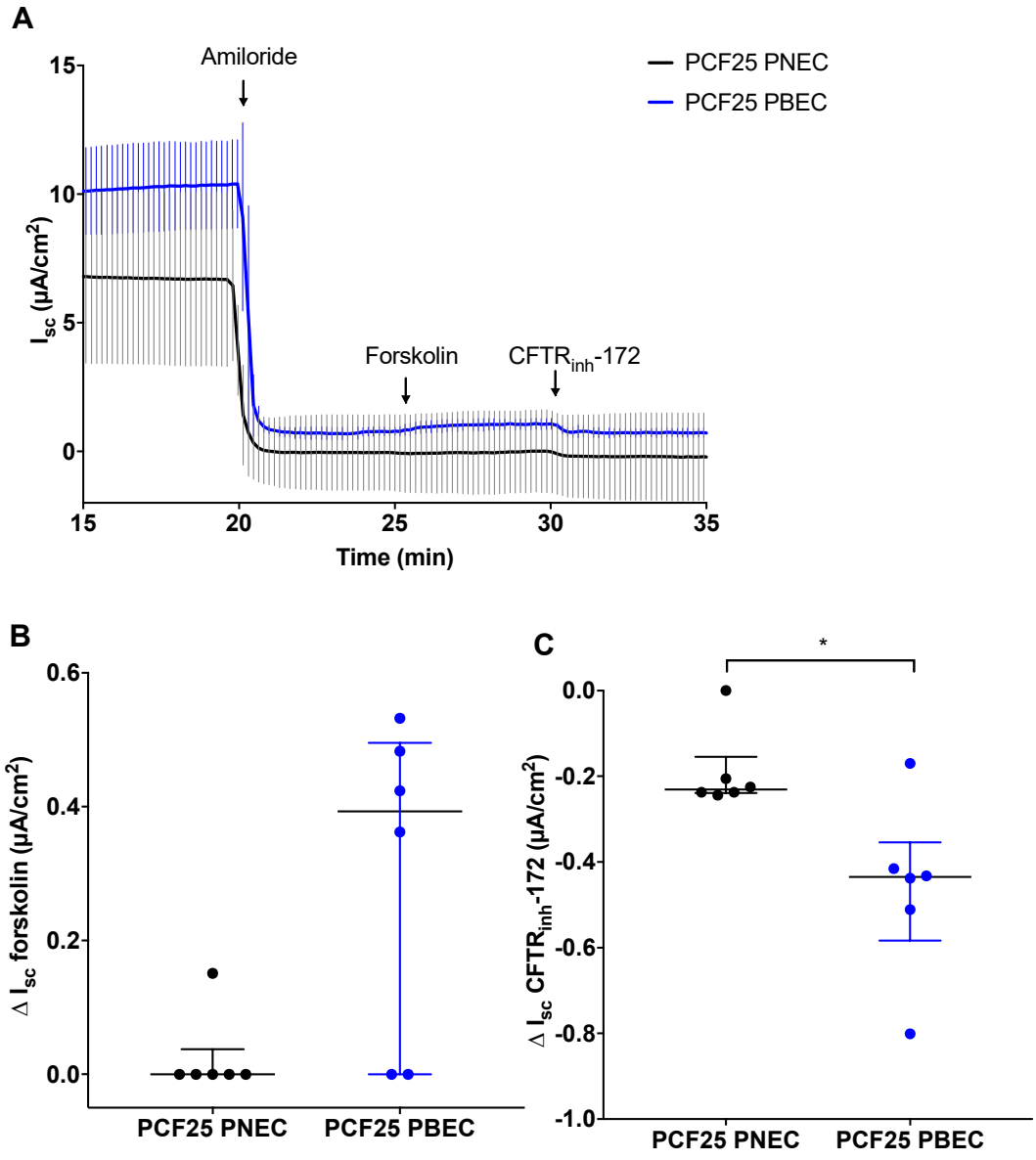

Figure 71: Paired assessment of short circuit current responses to forskolin and $CFTR_{inh}$-172 in PNEC and PBEC cultures derived from the CF PCF25 donor

Ussing chamber traces for PNEC and PBEC cultures isolated from the CF PCF25 donor (F508del/F508del) are shown in A. The lines represents the mean short circuit current (I_{sc}) with error bars for the SD (PNEC in black, PBEC in blue, n=6 inserts for each culture type). The change in I_{sc} (ΔI_{sc}) after forskolin (B) and $CFTR_{inh}$-172 (C) addition was calculated for each experiment. Data is presented as median ±IQR and analysed with Mann-Whitney test, * p=0.04, PNEC: n=6 inserts, PBEC: n=6 inserts.

4.4.9 Assessing the relationship between short circuit current responses to forskolin and CFTR$_{inh}$-172

In these experiments, forskolin and CFTR$_{inh}$-172 have been utilised as a measure of CFTR function. Given the different mechanisms of action of both reagents, it may be over simplistic to assume that responses are negatively correlated i.e. a positive I_{sc} response to forskolin is related to a negative response of similar magnitude to CFTR$_{inh}$-172. To further explore the relationship between the two reagents in PNEC and PBECs, linear regression analysis was performed. As shown in Figure 72, there is a clear correlation between the forskolin-induced and CFTR$_{inh}$-172-sensitive I_{sc} in non-CF PNECs (R^2 = 0.07, p<0.0001). The negativity of this correlation arises from the decrease in I_{sc} by CFTR$_{inh}$-172 (i.e. a greater negative CFTR$_{inh}$-172-sensitive I_{sc} signifies a larger response). This relationship was not paralleled in non-CF PBECs (R^2 = 0.49, p=0.19). In view of the relative specificity of CFTR$_{inh}$-172 for CFTR inhibition, this suggests that in this cohort of cultures, forskolin may have a relatively higher specificity for CFTR activation in non-CF PNECs than PBECs.

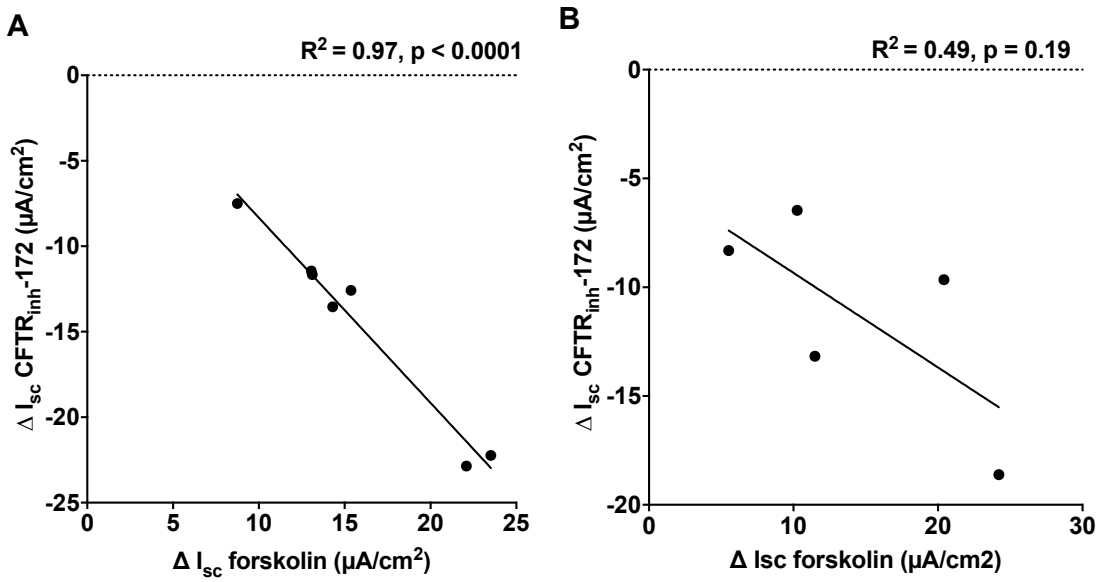

Figure 72: Linear regression analysis for short circuit current responses to forskolin and CFTR$_{inh}$-172 in non-CF PNEC and PBEC cultures

Linear regression analysis was performed to investigate the relationship between the forskolin-induced (ΔI_{sc} forskolin) and CFTR$_{inh}$-172-sensitive (ΔI_{sc} CFTR$_{inh}$-172) responses in differentiated non-CF PNECs (A) and PBECs (B). R^2 is the coefficient of determination whereby 0.0 indicates no linear relationship and 1.0 indicates a perfect linear relationship.

4.4.10 Assessment of intra-donor variability of short circuit current responses to amiloride, forskolin and CFTR$_{inh}$-172

Grouped analyses in Figure 52 and Figure 65 of I_{sc} responses to amiloride, forskolin and CFTR$_{inh}$-172, respectively, represent the median I_{sc} responses with the IQR for each group of cultures and clearly provide an impression of the inter-donor variability evident in each culture group. This was particularly notable in the amiloride-sensitive I_{sc} in PNECs, and the forskolin-induced I_{sc} in all non-CF cultures. However, it is important to also consider the extent of the intra-donor variability i.e. the variation in I_{sc} responses between culture inserts obtained from the same donor. To ascertain the magnitude of intra-donor variability, individual responses measured in each culture insert per donor are shown and grouped by culture type in Figure 73 to Figure 76 below. All Ussing chamber experiments were performed in at least 2 culture inserts derived from each donor.

The intra-donor variability in response to amiloride was predominantly greater in PNECs derived from both non-CF and CF donors as shown in Figure 73 and Figure 75, respectively. Amongst non-CF PNECs, the greatest variability in amiloride-sensitive I_{sc} was seen in cultures isolated from PWT13 (mean -25.2 $\mu A/cm^2 \pm$ SD 7.7). In CF PNECs, this was greatest in PCF26 PNECs (-17.9 $\mu A/cm^2 \pm 7.4$). Interestingly, the intra-donor variability in amiloride-sensitive I_{sc} did not seem to relate to the variability in responses to forskolin and CFTR$_{inh}$-172, as best demonstrated in non-CF PNECs. For example, although the variability in the amiloride-sensitive I_{sc} was lowest in cultures isolated from PWT4 (mean -13.1 $\mu A/cm^2 \pm 1.9$), these cultures showed the largest variability in responses to forskolin and CFTR$_{inh}$-172 (forskolin: 14.3 $\mu A/cm^2 \pm 8.7$; CFTR$_{inh}$-172: -13.5 $\mu A/cm^2 \pm 9.7$), suggesting no relationship between the extent of variability in ENaC versus CFTR function.

In non-CF cultures, forskolin-induced intra-donor variability in I_{sc} was apparent in both PNEC and PBECs. The greatest variability was found in PWT4 cultures as mentioned above. In non-CF PBECs, cultures derived from PWT11 showed the greatest intra-donor variability (forskolin: 11.5 $\mu A/cm^2 \pm 7.5$; CFTR$_{inh}$-172: -13.1 $\mu A/cm^2 \pm 4.0$). Notably, intra-donor variability in the CFTR$_{inh}$-172-sensitive I_{sc} was more pronounced in PNECs versus PBECs. Overall, these findings have shown that there is evidence of intra-donor variability in I_{sc} responses to amiloride, forskolin and CFTR$_{inh}$-172, and the extent of this variability is predominantly greater in PNECs versus PBECs.

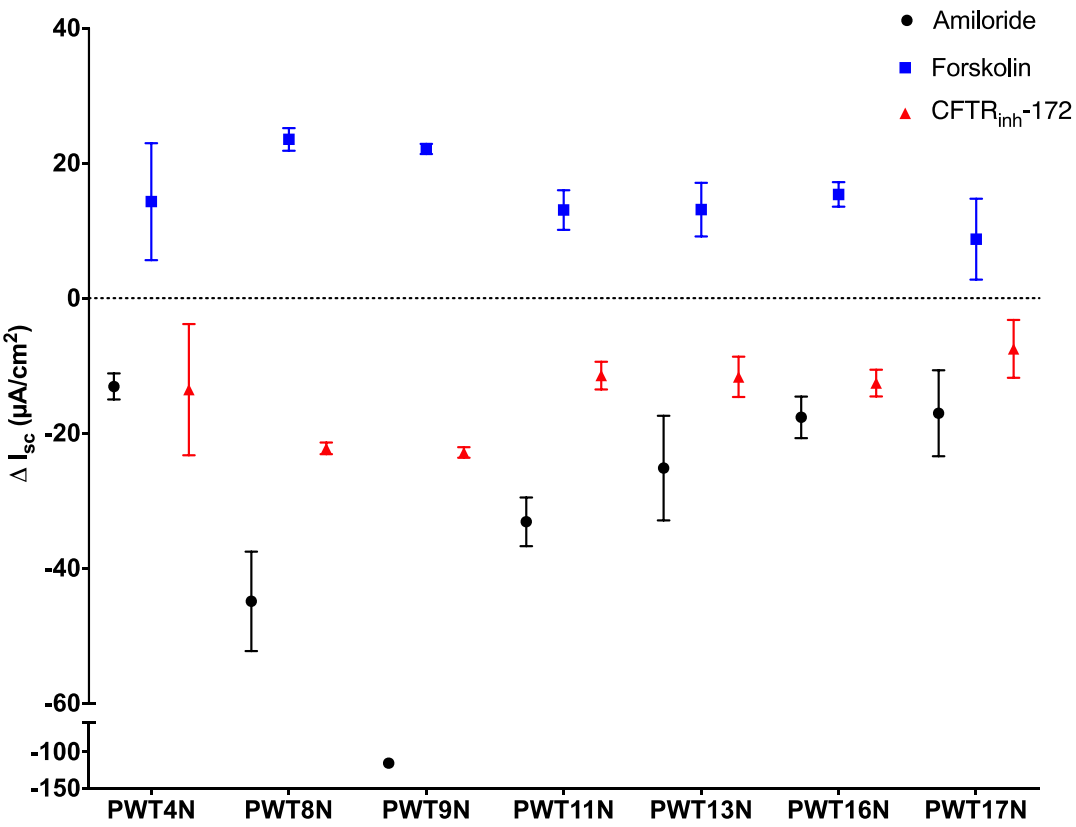

Figure 73: Assessment of intra-donor variability in short circuit current responses to amiloride, forskolin and CFTR$_{inh}$-172 in non-CF PNEC cultures

Intra-donor variability of short circuit current responses (ΔI_{sc}) to amiloride, forskolin and CFTR$_{inh}$-172 were assessed in non-CF PNEC ALI cultures. Data is presented as the mean ΔI_{sc} response ± SD. PWT4N: n=2 inserts; PWT8N: n=4 inserts; PWT9N: n=2 inserts; PWT11N: n=5 inserts; PWT13N: n=3 inserts; PWT16N: n=3 inserts; PWT17N: n=6 inserts.

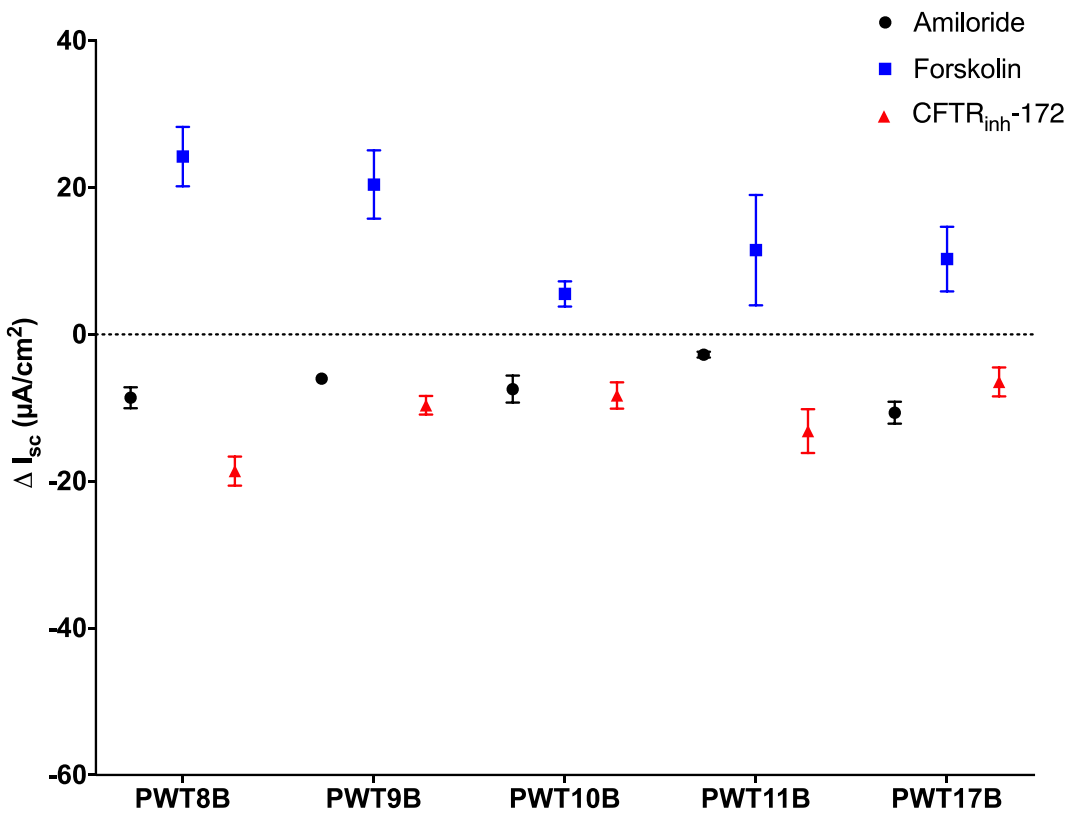

Figure 74: Assessment of intra-donor variability in short circuit current responses to amiloride, forskolin and CFTR$_{inh}$-172 in non-CF PBEC cultures

Intra-donor variability of short circuit current responses (ΔI_{sc}) to amiloride, forskolin and CFTR$_{inh}$-172 were assessed in non-CF PBEC ALI cultures. Data is presented as the mean ΔI_{sc} response ± SD. PWT8B: n=4 inserts; PWT9B: n=2 inserts; PWT10B: n=3 inserts; PWT11B: n=6 inserts; PWT17B: n=6 inserts.

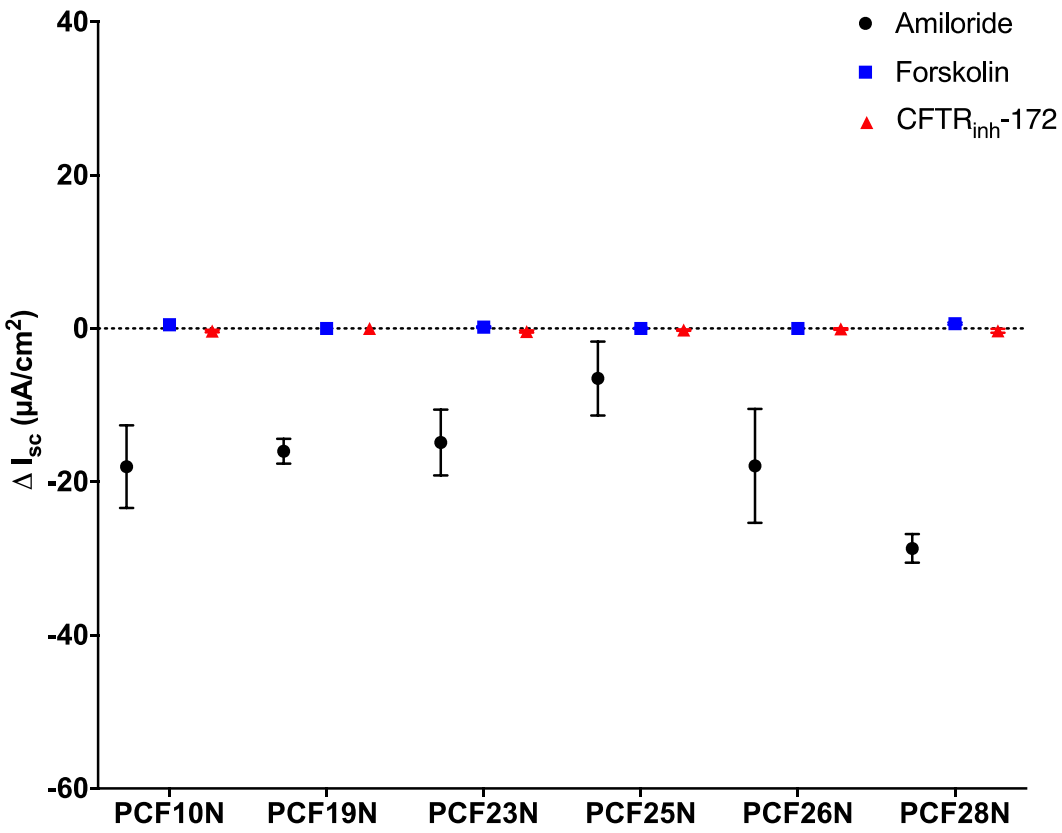

Figure 75: Assessment of intra-donor variability in short circuit current responses to amiloride, forskolin and CFTR$_{inh}$-172 in CF PNEC cultures

Intra-donor variability of short circuit current responses (ΔI_{sc}) to amiloride, forskolin and CFTR$_{inh}$-172 were assessed in CF PNEC ALI cultures. Data is presented as the mean ΔI_{sc} response ± SD. PCF10N: n=3 inserts; PCF19N: n=3 inserts; PCF23N: n=6 inserts; PCF25N: n=3 inserts; PCF26N: n=3 inserts; PCF28N: n=2 inserts.

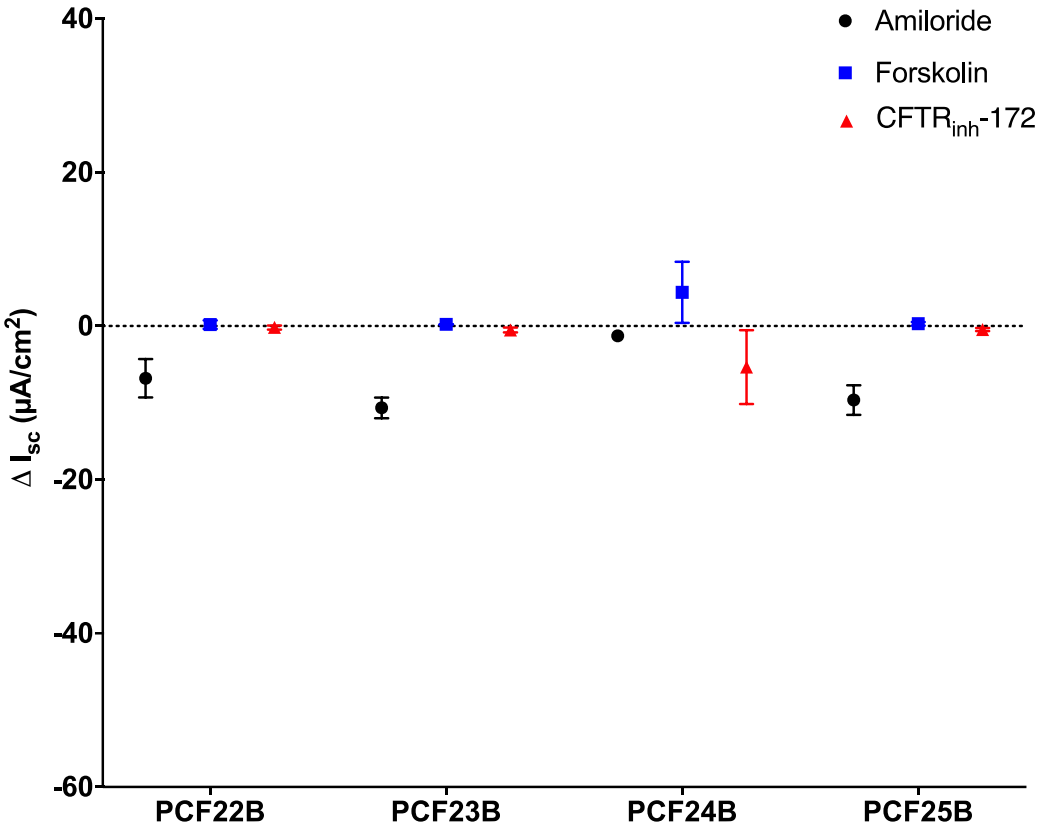

Figure 76: Assessment of intra-donor variability in short circuit current responses to amiloride, forskolin and $CFTR_{inh}$-172 in CF PBEC cultures

Intra-donor variability of short circuit current responses (ΔI_{sc}) to amiloride, forskolin and $CFTR_{inh}$-172 were assessed in CF PBEC ALI cultures. Data is presented as the mean ΔI_{sc} response ± SD. PCF22B: n=2 inserts; PCF23B: n=6 inserts; PCF24B: n=3 inserts; PCF25B: n=6 inserts.

4.4.11 Functional characterisation of the R751L mutation using the primary airway epithelial culture model

As evident in Figure 65, CF PBEC cultures derived from the donor with the *F508del/R751L* genotype (PCF24) demonstrated larger responses to forskolin and $CFTR_{inh}$-172 compared with cultures obtained from CF participants with more severe mutations. This particular participant clinically had a mild phenotype with a diagnostic sweat chloride at diagnosis of 83 mmol/L and features of pancreatic sufficiency. At present, there is no reported detailed characterisation of this genotype and reported Ussing chamber experiments in this PhD relating to this mutation are novel.

Figure 77 demonstrates the mean I_{sc} responses in 3 PBEC culture inserts derived from this participant. To investigate the relative magnitude of CFTR function in F508del/R751L, forskolin-induced I_{sc} responses were compared with PBECs derived from non-CF and F508del homozygous participants (i.e. a severe clinical phenotype). These results are shown below in Figure 77. Although the magnitude of the forskolin-induced I_{sc} associated with F508del/R751L was less than the median I_{sc} evident in non-CF PBECs (F508del/R751L: median 4.4 $\mu A/cm^2$, IQR 4.0 to 4.4 versus 18.3 $\mu A/cm^2$, IQR 10.2 to 24.0), it is greater than that evident in PBECs isolated from F508del homozygous donors (0.3 $\mu A/cm^2$, IQR 0 to 0.5). These findings correlate with the relatively mild phenotype evident in this CF donor, and the effects of *R751L* on CFTR channel function warrant further investigation. No differences were found with the magnitude of amiloride-sensitive I_{sc} in the F508del/R751L cultures (-1.3 $\mu A/cm^2$, IQR -1.0 to -1.6) compared with F508del homozygous (-8.2 $\mu A/cm^2$, IQR -6.7 to -9.6) and non-CF cultures (-7.4 $\mu A/cm^2$, IQR -4.4 to -9.6).

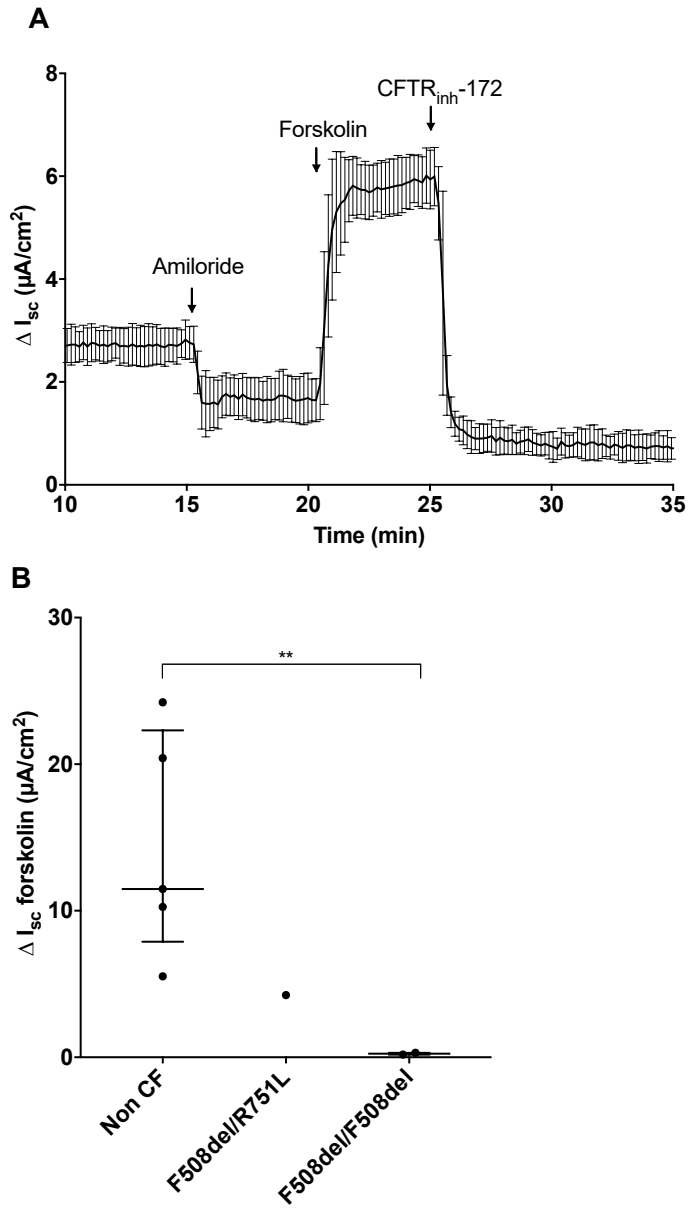

Figure 77: Short circuit current responses in PBEC cultures derived from a CF donor with the *F508/R751L* genotype

PBEC culture inserts derived from the CF PCF24B (F508/R751L) were mounted in the Ussing chamber and bathed apically and basolaterally in 125 mM chloride Krebs. Resultant short circuit current (I_{sc}) responses to amiloride, forskolin and $CFTR_{inh}$-172 are shown in A; lines represent mean with error bars for SD; n= 3 inserts.

Changes in the forskolin-induced I_{sc} (ΔI_{sc} forskolin) were compared with responses seen in non-CF PBECs and CF PBECs derived from F508del/F508del donors (B). Each point represents the mean ΔI_{sc} for each donor. Data is presented as median ± IQR and analysed with Kruskal-Wallis and post hoc Dunn's multiple comparison test; **p<0.01; non-CF PBECs (n=5 donors, 21 inserts), F508del/R751L donor (n=1 donor, 3 inserts), CF PBECs (n=2 donors, 8 inserts).

4.5 Discussion

4.5.1 Functional expression of ENaC does not differ in CF versus non-CF differentiated paediatric primary nasal and bronchial epithelial cultures

Overall, investigation of the amiloride-sensitive I_{sc} in this cohort of paediatric cultures has not shown any significant changes in CF versus non-CF epithelia in both PNECs and PBECs. These findings are contrary to the previously reported enhancement of ENaC activity in CF and subsequent sodium hyperabsorption in the absence of functional CFTR. Nasal PD *in vivo* assessment has shown a greater response to amiloride in CF versus non-CF subjects (Knowles et al., 1983). *In vitro* studies have demonstrated greater apical sodium conductance in freshly excised nasal tissue and submerged confluent nasal epithelial cells, both derived from nasal polyp tissue in CF and non-CF donors (Boucher et al., 1986, Boucher et al., 1988, Mall et al., 1998).

However, in addition to the results obtained in this PhD, there are also conflicting results from other studies, including a report which found no differences in response to amiloride on transepithelial conductance in primary ALI tracheal and bronchial cultures derived from explanted lung tissue of 261 non-CF and 74 CF donors (Itani et al., 2011). Furthermore, this group did not find any differences in the net rate of sodium absorption in CF versus non-CF epithelia. Interestingly, the amiloride-sensitive I_{sc} was greater in CF epithelia, but this was caused by a loss of chloride conductance due to dysfunctional CFTR rather than an increase in sodium conductance (Itani et al., 2011). In non-CF epithelia, the amiloride-induced apical hyperpolarisation increased the driving force for chloride secretion, resulting in a greater reduction in the amiloride-sensitive I_{sc} compared with CF epithelia which lack functional CFTR (Itani et al., 2011).

There have also been previous reports of anatomical variations in amiloride-sensitivity. *In vivo* assessment of nasal transepithelial voltage response to amiloride in the newborn pig model showed greater responses in CF versus non-CF pigs (Chen et al., 2010). However, these findings were not reproduced in tracheal epithelia, where results were similar. Furthermore, *in vivo* investigation of PD in children has shown more negative transepithelial voltages in tracheal versus lower airways (Davies et al., 2005). Interestingly, in the same study, responses were more negative in CF versus non-CF adult subjects in all airway regions, suggesting that age and hence disease severity may affect ENaC function (Davies et al., 2005). It is

recognised that proteolytic ENaC activation by serine proteases such as neutrophil elastase increases the amiloride-sensitive current in bronchial epithelial cell lines, and it is possible that this could contribute to greater responses seen in older subjects with more severe disease (Caldwell et al., 2005).

Clearly, the question regarding an increased ENaC function in the CF airway remains debateable. Variations in participant age, degree of inflammation, infection status and disease severity may contribute to the differences seen in this PhD and other previous studies. Furthermore, there are reported SNPs in ENaC that are associated with variations in ENaC surface expression and function (Rauh et al., 2010). Differences may also arise from a number of other potential causes including experimental variations in tissue type (i.e. nasal polyp versus turbinate, bronchial brushing versus explanted tissue, nasal versus bronchial epithelia), culture conditions (ALI versus submerged; seeding density), stages of epithelial differentiation and experimental conditions used for Ussing chamber experiments.

All paediatric cultures in this study showed high levels of *α-ENaC* expression compared with the other subunits. Despite the lack of difference in the amiloride-sensitive I_{sc}, expression of all three subunits was increased in CF versus non-CF PBECs. This was different in PNECs, where only *β-ENaC* was increased in CF versus non-CF cultures. Analysis in both non-CF and CF groups suggested lower fold changes in PNECs versus PBECs.

The importance of relative subunit expression for ENaC function is exemplified in a number of diseases. For example, mutations in β and γ-ENaC have been associated with the autosomal dominant disease Liddle syndrome, which leads to constitutive ENaC activation in the distal renal epithelium causing severe hypertension (Shimkets et al., 1994, Prince and Welsh, 1999). The systemic form of type 1 pseudohypoaldosteronism can be caused by mutations in each of the three ENaC subunits in multiple tissue sites causing renal salt wasting episodes and lower respiratory tract infections (Chang et al., 1996, Strautnieks et al., 1996). There have been 2 reported cases of β-ENaC mutations in patients with a 'CF-like' disease with pulmonary infections and elevated sweat chloride (Sheridan et al., 2005). Furthermore, the development of the transgenic over-expressing β-ENaC mouse is used as a model to investigate CF-like lung disease (Mall et al., 2004).

Relative contribution of ENaC subunit to resultant channel function has been assessed by injection of each subunit isolated from rat colonic epithelia into *Xenopus*

oocytes and subsequent measurement of amiloride-sensitive currents (Canessa et al., 1994, Bonny et al., 1999). Presence of α-ENaC alone was sufficient to induce an amiloride-sensitive current, however, this response was potentiated by over 100 times in the presence of all three subunits, which was later confirmed as equalling 2 % of total ENaC function (Canessa et al., 1994, Bonny et al., 1999). This increased to 15 % when either α and β or α and γ subunits were co-expressed (Bonny et al., 1999). Both studies confirmed that β and γ-ENaC failed to produce any currents in isolation, which increased to 15 % when either subunit was co-expressed with α-ENaC (Canessa et al., 1994, Bonny et al., 1999). In contrast to the study by Canessa et al, Bonney et al were able to demonstrate ENaC activity when β and γ-ENaC where co-expressed to around 2 % total function. In addition to potentiating overall ENaC activity, α-ENaC facilitates trafficking of β and γ-ENaC to the plasma membrane, while β and γ subunits are required for plasma membrane stabilisation (Gaillard et al., 2010).

The overall variation seen in ENaC-subunit *mRNA* expression in this PhD may account for lack of correlation seen with functional assessment of amiloride-sensitive I_{sc}. Similar oscillations in subunit expression in individual donors have been previously reported in nasal epithelial cultures, however, these authors were able to demonstrate upregulation of all 3 subunits in CF versus non-CF nasal cultures isolated from nasal polyp tissue (Bangel et al., 2008). This variability may reflect genuine differences in ENaC assembly and composition of subunits in different cellular populations, therefore making it difficult to make reliable assessments of such correlations. Two different ENaC populations have been described at the plasma membrane; basally active cleaved channels and uncleaved 'near silent' channels (Caldwell et al., 2005). However, it remains to be determined as to how these channels are distributed within distinct cellular populations. Furthermore, post transcriptional modifications of ENaC are likely to limit the value and weighting of *mRNA* expression analysis. Detailed exploration of protein expression would be useful to help explore this area further.

Although the numbers were small, paired analysis of PNEC/PBEC cultures isolated from the same donors did provide some useful information regarding variations in ENaC function and expression at the two culture sites. Overall, findings suggested that in the paired non-CF cultures, the amiloride-sensitive I_{sc} and *α-ENaC* expression were increased in nasal versus bronchial tissue. This paralleled the grouped

analyses of all non-CF cultures. Investigation of anatomical variations of ENaC subunit expression in non-CF airways has previously been performed in non-CF adults (Pitkänen et al., 2001). Nasal, bronchial and peripheral lung tissue were isolated from volunteers undergoing lobectomy for malignancy. Using RT-PCR, these authors found relatively higher levels of *α-ENaC* in nasal tissue. However, they also found increasing proportions of *β* and *γ-ENaC* with distal airway progression, which was not evident in the paediatric paired non-CF cultures (Pitkänen et al., 2001).

Analysis in paired CF cultures revealed the reverse situation, where amiloride-sensitive I_{sc} and *α-ENaC* expression were increased in PBECs. Unfortunately, there are no similar studies to compare these findings with, and this does warrant further investigation. Although the numbers are too small to perform any formal assessment of correlation in the paired cultures, there is a suggestion that *α-ENaC* expression was associated with an increase in the amiloride-sensitive I_{sc}.

Finally, it should be noted that although Ussing chamber experiments are widely employed to assess the epithelial function of ion channels such as ENaC, there are limitations with this technique. Under normal thin film conditions, the ASL overlying the airway epithelium is around 7-10 μm in height (Gaillard et al., 2010). In the Ussing chamber system, epithelial monolayers are mounted and bathed in significantly larger volumes, in this case 5 mL in each compartment. ENaC is subsequently proteolytically cleaved and activated in an attempt to restore ASL volume back to the normal height (Gaillard et al., 2010). This has been observed anecdotally on initial mounting of epithelia in the Ussing chamber, where the basal I_{sc} showed an initial increase (see Figure 51). Since this basal I_{sc} contributes to the majority of the amiloride-sensitive I_{sc}, it is most likely caused by ongoing ENaC activation at the plasma membrane. However, all assessments of the amiloride-sensitive I_{sc} were performed after a period of 15-20 minutes, to enable basal I_{sc} stabilisation prior to amiloride addition.

4.5.2 CFTR functional expression does not differ significantly between differentiated paediatric primary nasal and bronchial epithelial cultures

Investigation of CFTR-mediated chloride secretion in this cohort of paediatric cultures has not revealed any differences between the magnitude of both forskolin-induced and $CFTR_{inh}$-172-sensitive I_{sc} responses in PNECs versus PBECs. This therefore

demonstrates the suitability of PNECs for exploration of CFTR function using this experimental approach.

As expected the responses to both reagents were greater in non-CF versus CF cultures. However, the lack of significance seen amongst PBECs may be in part explained by the relatively small sample size, which was limited by the initial challenges faced with PBEC culture success. The non-parametric Kruskal-Wallis test was used for all Ussing chamber analyses. Normality was formally tested with Shapiro-Wilk assessment; however, this did not show normality across all culture groups. In view of the need to make reliable comparisons between CF/non-CF and PNEC/PBEC cultures and the difficulties of accurately testing for normality in small sample sizes, non-parametric analyses were used to investigate relationships between each culture group and maintain appropriate application of statistical comparisons. Interestingly, application of the parametric one-way ANOVA revealed findings to be significantly different between non-CF and CF PBECs (forskolin-induced I_{sc}: p=0.003), however without reliably assessing for normality, the decision was made not to use this analysis.

Forskolin has been widely employed for the *in vitro* assessment of CFTR secretory function in a range of studies including those that have investigated the role of potentiators and correctors in patient-derived epithelial cultures (Van Goor et al., 2009a, Ahmadi et al., 2017, Pranke et al., 2017). This was the rationale for selecting forskolin to investigate CFTR-mediated chloride secretion in this PhD to enable comparable analyses of results. As previously mentioned, CFTR is activated by PKA-mediated phosphorylation at multiple phosphorylation sites on the R domain (Bozoky et al., 2013). *In vitro,* this can be achieved with forskolin which acts to elevate cytosolic cAMP levels via direct (i.e. protein-independent) activation of adenylate cyclase (Moran and Zegarra-Moran, 2008), and subsequent PKA.

Concentrations of up to 10 μM forskolin are sufficient to activate CFTR with higher concentrations demonstrating non-specific responses (Moran and Zegarra-Moran, 2008). The initial peak and plateau response has been noted and suggested to occur due to limited activity of the basolateral Na/K/2Cl co-transporter and subsequent failure to maintain cytosolic chloride (Li et al., 2004). This could be investigated further by permeabilising the basolateral membrane to eliminate the effects of channels involved in generating a chloride gradient (Li et al., 2004). Although this may be a potential explanation for this type of response evident in some paired

PBEC cultures in this study, it does not explain why this finding was not apparent in PNECs. It is possible that there are variations in Na/K/2Cl functional expression in the two culture types and does requires further investigation. The phosphodiesterase inhibitor, 3-isobutyl-1-methylxanthine (IBMX), can also be used in conjunction with forskolin to augment CFTR activation, however, addition of this reagent also affects the gating properties of CFTR, and so it was not selected for use in this PhD (Moran and Zegarra-Moran, 2008).

The thiazolidinone $CFTR_{inh}$-172 is a relatively specific and reversible CFTR inhibitor with a significantly greater potency than other inhibitors such as glibenclamide and niflumic acid (Taddei et al., 2004). It works by reducing channel open probability and increases the time spent in the closed state, suggesting alteration of channel gating by binding to NBD1 as opposed to blockage of the channel pore as is the case with many alternative inhibitors (Taddei et al., 2004). GlyH-101, was later identified as another CFTR inhibitor, but despite its favourable property of improved water solubility, it was found to have additional inhibitory effects on alternative chloride conductance pathways, including SLC26A9 and CaCC (Bertrand et al., 2009, Melis et al., 2014). It was therefore not utilised in this PhD due to the requirement for TMEM16A investigation and the potential for unintended inhibition of CaCC.

Linear regression analysis of resultant ΔI_{sc} responses to forskolin and $CFTR_{inh}$-172 in non-CF PNECs showed that the two responses were significantly correlated. This suggested that in view of the relative specificity of $CFTR_{inh}$-172-mediated CFTR inhibition, forskolin may also be relatively specific for CFTR activation. The lack of correlation evident in non-CF PBECs could be explained by cAMP-activation of non-CFTR channels, such as cAMP-sensitive potassium channels as well as ion transporters such as the basolateral Na/K/2Cl cotransporter, the apical sodium/bicarbonate exchanger and the SLC26 co-transporters (Cuthbert et al., 1999, Haas and Forbush Iii, 2000, Frizzell and Hanrahan, 2012). Furthermore, co-expression of wild type CFTR and an alternative chloride channel, SLC26A9, in HEK 293 cells has shown enhanced forskolin-stimulated currents (Bertrand et al., 2009). Therefore, more selective activation of CFTR and knowledge of alternative chloride channel response and function would be beneficial in PBEC-related studies that require detailed exploration of CFTR activation including response to modulator therapies.

Although paired culture assessment did not show any differences between forskolin responses in PNEC and PBECs derived from both non-CF and CF donors, there were two occasions where the $CFTR_{inh}$-172 responses differed. In the non-CF PWT8 donor, the response was greater in PNECs versus PBECs. The reverse of this was true in the CF PCF25 cultures, where a greater response was evident in PBECs. The exact reason for this remains unclear and could be further investigated by assessing CFTR expression by Western blot or immunofluorescence to determine potential relationships of expression with functional CFTR. However, this is unlikely to have any significant implications for the application of PNECs in CF research, but is an important consideration.

4.5.3 There is evidence of inter- and intra-donor variability in Ussing chamber responses to amiloride, forskolin and $CFTR_{inh}$-172

There was notable variability in the responses to amiloride, forskolin and $CFTR_{inh}$-172 between cultures derived from different donors. Although it is important to recognise that channel expression and function may be affected by the tissue culture process and culture quality, all cultures were subject to the same processes and conditions including seeding density. Therefore, this inter-donor variability is likely to reflect the underlying variations in amiloride and CFTR function evident in cultures derived from the different donors. This is further exemplified by the presence of CFTR-mediated chloride secretion evident in cultures derived *F508del/R751L* and the absence of response in cultures representing severe CF mutations, therefore in keeping with the clinical phenotype.

It is important to recognise that cultures in the non-CF group were not isolated from completely healthy participants. As described in Chapter 3, the predominant reasons for clinical bronchoscopy in this group were to investigate recurrent LRTI, chronic cough and wheeze. This could potentially impact upon variations in ion transport in the airway, however, this study is not adequately powered to draw any sensible conclusions relating to this. Nevertheless, *in vitro* studies have recognised additional factors that may affect CFTR function. These include chronic exposure to β_2-agonists (which are used clinically to treat chronic wheeze), exposure to second-hand cigarette smoke and additional disorders of mucostasis and subsequent ASL dehydration including non-allergic asthma and non-CF bronchiectasis (Brewington et al., 2018a, Savitski et al., 2009, Schulz and Tümmler, 2016). However, for the non-CF cultures used in this PhD to investigate I_{sc} responses, sweat tests were

performed in 5 out of 8 children and reported to be normal, suggesting normal CFTR-mediated chloride function in these participants.

There was also evidence of variability between different culture inserts isolated from individual donors. This intra-donor variability may have arisen from different baseline levels of CFTR activation in different culture inserts, therefore impacting upon the degree of cAMP-mediated activation by forskolin (Moran and Zegarra-Moran, 2008). Culture quality should also be considered as a potential factor; however, ALI culture inserts displaying adequate TEER values and epithelial characteristics as described in Chapter 3 were carefully selected to perform all Ussing chamber experiments. Importantly, this assessment of intra-donor variability is limited by failure to compare consistent numbers of culture inserts for each donor analysed.

Indeed, the extent of intra and inter-donor variability of TEER in response to pharmacological agents such as amiloride has been comprehensively assessed in PNECs isolated from healthy volunteers (Tosoni et al., 2016). As with this PhD, the data was found to be non-parametric in nature (Tosoni et al., 2016). By varying their protocol with amiloride addition either before or after forskolin and $CFTR_{inh}$-172, no differences were evident in the resultant change in amiloride-induced TEER, suggesting that ENaC functional expression was innate to an individual donor's epithelium (Tosoni et al., 2016). Furthermore, Tosoni et al. did not find any correlation with the magnitude of the amiloride and forskolin responses, further highlighting the complexities of epithelial ion transport.

4.6 Conclusion

In this cohort of paediatric cultures, no differences were seen in the amiloride-sensitive I_{sc} in CF versus non-CF cultures in both PNEC and PBEC groups, further highlighting that the relationship between ENaC and CFTR remains in question. Responses were significantly greater in non-CF PNECs versus PBECs. This may be relevant where detailed ENaC assessment is performed in PNECs and translated to lower airway disease. Although the numbers are small, analyses from paired cultures do provide some useful insights with respect to relative changes in ENaC expression in the two anatomical sites. However, differences were not apparent in CF cultures, and therefore may not have significant implications.

No differences were evident in the assessment of I_{sc} responses to forskolin and $CFTR_{inh}$-172 in PNEC versus PBEC cultures, suggesting that under these experimental conditions, paediatric PNECs are a representative tool to investigate CFTR airway function. The presence of inter-donor variability in Ussing chamber responses may be related to TEER variability previously reported in Chapter 3. However, given the consistency of culture conditions it is likely to be a true reflection of variability in cultures derived from different participants.

The findings in this chapter have demonstrated the feasibility of using cultured paediatric airway epithelial cells to investigate ion transport profiles relating to ENaC and CFTR function in Ussing chamber experiments. Although adult primary bronchial cultures have been previously established in the current laboratory environment and utilised in Ussing chamber experiments, the work performed in this PhD was the first instance of applying this technique to paediatric ALI cultures. This has been exceptionally valuable, not only to facilitate the work required for this PhD but will establishment of this process will also be beneficial for future work involving paediatric CF ALI cultures.

5 Chapter 5: Investigating the expression and function of TMEM16A in differentiated paediatric primary nasal and bronchial epithelial cultures derived from children with and without cystic fibrosis

5.1 Introduction

Chloride secretion into the ASL is achieved through a combined effect of basolateral chloride entry via the Na/K/2Cl co transporter and apical channels that facilitate chloride transport. It has long been recognised that CFTR is co-expressed with other chloride channels, including CaCCs (Boucher et al., 1989). Although CFTR is the major contributor to maintaining ASL volume under basal conditions, acute CaCC stimulation can also increase ASL height, therefore potentially providing an alternative approach to restoring ASL volume and reducing ASL hydration in CF (Tarran et al., 2002).

Having established the feasibility of utilising paediatric PNEC and PBEC cultures to explore their ion transport profiles, the next focus of this research was to investigate the presence of CaCCs and their relative contribution to chloride secretion in paediatric airway epithelial cultures. Furthermore, the specific presence of TMEM16A has not previously been assessed in paediatric PNEC or PBEC cultures. Since the identification of TMEM16A ten years ago, there has been a large body of work investigating the expression and modulation of the channel in the airway, the majority of which has been performed using established cell lines (HEK 293, human bronchial epithelial) or PBEC cultures isolated from explanted lung tissue (Jung et al., 2013, Scudieri et al., 2012a, Ruffin et al., 2013, Caci et al., 2015, Ousingsawat et al., 2011, Gorrieri et al., 2016). At the time of this PhD, there was a lack of information regarding both CaCC and TMEM16A in the paediatric airway, including details regarding expression and function.

The work carried out in this chapter will investigate the role of CaCC in paediatric epithelial cultures developed in this PhD, with a view to investigating TMEM16A function and expression using experimental techniques described in preceding chapters.

5.2 Hypotheses

- Differentiated paediatric PNEC and PBEC ALI cultures can be used in Ussing chamber experiments to explore the function of CaCC.
- TMEM16A is expressed in differentiated paediatric PNEC and PBEC cultures.

5.3 Aims

The specific aims of this chapter were to:

- Investigate the function and expression of CaCC in paediatric differentiated ALI cultures using Ussing chamber experiments and determine any differences between PNECs and PBECs derived from non-CF and CF participants
- Investigate the function and expression of TMEM16A in these cultures.

5.4 Results

5.4.1 Assessment of calcium activated chloride channel function

To investigate CaCC-mediated chloride secretion, Ussing chamber experiments were performed in differentiated paediatric PNEC and PBEC ALI cultures. A Krebs solution containing 125 mM chloride was added to the apical and basolateral compartments and maintained at 5 % CO_2 and 37 °C. All experiments described in this chapter involved the initial addition of amiloride, forskolin and $CFTR_{inh}$-172 as previously outlined in Chapter 4 and performed from 25d to 33d ALI. UTP (100 μM) was subsequently added to the apical compartment to activate CaCC (Mason et al., 1991). The resultant I_{sc} and TEER were measured and calculated as previously described in Chapter 2 section 2.5. Although CaCC-mediated chloride secretion via P2Y2 receptor stimulation can be stimulated equally well with ATP and UTP, UTP was selected for these Ussing chamber experiments due to its additional activity on airway P2Y4 receptors, therefore maximising the resultant I_{sc} response (Lazarowski and Boucher, 2009). Furthermore, whereas ATP hydrolysis produces adenosine which modulates anion secretion via cAMP-dependent CFTR regulation, the hydrolysis product of UTP, uridine, does not have this effect, thereby minimising alternative mechanisms for UTP-induced chloride secretion (Paradiso et al., 2000).

To exemplify the nature of the response evident with UTP addition, representative Ussing chamber traces for I_{sc} and TEER responses to UTP in a non-CF culture are shown in Figure 78. Addition of UTP caused a rapid I_{sc} increase by 6.6 μA/cm^2 due to calcium activated chloride secretion, but unlike CFTR, the response was transient with spontaneous return to baseline of 1.9 μA/cm^2 without the need for pharmacological channel inhibition. The was accompanied by a TEER decrease of 110 Ω.cm^2 due to enhanced CaCC-mediated chloride conductance.

To investigate this further in paediatric PNEC and PBEC ALI cultures isolated from non-CF and CF donors, Ussing chamber experiments were performed to investigate the effects of apical UTP addition in 7 non-CF PNEC, 5 non-CF PBEC, 5 CF PNEC and 1 CF PBEC (Figure 79) cultures. In addition to the peak UTP-induced I_{sc} (ΔI_{sc}), the area under the curve (AUC) was also calculated as a measure of total UTP-induced I_{sc} as previously described in Chapter 2 section 2.5. As shown in Figure 79, in non-CF cultures, the UTP-induced I_{sc} in PNECs was similar to the response in PBECs (non-CF PNEC: median 3.3 μA/cm^2, IQR 1.8 to 5.5 versus non-CF PBEC: 2.4

μA/cm^2, IQR 1.8 to 3.4, p=0.48). No differences were found in the total UTP-induced I_{sc} (non-CF PNEC: median 9.0 μA/cm^2.min, IQR 5.2 to 25.1 versus non-CF PBEC: 9.2 μA/cm^2.min, IQR 5.7 to 9.8, p=0.56). Cultures isolated from one particular donor (PWT9) demonstrated the largest UTP-induced I_{sc} increase (mean 12.5 μA/cm^2 ± SD 0.27) and total response (120.9 μA/cm^2.min ± SD 0.14). Interestingly this was the same donor that had the greatest amiloride-sensitive I_{sc} as shown in Chapter 4 Figure 52.

In PNECs, the median UTP-induced I_{sc} in CF PNECs was 2.4 μA/cm^2, IQR 1.0 to 6.4, which was not statistically different to non-CF PNECs (p=0.67). This was paralleled with similar changes in the total UTP-induced I_{sc} for both groups (CF PNECs: 9.7μA/cm^2.min, IQR 3.4 to 21.2, p=0.66). Statistical comparisons could not be made involving CF PBECs because it was only possible to determine the peak UTP-induced I_{sc} in 1 CF PBEC for reasons explained below in section 5.4.3 .

Further investigation into the UTP-induced I_{sc} responses were investigated in paired PNEC/PBEC cultures isolated from 2 non-CF culture pairs. Cultures derived from the PWT8 donor (Figure 80) showed a 2-fold increase in the UTP-induced I_{sc} in PNECs compared with PBECs, however, this was not statistically significant (PNEC median: 4.6 μA/cm^2, IQR 4.6 to 4.7 PBEC: 2.3 μA/cm^2, IQR 2.3 to 2.6 versus; p=0.1). This was associated with a 3-fold AUC increase in PNECs, but again this was not statistically significant (PNEC median: 27.3 μA/cm^2.min, IQR 19.2 TO 28.8 versus PBEC: 8.4 μA/cm^2.min, IQR 8.4 to 9.6; p=0.1). Findings were similar in PWT11 cultures (Figure 81), whereby the UTP-induced I_{sc} was 3-fold greater in PNECs (PNEC median 5.5 μA/cm^2, IQR 4.4 to 6.6 versus PBEC: 1.6 μA/cm^2, IQR 1.3 to 2.5; p=0.2). The AUC was also greater in the PNECs but not statistically significant (PNEC median: 23.1 μA/cm^2.min, IQR 17.1 to 29.1 versus PBEC: 4.7 μA/cm^2.min, IQR 4.4 to 5.0; p=0.2).

Overall, this assessment did not reveal any differences between paediatric PNEC and PBEC non-CF and CF ALI cultures. However, analysis in paired non-CF cultures suggested greater responses to UTP in PNECs versus PBECs.

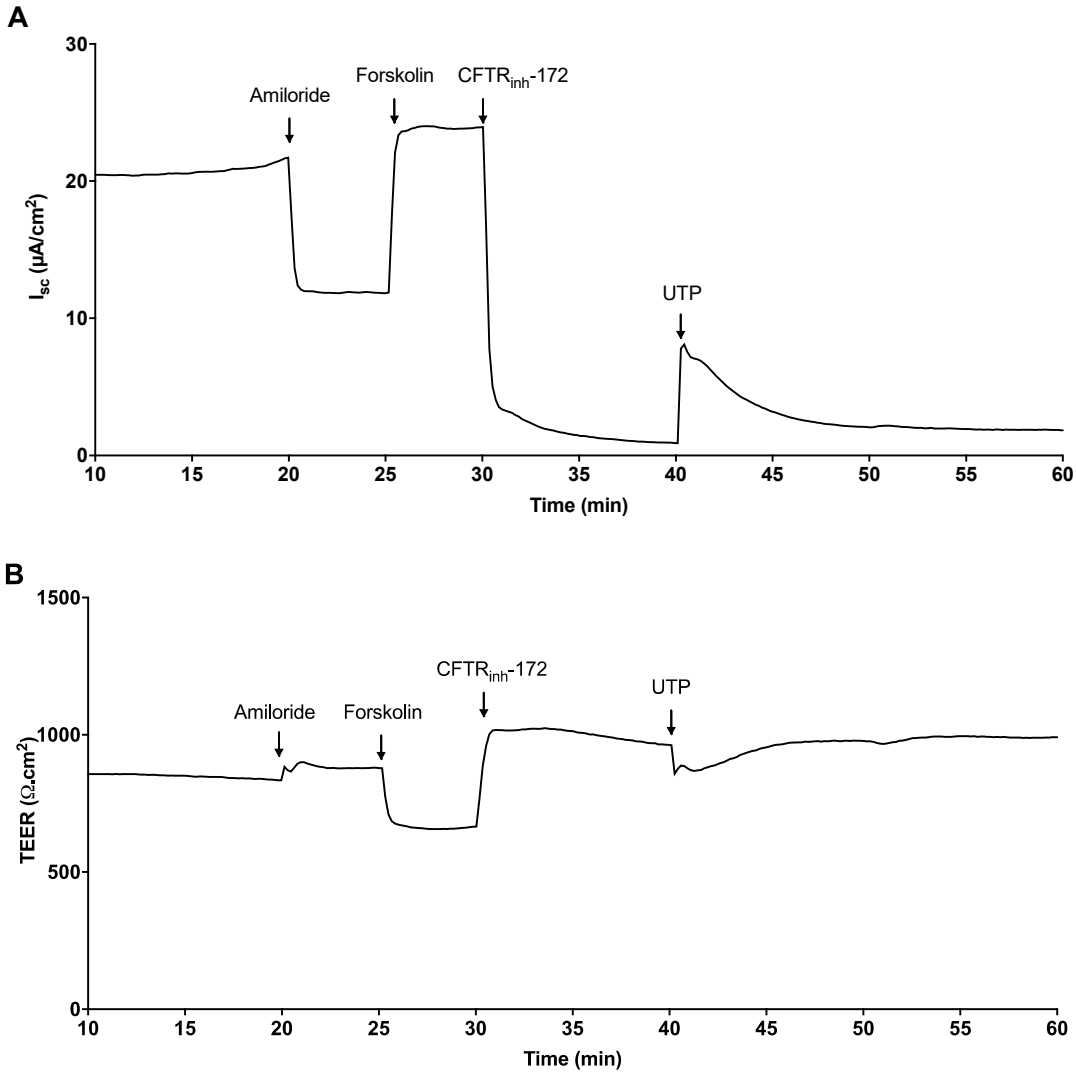

Figure 78: Representative Ussing chamber traces of the UTP-induced short circuit current and transepithelial electrical resistance response in a non-CF PNEC culture

A PNEC ALI culture insert derived from the non-CF PWT11N donor was mounted in the Ussing chamber and bathed apically and basolaterally in 125 mM chloride Krebs solution. After a 20-minute period of stabilisation, 10 μM amiloride was added to the apical compartment, followed by 10 μM forskolin and 20 μM $CFTR_{inh}$-172 at 25 and 30 minutes respectively. Resultant short circuit current (I_{sc}) and transepithelial electrical resistance (TEER) responses were recorded as shown in A and B respectively.

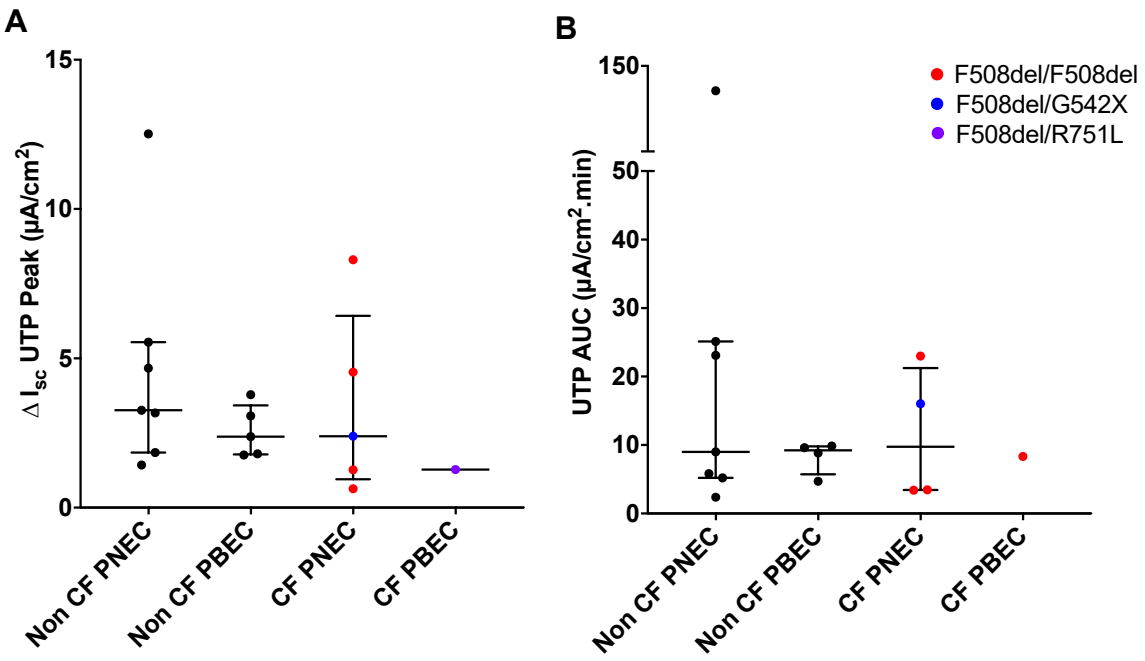

Figure 79: Assessment of the peak and total UTP-induced short circuit current in paediatric differentiated non-CF and CF PNEC and PBEC cultures

The UTP-induced change in peak short circuit current (ΔI_{sc} UTP peak) was assessed in differentiated PNEC and PBECs from 25 to 33d ALI in Ussing chamber experiments and shown in A. The area under the curve (AUC) was calculated for each response and shown in B. Each point represents the mean UTP-induced I_{sc} or AUC for each donor investigated. Data is presented as median ± IQR and analysed with Kruskal-Wallis and post hoc Dunn's multiple comparison test with no significant differences found. Non-CF PNECs (n=7 donors, 16 inserts), non-CF PBECs (n=5, 12 inserts), CF PNECs (n=5, 10 inserts), CF PBECs (n=1, 3 inserts). *CFTR* mutations for each CF donor are colour-coded as shown in the legend.

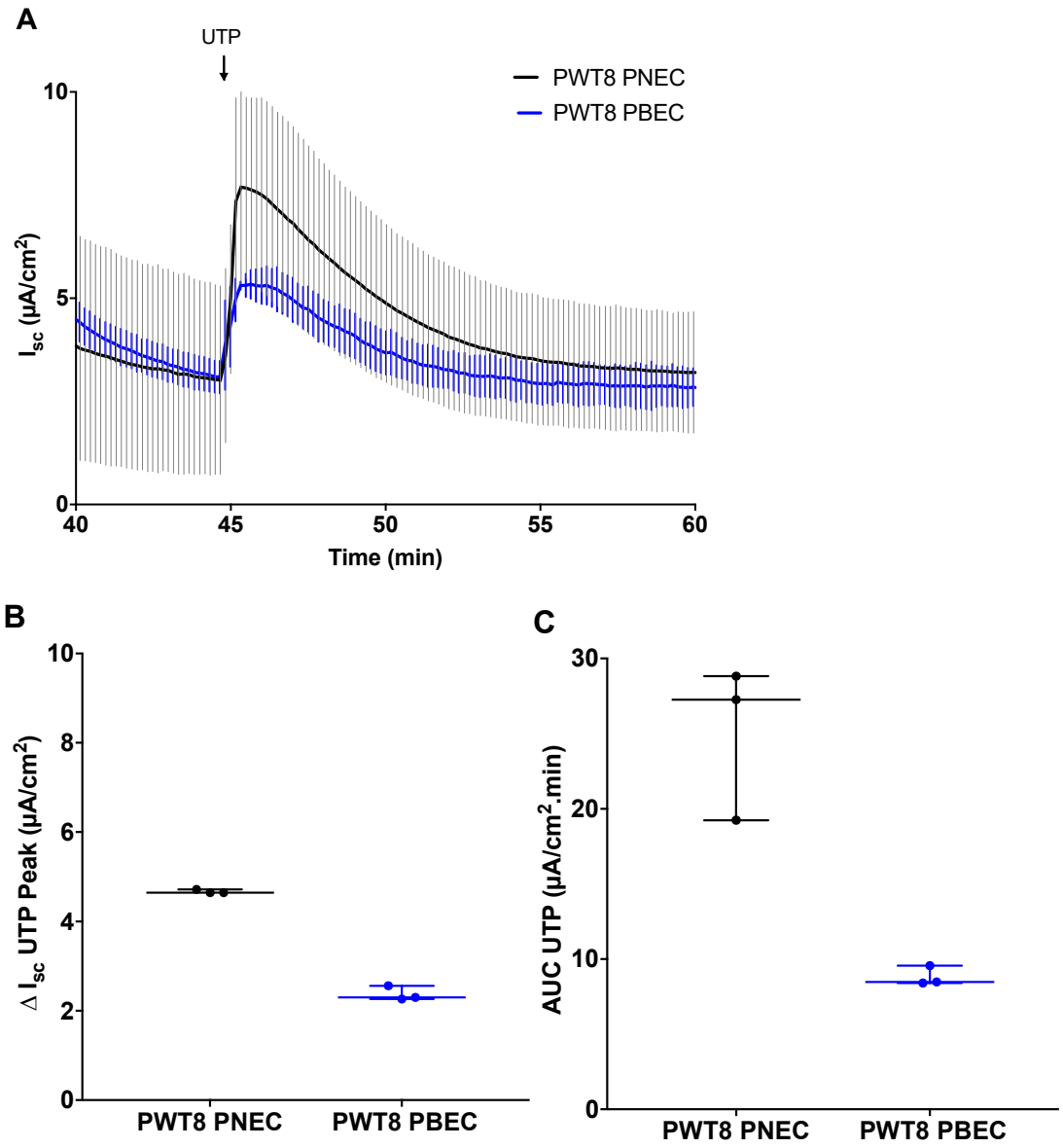

Figure 80: Paired assessment of UTP-induced short circuit current in PNEC and PBEC cultures derived from the non-CF PWT8 donor

Ussing chamber traces for PNEC and PBEC cultures isolated from the non-CF PWT8 donor are shown in A. Lines represents the mean short circuit current (I_{sc}) with error bars for the SD (PNEC in black, PBEC in blue, n=3 inserts for each culture type). The change in peak short circuit current (ΔI_{sc}) and area under the curve (AUC) after UTP addition were calculated and shown in B and C respectively. Data is presented as median ±IQR and analysed with Mann-Whitney test; p=0.1 for B and C. PNEC: n=3 inserts, PBEC: n=3 inserts.

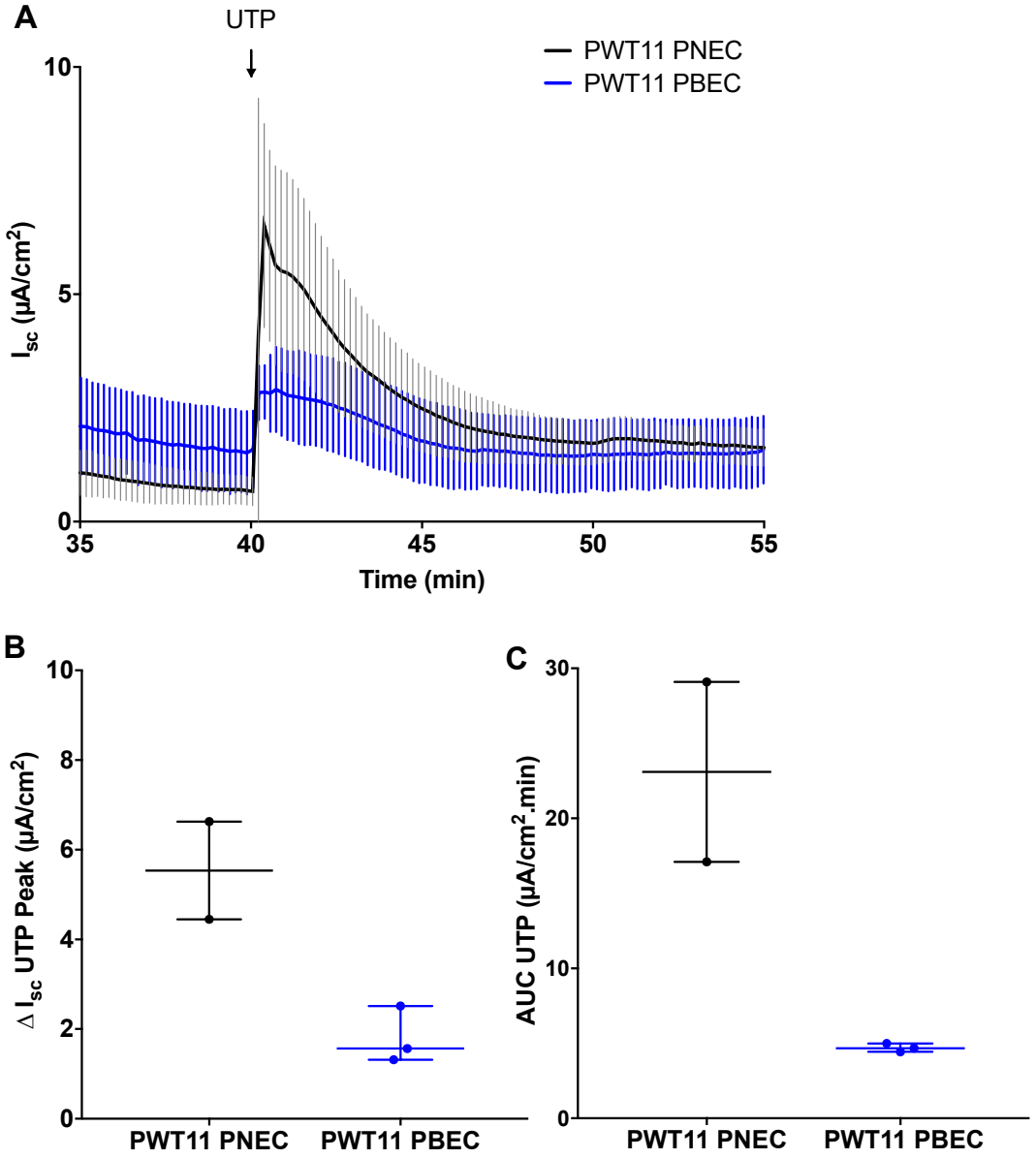

Figure 81: Paired assessment of UTP-induced short circuit current in PNEC and PBEC cultures derived from the non-CF PWT 11 donor

Ussing chamber traces for PNEC and PBEC cultures isolated from the non-CF PWT11 donor are shown in A. Lines represents the mean short circuit current (I_{sc}) with error bars for the SD (PNEC in black, n=2 inserts, PBEC in blue, n=3 inserts). The change in I_{sc} (ΔI_{sc}) and area under the curve (AUC) after UTP addition were calculated and shown in B and C respectively. Data is presented as median ±IQR and analysed with Mann-Whitney test; p=0.2 for B and C. PNEC: n=2 inserts, PBEC: n=3 inserts.

5.4.2 Assessment of relative chloride transport by CFTR and CaCC

Although CFTR is the principal channel involved in airway epithelial chloride secretion, it also transports bicarbonate into the ASL, with a relative permeability to chloride transport of 25 % (Tang et al., 2009). Investigation of relative chloride permeability by CaCC would be difficult to assess within the capacity of this PhD, however, assessment of CaCC-mediated chloride transport was assessed to ascertain its role in chloride secretion in paediatric airway epithelial cultures.

To determine the relative proportion of chloride transported by CaCC, the effect of chloride removal from Ussing chamber solutions was compared using 125 mM chloride with chloride free (0 mM) Krebs solutions. The composition of these solutions has been previously described in Chapter 2 section 2.5. Representative Ussing chamber traces demonstrating the responses seen in both 125 mM and 0 mM chloride Krebs are shown below in Figure 82. These experiments were performed in PNEC and PBEC cultures isolated from the non-CF PWT8 donor. It is evident that in both cases, removal of chloride resulted in a reduction in responses to amiloride, forskolin, $CFTR_{inh}$-172 and UTP.

The effect of chloride removal was investigated in 3 PNEC and 3 PBEC non-CF cultures. As shown in Figure 83, responses to forskolin were significantly reduced in 0 mM chloride (125mM chloride: 22.0 $\mu A/cm^2$, IQR 12.1 to 24.9 versus 0 mM chloride: 1.4$\mu A/cm^2$, IQR 0.9 to 2.4, p=0.002). This was also the case with the $CFTR_{inh}$-172-sensitive I_{sc} (125 mM chloride: -16.1 $\mu A/cm^2$, IQR -9.3 to -23.7 versus 0 mM chloride: -2.5 $\mu A/cm^2$, IQR -1.2 to -3.9, p=0.002). Each response was calculated as a percentage response relative to 125 mM chloride (which was given a value of 100 %). As shown in Figure 83, the percentage forskolin-induced I_{sc} responses in 0 mM chloride in both PNECs and PBECs were significantly less than responses seen at 125 mM chloride (PNEC: 8.6 % $\pm$4.9; p=0.03; PBEC: 10.7 % $\pm$5.5, p=0.04). The percentage responses for $CFTR_{inh}$-172-sensitive I_{sc} at 0 mM chloride were also reduced but the findings did not reach statistical significance (PNEC: 10.6 % $\pm$4.3, p=0.11; PBEC: 21.5 % $\pm$5.3, p>0.99).

The effects of chloride removal on the resultant UTP-induced I_{sc} were next investigated in 8 cultures (non-CF PNEC, non-CF PBEC and CF PNEC). Although there was a reduction in the UTP-induced I_{sc} in 0 mM chloride in all cultures as shown in Figure 84, the changes were not statistically significant (125 mM chloride:

2.4 μA/cm^2, IQR 1.9 to 4.2 versus 0 mM 1.5 μA/cm^2, IQR 0.8 to 2.7, p=0.1). The percentage UTP-induced I_{sc} response in 0 mM chloride relative to 125 mM in all three culture groups were all reduced, but only statistically significant in the non-CF PNECs (non-CF PNEC: 49.8 % ±7.6, p=0.04; non-CF PBEC: 78.4 % ±21.5, p=0.52; CF PNEC: 46.6 % ±21.2, p=0.09). Notably, UTP-induced I_{sc} responses in all 3 groups in 0 mM chloride conditions were proportionally greater than those evident with forskolin and $CFTR_{inh}$-172.

Overall these results have shown that in this cohort of paediatric cultures, as predicted, CFTR was predominantly involved in chloride secretion. Importantly, the relative contribution of CaCC-mediated chloride transport was proportionately less than CFTR. Aside from the non-CF PNECs, there were no differences in the UTP-induced I_{sc} in chloride and chloride-free conditions. The large residual I_{sc} response, the effect of which was greatest in non-CF PBECs, could be secondary to bicarbonate transport, but confirmation of this would require further detailed investigation.

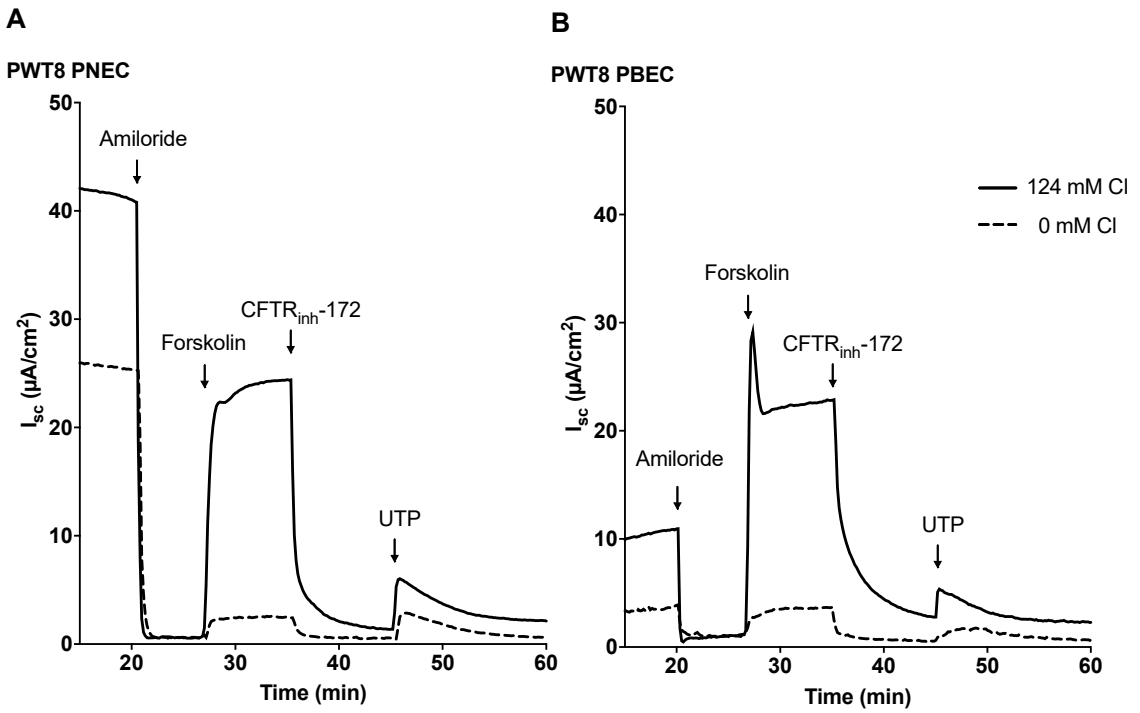

Figure 82: Representative trace of UTP-induced short circuit current in 125 mM and 0 mM chloride Krebs in PNEC and PBEC cultures isolated from a non-CF donor

PNEC and PBEC ALI culture inserts derived from the non-CF PWT8 donor were mounted in the Ussing chamber and bathed apically and basolaterally in 125 mM chloride Krebs solution. After a 20-minute period of stabilisation, 10 μM amiloride was added to the apical compartment, followed by 10 μM forskolin, 20 μM $CFTR_{inh}$-172 and 100 μM UTP at 25, 35 and 45 minutes respectively. This was repeated in 0 mM chloride Krebs solution. Resultant short circuit current (I_{sc}) responses for the PNEC (A) and PBEC cultures (B) are shown above at 125 mM chloride (solid black line) and 0 mM chloride (dashed black line); n=1 insert for each culture type.

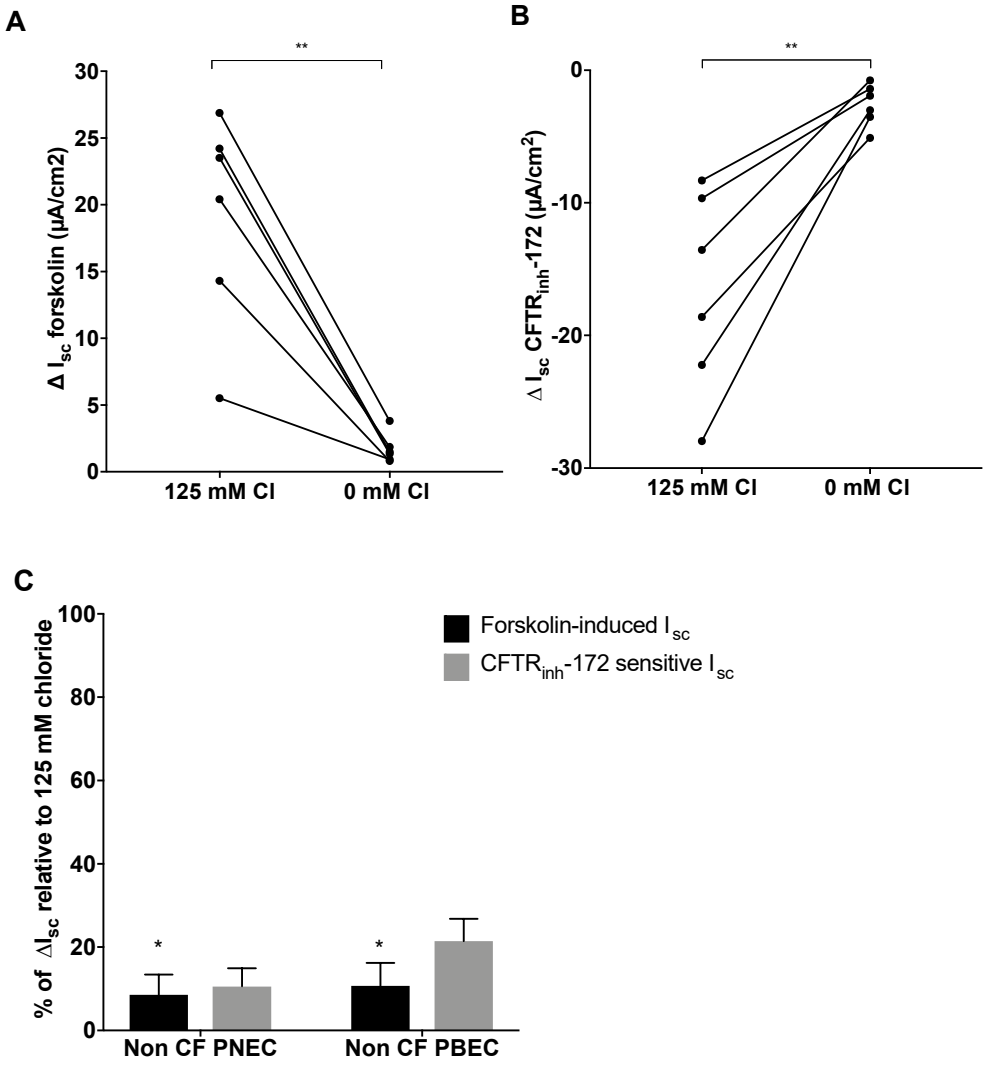

Figure 83: Short circuit responses to forskolin and $CFTR_{inh}$-172 in 125 mM and 0 mM chloride Krebs in non-CF PNEC and PBEC cultures

Resultant short circuit current responses to forskolin and $CFTR_{inh}$-172 (ΔI_{sc}) are shown in A and B respectively at 125 mM and 0 mM chloride solutions. Each point represents the mean ΔI_{sc} for each donor; each line represents individual donors. Data was analysed using the Mann-Whitney test; p=0.002 for forskolin and $CFTR_{inh}$-172. The percentage ΔI_{sc} at 0 mM relative to 125 mM chloride was calculated as shown in C. Bars represent mean percentage ±SD. Data is analysed using Kruskal-Wallis and post hoc Dunn's multiple comparison test; non-CF PNEC 0 mM versus 125 mM chloride ΔI_{sc} forskolin: p=0.03; non-CF PBEC 0 mM versus 125 mM chloride ΔI_{sc} $CFTR_{inh}$-172: p=0.04 for; non-CF PNECs n=3 donors (10 inserts); non-CF PBECs n=3 donors (9 inserts).

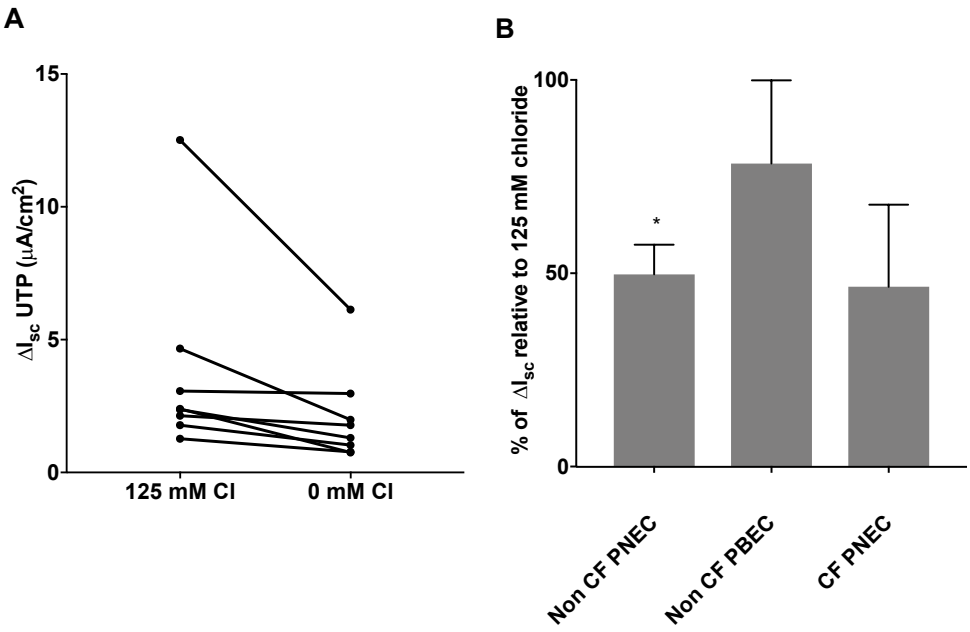

Figure 84: Short circuit current responses to UTP in 125 mM and 0 mM chloride Krebs in PNEC and PBEC cultures

Resultant short circuit current responses to UTP (ΔI_{sc}) at 125 mM and 0 mM chloride solutions are shown in A. Each point represents the mean ΔI_{sc} for each donor; each line represents individual donors. Data analysed using the Mann-Whitney test with no statistical differences found. Percentage ΔI_{sc} at 0 mM chloride relative to 125 mM chloride was calculated as shown in B. Bars represent mean percentage ± SD. Data is analysed using Kruskal-Wallis and post hoc Dunn's multiple comparison test; non-CF PNEC 0 mM versus 125 mM: p=0.04; non-CF PBEC. 0 mM versus 125 mM: p=0.54, CF PBEC 0 mM versus 125 mM: p=0.09; non-CF PNECs n=3 donors (6 inserts); non-CF PBECs n=3 donors (6 inserts); CF PNECs: n=2 donors (5 inserts).

5.4.3 Investigation of the atypical UTP-induced short circuit current responses

In a cohort of ALI cultures, apical UTP addition in Ussing chamber experiments resulted in responses that were not characteristic of CaCC activation. This occurred in 3 CF PBECs, 1 non-CF PBEC and 1 CF PNEC culture. It was not possible to reliably calculate the UTP-mediated CaCC activation in these cultures, and although I_{sc} changes were present, results from these cultures were omitted from the above comparisons and analyses.

Apical UTP addition in these circumstances resulted in a downward deflection in I_{sc} response, which is contrary to the characteristic upward change caused by CaCC-mediated chloride secretion under these experimental conditions. To demonstrate this effect, representative Ussing chamber traces from paired PNEC/PBEC cultures isolated from the PCF23 CF donor are shown in Figure 85. Panel A demonstrates the negative I_{sc} responses seen in both PNEC and PBECs, with a smaller response evident in PNECs (PNEC: -2.5 $\mu A/cm^2 \pm$ SD 3.2 versus PBEC: -12.2 $\mu A/cm^2 \pm 3.9$; mean responses derived from 2 culture inserts from each donor). Corresponding TEER changes are shown in panel B, where there was an associated TEER reduction of similar magnitudes resulting from increased channel conductance (PBEC: -308.8 $\Omega.cm^2 \pm 68.4$; PNEC: -312 308.8 $\Omega.cm^2 \pm 37.0$).

Similar to the changes seen with CaCC activation, these I_{sc} responses were transient, raising the possibility of an alternative UTP-mediated calcium activated channel. UTP-induced CaCC activation characteristically results in a positive I_{sc}, resulting from the outward flux of anions i.e. chloride ion secretion. However, the alternative resultant negative I_{sc} responses were likely caused by an outward flux of cations. This together with their transient nature led to the hypotheses that they were secondary to UTP-mediated activation of large conductance calcium activated potassium (BK) channels.

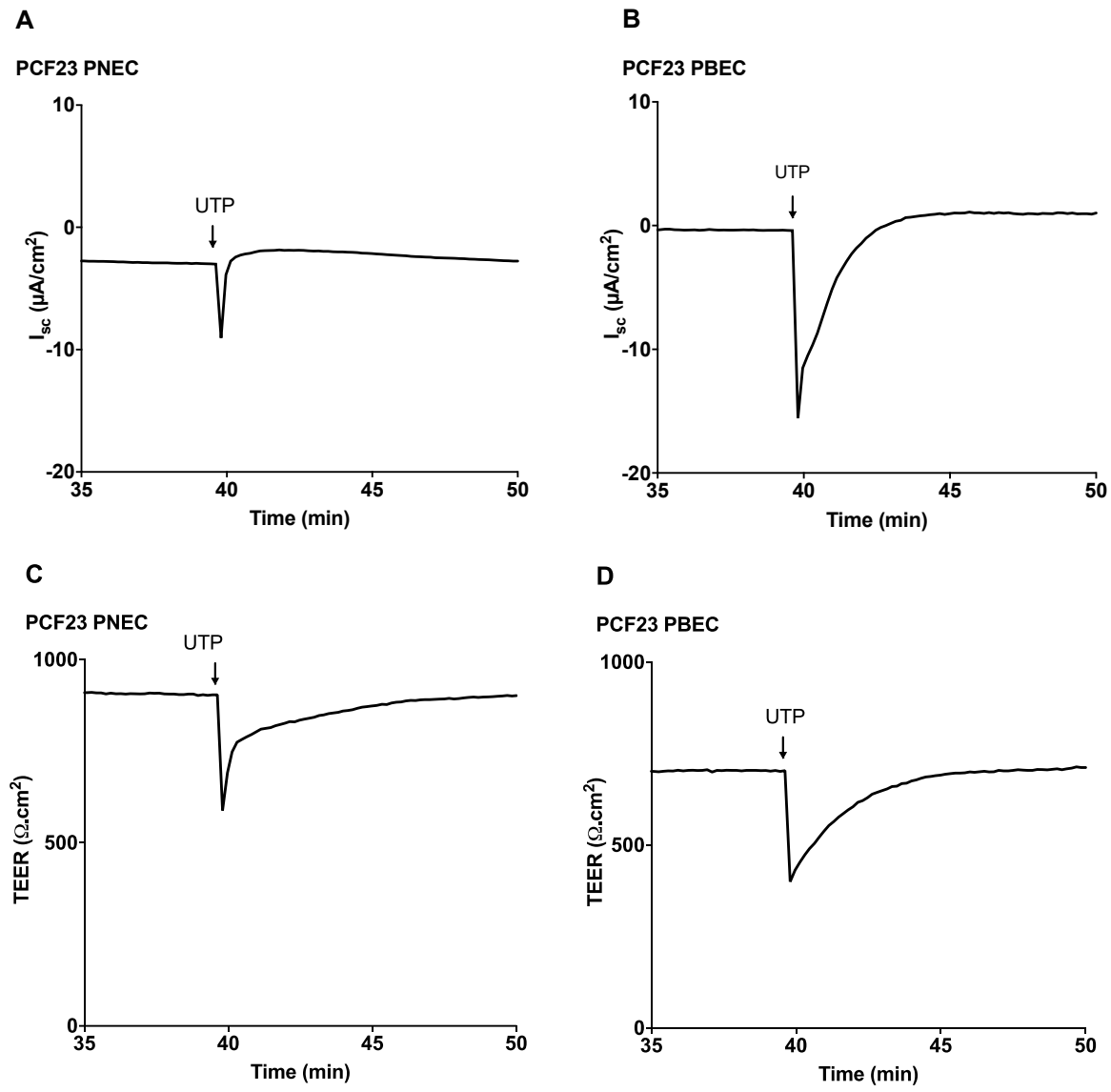

Figure 85: Representative Ussing chamber traces of the UTP-induced short circuit current and transepithelial electrical resistance response in PNEC and PBEC cultures derived from the PCF23 donor

Ussing chamber short circuit current (I_{sc}) traces for PNEC (A) and PBEC (B) cultures isolated from the PCF23 donor (F508del/2896delA) are shown. Corresponding transepithelial resistance (TEER) traces for PNECs and PBECs are shown in C and D respectively; n=1 culture insert for each condition.

5.4.4 Effects of barium chloride and BAPTA-AM on the atypical UTP-induced short circuit current response

To investigate this hypothesis, barium chloride ($BaCl_2$), a non-selective BK channel inhibitor, was added to the apical Ussing chamber compartment to determine its effects on the resultant I_{sc} in the PCF23 PNEC/PBEC cultures (2 culture inserts were used for each PBEC/PNEC). As demonstrated in Figure 86, apical addition of $BaCl_2$ prior to UTP eliminated the negative I_{sc} that was previously evident in the PNEC cultures, with a resultant positive I_{sc} response of 2.4 $\mu A/cm^2 \pm 0.6$ and a reduction in TEER decline (-77.1 $\Omega.cm^2 \pm 68.3$). In the PBECs, the UTP-induced I_{sc} remained negative after $BaCl_2$ addition, however, the magnitude of both I_{sc} and TEER responses were reduced (I_{sc}: -2.4 4 $\mu A/cm^2 \pm 2.2$; TEER: -69.9 $\Omega.cm^2 \pm 3.5$). Of note, the response at the time of $BaCl_2$ addition evident in Figure 86 was likely secondary to artefact and was not present in other experiments involving $BaCl_2$ addition.

To investigate if these negative I_{sc} responses were calcium-mediated, cell cultures were pre-treated with the calcium-selective cell permeator, BAPTA-AM (50 μM), for 60 minutes prior to performing Ussing chamber experiments to determine effects on UTP-induced I_{sc} and TEER. This was performed in the PCF25 PNEC/PBEC culture pair. Resultant traces together with changes in I_{sc} response are shown (Figure 87). Untreated PCF25 PNEC cultures demonstrated characteristic I_{sc} responses to UTP albeit small (1.1 $\mu A/cm^2$). In contrast, the PBEC culture showed a rapid UTP-induced decline in I_{sc} of -1.2 $\mu A/cm^2$ followed by an increase of 2.5 $\mu A/cm^2$. This was consistently evident in these PBEC cultures, suggesting a combination of potassium conductance and chloride secretion.

BAPTA-AM treatment in PNECs did not alter the resultant UTP-induced I_{sc} (untreated: 0.6 $\mu A/cm^2 \pm 0.4$; BAPTA-AM: 0.7 $\mu A/cm^2 \pm 0.2$). Notably, there was a 2-fold reduction in the resultant negative and positive induced-I_{sc} in PBECs (negative I_{sc} untreated: -2.8 $\mu A/cm^2 \pm 2.2$ versus BAPTA-AM: -1.3 $\mu A/cm^2 \pm 0.5$; positive I_{sc} untreated: 3.9 $\mu A/cm^2 \pm 2.0$ versus BAPTA-AM: 1.8 $\mu A/cm^2 \pm 1.3$). Experiments were performed in 2 culture inserts from each donor for each condition and therefore formal statistical analysis was not performed. However, these results suggested that calcium chelation reduced the UTP-induced responses in these PBECs, with no effect seen in PNECs. This could be explained by the relatively small UTP-induced I_{sc} present in untreated cultures or requirement for optimisation of the protocol used for BAPTA-AM addition in primary cultures.

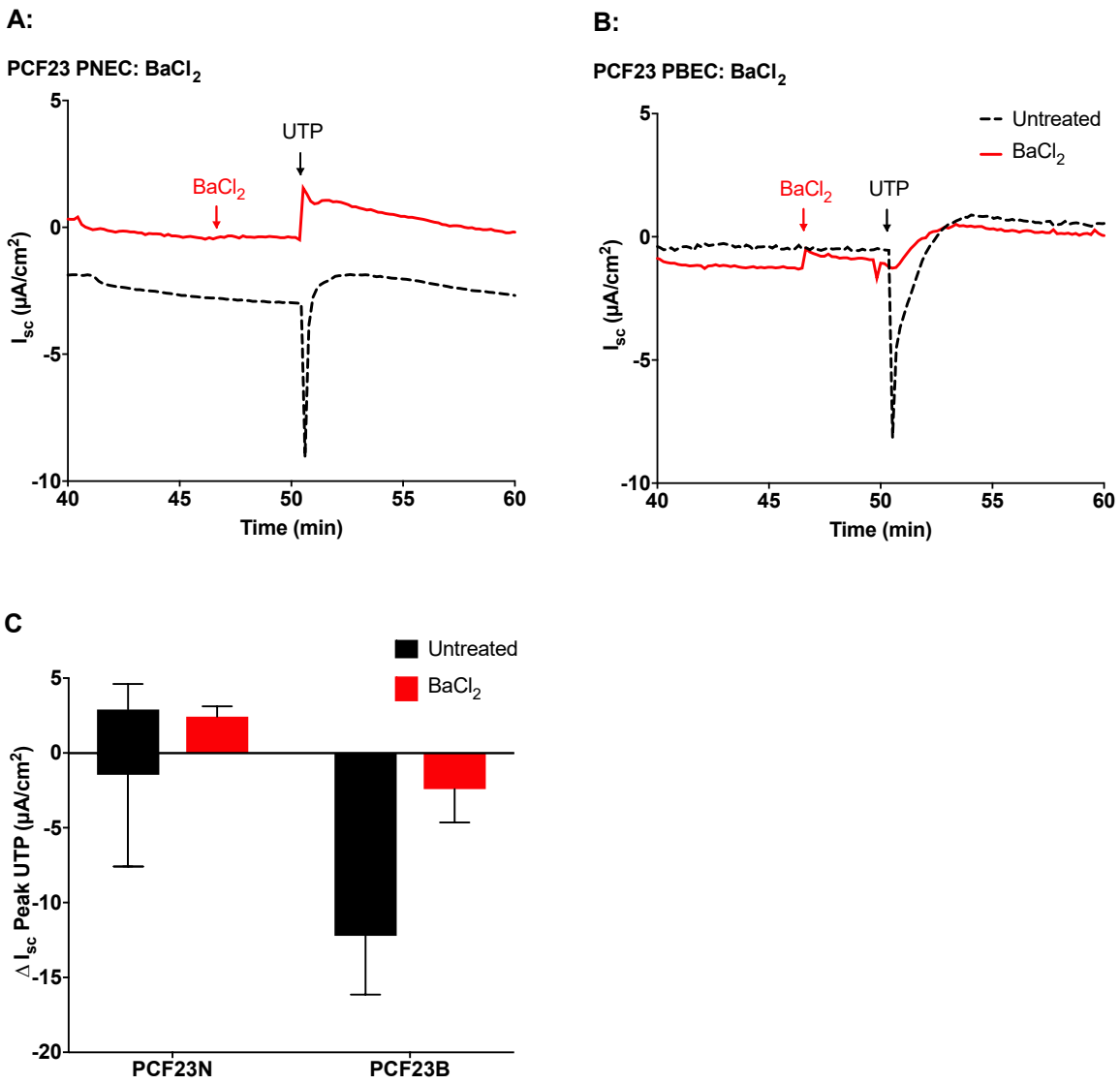

Figure 86: Representative Ussing chamber traces demonstrating the effects of barium chloride on the UTP-induced short circuit current response in PNEC and PBEC cultures derived from the CF PCF23 donor

Ussing chamber short circuit current (I_{sc}) traces for PNEC (A) and PBEC (B) cultures isolated from the CF PCF23 donor (F508del/2896delA) are shown. Barium chloride ($BaCl_2$) was added 5 minutes prior to UTP addition. The resultant change in peak short circuit current (ΔI_{sc}) was calculated (C). Bars represent mean ± SD; untreated: n=3 inserts for each culture type; $BaCl_2$: n=2 culture inserts for each culture type (statistical tests not applied).

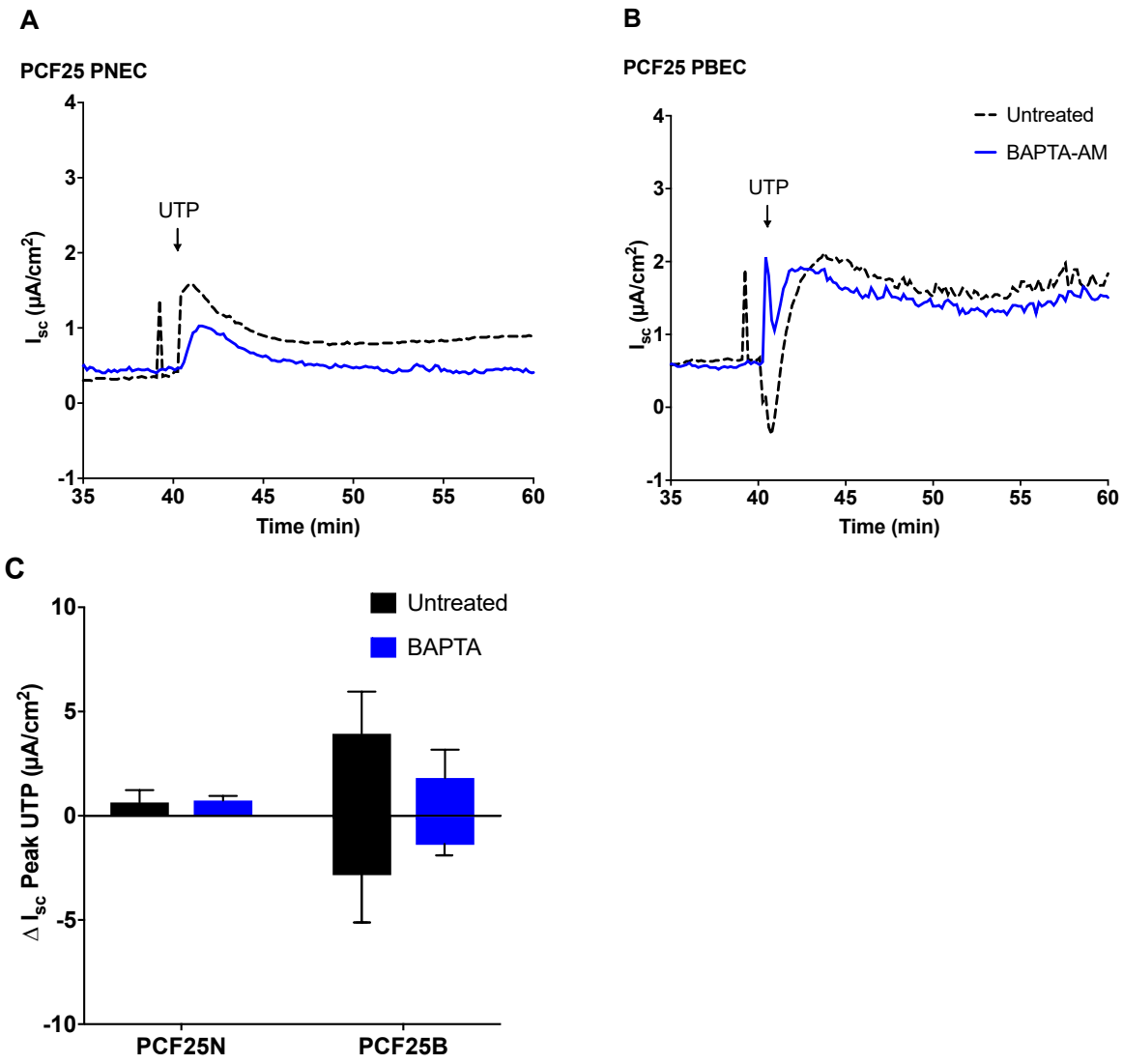

Figure 87: Representative Ussing chamber traces demonstrating the effects of BAPTA-AM pre-treatment on the UTP- induced short circuit current response in PNEC and PBEC cultures derived from the CF PCF25 donor

Ussing chamber short circuit current (I_{sc}) traces for PNEC (A) and PBEC (B) cultures isolated from the CF PCF25 donor (F508del/F508del) are shown above. Cell cultures were treated with 50 μM BAPTA-AM for 60 minutes prior to the Ussing chamber experiment. The resultant change in peak UTP-induced short circuit current (ΔI_{sc}) was calculated (C). Bars represent mean ± SD; untreated: n=2 inserts for each culture type; BAPTA-AM: n=2 culture inserts for each culture type (statistical tests not applied).

5.4.5 Assessment of chloride-dependence of the atypical UTP-induced short circuit current response

To determine the chloride-dependent nature of this negative UTP-induced I_{sc} response, Ussing chamber experiments were performed in 125 mM and 0 mM chloride Krebs. These experiments were carried out in paired non-CF PWT17 PNEC and PBEC cultures (Figure 88). Due to a limited number of available culture inserts, 1 insert was used for each assessment. In 125 mM chloride. The resultant UTP-induced I_{sc} in PNECs was positive in 125 mM chloride (3.8 $\mu A/cm^2$), which was negative in chloride free conditions (-0.9 $\mu A/cm^2$). In 125 mM chloride, the response in PBECs was initially negative (-5.3 $\mu A/cm^2$), followed by an increase by 4.7 $\mu A/cm^2$ from baseline. Chloride removal eliminated the positive I_{sc} component and the resultant negative I_{sc} predominated. This modification in I_{sc} response was also evident in the CF PCF22 PBEC culture as shown in Figure 89. In all cases, there was an associated decrease in resistance, again suggesting an increase in conductance (data not shown). The results obtained for the Ussing chamber experiments performed in 0 mM chloride suggested that the UTP-induced negative response was caused by chloride-independent channel activation.

Overall, experiments investigating the effects $BaCl_2$ and BAPTA in conjunction with assessment in chloride free conditions suggested that these responses were secondary to the UTP-induced activation of BK channels. This was not explored further during this PhD but does require further investigation using inhibitors of specific BK channels together with the exploration of BK channel expression in differentiated ALI cultures.

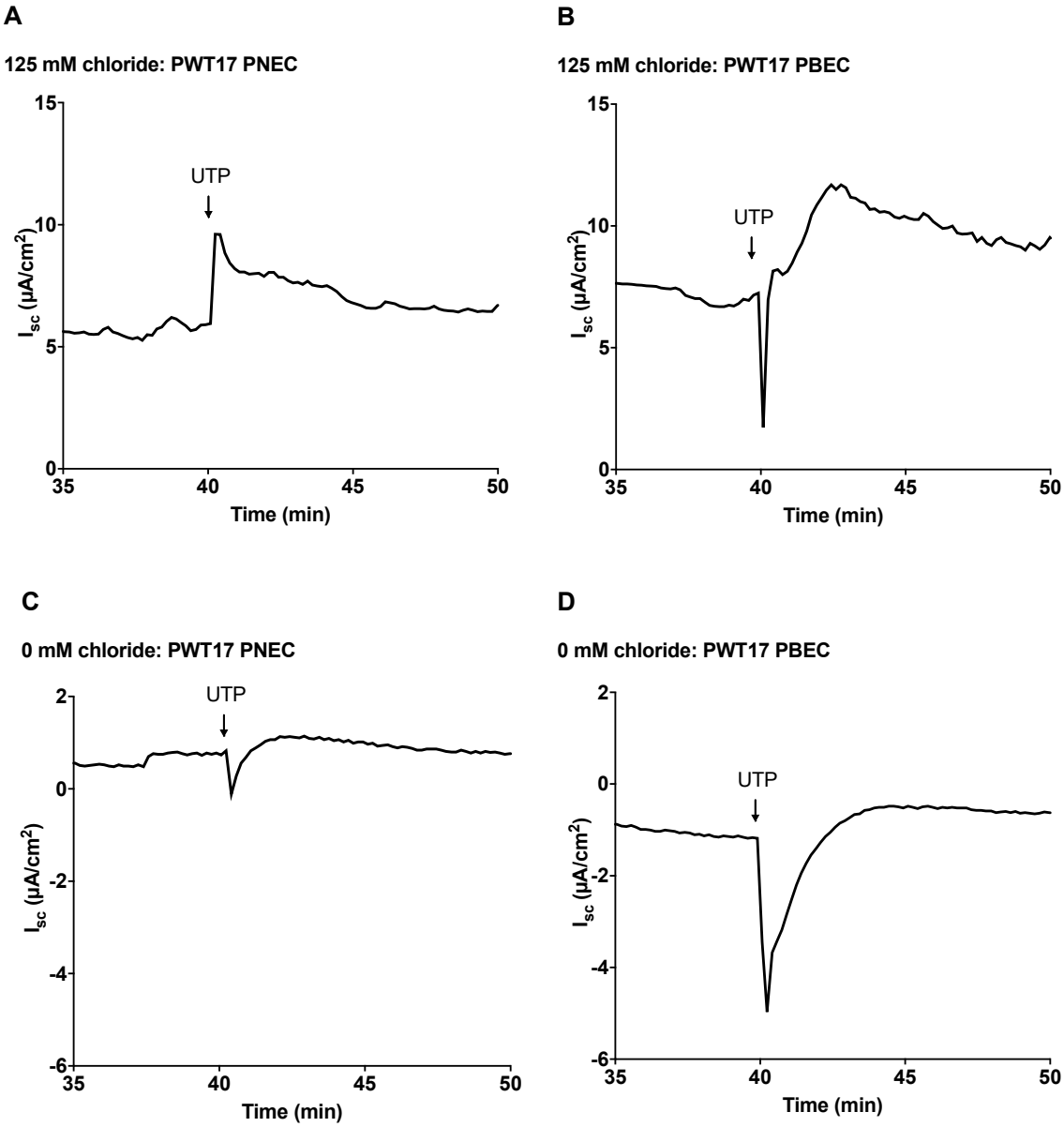

Figure 88: Representative Ussing chamber traces demonstrating the UTP-induced short circuit current in 125 mM and 0 mM chloride Krebs solutions in PNEC and PBEC cultures derived from the non-CF PWT17 donor

Ussing chamber short circuit current (I_{sc}) traces for PNEC and PBEC cultures isolated from the non-CF PWT17 donor are shown above in 125 mM chloride (A and B) and 0 mM chloride (C and D); n=1 culture insert for each condition.

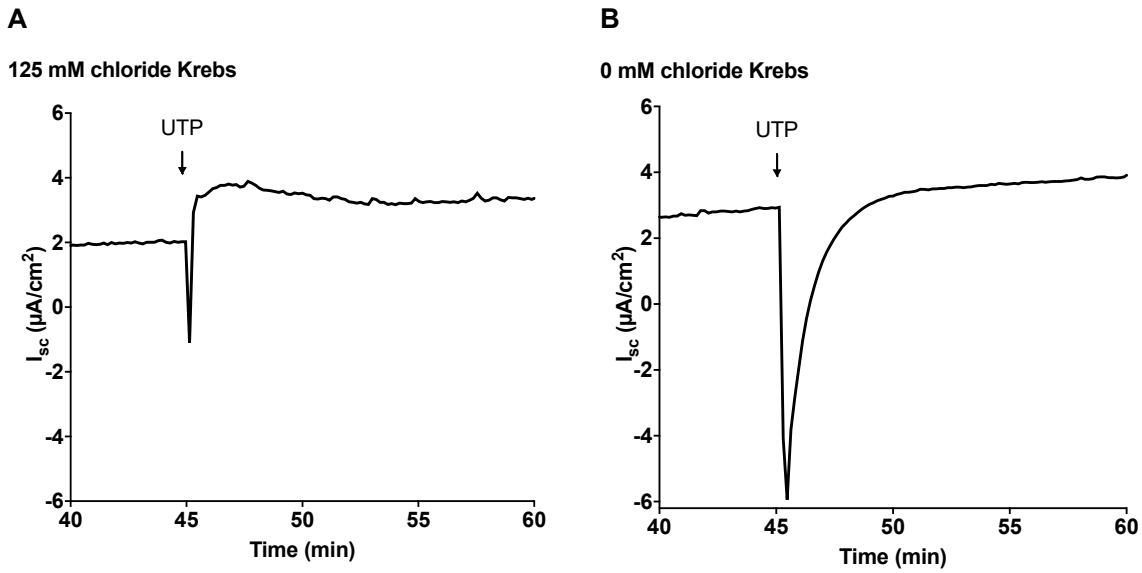

Figure 89 : Representative Ussing chamber traces for the UTP-induced short circuit current response in 125 mM and 0 mM chloride Krebs in PBEC cultures derived from the CF PCF22 donor

Ussing chamber short circuit current (I_{sc}) traces for PBEC cultures isolated from the CF PCF22B donor (F508del/F508del) are shown above in 125 mM chloride (A) and 0 mM chloride (B); n=1 culture insert for each condition.

5.4.6 Assessment of TMEM16A activation with the small molecule activator Eact in paediatric primary nasal epithelial cultures

Although purinergic agonists such as UTP are useful to determine the functional expression of CaCC in paediatric ALI cultures in Ussing chamber experiments, alternative agonists are required to enable the specific investigation of TMEM16A. In 2011, the small molecule Eact was discovered by high throughput screening of over 100,000 compounds as a potent putative activator of TMEM16A (Namkung et al., 2011b). Its mechanism of action is thought to be calcium-independent, through direct binding to the calcium binding site on TMEM16A (Namkung et al., 2011b). The effects of Eact were investigated during this PhD in Ussing chamber experiments involving paediatric differentiated ALI cultures at 25 to 33d ALI.

Initial evaluation was performed using conditions as previously described, with the application of 125 mM chloride Krebs to both Ussing chamber compartments, and the initial apical addition of amiloride, forskolin and $CFTR_{inh}$-172 as previously described. The Eact-induced I_{sc} relative to UTP was first established and investigated in PNEC cultures derived from a CF donor. As shown by the representative Ussing chamber traces in Figure 90, the Eact-induced I_{sc} was comparatively small (Eact: 0.7 $\mu A/cm^2$; UTP: 8.1 $\mu A/cm^2$).

To determine if this Eact-induced response could be augmented, a chloride gradient was established using 40 mM chloride Krebs apically and 125 mM chloride Krebs basolaterally (as previously described in Chapter 2 section 2.5) in PNEC cultures derived from the PWT4 donor. Responses using this chloride gradient were compared with experiments performed with 125 mM and 0 mM chloride solutions. Representative I_{sc} and TEER traces for each condition results are shown below in Figure 91 and summarised in Table 19. Due to limited culture insert availability, these experiments were performed only once, and therefore provide only descriptive data. Introduction of a chloride gradient increased the forskolin-induced I_{sc} (26.4 $\mu A/cm^2$) compared with 125 mM (20.4 $\mu A/cm2$) and 0 mM chloride (1.2 $\mu A/cm^2$) conditions. In these cultures, introduction of a chloride gradient did not alter the resultant UTP-induced I_{sc} compared with 125 mM chloride (2.4 $\mu A/cm^2$ versus 2.2 $\mu A/cm^2$). Eact induced-I_{sc} responses were evident in both 125 mM chloride and with the presence of a chloride gradient, however the nature of response differed in the 2 conditions, as evident in Figure 91 and Table 19. In 125 mM chloride Krebs, there was a gradual increase in the Eact-induced I_{sc}, with a peak response of 1.4 $\mu A/cm^2$, occurring 5 min

after Eact addition, followed by a return to a baseline of 0.2 μA/cm^2. With a chloride gradient, the Eact-induced I_{sc} was greater at 2.3 μA/cm^2, peaking 10 min after Eact addition. Furthermore, although the total duration of Eact response cannot be determined in these experiments due to the subsequent addition of UTP, the I_{sc} increase was more sustained, and had reduced by only 0.4 μA/cm^2 from the peak value at this time. The Eact-induced I_{sc} was the lowest in 0 mM chloride of 0.3 μA/cm^2 and the total response was much shorter in duration.

In all chloride containing Krebs solutions, Eact addition was associated with a TEER reduction, indicating increased chloride secretion. Although there was an initial decline in TEER in 0 mM chloride that could attributed to bicarbonate secretion, there was a subsequent complete loss of TEER and large reduction in I_{sc} after UTP addition. This sudden decline was likely caused by epithelial cell damage, resulting in loss of tight junction integrity and subsequent leakage of ions. Experiments were well tolerated in other conditions.

The effect of a chloride gradient on the Eact-induced I_{sc} was explored further in differentiated PNEC cultures isolated from 3 non-CF and 5 CF donors at 25 to 33d ALI. PNECs derived from 1 of each non-CF and CF donors did not respond (data not shown). It is evident from Figure 92 that in Eact responders, there was considerable intra-donor variability in the peak induced I_{sc}, and although donor numbers were small, this variability was greater in non-CF cultures. The peak Eact induced I_{sc} was 3.2-fold greater in non-CF PNECs, however this was not statistically significant (non-CF: 1.9 μA/cm^2, IQR 1.2 to 2.7 versus CF: 0.6 μA/cm^2, IQR 0.5 to 1.1, p=0.13). This was paralleled with a suggested higher total Eact-induced I_{sc} in the non-CF group (non-CF: 28.3 μA/cm^2.min, IQR 24.7 to 32.0 versus CF: 6.4 μA/cm^2.min, IQR 3.4 to 22.2; p=0.27). Overall, these results suggested that treatment with Eact generated an I_{sc} in these cultures and the effects were greatest in non-CF PNECs. The lack of statistical significance is likely due to limited culture numbers.

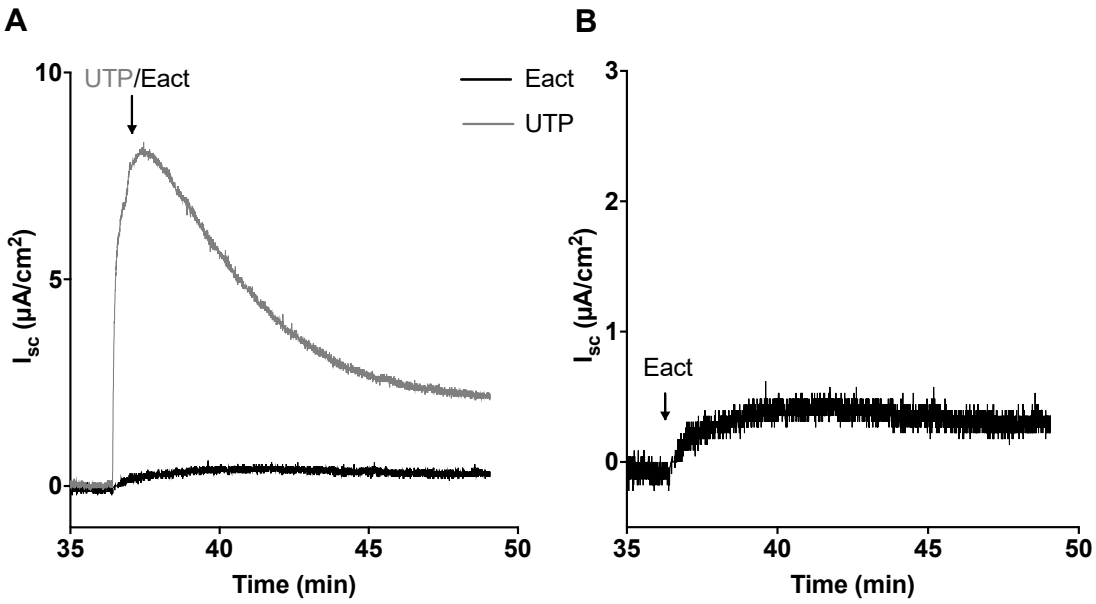

Figure 90: Representative Ussing chamber trace demonstrating short circuit current responses to UTP and Eact in a CF PNEC culture

A PNEC ALI culture insert the CF PCF10N donor (F508del/F508del) was mounted in the Ussing chamber and bathed apically and basolaterally in 125 mM chloride Krebs. After the addition of amiloride, forskolin and $CFTR_{inh}$-172 (not shown) either 100 μM UTP (grey) or 10 μM Eact (black) were added apically. Resultant short circuit current (I_{sc}) responses are shown in A. The magnified Eact-induced I_{sc} response is shown in B.

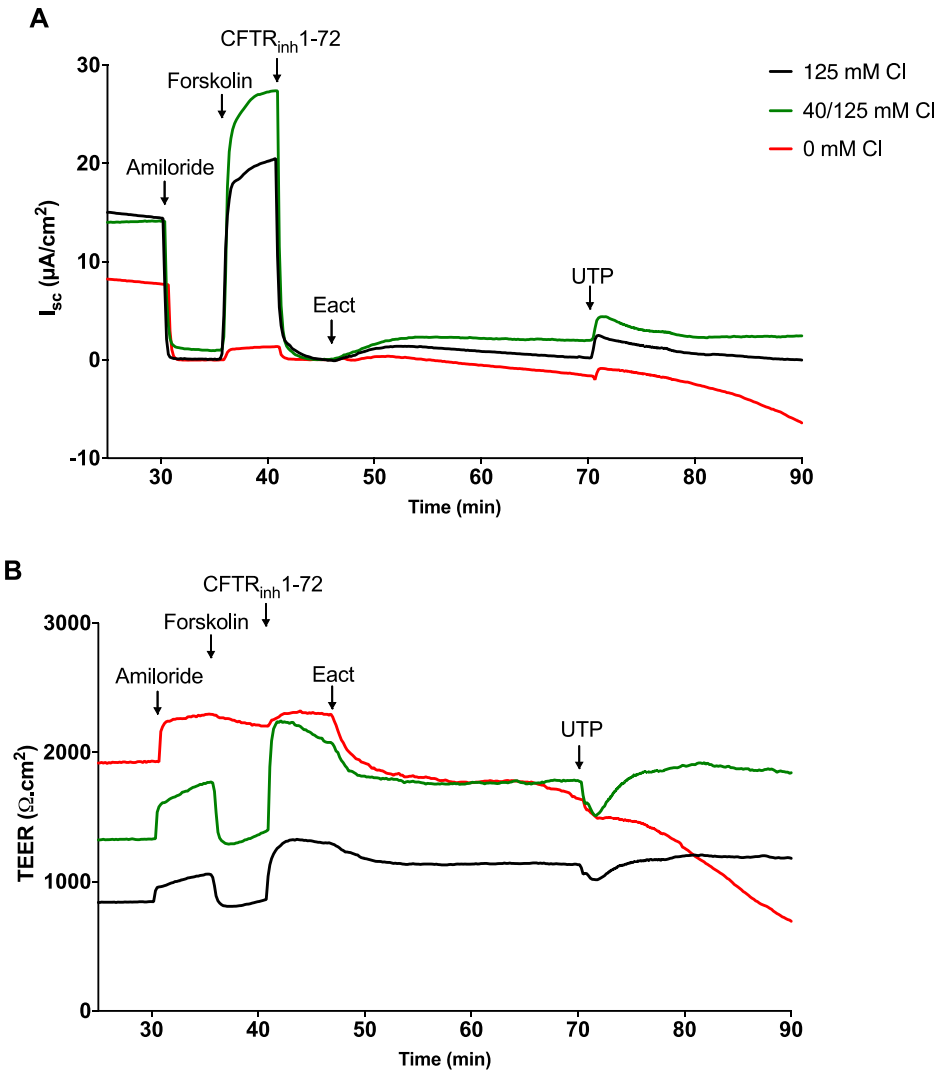

Figure 91: Representative short circuit current and transepithelial electrical resistance responses demonstrating the effects of chloride concentration in PNEC cultures derived from a non-CF donor

PNEC culture inserts derived from the non-CF PWT4 donor were mounted in the Ussing chamber and bathed bilaterally in 125 mM or 0 mM chloride, or in a 40/125 mM apical to basolateral chloride gradient. After a period of stabilisation, 10 µM amiloride, 10 µM forskolin, 20 µM $CFTR_{inh}$-172, 10 µM Eact and 100 µM UTP were added apically at 30, 35, 40, 50 and 70 minutes respectively. Resultant short circuit current (I_{sc}) and corresponding transepithelial electrical resistance (TEER) were measured as shown in A and B respectively; n=1 culture insert for each condition.

Measurement	0 mM chloride	125 mM chloride	40/125 mM chloride
Peak Δ I_{sc} ($\mu A/cm^2$)	0.3	1.4	2.2
AUC ($\mu A/cm^2$.min)	1.4	19.0	44.6
Duration (min)	6.5	25	> 25
Δ TEER ($\Omega.cm^2$)	-486	-134	-289

Table 19: Ussing chamber responses to Eact in 0 mM chloride, 125 mM chloride and a 40mM/125mM apical to basolateral chloride gradient in PNEC cultures isolated from the non-CF PWT4 donor

Abbreviations: ΔI_{sc}: change in short circuit current; AUC: area under the curve; TEER: transepithelial resistance.

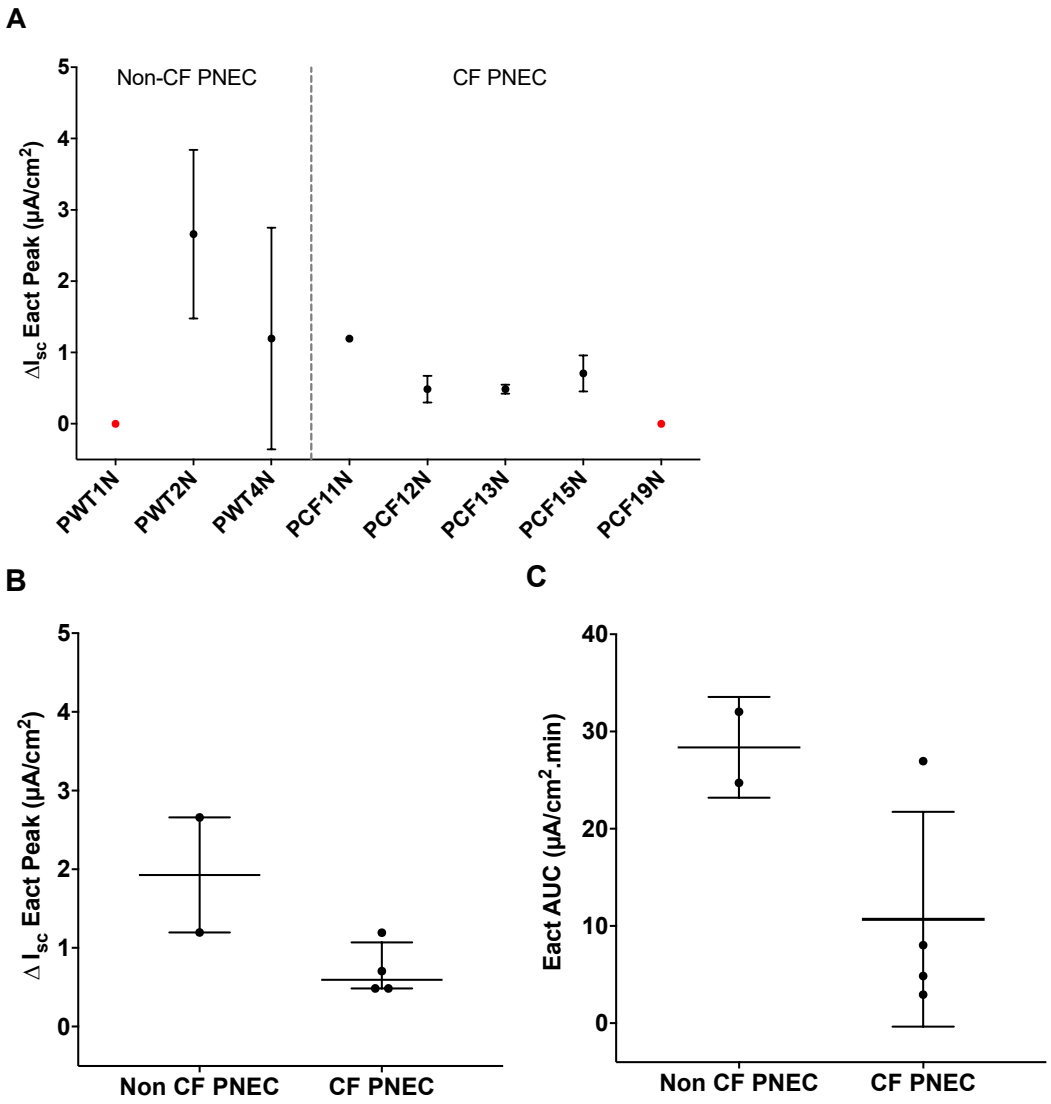

Figure 92: Assessment of Eact-induced short circuit current in non-CF and CF PNEC cultures

The Eact-induced change in peak short circuit current (ΔI_{sc}) was assessed in differentiated non-CF and CF PNECs in Ussing chamber experiments. Responses seen in each donor are shown in A, where each point represents the mean response ± SD. Donors with no response to Eact are shown in red. Combined Eact peak ΔI_{sc} and total (AUC) responses for non-CF and CF PNECs are shown in B and C respectively. Data is presented as median ± IQR and analysed with Mann Whitney test with no significant differences found. Non-CF PNECs (n=2 donors, 4 inserts), CF PNECs (n=4, 11 inserts).

5.4.7 Investigation of the effects of IL-4 on TMEM16 activation with Eact in paediatric primary nasal epithelial cultures

It has been shown previously by other groups that treatment of primary airway epithelial cultures with cytokines such as IL-4 or IL-13 promote a pro-secretory profile due to decreases in the amiloride-sensitive I_{sc} and increases in the forskolin and CaCC-induced responses (Danahay et al., 2002, Galietta et al., 2002, Gorrieri et al., 2016). In view of the relatively small magnitude of the Eact-induced I_{sc} described in the previous section, cell cultures were treated with IL-4 to determine if these responses could be enhanced.

Representative Ussing chamber traces demonstrating the comparative responses in vehicle control or IL-4 treated cultures for PNEC cultures derived from a non-CF and CF donor are shown in Figure 93 and Figure 94 respectively. As shown in Figure 93, the amiloride-sensitive I_{sc} in the PWT2 PNEC was reduced from -135 to -14.9 $\mu A/cm^2$. There was no effect on the forskolin and $CFTR_{inh}$-172 responses. In these cultures, there was no Eact-induced I_{sc}, however, IL-4 treatment resulted in a small response of 0.5 $\mu A/cm^2$ as shown in this figure. The UTP-induced I_{sc} demonstrated in this figure increased over 3 times with IL-4 treatment from 13.6 to 44.7 $\mu A/cm^2$. Representative I_{sc} traces for PCF15 PNEC cultures in Figure 94 showed a similar picture, with a decrease in the amiloride-sensitive I_{sc} from -11.0 to -2.5 $\mu A/cm^2$ and an increase in the UTP-induced I_{sc} from 6.7 to 19.8 $\mu A/cm^2$. However, IL-4 treatment did not affect the magnitude of the Eact-induced I_{sc} (0.5 $\mu A/cm^2$).

Responses to Eact in control and IL-4 treated cultures were assessed in PNECs derived from 2 non-CF and 2 CF donors as shown in Figure 95. IL-4 treatment increased the Eact-induced I_{sc} in all cultures aside from PCF15. All three culture inserts derived from the PWT1 donor did not show an Eact response in control conditions, but there was a suggested increase with IL-4 treatment (IL-4: 0.5 $\mu A/cm^2$, IQR 0.3 to 0.8, p=0.1). PWT2 PNECs showed the greatest Eact-induced I_{sc} under control conditions (2.7 $\mu A/cm^2$, IQR 1.8 to 3.5), which in 1 culture insert was increased by IL-4 treatment to 8.7 $\mu A/cm^2$. IL-4 treatment in cultures derived from PCF13N suggested an increase in the Eact-induced I_{sc} by 179 % (control: 0.43 $\mu A/cm^2$, IQR 0.4 to 0.5 versus IL-4: 1.3 $\mu A/cm^2$, IQR 1.2 to 1.5 , p=0.2).

Comparable UTP-induced I_{sc} responses in IL-4 treated cultures (1 non-CF and 2 CF PNECs) are also shown in Figure 95. In all cases, IL-4 treatment demonstrated large

increases in the UTP-induced I_{sc}. Notably this was also evident in the PCF15 cultures, which had failed to show a response with Eact. For completion, the comparable responses to amiloride, forskolin and $CFTR_{inh}$-172 are shown in Figure 96. As expected, all cultures demonstrated reductions in the amiloride-sensitive I_{sc} after IL-4 treatment. Cultures derived from PWT1 did not demonstrate an increase in the forskolin-induced I_{sc}, but there was a larger response to $CFTR_{inh}$-172. PWT2N did show enhanced CFTR activity with IL-4 treatment. Notably, it was possible to increase I_{sc} responses to forskolin and $CFTR_{inh}$-172 in the PCF15 PNEC cultures by 214 % and 117 % respectively.

These results indicate treatment with IL-4 produced expected responses in ENaC, CFTR and CaCC-mediated ion transport. It was possible to enhance the activity of Eact with IL-4 treatment, but this was not consistently possible in all cultures investigated.

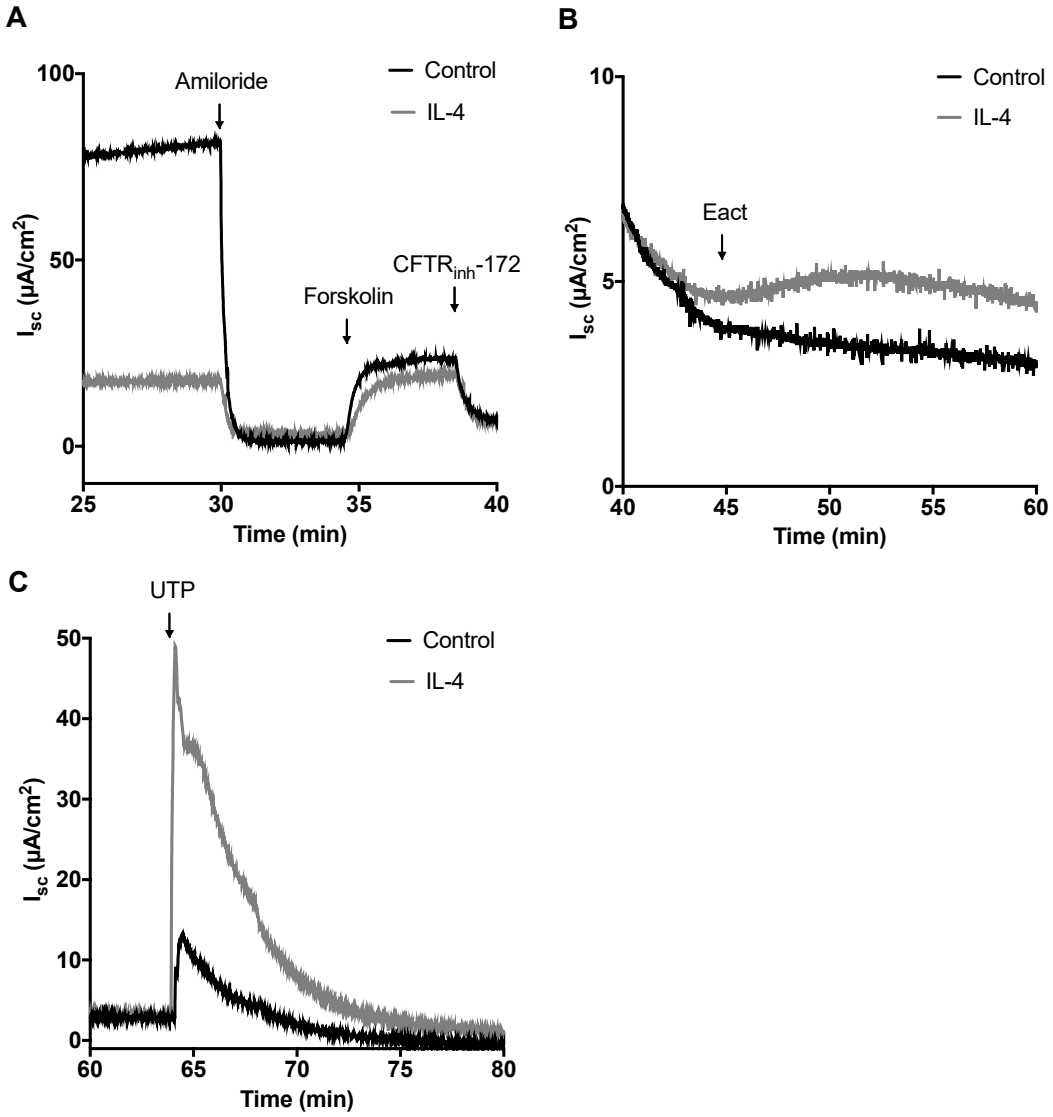

Figure 93: Representative Ussing chamber traces demonstrating the effects of IL-4 treatment in PNEC cultures derived from a non-CF donor

PNEC culture inserts derived from the non-CF PWT1 donor were mounted in the Ussing chamber and bathed bilaterally in a 40/125 mM chloride gradient. After a period of stabilisation, 10 μM amiloride, 10 μM forskolin and 20 μM $CFTR_{inh}$-172 were added apically at 30, 35, and 40 minutes respectively as shown in A. 10 μM Eact was added at 45 minutes followed by 100 μM UTP as shown in B and C respectively. The representative traces shown above demonstrate I_{sc} responses for culture inserts either treated with 10 ng IL-4 (grey) or vehicle control (black) for 24 hours; n=1 culture insert for each condition.

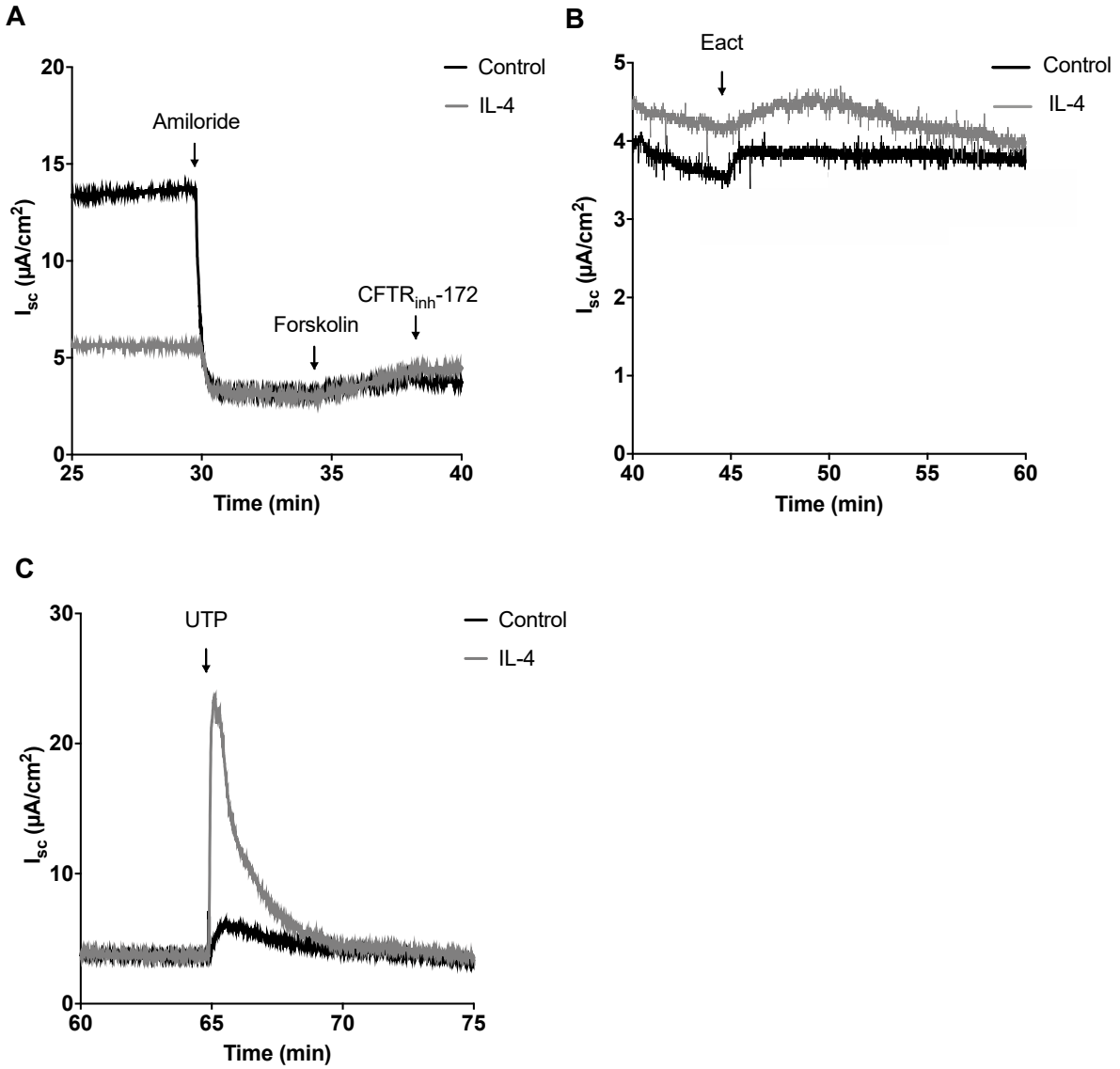

Figure 94: Representative Ussing chamber traces demonstrating the effects of IL-4 treatment in PNEC cultures derived from a CF donor

PNEC culture inserts derived from the CF PCF15 donor were mounted in the Ussing chamber and bathed bilaterally in a 40/125 mM chloride gradient. After a period of stabilisation, 10 μM amiloride, 10 μM forskolin and 20 μM $CFTR_{inh}$-172 were added apically at 30, 35, and 40 minutes respectively as shown in A. 10 μM Eact was added at 45 minutes followed by 100 μM UTP as shown in B and C respectively. The representative traces shown above demonstrate I_{sc} responses for culture inserts either treated with 10 ng IL-4 (black) or vehicle control (grey) for 24 hours; n=1 culture insert for each condition.

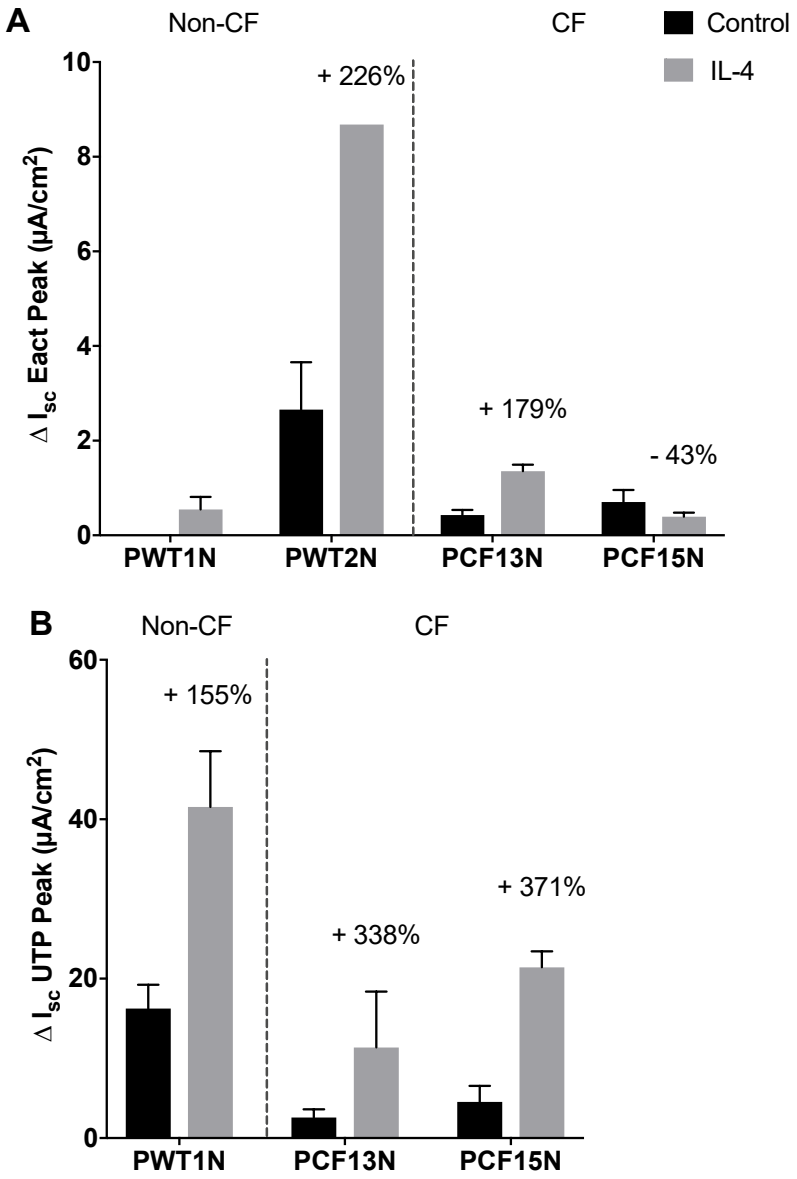

Figure 95: Effects of IL-4 treatment of the peak UTP and Eact-induced short circuit current responses in non-CF and CF PNEC cultures

Cultures were treated with vehicle control (black) or IL-4 (grey) for 24 hours and investigated in Ussing chamber experiments. The resultant Eact and UTP-induced change in peak short circuit current (ΔI_{sc}) are shown in A and B respectively. Data is presented as the mean I_{sc} response ± SD and analysed with Mann Whitney test with no significant differences found. Percentage increases in I_{sc} in IL-4 treated cultures are included. PWT1N: n=6 inserts; PWT2N: n=3 (1 for IL-4); PCF13N: n=5; PCF15N: n=9.

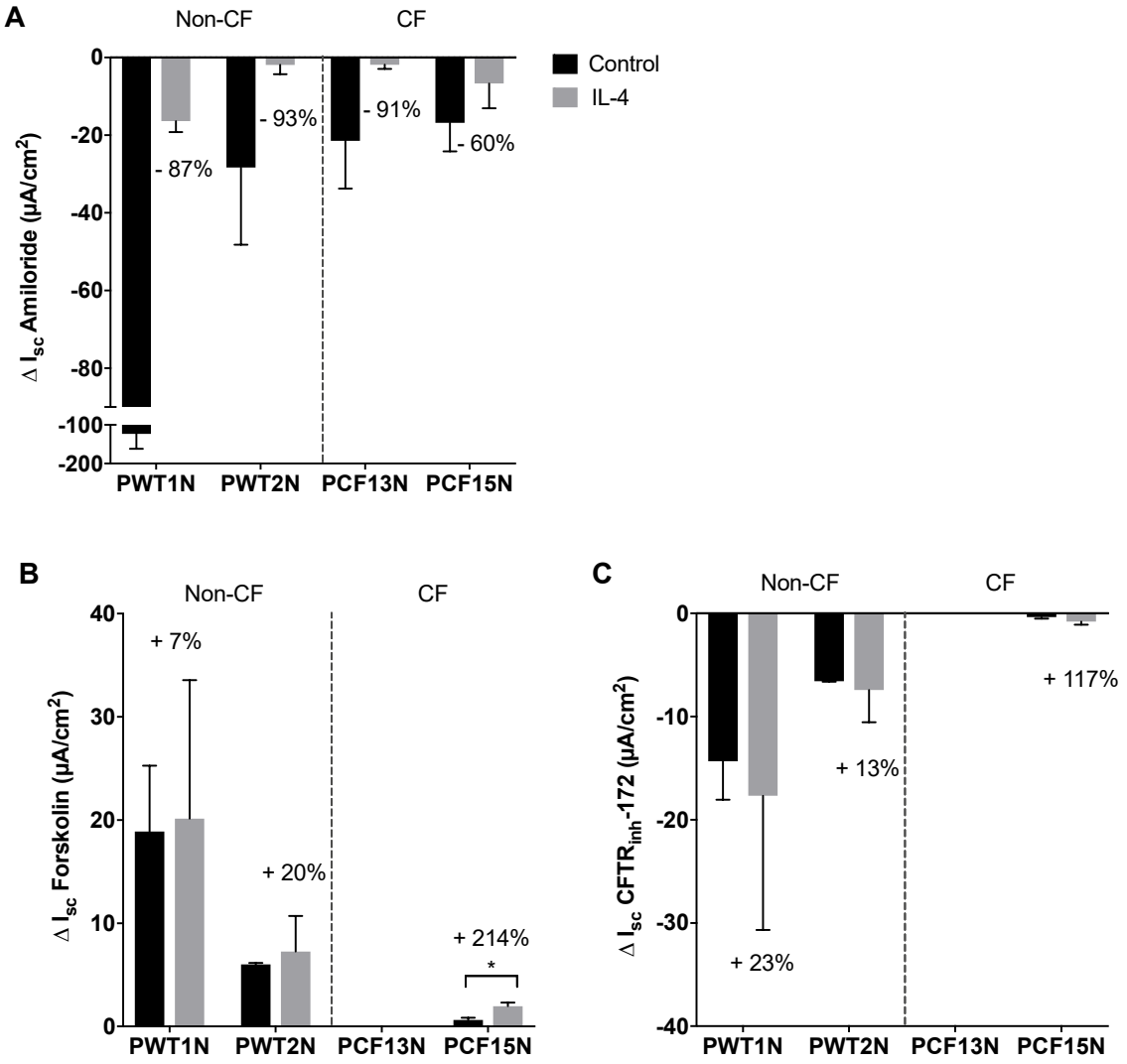

Figure 96: Effects of IL-4 treatment on short circuit current responses to amiloride, forskolin and $CFTR_{inh}$-172 in non-CF and CF PNECs

Cultures were treated with vehicle control (black) or IL-4 (grey) for 24 hours and investigated in Ussing chamber experiments. The resultant short circuit responses (ΔI_{sc}) to amiloride, forskolin and $CFTR_{inh}$-172 are shown in A,B and C respectively. Data presented as the mean I_{sc} response ± SD and analysed with Mann Whitney test; PCF15N $CFTR_{inh}$-172; p=0.02. Percentage increases in I_{sc} in IL-4 treated cultures are included. PWT1N: n=6 inserts; PWT2N: n=4; PCF13N: n=5; PCF15N: n=9.

5.4.8 Investigation of Eact addition in differentiated paediatric CF primary bronchial epithelial cultures

The effects of Eact in PNECs were more sustained than the typical UTP-induced I_{sc} therefore supporting previous published data to suggest that Eact activates TMEM16A via calcium-independent mechanisms (Namkung et al., 2011b). It was uncertain as to how the CF PBEC cultures would respond, given their uncharacteristic response to UTP as previously detailed in section 5.4.3.

To firstly ascertain the nature of Eact-induced I_{sc} in CF PBECs and secondly determine any potential effects of application of both Eact and UTP in the same culture inserts, Ussing chamber experiments were performed in PBEC cultures derived from a CF donor (PCF22). Experiments were first performed using 125 mM chloride Krebs in both apical and basolateral compartments as previously described, with the initial addition of amiloride, forskolin and $CFTR_{inh}$-172. UTP (100 μM) was next added apically, followed by Eact (10 μM) after 20 minutes; these were alternated in separate culture inserts for comparative assessment. Two culture inserts were used for each assessment and the mean I_{sc} and TEER were assessed as shown in Figure 97.

As shown in Figure 97A, apical UTP addition initially caused a downward deflection in the I_{sc} by a mean of -1.9 $\mu A/cm^2 \pm$ SD 1.6 followed by an increase from baseline of 2.0 $\mu A/cm^2 \pm 0.1$. This was associated with a mean TEER reduction of -146 $\Omega.cm^2 \pm$ SD 25 due to an increase in ion conductance (Figure 97B). As previously described, this was most likely secondary to a combination of BK and CaCC activation. After a steady baseline I_{sc}, subsequent Eact addition resulted in a further I_{sc} decline by -4.3 $\mu A/cm^2 \pm 1.1$ associated with an initial drop in TEER by -167 $\Omega.cm^2 \pm 4.0$. However, after this initial I_{sc} decline, there was a disproportionate I_{sc} increase associated with a decline in resistance to near 0 levels over a 20 min period. This latter finding suggested that the epithelial monolayer was damaged, resulting in paracellular ion transport. Figure 97C and Figure 97D demonstrate the effects on I_{sc} and TEER of Eact addition prior to UTP. Although Eact addition caused a small initial decrease in I_{sc}, there was an associated reduction in TEER by -163 $\Omega.cm^2 \pm 53$. This was followed by a gradual loss of TEER in conjunction with a gradual I_{sc} increase, again suggesting epithelial damage. Although UTP was added as shown, there was no response due to the ongoing decline of monolayer integrity.

These results revealed an atypical UTP-induced I_{sc} response, whereby there was an initial downward deflection followed by an upward change, suggesting a combination of BK and CaCC activation. Eact had been well tolerated in PNECs, however its addition in these PBECs either pre or post UTP resulted in epithelial damage and complete loss of resistance. It was hypothesised that these detrimental effects were secondary to non-CaCC channel activation and in view of the previously described effects of UTP on probable BK channel activation, it was hypothesised that these channels may predominate in the CF PBEC cultures and that like UTP, Eact was also demonstrating a similar secondary effect.

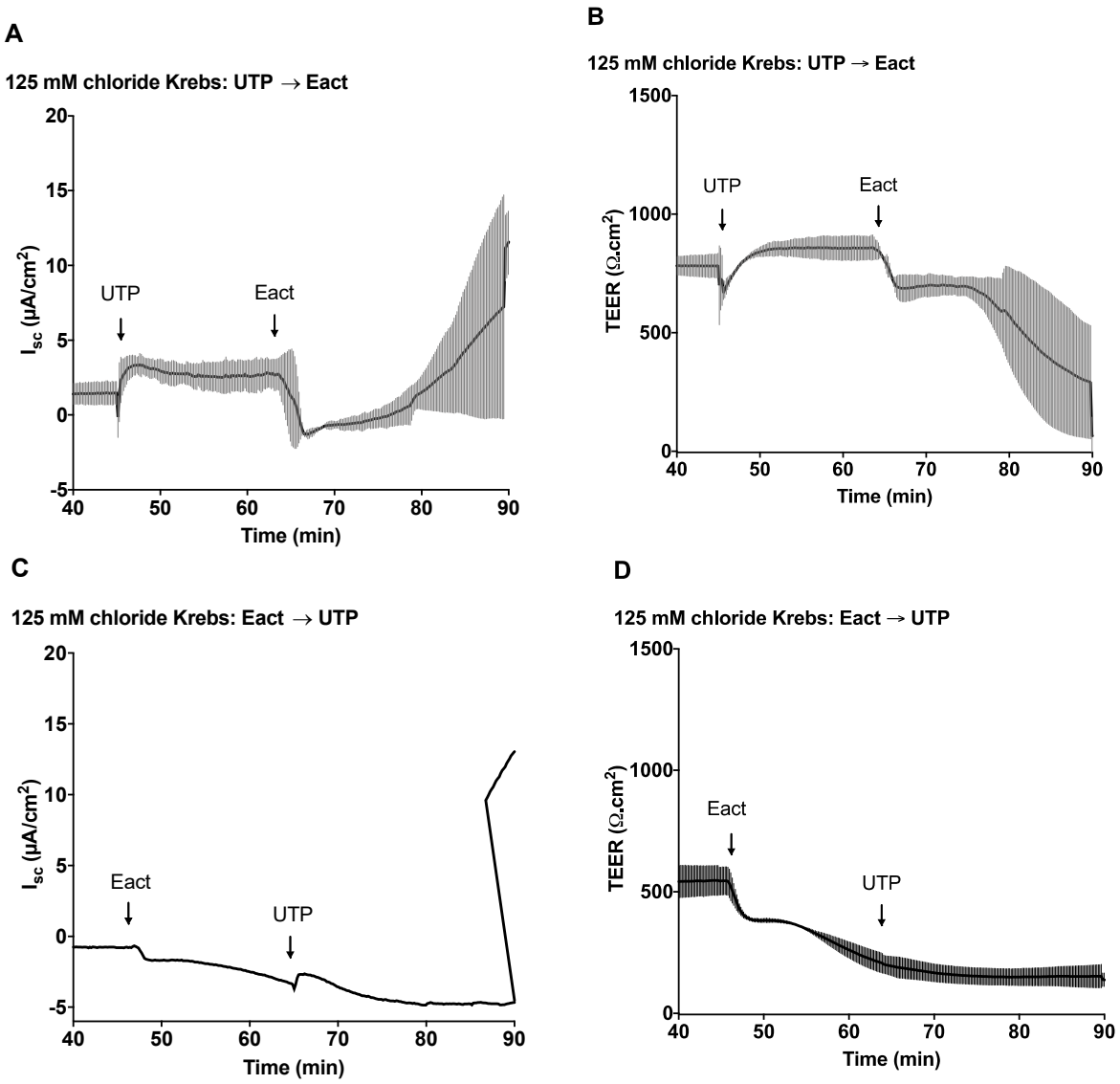

Figure 97: Representative Ussing chamber traces demonstrating the UTP-and Eact induced short circuit current responses in 125 mM chloride in PBEC cultures derived from the CF PCF22 donor

Ussing chamber short circuit current (I_{sc}) and transepithelial resistance (TEER) traces for PBEC cultures isolated from the CF PCF22B donor (F508del/F508del) are shown above in 125 mM chloride with the initial addition of UTP followed by Eact (A) with the corresponding TEER responses (B). I_{sc} (C)and TEER (D) responses for the alternative addition of Eact added prior to UTP are shown; n=2 inserts for A, B and D, n=1 insert for C.

5.4.9 Assessment of chloride-dependence of the atypical Eact-induced short circuit current response

To determine the chloride-dependent nature of this atypical Eact-induced I_{sc} response, Ussing chamber experiments involving PCF22 PBECs were firstly repeated in 0 mM chloride Krebs to determine the chloride-dependence of the Eact response. As shown in Figure 98A and B, initial application of UTP in 0 mM chloride abolished the secondary upward I_{sc} that was evident in 125 mM chloride, and resultant UTP-induced I_{sc} and TEER responses were reduced, to -8.7 $\mu A/cm^2$ $\pm$0.2 and -333 $\Omega.cm^2$ $\pm$17 respectively. Similar to 125 mM chloride conditions, the response was transient, with a return to a stable I_{sc} baseline and TEER recovery. Eact addition showed a similar response to that seen at 125 mM chloride, however, the induced response was greater at -8.3 $\mu A/cm^2$ $\pm$0.1. However, once again Eact addition was followed by a large I_{sc} increase and loss of TEER. As shown Figure 98C and D, initial Eact addition prior to UTP generated a larger negative deflection in I_{sc} at 0 mM compared with 125 mM chloride of -9.9 $\mu A/cm^2$ $\pm$2.2. Once again, the effects of UTP were not determined due to a complete loss of TEER.

These results for the experiments performed in both 125 mM and 0 mM chloride are summarised in Figure 99, with detrimental effects of Eact application in these CF PBEC cultures apparent both pre and post UTP addition. As with UTP, the magnitude of the initial Eact-induced I_{sc} was greater in 0 mM chloride conditions (UTP: p=0.008; Eact: p=0.05) suggesting also potential involvement of calcium activated BK channels.

To determine if the above responses were consistently evident in CF PBECs, Eact assessment was next performed in PBEC cultures derived from a different donor, PCF23. These cultures had also previously shown negative UTP-induced I_{sc} with an associated decrease in TEER (as previously shown in Figure 85). Like the PCF22 PBEC cultures, Eact addition after UTP in PCF23 cultures resulted in a negative I_{sc} Figure 100A). However, the resultant I_{sc} response together with the associated TEER reduction was transient, showing signs of recovery, with no apparent effect on epithelial monolayer integrity (Figure 100B). Eact application prior to UTP resulted in a similar effect to that seen with PCF22B PBECs, whereby there was a decline in TEER demonstrating loss of epithelial resistance as evident in Figure 100C and D.

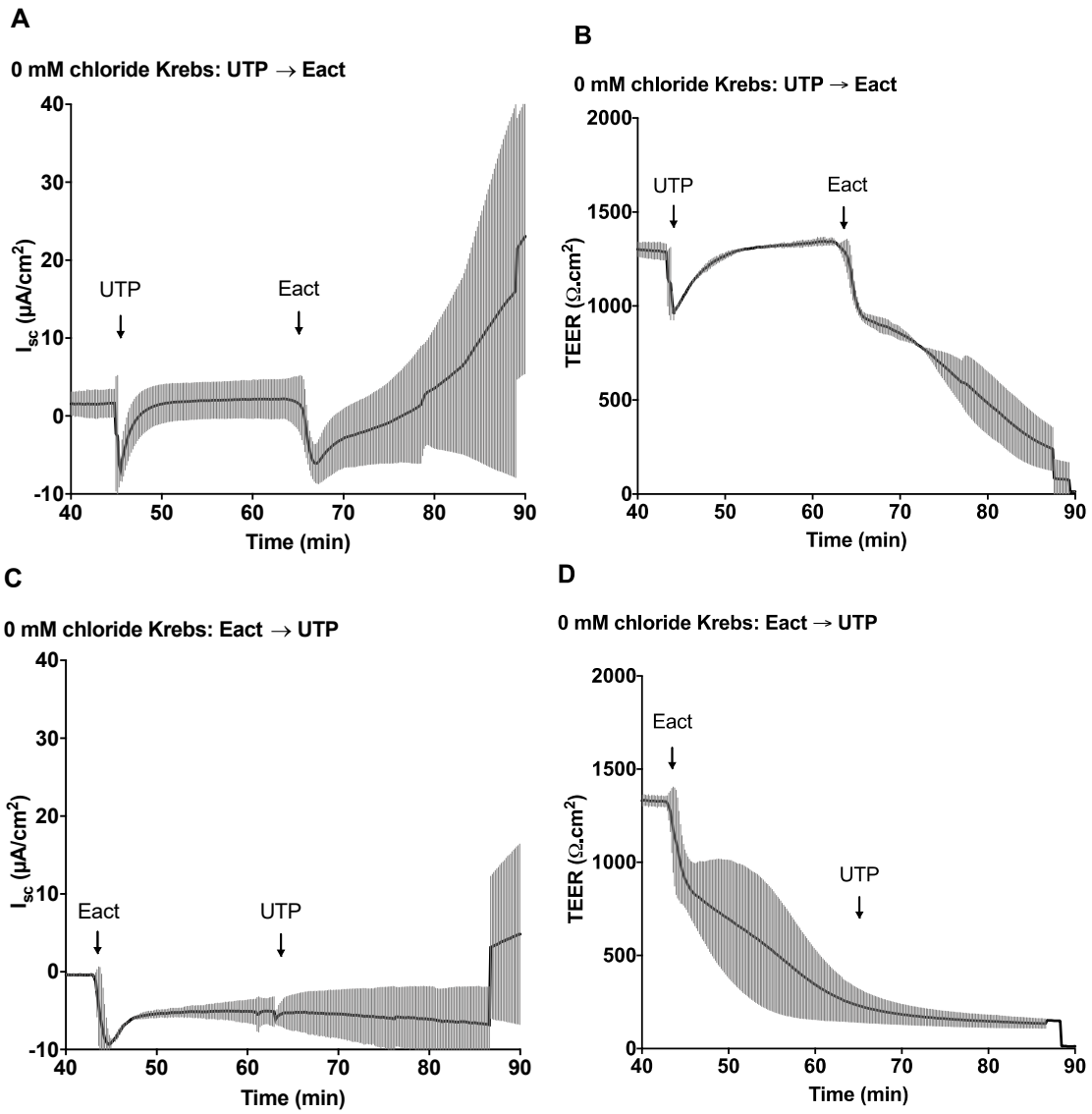

Figure 98: Representative Ussing chamber traces demonstrating the UTP-and Eact induced short circuit current responses in 0 mM chloride in PBEC cultures derived from the CF PCF22 donor

Ussing chamber short circuit current (I_{sc}) and transepithelial resistance (TEER) traces for PBEC cultures isolated from the CF PCF22B donor (F508del/F508del) are shown above in 0 mM chloride with the initial addition of UTP followed by Eact (A) with the corresponding TEER responses (B). I_{sc} (C)and TEER (D) responses for the alternative addition of Eact added prior to UTP are shown; n=2 inserts for each condition.

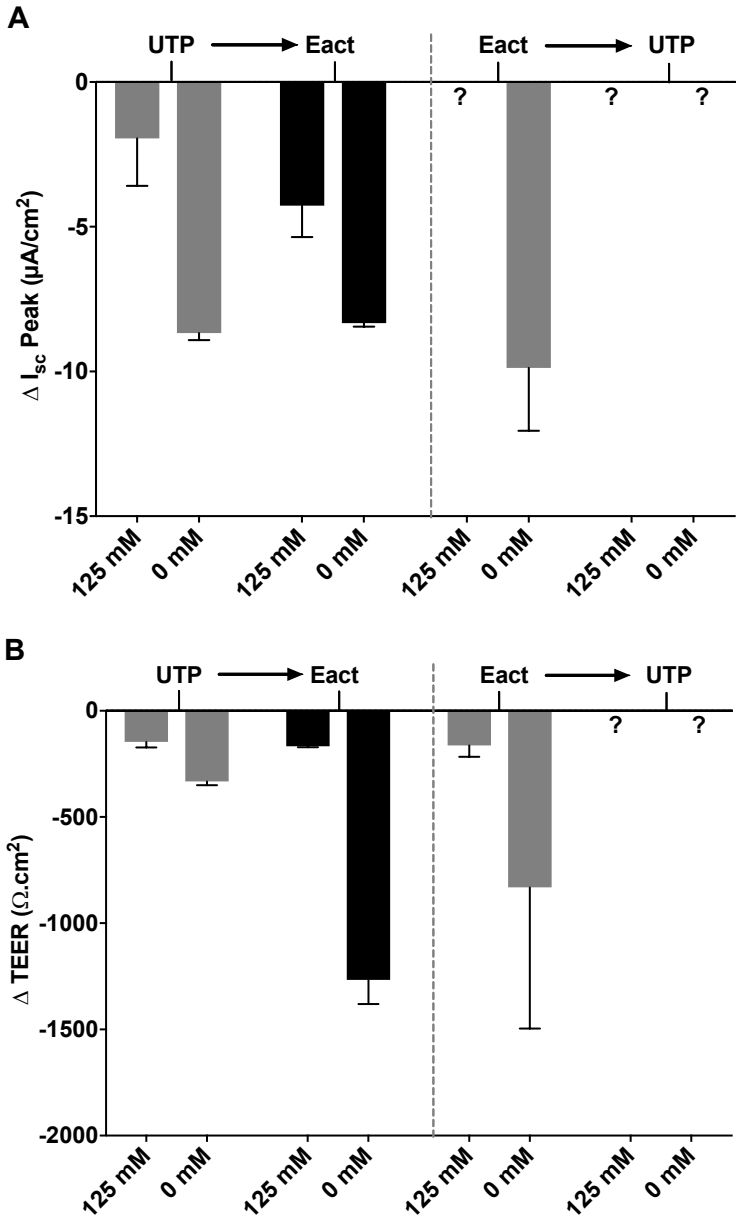

Figure 99: Resultant short circuit current and transepithelial resistance responses to UTP and Eact addition in 125 mM and 0 mM chloride in PBECs isolated from the CF PCF22 donor

The resultant short circuit (ΔI_{sc}) and transepithelial resistance (ΔTEER) in 125 mM and 0 mM chloride Krebs are shown in A and B respectively. The effects of UTP followed by Eact addition are demonstrated in addition to the alternative application of Eact followed by UTP. Data is presented as the mean response ± SD; n=2 inserts for each condition therefore statistical analysis not performed.

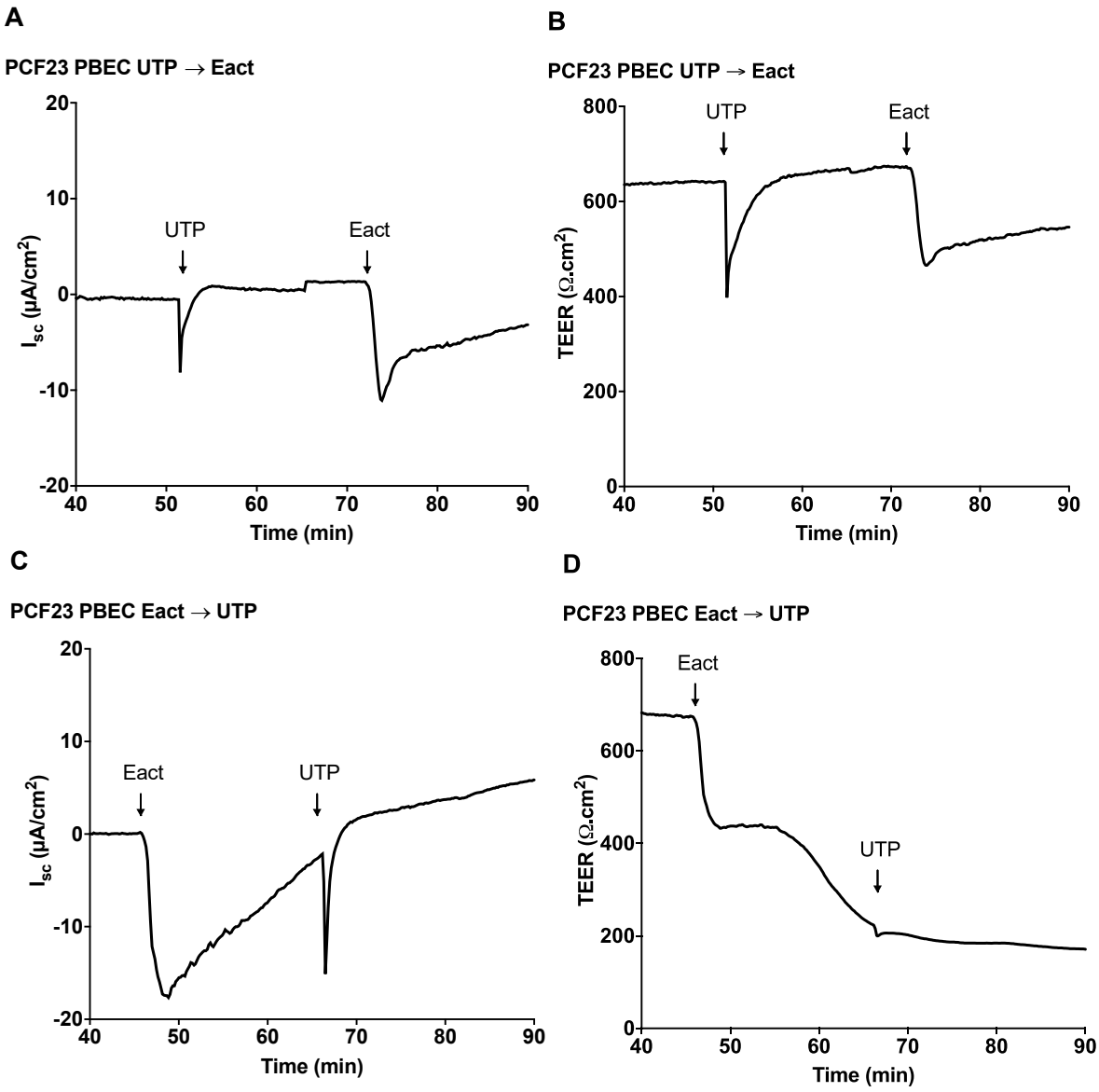

Figure 100: Representative Ussing chamber traces of short circuit current and transepithelial electrical resistance responses to UTP and Eact in PBEC cultures derived from the CF PCF23 donor

Ussing chamber short circuit current (I_{sc}) and transepithelial resistance (TEER) traces for PBEC cultures isolated from the CF PCF23 donor (F508del/2896delA) are shown above with the initial addition of UTP followed by Eact (A) with the corresponding TEER responses (C). I_{sc} (C)and TEER (D) responses for the alternative addition of Eact added prior to UTP are shown; n=1 insert for each condition.

5.4.10 Effects of barium chloride and BAPTA-AM on the atypical Eact-induced short circuit current response

It was possible that these effects were also secondary to BK channel activation and the effects of channel inhibition with $BaCl_2$ were next investigated as shown in Figure 101A and B. Furthermore, in view of the suggestion that these effects were calcium-mediated, the calcium-selective cell permeator, BAPTA-AM was applied to the cultures as previously described to determine any modification in resultant I_{sc} and TEER as shown in Figure 101C and D, with a summary provided in Figure 102.

Addition of $BaCl_2$ resulted in an overall reduction in the UTP-induced I_{sc}. Both the magnitude of the UTP and Eact-induced decline in I_{sc} and resultant TEER in these PBECs were reduced following the addition of $BaCl_2$ or pre-treatment with BAPTA-AM. Overall $BaCl_2$ treatment reduced the UTP-induced I_{sc} by 5-fold from -12.2 $\mu A/cm^2 \pm$ SD3.9 to -2.4 $\mu A/cm^2 \pm 3.9$ with a similar reduction in TEER from -308.8 $\Omega.cm.^2 \pm 68.4$ to 70 $\Omega.cm.^2 \pm 3.5$. The effect of $BaCl_2$ on the Eact-induced I_{sc} was less pronounced with a 3-fold reduction in both I_{sc} and TEER from -17.9 $\mu A/cm^2 \pm 6.5$ to -5.5 $\mu A/cm^2 \pm 0.9$ and -262.3 $\Omega.cm.^2 \pm 61$ to -87.0 $\Omega.cm.^2 \pm 12.9$ respectively. BAPTA-AM pre-treatment had a smaller effect on the UTP-induced I_{sc} and TEER to -4.1 $\mu A/cm^2 \pm 2.9$ and -131.1 $\Omega.cm.^2 \pm 91$ respectively. This was also the case for the Eact-induced I_{sc} with a resultant I_{sc} and TEER changes of -7.6 $\mu A/cm^2 \pm 8.8$ and -91.0 $\Omega.cm.^2 \pm 104$.

The effects of $BaCl_2$ and BAPTA-AM were also investigated in PNEC cultures derived from the same PCF23 donor, and the results have been summarised in Figure 103. As previously shown in section 5.4.4, these PNECs demonstrated both negative and positive I_{sc} deflections. In these cultures, addition of both $BaCl_2$ and BAPTA-AM had similar effects, whereby there was complete resolution of the negative I_{sc} deflection. However, responses to both reagents were less pronounced than in the PBECs.

To demonstrate that the relationship between Eact and UTP was not confined to CF PBECs, resultant I_{sc} traces for paired cultures obtained from the PWT8 donor are shown in Figure 104. Experiments were performed to assess the effect of UTP/Eact addition in the same culture inserts, and to ascertain any changes in chloride free Krebs solutions. As shown in this figure, in 125 mM chloride, UTP addition in PBEC and PNEC cultures was in keeping with CaCC activation when applied first. Eact did

not cause an I_{sc} change in PNECs. In PBECs, it caused a negative change in I_{sc}, which when applied first, prevented a UTP response in PBECs, and modified the response in PNECs to comprise a negative component. In 0 mM chloride, Eact caused a negative I_{sc} in all cases, the effect of which was greatest in PBECs. It was not possible to explore this further in these cultures due to limited culture insert availability.

Overall these results indicate that in the PBECs investigated, the UTP and Eact-induced I_{sc} responses suggested activation of alternative calcium-mediated channels with the potential involvement of BK channels. Non-selective inhibition of these channels with $BaCl_2$, and pre-treatment with the calcium chelator BAPTA-AM showed some evidence of reduction in the magnitude of the I_{sc} in CF PBECs and modification of the response in the PCF23 PNEC investigated. However, addition of these reagents did not eliminate the responses completely, suggesting that other mechanisms may be involved or further optimisation of these protocols are required in primary ALI cultures. Further investigation is required to investigate the effects of BK channel inhibition and BAPTA-AM on the Eact-induced I_{sc} alone.

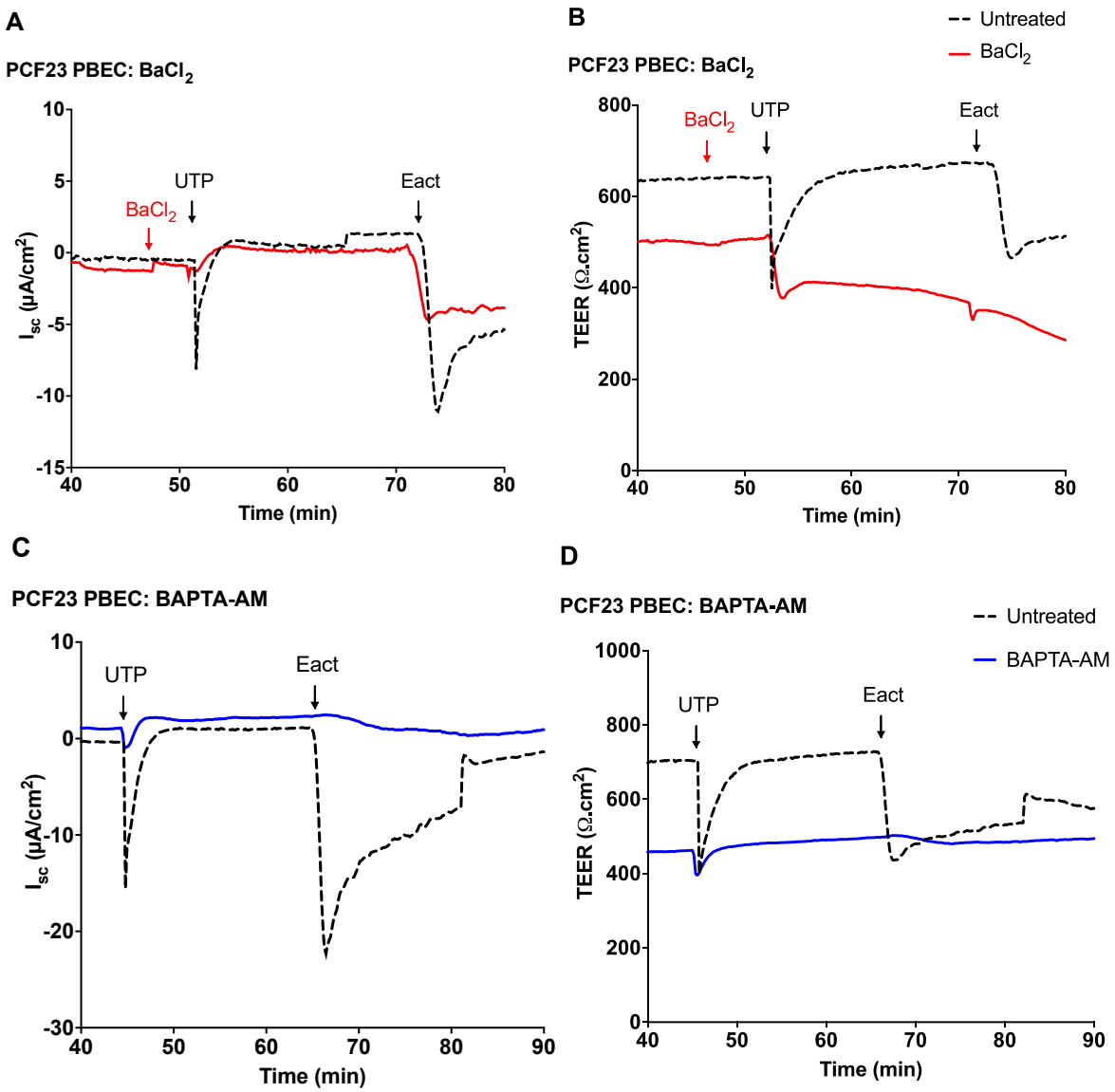

Figure 101: Representative Ussing chamber traces demonstrating the effects of barium chloride and BAPTA-AM on the UTP and Eact-induced short circuit current and transepithelial resistance responses in PBEC cultures isolated from the CF PCF23 donor

Ussing chamber short circuit current (I_{sc}) and transepithelial resistance (TEER) traces for PBEC cultures isolated from the CF PCF23 donor (F508del/2896delA) are shown above. Barium chloride ($BaCl_2$) was added 5 minutes prior to UTP addition and Eact was subsequently added as shown with resultant I_{sc} (A) and TEER (B) responses.

In a separate experiment cell culture inserts were treated with 50 µM BAPTA-AM for 60 minutes prior to the Ussing chamber experiment. UTP and Eact were subsequently added as shown with resultant I_{sc} (C) and TEER (D) responses; n=1 insert for each culture type.

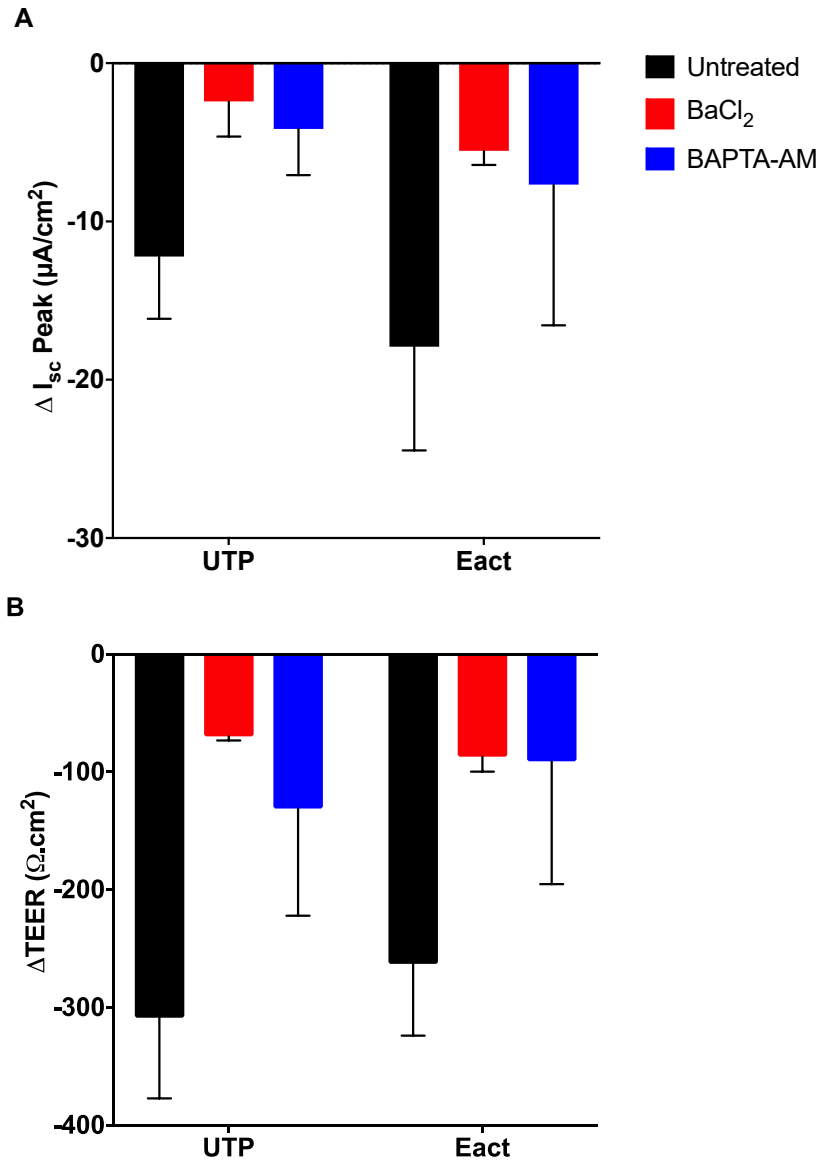

Figure 102: Effects of barium chloride and BAPTA-AM on short circuit current and transepithelial resistance measurements in PBEC cultures derived from the CF PCF23 donor

The resultant changes in peak UTP and Eact-induced short circuit current (ΔI_{sc}) and transepithelial resistance (ΔTEER) were determined in response to treatment with barium chloride (BaCl2) and BAPTA-AM as previously described in PBEC cultures derived from the PCF 23 donor (F508del/2896delA). Bars represent mean ± SD; n=2 culture inserts for each condition (no statistical test applied).

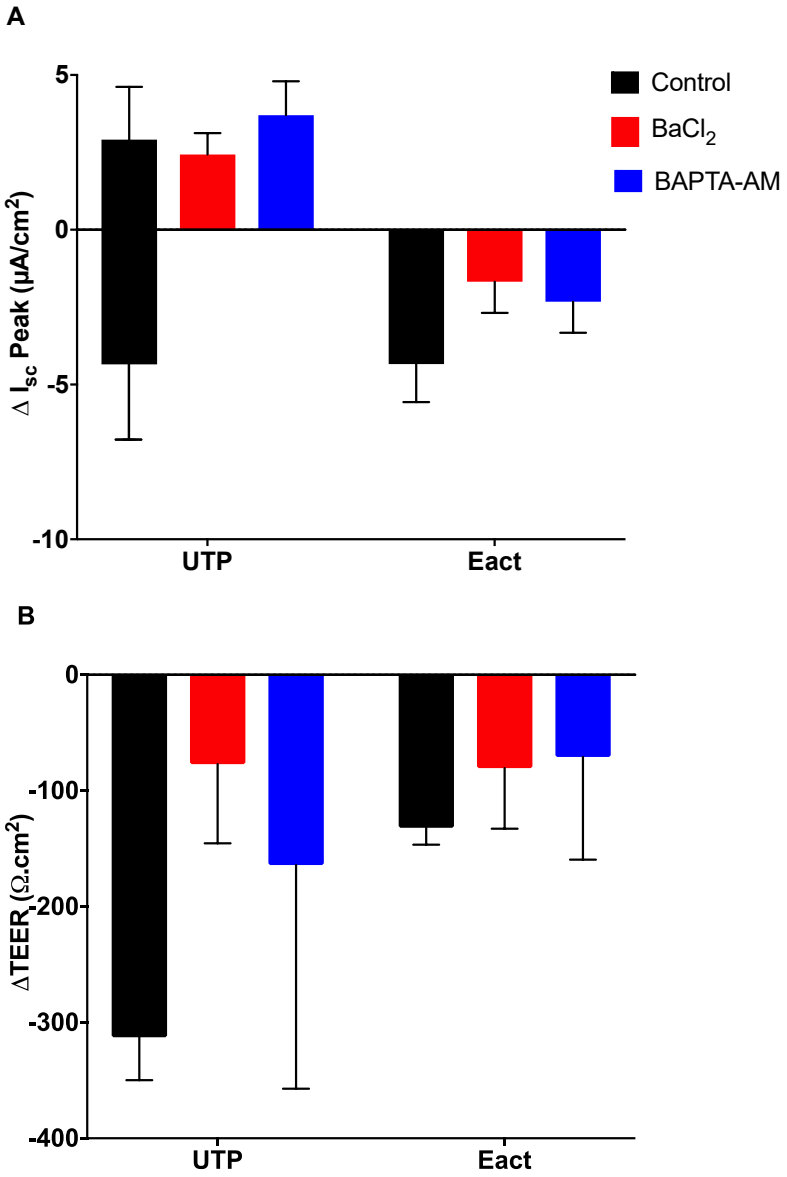

Figure 103: Effects of barium chloride and BAPTA-AM on short circuit current and transepithelial resistance measurements in PNEC cultures derived from the CF PCF23 donor

The resultant changes in peak UTP and Eact-induced short circuit current (ΔI_{sc}) and transepithelial resistance (ΔTEER) were determined in response to treatment with barium chloride (BaCl2) and BAPTA-AM as previously described in PNEC cultures derived from the PCF 23 donor (F508del/2896delA). Bars represent mean ± SD; n=2 culture inserts for each condition (no statistical test applied).

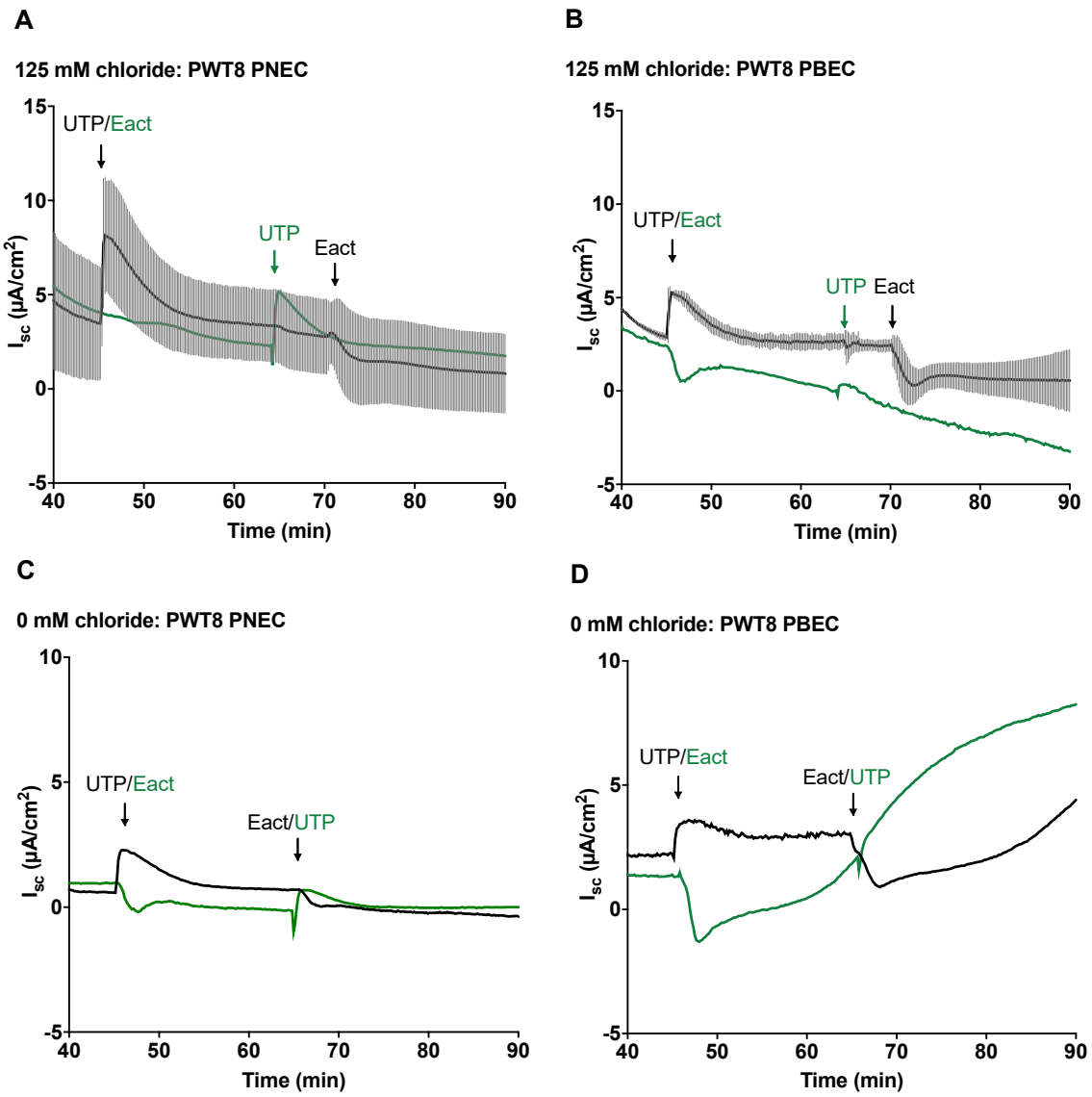

Figure 104: Representative Ussing chamber traces demonstrating the UTP-and Eact induced short circuit current responses in 125 mM and 0 mM chloride in PNEC and PBEC cultures derived from the non-CF PWT8 donor

Ussing chamber short circuit current (I_{sc}) traces for PNEC and PBEC cultures isolated from the non-CF PWT8 donor are shown above in 125 mM (A and B) and 0 mM chloride (C and D) conditions. Back lines represent UTP addition prior to Eact, green lines represent the reverse; n=2 inserts for PNECs and PBECs at 125 mM chloride where UTP was added first., n=1 insert for remaining conditions.

5.4.11 The effects of TMEM16A inhibition with small molecule inhibitors: tannic acid and T16$_{inh}$-A01

In view of the relatively recent identification of TMEM16A, the development of small molecule inhibitors has been recent, with ongoing identification of new molecules during the timeframe of this PhD. By measuring the kinetics of iodide efflux using YFP fluorescence techniques in FRT cells, tannic acid was identified as a potent CaCC inhibitor, with no effects on CFTR function (Namkung et al., 2010b). An additional compound was identified by the same group, T16$_{inh}$-A01with improved specificity for TMEM16A inhibition (Namkung et al., 2011a). Assessment of T16$_{inh}$-A01 in airway epithelial cells revealed a small inhibition of the peak UTP-induced response with little effect on the total CaCC current (Namkung et al., 2011a).

During the initial stages of this PhD, effects of both tannic acid and T16$_{inh}$-A01 were first investigated in PNEC cultures derived from a CF donor (PCF5; Figure 105). Although performed only once, pre-treatment with either 100 μM tannic acid or 10 μM T16$_{inh}$-A01 5 minutes prior to UTP addition did not alter the peak UTP-induced I_{sc} response (untreated: 19.3 μA/cm^2; tannic acid: 18.3 μA/cm^2, T16$_{inh}$-A01: 18.1 μA/cm^2), but the total response, as measured by AUC, was clearly reduced with each inhibitor (untreated;81.6 μA/cm^2.min; tannic acid: 45 μA/cm^2.min; T16$_{inh}$-A01: 47.3 μA/cm^2.min). Application of tannic acid after UTP (Figure 106) caused a reduction in both the peak I_{sc} (untreated: 23.1 μA/cm^2; tannic acid: 16.9 μA/cm^2) and the AUC (untreated: 95.5 cm^2.min; tannic acid: 55.0 cm^2.min), however, the decline in the UTP-induced I_{sc} was gradual, as opposed to the immediate inhibitory effect that had previously been described in the literature (Namkung et al., 2010b).

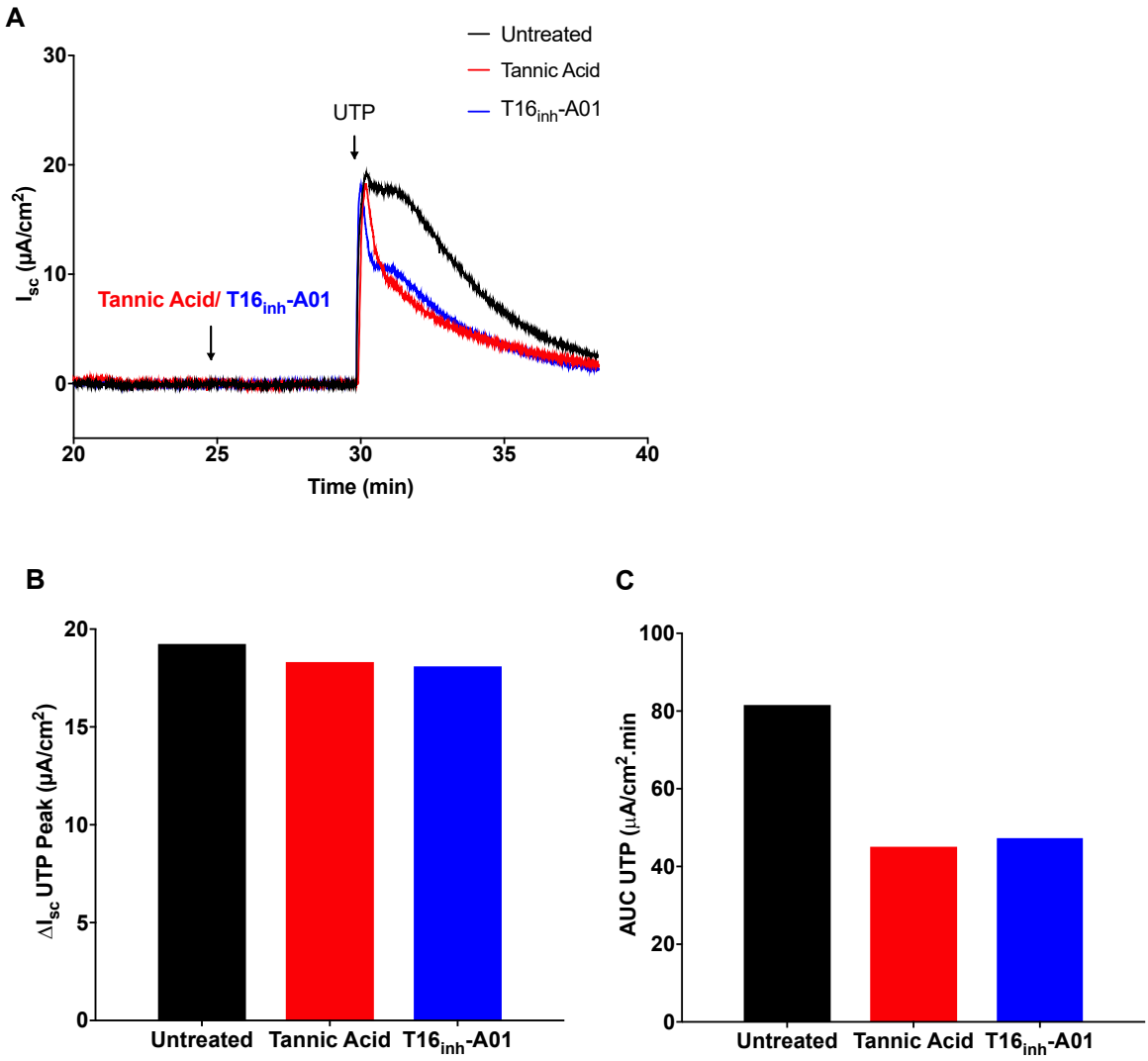

Figure 105: The effects of tannic acid and T16$_{inh}$-A01 pre-treatment on the peak and total UTP-induced short circuit current in PNEC cultures derived from the CF PCF5 donor

Ussing chamber short circuit current (I_{sc}) traces for PNEC cultures isolated from the CF PCF5 donor (F508del/F508del) are shown above (A) for untreated (black), tannic acid (red) and T16$_{inh}$-A01 (brown) treatment 5 minutes prior to UTP addition. Resultant changes in peak I_{sc} and area under the curve (AUC) are shown in B and C respectively; n=1 culture insert for each condition.

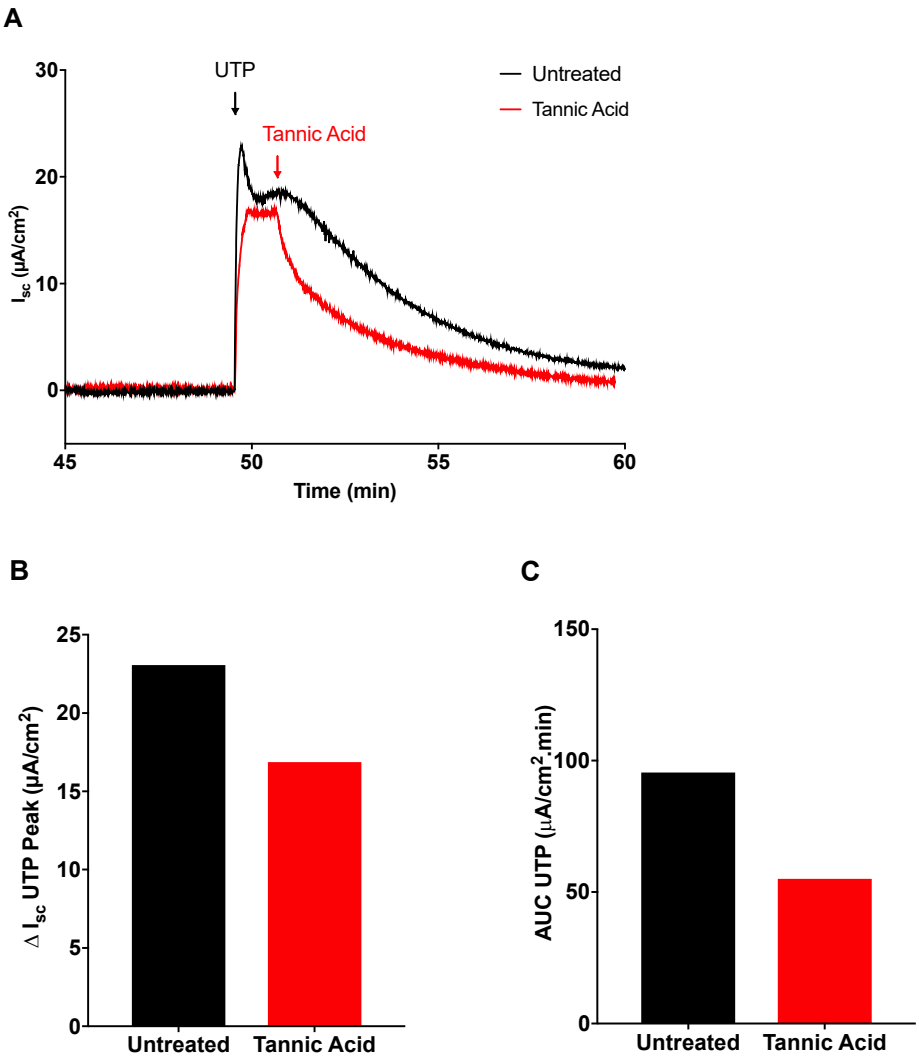

Figure 106: The effects of tannic acid treatment on the peak and total UTP-induced short circuit current in PNEC cultures derived from the CF PCF5 donor

Ussing chamber short circuit current (I_{sc}) traces for PNEC cultures isolated from the CF PCF5 donor (F508del/F508del) are shown above (A) for untreated (black) and tannic acid (red) treatment 2 minutes after UTP addition. Resultant changes in peak I_{sc} and area under the curve (AUC) are shown in B and C respectively; n=1 culture insert for each condition.

5.4.12 Inhibitory effects of the small molecule CaCCinh-A01 on TMEM16A

Although both tannic acid and $T16_{inh}$-A01 did demonstrate alterations in the UTP-induced I_{sc}, the activities of more potent new reagents were assessed with a view to enabling better characterisation of TMEM16A activity in primary cultures. This was of particular importance given the limitations of reliably using Eact as described above. The effects of an alternative TMEM16A inhibitor, $CaCCi_{nh}$-A01 (Namkung et al., 2011a), were investigated in paediatric ALI PNEC cultures derived from CF donors in Ussing chamber experiments. Representative I_{sc} traces taken from these experiments are shown in Figure 107. After the addition of amiloride, forskolin, and $CFTR_{inh}$-172 in 125 mM chloride solutions as previously described, 10 μM $CaCC_{inh}$-A01 was added apically 5 minutes prior to 100 μM UTP. As evident from these traces and as summarised in Figure 108, the greatest reductions in the peak and total induced I_{sc} were evident in cultures derived from PCF12 (70 % and 66 %, respectively). The peak UTP-induced I_{sc} was reduced in PCF11 and PCF15N cultures to a lesser degree (39 % and 31 %, respectively). However, the total UTP-induced response was greater in PCF11 and PCF15N cultures (25 % and 107 %, respectively), suggesting that $CaCC_{inh}$-A01 had inhibited only the initial phase of the UTP response, with no inhibitory effect on the subsequent plateau.

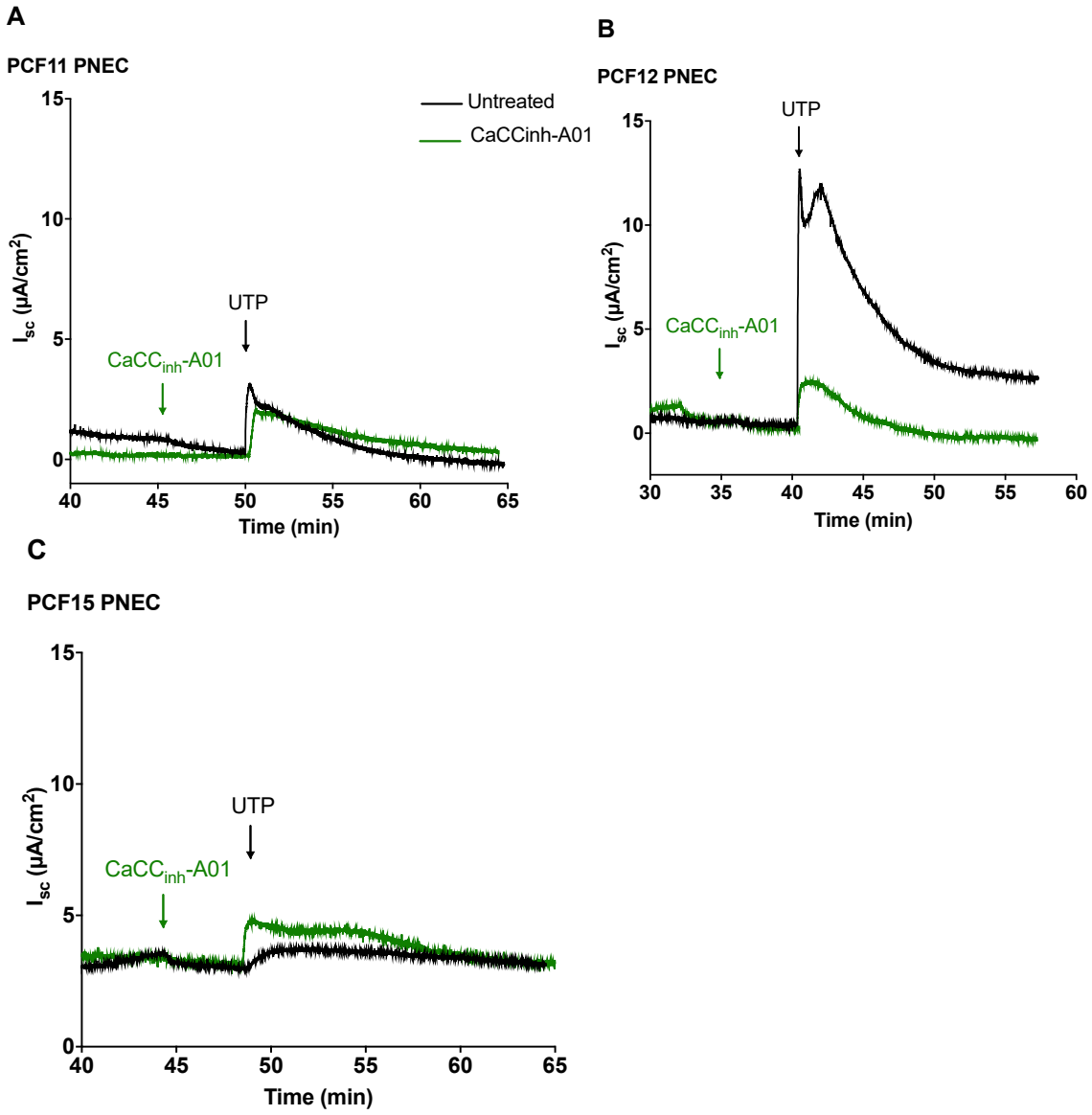

Figure 107: Representative Ussing chamber traces for the effects of CaCC$_{inh}$-A01 in PNEC cultures derived from 3 CF donors

Ussing chamber short circuit current (I_{sc}) traces for PNEC cultures isolated from the CF PCF11 (A), PCF12 (B) and PCF15 (B) donors (all F508del/F508del) are shown. Black lines represent UTP addition in untreated conditions, green lines represent CaCC$_{inh}$-A01 addition 5 minutes prior to UTP; n=1 inserts for each condition.

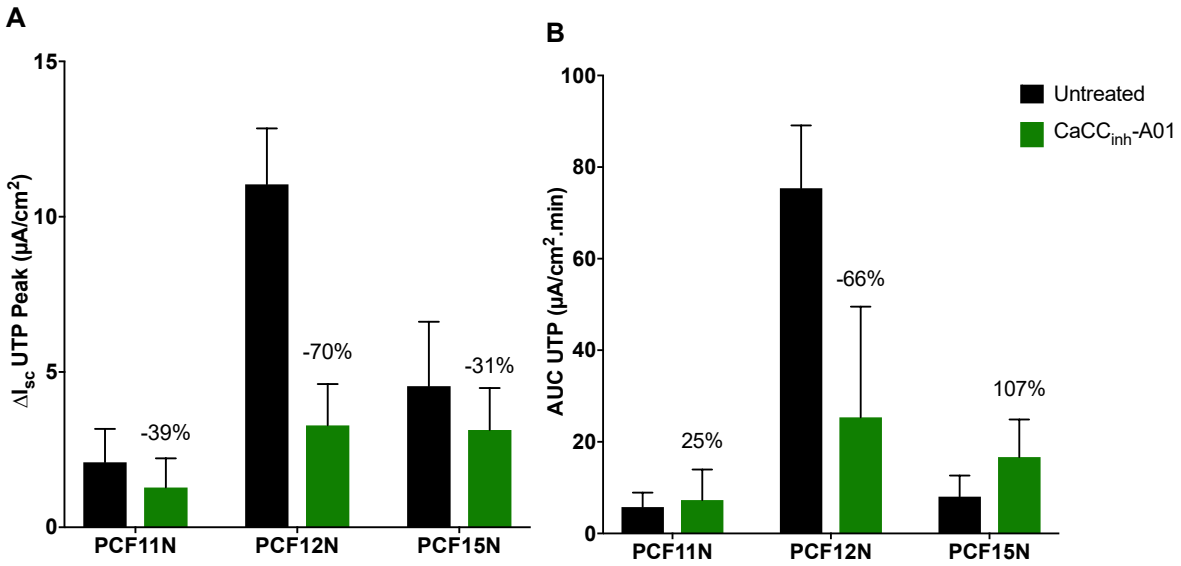

Figure 108: The effects of $CaCC_{inh}$-A01 on the peak and total UTP-induced short circuit current in PNEC cultures derived from 3 CF donors

The resultant UTP-induced change in peak short circuit current responses (ΔI_{sc} UTP peak) for PNECs derived from the PCF11, PCF12 and PCF15 donors (all F508del/F508del) are shown in A for untreated (black) and $CaCC_{inh}$-A01 (green) treatment 5 minutes to UTP. The area under the curve (AUC) for total UTP-induced responses are shown in B. Data is presented as mean ± SD; n=2 inserts for each condition therefore statistical tests not applied.

5.4.13 Inhibitory effects of the small molecule Ani9 on TMEM16A

In the search for a more potent selective inhibitor of TMEM16A, a further cell based screening approach again utilising FRT cells and the YFP technique was more recently performed by Namkung *et al*, and the results published during this PhD (Seo et al., 2016). This screen revealed an alternative compound, Ani9, to be the most selective inhibitor of TMEM16A to date.

The effects of Ani9 compared with $CaCC_{inh}$-A01 on the UTP-induced I_{sc} were investigated in PNEC and PBEC cultures derived from the PWT17 donor. As previously performed, amiloride, forskolin, and $CFTR_{inh}$-172 were first added to the Ussing chamber using 125 mM chloride solutions, after which either 10 μM $CaCC_{inh}$-A01 or 10 μM Ani9 were apically added 5 minutes prior to UTP.

Representative I_{sc} traces taken from these experiments together with a summary of the I_{sc} changes are shown in Figure 109 and Figure 110 respectively. In PNEC cultures, both inhibitors reduced the peak and total UTP-induced I_{sc}. However, the percentage reduction in peak and total I_{sc} was greater with Ani9 ($CaCC_{inh}$-A01: 57 % and 26 %, respectively, versus Ani9: 79 % and 72 %, respectively).

PBEC cultures obtained from this donor had previously shown negative UTP-induced I_{sc} responses as detailed in section 5.4.5. The effects of both inhibitors on the percentage reduction of peak positive UTP-induced I_{sc} was more modest in comparison to PNECs ($CaCC_{inh}$-A01: 26 %; Ani9: 22 %). This was also the case with the total positive UTP-induced I_{sc} whereby there was a small increase of 7 % with $CaCC_{inh}$-A01, and a reduction of 14 % with Ani9. However, as evident from the traces in Figure 109, addition of both inhibitors also reduced the negative responses. It is difficult to explain this given the activity of these inhibitors against TMEM16A and not BK channels, however, more comprehensive assessment of this finding was not possible due to limited culture insert availability.

Overall, these results obtained with all small molecules investigated highlight the challenges associated with finding selective inhibitors of TMEM16A for use in Ussing chamber experiments involving primary ALI cultures. Although only investigated in a limited number of cultures, these results suggest a greater degree of inhibition with Ani9, however, its function in a larger group of cultures remains to be determined.

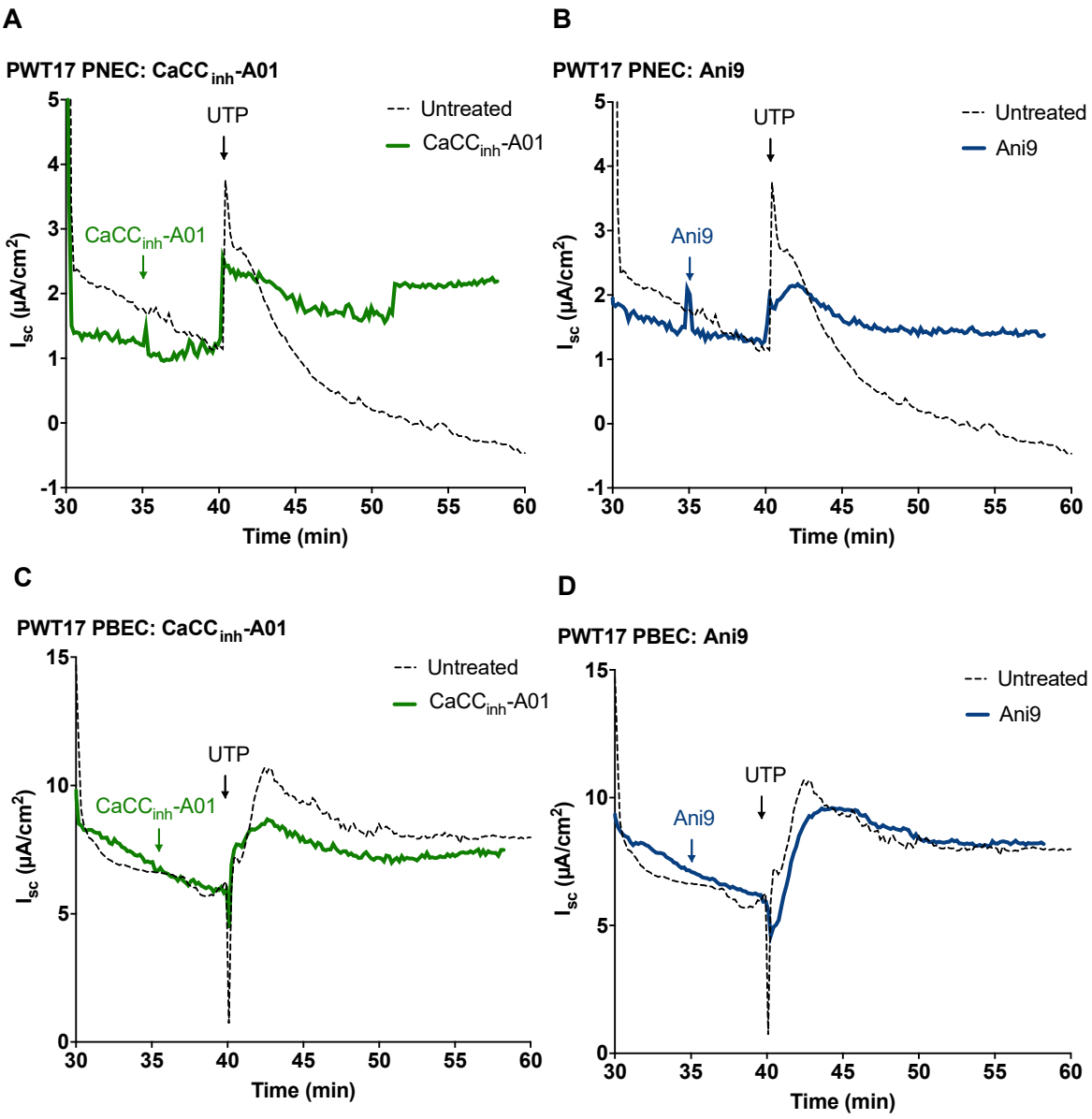

Figure 109: Representative Ussing chamber traces for the effects of $CaCC_{inh}$-A01 in PNEC and PBEC cultures derived from the non-CF PWT17 donor

Ussing chamber short circuit current (I_{sc}) traces for PNEC (A and B) and PBEC cultures (C and D) isolated from the non-CF PWT17 donor are shown. Black lines represent UTP addition in untreated conditions, green and blue lines represent the addition of $CaCC_{inh}$-A01 or Ani9 respectively 5 minutes prior to UTP; n=1 inserts for each condition.

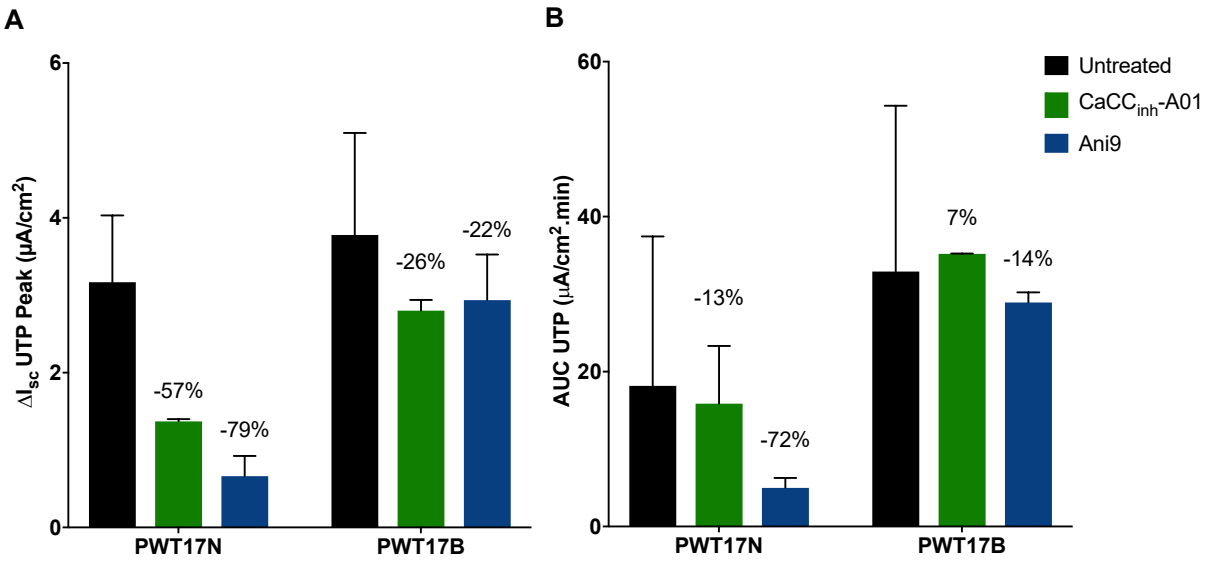

Figure 110: The effects of $CaCC_{inh}$-A01 and Ani9 on the peak and total UTP-induced short circuit current in PNEC and PBEC cultures derived from the non-CF PWT17 donor

The resultant UTP-induced change in peak short circuit current responses (ΔI_{sc} UTP peak) for PNECs and PBECs derived from PWT17 donor are shown in A for untreated (black), $CaCC_{inh}$-A01 (green) and Ani9 (blue) treatment 5 minutes to UTP. The area under the curve (AUC) for total UTP-induced response are shown in B. Data is presented as mean ± SD; n=2 inserts for each condition therefore statistical tests not applied.

5.4.14 Assessment of TMEM16A expression

To determine the relative mRNA expression of *TMEM16A* in differentiated paediatric ALI PNEC and PBEC cultures derived from non-CF and CF donors, RT-qPCR analysis was performed at 28d to 33d ALI as previously described in Chapter 2 section 2.7.

In non-CF cultures, no differences in *TMEM16A* expression were apparent in PBECs versus PNECs as shown in Figure 111A (1.1-fold change ±1.8) and this was paralleled by the lack of significance in the corresponding $2^{-\Delta CT}$ analysis of relative gene expression (p=0.32; Figure 112). Although there was a small increase in relative *TMEM16A* in CF PBECs versus CF PNECs (1.5-fold change ±0.7) as shown in Figure 111B, the $2^{-\Delta CT}$ analysis between the two groups was not statistically significant (p>0.99).

Gene expression and relative fold change analysis of *TMEM16A* was also performed to investigate any differences between disease groups in nasal and bronchial cultures as shown in Figure 111C and D. In nasal cultures, no differences were found between CF versus non-CF PNECs (0.8-fold change ±0.6) and there were no significant differences seen in $2^{-\Delta CT}$ analysis of gene expression for these comparisons (p>0.99). Although there was a 3.1-fold increase ±1.5 in CF PBECs versus non-CF PBECs, again the $2^{-\Delta CT}$ analysis was not significant (p>0.99), potentially attributable to the low donor number in the CF PBEC group.

To determine any potential relationship of *TMEM16A* expression with functional activity, correlation with the UTP-induced I_{sc} was investigated in differentiated ALI cultures where both experimental techniques were performed (Figure 113). Spearman rank correlation assessment of all ALI cultures did not reveal any relationship between *TMEM16A* and UTP-induced I_{sc} (r=0.24, p=0.4). Further subgroup analysis of each culture group did not reveal any correlations of *TMEM16A* mRNA expression with the UTP-induced I_{sc}.

As previously described in section 5.4.7, IL-4 treatment of ALI cultures increased the UTP-induced I_{sc}, with some suggestion of enhanced Eact activity in CF PNECs. IL-4 has previously been found to upregulate*TMEM16A* expression in cultured CF PBECs derived from explanted lung tissue (Gorrieri et al., 2016). To determine the effects of IL-4 treatment on *TMEM16A* expression in paediatric PNECs, RT-qPCR analysis was performed in PNEC cultures derived from 2 non-CF and 2 CF donors. As shown

in Figure 114, IL-4 treatment upregulated *TMEM16A* expression in both non-CF and CF PNECs. The magnitude of upregulation was similar in both groups compared with the controls in each group (non-CF PNECs: 115-fold ±135; CF PNECs: 102-fold ±77). Importantly, despite this upregulation, levels of TMEM16A expression in IL-4 treated PNECs as determined by the $2^{-\Delta CT}$ analysis were lower in the CF versus non-CF cultures (non-CF PNECs IL-4: 0.13 vs CF PNECs IL-4: 0.03). Statistical analysis was not possible due to the presence of only two donors from each group.

Expression and localisation of TMEM16A was also assessed using immunofluorescence and confocal microscopy in 8 paediatric ALI cultures which were fixed at 28 to 33d ALI. The protocol used for this technique has been previously described in Chapter 2, section 2.3.10. In all cases, immunofluorescence confirmed the presence of TMEM16A, with evidence of apical TMEM16A as shown in Figure 115.

The area of fluorescence intensity was calculated for each cell culture investigated as a measure of relative expression (Figure 116). The median area of fluorescence/cell was lower in non-CF cultures (non-CF: median 253.1 A.U. IQR 43.6 to 947.7 versus CF: 448 A.U. IQR 337.2 to 558.7). However, these findings were not significant (p=0.88) likely secondary to the low donor number in the CF group. Furthermore, there was considerable variability in the fluorescence intensity in the non-CF group.

Immunofluorescent assessment of TMEM16A was also performed in a CF PNEC culture that had been treated with IL-4 (Figure 115). IL-4 increased the area of fluorescence intensity (control: 337.2 A.U versus IL-4 865.7 A.U), with localisation of TMEM16A at the apical aspect of the PNEC epithelium. This was performed in cultures derived from one donor and would require further investigation in more participants.

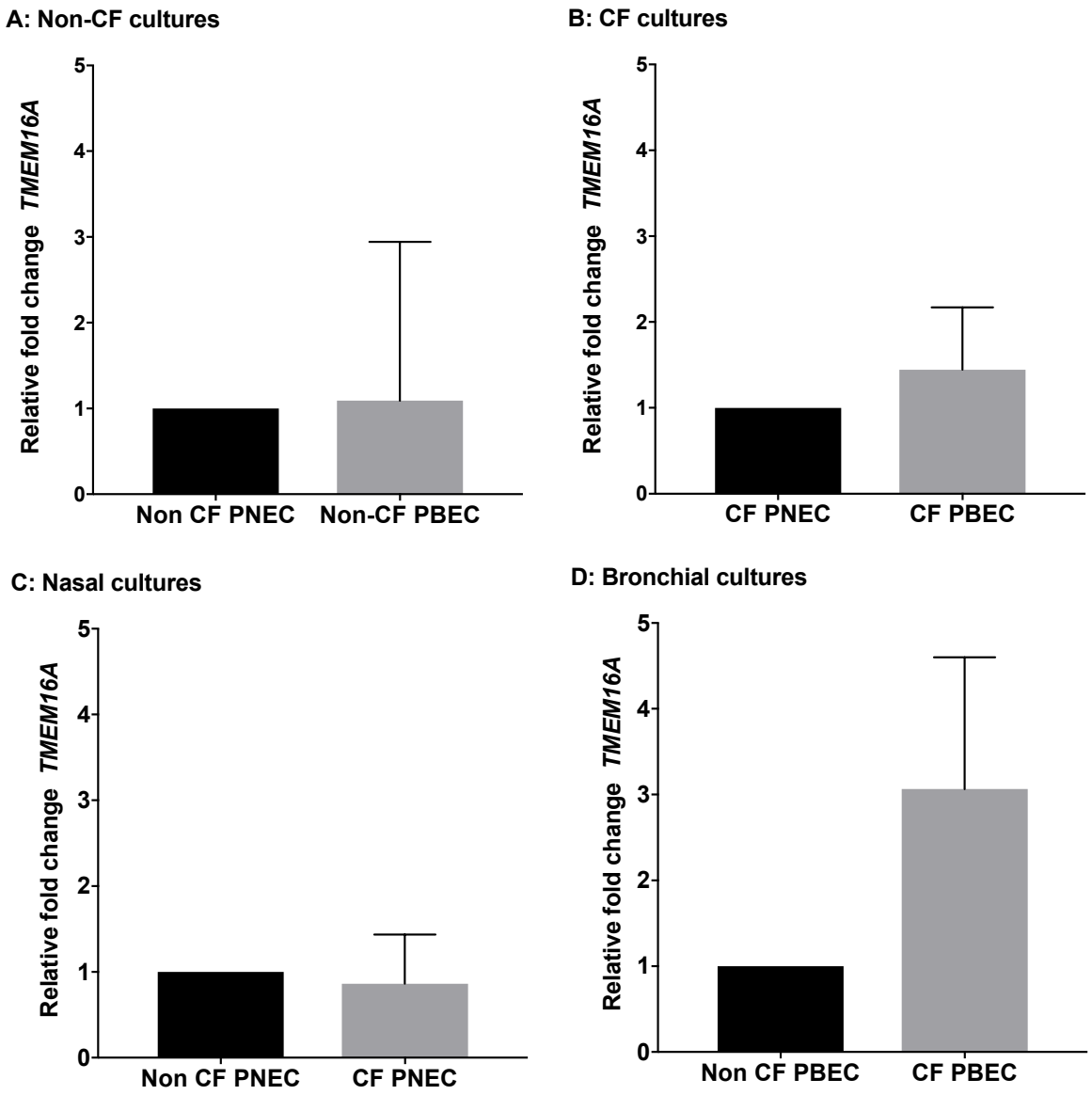

Figure 111: Relative fold change of *TMEM16A* in non-CF and CF cultures

Fold change of *TMEM16A* expression were determined in PNECs relative to PBECs in non-CF (A) and CF cultures (B) as assessed by RT-qPCR. This was also assessed in CF cultures relative to non-CF cultures in PNECs (C) and PBECs (D) non-CF PNECs (n=8 donors), non-CF PBECs (n=8 donors), CF PNECs (n=7 donors), CF PBECs (n=4 donors).

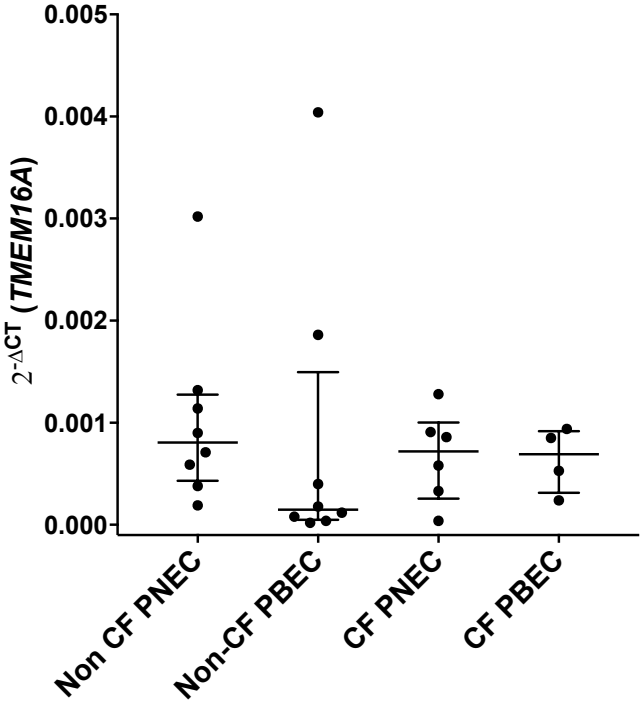

Figure 112: Relative gene expression of *TMEM16A* in non-CF and CF PNEC and PBEC cultures

TMEM16A expression was assessed in differentiated cultures using RT-qPCR. $2^{-\Delta CT}$ values were calculated to determine relative gene expression and complement data for relative fold change. Data is displayed as the median ±IQR and analysed with Kruskal-Wallis and post hoc Dunn's multiple comparison test with no statistical differences found; non-CF PNECs (n=8 donors), non-CF PBECs (n=8 donors); CF PNECs (n=7 donors), CF PBECs (n=4 donors).

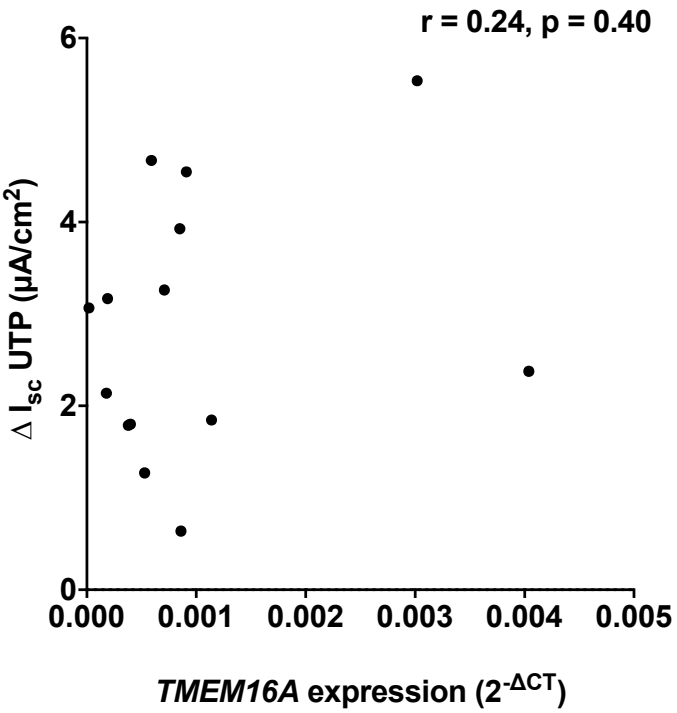

Figure 113: Correlation of *TMEM16A* expression with the UTP-induced short circuit current in all paediatric cultures

Spearman analysis of correlation was performed for expression of *TMEM16A* as measured by $2^{-\Delta CT}$ with corresponding assessment of UTP-induced short circuit current (I_{sc}) in all CF and non-CF PNEC and PBEC cultures. The correlation coefficient (r) was calculated whereby r of 1.0 indicates perfect correlation, 0.0 is no correlation and -1.0 refers to perfect inverse correlation; n=14.

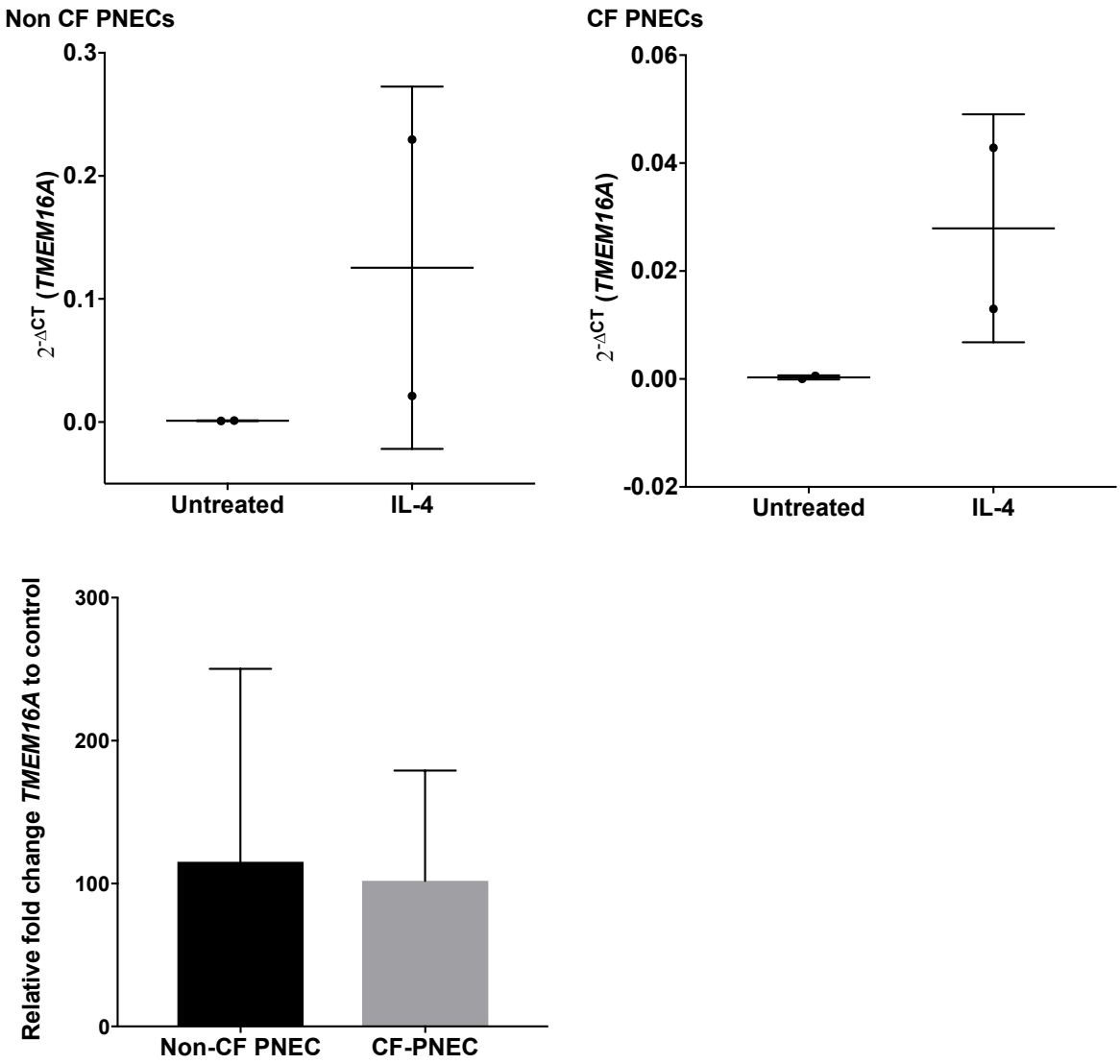

Figure 114: Effects of IL-4 treatment on *TMEM16A* mRNA expression in paediatric PNEC cultures

TMEM16A expression was assessed in differentiated PNEC cultures treated with either vehicle control or IL-4 using RT-qPCR. $2^{-\Delta CT}$ values were calculated to determine relative gene expression and complement data for relative fold change; non-CF PNECs (n=2 donors), CF PNECs (n=2 donors); no statistical analysis was performed.

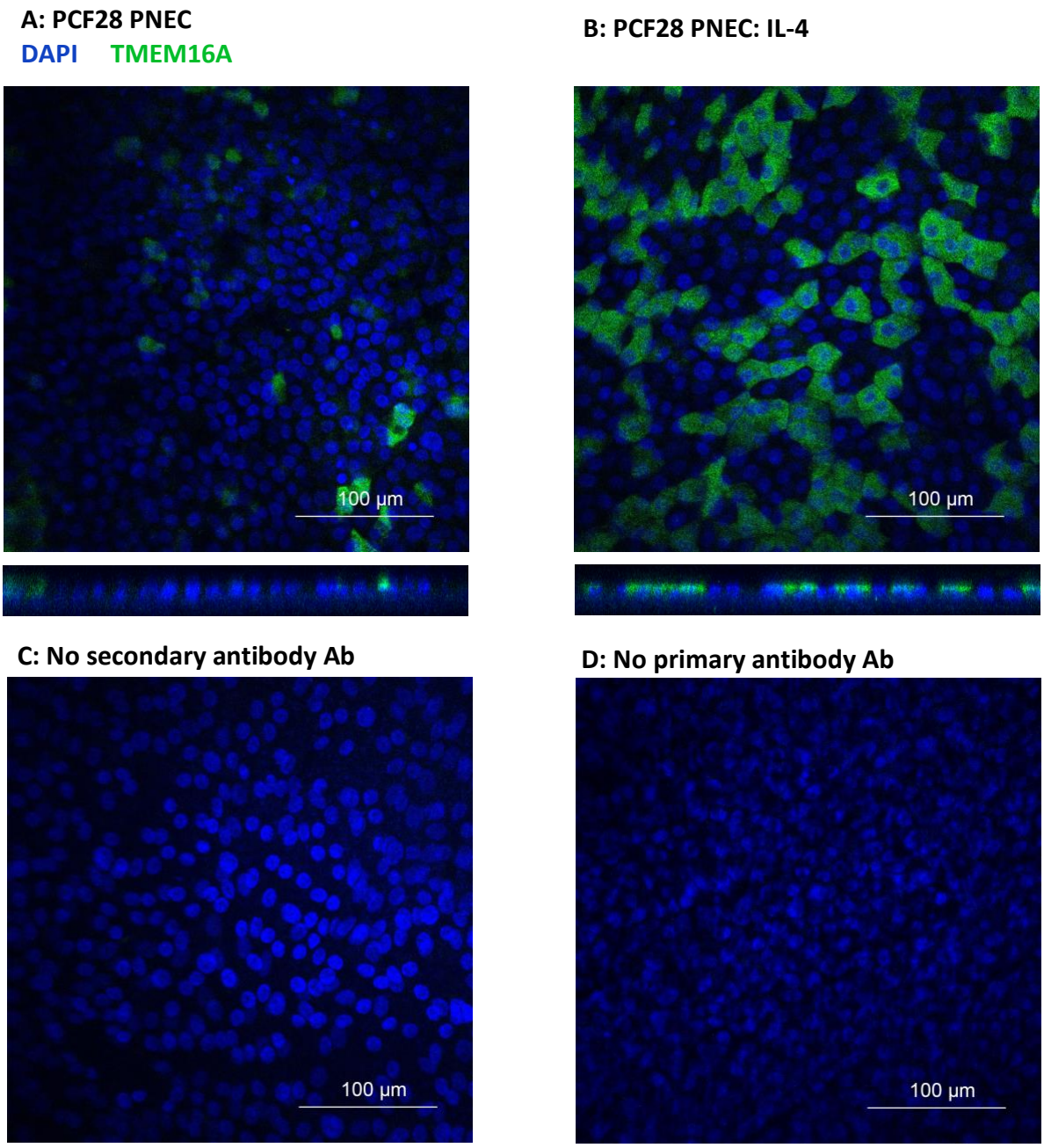

Figure 115: Detection of TMEM16A protein by immunofluorescence in differentiated CF PNEC cultures

A representative confocal image of immunofluorescent TMEM16A detection (green) in PNEC cultures derived from the CF PCF28 donor (F508del/F508del) is shown in A; nuclei stained with DAPI (blue). Staining in IL-4 treated PNECs is shown in B. No secondary/no primary antibody (Ab) controls are shown in C and D respectively; scales as shown.

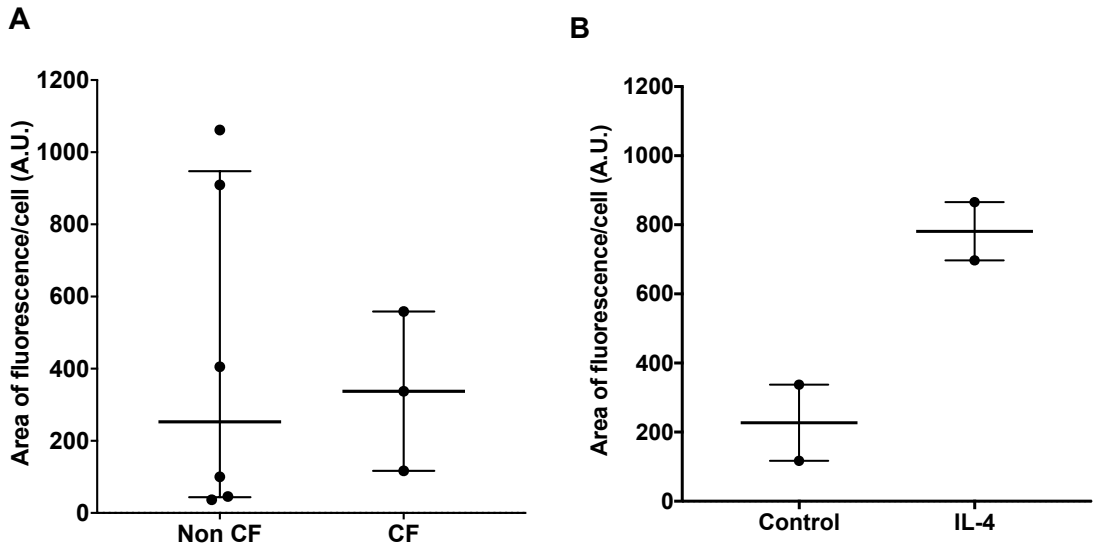

Figure 116: Quantification of TMEM16A immunofluorescence in IL-4 treated differentiated non-CF and CF PNEC cultures

Detection of TMEM16A by immunofluorescence and confocal microscopy was performed in differentiated non-CF and CF PNEC cultures as previously described. The area of fluorescence/cell was determined to quantify TMEM16A presence in non-CF and CF (A) and in IL-4 treated cultures (B). Each point represents a different donor and bars represent median ±IQR. A: Data analysed with Mann-Whitney test with no statistical differences found; n=6 non-CF donors, n=3 CF donors. B: n=2 CF donors for each group (no statistical test applied).

5.5 Discussion

5.5.1 CaCC function and expression does not differ significantly in non-CF versus CF paediatric primary airway epithelial cultures

It has been proposed that in the CF airway, CaCC is the key contributor to apical chloride secretion and large CaCC mediated changes in anion secretion have been found in CF relative to normal airway epithelial cells (Paradiso et al., 2000). As previously discussed in Chapter 1, section 1.6.4, CFTR has been found to inhibit endogenous CaCC activity and the purinergic response to CaCC is enhanced in the CF airway (Kunzelmann et al., 1997, Knowles et al., 1991, Ousingsawat et al., 2011). The results described in this chapter have not revealed any differences in the magnitude of the UTP-induced I_{sc} non-CF and CF PNECs suggesting similar levels of function in the non-CF and CF nasal epithelium.

However, it is important to acknowledge that the number of donors investigated in this PhD was small and further investigation with cultures derived from a larger cohort of participants is likely to be required. Nevertheless, there is limited assessment of CaCC function in paediatric ALI cultures in the literature to date, and these findings have demonstrated the feasibility of assessing CaCC expression by Ussing chamber experiments in paediatric differentiated ALI cultures.

It was interesting to note that despite no differences found between the UTP-induced I_{sc} in the total cohort of PNEC and PBEC cultures in the non-CF group, paired assessment did suggest an increased CaCC function in PNECs. However, given the limited number of paired cultures available for this assessment, this does require further investigation to determine the presence of any airway anatomical variations of CaCC function and expression assessed by the UTP-induced I_{sc}. RT-qPCR assessment of *TMEM16A* mRNA expression did not reveal any suggestion of variations in expression in PNECs versus PBECs in both non-CF and CF groups, however, again this assessment included the combined cohort of differentiated cultures and was limited to paired assessment of PNEC/PBEC culture pairs derived from the same donor.

Importantly, the relative contribution of CaCC to chloride secretion was smaller than that evident with CFTR, with a suggestion of greater bicarbonate transport in CF PNECs and non-CF cultures assessed. It is possible that the residual I_{sc} response evident in these primary cultures can be attributed to the bicarbonate secretory

properties of CaCC. This has significant implications for the potential role of CaCC and TMEM16A activation in counteracting the detrimental effects of dysfunctional CFTR on ASL acidification and dehydration through restoration of ASL pH and chloride transport. However, this does require further comprehensive assessment of firstly the UTP-induced I_{sc} changes in bicarbonate free conditions and secondly the specific inhibition of bicarbonate secretion with compounds such as acetazolamide (a carbonic anhydrase inhibitor) on the resultant forskolin and UTP-induced I_{sc} responses.

5.5.2 TMEM16A activation with Eact was achieved in paediatric primary nasal epithelial cultures

With respect to activation of TMEM16A with the putative small molecule Eact, it was possible to detect I_{sc} changes in the 6 out of 8 PNEC cultures investigated. However, these responses were small, ranging from 0.5 to 2.7 $\mu A/cm^2$, in comparison to the UTP-induced I_{sc}, which ranged from 0.6 to 12.5 $\mu A/cm^2$ and importantly investigation of the latter was performed without enforcement of a chloride gradient. Although the peak Eact-induced I_{sc} was relatively small, the total response as calculated by the area under the curve was larger, with a median value comparable to that seen with the UTP-induced I_{sc}. The characteristic rapid I_{sc} increase evident after apical UTP application occurs secondary to the activation of P2Y2, mobilisation of intracellular calcium stores and a rapid increase intracellular calcium concentration resulting in CaCC activation. The transient nature of the response is due to a combination of multiple effects, including rapid UTP hydrolysis, depletion of intracellular calcium stores and desensitisation of GPCR. This has limited the benefits of CaCC-activators to date as an alternative therapy for people with CF (Picher et al., 2004, Mason et al., 1991, Clarke et al., 1999).

Findings in this PhD suggested that Eact's mode of action was more sustained in comparison to UTP, which could be explained by its calcium-independent mode of action (Namkung et al., 2011b). However, this was not specifically assessed in this PhD. Eact-induced I_{sc} responses evident in this PhD were comparatively smaller than those found during the original identification and characterisation of Eact (Namkung et al., 2011b). Experiments performed in the latter study involved the stable expression of TMEM16A in FRT cells, membrane permeabilization methods and the investigation of I_{sc} using a chloride gradient. Although a gradient was applied in these

PhD experiments, the aim was to determine the relative magnitude of Eact-induced I_{sc} that could be achieved in primary airway epithelial cultures. Findings from this PhD revealed that TMEM16A was expressed in PNEC cultures, albeit at low levels. In view of the potential additional effects of UTP on calcium-activated potassium channels and therefore subsequent chloride secretion, it is possible that this did not occur with Eact, which could account for the relatively smaller magnitude of I_{sc} responses seen.

5.5.3 The activity of CaCC and TMEM16A could not be determined in paediatric CF primary bronchial epithelial cultures due to potential activation of calcium activated potassium channels

A major challenge encountered during the work outlined in this chapter related to the UTP-induced Ussing chamber I_{sc} responses that were not reflective of published characterisation of CaCC and occurred predominantly in CF PBECs. This prevented the inclusion of CF PBECs in overall UTP response analysis, and therefore hindered formal comparisons with the non-CF PBEC and CF PNEC culture groups. The most likely reason for the downward UTP response was secondary to BK channel activation, as suggested from the experimental work involving non-specific BK channel inhibition with $BaCl_2$ and augmentation of the response in chloride free conditions. Cultures were also treated with BAPTA-AM to clamp intracellular calcium levels as an effort to determine the calcium-dependence of these responses. It was anticipated that the resultant UTP-induced I_{sc} in BAPTA-AM treated cultures would be completely abolished. However, the response was modified, with a reduction in both the negative and positive I_{sc} components, as shown in Figure 87. Although the literature was comprehensively reviewed to ascertain an appropriate concentration and treatment duration for BAPTA-AM, these findings suggest that the protocol for administration does require optimisation in these primary cultures, perhaps by increasing both factors.

It is possible that this investigation of CaCC has generated novel data that could reflect the complexity of CaCC assessment and function. Many GPCRs are not confined solely to one G protein and it is possible that UTP is involved in the activation of other signalling pathways involving phosphatidylinositol phosphate (PIP)/PIP kinases and alternative kinases such as protein kinase B and D (Rosenbaum et al., 2009). This could result in the activation or inhibition of other channels and transporters that have an overall impact in the final I_{sc} response.

Although again only investigated in a small number of cultures, application of both $BaCl_2$ and BAPTA-AM modified the nature of the Eact-induced I_{sc} responses, suggesting it also led to calcium activated BK channel activity. However, unlike with UTP, in the CF PBEC cultures Eact addition resulted in a complete loss of I_{sc} and TEER suggesting epithelial damage. The exact cause of this is unknown. It is well recognised that high levels of intracellular calcium can cause apoptosis, and it is possible that this was the resultant effect of Eact in these cultures (Eggermont, 2004). However, this contradicts the proposed calcium independent nature of Eact (Namkung et al., 2011b). Although entirely anecdotal, discussion at relevant conferences with other researchers interested in this field have queried Eact's mode of TMEM16A activation and effects on intracellular calcium. Since its identification there are few studies in the literature that have utilised Eact to investigate airway TMEM16A function, making it difficult to determine if similar problems have been encountered by other research groups.

A major limitation of the results reported in relation to these UTP and Eact Ussing chamber responses is the descriptive nature of the data. Statistical analyses were not performed in circumstances where 2 or less culture inserts were used to assess an intervention, therefore limiting the value of the results obtained. Limited by the requirement of culture inserts for alternative experimental work together with problems encountered with culture failure, as described in Chapter 3 section 3.5.2, low numbers of remaining culture inserts were available to make detailed investigation of the underlying mechanisms involved. Furthermore, it was not possible to predict the occurrence of these UTP and Eact responses and they were only revealed in real-time during the Ussing chamber experiments. Nevertheless, it has been possible to propose potential involvement of BK channel activity. Had more culture inserts for these donors been available, further investigation would have involved the comprehensive investigation of calcium/potassium free Krebs solutions, application of reagents to modify the intracellular calcium environment including thapsigargin (to inhibit the uptake of intracellular calcium) and ionomycin (a calcium ionophore) and assessment of intracellular calcium concentrations.

BK channels are large conductance, voltage-dependent channels that are ubiquitously expressed and are present in the airway epithelium (Barrett et al., 1982, Manzanares et al., 2011). They consist of four subunits which regulate the calcium and voltage dependence of channel function (Manzanares et al., 2011). As opposed

to the membrane depolarisation that occurs with CaCC mediated chloride secretion, BK activation causes membrane hyperpolarisation due to potassium ion efflux. This provides/maintains the electrical driving force for sustained chloride secretion and therefore contributes towards maintenance of ASL hydration and MCC (Manzanares et al., 2011). It is possible that the paediatric PBEC cultures investigated in this PhD had higher levels of BK channel expression, thus leading to the negative UTP and Eact-induced I_{sc} responses.

Attempts were made to investigate relative mRNA expression of the BK channel pore forming subunit, *KCNMA1*, however, it was not possible within the timeframe of this PhD to optimise the primers to facilitate this investigation. This work could have been complemented by immunofluorescence and Western blot assessment to investigate levels and localisation of protein expression, together with the application of a more selective BK blocker, paxilline, in the Ussing chamber (Zaidman et al., 2017).

Recent published work has attributed the presence of hydrocortisone for purinergic BK channel activation channel in airway epithelial cultures via protein kinase C-dependent activation (Zaidman et al., 2017). Hydrocortisone has been shown to be necessary for the maintenance of ion transport properties in muco-ciliated differentiated PBECs (Zaidman et al., 2016). All PNEC and PBEC cultures in this PhD were grown and differentiated using a standardised protocol of cell culture components, included a consistent concentration of hydrocortisone. It is therefore difficult to attribute the presence of hydrocortisone to the findings in this PhD. However, BK channels are susceptible to post-transcriptional modifications, and the effects of the cell culture process on CF PBEC development should be considered (Zaidman et al., 2017).

5.5.4 Small molecule inhibitors demonstrated limited effects on TMEM16A inhibition in differentiated paediatric primary airway epithelial cultures

In view of the challenges faced with investigating TMEM16A activation, inhibition with recently developed small molecules was investigated to determine any effect in paediatric differentiated ALI cultures. Although both $CaCC_{inh}$-A01 and Ani9 demonstrated inhibition of the UTP-induced I_{sc}, investigation in one culture pair derived from PWT17, demonstrated Ani9 to have a larger inhibitory effect on the peak and total UTP-induced I_{sc} compared with $CaCC_{inh}$-A01.

Assessment in PBEC cultures was limited by suggested BK channel activity. However, of note, the nature of the UTP-induced I_{sc} was modified with both inhibitors, suggesting potential effects on reducing intracellular calcium concentration, thereby inhibiting BK channel as well as TMEM16A activity. This is contradictory to recent published data which has shown the effects of Ani9 to be independent of intracellular calcium signalling (Hahn et al., 2017). Of note, Ani9 application in this study completely abolished the UTP-induced I_{sc} (Hahn et al., 2017). However, these findings were obtained in TMEM16A transfected HEK293 cells and rat tracheal epithelial cells, which could account for failure of the UTP-induced I_{sc} to be abolished with Ani9 in human paediatric cultures in this present study.

Although both $CaCC_{inh}$-A01 and Ani9 have previously been shown to inhibit the UTP-induced I_{sc} response in alternative cellular models, this was not evident in paediatric cultures investigated in this PhD. This finding is important and is suggestive of a number of possibilities: i) TMEM16A does not form a significant component of CaCC-mediated airway chloride secretion (which has previously been suggested (Namkung et al., 2011a); ii) these small molecule inhibitors have a low specific potency for TMEM16A inhibition and iii) UTP is acting on alternative non-TMEM16A channels. Although all of these possibilities are feasible, the latter is an important consideration and is highly possible. Although UTP is employed for the purinergic activation of CaCC, previous investigation in primary bronchial cells has shown that UTP can induce CFTR-dependent chloride secretion via cAMP signalling (Namkung et al., 2010a). UTP was consistently added after CFTR inhibition in all Ussing chamber experiments, however re-application of $CFTR_{inh}$-172 after UTP could have helped determine any potential effects of UTP-mediated CFTR activation. Furthermore, it is also possible that the residual $CaCC_{inh}$-A01/Ani9 inhibited UTP-induced I_{sc} was the result of alternative non-TMEM16A CaCCs that remain to be characterised.

5.5.5 IL-4 upregulated TMEM16A expression in differentiated paediatric primary airway epithelial cultures

The effects of proinflammatory stimuli on the modification of airway epithelial ion transport properties has previously been recognised including the effects of IL-4 and IL-13 on inhibition of the amiloride-sensitive I_{sc}, enhancement of cAMP-mediated CFTR activation and increased responses to UTP (Galietta et al., 2002, Danahay et al., 2002). Indeed one of the three methods used to identify TMEM16A as an essential component of CaCC utilised this knowledge, whereby global gene

expression analysis was performed to identify proteins that were regulated by IL-4 (Caputo et al., 2008).

As a Th2 cytokine, IL-4 is implicated in respiratory diseases with features of mucus hypersecretion and goblet cell hyperplasia such as asthma (Daher et al., 1995, Steinke and Borish, 2001). Although CF is characterised by mucus hypersecretion, there is little evidence to demonstrate the exact relevance of IL-4 in the CF airway. Nevertheless, there is evidence to support the role of IL-4 in upregulating TMEM16A expression in bronchial epithelial cell lines and PBECs derived from explanted CF lung tissue (Scudieri et al., 2012a, Gorrieri et al., 2016).

This knowledge was utilised in this PhD to determine if TMEM16A expression could be enhanced in paediatric cultures. Treatment with IL-4 did demonstrate increases in both the UTP and Eact induced I_{sc} responses in paediatric PNEC cultures, with a paralleled suggestion of increased *TMEM16A* mRNA expression in both non-CF and CF PNECs. Furthermore, assessment by immunofluorescence in 2 CF PNEC cultures complemented these findings, with evidence of localisation to the apical aspect of the epithelium. Of note, the immunofluorescence work was demonstrated using only one anti-TMEM16A antibody, and although confirmation with an additional antibody would have been preferable, it was not possible to achieve any reliable staining despite considerable measures to optimise 2 alternative commercially available antibodies.

Reassuringly, the assessment of TMEM16A in IL-4 treated cultures complemented previously reported findings in bronchial cultures, further confirming the suitability of using paediatric PNECs for this work. Importantly, treatment was well tolerated by the cultures, with no detrimental effects on epithelial integrity as observed by TEER assessment.

There is limited data regarding *in vivo* airway concentrations of IL-4, however, both published BAL data in adult patients and the assessment of IL-4 and IL-13 in paediatric BAL samples in this PhD (Chapter 3 section 3.6.7) have shown elevated levels compared with non-CF participants (Bergin et al., 2013). Notably this finding was not present in cell culture supernatants, with no differences in the IL-4 and IL-13 between the CF and non-CF groups. However, it must be considered that this mode of investigation was utilised solely to augment channel function and it is difficult to translate this to the human CF airway. Furthermore, it would not be feasible to use this as a therapeutic strategy to increase TMEM16A function in CF, particularly given

the relatively large concentrations of IL-4 (in this case 10ng for 24 hours) required to achieve these outcomes. Although concentrations of IL-4 used to treat cell cultures are considerably greater than levels evident in BAL, the pro-secretory effects of such cytokines and impacts on ion transport are important considerations when assessing electrophysiological properties of the CF airway.

5.6 Conclusion

It has been possible to demonstrate the feasibility of using differentiated paediatric PNEC cultures to characterise CaCC and TMEM16A expression. No differences were evident in CaCC expression in PNEC cultures derived from non-CF and CF participants and although no differences were found between PNEC and PBEC cultures, paired assessment suggested increased CaCC function in PNECs derived from non-CF participants.

There was evidence to suggest the activation of BK channel expression in some paediatric cultures, with a predominance for PBECs derived from CF donors. This does require further exploration and investigation as outlined. Characterisation of TMEM16A with the application of known activators and inhibitors in Ussing chamber experiments has been demonstrated, despite the limited availability of reliable small molecules. Application of a combination of experimental techniques to complement Ussing chamber experiments, including RT-qPCR and immunofluorescence, has provided evidence to suggest that although present at low levels in the paediatric cultures, TMEM16A has potential for modulation in the paediatric airway.

6 Chapter 6: Investigation of TMEM16A activation with the novel C5 activating compound

6.1 Introduction

The work carried out in this PhD was closely associated with the research of a CF Trust funded Strategic Research Centre grant entitled “Non-CFTR approaches for CF therapy”, led by Dr Mike Gray. As part of this SRC, research groups of project collaborators Professor Karl Kunzelmann (University of Regensberg, Germany) and Professor Margarida Amaral (University of Lisbon, Portugal) had identified novel TMEM16A activating compounds as described below. Of the seven identified ‘C’ compounds that demonstrated potential, the C5 compound was selected for further investigation in this PhD. These first-generation compounds had not yet been investigated in primary airway epithelial cultures and as a result there was very little known about potential effects and activity using this *in vitro* model. The results described in this chapter are primarily descriptive in nature.

In addition to investigating any potential responses of the C5 compound in primary cultures using Ussing chamber experiments, the additional purpose of the work in this chapter was to determine the feasibility of utilising established paediatric primary ALI cultures to investigate newly developed molecules as a strategy for TMEM16A activation and CF therapy.

6.2 Hypotheses

- Differentiated paediatric PNEC and PBEC ALI cultures can be used in Ussing chamber experiments to explore the effects of C5, a novel TMEM16A activating compound.

6.3 Aims

The specific aims of this chapter were to:

- investigate the effects of C5 application in cultures derived from non-CF and CF donors using Ussing chamber experiments
- demonstrate the feasibility of utilising paediatric differentiated airway epithelial cultures established in this PhD to investigate the effects of novel small molecule targets for therapy

6.4 Results

6.4.1 Preliminary investigation of novel C5 compounds in HT29 cells

This work was performed by the research groups of Professors Kunzelmann and Amaral who kindly shared the preliminary data for the purposes of compound investigation in this PhD. Novel candidate molecules for TMEM16A activation were identified by the research groups of Professors Amaral and Kunzelmann using an in-silico approach of compounds structurally similar to Eact and investigated using the YFP halide assay. As detailed in Chapter 1, the YFP assay can be used as a measure of CaCC sensitivity. Cells expressing YFP are placed into an iodide rich solution and challenged with a calcium agonist. The resultant iodide flux results in rapid YFP fluorescence, the rate of which is proportionate to CaCC activity. In this case, YFP-expressing HT29 cells (human adenocarcinoma cell line) were transfected with TMEM16A and pre-incubated for 10 minutes with varying concentrations of the novel compounds. The rate of iodide quenching was assessed, revealing seven C compounds with significant increases in anion conductance. Compound C5 was selected as one of the key activating molecules and the YFP assay results are shown below relative to Eact (Figure 117). This preliminary investigation showed significant increases in iodide quenching at 10 and 50 μM C5 that were comparable to Eact.

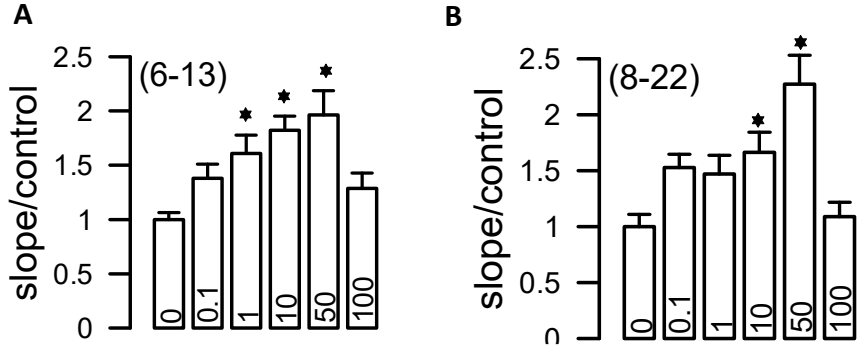

Figure 117: YFP iodide assay demonstrating the C5 activity in HT29 cells

This work was performed by the research groups of Professor Amaral and the data presented was kindly provided for the purposes of this PhD. HT29-YFP cells were pre-incubated with either Eact (A) or C5 (B) at 0.1, 1, 10, 50 and 100 μM concentrations for 10 minutes. Iodide quenching was assessed at 37 °C as a measure of anion conductance. Bars represent the mean ±SEM. Data analysed with one-way ANOVA; *p<0.05; A: n=6-13 experiments, B: n=8-22.

6.4.2 Effects of acute C5 treatment in paediatric primary nasal epithelial cultures derived from non-CF donors

The presence of any potential activity of C5 in paediatric primary cultures was firstly assessed in PNEC cultures derived from a non-CF donor, PWT11. The first priority was to ensure that the UTP-induced I_{sc} was characteristic of CaCC secretion, therefore responses to the standard protocol utilised in this PhD were first investigated. Ussing chamber experiments were performed using the standard protocol with an initial apical addition of amiloride, forskolin and $CFTR_{inh}$-172 as previously described in Chapter 2 section 2.5. As shown from the resultant traces below in Figure 118, the response to UTP was characteristic of CaCC mediated chloride secretion (mean UTP-induced I_{sc}: 5.5 μA/cm^2 ± SD 1.5), therefore enabling reliable future exploration of C5 effect on I_{sc} response and TMEM16A activity.

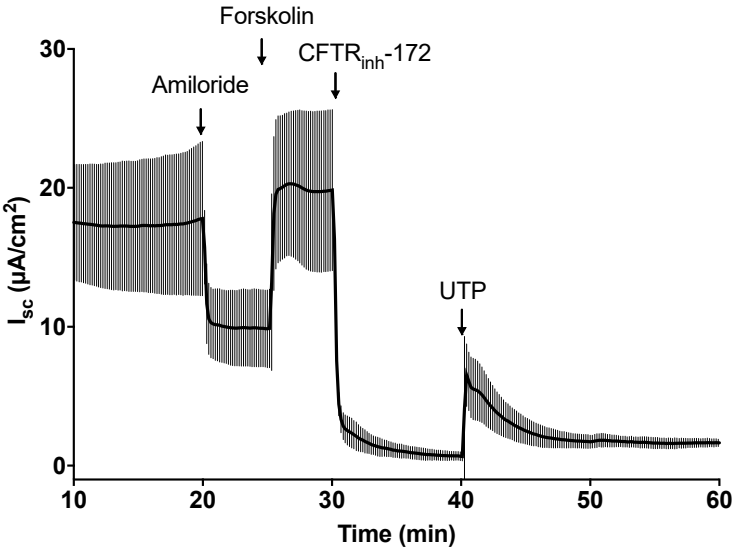

Figure 118: Short circuit current responses to amiloride, forskolin, $CFTR_{inh}$-172 and UTP in PNEC cultures derived from the non-CF PWT11 donor

Ussing chamber experiments were performed in 125 mM chloride as previously described. 100 μM amiloride, 10 μM forskolin, 20 μM $CFTR_{inh}$-172 and 100 μM UTP were added at 20, 25, 30 and 40 minutes respectively as shown. Lines represent the mean short circuit current (I_{sc}) responses with error bars for the SD; n=2 culture inserts.

The effect of C5 addition alone was next explored in cultures derived from this donor. All experiments involving C5 addition were performed using 125 mM chloride Krebs, with the preceding addition of amiloride, forskolin and $CFTR_{inh}$-172. Previous data from the Kunzelmann lab had demonstrated significant increases in iodide quenching in the YFP assay with 10 μM and 50 μM of C5. It was not possible to perform a formal dose response in primary cultures, namely due to the very limited amount of compound that was available for investigation. Concentrations of 10 μM and 20 μM C5 were therefore initially investigated. Representative Ussing chamber traces together with the resultant peak and total I_{sc} responses are shown in Figure 119. Both concentrations demonstrated increases in the C5-induced I_{sc}, however there were no significant differences found between the two concentrations (10 μM: 0.9 $\mu A/cm^2 \pm$ SD 0.5 versus 20 μM: 1.7 $\mu A/cm^2 \pm$ SD 0.2; p=0.4). C5 addition at 10 μM produced a significantly smaller peak I_{sc} response than UTP (p=0.04), but no significant differences were found between UTP and 20 μM C5 (p=0.8). Although no significant differences were found in peak response with 10 μM C5, there was a suggestion of a greater total I_{sc} response with C5 compared with 100 μM UTP (23.1$\mu A/cm^2$.min ± SD 8.4), which was larger with 20 μM C5 (10μM: 32.1 $\mu A/cm^2$.min ± SD 1.9; p=0.7; 20 μM: 36.0 $\mu A/cm^2$.min ± SD 3.6; p=0.1). These C5-induced I_{sc} changes were not accompanied by a reduction in TEER, and although there was a TEER decrease with UTP addition, this was small (-58.0 $\Omega.cm^2 \pm$ SD 66.5).

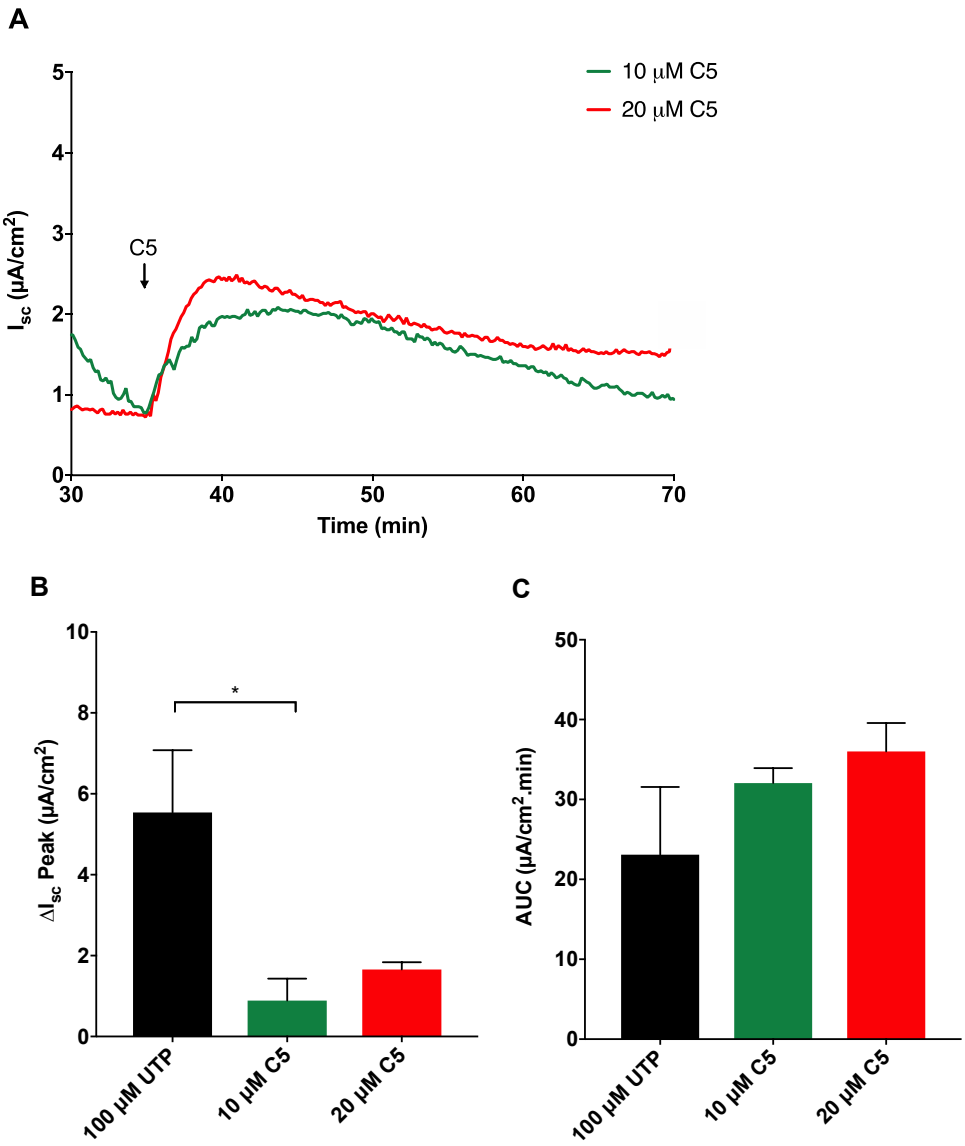

Figure 119: Short circuit current response to C5 in PNEC cultures derived from the non-CF PWT11 donor

Representative short circuit current (I_{sc}) responses for 10 μM (green) and 20 μM (red) C5 addition in PWT11 PNECs. The peak-induced I_{sc} (ΔI_{sc}) and area under the curve (AUC) as compared with 100 μM UTP (black) are shown in B and C respectively. Bars represent mean ± SD. Data analysed with Kruskal Wallis and Dunn's multiple comparisons tests; *p=0.04 for peak ΔI_{sc} for 100 μM UTP versus 10 μM C5; n=3 inserts for each condition.

6.4.3 C5 potentiation of the UTP-induced short circuit current

The next focus of work was to determine the ability of C5 to potentiate the UTP-induced $I_{sc.}$ Until now, 100 μM UTP had been used in Ussing chamber experiments to ensure maximal CaCC activation. However, for the investigation of UTP potentiation, a reduced concentration was required to prevent complete saturation of response. To ascertain an appropriate concentration of UTP for further assessment with C5, a dose response investigation was performed (Figure 120). The peak-induced I_{sc} was greatest after the initial application of 1 μM (4.2 μA/cm^2 ± SD 0.1) which was similar in magnitude to that seen at 100 μM as reported above. Increasing concentrations of UTP in the same culture insert resulted in a subsequent decrease in peak I_{sc} suggesting that P2Y2 receptors were desensitised and calcium stores were depleted at concentrations above 5 μM. A UTP concentration of 1 μM was therefore selected for use in conjunction with C5 so as not to diminish any potential effect of C5 on I_{sc}.

Ussing chamber experiments were performed to assess the effects of 1 μM UTP addition in conjunction with either 10 μM or 20 μM C5. The effects of C5 were assessed after the initial application of amiloride, forskolin and $CFTR_{inh}$-172 as with all previous experiments. The resultant peak and total I_{sc} responses are shown in Figure 121. There were no differences between the peak-induced I_{sc} between the UTP/C5 combinations at both C5 concentrations (1 μM UTP/10 μM C5: 6.2 μA/cm^2 ± SD 3.1 versus 1 μM UTP/20 μM C5: 6.6 μA/cm^2 ± SD 0.9; p>0.99). Furthermore, neither combination of UTP/C5 addition was significantly different to the peak-induced I_{sc} evident with either 1 μM UTP (1 μM UTP/10 μM C5: p=0.5; 1 μM UTP/20 μM C5: p>0.99) or 100 μM UTP (p>0.99 for both). The total I_{sc} for 1 μM UTP alone was 37.6 μA/cm^2.min ± SD 18.3. This was increased by 2.5-fold with 1 μM UTP/10 μM C5 (92.0μA/cm^2 ± SD 55.6; p=0.8) and 2.6-fold with 1 μM UTP/20 μM C5 (96.2 μA/cm^2 ± SD 15.3; p=0.3), however, these findings were not statistically significant.

These data suggest that C5 did produce small increases in I_{sc} when applied alone. The greatest effect was evident with the combination of C5 with 1 μM UTP, predominantly on the total induced I_{sc}. Furthermore, there was little difference between 10 μM and 20 μM when used in conjunction with UTP.

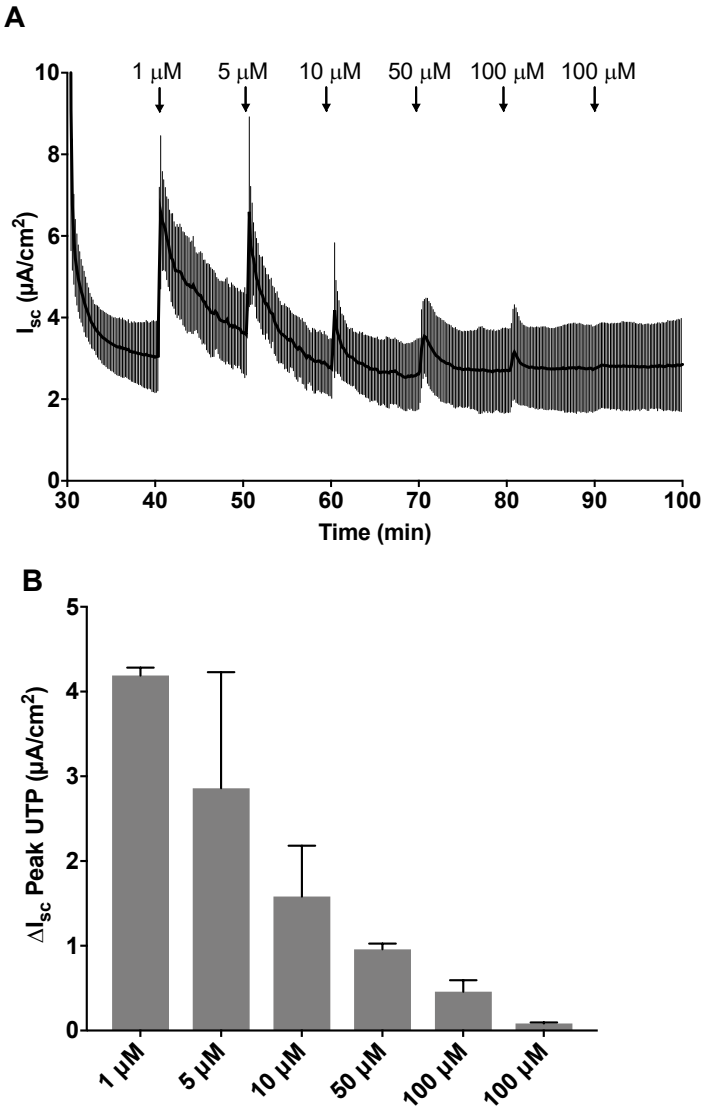

Figure 120: Effects of increasing UTP concentration on short circuit current response in PNEC cultures derived from the non-CF PWT11 donor

UTP was applied to the apical compartment of the Ussing chamber at the concentrations shown above in the same culture insert. Short circuit current responses (I_{sc}) are shown in A; lines represent the mean response with bars for the SD. The peak-induced I_{sc} (ΔI_{sc}) is shown in B; bars represent mean ± SD; n=2 culture inserts (statistical analysis not performed).

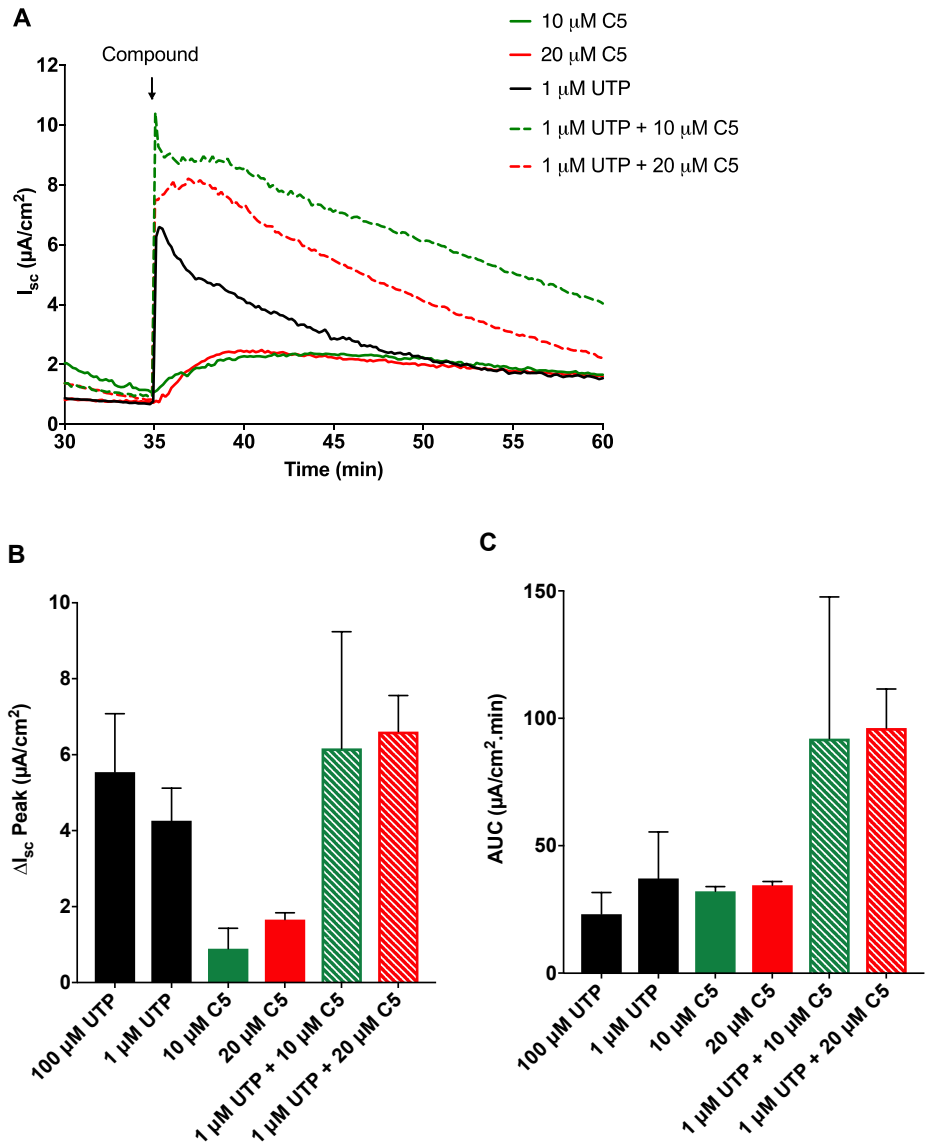

Figure 121: Effects of UTP and C5 on short circuit current response in PNEC cultures derived from the non-CF PWT11 donor

Representative short circuit current (I_{sc}) responses for 10 μM C5 (green solid line) and 20 μM C5 (red solid), 1 μM UTP (black), 1 μM UTP plus 10 μM C5 (green dashed) and 1 μM UTP plus 20 μM C5 (red dashed) addition in PNECs derived from the non-CF PWT11 donor. The peak-induced I_{sc} (ΔI_{sc}) and area under the curve (AUC) are shown in B and C respectively. Bars represent mean ± SD. Data analysed with Kruskal Wallis and Dunn's multiple comparisons test with no statistical differences found; n=4 culture inserts for1 μM UTP, n=3 culture inserts for all other conditions.

I_{sc} responses after acute apical addition of C5 5 minutes prior to UTP application were next assessed to determine any potential effects on further augmentation of the UTP-induced response. This was investigated in PNEC cultures derived from the non-CF PWT16 donor, which had demonstrated a peak UTP-induced I_{sc} at 100 μM of 1.8 μA/cm^2 ± SD 1.1 and total response of 8.9 μA/cm^2.min ± SD 2.4.

The effects of C5 treatment alone in these cultures was firstly established to determine any changes in I_{sc} as shown below in Figure 122. C5 concentration of 10 μM was selected for investigation based on results previously reported. Apical addition of C5 did increase the I_{sc} response, with peak and total responses of 2.7 μA/cm^2 ± SD 1.7 and 88.4 μA/cm^2.min ± SD 49.1, respectively, and although the total response was almost 10-fold greater than with UTP, this was not significant (p=0.2).

Initial apical addition of C5 was investigated with 1, 10 and 100 μM UTP to determine if pre-treatment induced any changes in the subsequent UTP response. It was only possible to investigate this in 1 culture insert for each condition due to limited culture availability. As shown in Figure 123, the apical addition of UTP alone at all 3 concentrations showed a biphasic response, with the rapid first peak demonstrating the largest UTP-induced I_{sc}. C5 addition 5 minutes prior to UTP reversed this effect at all 3 UTP concentrations, with a resultant larger second UTP-induced peak I_{sc} increase. Although the I_{sc} traces showed in Figure 123 show some features of instability, the initial resting TEER for these cultures were all in the range of 747 to 955 Ω.cm^2, indicating adequate tight junction integrity and suitability of these culture inserts for this assessment. The changes in these peak UTP-induced I_{sc} responses are shown in Figure 124 whereby the largest UTP-induced I_{sc} after C5 addition was evident with 100 μM UTP.

Interestingly pre-treatment of C5 at UTP concentrations of 10 and 100 μM produced a $CaCC_{inh}$-A01-sensitive I_{sc}, indicating that at these concentrations, the resultant augmented responses involved TMEM16A activation. These responses were also bumetanide-sensitive, suggesting involvement of C5/UTP-mediated chloride secretion. Importantly, the UTP-induced I_{sc} alone was not sensitive to $CaCC_{inh}$-A01, suggesting minimal TMEM16A-mediated chloride secretion under these conditions. Of note, the TEER did not change with C5 addition in all circumstances (not shown). However, addition of $CaCC_{inh}$-A01 with C5/UTP did show increases in TEER (10 μM UTP: 80 Ω.cm^2; 100 μM UTP: 120 Ω.cm^2) further confirming inhibition of TMEM16A-mediated ion transport.

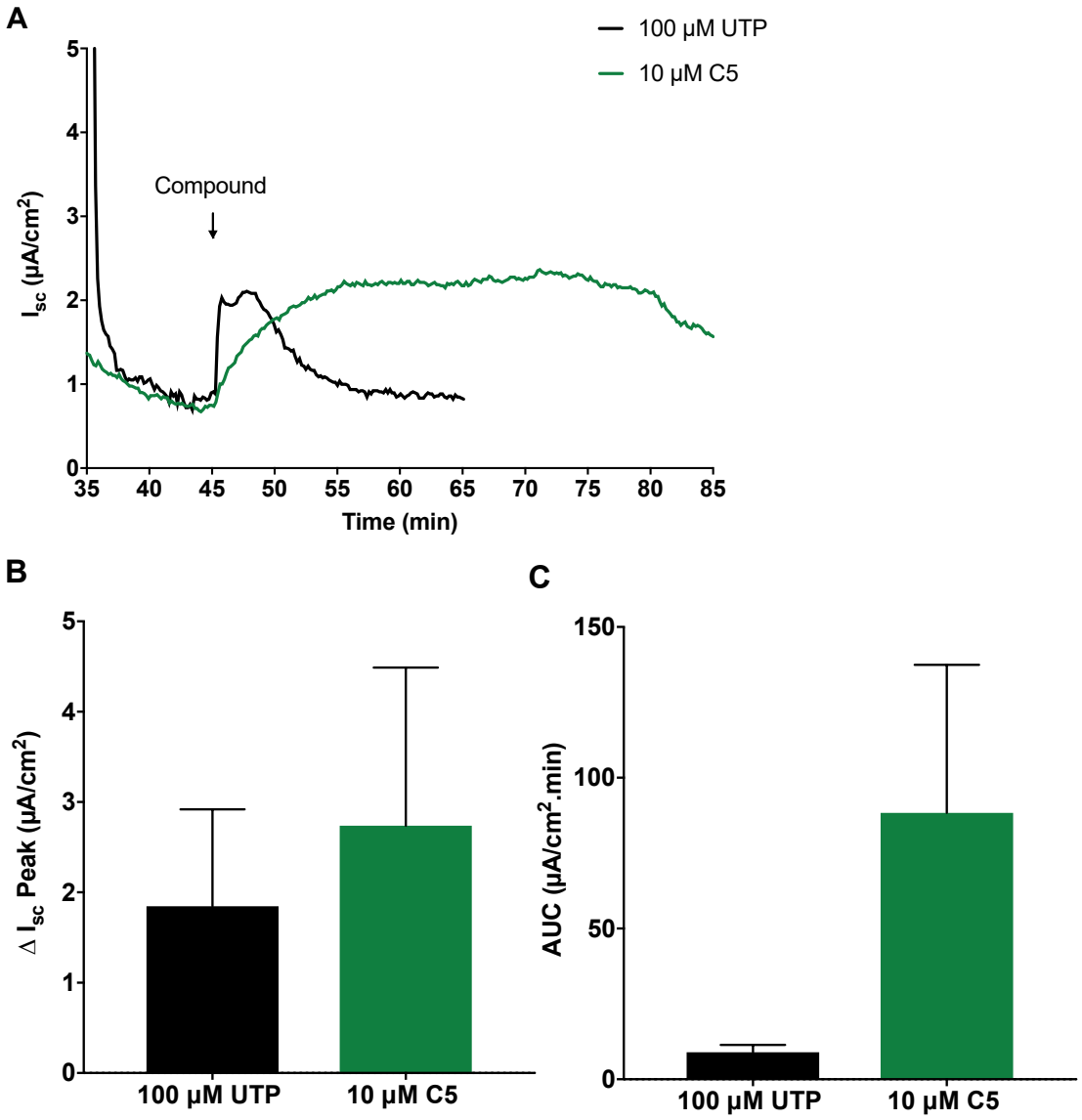

Figure 122: Short circuit current response to C5 in PNEC cultures derived from the non-CF PWT16 donor

Representative short circuit current (I_{sc}) responses for 10 µM C5 (green) and 100 µM UTP (black) in PNECs derived from the non-CF PWT16 donor. The peak-induced I_{sc} (ΔI_{sc}) and area under the curve (AUC) are shown in B and C respectively. Bars represent mean ± SD. Data analysed with Kruskal Wallis and Dunn's multiple comparisons tests; p=0.4 for peak ΔI_{sc}; p=0.2 for AUC; n=3 inserts for each condition.

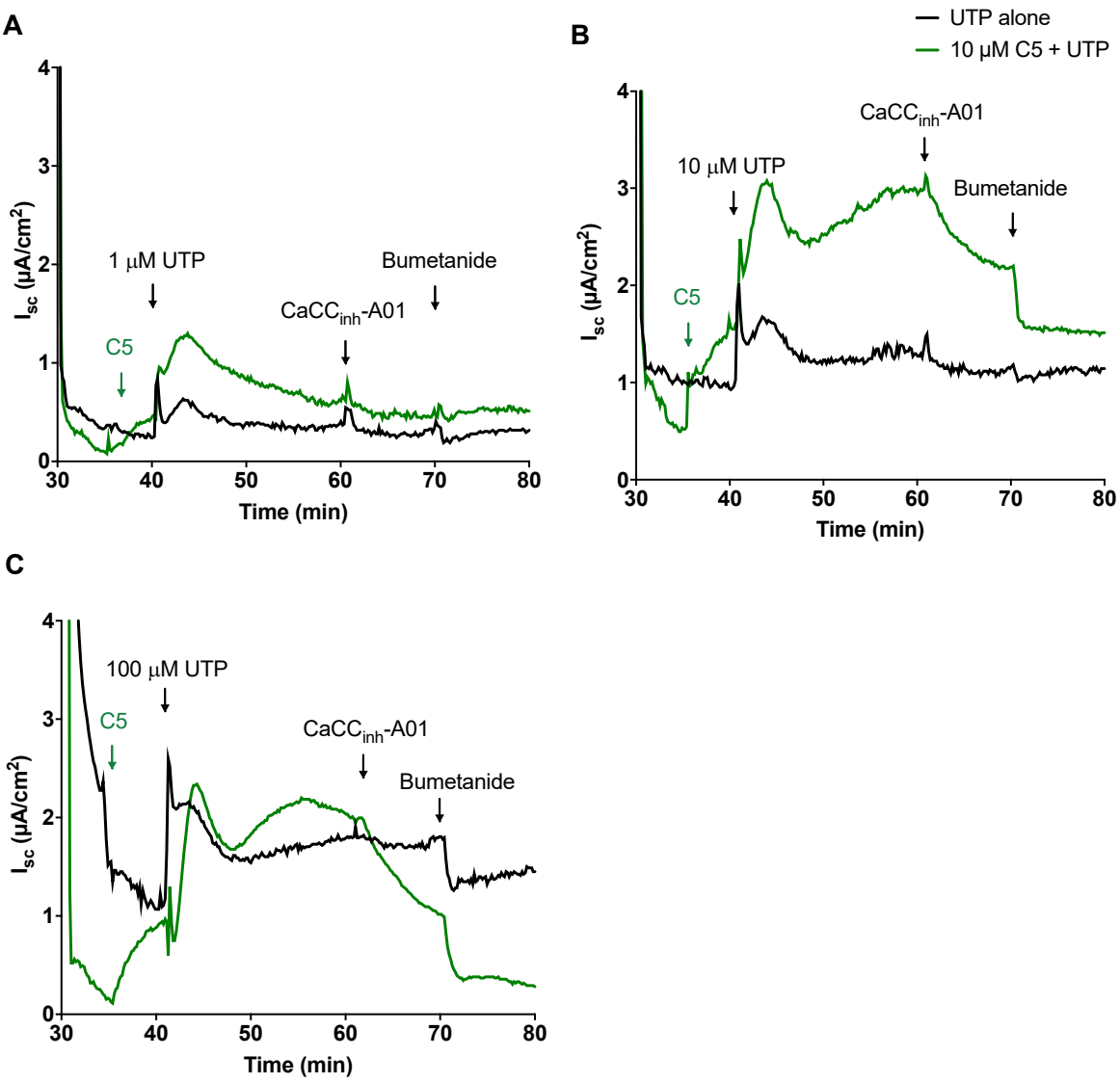

Figure 123: Representative Ussing chamber traces for acute C5 treatment with varying UTP concentrations in PNEC cultures derived from the non-CF PWT16 donor

Representative short circuit current (I_{sc}) responses for the addition of UTP alone (black line) or the 10 μM C5 added 5 minutes prior to UTP (green) at 1 μM UTP (A), 10 μM UTP (B) and 100 μM UTP (C) addition in PNECs derived from the non-CF PWT16 donor; n=1 for each condition.

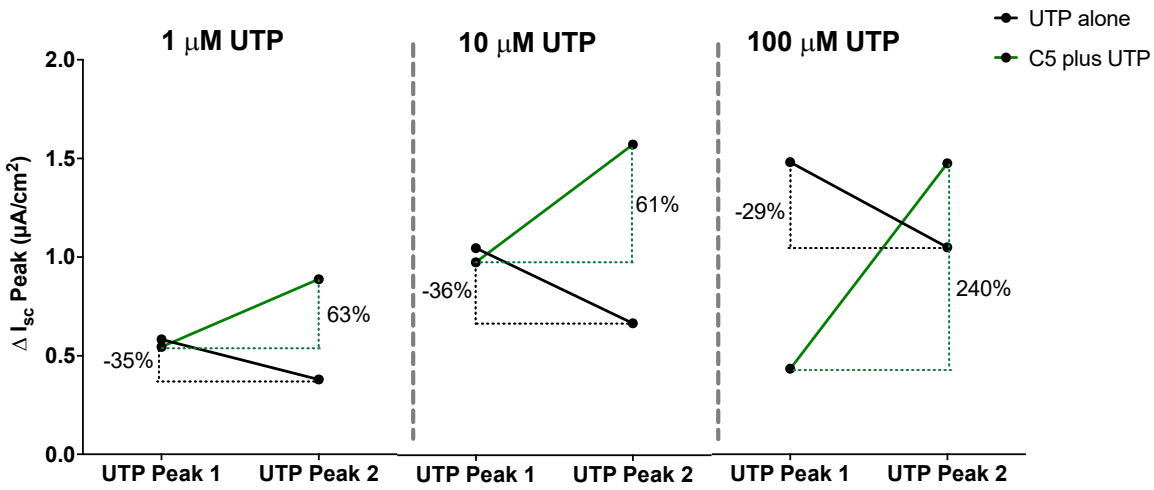

Figure 124: Effects of acute C5 treatment on the UTP-induced short circuit current peak response in PNEC cultures derived from the non-CF PWT16 donor

The percentage change of the UTP-induced short circuit current (ΔI_{sc}) for the second peak relative to the first peak was calculated for experiments where UTP was applied alone (black line) and where cultures were pre-treated with C5 for 5 minutes prior to UTP addition (green). This was calculated for 1 μM, 10 and 100 μM UTP.

6.4.4 Chronic C5 treatment in paediatric primary nasal epithelial cultures derived from non-CF donors

The effects of chronic C5 treatment were next assessed in PNEC cultures derived from the PWT16 donor. Cell cultures were treated with either a vehicle control or 10 μM C5 for 24h and 48h before performing Ussing chamber assessment of I_{sc} response to 1, 10 and 100 μM UTP. Amiloride, forskolin and $CFTR_{inh}$-172 were added prior to UTP as previously described and experiments were performed using 125 mM chloride Krebs solutions in both Ussing chamber compartments. This was performed in 1 culture insert for each condition due to a limited number of cultures remaining for this experimental work from this donor. Therefore this data is descriptive.

Responses were similar at all UTP concentrations and duration of C5 treatment; representative I_{sc} and TEER Ussing chamber traces for investigation of 100 μM UTP at 24h are shown in Figure 125 with resultant changes in I_{sc} at all UTP concentrations in Figure 126. It is difficult to ascertain the relative changes in the magnitude of responses with all 3 concentrations of UTP after 24h and 48h of C5 treatment because experiments were limited by the number of repeats. However, after both 24h and 48h of C5 treatment, there was clear modification of the resultant UTP-induced $I_{sc,}$ where the response was initially negative, followed by an increase. These changes were accompanied by a reduction in TEER. Notably, chronic C5 treatment at both 24h and 48h appeared to result in reductions in I_{sc} responses to both amiloride, forskolin and $CFTR_{inh}$-172, however these differences were only significant for $CFTR_{inh}$-172 after 48h treatment (DMSO: -12.0 $\mu A/cm^2 \pm$ SD versus 48h C5: -3 $\mu A/cm^2 \pm$ SD 1.1; p=0.04). DMSO treatment alone after 48h reduced the amiloride-sensitive and the UTP-induced I_{sc} on all occasions, suggesting off-target effects over this duration of treatment. C5 treatment for 24h was also investigated in a limited number of PNEC and PBEC cultures derived from the PWT17 donor, with similar changes seen (not shown).

Although chronic C5 treatment was tolerated in cultures derived from both donors, (as determined by maintenance of TEER), it failed to augment the UTP-induced I_{sc} , with additional off-target effects of modifying responses to UTP and reducing responses of other channels investigated.

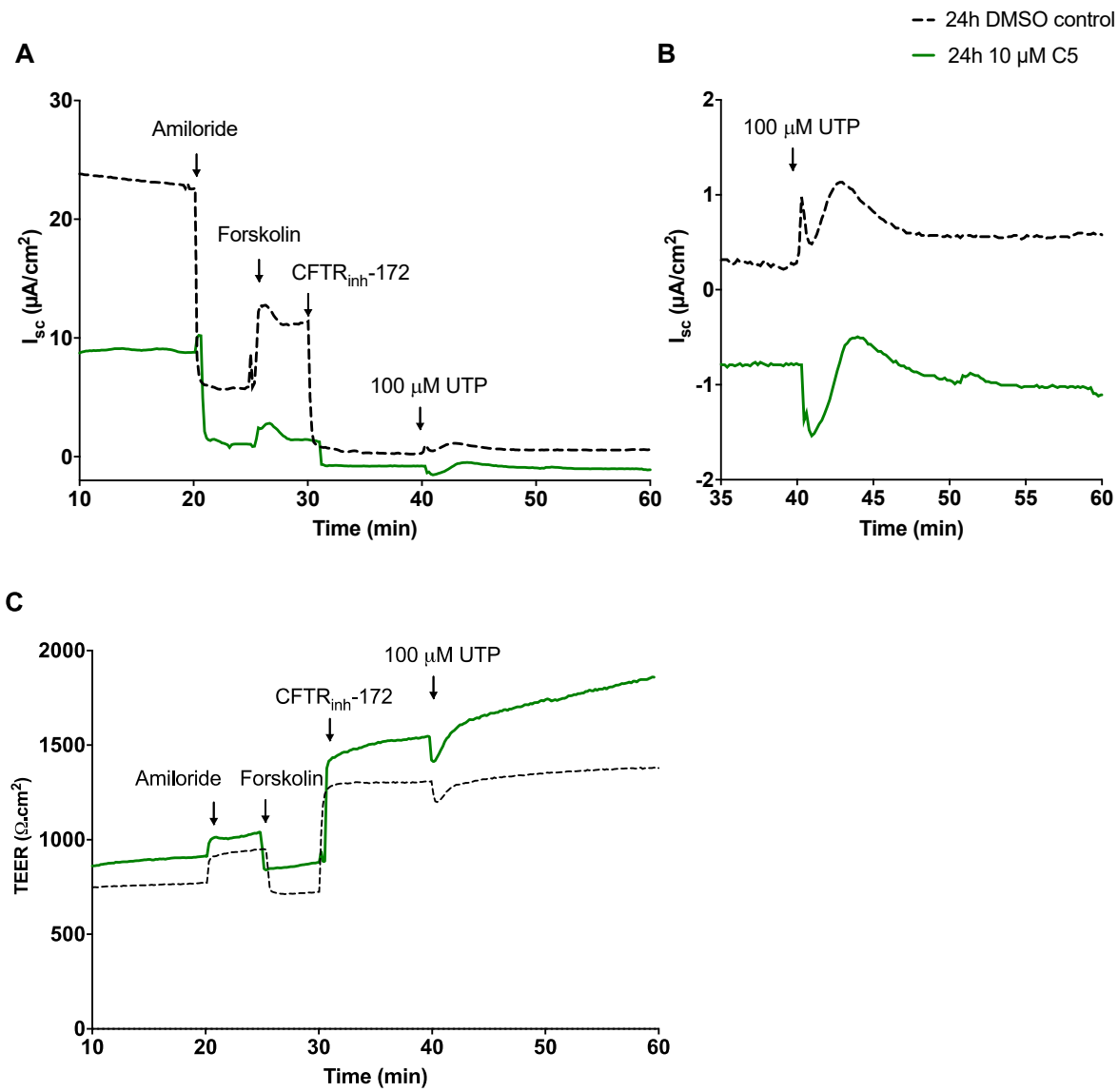

Figure 125: Representative Ussing chamber short circuit current and transepithelial resistance responses after 24h C5 treatment in PNEC cultures derived from the non-CF PWT16 donor

PNEC cultures derived from the non-CF PWT16 donor were treated with either 10 µM C5 or vehicle control (0.1 % DMSO) for 24h before performing Ussing chamber experiments and addition of 100 µM UTP. Representative short circuit current (I_{sc}) traces are shown in A, with expansion of the UTP-induced I_{sc} response shown in B. The corresponding transepithelial resistance (TEER) measurements are shown in C; n=1 culture insert for each condition.

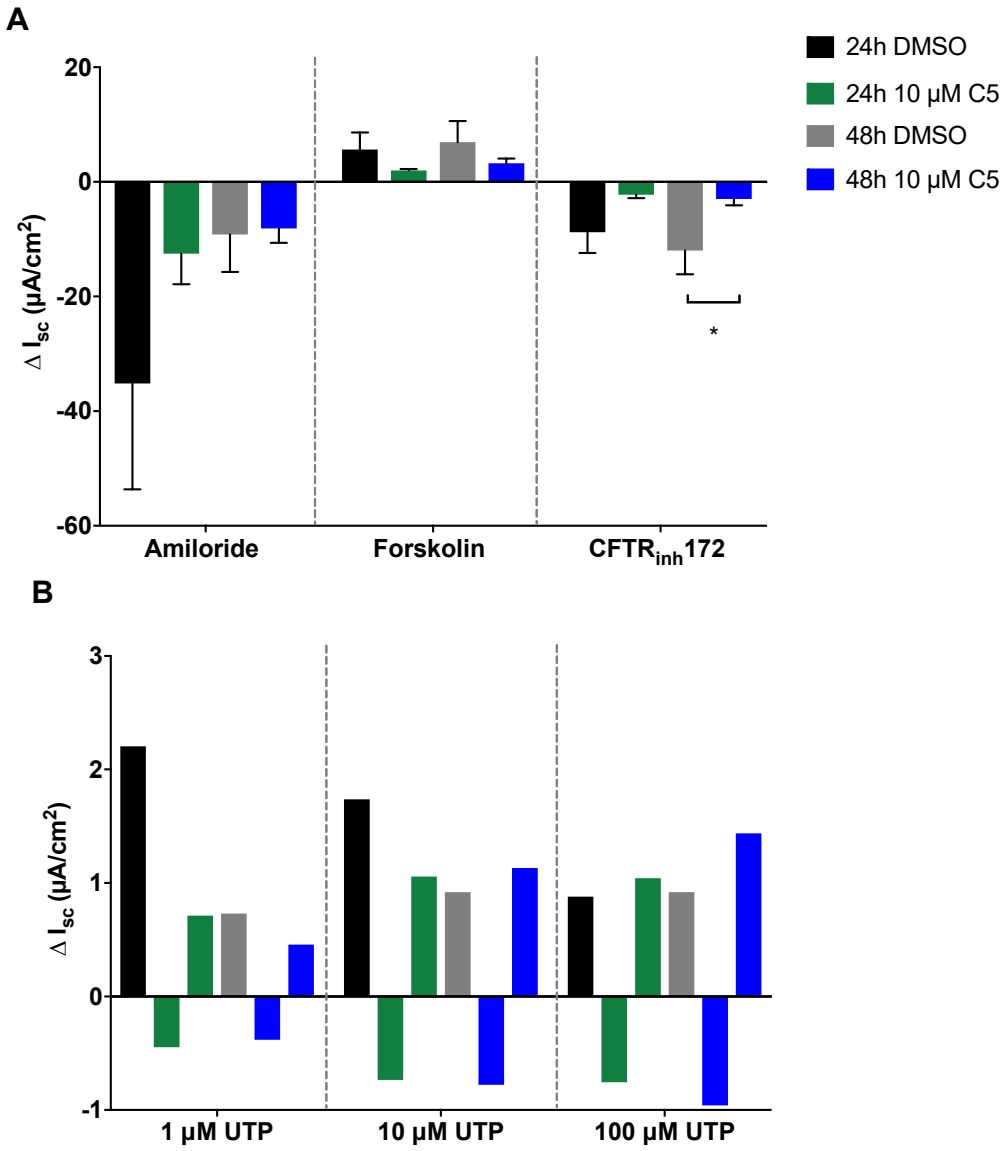

Figure 126: Effects of chronic C5 treatment on the short circuit current responses in PNEC cultures derived from the non-CF PWT16 donor

Changes in short circuit current response (ΔI_{sc}) to amiloride, forskolin and $CFTR_{inh}$-172 for 24h DMSO (black), 24h 10 µM C5 (green), 48h DMSO (grey) and 48h 10 µM C5 (blue) treatment in PNEC cultures derived from the non-CF PWT16 donor are shown in A. Bars represent mean ± SD. Data analysed with Kruskal Wallis and Dunn's multiple comparisons tests; p=0.04 for $CFTR_{inh}$-172 at 48h; n=3 culture inserts for each control and C5 condition. Resultant ΔI_{sc} for varying UTP concentrations after chronic C5 treatment are shown in B; n=1 culture insert for each control and C5 condition.

6.4.5 Effects of IL-4 treatment on C5 response in paediatric primary nasal epithelial cultures derived from CF donors

The effects of acute C5 treatment (10 μM) were assessed in cultures derived from 3 CF donors, PCF25 (F508del/ F508del), PCF26 (F508del/G542X) and PCF28 (F508del/F508del), all of which did not show any changes in C5-induced $I_{sc.}$ In view of the described effects of IL-4 treatment on the UTP and Eact-induced I_{sc}, PCF28 PNEC cultures were treated with IL-4 to investigate the effects of acute C5 treatment. PNEC cultures were treated with vehicle control or IL-4 (10ng) for 24 hours before assessing I_{sc} responses to either 1 μM UTP, 10 μM C5 or the combination of 10 μM C5 5 minutes prior to 1 μM UTP apical addition. Amiloride, forskolin and $CFTR_{inh}$-172 were added prior to these reagents as previously described and experiments were performed using 125 mM chloride Krebs solutions in both Ussing chamber compartments. Each experiment was performed using 2 PNEC culture inserts and the resultant I_{sc} traces together with the calculated peak and total I_{sc} are shown in Figure 127 and Figure 128 respectively. Statistical analyses were not performed due to the limited number of culture inserts.

In all circumstances, IL-4 treatment increased the peak I_{sc} response (1 μM UTP 3.1 $\mu A/cm^2 \pm$ SD 1.5 versus 10.0 $\mu A/cm^2 \pm$ SD 7.6; 10 μM C5: 0.2 $\mu A/cm^2 \pm 0.3$ versus 1.5 $\mu A/cm^2 \pm 0.3$; 1 μM UTP plus 10 μM C5: 3.6 $\mu A/cm^2 \pm$ SD 1.5 versus IL-4: 19.6 $\mu A/cm^2 \pm$ SD 7.6). IL-4 treatment did not increase the total I_{sc} response for 1 μM UTP alone (21.8 $\mu A/cm^2.min \pm$ SD 11.6 versus 23.4 $\mu A/cm^2.min \pm 8.0$). However, an increase was suggested for 10 μM C5 (17.1 $\mu A/cm^2.min \pm 13.2$ versus 30.0 $\mu A/cm^2.min \pm 7.6$) and the combination of 1 μM UTP plus 10 μM C5 (43.2 $\mu A/cm^2.min \pm 20.1$ versus 96.9 $\mu A/cm^2.min \pm 11.6$).

These findings suggest that unlike the responses in PWT16 cultures, the C5/UTP combination in PCF28 PNECs did not augment the peak UTP-induced I_{sc} response. However, the total UTP-induced response as assessed by AUC was increased by 2-fold with C5/UTP, and this was further augmented by 4-fold in IL-4 treated cultures.

Response to C5 alone was minimal (unlike mean response in PWT16 of 2.7 $\mu A/cm^2$, as reported above), however, it was increased by 7.5-fold with IL-4 treatment. This finding complements the previously described increase in TMEM16A immunofluorescence in PCF28 PNECs (Chapter 5 section 5.4.14). Of the 7 donors where C5 response was assessed with I_{sc} in conjunction with TMEM16A

immunofluorescence, the 2 non-CF C5-responders demonstrated the greatest degree of TMEM16A immunofluorescent expression and the 5 non-responders showed lower levels (Figure 129). These findings, together with investigation of TMEM16A *mRNA* expression (Chapter 5 section 5.4.14), suggests that C5 may be implicated in TMEM16A activation.

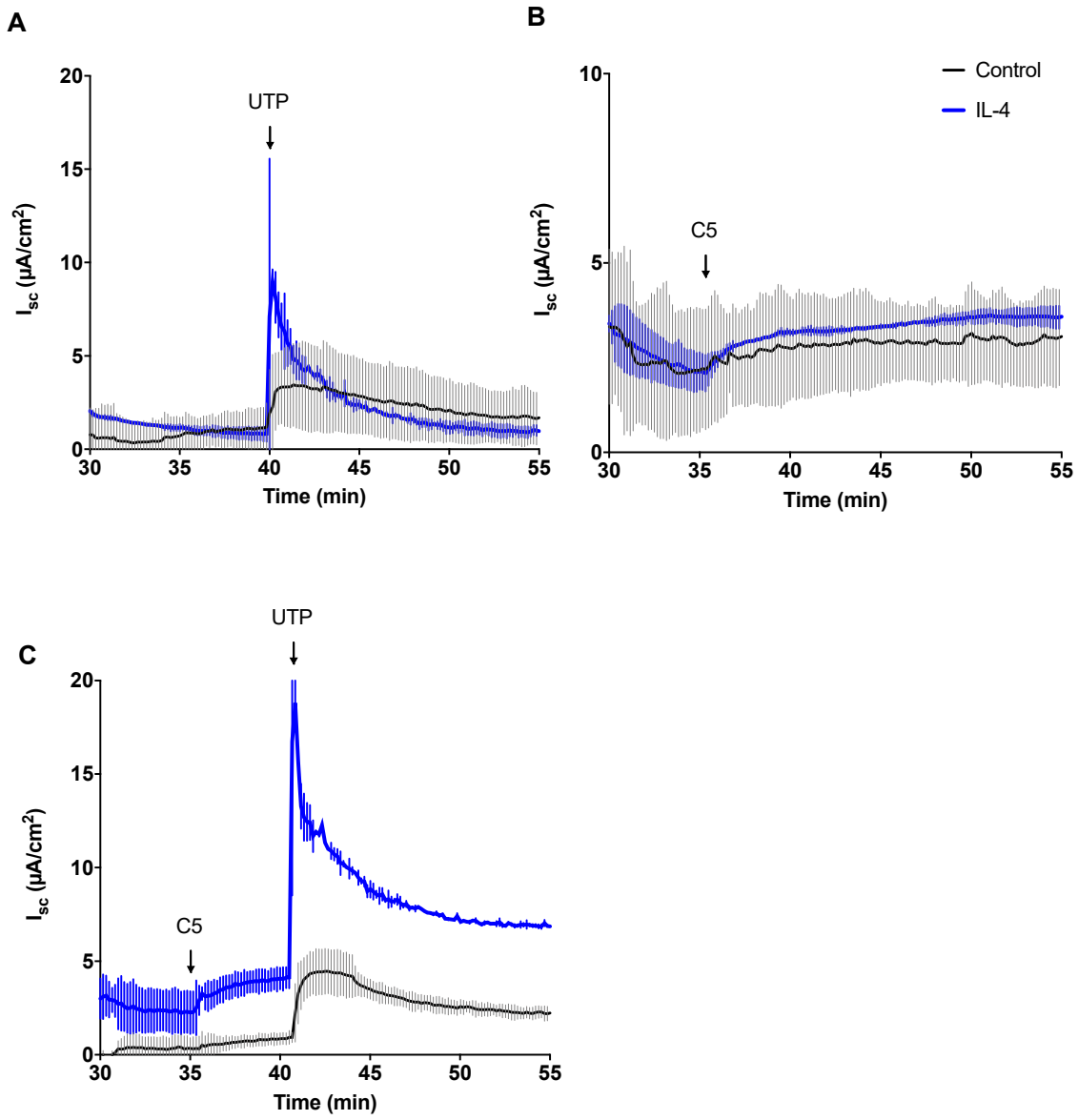

Figure 127: Effects of IL-4 treatment on short circuit current responses to C5 and UTP in PNECs derived from the CF PCF28 donor

Representative short circuit current (I_{sc}) responses to the addition of 1 μM UTP (A), 10 μM C5 (B) and 1 μM UTP/10 μM C5 together (C) in control (black line) and IL-4 (blue) treated PNECs derived from the CF PCF28 donor (F508del/F508del). Lines represent mean ± SD; n=2 culture inserts for each condition.

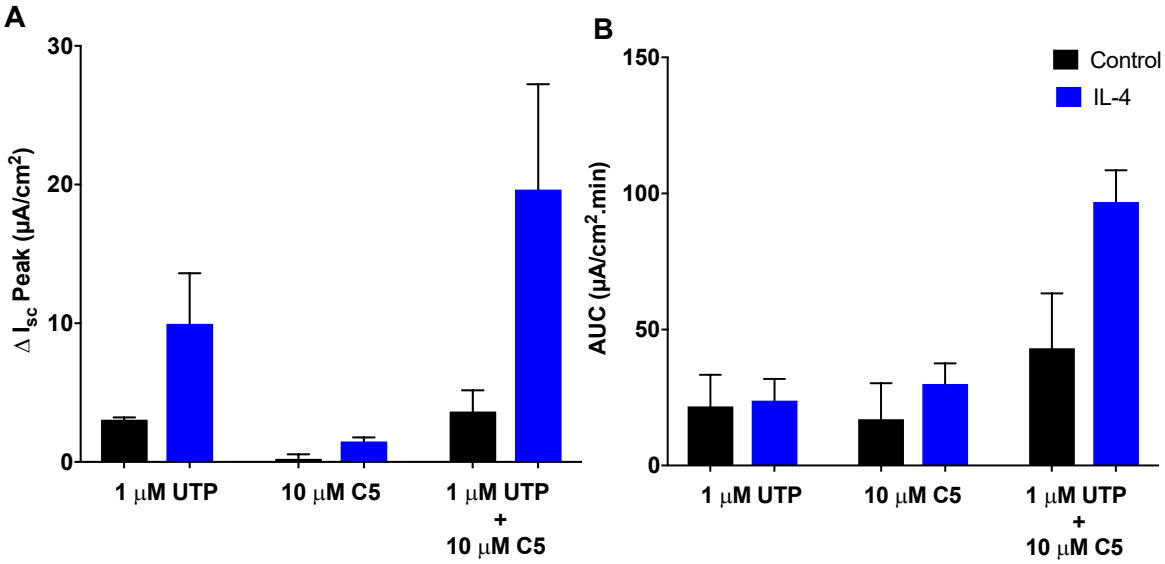

Figure 128: Effects of IL-4 treatment on the peak and total short circuit current responses to C5 and UTP in PNECs derived from the CF PCF28 donor

The effects of IL-4 treatment on the peak-induced short circuit current (ΔI_{sc}) and area under the curve (AUC) are for the addition of 1 μM UTP, 10 μM C5 and 1 μM UTP/10 μM C5 together are shown in A and B respectively for control (black) and IL-4 treated (blue) PNEC cultures derived from the CF PCF28 donor (F508del/F508del). Bars represent mean ± SD; n=2 culture inserts for each condition (statistical analysis not performed).

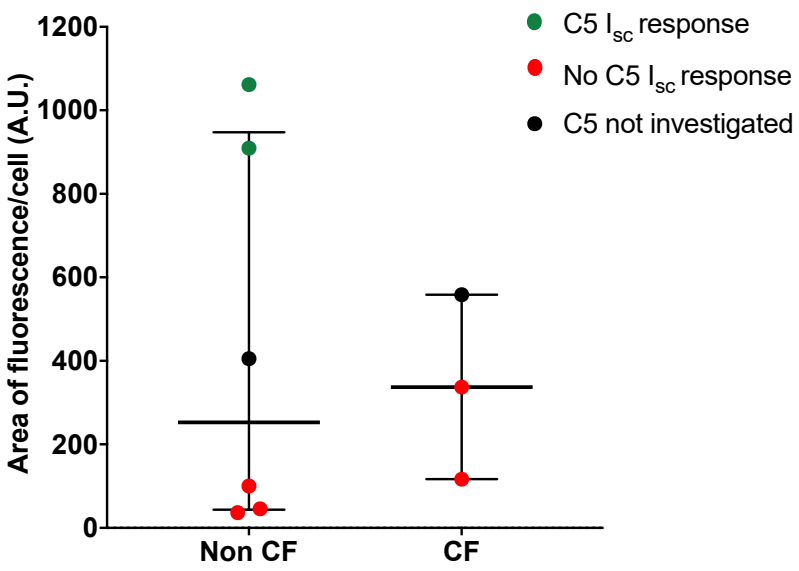

Figure 129: TMEM16A immunofluorescent detection in relation to C5-induced short circuit current response

Detection of TMEM16A by immunofluorescence and confocal microscopy was performed in differentiated non-CF and CF PNEC cultures as previously described. The area of fluorescence/cell was determined to quantify TMEM16A presence. Each point represents a different donor and bars represent median ±IQR. Data analysed with Mann-Whitney test with no statistical differences found; A: n=6 non-CF donors, n=3 CF donors. Corresponding short circuit current (I_{sc}) responses are colour coded according to responders (green) and non-responders (red) to C5 addition in Ussing chamber experiments. Black points indicate circumstances where the effect of C5 on I_{sc} was not assessed.

6.4.6 Effects of C5 treatment on intracellular calcium concentration in submerged nasal epithelial cultures

In contrast to the characteristic transient UTP-induced I_{sc} response, the above findings in differentiated PNEC ALI cultures with C5 addition could suggest either a sustained increase in intracellular calcium or a calcium-independent mode of action for C5-induced chloride secretion. To investigate this further, the effects of C5 on intracellular calcium concentration were assessed. This experimental work was performed by JinHeng Lin (PhD student, Dr Mike Gray) and assessed in submerged PNEC cultures derived from a non-CF (PWT19) and CF (PCF28) donor. Methods used were as previously described in Chapter 2, section 2.6, whereby cells were loaded with the ratiometric Fura-2 dye, and the changes in the ratio of 340:380 nm emission were proportional to changes in intracellular calcium ($[Ca^{2+}]_I$). Unfortunately, there was no corresponding Ussing chamber data for PWT19, however C5-induced I_{sc} responses for PCF28 have already been described.

C5 was first assessed after UTP addition, and this procedure was reversed to determine any potential relationship between the 2 reagents. In all cases, the peak 340:380 ratios, rate of increase and rate of recovery for PWT19 (Figure 130 and Figure 131) and PCF28 (Figure 132 and Figure 133) were calculated. Overall, C5 addition in PNECs derived from both PWT19 and PCF28 donors showed minimal increases in the $[Ca^{2+}]_I$ when applied before (PWT19: 348/380: 0.01 ± SD 0.008; PCF28N: 0.006 ± SD 0.0008) and after UTP (PWT19: 348/380: 0.01 ± SD 0.008; PCF28N: 0.004 ± SD 0.002).

Initial UTP application increased $[Ca^{2+}]_I$ to similar extents in cultures derived from both donors (PWT19N: 0.05 ±SD 0.02; PCF28N: 0.05 ± SD 0.01). In all cultures, C5 addition *after* UTP showed minimal changes in $[Ca^{2+}]_I$, (PWT19: 0.01 ± SD 0.008; PCF28N: 0.006 ±SD 0.0008). A second addition of UTP was also tested after C5 in PCF28N cultures to determine any potential effects of C5 on the subsequent UTP-induced $[Ca^{2+}]_I$, however, no differences were found (0.06 ± SD 0.03; $p>0.99$). This investigation of a second application of UTP was likely possible due to assessment of $[Ca^{2+}]_I$ using a perfused system (in contrast to the non-perfused Ussing chamber used in this PhD), which allowed recovery from P2Y2 receptor desensitisation.

C5 application prior to UTP did not affect this UTP-induced peak $[Ca^{2+}]_I$ compared to responses where UTP was applied first (PWT19N: 0.09 ± SD 0.02, $p>0.99$; PCF28N: 0.07 ± SD 0.04, $p>0.99$). Furthermore, C5 addition pre-UTP did not affect the

subsequent UTP-induced increase in $[Ca^{2+}]_I$ and rate of recovery compared to the initial application of UTP in PWT19 PNECs (rate: p>0.99; recovery: p=0.2). Although there was a suggestion that C5 affected the rate of UTP-induced $[Ca^{2+}]_I$ increase in PCF28 PNECs, the recovery was unchanged and findings were not significant (rate: p=0.4; recovery: p>0.99).

An additional observation from this work was the relatively larger ionomycin-induced increase in 340:380 ratio versus the UTP response in CF cultures (Figure 132) compared with non-CF cultures (Figure 130), suggesting a larger UTP-induced $[Ca^{2+}]_I$ increase in non-CF cultures, however, this would require further investigation in a larger cohort of cultures.

Overall, these findings suggested that C5 addition did not affect $[Ca^{2+}]_I$, and application after UTP did not modify the resultant changes in $[Ca^{2+}]_I$ kinetics. However, this was performed only in a limited number of culture inserts and although has provided some preliminary data, requires further investigation in a larger cohort of cultures.

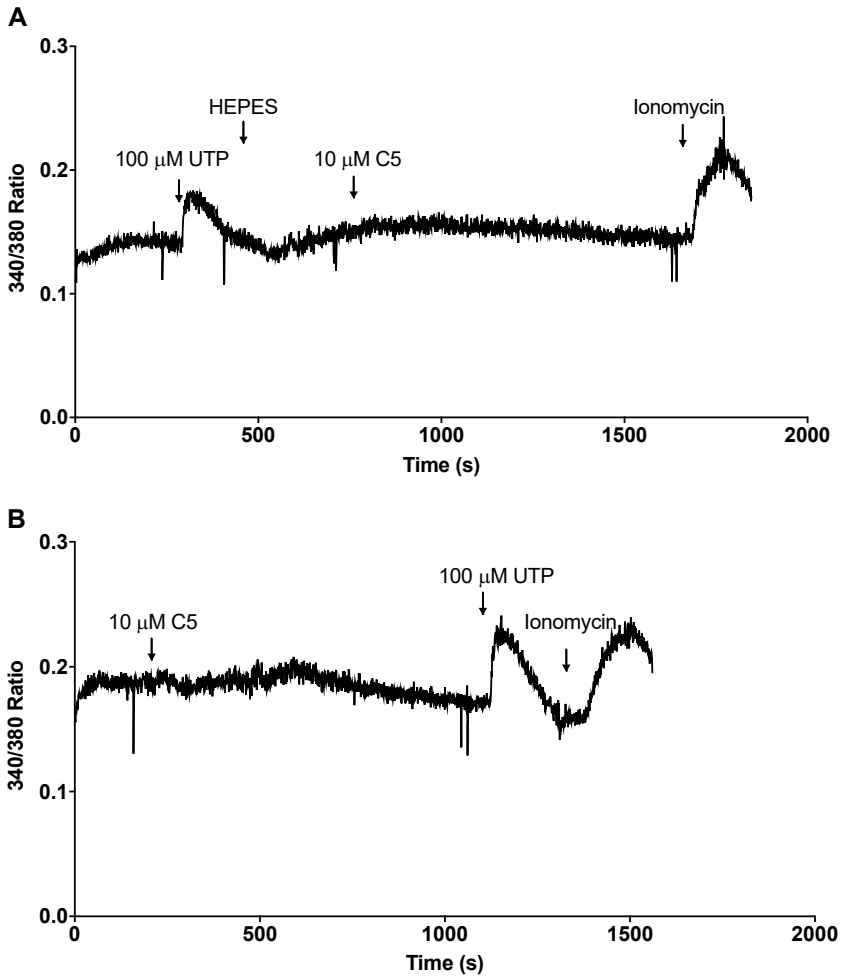

Figure 130: Effect of C5 and UTP addition on intracellular calcium in PNEC cultures derived from the non-CF PWT19 donor

Submerged PNEC cells derived from the non-CF PWT19 donor were grown to confluence and incubated with Fura-2 AM for 1 hour. After dye removal, cells were incubated with HEPES buffered solution at room temperature and mounted on a Nikon Fluor oil immersion microscope. Cells were alternately excited at 340 nm and 380 nm for 0.25 s continuously. Changes in the 340:380nm emission were proportional to changes in intracellular calcium concentration. The effects of initial UTP addition, followed by C5 (A) compared with the initial application of C5 followed by UTP (B) were investigated. The calcium ionophore, ionomycin, was used as a positive control.

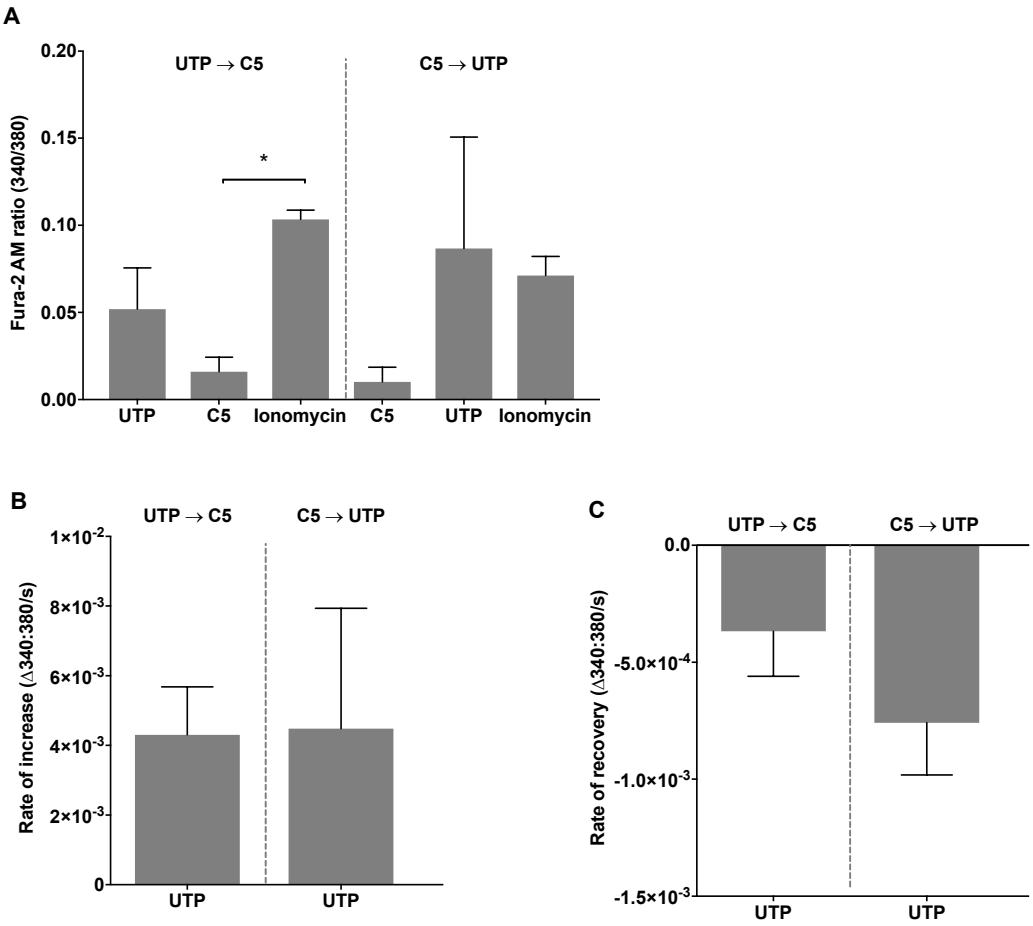

Figure 131: Kinetics of intracellular calcium changes induced by C5 and UTP in PNECs derived from the non-CF PWT19 donor

The Fura-2 340nm/380nm was used to calculate the peak increase in intracellular calcium concentration ($[Ca^{2+}]_{I,}$) where UTP was added prior to C5, and with the reverse protocol of C5 addition before UTP (A). Rate of UTP-induced $[Ca^{2+}]_{I,}$ increase (B) and rate of recovery of the UTP response (C) were calculated for each protocol.

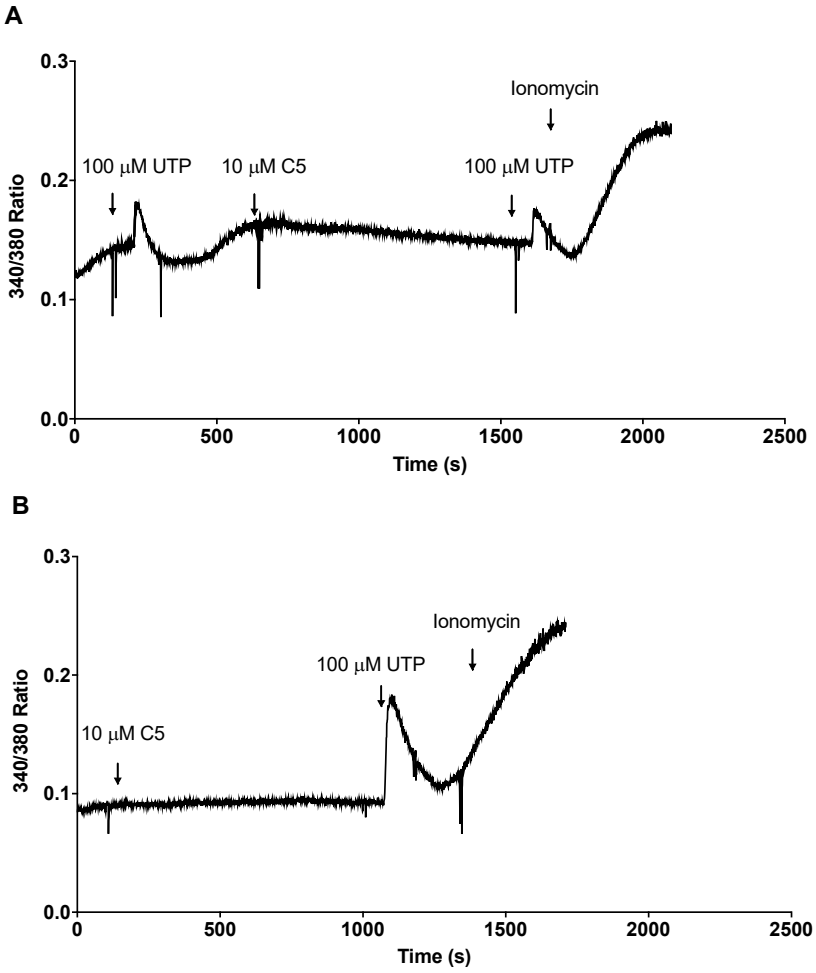

Figure 132: Effect of C5 and UTP on intracellular calcium in PNEC cultures derived from the CF PCF28 donor

Submerged PNEC cells derived from the CF PCF28 donor (F508del/F508del) were grown to confluence and incubated with Fura-2 AM for 1 hour. After dye removal, cells were incubated with HEPES buffered solution at room temperature and mounted on a Nikon Fluor oil immersion microscope. Cells were alternately excited at 340 nm and 380 nm for 0.25s continuously. Changes in the 340:380nm emission were proportional to changes in intracellular calcium concentration. The effects of initial UTP addition, followed by C5 and UTP (A) compared with the initial application of C5 followed by UTP (B) were investigated. The calcium ionophore, ionomycin, was used as a positive control.

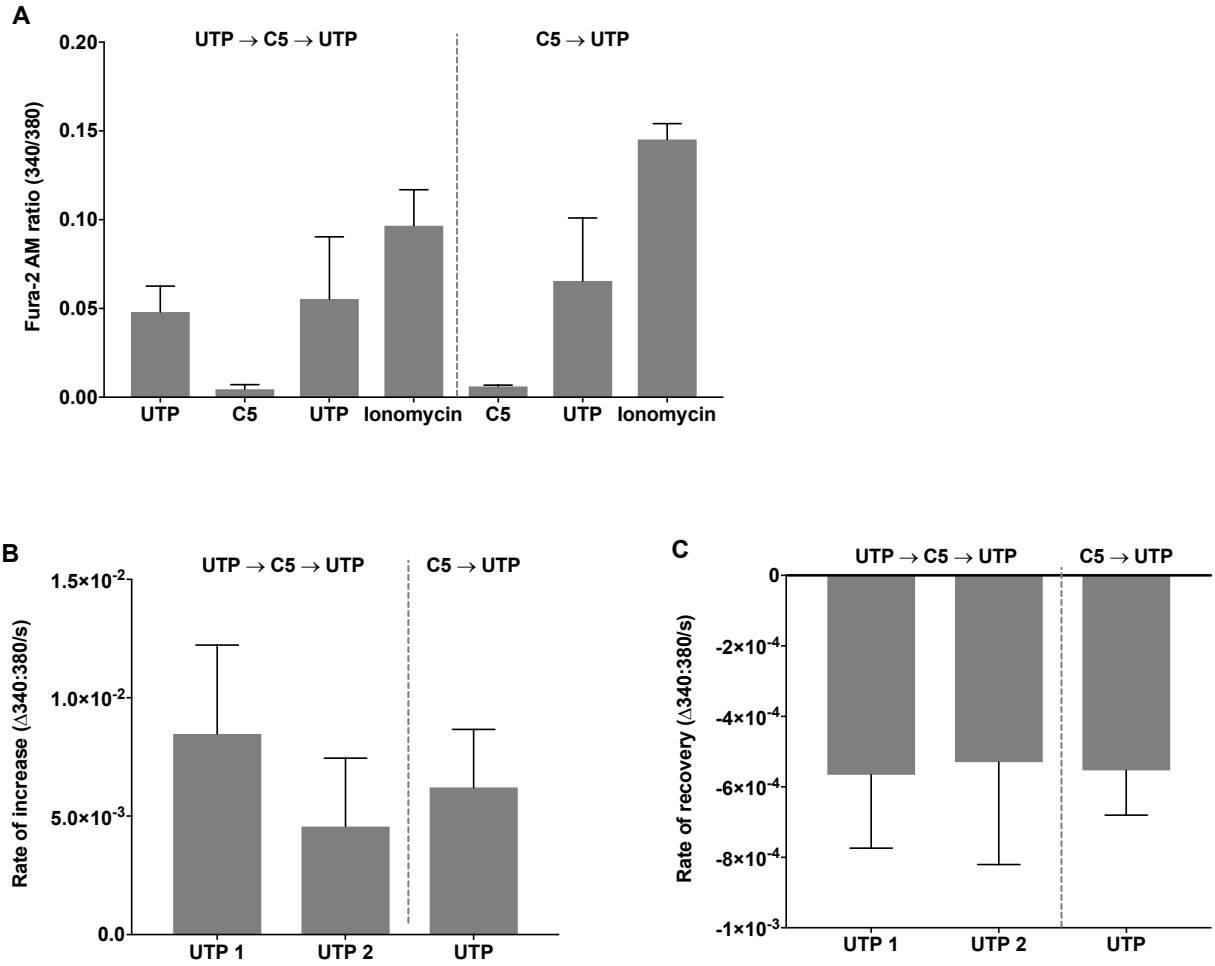

Figure 133: Kinetics of intracellular calcium changes induced by C5 and UTP from PNEC cultures derived from the CF PCF28 donor

The Fura-2 340nm/380nm was used to calculate the peak increase in intracellular calcium concentration ($[Ca^{2+}]_{I,}$) where UTP was added prior to C5 and UTP, and with the reverse protocol of C5 addition to UTP (A). Rate of UTP-induced $[Ca^{2+}]_{I,}$ increase (B) and rate of recovery of the UTP response (C) were calculated for each protocol.

6.5 Discussion

The results from the experimental work detailed in this chapter has demonstrated the feasibility of investigating the effects of the novel compound C5 on TMEM16A activity in differentiated paediatric PNEC ALI cultures. Importantly, although this compound has been previously assessed using alternative cell lines, this is the first study in airway epithelial cultures derived from humans. In summary, it has been possible to use Ussing chamber experiments to demonstrate that in a small number of non-CF PNEC cultures, addition of C5 alone demonstrated small, but more sustained, increases in I_{sc} response relative to UTP. Furthermore, it was possible to augment the UTP response by C5 pre-treatment, with enhanced peak and total I_{sc} changes that were suggestive of increased TMEM16A-mediated chloride secretion. In contrast, assessment of chronic treatment with C5 in these cultures was not consistent with TMEM16A activation, and in fact off target effects included inhibition of ENaC, CFTR and alteration of the UTP-induced response.

Importantly, a combination of 4 non-CF PNECs, 3 non-CF PBECs, 1 CF PNEC and 1 CF PBEC were investigated, of which responses were evident in only 2 non-CF PNECs. This is potentially explained by the relatively low levels of TMEM16A that are expressed, as evident by both RT-qPCR and immunofluorescence work. It was possible to generate a C5-induced I_{sc} after IL-4 treatment, and this could be a useful assessment tool for future work involving more detailed characterisation of this and similar compounds.

Although C5 application either with, or before UTP increased the I_{sc} response in the PWT16 cultures, further investigation did not show any changes in $[Ca^{2+}]_I$ secondary to C5 addition. Therefore the effect of C5 appeared to be independent of an increase in cytosolic calcium. However, it should be highlighted that the $[Ca^{2+}]_I$ experiments were performed in cultures derived from a different donor, PWT19. Submerged cultures required for $[Ca^{2+}]_I$ assessment were prepared at the start of the culture process and corresponding ALI cultures were not successful. It would have been highly valuable to follow through a comprehensive analysis involving assessment of I_{sc}, RT-qPCR, immunofluorescence and measurement of $[Ca^{2+}]_I$ in cultures obtained from each individual donor, however, this was not possible. A limitation of this technique used to assess $[Ca^{2+}]_I$ was use of undifferentiated submerged cultures, in contrast to the differentiated ALI cultures used in Ussing chamber experiments. However, this method was accessible at the time of performing this PhD, and

alternative methods to explore the effects of C5 on $[Ca^{2+}]_I$ in ALI cultures would be required in the future.

In view of the sustained nature of the C5 response, together with the lack of any substantial increase in $[Ca^{2+}]_I$, the augmented UTP-induced I_{sc} with C5 could have occurred secondary to calcium-independent chloride secretory mechanisms. Although UTP can be used as a purinergic agonist for CaCC activation in Ussing chamber experiments, previous investigation in primary bronchial cells has shown that UTP can induce CFTR-dependent chloride secretion via cAMP signalling (Namkung et al., 2010a). It is possible that C5 mediated a similar and more sustained I_{sc} increase, that was secondary to calcium-independent cAMP-mediated chloride secretion. This theory could be further supported by the limited C5 response in non-CF cultures only. However, all experiments were performed after inhibition of CFTR with $CFTR_{inh}$-172, suggesting that any cAMP-mediated chloride secretion was via alternative 'non-CFTR' channels and transporters. It was not possible to investigate this within the timeframe of this PhD, however, further clarification of the effects of C5 on the UTP-induced I_{sc} could be investigated by comparing the application of $CFTR_{inh}$-172 versus $CaCC_{inh}$-A01 or Ani9 to determine the relative contribution of CFTR and CaCC to the induced response. Furthermore, specific inhibitors of cAMP/PKA signalling such as H89, and assessment of intracellular calcium reduction (e.g. with BAPTA-AM) could be used to ascertain the underlying mechanisms involved and determine potential contributions of 'non-CFTR' channels.

6.6 Conclusion

Treatment of paediatric differentiated primary airway epithelial cultures with C5 has shown some evidence of changes in I_{sc} that suggest TMEM16A activation. This preliminary investigation of C5 response in primary cultures has potential to help direct future work including investigation in a wider range of cultures and assessment of other related compounds. Furthermore, this compound is the first of its generation, and assessment in human *in vitro* models will help to guide subsequent development of next generation compounds that may be of benefit in improving the ion transport defects that exist in CF.

Importantly the work carried out in this chapter has demonstrated the suitability of using paediatric PNEC cultures to investigate novel small molecule therapeutic targets.

7 Discussion

7.1 Introduction

This final discussion will summarise the key results described in this thesis together with the key strengths and limitations to complement previous discussions from each chapter. Finally, the chapter will conclude with considerations for future investigations that are needed to confirm and investigate the work detailed in this thesis.

7.2 Development of differentiated primary nasal and bronchial epithelial cell cultures from children with and without CF

The value of utilising patient-derived primary airway epithelial cultures for CF research has been validated through their recent role in the development of novel CFTR modulator therapies (Van Goor et al., 2009b). They have helped to provide a more accessible tool for research than animal models and have overcome the problems of karyotype instability associated with alternative immortalised cellular models. CF research in children remains important, namely in view of the recognised early onset of bronchiectasis which is progressive and life-limiting (Adam et al., 2013, Khan et al., 1995b, Sly et al., 2013). To facilitate the development of robust paediatric research models it is highly important that methods used to acquire research samples are minimally invasive and well tolerated. The suitability of PNECs as a surrogate for PBECs remains a long-standing yet pertinent question. Clearly if PNECs are found to be a representative research tool, they are well placed to facilitate paediatric research given the relative ease of nasal brushing sampling. However, the suitability of their role in CF remains in question, as highlighted by a recent review in the Journal of CF (Clancy et al., 2018).

A key aim of this PhD was to establish the relevance of paediatric-derived PNECs as a suitable model for CF research and validate their role as a drug discovery tool. The initial focus of work was to design the research study protocol and drive the ethical approval processes required to enable the research to take place in the Great North Children's Hospital and Newcastle University. As a paediatric speciality trainee, I was well placed to acknowledge the importance of designing a protocol that enabled the acquisition of nasal and bronchial brushings, whilst ensuring minimal distress to the research participants involved. Having previously worked closely with the CF clinical team and patients, I was able to obtain their valuable insight into research design and establishment within the hospital environment. Collecting both nasal and

bronchial brushings at the time of clinical bronchoscopy under general anaesthetic ensured that research procedures were minimally invasive.

However, the decision to sample brushings during a clinically indicated bronchoscopy limited the phenotype of the non-CF group to children who were being investigated for recurrent respiratory infections, persistent bacterial bronchitis, persistent wheeze and chronic cough. Although these children were comparatively healthier than those with CF, research findings related to BAL, cell culture inflammatory environment as assessed by cytokine levels should be interpreted with some caution.

ALI cultures derived from nasal and bronchial brushings demonstrated typical epithelial characteristics and features of muco-ciliary differentiation as assessed by morphology, TEER, epithelial marker detection by immunofluorescence and RT-qPCR and analysis of cytokine production. Despite the maintenance of consistent culture conditions differences in TEER measurements were found between PNECs and PBECs, with highest values evident in CF PNECs. The exact cause for this was unclear, but there have been comparable TEER values reported in the literature together with reductions in TEER after the application of a mucolytic to the culture surface (Sajjan et al., 2004). Furthermore, both intra and inter-donor variation of TEER measurement is a recognised finding (Tosoni et al., 2016).

Elevated mRNA expression of *Foxj1* mRNA in CF PBECs was an unanticipated finding. This was attributed to its role in promoting cilial differentiation and therefore a reflection of the role of cilia for MCT in lower airways. Furthermore, given the association of *Foxj1* with cilial motility and increasing levels of expression evident at later stages of ALI, reduced levels of expression in PNECs could be accounted for by their later onset of ciliagenesis (Jain et al., 2010).

Although the technique of growing adult PBECs from explanted lung tissue and bronchoscopic brushings was well established at the time of starting this PhD, paediatric cultures had not previously been developed. Considerable optimisation of techniques was therefore required, from sampling nasal and bronchial airways through to the ALI culture process, which accounted for the initial poor success rates. Infection rates significantly reduced and techniques for sampling and culture improved, but cultures did fail during the ALI process with no clear cause despite monitoring and assessment of controllable conditions. This highlights a key challenge associated with this model, however, culture success rates did improve during the course of the PhD. Importantly it was possible to develop paediatric PNEC and

PBEC culture models to investigate the aims of this PhD research and provide a valuable resource for future paediatric CF research in Newcastle.

7.3 Functional characterisation of ion transport profiles

At the time of starting this PhD, no published information was available relating to the ion transport profiles of paediatric ALI cultures including no direct comparisons of PNEC and PBEC cultures. In view of the major contributions of CFTR and ENaC to the maintenance of ASL hydration and composition, it was decided to compare the functional expression of these channels in the established PNEC and PBEC ALI cultures using Ussing chamber experiments.

This present work did not find any significant differences between the functional expression of ENaC in non-CF versus CF cultures in both PNECs and PBECs. RT-qPCR assessment of *ENaC* subunit expression showed α-*ENaC* to be the predominant subunit, which is unsurprising given the ability of this subunit to produce amiloride-sensitive I_{sc} changes without the other subunits. All three subunits had lower levels of expression in non-CF versus CF PBECs and overall expression was lower in PNECs. Overall there was considerable variability in all three subunits between different donors.

As described in detail in the discussion of Chapter 3, the lack of differences in I_{sc} responses found in this PhD contradicts the previously reported concept of sodium hyperabsorption in the CF airway (Knowles et al., 1983, Boucher et al., 1988, Mall et al., 1998). This could be explained by the young median age of the CF participants, relatively mild degree of lung disease and variations in experimental techniques used with these previously reported studies. However, the impact of CF and dysfunctional CFTR on ENaC remains under debate, with conflicting results in other studies (Itani et al., 2011). Evidently the investigation of ENaC functional expression is complex with additional factors including SNPs, variations in plasma membrane ENaC channel activity, experimental variations and culture conditions that likely to contribute to the changes in channel function and expression (Azad et al., 2009, Caldwell et al., 2005).

No significant differences were found with CFTR functional expression between PNECs and PBECs. Interestingly, the shape of the Ussing chamber I_{sc} response was different. This could have arisen from differences in the basolateral NaK2Cl cotransporter activity, therefore limiting apical CFTR-mediated chloride secretion (Li

et al., 2004). The experimental protocol used in Ussing chamber experiments to assess CFTR activation and inhibition could have included more detailed characterisation of CFTR-mediated apical chloride secretion. Pharmacological permeabilisation of the basolateral membrane with an ionophore would have eliminated the effects of basolateral channels involved in generating a chloride gradient, enabling more specific exploration of CFTR-mediated chloride secretion (Li et al., 2004). However, a key consideration in the experimental design was a protocol that enabled the investigation of ENaC, CFTR and CaCC in the same culture insert, whilst minimising the duration of time spent in the Ussing chamber. Addition of an ionophore would have increased this time, and potentially impacted on the assessment of alternative channels. Nevertheless, this is an important consideration for experiments that require detailed characterisation of CFTR.

The main experimental technique used in this PhD involved assessment of I_{sc} as a measure of net ion transport utilising Ussing chamber experiments. A non-perfused system was used, whereby all reagents remained in the chambers for the duration of the experiment. Although the system was continuously gassed, residual reagents may have impacted on subsequent channel responses. Perfused systems are commercially available but were not accessible for this PhD.

Alternative techniques are available to measure epithelial ion transport. For example, the patch clamp technique can be used to electrically isolate a small patch of membrane using a glass micropipette tip to measure single or multiple channel events (Moran and Zegarra-Moran, 2008). This method can help to overcome the variations in channel distribution and expression that are increasingly recognised to be present in epithelial monolayers and provides detailed characterisation of ion channels (Caldwell et al., 2005, Caputo et al., 2008). However, this technique is recognised to be technically challenging in primary epithelial cultures and was not used in this PhD. Alternative assessment of CFTR can be achieved via flux assays, for example the iodide flux assay that utilised CFTR's property of iodide permeability, with the addition of radiolabelled or fluorescent probes or fluorescently tagged cells (Moran and Zegarra-Moran, 2008). However, these techniques are generally reserved for high throughput screening assessment.

Ussing chamber assessment of I_{sc} is a widely adopted tool for the investigation of channel-mediated ion transport in CF research. It was deemed appropriate for application in this PhD in view of existing expertise within the lab environment and its

suitability for application with primary airway epithelial cultures. Importantly, this work demonstrated the feasibility of using paediatric PNECs for Ussing chamber experiments.

7.4 Investigating the expression and function of TMEM16A

Overall assessment of CaCC functional expression in differentiated paediatric cultures did not show any differences between PNEC and PBEC cultures in the non-CF group. Furthermore, no differences were found between non-CF and CF PNECs. CF PBECs demonstrated features of BK channel activation. Unfortunately, it was not possible to include these cultures in the CaCC and TMEM16A analyses and this was a significant limitation of this work performed.

The lack of reliable activators and inhibitors of TMEM16A limited the ability to perform detailed characterisation of TMEM16A-mediated ion transport using Ussing chamber experiments. Despite these challenges, it was possible to provide some evidence of Eact-induced increases in chloride secretion in addition to TMEM16A inhibition with the small molecules $CaCC_{inh}$-A01 and Ani9. These molecules did not completely eliminate the UTP-induced I_{sc}, and this does require further investigation as previously discussed.

Alternative methods were employed to assess the functional expression of TMEM16A including immunofluorescence and RT-qPCR. Both of these techniques revealed low levels of TMEM16A expression under basal conditions, which is consistent with the literature (Scudieri et al., 2012a, Gorrieri et al., 2016). This was an obstacle to detection of TMEM16A by immunofluorescence and the current protocol used in this PhD was developed after considerable optimisation. It was possible to upregulate TMEM16A expression with IL-4 and this was used as a tool to facilitate more detailed characterisation and verify expression in the paediatric airway. This was consistent with the literature relating to PBECs isolated from explanted CF lungs, thereby further validating the role of paediatric PNECs for this area of research (Scudieri et al., 2012b, Gorrieri et al., 2016).

Suggested UTP-induced BK channels activation in CF PBECs was an unanticipated finding. Although noted in one of each non-CF PBEC and PNEC culture type, this finding was relatively specific for CF PBECs. Of note, PBEC cultures derived from the CF participant with the less severe R751L/F508del mutation demonstrated a UTP-induced I_{sc} response characteristic of CaCC activation. It was possible to

investigate the hypotheses related to BK channel activation by inhibiting channels and reducing intracellular calcium levels. However, this analysis was significantly limited by the number of culture inserts available for comprehensive investigation and was predominantly descriptive.

Investigation of TMEM16A functional expression in paediatric PNEC ALI cultures has not previously been performed and this work has provided preliminary data which will help guide and facilitate future directions of work.

7.5 Investigation of TMEM16A activation with the novel C5 activating compound

The activity of a novel TMEM16A activator, C5, was investigated in the differentiated PNEC and PBEC ALI cultures using Ussing chamber experiments. A sustained C5-induced I_{sc} response was evident in PNEC cultures derived from 2 non-CF donors. This suggested C5-mediated chloride secretion with additional augmentation of the UTP-induced I_{sc}. Cultures did not respond to chronic C5 treatment, with a reduction in both ENaC and CFTR functional expression. The effects of C5 were calcium independent, suggesting either a similar mechanism of action to that proposed for Eact with direct binding to TMEM16A's calcium binding site or alternative activation of non-CaCC channels. Assessment of C5 was not possible in CF PBECs due to the difficulties mentioned previously.

This investigation of C5 was very preliminary and novel, performed for the first time in primary airway epithelial cultures. Further investigation was not possible due to time constraints, however, the work carried out in this PhD has provided some useful information to help guide future experiments and assessment of additional C compounds. Furthermore, it has validated the role of paediatric PNEC cultures developed in this PhD for their suitability in investigating responses to novel therapeutic targets.

7.6 Reflection: the application of differentiated paediatric primary nasal and bronchial epithelial cultures as an experimental model

The aims of this PhD were to establish paediatric PNEC and PBEC cultures isolated from non-CF and CF donors and utilise these to characterise epithelial and ion transport properties. This was with the objective of investigating the role of TMEM16A in the paediatric airway and responses to novel small molecule TMEM16A activators. The strategy employed in this PhD was to recruit multiple non-CF and CF

participants, with the objective of using the described experimental techniques to characterise cultures. The final numbers available for these analyses were limited by culture success rates and comprehensive analysis was limited by the number of culture inserts available. This was improved to some extent by moving from 6-well to 12-well plates and was facilitated by the upgrade of an Ussing chamber system in 2017 that was compatible for use with these smaller culture inserts.

There are recognised techniques for cell culture expansion, including the use of fibroblastic feeders or Rho-associated protein kinase (ROCK) inhibitors (Horani et al., 2013, Martinovich et al., 2017). In hindsight, the research focus at the start of my PhD could have been to optimise these expansion methods after establishing the paediatric culture models. This would have facilitated more detailed analyses of the key findings (e.g. variations in ENaC expression, BK channel characterisation, C5 compound investigation). However, this would have involved a huge body of work, particularly in view of my limited cell culture experience at the start of this PhD. In view of the time required for cell culture in addition to the experimental work, these investigations would have only been possible in a cultures derived from a small number of donors.

Detailed assessment of TMEM16A function has been performed by other research groups using cell lines and siRNA to overexpress TMEM16A and this approach could have been adopted for this PhD (Scudieri et al., 2012a). Preliminary work was performed at the start of this PhD with the bronchial epithelial CFBE41δ^- cell line, however, these did not produce reliable results in Ussing chamber experiments. Patient-derived primary cultures are recognised to be more representative of the *in vivo* airway environment and it was important to establish if TMEM16A was present in the paediatric airway. Furthermore, the degree of intra-donor variability evident with ENaC and CFTR functional expression in primary cultures would have not have been appreciated.

This thesis has demonstrated that ion channel functional in airway epithelial ALI cultures is complex. However, the work has provided some valuable information regarding the characterisation and comparisons of paediatric differentiated PNEC and PBEC ALI cultures that will help guide future research.

7.7 Future work

7.7.1 Functional characterisation of differentiated paediatric primary nasal and bronchial epithelial cultures

Paired assessment of ENaC and CaCC functional expression in PNEC and PBECs derived from the same donor did suggest that there could be differences in ENaC and CaCC, but analysis was limited by the number of repeated assessments in these cultures. Culture success rates have improved since then, including the ability to successfully establish paired cultures. To investigate these differences further, paired cultures would be expanded using the above-mentioned ROCK inhibitor technique. This method has since been optimised for use with paediatric PNEC and PBEC cultures by other members of the research group and would facilitate detailed assessment of Ussing chamber responses.

Detailed investigation of the functional expression of BK channels in paediatric CF PBECs is required. Future work would start with detailed BK channel characterisation using Ussing chamber experiments together with assessment of *mRNA* and protein expression for KCNMA1, the pore-forming structure of the channel. This investigation would be required in all culture types to determine selectivity for CF cultures. Importantly, the effects of different culture media on the expression of CaCC and KCNMA1 would also provide useful information relating to the contribution of culture conditions to BK channel expression.

In addition to assessing morphology and epithelial characterisation, the work is this thesis has predominantly focussed on the ion transport profiles of established cultures. To help determine any differences between paediatric PNEC and PBEC cultures harvested from both non-CF and CF donors, detailed analysis of the transcriptomic profile could be performed using techniques such as RNAseq, and data collection for this for paired non-CF and CF cultures is underway.

Assessment of ASL parameters including ASL height and pH would be highly valuable to determine any variations between PNECs and PBECs and ascertain how these relate to ion transport profiles. Techniques to enable the dynamic assessment of pH in ALI cultures has been carefully optimised by a member of the research group and assessment in paediatric cultures would help contribute to the growing body of literature around this area.

7.7.2 Assessment of TMEM16A in differentiated paediatric primary nasal and bronchial epithelial cultures

To complement the RT-qPCR analysis of channel *mRNA* expression, future work would involve techniques such as Western blot to investigate TMEM16A protein expression in paediatric CF cultures and further elucidate any differences between PNECs versus PBECs. These techniques are described in the literature and could be consulted to help optimise protocols in paediatric cultures (Gorrieri et al., 2016). In view of the relative low levels of TMEM16A under basal conditions, it would be useful to determine how much is expressed relative to CFTR in paediatric cultures.

Detailed assessment of TMEM16A localisation is required in paediatric cultures, with particular reference to co-localisation with CFTR and epithelial cell types. TMEM16A overexpression has been associated with goblet cell hyperplasia and this requires comparable investigation in paediatric cultures (Scudieri et al., 2012a).

Immunostaining of TMEM16A has previously been performed in adult bronchial tissue (Ousingsawat et al., 2009). Assessment in paediatric-derived airway tissue would help to determine any variations with age and disease severity. However, bronchial tissue is relatively difficult to acquire due to the relative infrequency of paediatric lung transplantation and mucosal biopsy. Alternatively, nasal polyp tissue could be an alternative model, and although this would be achievable in CF, may prove more difficult with control tissue.

7.7.3 Investigation of novel TMEM16A activators and their role as a potential CF therapeutic avenue

Comprehensive characterisation of C5-induced I_{sc} responses is required in expanded cell cultures that responded to C5. This would involve application of current TMEM16A inhibitors and modification of the Ussing chamber solutions to permit investigation of chloride and calcium dependence of responses.

If C5 is determined to have consistent benefits and characteristics of TMEM16A activation, the clinical relevance of these compounds for CF therapy could be investigated by assessing impact on ASL height, pH, airway inflammation and mucociliary clearance. At least 2 further C compounds demonstrated potential benefits for TMEM16A in preliminary work performed by Professor Amaral's lab in HT29 cells and these would require investigation using above-mentioned methods.

A higher throughput assay based on the forskolin-induced assay currently utilised in organoid cultures could be developed to investigate the effects of a panel of C compounds on improving ASL volume (Dekkers et al., 2013).

7.7.4 Clinical relevance of the paediatric primary air liquid interface epithelial culture model

Having demonstrated the value of paediatric PNEC ALI cultures, the comparisons made in this PhD could be further validated by PNECs derived from completely healthy children. This would be achievable given the minimally invasive nature of nasal brushing and would further increase the variety of CF patients by enabling sampling from a range of disease severities.

The inter-donor variability in ion transport profiles and channel expression demonstrated in this PhD has emphasised the need for future work to focus on comprehensively characterising responses in individual donors, rather than grouping data together from different donors, to facilitate personalised assessment of channel function and response to novel therapeutic targets. In this PhD, this has been exemplified by the findings relating to the CF donor with the R751L/F508del mutation, and the residual CFTR functional expression that was found with Ussing chamber experiments. This novel and exciting finding was selected as an oral presentation at the European CF Society conference this year and has facilitated collaborations with other CF research groups that will assist with detailed characterisation of this mutation. Further understanding of the phosphorylation or gating mechanisms affected with this mutation, and potential responses to small molecule CFTR modulators may have clinical implications for patients with this specific mutation.

7.8 Concluding remarks

This present work has described the establishment of a research programme to facilitate the sampling of nasal and bronchial brushings to develop differentiated paediatric PNEC and PBEC ALI cultures. The ion transport profiles have been characterised in these cultures, including the assessment of TMEM16A functional expression and response to novel activating compounds. Furthermore, the work has demonstrated that paediatric PNECs do provide a representative CF research model and are a valuable resource to facilitate a personalised approach to investigating ion transport profiles and responses to novel therapeutic targets.

Appendix A: Ethical approval, consent forms and parent and participant information literature

NHS
Health Research Authority
NRES Committee North East - Newcastle & North Tyneside 1
Jarrow Business Centre
Room 001
Viking Industrial Park
Rolling Mill Road
Jarrow
NE32 3DT

Telephone: 0191 428 3384

08 September 2015

Dr Malcolm Brodlie
Great North Children's Hospital
Old Children's Outpatients Department
Newcastle upon Tyne
NE1 4LP

Dear Dr Brodlie

Study title:	**Functional characterisation of the airway epithelium in children**
REC reference:	**15/NE/0215**
Protocol number:	**7494**
IRAS project ID:	**178672**

Thank you for your letter of 19th August 2015, responding to the Committee's request for further information on the above research and submitting revised documentation.

The further information has been considered on behalf of the Committee by the Chair.

We plan to publish your research summary wording for the above study on the HRA website, together with your contact details. Publication will be no earlier than three months from the date of this favourable opinion letter. The expectation is that this information will be published for all studies that receive an ethical opinion but should you wish to provide a substitute contact point, wish to make a request to defer, or require further information, please contact the REC Assistant, Sarah Prothero, nrescommittee.northeast-newcastleandnorthtyneside1@nhs.net. Under very limited circumstances (e.g. for student research which has received an unfavourable opinion), it may be possible to grant an exemption to the publication of the study.

Confirmation of ethical opinion

On behalf of the Committee, I am pleased to confirm a **favourable** ethical opinion for the above research on the basis described in the application form, protocol and supporting documentation as revised, subject to the conditions specified below.

Participant Identification Number:

Affix patient sticker here:

CONSENT FORM

(For parent/person with parental responsibility)

Title of Study: Characterisation of the Airway Epithelium in Children
Researcher: Dr Malcolm Brodlie
Consultant in Paediatric Respiratory Medicine

Please initial box

1. I confirm that I have read and understand the information sheet dated ..... version ..... for the above study and have had the opportunity to ask questions. ☐

2. I understand participation is voluntary and that I am free to withdraw at any time, without giving any reason and without my child's medical care or legal rights being affected. ☐

3. I understand that relevant sections of my child's medical notes and data collected during the study may be looked at by responsible individuals from the NHS Trust or from regulatory authorities, where it is relevant to my child taking part in this research. I give permission for these individuals to have access to my child's records. ☐

4. I agree to my child taking part in the above study including the taking and storing of blood, nasal and lower airway brushings and broncho-alveolar lavage samples as described in the patient information sheet. ☐

Name of Patient ☐ ☐ ☐ ☐

Name of Parent ☐ ☐ Date ☐ ☐ ☐ Signature ☐

Name of Person taking consent (if different from researcher) ☐ ☐ Date ☐ ☐ ☐ Signature ☐

Researcher ☐ ☐ ☐ ☐ Date ☐ ☐ ☐ Signature ☐

Participant Identification Number:

Affix patient sticker here:

ASSENT FORM

(To be completed by child with their parent/guardian)

Title of Study: Characterisation of the Airway Epithelium in Children

Researcher: Dr Malcolm Brodlie
Consultant in Paediatric Respiratory Medicine

		Yes	No
1.	Have you read (or had read to you) the information sheet about this project?	☐	☐
2.	Has somebody else explained what this project is about?	☐	☐
3.	Do you understand what this project is about?	☐	☐
4.	Have you been given the chance to ask questions about this project?	☐	☐
5.	Have you understood the answers that you have been given to your questions?	☐	☐
6.	Do you understand that you can stop taking part in this project at any time?	☐	☐
7.	Are you happy to take part?	☐	☐

If any answers are 'no', or you don't want to take part, don't sign your name!

If you do want to take part, you can write your name below

---------- ---------- ----------

Your name Date

The doctor who explained this project needs to sign their name too:

---------- ---------- ----------

Print Name Date Signature

"Characterisation of the Airway Epithelium in Children"

This information sheet is for:
Parents/Guardians of children without CF who are having a bronchoscopy

Investigators: Dr Malcolm Brodlie, Consultant in Paediatric Respiratory Medicine, Great North Children's Hospital
Dr Iram Haq, Clinical Research Fellow, Great North Children's Hospital

We would like to invite your child to take part in our research study. Before you decide whether or not you would like to take part, we would like to explain why the research is being done, and what it will involve for your child. Please the take the time to read the following information carefully. One of our team can go through this information with you and answer any questions you may have.

What is the study about?

Cystic fibrosis (CF) is the most common inherited condition in the UK. In CF, the body makes very thick mucus. This mainly affects the lungs and digestive system. In the lungs this mucus is very difficult to clear, causing infections and severe lung damage. Children with CF need intensive treatment regimes to help manage their symptoms. Despite this, CF is life shortening. Research is important to help us understand more about CF and develop new treatments so people with CF can live longer and healthier lives.

Research scientists can learn more about CF and investigate new treatments by studying cells that come directly from the lining of the lower airways. These cells are collected using a brush during a bronchoscopy and grown in a laboratory for research.

Collecting nasal cells, cells from the nose, may also give us the same information about CF as the lower airways. Nasal cells can be collected from a person when they are awake. This is a more simple procedure that can be done without an anaesthetic.

In our study, we would like to compare nasal cells with lower airway cells. We will look at these cells in a research laboratory and measure different properties that are important in CF. We will look at how these compare with children that do not have CF. If we find that nasal cells are similar to lower airway cells, this will provide us and other researchers with valuable information about using nasal cells in future CF research. Given how simple it is to collect nasal cells, large numbers could be collected. This could bring researchers closer to finding more treatments for CF. Our study will help us find out more about how children with CF are different. Studying these cells will also help researchers learn more about other airways diseases in children.

Why has my child been invited?

Your child has been invited to take part in this study because they are attending hospital for a bronchoscopy. During the anaesthetic, we would like to collect some samples that would not otherwise be possible. Your child does not have CF, and so we will be able to compare their samples with children that have CF.

Does my child have to take part?

No. It is up to you and your child (where possible) to decide if you want to take part. If you do decide to take part, you are both free to withdraw from the study at any time without giving a reason. Your decisions will not affect your child's standard of care.

What will happen if I agree for my child to take part?

- If you agree to take part, we will ask you to sign a consent form. If your child is old enough and able to understand the research, they can write their name on the assent form.
- With your permission, we will collect information about your child's health and medical information from their medical records.
- Your child will attend for a bronchoscopy as planned by their clinical team.

What samples will be collected during the bronchoscopy?

- **Collection of blood**

  As is normal before the bronchoscopy, a drip (cannula) will be inserted into your child. Blood will be taken from this drip for the study. No extra needles will be needed. The blood will be tested for glucose levels and the rest of the blood will be kept for the study to look at other tests that are important in CF.

- **Collection of airway brushings**

  A soft brush will be used to brush some cells from the surface of the airways inside each nostril, and from the lower airways. These cells will be grown in the research laboratory to look at factors that are important in CF. Your child will not feel anything whilst these samples are collected because they will be asleep.

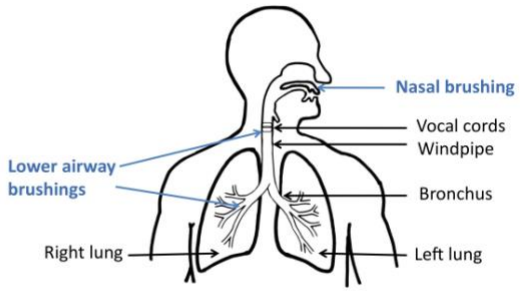

Location of airway brushings
The bronchoscope (flexible telescope) will be passed down the nose, into the windpipe, down the bronchus (large airway) and into the lower airways.

Nasal brushings will be taken from inside the nose.
Lower airway brushings will be taken from the lower airways (from below the vocal cords and the lower smaller airways).

- **Collection of a broncho-alveolar lavage (washing from the lower airway) and lower airway secretions**

  During the bronchoscopy, the lungs can be washed with a small amount of salt-water. This is called a broncho-alveolar lavage, and is usually taken to look for infection inside the lungs. We will collect some of this for the study. It isn't always performed, and may be collected specifically for our study. We will also try and collect some of the suctioned secretions that would normally be discarded during the bronchoscopy.

Are there any disadvantages to my child taking part in this study?

Collection of the research samples will add around 10 minutes onto the procedure. This should not cause any significant problems with your child or change their recovery after the bronchoscopy.

We have performed many brushings in children in Newcastle. Very occasionally, there can be mild bleeding from inside the nose. This is very short-lived and does not need any additional treatment.

Sometimes children can have a high temperature after a washing is taken from the airway. Again, this is usually short-lived.

Are there any benefits to my child taking part in this study?

There are no direct benefits to your child taking part in this study. However, your child will be part of research that will help us understand more about CF in children and find treatments for CF in the future.

Will information about my child be kept confidential and how?

Yes. All personal information on your child will be kept confidential. Only people involved in the study will have access to this information. All samples used in the study will be anonymised with a code. We will follow ethical and legal practice to make sure that all personal information about your child will be kept secure and confidential.

Has anyone reviewed this study?

All research carried out in the NHS is looked at by an independent group of people called a Research Ethics Committee. This is to protect you and your child's safety, rights, dignity and respect. The Newcastle and North Tyneside 1 Research Ethics Committee have reviewed this study.

The study has also been independently scientifically reviewed by an expert in this field.

How is the study being funded?

This study is being funded by Newcastle University. The money from this funding is being used to pay for one of the clinical researcher's salary. It is also being used to pay for the collection and testing of the samples that will be looked at in the study. None of the doctors or nurses asking you to help with the study will make any extra money if you agree to take part.

What will happen to the results of the study?

This study is part of an educational research project. Findings from the study will be written in a research project, and may be published in medical journals. However, personal information about you or your child will not be available from what is written.

Will I learn the results of the study?

If you and your child are interested, we can give you a copy of the results after the study has finished.

What will happen to the samples that have been collected?

Samples collected for the study will be stored in the research laboratory until the study is finished.

The airway cells that are grown will be stored in an appropriate research laboratory so that they can be used in future research looking at lung diseases in children. Your child's personal information will be kept confidential.

Where can I get more information?

If you require any further information regarding the study, you can contact the investigators who are based at the Great North Children's Hospital.

If you wish to speak to one of the doctors working in the Respiratory Department, you can speak to Dr Christopher O'Brien, Consultant in Paediatric Respiratory Medicine.

What if there are any problems?

If you have any concerns about any aspect of the study, you can speak to any of the researchers. If there is still a problem and you wish to make a formal complaint, you can contact the Patient Advice and Liaison Service.

Contacts

Research Contact:
Dr Malcolm Brodlie
Great North Children's Hospital
Queen Victoria Road
Newcastle upon Tyne
NE1 4LP

Patient Advice and Liaison Service:
Freepost: RLTC-SGHH-EGXJ
North of Tyne PALS
The Old Stables
Grey's Yard
Morpeth
NE61 1QD

What now?

If you and your child have decided that you would like to take part, please let the doctors and nurses know when you come to hospital, and someone from the study team will come and speak to you.

CF can have a significant impact on the lives of affected children, adults and their families. If you agree to take part in the study, you will be providing us with some very important information that will help us understand more about CF in children and how we may treat CF in the future. We are very grateful for this, and would like to thank you and your child for helping us with this study.

If you decide not to take part, we appreciate very much the time you have taken to read this, and would like to thank you for doing this.

"Characterisation of the Airway Epithelium in Children"

This information sheet is intended for:
Parents/Guardians of children with Cystic Fibrosis who are having a bronchoscopy

Investigators: Dr Malcolm Brodlie, Consultant in Paediatric Respiratory Medicine,
Great North Children's Hospital
Dr Iram Haq, Clinical Research Fellow, Great North Children's Hospital

We would like to invite your child to take part in our research study. Before you decide whether or not you would like to take part, we would like to explain why the research is being done, and what it will involve for your child. Please the take the time to read the following information carefully. One of our team can go through this information with you and answer any questions you may have.

What is the study about?

Cystic fibrosis (CF) is the most common inherited condition in the UK. In CF, the body makes very thick mucus. This mainly affects the lungs and digestive system. In the lungs, this mucus is very difficult to clear, causing infections and severe lung damage. Children with CF need intensive treatment regimes to help manage their symptoms. Despite this, CF is life shortening. Research is important to help us understand more about CF and develop new treatments so people with CF can live longer and healthier lives.

Research scientists can learn more about CF and investigate new treatments by studying cells that come directly from the lining of the lower airways. These cells are collected using a brush during a bronchoscopy and grown in a laboratory for research.

Collecting nasal cells, cells from the nose, may also give us the same information about CF as the lower airways. Nasal cells can be collected from a person when they are awake. This is a more simple procedure that can be done without an anaesthetic.

In our study, we would like to compare nasal cells with lower airway cells. We will look at these cells in a research laboratory and measure different properties that are important in CF. We will look at how these compare with children that do not have CF. If we find that nasal cells are similar to lower airway cells, this will provide us and other researchers with valuable information about using nasal cells in future CF research. Given how simple it is to collect nasal cells, large numbers could be collected. This could bring researchers closer to finding more treatments for CF. Our study will help us find out more about how children with CF are different. Studying these cells will also help researchers learn more about other airways diseases in children.

Why has my child been invited?

Your child has been invited to take part in this study because they are attending hospital for a bronchoscopy. During the anaesthetic, we would like to collect some samples that would not otherwise be possible. Your child has CF, and we will compare their samples with those collected from children that don't have CF.

Does my child have to take part?

No. It is up to you and your child (where possible) to decide if you want to take part. If you do decide to take part, you are both free to withdraw from the study at any time without giving a reason. Your decisions will not affect your child's standard of care.

What will happen if I agree for my child to take part?

- If you agree to take part, we will ask you to sign a consent form. If your child is old enough and able to understand the research, they can write their name on the assent form.
- With your permission, we will collect information about your child's health and medical information from their medical records.
- Your child will attend for a bronchoscopy as planned by their clinical team.

What samples will be collected during the bronchoscopy?

- **Collection of blood**

  As is normal before the bronchoscopy, a drip (cannula) will be inserted into your child. Blood will be taken from this drip for the study. No extra needles will be needed. The blood will be tested for glucose levels and the rest of the blood will be kept for the study to look other tests that are important in CF.

- **Collection of airway brushings**

  A soft brush will be used to brush some cells from the surface of the airways inside each nostril, and from the lower airways. These cells will be grown in the research laboratory to look at important factors that are important in CF. Your child will not feel anything whilst these samples are collected because they will be asleep.

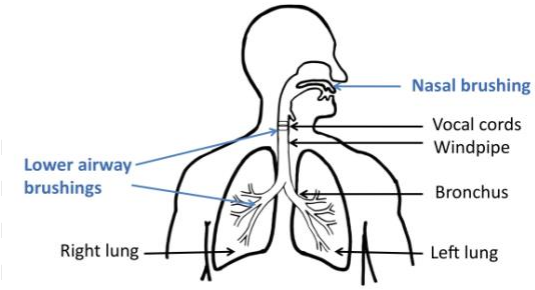

Location of airway brushings
The bronchoscope (flexible telescope) will be passed down the nose, into the windpipe, down the bronchus (large airway) and into the lower airways.

Nasal brushings will be taken from inside the nose.
Lower airway brushings will be taken from the lower airways (from below the vocal cords and the lower smaller airways).

- **Collection of a broncho-alveolar lavage (washing from the lower airway) and lower airway secretions**

  During the bronchoscopy, the lungs can be washed with a small amount of salt-water. This is called a broncho-alveolar lavage, and is usually taken to look for infection. This often applies to children with CF, and we will collect some of this for the study. It isn't always performed, and may be collected specifically for our study.

We will also try and collect some of the suctioned secretions that would normally be discarded during the bronchoscopy.

Are there any disadvantages to my child taking part in this study?

Collection of the research samples will add around 10 minutes onto the procedure. This should not cause any significant problems with your child or change their recovery after the bronchoscopy.

We have performed many brushings in children in Newcastle. Very occasionally, there can be mild bleeding from inside the nose. This is very short-lived and does not need any additional treatment.

Sometimes children can have a high temperature after a washing is taken from the airway. Again, this is usually short-lived.

Are there any benefits to my child taking part in this study?

There are no direct benefits to your child taking part in this study. However, your child will be part of research that will help us understand more about CF in children and find treatments for CF in the future.

Will information about my child be kept confidential and how?

Yes. All personal information on your child will be kept confidential. Only people involved in the study will have access to this information. All samples used in the study will be anonymised with a code. We will follow ethical and legal practice to make sure that all personal information about your child will be kept secure and confidential.

Has anyone reviewed this study?

All research carried out in the NHS is looked at by an independent group of people called a Research Ethics Committee. This is to protect you and your child's safety, rights, dignity and respect. The Newcastle and North Tyneside 1 Research Ethics Committee have reviewed this study.

The study has also been independently scientifically reviewed by an expert in this field.

How is the study being funded?

This study is being funded by Newcastle University. The money from this funding is being used to pay for one of the clinical researcher's salary. It is also being used to pay for the collection and testing of the samples that will be looked at in the study. None of the doctors or nurses asking you to help with the study will make any extra money if you agree to take part.

What will happen to the results of the study?

This study is part of an educational research project. Findings from the study will be written in a research project, and may also be published in medical journals. However, personal information about you or your child will not be available from what is written.

Will I learn the results of the study?

If you and your child are interested, we can give you a copy of the results after the study has finished.

What will happen to the samples that have been collected?

Samples collected for the study will be stored in the research laboratory until the study is finished.

The airway cells that are grown will be stored in an appropriate research laboratory so that they can be used in future research looking at lung diseases in children. Your child's personal information will be kept confidential.

Where can I get more information?

If you require any further information regarding the study, you can contact the investigators who are based at the Great North Children's Hospital.

If you wish to speak to one of the doctors working in the Respiratory Department, you can speak to Dr Christopher O'Brien, Consultant in Paediatric Respiratory Medicine.

What if there are any problems?

If you have any concerns about any aspect of the study, you can speak to any of the researchers. If there is still a problem and you wish to make a formal complaint, you can contact the Patient Advice and Liaison Service.

Contacts

Research Contact:
Dr Malcolm Brodlie
Great North Children's Hospital
Queen Victoria Road
Newcastle upon Tyne
NE1 4LP

Patient Advice and Liaison Service
Freepost: RLTC-SGHH-EGXJ
North of Tyne PALS
The Old Stables,
Grey's Yard
Morpeth
NE61 1QD

What now?

If you and your child have decided that you would like to take part, please let the doctors and nurses know when you come to hospital, and someone from the study team will come and speak to you.

CF can have a significant impact on the lives of affected children, adults and their families. If you agree to take part in the study, you will be providing us with some very important information that will help us understand more about CF in children and how we may treat CF in the future. We are very grateful for this, and would like to thank you and your child for helping us with this study.

If you decide not to take part, we appreciate very much the time you have taken to read this, and would like to thank you for doing this.

"Characterisation of the Airway Epithelium in Children"

This leaflet is for:
Children aged 11 to 15 years without Cystic Fibrosis who are having a bronchoscopy

Investigators: Dr Malcolm Brodlie, Consultant in Paediatric Respiratory Medicine, Great North Children's Hospital
Dr Iram Haq, Clinical Research Fellow, Great North Children's Hospital

We are inviting you to take part in our research study. Before you decide if you want to join in, it's important you understand why it is being done and what it will involve for you. Please read this leaflet carefully. Talk to your family, friends, doctors or nurses if you want to and ask us if you have any questions.

What is the study all about?

Cystic fibrosis (CF) is a disease that affects the lungs. The body makes very thick mucus, which is very hard to get rid of and causes lung infections. People with CF need to take lots of medicines every day and do regular physiotherapy to help get rid of this mucus. The lungs can still be badly damaged making people with CF very unwell. Research is important to help us learn more about why CF happens, and how we can help people with CF live longer.

Scientists can learn about new CF treatments by studying cells that come from the lower airways of the body's breathing system. These are collected using a brush when a person has a bronchoscopy and grown in a laboratory for scientific experiments.

Collecting cells from inside the nose (nasal cells) may also tell us important information about CF. These are collected easily without an anesthetic when someone is awake.

In our study, we would like to compare nasal cells to lower airway cells. We will grow them in a research laboratory, and measure things that are important in CF. We will compare these with cells from children that don't have CF. If nasal cells are similar to lower airway cells, they could be used more in CF research. Lots of cells could be used because they are easier to collect. This would help scientists perform more research experiments to help find treatments for CF.

Our study will help us to find out if we can use nasal cells in CF research, and more about how children with CF are different. Studying nasal and lower airway cells will also help researchers find out more about other lung diseases in children.

Why have I been invited?

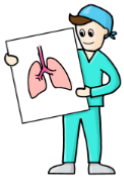

You have been invited to take part because you are coming to hospital for a bronchoscopy. We will collect some samples during the bronchoscopy that will help with our research. You don't have CF, and so we will be able to compare your samples with children that have CF.

Do I have to take part?

No. If you decide not to take part, it will not affect how your doctors and nurses look after you.

What happens if I want to take part?

- We will ask you to sign a form giving your assent if you are able to do this.
- We will give you a copy of this information for you to keep.
- You can stop taking part in the study at any time during the research. You won't have to give us a reason for deciding to stop.

What will I have to do?

We will collect some samples from you when you have the bronchoscopy.

- **Blood sample**

  Before starting the bronchoscopy, a drip (cannula) is normally put into by doctors in the theatre room. We will collect some blood from this drip for our study. No extra needles will be needed.

- **Brushing samples**

  A soft brush will be used to pick up some cells from inside your nose and lower down the airways. You will not feel anything because you will be asleep. These cells will be studied in the research laboratory.

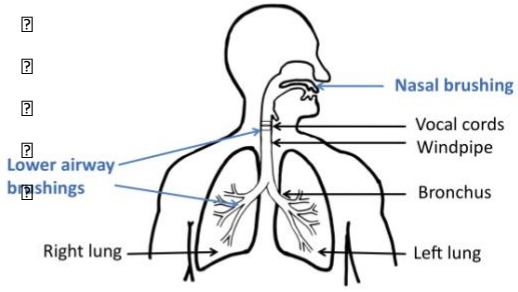

Location of airway brushings
The bronchoscope (flexible telescope) will be passed down the nose, into the windpipe, down the bronchus (large airway) and into the lower airways.

Nasal brushings will be taken from inside the nose.
Lower airway brushings will be taken from the lower airways (from below the vocal cords and the lower smaller airways).

- **Washings and secretions from the lower airways**

  During the bronchoscopy, a washing can be taken from the lungs using salty water, to look for infections inside the lungs. We will collect some of this for our study. This isn't always done and we may collect it especially for our study. We will look for bugs and other important factors in CF. We will also try and collect any suctioned secretions that would have normally been thrown away.

Is there anything I should worry about?

It will take around 10 minutes to take these samples. You will be asleep when you have the bronchoscopy, and so you won't feel anything.

Brushings are taken in Newcastle without any problems. Sometimes there can be a very small bleed from the area that is brushed, but this stops by itself very quickly.

Many washings are taken in Newcastle. You may have a mild temperature later that day. This usually is for a very short time and gets better by itself.

What are the benefits in taking part?

You will not directly benefit from taking part. However, you will be helping us learn more about CF, and how we may treat it in the future.

Will information collected about me be kept confidential?

Yes. Your information will be kept confidential and safe. We will only tell people who have a right to know that you are taking part in the study.

This study is part of an educational project, which will be written up as a research project. We may also write up this study in a medical journal, but you and your parents/guardian won't be identifiable from what is written. If you want to find out the study results, we give you a copy of the results after the study has finished.

Has anyone reviewed this study?

All research in the NHS is looked at by an independent group of people called the Research Ethics Committee. This makes sure that the research is fair. The Newcastle and North Tyneside 1 Research Ethics Committee has checked our study. An expert doctor for lung problems in children has also checked the study.

How is the study being funded?

This study is being funded by Newcastle University. The money from this funding is being used to pay for one of the research doctor's salary. It is also being used to pay for the collection and testing of the samples that will be looked at in the study. None of the doctors or nurses asking you to help with the study will make any extra money if you agree to take part.

What will happen to my samples when the study has finished?

Samples collected for the study will be stored in the research laboratory until the study is over.

The airway cells that are grown will be stored so that they can be used in future research looking at lung diseases in children. Your personal information will be kept confidential.

Where can I get more information?

If you want any more information about the study, you can speak to us or your doctors and nurses at the Great North Children's Hospital.

If you have any questions or are unhappy about anything, speak to your parents. Either they or you can ask to speak to one of the researchers, who will do their best to help you.

Research Contact:

Dr Malcolm Brodlie, Consultant in Paediatric Respiratory Medicine, GNCH 0191 2336161, extension 25089

What now?

Please have a think about if you want to take part and talk to your family, doctors and nurses about the study if you want to.

If you and your parents agree, let the doctors and nurses know, and someone from the study team will come and speak to you.

Your doctors and nurses will look after you in the same way whether or not you take part.

Whatever you decide, we thank you for reading this, and hope your stay in hospital goes well.

"Characterisation of the Airway Epithelium in Children"

This leaflet is for:
Children aged 11 to 15 years with Cystic Fibrosis who are having a bronchoscopy

Investigators: Dr Malcolm Brodlie, Consultant in Paediatric Respiratory Medicine, Great North Children's Hospital
Dr Iram Haq, Clinical Research Fellow, Great North Children's Hospital

We are inviting you to take part in our research study. Before you decide if you want to join in, it's important you understand why it is being done and what it will involve for you. Please read this leaflet carefully. Talk to your family, friends, doctors or nurses if you want to and ask us if you have any questions.

What is the study all about?

As you know, cystic fibrosis (CF) is a disease that affects the lungs. The body makes very thick mucus, which is very hard to get rid of and causes lung infections. People with CF need to take lots of medicines every day and do regular physiotherapy to help get rid of this mucus. The lungs can still be badly damaged making people with CF very unwell. Research is important to help us learn more about why CF happens, and how we can help people with CF live longer.

Scientists can learn about new CF treatments by studying cells that come from the lower airways in the body's breathing system. These are collected using a brush when a person has a bronchoscopy and are grown in a laboratory for scientific experiments.

Collecting cells from inside the nose (nasal cells) may also tell us important information about CF. These are collected easily without an anesthetic when someone is awake.

In our study, we would like to compare nasal cells to lower airway cells. We will grow them in a research laboratory, and measure things that important in CF. We will compare these with cells from children that don't have CF. If nasal cells are similar to lower airway cells, they could be used more in CF research. Lots of cells could be used because they are easier to collect. This would help scientists perform more research experiments to help find treatments for CF.

Our study will help us to find out if we can use nasal cells in CF research, and more about how children with CF are different. Studying nasal and lower airway cells will also help researchers find out more about other lung diseases in children.

Why have I been invited?

You have been invited to take part because you are coming to hospital for a bronchoscopy. We will collect some samples during the bronchoscopy that will help with our research. We will compare your samples with children that don't have CF.

Do I have to take part?

No. If you decide not to take part, it will not affect how your doctors and nurses look after you.

What happens if I want to take part?

- We will ask you to sign a form giving your assent if you are able to do this.
- We will give you a copy of this information for you to keep.
- You can stop taking part in the study at any time during the research. You won't have to give us a reason for deciding to stop.

What will I have to do?

We will collect some samples from you when you have the bronchoscopy.

- **Blood sample**

Before starting the bronchoscopy, a drip (cannula) is normally put into by doctors in the theatre room. We will collect some blood from this drip for our study. No extra needles will be needed.

- **Brushing samples**

A soft brush will be used to pick up some cells from inside your nose and lower down the airways. You will not feel anything because you will be asleep. These cells will be studied in the research laboratory.

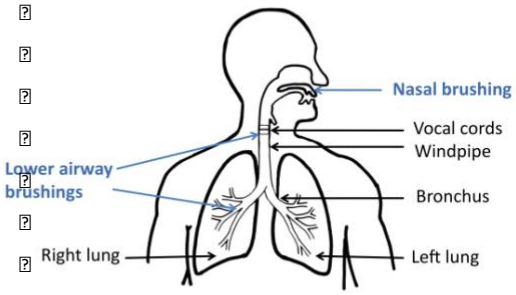

Location of airway brushings
The bronchoscope (flexible telescope) will be passed down the nose, into the windpipe, down the bronchus (large airway) and into the lower airways.

Nasal brushings will be taken from inside the nose.
Lower airway brushings will be taken from the lower airways (from below the vocal cords and the lower smaller airways).

- **Washings and secretions from the lower airways**

During the bronchoscopy, a washing can be taken from the lungs using salty water, to look for infections inside the lungs. We will collect some of this for our study. This is usually done in children with CF, but we may collect it especially for our study. We will look for bugs and other important factors in CF. We will also try and collect any suctioned secretions that would have normally been thrown away.

Is there anything I should worry about?

It will take around 10 minutes to take these samples. You will be asleep when you have the bronchoscopy, and so you won't feel anything.

Brushings are taken in Newcastle without any problems. Sometimes there can be a very small bleed from the area that is brushed, but this stops by itself very quickly.

Many washings are taken in Newcastle. You may have a mild temperature later that day. This usually is for a very short time and gets better by itself.

What are the benefits in taking part?

You will not directly benefit from taking part. However, you will be helping us learn more about CF, and how we may treat it in the future.

Will information collected about me be kept confidential?

Yes. Your information will be kept confidential and safe. We will only tell people who have a right to know that you are taking part in the study.

This study is part of an educational project, which will be written up as a research project. We may also write up this study in a medical journal, but you and your parents/guardian won't be identifiable from what is written. If you want to find out the study results, we give you a copy of the results after the study has finished.

Has anyone reviewed this study?

All research in the NHS is looked at by an independent group of people called the Research Ethics Committee. This makes sure that the research is fair. A Research Ethics Committee has checked our study. An expert doctor for lung problems in children has also checked the study.

How is the study being funded?

This study is being funded by Newcastle University. The money from this funding is being used to pay for one of the research doctor's salary. It is also being used to pay for the collection and testing of the samples that will be looked at in the study. None of the doctors or nurses asking you to help with the study will make any extra money if you agree to take part.

What will happen to my samples when the study has finished?

Samples collected for the study will be stored in the research laboratory until the study is over.

The airway cells that are grown will be stored so that they can be used in future research looking at lung diseases in children. Your personal information will be kept confidential.

Where can I get more information?

If you want any more information about the study, you can speak to us or your doctors and nurses at the Great North Children's Hospital.

If you have any questions or are unhappy about anything, speak to your parents. Either they or you can ask to speak to one of the researchers, who will do their best to help you.

Research Contact:

Dr Malcolm Brodlie, Consultant in Paediatric Respiratory Medicine, GNCH 0191 2336161, extension 25089

What now?

Please have a think about if you want to take part and talk to your family, doctors and nurses about the study if you want to.

If you and your parents agree, let the doctors and nurses know, and someone from the study team will come and speak to you.

Your doctors and nurses will look after you in the same way whether or not you take part.

Whatever you decide, we thank you for reading this, and hope your stay in hospital goes well.

"Characterisation of the Airway Epithelium in Children"

This leaflet is for:
Children aged 6 to 10 years without Cystic Fibrosis
who are having a bronchoscopy

Investigators: Dr Malcolm Brodlie, Consultant in Paediatric Respiratory Medicine,
Great North Children's Hospital
Dr Iram Haq, Clinical Research Fellow, Great North Children's Hospital

What is the study all about?

We are asking you if you would like to join in a research study about cystic fibrosis, or CF. People with CF get lots of chest infections and breathing problems. We would like to learn more about children with and without CF so that we can try and help treat it.

Why am I being asked to take part?

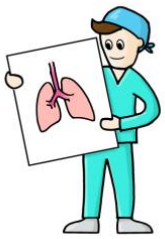

You are coming to hospital to have a special camera test called a bronchoscopy to have a look inside your chest. You don't have CF, but we would like to collect some samples from you. This will help us learn more about how children with CF are different.

Do I have to take part?

No. You don't have take part if you don't want to.

If you take part and want to stop any time, you can tell your parents, doctors or nurses. They won't be cross with you.

What will I have to do?

When you come to hospital for your bronchoscopy, we will collect some samples from you while you are asleep.

- Before starting the bronchoscopy, a drip (plastic tube) is put into your arm by the doctors. You will be asleep at this time. We will collect some blood from this drip for our study. There won't be any extra needles.

- While you are asleep, we will wash and take some fluid from your chest. We will also use a very small brush to brush some cells from inside your nose and your chest. You won't feel any of these things happening.

Is there anything that might upset me?

You will be asleep when we take these samples and so you won't feel anything.

Sometimes you can feel hot later on after the washing is taken, but this gets better very quickly. Lots of these samples are taken at this hospital and there aren't usually any problems.

Will joining in help me?

Joining in won't help you, but what we learn from the study may help us know more about CF and how to help children that have it.

Will anyone else know I am doing this?

We will keep your details private. We will only tell people who have a right to know.

We will write up this study as a project and in medical journals, but we won't write anything about your private details.

Did anyone else check that this study is OK to do?

Before any research can happen, it has to be looked at by a group of people from a Research Ethics Committee. They make sure that the research is fair. This study has been looked at by the Research Ethics Committee and an expert doctor for children's lung problems.

What if there are any problems?

If you have any questions or problems during the study, speak to your parents, or doctors and nurses who will be able to help you.

What now?

Please think about if you want to join in and talk to your mum and dad. You can talk to the doctors and nurses that look after you if you want to.

If you and your parents agree, let the doctors and nurses know, and someone from the study team will come and speak to you.

Your doctors and nurses will look after you just the same whether or not you join in.

Thank you for reading this. We hope your stay in hospital goes well.

"Characterisation of the Airway Epithelium in Children"

This leaflet is for:
Children aged 6 to 10 years with Cystic Fibrosis
who are having a bronchoscopy

Investigators: Dr Malcolm Brodlie, Consultant in Paediatric Respiratory Medicine,
Great North Children's Hospital
Dr Iram Haq, Clinical Research Fellow, Great North Children's Hospital

What is the study all about?

We are asking you if you would like to join in a research study about cystic fibrosis, or CF. People with CF get lots of chest infections and breathing problems. We would like to learn more about children with and without CF so we can try and help treat it.

Why am I being asked to take part?

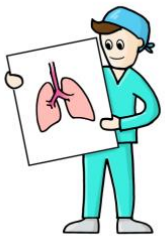

You have CF and are coming to hospital to have a special camera test called a bronchoscopy to have a look inside your chest. We would like to collect some samples from you when you have this.

Do I have to take part?

No. You don't have take part if you don't want to.

If you take part and want to stop any time, you can tell your parents, doctors or nurses. They won't be cross with you.

What will I have to do?

When you come to hospital for your bronchoscopy, we will collect some samples from you while you are asleep.

- Before starting the bronchoscopy, a drip (plastic tube) is put into your arm by the doctors. You will be asleep at this time. We will collect some blood from this drip for our study. There won't be any extra needles.

- While you are asleep, we will wash and take some fluid from your chest. We will also use a very small brush to brush some cells from inside your nose and your chest. You won't feel any of these things happening.

Is there anything that might upset me?

You will be asleep when we take these samples and so you won't feel anything.

Sometimes you can feel hot later on after the washing is taken, but this gets better very quickly. Lots of these samples are taken at this hospital and there aren't usually any problems.

Will joining in help me?

Joining in won't help you, but what we learn from the study may help know more about CF and how to help children that have it.

Will anyone else know I am doing this?

We will keep your details private. We will only tell people who have a right to know.

We will write up this study as a project and in medical journals, but we won't write anything about your private details.

Did anyone else check that this study is OK to do?

Before any research can happen, it has to be looked at by a group of people from a Research Ethics Committee. They make sure that the research is fair. This study has been looked at by a Research Ethics Committee and an expert doctor for children's lung problems.

What if there are any problems?

If you have any questions or problems during the study, speak to your parents, or doctors and nurses who will be able to help you.

What now?

Please think about if you want to join in and talk to your mum and dad. You can talk to the doctors and nurses that look after you if you want to.

If you and your parents agree, let the doctors and nurses know, and someone from the study team will come and speak to you.

Your doctors and nurses will look after you just the same whether or not you join in.

Thank you for reading this. We hope your stay in hospital goes well.

The Newcastle upon Tyne Hospitals NHS
NHS Foundation Trust

THE great north CHILDREN'S HOSPITAL

Hello!

My name is Fudge.

I am here to tell you about a special test.

Your name is:

_____

"Characterisation of the Airway Epithelium in Children"
Investigators: Dr Malcolm Brodlie, Dr Iram Haq
Participant information sheet (5 years and under) Version 1.0
29.7.15

Colour this picture in!

You are coming to hospital for a special test.

This will let the doctors look inside your chest.

We would like to do some more tests at the same time.

You will be asleep and won't feel anything.

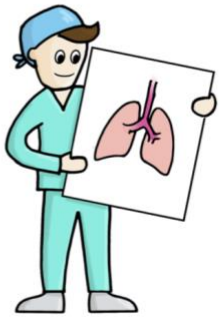

After the test you will rest in hospital.

Later on, when the doctors and nurses are happy, you can go home!

Appendix B: Academic achievements during this PhD

Funding

Wellcome Trust Clinical Research Training Fellowship, July 2016

Publications

Haq IJ, Harris C, Taylor J, McKean MC, Brodlie M. Should we use Montelukast in wheezy children? Arch Dis Child. 2017 Nov;102(11):997-998. doi:10.1136/archdischild-2017-312655.

Zainal Abidin N, **Haq IJ**, Gardner AI, Brodlie M. Ataluren in cystic fibrosis: development, clinical studies and where are we now? *Expert Opin Pharmacother.* 2017 Sep;18(13):1363-1371. doi: 10.1080/14656566.2017.1359255.

Ibrahim SH, Turner MJ, Saint-Criq V, Garnett J, **Haq IJ**, Brodlie M, Ward C, Borgo C, Salvi M, Venerando A, Gray MA. CK2 is a key regulator of SLC4A2-mediated Cl^-/$HCO3^-$ exchange in human airway epithelia. *Pflugers Arch.* 2017 Apr 28. doi: 10.1007/s00424-017-1981-3.

Haq IJ, Battersby AC, Eastham K, McKean M. Community acquired pneumonia in children. *BMJ.* 2017 Mar 2;356:j686. doi: 10.1136/bmj.j686.

Haq IJ, Gardner A, Brodlie M. A multifunctional bispecific antibody against Pseudomonas aeruginosa as a potential therapeutic strategy. *Ann Trans Med.* 2016 Jan;4(1):12. doi: 10.3978/j.issn.2305-5839.2015.10.10.

Haq IJ, Gray MA, Garnett JP, Ward C, Brodlie M. Airway surface liquid homeostasis in cystic fibrosis: pathophysiology and therapeutic targets. *Thorax*. 2015; 10.1136/thoraxjnl-2015-207588.

Brodlie M, **Haq IJ**, Roberts K, Elborn JS. Targeted therapies to improve CFTR function in cystic fibrosis. *Genome Medicine 2015*; doi: 10.1186/s13073-015-0223-6.

Oral presentations

‘Using the nose to investigate novel therapeutic avenues in cystic fibrosis’, invited speaker at the Clinical Academic Training Pathway Scientific Meeting September 2018, Newcastle University, Newcastle upon Tyne.

‘First functional characterisation of the *R751L CFTR* mutation using an *ex vivo* primary airway epithelial cell culture model’, European Cystic Fibrosis Conference June 2018, Belgrade, Serbia.

‘Functional characterisation of the airway epithelium in children with cystic fibrosis’, Annual Northern Cystic Fibrosis Meeting February 2018, Centre for Life, Newcastle upon Tyne.

‘Use of primary airway epithelial cells from children with cystic fibrosis to investigate novel anoctamin 1 activators’, Newcastle, Edinburgh, Cambridge and Sheffield Scientific Collaborative Meeting November 2017, Sheffield.

‘A case of lobar lung transplantation in a boy with cystic fibrosis’, Northern Paediatric Respiratory Spring Meeting March 2016, Newcastle upon Tyne.

‘Asthma: getting the diagnosis right’, educational session for primary care physicians March 2016, Newcastle University.

‘My experience of paediatric training in the Northern Deanery’, invited speaker at the MBBS careers day June 2016, Newcastle University.

‘Research in paediatrics: a trainee’s perspective’, invited speaker at the Great North Children’s Hospital Research Community Meeting February 2016, Newcastle upon Tyne.

‘Lung research for children at the Great North Children’s Hospital’, Invited speaker at the North-East Young People’s Advisory Group for Research September 2015, Sir James Spence Institute, Royal Victoria Infirmary, Newcastle upon Tyne

Poster presentations

‘Use of *ex vivo* paediatric primary nasal epithelial cultures to investigate TMEM16A as a potential therapeutic target in children with cystic fibrosis’, European Cystic Fibrosis Conference June 2018, Belgrade, Serbia.

‘Characterisation of primary paediatric nasal epithelial cells as a model system to investigate TMEM16A as a therapeutic avenue in CF, European Cystic Fibrosis Basic Science Conference April 2018, Loutraki, Greece.

‘A paediatric primary nasal epithelial cell culture model to investigate bypass channels as a therapeutic target in cystic fibrosis’, European Cystic Fibrosis Basic Science Conference April 2017, Albufeira, Portugal.

‘A paediatric primary nasal epithelial cell culture model to investigate bypass channels as a therapeutic target in cystic fibrosis’, Institute of Cellular Medicine Directors Day June 2017, (poster prize awarded), Newcastle University, Newcastle upon Tyne

‘A paediatric primary nasal epithelial cell culture model to investigate bypass channels as a therapeutic target in cystic fibrosis’, Great North Children’s Research Community Conference March 2017, The Sage, Gateshead.

‘Airway epithelial cells from children with cystic fibrosis to investigate novel anoctamin 1 activators’, Newcastle Academic Health Partners Research Day June 2016, Newcastle University, Newcastle upon Tyne.

*‘*Airway epithelial cells from children with cystic fibrosis to investigate novel anoctamin 1 activators’, Young Person’s Advisory Group North East Research Conference December 2016, The Hancock Museum, Newcastle upon Tyne.

Additional academic activities

Editorial board member for ‘Beat Asthma’ – online resource for children and young people with asthma, September 2017.

Invited interview with the BMJ for review on community acquired pneumonia in children doi: 10.1136/bmj.j686, February 2017 (available online).

Invited reviewer for the BMJ, BMJ Paediatrics Open and BMC Pulmonary Medicine.

References

Abdullah, L., et al. 2012. Studying mucin secretion from human bronchial epithelial cell primary cultures. *Mucins Methods and Protocols.* New York: Springer, 259-78.

Abou Alaiwa, M. H., et al. 2014. Neonates with cystic fibrosis have a reduced nasal liquid pH; a small pilot study. *J Cyst Fibros,* 13, (4)**,** 373-7.

Adam, R. J., et al. 2013. Air trapping and airflow obstruction in newborn cystic fibrosis piglets. *Am J Respir Crit Care Med,* 188, (12)**,** 1434-41.

Ahmadi, S., et al. 2017. Phenotypic profiling of CFTR modulators in patient-derived respiratory epithelia. *NPJ Genom Med,* 2, (1)**,** 1-10.

Alexander, C. L., et al. 2008. The risk of gastrointestinal malignancies in cystic fibrosis. *J Cyst Fibros,* 7, (1)**,** 1-6.

Alikadic, S., et al. 2011. Ciliary beat frequency in nasal and bronchial epithelial cells in patients with cystic fibrosis. *Eur Respir J,* 38, (Suppl 55).

Alton, E. W. F. W., et al. 2015. Repeated nebulisation of non-viral CFTR gene therapy in patients with cystic fibrosis: a randomised, double-blind, placebo-controlled, phase 2b trial. *Lancet Respir Med,* 3, (9)**,** 684-691.

Alton, E. W. F. W., et al. 2017. Preparation for a first-in-man lentivirus trial in patients with cystic fibrosis. *Thorax,* 72, 137-147.

Awadalla, M., et al. 2014. Early Airway Structural Changes in Cystic Fibrosis Pigs as a Determinant of Particle Distribution and Deposition. *Ann Biomed Eng,* 42, (4)**,** 915-927.

Azad, A. K., et al. 2009. Mutations in the amiloride-sensitive epithelial sodium channel in patients with cystic fibrosis-like disease. *Hum Mutat,* 30, (7)**,** 1093-1103.

Bangel, N., et al. 2008. Upregulated expression of ENaC in human CF nasal epithelium. *J Cyst Fibros,* 7, (3)**,** 197-205.

Barrett, J. N., et al. 1982. Properties of single calcium-activated potassium channels in cultured rat muscle. *J Physiol,* 331, 211-230.

Benedetto, R., et al. 2017. Epithelial Chloride Transport by CFTR Requires TMEM16A. *Sci Rep,* 7, (1)**,** 12397.

Bergin, D. A., et al. 2013. Airway inflammatory markers in individuals with cystic fibrosis and non-cystic fibrosis bronchiectasis. *J Inflamm Res,* 6, 1-11.

Bernacki, S. H., et al. 1999. Mucin Gene Expression during Differentiation of Human Airway Epithelia In Vitro. *Am J Respir Cell Mol Biol,* 20, (4)**,** 595-604.

Bertrand, C. A., et al. 2009. SLC26A9 is a constitutively active, CFTR-regulated anion conductance in human bronchial epithelia. *J Gen Physiol,* 133, (4)**,** 421-438.

Birket, S. E., et al. 2014. A functional anatomic defect of the cystic fibrosis airway. *Am J Respir Crit Care Med,* 190, (4)**,** 421-32.

Blume, L. F., et al. 2010. Temperature corrected transepithelial electrical resistance (TEER) measurement to quantify rapid changes in paracellular permeability. *Pharmazie,* 65, (1)**,** 19-24.

Bonny, O., et al. 1999. Functional expression of a pseudohypoaldosteronism type I mutated epithelial Na(+) channel lacking the pore-forming region of its α subunit. *J. Clin. Invest,* 104, (7)**,** 967-974.

Boucher, R. C., et al. 1989. Chloride secretory response of cystic fibrosis human airway epithelia. Preservation of calcium but not protein kinase C- and A-dependent mechanisms. *J Clin Invest,* 84, (5)**,** 1424-1431.

Boucher, R. C., et al. 1988. Evidence for reduced Cl- and increased Na+ permeability in cystic fibrosis human primary cell cultures. *J Physiol,* 405, 77-103.

Boucher, R. C., et al. 1986. Na+ transport in cystic fibrosis respiratory epithelia. Abnormal basal rate and response to adenylate cyclase activation. *J Clin Invest,* 78, (5)**,** 1245-1252.
Bozoky, Z., et al. 2013. Regulatory R region of the CFTR chloride channel is a dynamic integrator of phospho-dependent intra- and intermolecular interactions. *Proc Natl Acad Sci U S A,* 110, (47)**,** E4427-E4436.
Brewington, J. J., et al. 2018a. Chronic β2AR stimulation limits CFTR activation in human airway epithelia. *JCI Insight,* 3, (4)**,** e93029.
Brewington, J. J., et al. 2018b. Brushed nasal epithelial cells are a surrogate for bronchial epithelial CFTR studies. *JCI Insight,* 3, (13)**,** e99385.
Brodlie, M., et al. 2015. Targeted therapies to improve CFTR function in cystic fibrosis. *Genome Med,* 7, (101)**,** 1-16.
Brodlie, M., et al. 2011. Raised interleukin-17 is immunolocalised to neutrophils in cystic fibrosis lung disease. *Eur Respir J,* 37, (6)**,** 1378-1385.
Brodlie, M., et al. 2010. Primary bronchial epithelial cell culture from explanted cystic fibrosis lungs. *Exp Lung Res,* 36, (2)**,** 101-110.
Burgel, P.-R., et al. 2015. Future trends in cystic fibrosis demography in 34 European countries. *Eur Respir J,* 46, 133-141.
Button, B., et al. 2012. A Periciliary Brush Promotes the Lung Health by Separating the Mucus Layer from Airway Epithelia. *Science,* 337, (6097)**,** 937-941.
Caci, E., et al. 2015. Upregulation of TMEM16A Protein in Bronchial Epithelial Cells by Bacterial Pyocyanin. *PloS one,* 10, (6)**,** e0131775.
Caldwell, R. A., et al. 2005. Neutrophil elastase activates near-silent epithelial Na+ channels and increases airway epithelial Na+ transport. *Am J Physiol Lung Cell Mol Physiol,* 288, (5)**,** L813-L819.
Canessa, C. M., et al. 1994. Amiloride-sensitive epithelial Na+ channel is made of three homologous subunits. *Nature,* 367, 463-467.
Caputo, A., et al. 2008. TMEM16A, A Membrane Protein Associated with Calcium-Dependent Chloride Channel Activity. *Science,* 322, (5901)**,** 590-594.
Chang, S. S., et al. 1996. Mutations in subunits of the epithelial sodium channel cause salt wasting with hyperkalaemic acidosis, pseudohypoaldosteronism type 1. *Nat Genet,* 12, 248.
Chen, J.-H., et al. 2010. Loss of anion transport without increased sodium absorption characterizes newborn porcine cystic fibrosis airway epithelia. *Cell,* 143, (6)**,** 911-923.
Chen, J. S., et al. 2017. Enhanced proofreading governs CRISPR-Cas9 targeting accuracy. *Nature,* 550, (7676)**,** 407-410.
Clancy, J. P., et al. 2018. CFTR modulator theratyping: Current status, gaps and future directions. *J Cyst Fibros,* Article in press.
Clarke, L. L., et al. 1994. Relationship of a non-cystic fibrosis transmembrane conductance regulator-mediated chloride conductance to organ-level disease in Cftr(-/-) mice. *Proc Am Thorac Soc,* 91, (2)**,** 479-483.
Clarke, L. L., et al. 1999. Desensitization of P2Y2receptor-activated transepithelial anion secretion. *American Journal of Physiology-Cell Physiology,* 276, (4)**,** C777-C787.
Coakley, R. D., et al. 2003. Abnormal surface liquid pH regulation by cultured cystic fibrosis bronchial epithelium. *Proc Natl Acad Sci U S A,* 100, (26)**,** 16083-8.
Colledge, W. H., et al. 1995. Generation and characterization of a ΔF508 cystic fibrosis mouse model. *Nat Genet,* 10, 445.
Comer, D. M., et al. 2012. Comparison of nasal and bronchial epithelial cells obtained from patients with COPD. *PloS one,* 7, (3)**,** e32924.

Contreras, R. G., et al. 2002. E-Cadherin and tight junctions between epithelial cells of different animal species. *Pflugers Arch,* 444, (4), 467-475.
Cuthbert, A. W., et al. 1999. Activation of Ca2+- and cAMP-sensitive K+ channels in murine colonic epithelia by 1-ethyl-2-benzimidazolone. *American Journal of Physiology-Cell Physiology,* 277, (1), C111-C120.
Cystic Fibrosis Trust 2004. *Pseudomonas aeruginosa* infection in people with cystic fibrosis. Suggestions for Prevention and Infection Control. Second edition. November 2004.
Cystic Fibrosis Trust 2011. Cystic Fibrosis Trust: Standards for the Clinical Care of Children and Adults with Cystic Fibrosis in the UK. Second edition. December 2011 (updated 01.11.2016).
Daher, S., et al. 1995. Interleukin-4 and soluble CD23 serum levels in asthmatic atopic children. *J Investig Allergol Clin Immunol,* 5, (5), 251-254.
Danahay, H., et al. 2002. Interleukin-13 induces a hypersecretory ion transport phenotype in human bronchial epithelial cells. *Am J Physiol Lung Cell Mol Physiol,* 282, (2), L226-L236.
Dang, S., et al. 2017. Cryo-EM structures of the TMEM16A calcium-activated chloride channel. *Nature,* 552, 426.
Davies, J. C., et al. 2005. Potential Difference Measurements in the Lower Airway of Children with and without Cystic Fibrosis. *Am J Respir Crit Care Med,* 171, (9), 1015-1019.
Davies, J. C., et al. 2013. Efficacy and Safety of Ivacaftor in Patients Aged 6 to 11 Years with Cystic Fibrosis with a G551D Mutation. *Am J Respir Crit Care Med,* 187, (11), 1219 - 1225.
De Blic, J., et al. 2000. Bronchoalveolar lavage in children. ERS Task Force on bronchoalveolar lavage in children. European Respiratory Society. *Eur Respir J,* 15, 217-231.
De Courcey, F., et al. 2012. Development of primary human nasal epithelial cell cultures for the study of cystic fibrosis pathophysiology. *Am J Physiol Cell Physiol,* 303, (11), C1173-9.
Dekkers, J. F., et al. 2013. A functional CFTR assay using primary cystic fibrosis intestinal organoids. *Nat Med,* 19, 939.
Delaney, S. J., et al. 1996. Cystic fibrosis mice carrying the missense mutation G551D replicate human genotype-phenotype correlations. *EMBO J,* 15, (5), 955-963.
Deterding, R., et al. 2005. Safety and tolerability of denufosol tetrasodium inhalation solution, a novel P2Y2 receptor agonist: Results of a phase 1/phase 2 multicenter study in mild to moderate cystic fibrosis. *Pediatr Pulmonol,* 39, (4), 339-348.
Döring, G., et al. 2007. Clinical trials in cystic fibrosis. *J Cyst Fibros,* 6, (2), 85-99.
Downey, D. G., et al. 2009. Neutrophils in cystic fibrosis. *Thorax,* 64, 81-88.
Eggermont, J. 2004. Calcium-activated Chloride Channels. *Proc Am Thorac Soc,* 1, (1), 22-27.
Elborn, J. S. 2016. Cystic fibrosis. *Lancet,* 388, (10059), 2519-2531.
Elborn, J. S., et al. 1991. Cystic fibrosis: current survival and population estimates to the year 2000. *Thorax,* 46, (12), 881.
Evans, M. J., et al. 1989. The Role of Basal Cells in Attachment of Columnar Cells to the Basal Lamina of the Trachea. *Am J Respir Cell Mol Biol,* 1, (6), 463-470.
Ferrera, L., et al. 2009. Regulation of TMEM16A Chloride Channel Properties by Alternative Splicing. *J Biol Chem,* 284, (48), 33360-33368.
Fischer, H. & Widdicombe, J. H. 2006. Mechanisms of Acid and Base Secretion by the Airway Epithelium. *J Membr Biol,* 211, (3), 139-50.

Forrest, I. A., et al. 2005. Primary airway epithelial cell culture from lung transplant recipients. *Eur Respir J,* 26, (6)**,** 1080-1085.
Frizzell, R. A. & Hanrahan, J. W. 2012. Physiology of Epithelial Chloride and Fluid Secretion. *Cold Spring Harb Perspect Med,* 2, (6)**,** a009563.
Fu, Y., et al. 2014. Improving CRISPR-Cas nuclease specificity using truncated guide RNAs. *Nat Biotechnol,* 32, 279.
Fulcher, M. L., et al. 2005. Well-differentiated human airway epithelial cell cultures. *Methods Mol Med,* 107, 183-206.
Gaga, M., et al. 2001. Histological similarities nasal and lower airways. *Eur Respir J,* 18, 1-15.
Gaillard, E. A., et al. 2010. Regulation of the epithelial Na+ channel and airway surface liquid volume by serine proteases. *Pflugers Arch,* 460, (1)**,** 1-17.
Galietta, L. J. V., et al. 2002. IL-4 Is a Potent Modulator of Ion Transport in the Human Bronchial Epithelium In Vitro. *J Immunol,* 168, 839-845.
Gallos, G., et al. 2013. Functional expression of the TMEM16 family of calcium-activated chloride channels in airway smooth muscle. *Am J Physiol Lung Cell Mol Physiol,* 305, (9)**,** L625-L634.
Garcia, M. a. S., et al. 2009. Normal mouse intestinal mucus release requires cystic fibrosis transmembrane regulator–dependent bicarbonate secretion. *J Clin Invest,* 119, (9)**,** 2613-2622.
Garcia-Caballero, A., et al. 2009. SPLUNC1 regulates airway surface liquid volume by protecting ENaC from proteolytic cleavage. *Proc Natl Acad Sci U S A,* 106, (27)**,** 11412-7.
Garratt, L. W., et al. 2014. Determinants of culture success in an airway epithelium sampling program of young children with cystic fibrosis. *Exp Lung Res,* 40, (9)**,** 447-459.
Gentzsch, M., et al. 2010. The Cystic Fibrosis Transmembrane Conductance Regulator Impedes Proteolytic Stimulation of the Epithelial Na+ Channel. *J Biol Chem,* 285, (42)**,** 32227-32232.
Gorrieri, G., et al. 2016. Goblet Cell Hyperplasia Requires High Bicarbonate Transport To Support Mucin Release. *Sci Rep,* 6, 36016.
Groneberg, D. A., et al. 2002. Expression of MUC5AC and MUC5B mucins in normal and cystic fibrosis lung. *Respir Med,* 96, (2)**,** 81-86.
Grubb, B. R., et al. 2012. Transgenic hCFTR expression fails to correct β-ENaC mouse lung disease. *Am J Physiol Lung Cell Mol Physiol,* 302, (2)**,** L238-L247.
Grubb, B. R., et al. 1994. Anomalies in ion transport in CF mouse tracheal epithelium. *Am J Physiol Cell Physiol,* 267, (1)**,** C293-C300.
Gruenert, D. C., et al. 1995. Culture and transformation of human airway epithelial cells. *Am J Physiol,* 268, (3 Pt 1)**,** L347-360.
Gruenert, D. C., et al. 2004. Established cell lines used in cystic fibrosis research. *J Cyst Fibros,* 3 Suppl 2, 191-6.
Guggino, W. B. & Stanton, B. A. 2006. New insights into cystic fibrosis: molecular switches that regulate CFTR. *Nat Rev Mol Cell Biol,* 7, 426.
Guo-Parke, H., et al. 2013. Relative Respiratory Syncytial Virus Cytopathogenesis in Upper and Lower Respiratory Tract Epithelium. *Am J Respir Crit Care Med,* 188, (7)**,** 842-851.
Gustafsson, J. K., et al. 2012. Bicarbonate and functional CFTR channel are required for proper mucin secretion and link cystic fibrosis with its mucus phenotype. *The Journal of experimental medicine,* 209, (7)**,** 1263-72.
Gutierrez, J. P., et al. 2001. Interlobar differences in bronchoalveolar lavage fluid from children with cystic fibrosis. *Eur Respir J,* 17, 281-286.

Haas, M. & Forbush Iii, B. 2000. The Na-K-Cl Cotransporter of Secretory Epithelia. *Annual Review of Physiology,* 62, (1), 515-534.
Hahn, A., et al. 2017. Cellular distribution and function of ion channels involved in transport processes in rat tracheal epithelium. *Physiological Reports,* 5, (12), e13290.
Haq, I. J., et al. 2015. Airway surface liquid homeostasis in cystic fibrosis: pathophysiology and therapeutic targets. *Thorax,* 71, 284-287.
Harrison, P. T., et al. 2018. Gene editing and stem cells. *J Cyst Fibros,* 17, (1), 10-16.
Hartsock, A. & Nelson, W. J. 2008. Adherens and tight junctions: Structure, function and connections to the actin cytoskeleton. *Biochem Biophys Acta Biomembr,* 1778, (3), 660-669.
Hartzell, C., et al. 2004. Calcium activated chloride channels. *Annu Rev Physiol,* 67, (1), 719-758.
Harvey, P. R., et al. 2011. Measurement of the airway surface liquid volume with simple light refraction microscopy. *Am J Respir Cell Mol Biol,* 45, (3), 592-9.
Henderson, A. G., et al. 2014. Cystic fibrosis airway secretions exhibit mucin hyperconcentration and increased osmotic pressure. *J Clin Invest,* 124, (7), 3047-3060.
Hirsh, A. J., et al. 2004. Evaluation of Second Generation Amiloride Analogs as Therapy for Cystic Fibrosis Lung Disease. *J Pharmacol Exp Ther,* 311, 929-938.
Horani, A., et al. 2013. Rho-Associated Protein Kinase Inhibition Enhances Airway Epithelial Basal-Cell Proliferation and Lentivirus Transduction. *Am J Respir Cell Mol Biol,* 49, (3), 341-347.
Houwen, R. H., et al. 2010. Defining DIOS and Constipation in Cystic Fibrosis With a Multicentre Study on the Incidence, Characteristics, and Treatment of DIOS. *J Pediatr Gastroenterol Nutr,* 50, (1), 38-42.
Huang, F., et al. 2009. Studies on expression and function of the TMEM16A calcium-activated chloride channel. *Proc Am Thorac Soc,* 106, 21413-21418.
Huang, S. X. L., et al. 2014. Highly efficient generation of airway and lung epithelial cells from human pluripotent stem cells. *Nat Biotechnol,* 32, (1), 84-91.
Hwang, T.-C. & Sheppard, D. N. 2009. Gating of the CFTR Cl− channel by ATP-driven nucleotide-binding domain dimerisation. *J Physiol,* 587, (10), 2151-2161.
Itani, O. A., et al. 2011. Human cystic fibrosis airway epithelia have reduced Cl− conductance but not increased Na+ conductance. *Proc Am Thorac Soc,* 108, (25), 10260-10265.
Jain, R., et al. 2010. Temporal Relationship between Primary and Motile Ciliogenesis in Airway Epithelial Cells. *Am J Respir Cell Mol Biol,* 43, (6), 731-739.
Janoff, A., et al. 1979. Lung injury induced by leukocytic proteases. *Am J Pathol,* 97, (1), 111-136.
Jung, J., et al. 2013. Dynamic modulation of ANO1/TMEM16A HCO3− permeability by Ca2+/calmodulin. *Proc Am Thorac Soc,* 110, (1), 360-365.
Kent, G., et al. 1996. Phenotypic Abnormalities in Long-Term Surviving Cystic Fibrosis Mice. *Pediatr Res,* 40, 233.
Kerem, E., et al. 2014. A randomized placebo-controlled trial of ataluren for the treatment of nonsense mutation cystic fibrosis. *Lancet Respir Med,* 2, (7), 539-547.
Khan, T. Z., et al. 1995a. Early pulmonary inflammation in infants with cystic fibrosis. *Am J Respir Crit Care Med,* 151, (4), 1075-1082.

Khan, T. Z., et al. 1995b. Early Pulmonary Inflammation in Infants with Cystic Fibrosis. *Am J Respir Crit Care Med,* 151, (4)**,** 1075-1082.
Knight, D. A. & Holgate, S. T. 2003. The airway epithelium: Structural and functional properties in health and disease. *Respirology,* 8, (4)**,** 432-446.
Knowles, M., et al. 1983. Relative ion permeability of normal and cystic fibrosis nasal epithelium. *J. Clin. Invest,* 71, (5)**,** 1410-1417.
Knowles, M. R., et al. 1990. A Pilot Study of Aerosolized Amiloride for the Treatment of Lung Disease in Cystic Fibrosis. *N Engl J Med,* 322, (17)**,** 1189-1194.
Knowles , M. R., et al. 1991. Activation by Extracellular Nucleotides of Chloride Secretion in the Airway Epithelia of Patients with Cystic Fibrosis. *N Engl J Med,* 325, (8)**,** 533-538.
Kunzelmann, K., et al. 1997. The cystic fibrosis transmembrane conductance regulator attenuates the endogenous Ca2+ activated Cl– conductance of Xenopus oocytes. *Pflugers Arch,* 435, (1)**,** 178-181.
Kunzelmann, K., et al. 2012. Airway epithelial cells—Functional links between CFTR and anoctamin dependent Cl− secretion. *Int J Biochem Cell Biol,* 44, (11)**,** 1897-1900.
Lazarowski, E. R. & Boucher, R. C. 2009. Purinergic receptors in airway epithelia. *Curr Opin Pharmacol,* 9, (3)**,** 262-267.
Lee, H. J., et al. 2015a. Thick airway surface liquid volume and weak mucin expression in pendrin-deficient human airway epithelia. *Physiol Rep,* 3, (8)**,** e12480.
Lee, J., et al. 2015b. Two helices in the third intracellular loop determine anoctamin 1 (TMEM16A) activation by calcium. *Pflugers Arch,* 467, (8)**,** 1677-1687.
Li, H., et al. 2004. Transepithelial electrical measurements with the Ussing chamber. *J Cyst Fibros,* 3, 123-126.
Li, Z., et al. 2012. Regional Differences in the Evolution of Lung Disease in Children with Cystic Fibrosis. *Pediatr Pulmonol,* 47, (7)**,** 635-640.
Lin, H., et al. 2007. Air-Liquid Interface (ALI) Culture of Human Bronchial Epithelial Cell Monolayers as an in vitro Model for Airway Drug Transport Studies. *J Pharm Sci,* 96, (2)**,** 341-350.
Lin, J., et al. 2015. TMEM16A mediates the hypersecretion of mucus induced by Interleukin-13. *Exp Cell Res,* 334, (2)**,** 260-269.
Mall, M., et al. 1998. The amiloride-inhibitable Na+ conductance is reduced by the cystic fibrosis transmembrane conductance regulator in normal but not in cystic fibrosis airways. *J. Clin. Invest,* 102, (1)**,** 15-21.
Mall, M., et al. 2003. Modulation of Ca2+-Activated Cl- Secretion by Basolateral K+ Channels in Human Normal and Cystic Fibrosis Airway Epithelia. *Pediatr Res,* 53, (4)**,** 608-618.
Mall, M., et al. 2004. Increased airway epithelial Na+ absorption produces cystic fibrosis-like lung disease in mice. *Nat Med,* 10, (5)**,** 487-493.
Mall, M. A. & Galietta, L. J. V. 2015. Targeting ion channels in cystic fibrosis. *J Cyst Fibros,* 14, (5)**,** 561-570.
Mall, M. A., et al. 2008. Development of Chronic Bronchitis and Emphysema in β-Epithelial Na+ Channel–Overexpressing Mice. *Am J Respir Crit Care Med,* 177, (7)**,** 730-742.
Manunta, M. D. I., et al. 2017. Delivery of ENaC siRNA to epithelial cells mediated by a targeted nanocomplex: a therapeutic strategy for cystic fibrosis. *Sci Rep,* 7, (1)**,** 700.
Manzanares, D., et al. 2011. Functional Apical Large Conductance, Ca2+-activated, and Voltage-dependent K+ Channels Are Required for Maintenance of Airway Surface Liquid Volume. *J Biol Chem,* 286, (22)**,** 19830-19839.

Marchant, J. M., et al. 2008. Prospective assessment of protracted bacterial bronchitis: Airway inflammation and innate immune activation. *Pediatr Pulmonol,* 43, (11)**,** 1092-1099.
Martinovich, K. M., et al. 2017. Conditionally reprogrammed primary airway epithelial cells maintain morphology, lineage and disease specific functional characteristics. *Sci Rep,* 7, (1)**,** 17971.
Mason, S. J., et al. 1991. Regulation of transepithelial ion transport and intracellular calcium by extracellular ATP in human normal and cystic fibrosis airway epithelium. *Br J Pharmacol,* 103, (3)**,** 1649-1656.
Mathee, K., et al. 1999. Mucoid conversion of Pseudomonas aeruginos by hydrogen peroxide: a mechanism for virulence activation in the cystic fibrosis lung. *Microbiology,* 145, (6)**,** 1349-1357.
Matsui, H., et al. 2006. A physical linkage between cystic fibrosis airway surface dehydration and Pseudomonas aeruginosa biofilms. *Proc Am Thorac Soc,* 103, (48)**,** 18131.
Mcdougall, C. M., et al. 2008. Nasal epithelial cells as surrogates for bronchial epithelial cells in airway inflammation studies. *Am J Respir Cell Mol Biol,* 39, (5)**,** 560-8.
Mckone, E. F., et al. Long-term safety and efficacy of ivacaftor in patients with cystic fibrosis who have the Gly551Asp-*CFTR* mutation: a phase 3, open-label extension study (PERSIST). *Lancet Respir Med,* 2, (11)**,** 902-910.
Mcnamara, P. S., et al. 2008. Comparison of techniques for obtaining lower airway epithelial cells from children. *Eur Respir J,* 32, (3)**,** 763-8.
Mcshane, D., et al. 2003. Airway surface pH in subjects with cystic fibrosis. *Eur Respir J,* 21, (1)**,** 37-42.
Meachery, G., et al. 2008. Outcomes of lung transplantation for cystic fibrosis in a large UK cohort. *Thorax,* 63, 725-731.
Melis, N., et al. 2014. Revisiting CFTR inhibition: a comparative study of CFTR(inh)-172 and GlyH-101 inhibitors. *Br J Pharmacol,* 171, (15)**,** 3716-3727.
Miledi, R. 1982. A calcium-dependent transient outward current in Xenopus laevis oocytes. 215, (1201)**,** 491-7.
Moran, A., et al. 2009. Cystic Fibrosis–Related Diabetes: Current Trends in Prevalence, Incidence, and Mortality. *Diabetes Care,* 32, 1626-1631.
Moran, O. & Zegarra-Moran, O. 2008. On the measurement of the functional properties of the CFTR. *J Cyst Fibros,* 7, (6)**,** 483-494.
Mosler, K., et al. 2008. Feasibility of nasal epithelial brushing for the study of airway epithelial functions in CF infants. *J Cyst Fibros,* 7, (1)**,** 44-53.
Nakayama, K., et al. 2002. Acid Stimulation Reduces Bactericidal Activity of Surface Liquid in Cultured Human Airway Epithelial Cells. *Am J Respir Cell Mol Biol,* 26, (1)**,** 105-113.
Namkung, W., et al. 2010a. CFTR-Adenylyl Cyclase I Association Responsible for UTP Activation of CFTR in Well-Differentiated Primary Human Bronchial Cell Cultures. *Mol Biol Cell,* 21, (15)**,** 2639-2648.
Namkung, W., et al. 2011a. TMEM16A Inhibitors Reveal TMEM16A as a Minor Component of Calcium-activated Chloride Channel Conductance in Airway and Intestinal Epithelial Cells. *J Biol Chem,* 286, (3)**,** 2365-2374.
Namkung, W., et al. 2010b. Inhibition of Ca2+-activated Cl− channels by gallotannins as a possible molecular basis for health benefits of red wine and green tea. *FASEB J,* 24, (11)**,** 4178-4186.
Namkung, W., et al. 2011b. Small-molecule activators of TMEM16A, a calcium-activated chloride channel, stimulate epithelial chloride secretion and intestinal contraction. *FASEB J,* 25, (11)**,** 4048-4062.

Ni, Y.-L., et al. 2014. Activation and Inhibition of TMEM16A Calcium-Activated Chloride Channels. *PloS one,* 9, (1), e86734.
Nixon, L. S., et al. 1998. Circulating Immunoreactive Interleukin-6 in Cystic Fibrosis. *Am J Respir Crit Care Med,* 157, (6), 1764-1769.
O'sullivan, B. P. & Freedman, S. D. 2009. Cystic fibrosis. *Lancet,* 373, (9678), 1891-1904.
Ogilvie, V., et al. 2011. Differential global gene expression in cystic fibrosis nasal and bronchial epithelium. *Genomics,* 98, (5), 327-36.
Okiyoneda, T., et al. 2010. Peripheral Protein Quality Control Removes Unfolded CFTR from the Plasma Membrane. *Science,* 329, 805-810.
Olympus. 2017. *Solutions for bronchoscopy* [Online]. Germany. Available: https://ssd.olympus.eu/medical/en/medical_systems/contact___support/media centre/media_detail_99008.jsp [Accessed].
Ousingsawat, J., et al. 2011. CFTR and TMEM16A are Separate but Functionally Related Cl Channels. *Cell Physiol Biochem,* 28, (4), 715-724.
Ousingsawat, J., et al. 2009. Loss of TMEM16A Causes a Defect in Epithelial Ca2+-dependent Chloride Transport. *J Biol Chem,* 284, (42), 28698-28703.
Pack, R. J., et al. 1981. The cells of the tracheobronchial epithelium of the mouse: a quantitative light and electron microscope study. *J Anat,* 132, (Pt 1), 71-84.
Paradiso, A. M., et al. 2000. Polarized Signaling via Purinoceptors in Normal and Cystic Fibrosis Airway Epithelia. *J Gen Physiol,* 117, (1), 53.
Pedersen, S. S., et al. 1992. Role of alginate in infection with mucoid Pseudomonas aeruginosa in cystic fibrosis. *Thorax,* 47, 6-13.
Pezzulo, A. A., et al. 2012. Reduced airway surface pH impairs bacterial killing in the porcine cystic fibrosis lung. *Nature,* 487, (7405), 109-13.
Picher, M., et al. 2004. Metabolism of P2 Receptor Agonists in Human Airways: implications for mucociliary clearance and cystic fibrosis. *J Biol Chem,* 279, (19), 20234-20241.
Pier, G. B., et al. 1991. Complement deposition by antibodies to Pseudomonas aeruginosa mucoid exopolysaccharide (MEP) and by non-MEP specific opsonins. *J Immunol,* 147, 1869-1876.
Pillarisetti, N., et al. 2011. Infection, inflammation, and lung function decline in infants with cystic fibrosis. *Am J Respir Crit Care Med,* 184, (1), 75-81.
Pitkänen, O. M., et al. 2001. Expression of α -, β -, and γ -hENaC mRNA in the Human Nasal, Bronchial, and Distal Lung Epithelium. *Am J Respir Crit Care Med,* 163, (1), 273-276.
Pranke, I. M., et al. 2017. Correction of CFTR function in nasal epithelial cells from cystic fibrosis patients predicts improvement of respiratory function by CFTR modulators. *Sci Rep,* 7, (1), 7375.
Prince, L. S. & Welsh, M. J. 1999. Effect of subunit composition and Liddle's syndrome mutations on biosynthesis of ENaC. *Am J Physiol Cell Physiol,* 276, (6), C1346-C1351.
Pringle, E. J., et al. 2012. Nasal and bronchial airway epithelial cell mediator release in children. *Pediatr Pulmonol,* 47, (12), 1215-25.
Qiagen 2014. AllPrep RNA/Protein Handbook.
Qu, Z. & Hartzell, H. C. 2000. Anion Permeation in Ca(2+)-Activated Cl(−) Channels. *J Gen Physiol,* 116, (6), 825-844.
Ramsey, B. W., et al. 2011. A CFTR Potentiator in Patients with Cystic Fibrosis and the G551D Mutation. *N Engl J Med,* 365, (18), 1663-1672.
Randell, S. H., et al. 2006. Effective Mucus Clearance Is Essential for Respiratory Health. *Am J Respir Cell Mol Biol,* 35, (1), 20-28.

Ratcliff, R., et al. 1993. Production of a severe cystic fibrosis mutation in mice by gene targeting. *Nat Genet,* 4, 35.
Ratjen, F., et al. 2015. Cystic fibrosis. *Nat Rev Dis Primers,* 1, 1-19.
Ratjen, F., et al. 2012. Long term effects of denufosol tetrasodium in patients with cystic fibrosis. *J Cyst Fibros,* 11, (6)**,** 539-549.
Ratjen, F., et al. 2017. Efficacy and safety of lumacaftor and ivacaftor in patients aged 6 -11 years with cystic fibrosis homozygous for F508del-CFTR: a randomised, placebo-controlled phase 3 trial. *Lancet Respir Med,* 5, (7)**,** 557-567.
Rauh, R., et al. 2010. A mutation of the epithelial sodium channel associated with atypical cystic fibrosis increases channel open probability and reduces Na+ self inhibition. *J Physiol,* 588, (8)**,** 1211-1225.
Riordan, J., et al. 1989. Identification of the cystic fibrosis gene: cloning and characterization of complementary DNA. *Science,* 245, (4922)**,** 1066-1073.
Rock, J. R., et al. 2009. Transmembrane Protein 16A (TMEM16A) Is a Ca2+-regulated Cl– Secretory Channel in Mouse Airways. *J Biol Chem,* 284, (22)**,** 14875-14880.
Rogers, C. S., et al. 2008. Disruption of the *CFTR* Gene Produces a Model of Cystic Fibrosis in Newborn Pigs. *Science,* 321, (5897)**,** 1837.
Rosen, B. H., et al. 2018. Animal and model systems for studying cystic fibrosis. *J Cyst Fibros,* 17, (2)**,** S28-S34.
Rosenbaum, D. M., et al. 2009. The structure and function of G-protein-coupled receptors. *Nature,* 459, (7245)**,** 356-363.
Rossi, U. G. & Owens, C. M. 2005. The radiology of chronic lung disease in children. *Arch Dis Child,* 90, 601-607.
Rowe, S. M., et al. 2017. Tezacaftor–Ivacaftor in Residual-Function Heterozygotes with Cystic Fibrosis. *N Engl J Med,* 377, (21)**,** 2024-2035.
Rozmahe, R., et al. 1996. Modulation of disease severity in cystic fibrosis transmembrane conductance regulator deficient mice by a secondary genetic factor. *Nat Genet,* 12, 280.
Ruffin, M., et al. 2013. Anoctamin 1 dysregulation alters bronchial epithelial repair in cystic fibrosis. *Biochim Biophys Acta,* 1832, (12)**,** 2340-51.
Rymut, S. M., et al. 2013. Reduced microtubule acetylation in cystic fibrosis epithelial cells. *Am J Physiol Lung Cell Mol Physiol,* 305, (6)**,** L419-L431.
Sahin-Yilmaz, A. & Naclerio, R. M. 2011. Anatomy and Physiology of the Upper Airway. *Proc Am Thorac Soc,* 8, (1)**,** 31-39.
Sajjan, U., et al. 2004. Responses of Well-Differentiated Airway Epithelial Cell Cultures from Healthy Donors and Patients with Cystic Fibrosis to Burkholderia cenocepacia Infection. *Infect Immun,* 72, (7)**,** 4188-4199.
Satir, P. & Christensen, S. T. 2007. Overview of Structure and Function of Mammalian Cilia. *Annu Rev Physiol,* 69, (1)**,** 377-400.
Savitski, A. N., et al. 2009. Secondhand smoke inhibits both Cl- and K+ conductances in normal human bronchial epithelial cells. *Respiratory Research,* 10, (1)**,** 120.
Schmittgen, T. D. & Livak, K. J. 2008. Analyzing real-time PCR data by the comparative CT method. *Nat Protoc,* 3, 1101.
Scholte, B. J., et al. 2004. Animal models of cystic fibrosis. *J Cyst Fibros,* 3, 183-190.
Schreiber, M. & Salkoff, L. 1997. A novel calcium-sensing domain in the BK channel. *Biophys J,* 73, (3)**,** 1355-1363.
Schroeder, B. C., et al. 2008. Expression cloning of TMEM16A as a calcium-activated chloride channel subunit. *Cell,* 134, (6)**,** 1019-1029.

Schultz, A., et al. 2017. Airway surface liquid pH is not acidic in children with cystic fibrosis. *Nat Commun,* 10, (8)**,** 1409.
Schulz, A. & Tümmler, B. 2016. Non-allergic asthma as a CFTR-related disorder. *Journal of Cystic Fibrosis,* 15, (5)**,** 641-644.
Scudieri, P., et al. 2012a. Association of TMEM16A chloride channel overexpression with airway goblet cell metaplasia. *J Physiol,* 590, (23)**,** 6141-6155.
Scudieri, P. & Galietta, L. J. V. 2016. TMEM16 Proteins (Anoctamins) in Epithelia. *Ion Channels and Transporters of Epithelia in Health and Disease.* Springer, 553-568.
Scudieri, P., et al. 2013. TMEM16A–TMEM16B chimaeras to investigate the structure–function relationship of calcium-activated chloride channels. *Biochem J,* 452, 443-455.
Scudieri, P., et al. 2012b. The anoctamin family: TMEM16A and TMEM16B as calcium-activated chloride channels. *Exp Physiol,* 97, (2)**,** 177-183.
Seo, Y., et al. 2016. Ani9, A Novel Potent Small-Molecule ANO1 Inhibitor with Negligible Effect on ANO2. *PloS one,* 11, (5)**,** e0155771.
Serrano, C., et al. 2005. Rhinitis and asthma: one airway, one disease. *Arch Bronconeumol,* 41, (10)**,** 569-78.
Sheridan, M. B., et al. 2005. Mutations in the beta-subunit of the epithelial Na+ channel in patients with a cystic fibrosis-like syndrome. *Hum Mol Genet,* 14, (22)**,** 3493-3498.
Shimkets, R. A., et al. 1994. Liddle's syndrome: Heritable human hypertension caused by mutations in the β subunit of the epithelial sodium channel. *Cell,* 79, (3)**,** 407-414.
Sly, P. D., et al. 2013. Risk Factors for Bronchiectasis in Children with Cystic Fibrosis. *New England Journal of Medicine,* 368, (21)**,** 1963-1970.
Smith, J. J., et al. 1996. Cystic Fibrosis Airway Epithelia Fail to Kill Bacteria Because of Abnormal Airway Surface Fluid. *Cell,* 85, (2)**,** 229-236.
Snouwaert, J. N., et al. 1992. An Animal Model for Cystic Fibrosis Made by Gene Targeting. *Science,* 257, 1083-1088.
Srinivasan, B., et al. 2015. TEER Measurement Techniques for In Vitro Barrier Model Systems. *J Lab Autom,* 20, (2)**,** 107-126.
Steinke, J. W. & Borish, L. 2001. Th2 cytokines and asthma — Interleukin-4: its role in the pathogenesis of asthma, and targeting it for asthma treatment with interleukin-4 receptor antagonists. *Respir Res,* 2, (2)**,** 66-70.
Stephan, A. B., et al. 2009. ANO2 is the cilial calcium-activated chloride channel that may mediate olfactory amplification. *Proc Am Thorac Soc,* 106, 11776-11781.
Stephenson, A. L., et al. 2015. Clinical and demographic factors associated with post-lung transplantation survival in individuals with cystic fibrosis. *J Heart Lung Transplant,* 34, (9)**,** 1139-1145.
Stewart, C. E., et al. 2012. Evaluation of Differentiated Human Bronchial Epithelial Cell Culture Systems for Asthma Research. *J Allergy,* 2012, 943982.
Stick, S. M., et al. 2009. Bronchiectasis in Infants and Preschool Children Diagnosed with Cystic Fibrosis after Newborn Screening. *J Pediatr,* 155, (5)**,** 623-628.e1.
Stöhr, H., et al. 2009. TMEM16B, A Novel Protein with Calcium-Dependent Chloride Channel Activity, Associates with a Presynaptic Protein Complex in Photoreceptor Terminals. *J Neurosci,* 29, 6809-6818.
Strautnieks, S. S., et al. 1996. A novel spice–site mutation in the γ subunit of the epithelial sodium channel gene in three pseudohypoaldosteronism type 1 families. *Nat Genet,* 13, 248.
Stutts, M. J., et al. 1995. CFTR as a cAMP-dependent regulator of sodium channels. *Science,* 269, (5225)**,** 847-850.

Sun, X., et al. 2010. Disease phenotype of a ferret CFTR-knockout model of cystic fibrosis. *J Clin Invest,* 120, (9)**,** 3149-3160.
Taddei, A., et al. 2004. Altered channel gating mechanism for CFTR inhibition by a high-affinity thiazolidinone blocker. *FEBS Letters,* 558, (1)**,** 52-56.
Taggart, C., et al. 2000. Increased elastase release by CF neutrophils is mediated by tumor necrosis factor-α and interleukin-8. *Am J Physiol Lung Cell Mol Physiol,* 278, (1)**,** L33-L41.
Tam, A., et al. 2011. The airway epithelium: more than just a structural barrier. *Ther Adv Respir Dis,* 5, (4)**,** 255-273.
Tan, H.-L., et al. 2011. The Th17 Pathway in Cystic Fibrosis Lung Disease. *Am J Respir Crit Care Med,* 184, (2)**,** 252-258.
Tang, L., et al. 2009. Mechanism of direct bicarbonate transport by the CFTR anion channel. *J Cyst Fibros,* 8, (2)**,** 115-121.
Tarran, R., et al. 2002. Regulation of murine airway surface liquid volume by CFTR and Ca2+-activated Cl- conductances. *J. Gen Physiol,* 120, (0022-1295 (Print))**,** 407-418.
Tate, S., et al. 2002. Airways in cystic fibrosis are acidified: detection by exhaled breath condensate. *Thorax,* 57, (11)**,** 926-929.
Taylor-Cousar, J. L., et al. 2017. Tezacaftor–Ivacaftor in Patients with Cystic Fibrosis Homozygous for Phe508del. *N Engl J Med,* 377, (21)**,** 2013-2023.
Thavagnanam, S., et al. 2014. Nasal Epithelial Cells Can Act as a Physiological Surrogate for Paediatric Asthma Studies. *PloS one,* 9, (1)**,** e85802.
Tian, Y., et al. 2011. Calmodulin-dependent activation of the epithelial calcium-dependent chloride channel TMEM16A. *FASEB J,* 25, (3)**,** 1058-1068.
Tiringer, K., et al. 2013. A Th17- and Th2-skewed cytokine profile in cystic fibrosis lungs represents a potential risk factor for Pseudomonas aeruginosa infection. (1535-4970 (Electronic)).
Tosoni, K., et al. 2016. Using Drugs to Probe the Variability of Trans-Epithelial Airway Resistance. *PloS one,* 11, (2)**,** e0149550.
Ussing, H. & Zerahn, K. 1951. Active transport of sodium as the source of electric current in the short-circuited isolated frog skin. *Acta Physiol,* 25, (0001-6772 (Print))**,** 110-27.
Van Goor, F., et al. 2009a. Rescue of CF airway epithelial cell function in vitro by a CFTR potentiator, VX-770. *Proc Am Thorac Soc,* 106, (44)**,** 18825-18830.
Van Goor, F., et al. 2009b. Rescue of CF airway epithelial cell function in vitro by a CFTR potentiator, VX-770. *Proceedings of the National Academy of Sciences,* 106, 18825-18830.
Vergani, P., et al. 2005. CFTR channel opening by ATP-driven tight dimerization of its nucleotide-binding domains. *Nature,* 433, 876.
Verkman, A. S., et al. 2003. Role of airway surface liquid and submucosal glands in cystic fibrosis lung disease. *American Journal of Physiology - Cell Physiology,* 284, (1)**,** C2-C15.
Vertex Pharamceuticals Incorporated 2018. Vertex Initiates First Phase 3 Study of VX-659, Tezacaftor and Ivacaftor as a Triple Combination Regimen for People with Cystic Fibrosis.
Wainwright, C. E., et al. 2015. Lumacaftor–Ivacaftor in Patients with Cystic Fibrosis Homozygous for Phe508del CFTR. *N Engl J Med,* 373, 220-231.
Waldmann, R., et al. 1995. Molecular Cloning and Functional Expression of a Novel Amiloride-sensitive Na+ Channel. *J Biol Chem,* 270, (46)**,** 27411-27414.
Walker, M. P., et al. SPX-101 Is a Novel ENaC-Targeted Therapeutic for Cystic Fibrosis that Restores Mucus Transport. C67. Suppurative lung diseases in children, 2017. American Thoracic Society, A7674-A7674.

Walters, E. H. & Gardiner, P. V. 1991. Bronchoalveolar lavage as a research tool. *Thorax,* 46, (9), 613-618.
Wang, H., et al. 2016. CRISPR/Cas9 in Genome Editing and Beyond. *Annu Rev Biochem,* 85, (1), 227-264.
Wang, H., et al. 2017. Cell-specific mechanisms of TMEM16A Ca2+-activated chloride channel in cancer. *Mol Cancer,* 16, (1), 152.
Wei, L., et al. 1999. Interaction between calcium-activated chloride channels and the cystic fibrosis transmembrane conductance regulator. *Pflugers Arch,* 438, (5), 635-641.
Welsh, M. J. & Smith, A. E. 1993. Molecular mechanisms of CFTR chloride channel dysfunction in cystic fibrosis. *Cell,* 73, (7), 1251-1254.
Whiting, P., et al. 2014. Ivacaftor for the treatment of patients with cystic fibrosis and the G551D mutation: a systematic review and cost-effectiveness analysis. *Health Technol Assess,* 18, (18).
Wichmann, L., et al. 2018. Incorporation of the delta-subunit into the epithelial sodium channel (ENaC) generates protease-resistant ENaCs in Xenopus laevis. *J Biol Chem*.
Widdicombe, J. H. & Widdicombe, J. G. 1995. Regulation of human airway surface liquid. *Respir Physiol,* 99, (1), 3-12.
Widdicombe, J. H. & Wine, J. J. 2015. Airway Gland Structure and Function. *Physiol Rev,* 95, (4), 1241-1319.
Worlitzsch, D., et al. 2002. Effects of reduced mucus oxygen concentration in airway Pseudomonas infections of cystic fibrosis patients. *J Clin Invest,* 109, (3), 317-325.
Wu, C.-J., et al. 2013. Epithelial Cell Adhesion Molecule (EpCAM) Regulates Claudin Dynamics and Tight Junctions. *J Biol Chem,* 288, (17), 12253-12268.
Xiao, Q., et al. 2011. Voltage- and calcium-dependent gating of TMEM16A/Ano1 chloride channels are physically coupled by the first intracellular loop. *Proc Am Thorac Soc,* 108, 8891-8896.
Yaghi, A., et al. 2010. Primary Human Bronchial Epithelial Cells Grown from Explants. *J Vis Exp*, (37), 1789.
Yang, Y. D., et al. 2008. TMEM16A confers receptor-activated calcium-dependent chloride conductance. *Nature,* 455, (7217), 1210-1215.
You, Y., et al. 2004. Role of f-box factor foxj1 in differentiation of ciliated airway epithelial cells. *Am J Physiol Lung Cell Mol Physiol,* 286, (4), L650-L657.
Yu, K., et al. 2012. Explaining Calcium-Dependent Gating of Anoctamin-1 Chloride Channels Requires a Revised Topology. *Circ Res,* 110, (7), 990-999.
Yu, K., et al. 2014. Activation of the Ano1 (TMEM16A) chloride channel by calcium is not mediated by calmodulin. *J Gen Physiol,* 143, 253-267.
Yu, X., et al. 2008. Foxj1 transcription factors are master regulators of the motile ciliogenic program. *Nat Genet,* 40, 1445.
Zabner, J., et al. 2005. CFTR DeltaF508 mutation has minimal effect on the gene expression profile of differentiated human airway epithelia. *Am J Physiol Lung Cell Mol Physiol,* 289, (4), L545-53.
Zaidman, N. A., et al. 2016. Differentiation of human bronchial epithelial cells: role of hydrocortisone in development of ion transport pathways involved in mucociliary clearance. *Am J Physiol Cell Physiol,* 311, (2), C225-C236.
Zaidman, N. A., et al. 2017. Large-conductance Ca2+-activated K+ channel activation by apical P2Y receptor agonists requires hydrocortisone in differentiated airway epithelium. *The Journal of Physiology,* 595, (14), 4631-4645.

Zeiher, B. G., et al. 1995. A mouse model for the delta F508 allele of cystic fibrosis. *J Clin Invest,* 96, (4)**,** 2051-2064.
Zhang, C.-H., et al. 2013. The Transmembrane Protein 16A Ca2+-activated Cl− Channel in Airway Smooth Muscle Contributes to Airway Hyperresponsiveness. *Am J Respir Crit Care Med,* 187, (4)**,** 374-381.
Zolin, A., et al. 2017. European Cystic Fibrosis Society Patient Registry Annual Report 2016. Denmark.